POWER ELECTRONICS

CIRCUITS, DEVICES, AND APPLICATIONS

THIRD EDITION



MUHAMMAD H. RASHID

Power Electronics

Circuits, Devices, and Applications

Muhammad.H.Rashid Power Electronics Circuits, Devices & Applications - PowerEn.ir

Muhammad Harunur Rashid

Ph.D., Fellow IEE
Professor of Electrical Engineering
PURDUE UNIVERSITY Calumet





Prentice Hall, Englewood Cliffs, New Jersey 07632



Contents

PREFACE xvii

ACKNOWLEDGMENTS xx

CHAPTER 1 INTRODUCTION 1

1-1 Applications of Power Electronics, 1
1-2 Power Semiconductor Devices, 3
1-3 Control Characteristics of Power Devices, 8
1-4 Types of Power Electronic Circuits, 8
1-5 Design of Power Electronics Equipment, 12
1-6 Peripheral Effects, 13
Summary, 13
References, 14
Review Questions, 14

CHAPTER 2 DIODE CIRCUITS AND RECTIFIERS 15

2-1 Introduction, 15
2-2 Diodes with *RC* and *RL* Loads, 15
2-3 Diodes with *LC* and *RLC* Loads, 18
2-4 Freewheeling Diodes, 23
2-5 Recovery of Trapped Energy with a Diode, 25
2-6 Single-Phase Half-Wave Rectifiers, 29
2-7 Performance Parameters, 29
2-8 Single-Phase Full-Wave Rectifiers, 33
2-9 Multiphase Star Rectifiers, 38
2-10 Three-Phase Bridge Rectifiers, 41
2-11 Rectifier Circuit Design, 44
2-12 Effects of Source and Load Inductances, 49
Summary, 50
References, 51
Review Questions, 51
Problems, 52

CHAPTER 3 THYRISTOR COMMUTATION TECHNIQUES 56

3-1 Introduction, 56
3-2 Natural Commutation, 57
3-3 Forced Commutation, 57
3-3.1 Self-Commutation, 58
3-3.2 Impulse Commutation, 60
3-3.3 Resonant Pulse Commutation, 64
3-3.4 Complementary Commutation, 67
3-3.5 External Pulse Commutation, 69
3-3.6 Load-Side Commutation, 69
3-3.7 Line-Side Commutation, 69
3-4 Commutation Circuit Design, 71
3-5 Commutation Capacitors, 74
Summary, 74
References, 74
Review Questions, 75
Problems, 75

CHAPTER 4 CONTROLLED RECTIFIERS 77

4-1 Introduction, 77
4-2 Principle of Phase-Controlled Converter Operation, 78
4-3 Single-Phase Semiconverters, 80
4-4 Single-Phase Full Converters, 84
4-5 Single-Phase Dual Converters, 87

4-6 Single-Phase Series Converters, 90
4-7 Three-Phase Half-Wave Converters, 95
4-8 Three-Phase Semiconverters, 99
4-9 Three-Phase Full Converters, 101
4-10 Three-Phase Dual Converters, 105
4-11 Power Factor Improvements, 107
4-11.1 Extinction Angle Control, 108
4-11.2 Symmetrical Angle Control, 110
4-11.3 Pulse-Width-Modulation Control, 112
4-11.4 Sinusoidal Pulse-Width Modulation, 114
4-12 Design of Converter Circuits, 115
4-13 Effects of Load and Source Inductances, 117
Summary, 119
References, 119
Review Questions, 120
Problems, 121

CHAPTER 5 STATIC SWITCHES 124

5-1 Introduction, 124
5-2 Single-Phase AC Switches, 125
5-3 Three-Phase AC Switches, 127
5-4 Three-Phase Reversing Switches, 127
5-5 AC Switches for Bus Transfer, 130
5-6 DC Switches, 130
5-7 Solid-State Relays, 132
5-8 Design of Static Switches, 133
Summary, 134
References, 134
Review Questions, 134
Problems, 135

CHAPTER 6 AC VOLTAGE CONTROLLERS 137

6-1 Introduction, 137
6-2 Principle of On–Off Control, 138
6-3 Principle of Phase Control, 140
6-4 Single-Phase Bidirectional Controllers with Resistive Loads, 142
6-5 Single-Phase Controllers with Inductive Loads, 145
6-6 Three Phase Half-Wave Controllers, 148
6-7 Three-Phase Full-Wave Controllers, 154
6-8 Three-Phase Bidirectional Delta-Connected Controllers, 157
6-9 Single-Phase Transformer Tap Changers, 161
6-10 Cycloconverters, 166

6-10.1 Single-Phase Cycloconverters, 166
6-10.2 Three-Phase Cycloconverters, 168
6-10.3 Reduction of Output Harmonics, 169
6-11 Design of AC Voltage-Controller Circuits, 172
6-12 Effects of Source and Load Inductances, 175
Summary, 176
References, 176
Review Questions, 176
Problems, 177

CHAPTER 7 DC CHOPPERS 180

7-1 Introduction, 180
7-2 Principle of Step-Down Operation, 180
7-3 Step-Down Choppers with *RL* Load, 183
7-4 Principle of Step-Up Operation, 186
7-5 Performance Parameters, 189
7-6 Switching-Mode Regulators, 189
7-6.1 Buck Regulators, 190
7-6.2 Boost Regulators, 193
7-6.3 Buck–Boost Regulators, 196
7-6.4 Cúk Regulators, 199
7-6.5 Limitations of Single-Stage Conversion, 204
7-7 Thyristor Chopper Circuits, 204
7-7.1 Impulse-Commutated Choppers, 205
7-7.2 Effects of Source and Load Inductance, 210
7-7.3 Impulse-Commutated Three-Thyristor Choppers, 210
7-7.4 Resonant Pulse Choppers, 212
7-8 Chopper Circuit Design, 215
7-9 Magnetic Considerations, 221
Summary, 221
References, 221
Review Questions, 222
Problems, 223

CHAPTER 8 INVERTERS 226

8-1 Introduction, 226
8-2 Principle of Operation, 227
8-3 Performance Parameters, 228
8-4 Single-Phase Bridge Inverters, 230
8-5 Three-Phase Inverters, 233
8-6 Voltage Control of Single-Phase Inverters, 239
8-6.1 Single-Pulse-Width Modulation, 240

8-6.2 Multiple-Pulse-Width Modulation, 241
8-6.3 Sinusoidal Pulse-Width Modulation, 243
8-6.4 Modified Sinusoidal Pulse-Width Modulation, 245
8-6.5 Phase-Displacement Control, 246
8-7 Voltage Control of Three-Phase Inverters, 247
8-8 Harmonic Reductions, 248
8-9 Series Resonant Inverters, 251
8-9.1 Series Resonant Inverters with Unidirectional Switches, 252
8-9.2 Series Resonant Inverters with Bidirectional Switches, 259
8-10 Forced-Commutated Thyristor Inverters, 264
8-10.1 Auxiliary-Commutated Inverters, 265
8-10.2 Complementary-Commutated Inverters, 266
8-11 Current-Source Inverters, 273
8-12 Variable DC Link Inverter, 276
8-13 Inverter Circuit Design, 276
8-14 Magnetic Considerations, 279
Summary, 279
References, 279
Review Questions, 280
Problems, 281

CHAPTER 9 POWER SUPPLIES 284

9-1 Introduction, 284
9-2 DC Power Supplies, 285
9-2.1 Switched-Mode DC Power Supplies, 285
9-2.2 Resonant DC Power Supplies, 288
9-2.3 Bidirectional Power Supplies, 289
9-3 AC Power Supplies, 290
9-3.1 Switched-Mode AC Power Supplies, 290
9-3.2 Resonant AC Power Supplies, 291
9-3.3 Bidirectional AC Power Supplies, 291
9-4 Multistage Conversions, 292
9-5 Magnetic Considerations, 293
Summary, 294
References, 294
Review Questions, 294
Problems, 295

CHAPTER 10 DC DRIVES 296

10-1 Introduction, 296
10-2 Basic Characteristics of DC Motors, 297
10-3 Single-Phase Drives, 300
10-3.1 Single-Phase Half-Wave Converter Drives, 301

10-3.2 Single-Phase Semiconverter Drives, 302
10-3.3 Single-Phase Full-Converter Drives, 303
10-3.4 Single-Phase Dual-Converter Drives, 304
10-4 Three-Phase Drives, 307
10-4.1 Three-Phase Half-Wave Converter Drives, 308
10-4.2 Three-Phase Semiconverter Drives, 308
10-4.3 Three-Phase Full-Converter Drives, 308
10-4.4 Three-Phase Dual-Converter Drives, 309
10-5 Chopper Drives, 313
10-5.1 Principle of Power Control, 313
10-5.2 Principle of Regenerative Brake Control, 315
10-5.3 Principle of Rheostatic Brake Control, 317
10-5.4 Principle of Combined Regenerative and Rheostatic Brake Control, 319
10-5.5 Two/Four-Quadrant Chopper Drives, 319
10-5.6 Multiphase Choppers, 321
10-6 Closed-Loop Control of DC Drives, 323
10-6.1 Open-Loop Transfer Function, 324
10-6.2 Closed-Loop Transfer Function, 328
10-6.3 Phase-Locked-Loop Control, 330
10-6.4 Microcomputer Control of DC Drives, 332
Summary, 333
References, 333
Review Questions, 334
Problems, 335

CHAPTER 11 AC DRIVES 339

11-1 Introduction, 339
11-2 Induction Motor Drives, 340
11-2.1 Performance Characteristics, 341
11-2.2 Stator Voltage Control, 347
11-2.3 Rotor Voltage Control, 349
11-2.4 Frequency Control, 356
11-2.5 Voltage and Frequency Control, 358
11-2.6 Current Control, 361
11-2.7 Voltage, Current, and Frequency Control, 364
11-2.8 Closed-Loop Control of Induction Motors, 365
11-3 Synchronous Motor Drives, 369
11-3.1 Cylindrical Rotor Motors, 370
11-3.2 Salient-Pole Motors, 373
11-3.3 Reluctance Motors, 374
11-3.4 Permanent-Magnet Motors, 375
11-3.5 Closed-Loop Control of Synchronous Motors, 376

Summary, 377
References, 378
Review Questions, 379
Problems, 380

CHAPTER 12 POWER SEMICONDUCTOR DIODES 383

12-1 Introduction, 383
12-2 Diode Characteristics, 383
12-3 Power Diode Types, 386
12-3.1 General-Purpose Diodes, 386
12-3.2 Fast-Recovery Diodes, 387
12-3.3 Schottky Diodes, 387
12-4 Performance Parameters, 388
12-5 Effects of Forward and Reverse Recovery Time, 402
12-6 Series-Connected Diodes, 406
12-7 Parallel-Connected Diodes, 408
Summary, 409
Review Questions, 409
Problems, 410

CHAPTER 13 POWER TRANSISTORS 412

13-1 Introduction, 412
13-2 Bipolar Junction Transistors, 413
13-2.1 Steady-State Characteristics, 413
13-2.2 Switching Characteristics, 418
13-2.3 Performance Parameters, 424
13-2.4 Base Drive Control, 436
13-3 Power MOSFETs, 440
13-3.1 Steady-State Characteristics, 442
13-3.2 Switching Characteristics, 444
13-3.3 Performance Parameters, 445
13-3.4 Gate Drive, 452
13-4 MOSIGTs, 452
13-5 Series and Parallel Operation, 457
13-6 *di/dt* and *dv/dt* Limitations, 458
13-7 Isolation of Gate and Base Drives, 461
13-7.1 Pulse Transformers, 462
13-7.2 Optocouplers, 462
Summary, 463
References, 464
Review Questions, 464
Problems, 466

CHAPTER 14 THYRISTORS 468

14-1 Introduction, 468
14-2 Thyristor Characteristics, 468
14-3 Two-Transistor Model of Thyristor, 470
14-4 Thyristor Turn-On, 472
14-5 *di/dt* Protection, 474
14-6 *dv/dt* Protection, 476
14-7 Thyristor Turn-Off, 478
14-8 Thyristor Types, 479
14-8.1 Phase Control Thyristors, 480
14-8.2 Fast-Switching Thyristors, 480
14-8.3 Gate-Turn-Off Thyristors, 481
14-8.4 Bidirectional Triode Thyristors, 482
14-8.5 Reverse-Conducting Thyristors, 482
14-8.6 Static Induction Thyristors, 483
14-8.7 Light-Activated Silicon-Controlled Rectifiers, 484
14-8.8 FET-Controlled Thyristors, 484
14-9 Performance Parameters, 485
14-9.1 SCR Parameters, 485
14-9.2 GTO Parameters, 494
14-10 Series Operation of Thyristors, 504
14-11 Parallel Operation of Thyristors, 507
14-12 Thyristor Firing Circuits, 507
Summary, 509
References, 510
Review Questions, 510
Problems, 511

CHAPTER 15 PROTECTION OF DEVICES AND CIRCUITS 514

15-1 Introduction, 514
15-2 Cooling and Heat Sinks, 514
15-3 Snubber Circuits, 520
15-4 Reverse Recovery Transients, 521
15-5 Supply- and Load-Side Transients, 527
15-6 Voltage Protection by Seleniun Diodes and Metal-Oxide Varistors, 529
15-7 Current Protections, 531
15-7.1 Fusing, 531
15-7.2 Fault Current with AC Source, 538
15-7.3 Fault Current with DC Source, 540
Summary, 541
References, 541
Review Questions, 542
Problems, 542

APPENDIX A THREE-PHASE CIRCUITS 545

APPENDIX B MAGNETIC CIRCUITS 549

APPENDIX C SWITCHING FUNCTIONS OF CONVERTERS 554

APPENDIX D TRANSIENT ANALYSIS 560

APPENDIX E FOURIER ANALYSIS 564

APPENDIX F LISTING OF COMPUTER PROGRAMS IN IBM-PC BASICA 567

BIBLIOGRAPHY 578

INDEX 580




POWEREN.IR

Preface

Power electronics deals with the applications of solid-state electronics for the control and conversion of electric power. Conversion techniques require the switching on and off of power semiconductor devices. Low-level electronics circuits, which normally consist of integrated circuits and discrete components, generate the required gating signals for the power devices. Integrated circuits and discrete components are being replaced by microprocessors.

An ideal power device should have no switching-on and -off limitations in terms of turn-on time, turn-off time, current, and voltage handling capabilities. Power semiconductor technology is rapidly developing fast switching power devices with increasing voltage and current limits. Power switching devices such as power BJTs, power MOSFETs, MOSIGTs, SCRs, TRIACS, GTOs, and other semiconductor devices are finding increasing applications in a wide range of products. With the availability of faster switching devices, the applications of modern microprocessors in synthesizing the control strategy for gating power devices to meet the conversion specifications are widening the scope of power electronics. The potential applications of power electronics is yet to be fully explored.

The time allocated to a course on power electronics in a typical undergraduate curriculum is normally only one semester. Power electronics has already advanced to the point where it is difficult to cover the entire subject in a one-semester course. The fundamentals of power electronics are well established and they do not change

rapidly. However, the device characteristics are changing continuously. *Power Electronics*, which employs the top-down approach, covers conversion techniques first, and then applications and device characteristics. It emphasizes the fundamental principles of power conversions. The book is divided into five parts:

1. Introduction—Chapter 1
2. Commutation techniques of SCRs and power conversion techniques—Chapters 2, 3, 4, 6, 7, and 8
3. Applications—Chapters 5, 9, 10, and 11
4. Devices—Chapters 12, 13, and 14
5. Protections—Chapter 15

Topics like three-phase circuits, magnetic circuits, switching functions of converters, dc transient analysis, and Fourier analysis are reviewed in the Appendixes.

Power Electronics is intended as a textbook for a course on "power electronics/static power converters" for junior or senior undergraduate students in electrical and electronic engineering. It could also be used as a textbook for graduate students and could be a reference book for practicing engineers involved in the design and applications of power electronics. The prerequisites would be courses on basic electronics and basic electrical circuits. The content of *Power Electronics* is beyond the scope of a one-semester course. For an undergraduate course, Chapters 1 to 9 should be adequate to provide a strong background on power electronics. Chapters 9 to 15 could be left for other courses or included in a graduate course.

Muhammad H. Rashid
Munster, Indiana

COMMENTS ON THE ENCLOSED FLOPPY DISK

A floppy disk has been enclosed with this text. It contains 51 programs written in Advanced BASIC and saved in ASCII characters. These programs can be used for the solutions of some worked-out examples and generating data for some figures, especially with pulse width modulation. The filenames on the disk begin with 'EX' for worked-out examples and 'FIG' for figures. For example, Figure 4-14 has a filename of 'FIG-14'. The filenames can be listed by directory listing. The disk has a double-sided 360 kB format readable by any personal computer with a PC-DOS or an MS-DOS 2 or 3 operating system, such as IBM PC, XT or AT. Questions regarding the software may be directed to the author:

Dr. Muhammad H. Rashid
Professor of Electrical Engineering
PURDUE UNIVERSITY Calumet
Hammond, Indiana 46323

PROGRAMS ON THE DISKETTE

EX2-16 .BAS
EX3-4 .BAS
EX3-5 .BAS
EX3-9 .BAS
EX3-10 .BAS
Ex3-12 .BAS
Ex4-6 .BAS
Ex4-12 .BAS
Ex4-13 .BAS
FIG4-14 .BAS
FIG4-15 .BAS
EX6-4 .BAS
EX6-5 .BAS
Ex6-6 .BAS
Ex6-7 .BAS
Ex6-8 .BAS
Ex6-9 .BAS
Ex6-12 .BAS
EX7-2 .BAS
EX8-3 .BAS
Ex8-7 .BAS
Ex8-9 .BAS
EX8-10 .BAS
EX8-11 .BAS
EX8-12 .BAS
Ex8-13 .BAS
EX8-14 .BAS
FIG8-11 .BAS
FIG8-13 .BAS
FIG8-15 .BAS
EX11-1 .BAS
Ex11-2 .BAS
Ex11-3 .BAS
Ex11-4 .BAS
EX11-6 .BAS
EX11-7 .BAS
Ex11-8 .BAS
Ex11-9 .BAS
EX11-10 .BAS
FIG11-3 .BAS
FIG11-4 .BAS
FIG11-9 .BAS
FIG11-12.BAS
EX12-1 .BAS
Ex12-2 .BAS
Ex12-3 .BAS
Ex12-4 .BAS
Ex12-5 .BAS
EX15-2 .BAS
EX15-3 .BAS
EX15-4 .BAS

Acknowledgments

I would like to thank the following reviewers for their comments and suggestions:

Ashoka K. S. Bhat—University of Victoria, Canada
Fred Brockhurst—Rose-Hulman Institute of Technology
Joseph M. Crowley—University of Illinois, Urbana–Champaign
Mehrad Ehsani—Texas A&M University
Shahidul I. Khan—Concordia University, Canada
Peter Lauritzen—University of Washington
Marrija Ilic-Spong—University of Illinois, Urbana–Champaign

It has been a great pleasure working with the editor, Tim Bozik, and his assistant, Kitty Monahan. Finally, I would thank my family for their love, patience, and understanding.

Power Electronics

1

Introduction

1-1 APPLICATIONS OF POWER ELECTRONICS

The demand for control of electric power for electric motor drive systems and industrial controls existed for many years, and this led to early development of the Ward–Leonard system to obtain a variable dc voltage for the control of dc motor drives. Power electronics have revolutionized the concept of power control for power conversion and for control of electrical motor drives.

Power electronics combine power, electronics, and control. Control deals with the steady-state and dynamic characteristics of closed-loop systems. Power deals with the static and rotating power equipment for the generation, transmission, and distribution of electric power. Electronics deal with the solid-state devices and circuits for signal processing to meet the desired control objectives. *Power electronics* may be defined as the applications of solid-state electronics for the control and conversion of electric power. The interrelationship of power electronics with power, electronics, and control is shown in Fig. 1-1.

Power electronics is based primarily on the switching of the power semiconductor devices. With the development of power semiconductor technology, the power-handling capabilities and the switching speed of the power devices have improved tremendously. The development of microprocessors/microcomputer

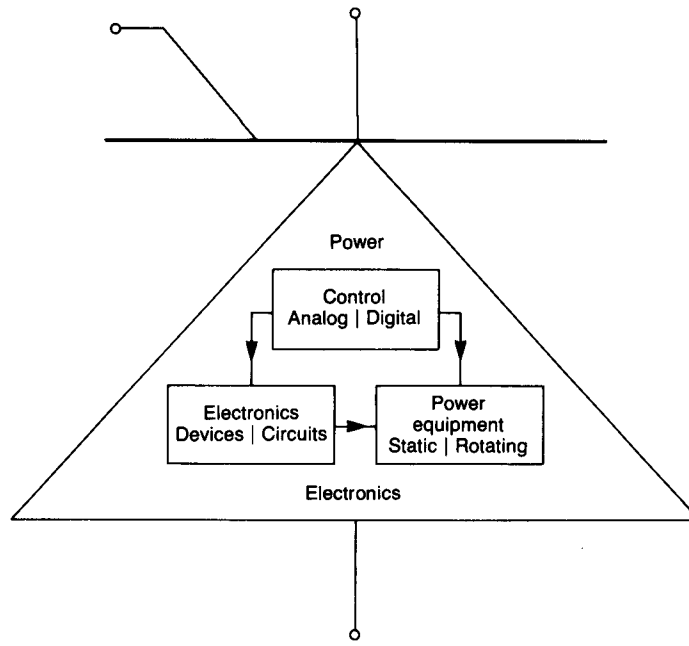


Figure 1-1 Relationship of power electronics to power, electronics and control.

technology has a great impact on the control and synthesizing the control strategy for the power semiconductor devices.

Power electronics have already found an important place in modern technology and are now used in a great variety of high-power products, including heat controls, light controls, motor controls, power supplies, vehicle propulsion systems, and high-voltage direct-current (HVDC) systems. It is difficult to draw the boundaries for the applications of power electronics; especially with the present trends in the development of power devices and microprocessors, the upper limit is undefined. Table 1-1 shows some applications of power electronics.

1-2 POWER SEMICONDUCTOR DEVICES

Since the first thyristor of silicon-controlled rectifier (SCR) was developed in late 1957, there have been tremendous advances in the power semiconductor devices. Until 1970, the conventional thyristors had been exclusively used for power control in industrial applications. Since 1970, various types of power semiconductor devices were developed and became commercially available. These can be divided broadly into four types: (1) power diodes, (2) thyristors, (3) power bipolar junction transistors (BJTs), and (4) power MOSFETs. The thyristors can be subdivided into seven types: (a) forced-commutated thyristor, (b) line-commutated thyristor, (c) gate-turn-off thyristor (GTO), (d) reverse-conducting thyristor (RCT), (e) static induction thyristor (SITH), (f) gate-assisted turn-off thyristor (GATT), and (g)

TABLE 1-1 SOME APPLICATIONS OF POWER ELECTRONICS

Advertising	Magnets
Air conditioning	Mass transits
Aircraft power supplies	Mercury-arc lamp ballasts
Alarms	Mining
Appliances	Model trains
Audio amplifiers	Motor controls
Battery charger	Motor drives
Blenders	Movie projectors
Blowers	Nuclear reactor control rod
Boilers	Oil well drilling
Burglar alarms	Oven controls
Cement kiln	Paper mills
Chemical processing	Particle accelerators
Clothes dryers	People movers
Computers	Phonographs
Conveyers	Photocopies
Cranes and hoists	Photographic supplies
Dimmers	Power supplies
Displays	Printing press
Electric blankets	Pumps and compressors
Electric door openers	Radar/sonar power supplies
Electric dryers	Range surface unit
Electric fans	Refrigerators
Electric vehicles	Regulators
Electromagnets	RF amplifiers
Electromechanical electroplating	Security systems
Electronic ignition	Servo systems
Electrostatic precipitators	Sewing machines
Elevators	Solar power supplies
Fans	Solid-state contactors
Flashers	Solid-state relays
Food mixers	Space power supplies
Food warmer trays	Static circuit breakers
Forklift trucks	Static relays
Furnaces	Steel mills
Games	Synchronous machine starting
Garage door openers	Synthetic fibers
Gas turbine starting	Television circuits
Generator exciters	Temperature controls
Grinders	Timers
Hand power tools	Toys
Heat controls	Traffic signal controls
High-frequency lighting	Trains
High-voltage dc (HVDC)	TV deflections
Induction heating	Ultrasonic generators
Laser power supplies	Uninterruptible power supplies
Latching relays	Vacuum cleaners
Light dimmers	VAR compensation
Light flashers	Vending machines
Linear induction motor controls	VLF transmitters
Locomotives	Voltage regulators
Machine tools	Washing machines
Magnetic recordings	Welding

Source: Ref. 5.

light-activated silicon-controlled rectifier (LASCR). Static induction transistors are also commercially available.

Power diodes are of three types: general purposes, high speed (or fast recovery), and Schottky. General-purpose diodes are available up to 3000 V, 3500 A, and the rating of fast-recovery diodes can go up to 3000 V, 1000 A. The reverse recovery time varies between 0.1 and 5 μs. The fast-recovery diodes are essential for high-frequency switching of power converters. A diode has two terminals: a cathode and an anode. Schottky diodes have low on-state voltage and very small recovery time, typically nanoseconds. The leakage current increases with the voltage rating and their ratings are limited to 100 V, 300 A. A diode conducts when its anode voltage is higher than that of the cathode; and the forward voltage drop of a power diode is vey low, typically 0.5 and 1.2 V. If the cathode voltage is higher than its anode voltage, a diode is said to be in a *blocking mode*. Figure 1-2 shows various configurations of general-purpose diodes, which basically fall into two types. One is called a *stud* or *stud-mounted* type and the other is called a *disk* or *press pak* or *hockey puck* type. In a stud-mounted type, either the anode or the cathode could be the stud.

A thyristor has three terminals: an anode, a cathode, and a gate. When a small current is passed through the gate terminal to cathode, the thyristor conducts, provided that the anode terminal is at a higher potential than the cathode. Once a thyristor is in a conduction mode, the gate circuit has no control and the thyristor continues to conduct. When a thyristor is in a conduction mode, the forward voltage drop is very small, typically 0.5 to 2 V. A conducting thyristor can be turned off by making the potential of the anode equal to or less than the cathode potential. The line-commutated thyristors are turned off due to the sinusoidal nature of the input voltage, and forced-commutated thyristors are turned off by an extra circuit called *commutation circuitry*. Figure 1-3 shows various configurations of phase control (or line-commutated) thyristors: stud, hockey puck, flat, and pins types.

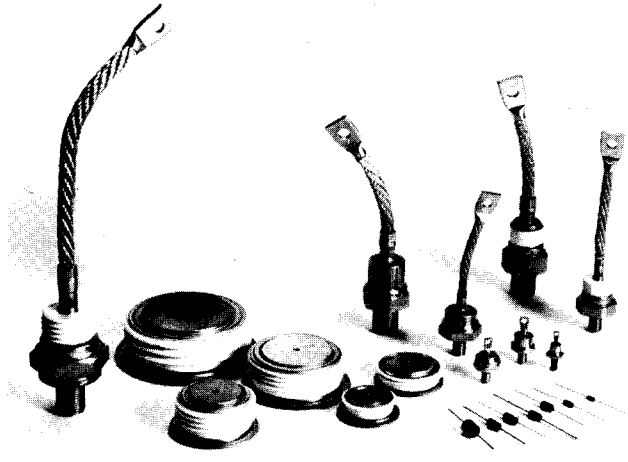


Figure 1-2 Various general-purpose diode configurations. (*Courtesy of Powerex, Inc.*)

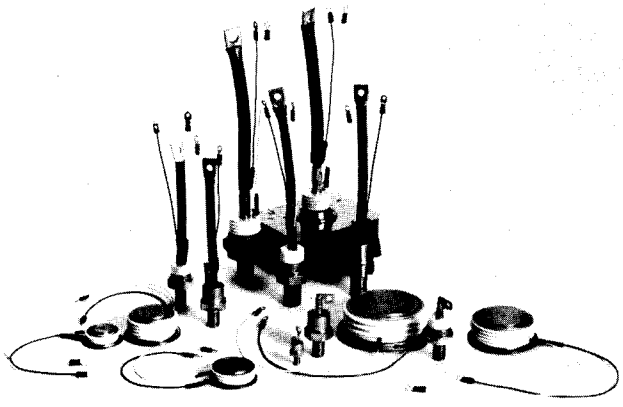


Figure 1-3 Various thyristor configurations. (*Courtesy of Powerex, Inc.*)

Natural or line-commutated thyristors are available with ratings up to 2500 V, 4000 A (and 5000 V, 2500 A). The *turn-off time* of high-speed reverse-blocking thyristors have been improved substantially and it is possible to have 10 to 20 μs in a 1200-V, 2000-A thyristor. The *turn-off time* is defined as the time interval between the instant when the principal current has decreased to zero after external switching of the principal voltage circuit, and the instant when the thyristor is capable of supporting a specified principal voltage without turning on [2]. RCTs and GATTs are widely used for high-speed switching, especially in traction applications. An RCT can be considered as a thyristor with an inverse-parallel diode. RCTs are available up to 2500 V, 1000 A (and 400 A in reverse conduction) with a switching time of 40 μs. GATTs are available up to 1200 V, 400 A with a switching speed of 8 μs. LASCRs, which are available up to 6000 V, 1500 A, with a switching speed of 200 to 400 μs, are suitable for high-voltage power systems, especially in HVDC. For low-power ac applications, TRIACs are widely used in all types of simple heat controls, light controls, motor controls, and ac switches. The characteristics of TRIACs are similar to two thyristors connected in inverse parallel and having only one gate terminal. The current flow through a TRIAC can be controlled in either direction.

GTOs and SITHs are self-turned-off thyristors. GTOs and SITHs are turned on by applying a short positive pulse to the gates and are turned off by the applications of short negative pulse to the gates. They do not require any commutation circuit. GTOs are very attractive for forced commutation of converters and are available up to 2500 V, 1000 A. SITHs are expected to be applied for medium-power converters with a frequency of several hundred kilohertz and beyond the frequency range of GTOs. Figure 1-4 shows various configurations of GTOs.

High-power bipolar transistors are commonly used in power converters at a frequency below 10 kHz and are effectively applied in the power ratings up to 100 kW and 1000 V. The various configurations of bipolar power transistors are shown in Fig. 13-2. A bipolar transistor has three terminals: base, emitter, and collector. It is normally operated as a switch in the common-emitter configuration. As long as the base of an NPN transistor is at a higher potential than the emitter and the

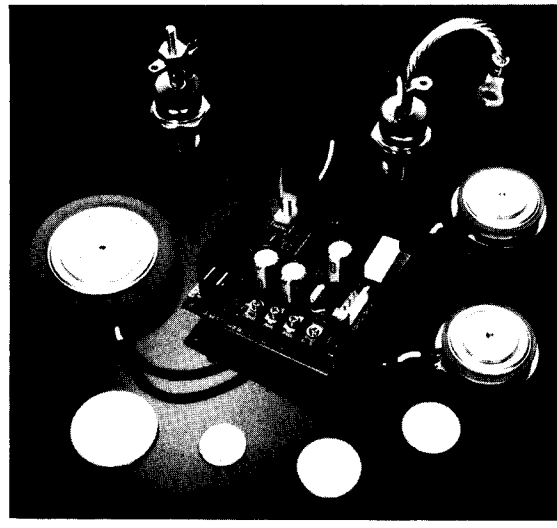


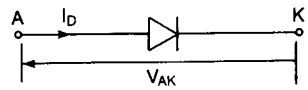
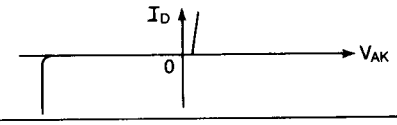
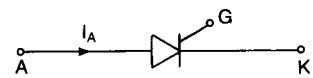
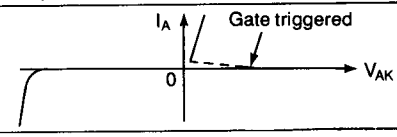
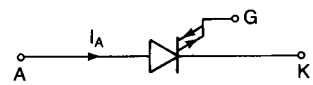
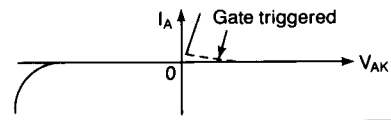
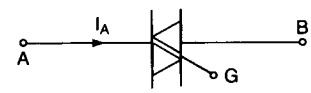
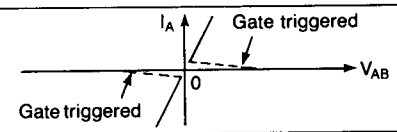
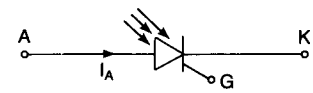
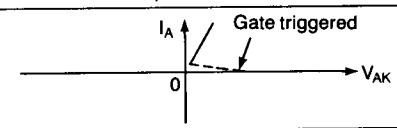
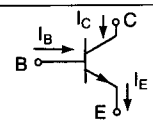
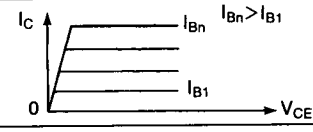
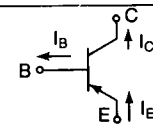
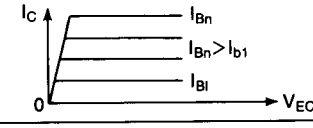
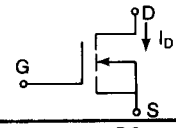
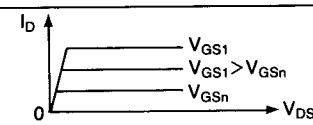
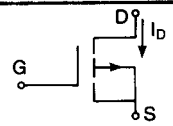
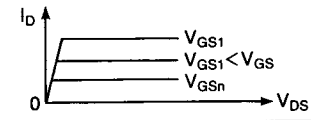
Figure 1-4 Gate-turn-off thyristors. (*Courtesy of International Rectifier*)

TABLE 1-2 RATINGS OF POWER SEMICONDUCTOR DEVICES

Type		Voltage/current rating	Switching time (μs)	On voltage/current
Diodes	General purpose	3000 V/3500 A		1.6 V/10 kA
	High speed	3000 V/1000 A	2–5	3 V/3000 A
	Schottky	40 V/60 A	0.23	0.58 V/60 A
Forced-turned-off thyristors	Reverse blocking	3000 V/1000 A	400	2.5 V/10 kA
	High speed	1200 V/1500 A	20	2.1 V/4500 A
	Reverse blocking	2500 V/400 A	40	2.7 V/1250 A
	Reverse conducting	2500 V/1000 A/R400 A	40	2.1 V/1000 A
	GATT	1200 V/400 A	8	2.8 V/1250 A
	Light triggered	6000 V/1500 A	200–400	2.4 V/4500 A
TRIACs		1200 V/300 A		1.5 V/420 A
Self-turned-off thyristors	GTO	3600 V/600 A	25	2.5 V/1000 A
	SITH	4000 V/2200 A	6.5	2.3 V/400 A
Power transistors	Single	400 V/250 A	9	1 V/250 A
		400 V/40 A	6	1.5 V/49 A
		630 V/50 A	1.7	0.3 V/20 A
	Darlington	900 V/200 A	40	2 V
SITs		1200 V/10 A	0.55	1.2 Ω
Power MOSFETS		500 V/8.6 A	0.7	0.6
		1000 V/4.7 A	0.9	2 Ω
		500 V/10 A	0.6	0.4 Ω

Source: Ref. 3.

TABLE 1-3 CHARACTERISTICS AND SYMBOLS OF SOME POWER DEVICES

Devices	Symbols	Characteristics
Diode		
Thyristor		
GTO		
TRIAC		
LASCR		
NPN BJT		
PNP BJT		
N-Channel MOSFET		
P-Channel MOSFET		

base current is sufficiently large to drive the transistor in the saturation region, the transistor remains on, provided that the collector-to-emitter junction is properly biased. The forward drop of a conducting transistor is in the range 0.5 to 1.5 V. If the base drive voltage is withdrawn, the transistor remains in the nonconduction (or off) mode.

Power MOSFETs are used in high-speed power converters and are available at a relatively low power rating in the range of 1000 V, 50 A at a frequency range of several tens of kilohertz. The various power MOSFETs of different sizes are shown in Fig. 13-22. The ratings of commercially available power semiconductor devices are shown in Table 1-2, where the on-voltage is the on-state voltage drop of the device at the specified current. Table 1-3 shows the v–i characteristics and the symbols of commonly used power semiconductor devices.

1-3 CONTROL CHARACTERISTICS OF POWER DEVICES

The power semiconductor devices can be operated as switches by applying control signals to the gate terminal of thyristors (and to the base of bipolar transistors). The required output is obtained by varying the conduction time of these switching devices. Figure 1-5 shows the output voltages and control characteristics of commonly used power switching devices. Once a thyristor is in a conduction mode, the gate signal of either positive or negative magnitude has no effect and this is shown in Fig. 1-5a. When a power semiconductor device is in a normal conduction mode, there is a small voltage drop across the device. In the output voltage waveforms in Fig. 1-5, these voltage drops are considered negligible, and unless specified, this assumption is made throughout the following chapters.

The power semiconductor switching devices can be classified on the basis of:

1. Uncontrolled turn on and off (e.g., diode)
2. Controlled turn on and uncontrolled turn off (e.g., SCR)
3. Controlled turn on and off characteristics (e.g., BJT, MOSFET, GTO)
4. Continuous gate signal requirement (BJT, MOSFET)
5. Pulse gate requirement (e.g., SCR, GTO)
6. Bipolar voltage-withstanding capability (SCR)
7. Unipolar voltage-withstanding capability (BJT, MOSFET, GTO)
8. Bidirectional current capability (TRIAC, RCT)
9. Unidirectional current capability (SCR, GTO, BJT, MOSFET, diode)

1-4 TYPES OF POWER ELECTRONIC CIRCUITS

For the control of electric power or power conditioning, the conversion of electric power from one form to another is necessary and the switching characteristics of the power devices permit these conversions. The static power converters perform

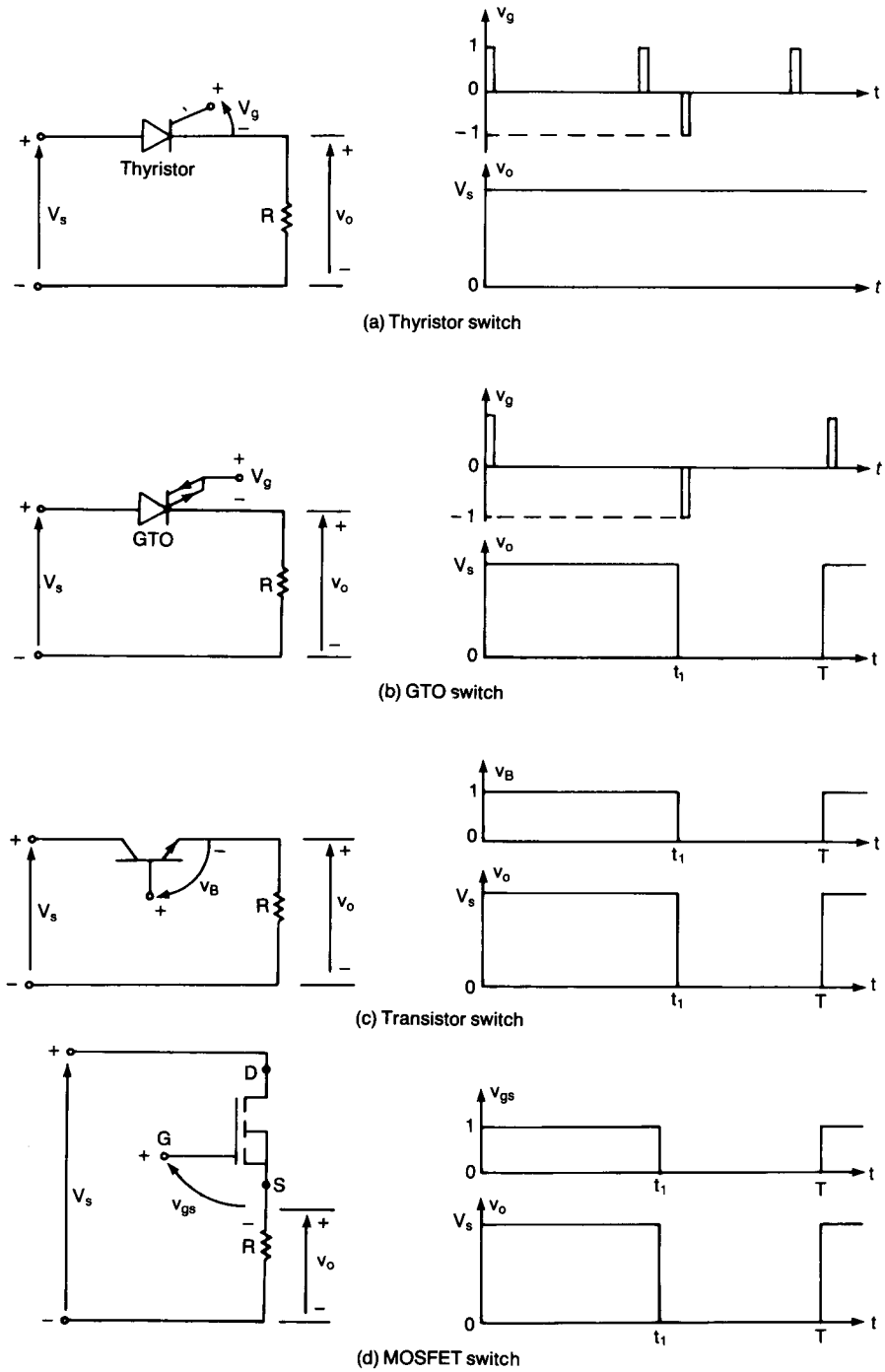


Figure 1-5 Control characteristics of power switching devices.

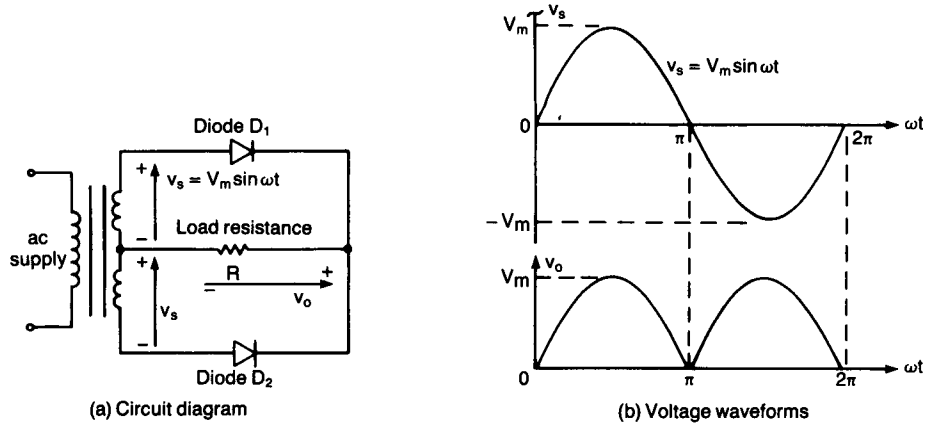


Figure 1-6 Single-phase rectifier circuit.

these functions of power conversions. A converter may be considered as a switching matrix. The power electronics circuits can be classified into six types:

1. Diode rectifiers
2. ac–dc converters (controlled rectifiers)
3. ac–ac converters (ac voltage controllers)
4. dc–dc converters (dc choppers)
5. dc–ac converters (inverters)
6. Static switches

Rectifiers. A diode rectifier circuit converts ac voltage into a fixed dc voltage and is shown in Fig. 1-6. The input voltage to the converter could be either single-phase or three-phase.

ac–dc converters. A single-phase converter with two natural commutated thyristors is shown in Fig. 1-7. The average value of the output voltage can be controlled by varying the conduction time of thyristors. The input could be a single or three-phase source. These converters are also known as *controlled rectifiers*.

ac–ac converters. These converters are used to obtain a variable ac output voltage from a fixed ac source and a single-phase converter with a TRIAC is shown in Fig. 1-8. The output voltage is controlled by varying the conduction time of a TRIAC. These types of converters are also known as *ac voltage controllers*.

dc–dc converters. A dc–dc converter is also known as a *chopper* or *switching regulator* and a transistor chopper is shown in Fig. 1-9. The average output voltage is controlled by varying the conduction of transistor, t_1. If T is the chopping period, then $t_1 = \delta T$. δ is called as the *duty cycle* of chopper.

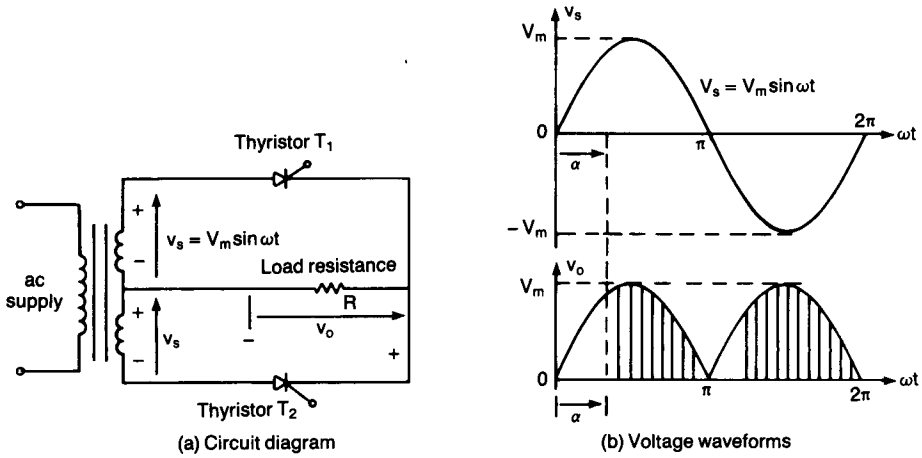


Figure 1-7 Single-phase ac–dc converter.

dc–ac converters. A dc–ac converter is also known as an *inverter*. A single-phase transistor inverter is shown in Fig. 1-10. If transistors Q_1 and Q_2 conduct for one-half period and Q_3 and Q_4 conduct for the other half, the output voltage is of alternating form. The output voltage can be controlled by varying the conduction time of transistors.

Static switches. Since the power devices can be operated as static switches or contactors, the supply to these switches could be either ac or dc and the switches are called as *ac static switches* or *dc switches*.

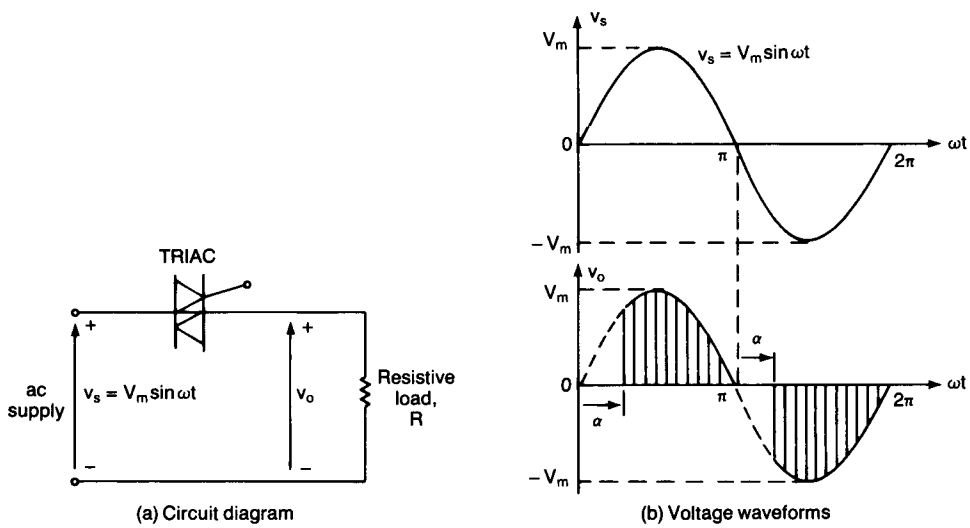


Figure 1-8 Single-phase ac–ac converter.

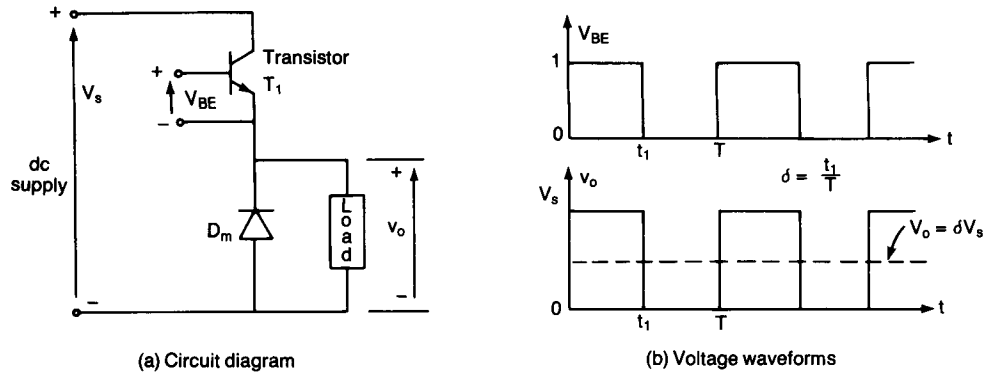


Figure 1-9 Dc–dc converter.

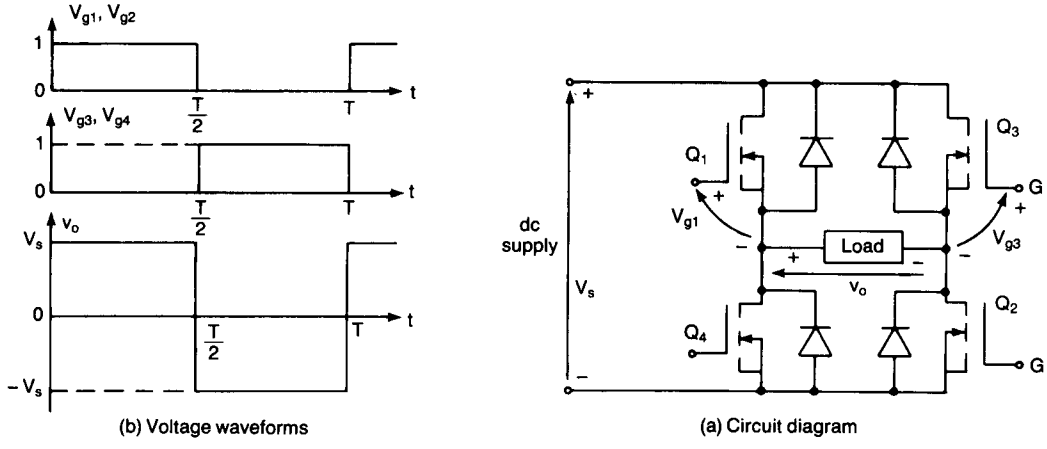


Figure 1-10 Single-phase dc–ac converter.

1-5 DESIGN OF POWER ELECTRONICS EQUIPMENT

The design of a power electronics equipment can be divided into four parts:

1. Design of power circuits
2. Protection of power devices
3. Determination of the control strategy
4. Design of logic and gating circuits

In the chapters that follow, various types of power electronic circuits are described and analyzed. In the analysis, the power devices are assumed as ideal switches; and effects of circuit stray inductance, circuit resistances, and source inductance are neglected. The practical power devices and circuits differ from these ideal conditions and the designs of the circuits are also affected. However, in the early stage of the design, the simplified analysis of a circuit is very useful to

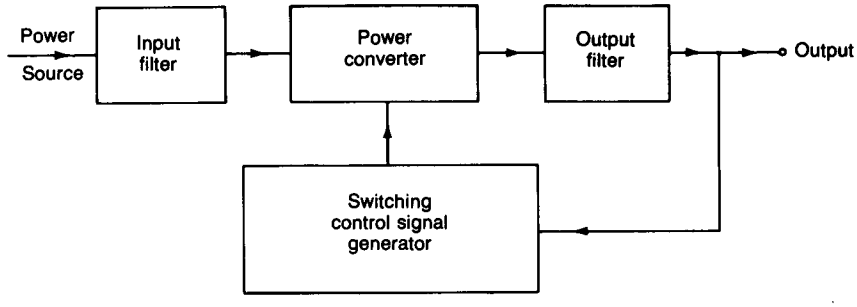


Figure 1-11 Generalized power converter structure.

understand the operation of the circuit and to establish the characteristics and control strategy.

Before a prototype is built, the designer should investigate the effects of the circuit parameters (and devices imperfections) and should modify the design if necessary. Only after the prototype is built and tested, the designer can be confident about the validity of the design and can estimate more accurately some of the circuit parameters (e.g., stray inductance).

1-6 PERIPHERAL EFFECTS

The operations of the power converters are based mainly on the switching of power semiconductor devices; and as a result the converters introduce current and voltage harmonics into the supply system and on the output of the converters. These can cause problems of distortion of the output voltage, harmonic generation into the supply system, and interference with the communication and signaling circuits. It is normally necessary to introduce filters on the input and output of a converter system to reduce the harmonic level to an acceptable magnitude. Figure 1-11 shows the block diagram of a generalized power converter.

The control strategy for the power converters plays an important part on the harmonic generation and output waveform distortion, and can be aimed to minimize or reduce these problems. The power converters can cause radio-frequency interference due to electromagnetic radiation and the gating circuits may generate erroneous signals. This interference can be avoided by *grounded shielding*.

SUMMARY

As the technology for the power semiconductor devices and integrated circuits develops, the potential for the applications of power electronics becomes wider. There are already many power semiconductor devices that are commercially available; however, the development in this direction is continuing. The power converters fall generally into six categories: (1) rectifiers, (2) ac–dc converters, (3) ac–ac converters, (4) dc–dc converters, (5) dc–ac converters, and (6) static switches. The

design of power electronics circuits requires designing the power and control circuits. The voltage and current harmonics that are generated by the power converters can be reduced (or minimized) with a proper choice of the control strategy.

REFERENCES

1. R. G. Hoft, "Historical review, present status and future prospects," *International Power Electronics Conference*, Tokyo, 1983, pp. 6–18.
2. General Electric, D. R. Grafham and F. B. Golden, eds. *SCR Manual*, 6th ed., Englewood Cliffs, N.J.: Prentice-Hall, Inc., 1982.
3. F. Harashima, "State of the art on power electronics and electrical drives in Japan," *3rd IFAC Symposium on Control in Power Electronics and Electrical Drives*, Lausanne, Switzerland, 1983, Tutorial session and survey papers, pp. 23–33.
4. B. R. Pelly, "Power semiconductor devices—a status review," *IEEE Industry Applications Society International Semiconductor Power Converter Conference*, 1982, pp. 1–19.
5. R. G. Holt, *Semiconductor Power Electronics*, New York, N.Y.: Van Nostrand Reinhold Company, Inc., 1986.

REVIEW QUESTIONS

1–1. What is power electronics?
1–2. What are the various types of thyristors?
1–3. What is a commutation circuit?
1–4. What are the conditions for a thyristor to conduct?
1–5. How can a conducting thyristor be turned off?
1–6. What is a line commutation?
1–7. What is a forced commutation?
1–8. What is the difference between a thyristor and a TRIAC?
1–9. What is the gating characteristic of a GTO?
1–10. What is turn-off time of a thyristor?
1–11. What is a converter?
1–12. What is the principle of ac–dc conversion?
1–13. What is the principle of ac–ac conversion?
1–14. What is the principle of dc–dc conversion?
1–15. What is the principle of dc–ac conversion?
1–16. What are the steps involved in designing power electronics equipment?
1–17. What are the peripheral effects of power electronics equipment?
1–18. What are the differences in the gating characteristics of GTOs and thyristors?
1–19. What are the differences in the gating characteristics of thyristors and transistors?
1–20. What are the differences in the gating characteristics of BJTs and MOSFETs?

2

Diode Circuits and Rectifiers

2-1 INTRODUCTION

Semiconductor diodes have found many applications in electronics and electrical engineering circuits. Diodes are also widely used in power electronics circuits for conversion of electric power. The diode circuits that are commonly used in power electronics for signal processing are reviewed in this chapter. The applications of diodes for conversion of power from ac–dc are introduced. The ac–dc converters are commonly known as *rectifiers* and the diode rectifiers provide a fixed dc output voltage. For the sake of simplicity the diodes are considered to be ideal. By ideal, we mean that the reverse recovery time and the forward voltage drop are negligible.

2-2 DIODES WITH *RC* AND *RL* LOADS

Figure 2-1a shows a diode circuit with an *RC* load. When the switch S_1 is closed at $t = 0$, the charging current that flows through the capacitor is found from

$$V_s = v_R + v_c = v_R + \frac{1}{C}\int i\,dt + v_c\,(t = 0) \tag{2-1}$$

$$v_R = Ri \tag{2-2}$$

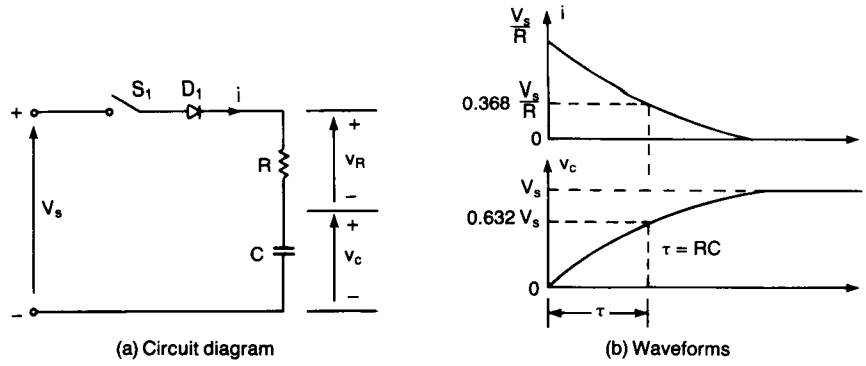


Figure 2-1 Diode circuit with RC load.

With the initial condition $v_c\,(t = 0) = 0$, the solution of Eq. (2-1) (which is derived in Appendix D.1) gives the charging current as

$$i(t) = \frac{V_s}{R} e^{-t/RC} \tag{2-3}$$

The capacitor voltage is

$$v_c(t) = \frac{1}{C}\int_0^t i\,dt = V_s(1 - e^{-t/RC}) \tag{2-4}$$

where $RC = \tau$ is the time constant of an RC load. The rate of change of the capacitor voltage is

$$\frac{dv_c}{dt} = \frac{V_s}{RC} e^{-t/RC} \tag{2-5}$$

and the initial rate of change of capacitor voltage (at $t = 0$) is obtained from Eq. (2-5):

$$\left.\frac{dv_c}{dt}\right|_{t=0} = \frac{V_s}{RC} \tag{2-6}$$

A diode circuit with an RL load is shown in Fig. 2-2a. When switch S_1 is closed at $t = 0$, the current through the inductor increases and is expressed as

$$V_s = v_L + v_R = L\frac{di}{dt} + Ri \tag{2-7}$$

With the initial condition $i(t = 0) = 0$, the solution of Eq. (2-7) (which is derived in Appendix D.2) yields

$$i(t) = \frac{V_s}{R}(1 - e^{-tR/L}) \tag{2-8}$$

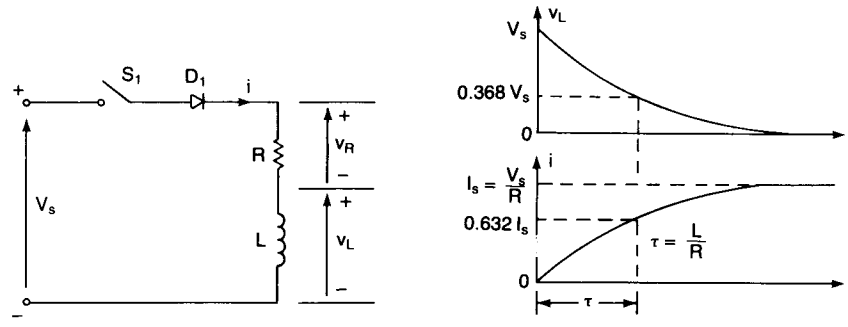


Figure 2-2 Diode circuit with *RL* load.

The rate of change of this current can be obtained from Eq. (2-8) as

$$\frac{di}{dt} = \frac{V_s}{L} e^{-tR/L} \tag{2-9}$$

and the initial rate of rise of the current (at $t = 0$) is obtained from Eq. (2-9):

$$\left.\frac{di}{dt}\right|_{t=0} = \frac{V_s}{L} \tag{2-10}$$

The voltage across the inductor is

$$v_L(t) = L\frac{di}{dt} = V_s e^{-tR/L} \tag{2-11}$$

where $L/R = \tau$ is the time constant of an *RL* load.

The waveforms for the voltage and current are shown in Fig. 2-2b. If $t >> L/R$, the voltage across the inductor tends to be zero and its current reaches a steady-state value of $I_s = V_s/R$. If an attempt is then made to open switch S_1, the energy stored in the inductor ($= 0.5Li^2$) will be transformed into a high reverse voltage across the switch and diode. This energy will be dissipated in the form of sparks across the switch; and the diode D_1 is likely to be damaged in this process. To overcome such a situation, a diode commonly known as a *freewheeling diode* is connected across an inductive load as shown in Fig. 2-8a.

Example 2-1

A diode circuit is shown in Fig. 2-3a with $R = 44\ \Omega$ and $C = 0.1\ \mu$F. The capacitor has an initial voltage, $V_0 = 220$ V. If the switch S_1 is closed at $t = 0$, determine the (a) peak diode current; (b) energy dissipated in the resistor, R; and (c) capacitor voltage at $t = 2\ \mu$s.

Solution The waveforms are shown in Fig. 2-3b.

(a) Equation (2-3) can be used with $V_s = V_0$ and the peak diode current is

$$I_p = \frac{220}{44} = 5\text{ A}$$

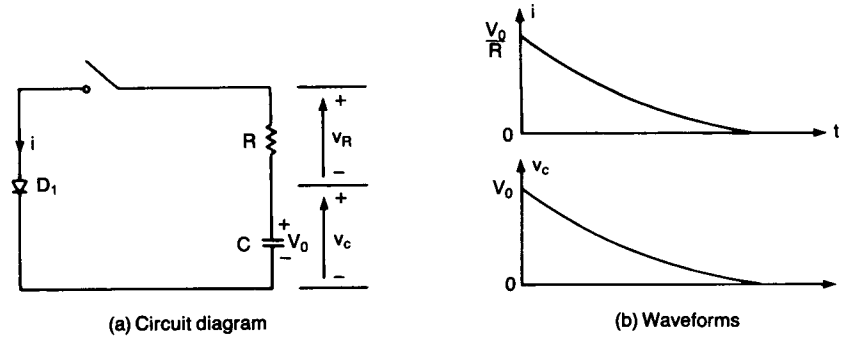


Figure 2-3 Diode circuit with *RC* load.

(b) The energy dissipated is

$$W = 0.5CV_0^2 = 0.5 \times 0.1 \times 10^{-6} \times 220^2 = 0.00242 \text{ J}$$

(c) For $RC = 0.1 \times 44 = 4.4$ μs and $t = t_1 = 2$ μs, the capacitor voltage is

$$v_c\,(t = 2\ \mu\text{s}) = 220 \times e^{-2/4.4} = 139.64 \text{ V}$$

2-3 DIODES WITH *LC* AND *RLC* LOADS

A diode circuit with an *LC* load is shown in Fig. 2-4a. When switch S_1 is closed at $t = 0$, the charging current of the capacitor is expressed as

$$V_s = L\frac{di}{dt} + \frac{1}{C}\int i\,dt + v_c\,(t = 0) \tag{2-12}$$

With initial conditions $i(t = 0) = 0$ and $v_c(t = 0) = 0$, Eq. (2-12) can be solved for the capacitor current as (in Appendix D.3)

$$i(t) = V_s\sqrt{\frac{C}{L}}\sin \omega t \tag{2-13}$$

$$= I_p \sin \omega t \tag{2-14}$$

where $\omega = 1/\sqrt{LC}$ and the peak current,

$$I_p = V_s\sqrt{\frac{C}{L}} \tag{2-15}$$

The rate of rise of the current is obtained from Eq. (2-13) as

$$\frac{di}{dt} = \frac{V_s}{L}\cos \omega t \tag{2-16}$$

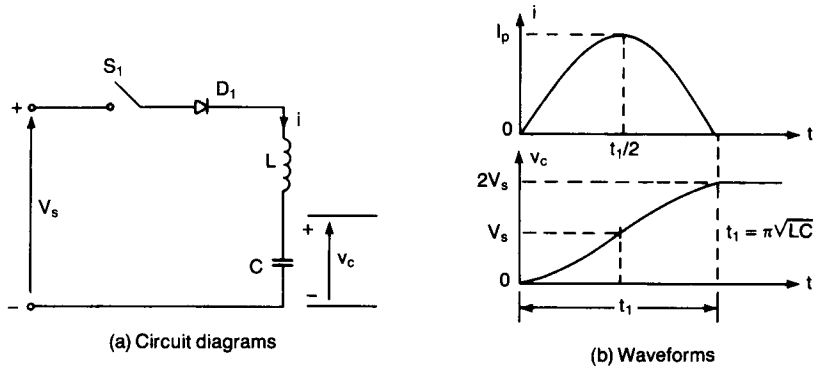


Figure 2-4 Diode circuit with *LC* load.

and Eq. (2-16) gives the initial rate of rise of the current (at $t = 0$) as

$$\left.\frac{di}{dt}\right|_{t=0} = \frac{V_s}{L} \tag{2-17}$$

The voltage across the capacitor can be derived as

$$v_c(t) = \frac{1}{C}\int_0^t i\,dt = V_s(1 - \cos \omega t) \tag{2-18}$$

At a time $t = t_1 = \pi\sqrt{LC}$, the diode current, i falls to zero and the capacitor is charged to $2V_s$. The waveforms for the voltage and current are shown in Fig. 2-4b.

Example 2-2

A diode circuit with an *LC* load is shown in Fig. 2-5a with the capacitor having an initial voltage, $V_0 = 220$ V, capacitance, $C = 20$ μF, and inductance, $L = 80$ μH. If the switch S_1 is closed at $t = 0$, determine the (a) peak current through the diode; (b) conduction time of the diode; and (c) steady-state capacitor voltage.

Solution (a) Using *Kirchhoff's voltage law* (KVL), we can write the equation for the current as

$$L\frac{di}{dt} + \frac{1}{C}\int i\,dt + v_c\,(t = 0) = 0$$

and the current with initial conditions of $i(t = 0) = 0$ and $v_c\,(t = 0) = -V_0$ is solved as

$$i(t) = V_0\sqrt{\frac{C}{L}}\sin \omega t$$

where $\omega = 1/\sqrt{LC} = 10^6/\sqrt{20 \times 80} = 25{,}000$ rad/s. The peak current,

$$I_p = V_0\sqrt{C/L} = 220\sqrt{\frac{20}{80}} = 110 \text{ A}$$

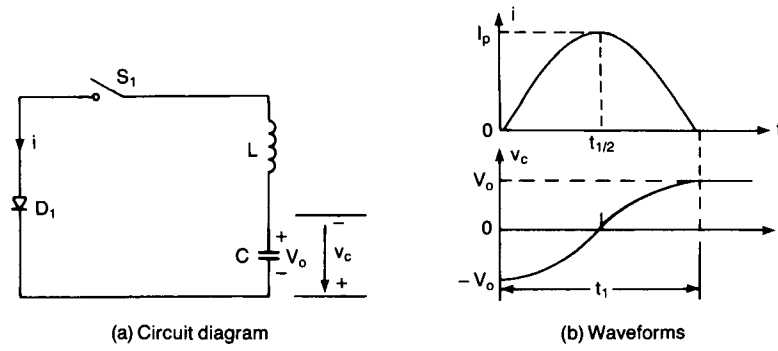


Figure 2-5 Diode circuit with LC load.

(b) At $t = t_1 = \pi\sqrt{LC}$, the diode current becomes zero and the conduction time of diode is

$$t_1 = \pi\sqrt{LC} = \pi\sqrt{20 \times 80} = 125.66\ \mu s$$

(c) The capacitor voltage can be shown to be

$$v_c(t) = \frac{1}{C}\int_0^t i\,dt - V_0 = -V_0 \cos \omega t$$

For $t = t_1 = 125.66\ \mu s$, $v_c\ (t = t_1) = 220$ V.

A diode circuit with an RLC load is shown in Fig. 2-6. If the switch S_1 is closed at $t = 0$, we can use the KVL to write the equation for the load current as

$$L\frac{di}{dt} + Ri + \frac{1}{C}\int i\,dt + v_c\,(t = 0) = V_s \tag{2-19}$$

with initial conditions $i\ (t = 0)$ and $v_c\ (t = 0) = V_0$. Differentiating Eq. (2-19) and dividing both sides by L gives

$$\frac{d^2i}{dt^2} + \frac{R}{L}\frac{di}{dt} + \frac{i}{LC} = 0 \tag{2-20}$$

Under steady-state conditions, the capacitor is charged to the source voltage V_s and the steady-state current will be zero. The forced component of the current in Eq. (2-20) is also zero. The current is due to the natural component.

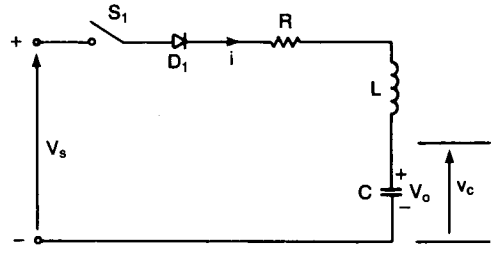


Figure 2-6 Diode circuit with RLC load.

The characteristic equation in Laplace's domain is

$$s^2 + \frac{R}{L}s + \frac{1}{LC} = 0 \tag{2-21}$$

and the roots of quadratic Eq. (2-21) are given by

$$s_{1,2} = -\frac{R}{2L} \pm \sqrt{\left(\frac{R}{2L}\right)^2 - \frac{1}{LC}} \tag{2-22}$$

Let us define two important properties of a second-order circuit: the *damping factor*,

$$\alpha = \frac{R}{2L} \tag{2-23}$$

and the *resonant frequency*,

$$\omega_0 = \frac{1}{\sqrt{LC}} \tag{2-24}$$

Substituting these into Eq. (2-22) yields

$$s_{1,2} = -\alpha \pm \sqrt{\alpha^2 - \omega_0^2} \tag{2-25}$$

The solution for the current, which will depend on the values of α and ω_0, would follow one of the three possible cases.

Case 1. If $\alpha = \omega_0$, the roots are equal, $s_1 = s_2$, and the circuit is called *critically damped*. The solution will be of the form

$$i(t) = (A_1 + A_2 t)e^{s_1 t} \tag{2-26}$$

Case 2. If $\alpha > \omega_0$, the roots are real and the circuit is said to be *overdamped*. The solution takes the form

$$i(t) = A_1 e^{s_1 t} + A_2 e^{s_2 t} \tag{2-27}$$

Case 3. If $\alpha < \omega_0$, the roots are complex and the circuit is said to be *underdamped*. The roots are

$$s_{1,2} = -\alpha \pm j\omega_r \tag{2-28}$$

where ω_r is called the *ringing frequency* (or damped resonant frequency) and $\omega_r = \sqrt{\omega_0^2 - \alpha^2}$. The solution takes the form

$$i(t) = e^{-\alpha t}(A_1 \cos \omega_r t + A_2 \sin \omega_r t) \tag{2-29}$$

and the current consists of a *damped or decaying sinusoidal*.

Note. The constants A_1 and A_2 can be determined from the initial conditions of the circuit. The ratio of α/ω_0 is commonly known as *damping ratio*, δ.

Example 2-3

In the second-order *RLC* circuit of Fig. 2-6, the source voltage, $V_s = 220$ V, inductance, $L = 2$ mH, capacitance, $C = 0.05$ μF, and resistance, $R = 160\ \Omega$. The initial value of the capacitor voltage is $V_0 = 0$. If the switch is closed at $t = 0$, determine (a) an expression for the current, $i(t)$, and (b) the conduction time of diode. (c) Draw a sketch of $i(t)$.

Solution (a) From Eq. (2-23), $\alpha = 160 \times 10^3/(2 \times 2) = 40{,}000$ rad/s and from Eq. (2-24), $\omega_0 = 1/\sqrt{LC} = 10^5$ rad/s.

$$\omega_r = \sqrt{10^{10} - 16 \times 10^8} = 91{,}652 \text{ rad/s}$$

Since $\alpha < \omega_0$, it is an underdamped circuit and the solution is of the form

$$i(t) = e^{-\alpha t}(A_1 \cos \omega_r t + A_2 \sin \omega_r t)$$

At $t = 0$, $i(t = 0) = 0$ and this gives $A_1 = 0$. The solution becomes

$$i(t) = e^{-\alpha t} A_2 \sin \omega_r t$$

The derivative of $i(t)$ gives

$$\frac{di}{dt} = \omega_r \cos \omega_r t A_2 e^{-\alpha t} - \alpha \sin \omega_r t A_2 e^{-\alpha t}$$

When the switch is closed at $t = 0$, the capacitor offers a low impedance and the inductor offers a high impedance. The initial rate of rise of the current is limited only by the inductor L. Thus at $t = 0$, the circuit di/dt is

$$\left.\frac{di}{dt}\right|_{t=0} = \omega_r A_2 = \frac{V_s}{L}$$

and the constant

$$A_2 = \frac{V_s}{\omega_r L} = \frac{220 \times 1000}{91{,}652 \times 2} = 1.2$$

The final expression for the current $i(t)$ is

$$i(t) = 1.2 \sin (91{,}652t) e^{-40{,}000t} \text{ A}$$

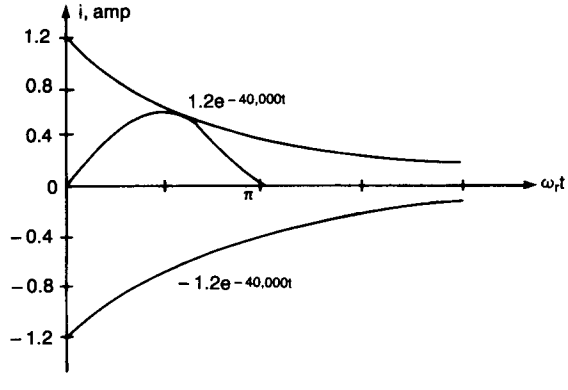


Figure 2-7 Current waveform for Example 2-3.

(b) The conduction time of the diode is given as

$$\omega_r t_1 = \pi \quad \text{or} \quad t_1 = \frac{\pi}{91{,}652} = 34.27\ \mu\text{s}$$

(c) The sketch for the current waveform is shown in Fig. 2-7.

2-4 FREEWHEELING DIODES

If the switch S_1 in Fig. 2-2a is closed for time t_1, a current is established through the load; and then if the switch is opened, a path must be provided for the current in the inductive load. This is normally done by connecting a diode D_m as shown in Fig. 2-8a, and this diode is usually called a *freewheeling diode*. The circuit operation can be divided into two modes. Mode 1 begins when the switch is closed at $t = 0$, and mode 2 begins when the switch is then opened. The equivalent circuits for the modes are shown in Fig. 2-8b. i_1 and i_2 are defined as the instantaneous currents for mode 1 and mode 2, respectively. t_1 and t_2 are the corresponding durations of these modes.

Mode 1. During this mode, the diode current, which is similar to Eq. (2-8), is

$$i_1(t) = \frac{V_s}{R}(1 - e^{-tR/L}) \tag{2-30}$$

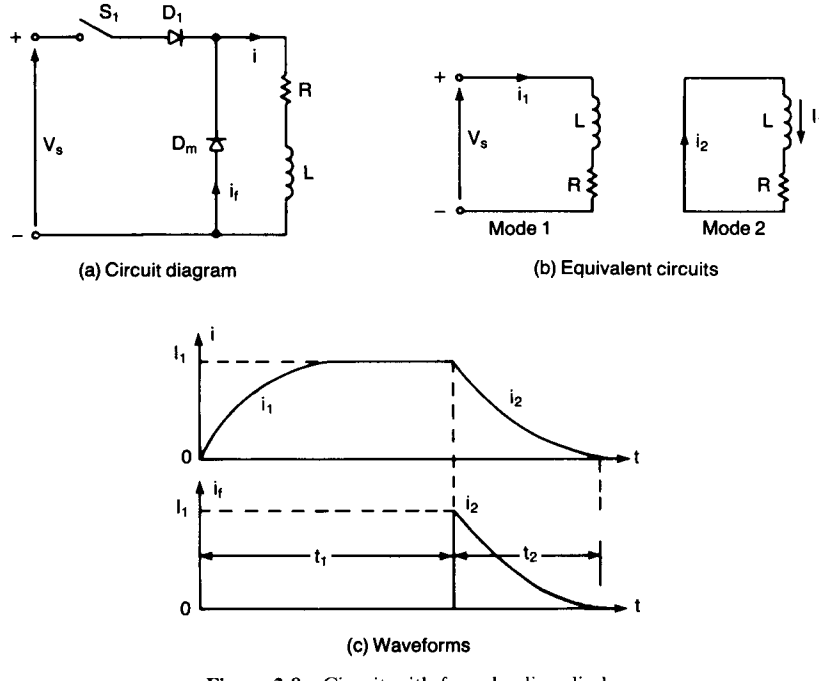


Figure 2-8 Circuit with freewheeling diode.

When the switch is opened at $t = t_1$ (at the end of this mode), the current at that time becomes

$$I_1 = i_1(t = t_1) = \frac{V_s}{R}(1 - e^{-t_1 R/L}) \tag{2-31}$$

If the time t_1 is sufficiently long, the current reaches a steady-state value and a steady-state current of $I_s = V_s/R$ flows through the load.

Mode 2. This mode begins when the switch is opened and the load current starts to flow through the freewheeling diode D_m. Redefining the time origin at the beginning of this mode, the current through the freewheeling diode is found from

$$0 = L\frac{di_2}{dt} + Ri_2 \tag{2-32}$$

with initial condition $i_2\ (t = 0) = I_1$. The solution of Eq. (2-32) gives the freewheeling current as

$$i_2(t) = I_1 e^{-tR/L} \tag{2-33}$$

and this current decays exponentially to zero at $t = t_2$ provided that $t_2 >> L/R$. The waveforms for the currents are shown in Fig. 2-8c.

Example 2-4

In Fig. 2-8a, the resistance is negligible ($R = 0$), source voltage, $V_s = 220$ V, and load inductance, $L = 220$ μH. (a) Draw the waveform for the load current if the switch is closed for a time $t_1 = 100$ μs and is then opened. (b) Determine the energy stored in the load inductor.

Solution (a) The circuit diagram is shown in Fig. 2-9a with a zero initial current.

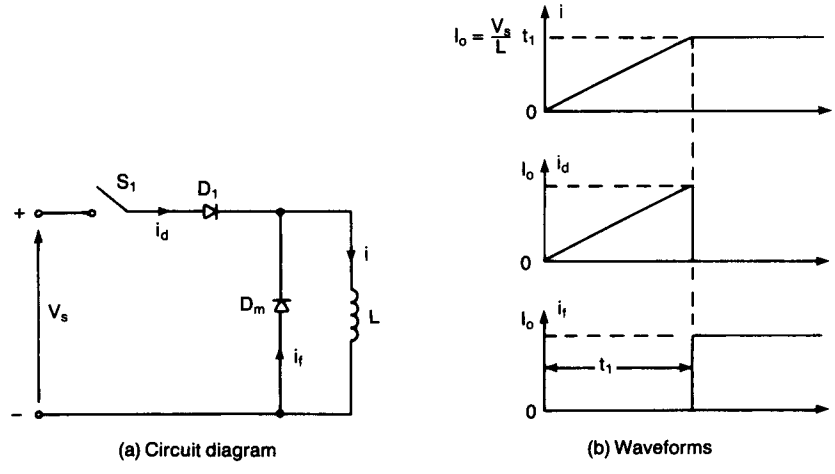


Figure 2-9 Diode circuit with L-load.

When the switch is closed at $t = 0$, the load current rises linearly and is expressed as

$$i(t) = \frac{V_s}{L}t$$

and at $t = t_1$, $I_0 = V_s t_1/L = 220 \times 100/220 = 100$ A.

(b) When the switch S_1 is opened at a time $t = t_1$, the load current starts to flow through the diode D_m. Since there is no dissipative (resistive) element in the circuit, the load current remains constant at $I_0 = 100$ A and the energy stored in the inductor is $0.5LI_0^2 = 1.1$ J. The current waveforms are shown in Fig. 2-9b.

2-5 RECOVERY OF TRAPPED ENERGY WITH A DIODE

In the ideal lossless circuit of Fig. 2-9a, the energy stored in the inductor is trapped there, because there is no resistance in the circuit. In a practical circuit it is desirable to improve the *efficiency* by returning the stored energy into the supply source. This can be achieved by adding a second winding to the inductor and connecting a diode D_1 as shown in Fig. 2-10a. The inductor behaves as a transformer. The transformer secondary is connected such that if v_1 is positive, then v_2 is negative, and vice versa, The secondary winding that facilitiates returning the stored energy to the source via diode D_1 is known as a *feedback winding*. Assuming a transformer with a magnetizing inductance of L_m, the equivalent circuit is as shown in Fig. 2-10b.

If the diode and secondary voltage (source voltage) are referred to the primary side of the transformer, the equivalent circuit is that shown in Fig. 2-10c. i_1 and i_2 define the primary and secondary currents of the transformer, respectively.

The *turns ratio* of an ideal transformer is defined as

$$a = \frac{N_2}{N_1} \tag{2-34}$$

The circuit operation can be divided into two modes. Mode 1 begins when the switch S_1 is closed at $t = 0$ and mode 2 begins when the switch is opened. The equivalent circuits for the modes are shown in Fig. 2-11a. t_1 and t_2 are durations of mode 1 and mode 2, respectively.

Mode 1. During this mode the switch is closed at $t = 0$. The diode D_1 is reverse biased and the current through the diode (secondary current) is a $i_2 = 0$ or $i_2 = 0$. Using the KVL in Fig. 2-11a, $V_s = (v_D - V_s)/a$ and this gives the reverse diode voltage as

$$v_D = V_s(1 + a) \tag{2-35}$$

Assuming that there is no initial current in the circuit, the primary current is the same as the switch current i_s and is expressed as

$$V_s = L_m \frac{di_1}{dt} \tag{2-36}$$

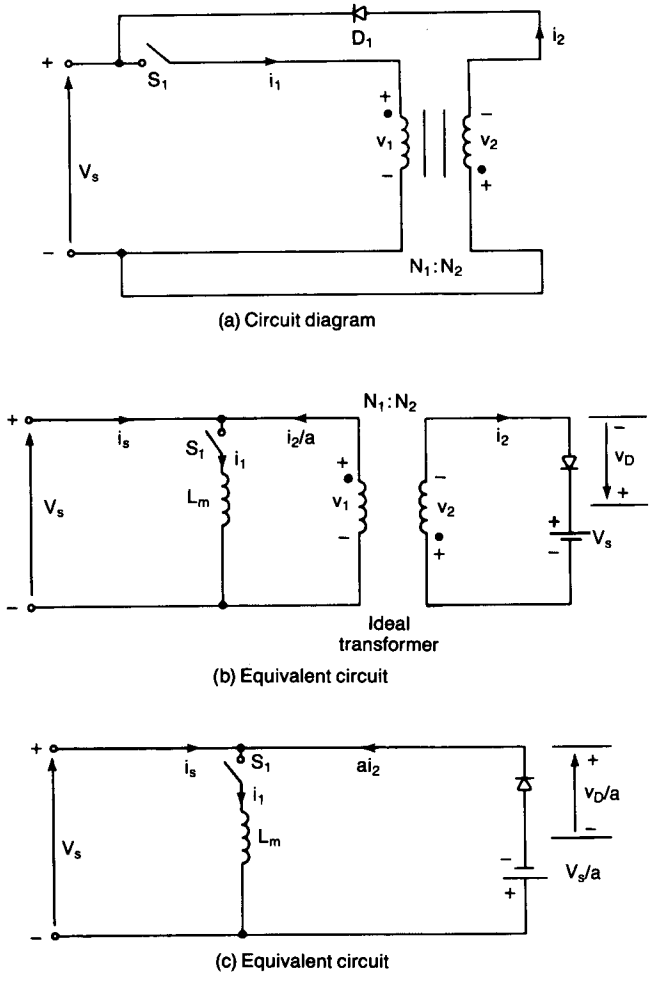


Figure 2-10 Circuit with energy recovery diode.

and this gives

$$i_1(t) = i_s(t) = \frac{V_s}{L_m} t \tag{2-37}$$

This mode is valid for $0 \leq t \leq t_1$ and ends when the switch is opened at $t = t_1$. At the end of this mode the primary current becomes

$$I_0 = \frac{V_s}{L_m} t_1 \tag{2-38}$$

Mode 2. During this mode the switch is opened, the voltage across the inductor is reversed and the diode D_1 is forward biased. A current flows through the transformer secondary and the energy stored in the inductor is returned to the

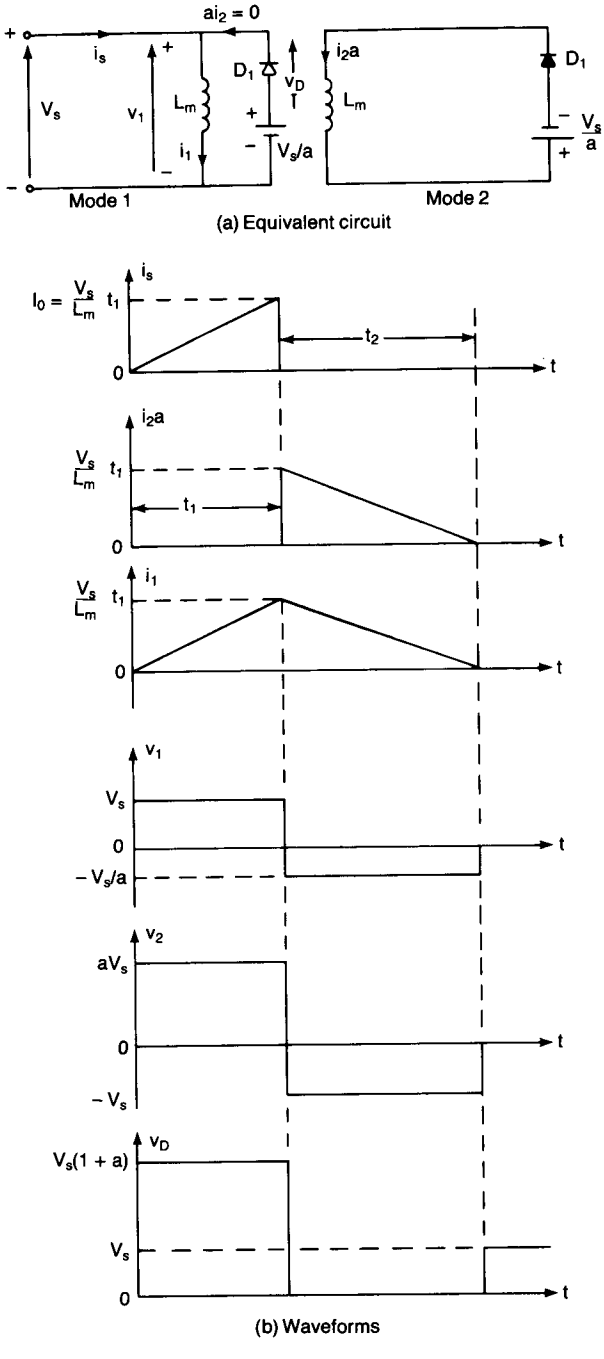


Figure 2-11 Equivalent circuits and waveforms.

source. Using the KVL and redefining the time origin at the beginning of this mode, the primary current is expressed as

$$L_m \frac{di_1}{dt} + \frac{V_s}{a} = 0 \tag{2-39}$$

with initial condition $i_1\ (t = 0) = I_0$, and we can solve the current as

$$i_1(t) = -\frac{V_s}{aL_m} t + I_0 \tag{2-40}$$

The conduction time of diode D_1 is found from the condition $i_1\ (t = t_2) = 0$ of Eq. (2-40) and is

$$t_2 = \frac{aL_m I_0}{V_s} = at_1 \tag{2-41}$$

Mode 2 is valid for $0 \leq t \leq t_2$. At the end of this mode at $t = t_2$, all the energy stored in the inductor L_m is returned to the source. The various waveforms for the currents and voltage are shown in Fig. 2-11b for $a = 10/6$.

Example 2-5

For the energy recovery circuit of Fig. 2-10a, the magnetizing inductance of the transformer is $L_m = 250\ \mu H$, $N_1 = 10$, and $N_2 = 100$. The leakage inductances and resistances of the transformer are negligible. The source voltage is $V_s = 220$ V and there is no initial current in the circuit. If the switch is closed for a time $t_1 = 50\ \mu s$ and is then opened; (a) determine the reverse voltage of diode D_1; (b) calculate the peak value of primary current; (c) calculate the peak value of secondary current; (d) determine the conduction time of diode D_1; and (e) determine the energy supplied by the source.

Solution The turns ratio is $a = N_2/N_1 = 100/10 = 10$.

(a) From Eq. (2-35) the reverse voltage of the diode,

$$v_D = 220 \times (1 + 10) = 2420 \text{ V}$$

(b) From Eq. (2-38) the peak value of the primary current,

$$I_0 = 220 \times \frac{50}{250} = 44 \text{ A}$$

(c) The peak value of the secondary current, $I_0' = I_0/a = 44/10 = 4.4$ A.

(d) From Eq. (2-41) the conduction time of the diode,

$$t_2 = 250 \times 44 \times \frac{10}{220} = 500\ \mu s$$

(e) The energy supplied by the source,

$$W = \int_0^{t_1} vi\, dt = \int_0^{t_1} V_s \frac{V_s}{L_m} t\, dt = \frac{1}{2} \frac{V_s^2}{L_m} t_1^2$$

Using Eq. (2-38) yields

$$W = 0.5 L_m I_0^2 = 0.5 \times 250 \times 10^{-6} \times 44^2 = 0.242 \text{ J}$$

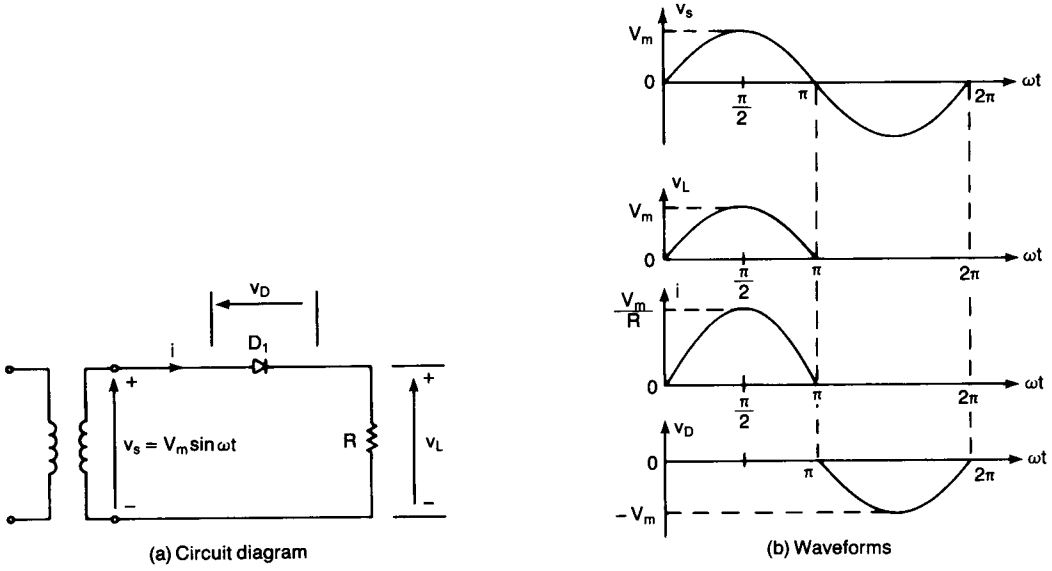


Figure 2-12 Single-phase half-wave rectifier.

2-6 SINGLE-PHASE HALF-WAVE RECTIFIERS

A *rectifier* is a circuit that converts an ac signal into a unidirectional signal. Diodes are used extensively in rectifiers. A single-phase half-wave rectifier is the simplest type and is not normally used in industrial applications. However, it is useful in understanding the principle of rectifier operation. The circuit diagram with a resistive load is shown in Fig. 2-12a. During the positive half-cycle of the input voltage, diode D_1 conducts and the input voltage appears across the load. During the negative half-cycle of the input voltage, the diode is in a *blocking condition* and the output voltage is zero. The waveforms for the input and output voltages are shown in Fig. 2-12b.

2-7 PERFORMANCE PARAMETERS

Although the output voltage as shown in Fig. 2-12b is dc, it is discontinuous and contains harmonics. There are different types of rectifier circuits and the performances of a rectifier are normally evaluated in terms of the following parameters:

The *average* value of the output (load) voltage, V_{dc}
The average value of the output (load) current, I_{dc}
The output *dc power*,

$$P_{dc} = V_{dc}I_{dc} \tag{2-42}$$

The *rms* value of the output voltage, V_{rms}
The *rms* value of the output current, I_{rms}

The output *ac power*,

$$P_{ac} = V_{rms}I_{rms} \tag{2-43}$$

The *efficiency* (or *rectification ratio*) of a rectifier, which is a figure of merit and permits us to compare the effectiveness, is defined as

$$\eta = \frac{P_{dc}}{P_{ac}} \tag{2-44}$$

The output voltage can be considered as being composed of two components: (1) the dc value, and (2) the ac component or ripple.

The *effective* (rms) value of the ac component of output voltage is

$$V_{ac} = \sqrt{V_{rms}^2 - V_{dc}^2} \tag{2-45}$$

The *form factor*, which is a measure of the shape of output voltage, is

$$FF = \frac{V_{rms}}{V_{dc}} \tag{2-46}$$

The *ripple factor*, which is a measure of the ripple content, is defined as

$$RF = \frac{V_{ac}}{V_{dc}} \tag{2-47}$$

Substituting Eq. (2-45) in Eq. (2-47), the ripple factor can be expressed as

$$RF = \sqrt{\left(\frac{V_{rms}}{V_{dc}}\right)^2 - 1} = \sqrt{FF^2 - 1} \tag{2-48}$$

The *transformer utilization factor* is defined as

$$TUF = \frac{P_{dc}}{V_sI_s} \tag{2-49}$$

where V_s and I_s are the rms voltage and rms current of the transformer secondary, respectively.

If ϕ is the angle between the fundamental components of the input current and voltage, ϕ is called the *displacement angle*. The *displacement factor* is defined as

$$DF = \cos\phi \tag{2-50}$$

The *harmonic factor* of the input current is defined as

$$HF = \left(\frac{I_s^2 - I_1^2}{I_1^2}\right)^{1/2} = \left[\left(\frac{I_s}{I_1}\right)^2 - 1\right]^{1/2} \tag{2-51}$$

where I_1 is the fundamental rms component of the input current. The input *power factor* is defined as

$$PF = \frac{V_sI_1}{V_sI_s}\cos\phi = \frac{I_1}{I_s}\cos\phi \tag{2-52}$$

Note. If the input current is purely sinusoidal, $I_1 = I_s$ and the power factor, PF, equals the displacement factor, DF. An ideal rectifier should have: $\eta = 100\%$, $V_{ac} = 0$, FF = 0, RF = 0, TUF = 1, HF = 0, and PF = 1.

Example 2-6

The rectifier in Fig. 2-12a has a purely resistive load of R. Determine the (a) efficiency; (b) form factor; (c) ripple factor; (d) transformer utilization factor; and (e) peak inverse voltage (PIV) of diode D_1.

Solution The average output voltage V_{dc} is defined as

$$V_{dc} = \frac{1}{T}\int_0^T v_L(t)\,dt \tag{2-53}$$

We can notice from Fig. 2-12b that $v_L(t) = 0$ for $T/2 \le t \le T$. Hence we have

$$V_{dc} = \frac{1}{T}\int_0^{T/2} V_m \sin \omega t\,dt = \frac{-V_m}{T}\left(\cos\frac{\omega T}{2} - 1\right)$$

But the frequency of the source is $f = 1/T$ and $\omega = 2\pi f$.

$$\begin{aligned} V_{dc} &= \frac{V_m}{\pi} = 0.318V_m \\ I_{dc} &= \frac{V_{dc}}{R} = \frac{0.318V_m}{R} \end{aligned} \tag{2-54}$$

The *root-mean-square* (rms) value of a periodic waveform is defined as

$$V_{rms} = \left[\frac{1}{T}\int_0^T v_L^2(t)\,dt\right]^{1/2} \tag{2-55}$$

For a sinusoidal voltage of $v_L(t) = V_m \sin \omega t$ for $0 \le t \le T/2$, the rms value of the output voltage is

$$\begin{aligned} V_{rms} &= \left[\frac{1}{T}\int_0^{T/2} (V_m \sin \omega t)^2\,dt\right]^{1/2} = \frac{V_m}{2} = 0.5V_m \\ I_{rms} &= \frac{V_{rms}}{R} = \frac{0.5V_m}{R} \end{aligned} \tag{2-56}$$

From Eq. (2-42), $P_{dc} = (0.318V_m)^2/R$, and from Eq. (2-43), $P_{ac} = (0.5V_m)^2/R$.

(a) From Eq. (2-44), the efficiency, $\eta = (0.318V_m)^2/(0.5V_m)^2 = 40.5\%$.

(b) From Eq. (2-46), the form factor, FF $= 0.5V_m/0.318V_m = 1.57$ or 157%.

(c) From Eq. (2-48), the ripple factor, RF $= \sqrt{1.57^2 - 1} = 1.21$ or 121%.

(d) The rms voltage of the transformer secondary is

$$V_s = \left[\frac{1}{T}\int_0^T (V_m \sin \omega t)^2\,dt\right]^{1/2} = \frac{V_m}{\sqrt{2}} = 0.707V_m \tag{2-57}$$

The rms value of the transformer secondary current is the same as that of the load:

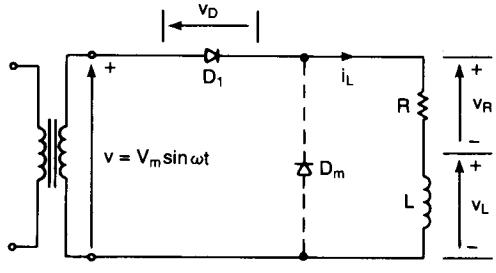
$$I_s = \frac{0.5V_m}{R}$$

The *volt-ampere* rating (VA) of transformer, VA = $V_s I_s$ = $0.707V_m \times 0.5V_m/R$.
From Eq. (2-49) TUF = $0.318^2/(0.707 \times 0.5)$ = 0.286.

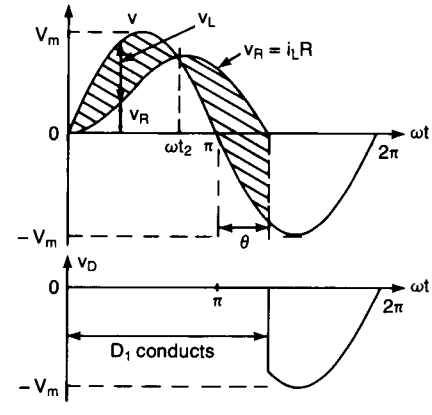
(e) The peak reverse (or inverse) blocking voltage, PIV = V_m.

Note. 1/TUF = 1/0.286 = 3.496 signifies that the transformer must be 3.496 times larger than that when it is being used to deliver power from a pure ac voltage. This rectifier has a high ripple factor, 121%; a low efficiency, 40.5%; and a poor TUF, 0.286. In addition, the transformer has to carry a dc current, and this results in a dc saturation problem of the transformer core.

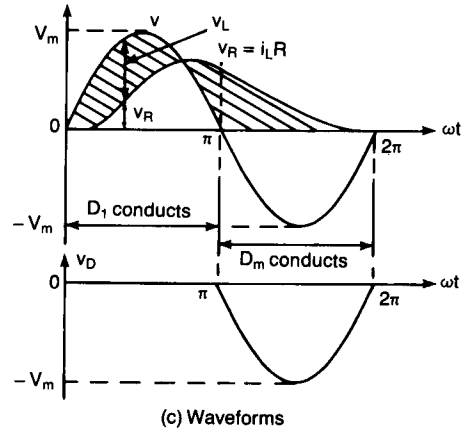
Let us consider the circuit of Fig. 2-12a with an *RL* load as shown in Fig. 2-13a. Due to inductive load, the conduction period of the diode D_1 will extend beyond 180° until the current becomes zero. The waveforms for the current and



(a) Circuit diagram



(b) Waveforms



(c) Waveforms

Figure 2-13 Half-wave rectifier with *RL* load.

voltage are shown in Fig. 2-13b. The average output voltage is

$$V_{dc} = \frac{V_m}{2\pi}\int_0^{\pi+\theta} \sin \omega t \, d(\omega t) = \frac{V_m}{2\pi}[-\cos \omega t]_0^{\pi+\theta}$$
$$= \frac{V_m}{2\pi}[1 - \cos(\pi + \theta)] \tag{2-58}$$

where $\theta = \tan^{-1}(\omega L/R)$ and $\omega = 2\pi f$. The average load current is $I_{dc} = V_{dc}/R$.

It can be noted from Eq. (2-58) that the average voltage (and current) can be increased by making $\theta = 0$, which is possible by adding a freewheeling diode D_m as shown in Fig. 2-13a with dashed lines. The effect of this diode is to prevent a negative voltage appearing across the load; and as a result, the magnetic stored energy is increased. At $t = t_1 = \pi/\omega$, the current from D_1 is transferred to D_m and this process is called *commutation* of diodes and the waveforms are shown in Fig. 2-13c. Depending on the load time constant, the load current may be discontinuous.

2-8 SINGLE-PHASE FULL-WAVE RECTIFIERS

A full-wave rectifier circuit with a center-tapped transformer is shown in Fig. 2-14a. Each half of the transformer with its associated diode acts as a half-wave rectifier and the output of a full-wave rectifier is shown in Fig. 2-14b. Since there is no dc current flowing through the transformer, there is no dc saturation problem of transformer core. The average output voltage is

$$V_{dc} = \frac{2}{T}\int_0^{T/2} V_m \sin \omega t \, dt = \frac{2V_m}{\pi} = 0.6366V_m \tag{2-59}$$

Instead of using a center-tapped transformer, we could use four diodes, as shown in Fig. 2-15a. During the positive half-cycle of the input voltage, the current flows to the load through diodes D_1 and D_2. During the negative cycle, diodes D_3 and D_4 conduct. The waveform for the output voltage is shown in Fig. 2-15b and is similar to that of Fig. 2-14b. The peak-inverse voltage of a diode is only V_m. This circuit is known as a *bridge rectifier.*

Example 2-7

If the rectifier in Fig. 2-14a has a purely resistive load of R, determine the (a) efficiency; (b) form factor; (c) ripple factor; (d) transformer utilization factor; and (e) peak inverse voltage (PIV) of diode D_1.

Solution From Eq. (2-59), the average output voltage is

$$V_{dc} = \frac{2V_m}{\pi} = 0.6366V_m$$

and the average load current is

$$I_{dc} = \frac{V_{dc}}{R} = \frac{0.6366V_m}{R} \tag{2-60}$$

The rms value of the output voltage is

$$V_{\text{rms}} = \left[\frac{2}{T}\int_0^{T/2} (V_m \sin \omega t)^2\, dt\right]^{1/2} = \frac{V_m}{\sqrt{2}} = 0.707V_m$$
$$I_{\text{rms}} = \frac{V_{\text{rms}}}{R} = \frac{0.707V_m}{R} \tag{2-61}$$

From Eq. (2-42), $P_{\text{dc}} = (0.6366V_m)^2/R$ and from Eq. (2-43), $P_{\text{ac}} = (0.707V_m)^2/R$.

(a) From Eq. (2-44), the efficiency, $\eta = (0.6366V_m)^2/(0.707V_m)^2 = 81\%$.

(b) From Eq. (2-46), the form factor, FF $= 0.707V_m/0.6366V_m = 1.11$.

(c) From Eq. (2-48), the ripple factor, RF $= \sqrt{1.11^2 - 1} = 0.482$ or 48.2%.

(d) The rms voltage of the transformer secondary, $V_s = V_m/\sqrt{2} = 0.707V_m$. The rms value of transformer secondary current, $I_s = 0.5V_m/R$. The volt-ampere rating (VA) of the transformer, VA $= 2V_sI_s = 2 \times 0.707V_m \times 0.5V_m/R$. From Eq. (2-49),

$$\text{TUF} = \frac{0.6366^2}{2 \times 0.707 \times 0.5} = 0.5732 = 57.32\%$$

(e) The peak reverse blocking voltage, PIV $= 2V_m$.

Note. The performance of a full-wave rectifier is significantly improved compared to that of a half-wave rectifier.

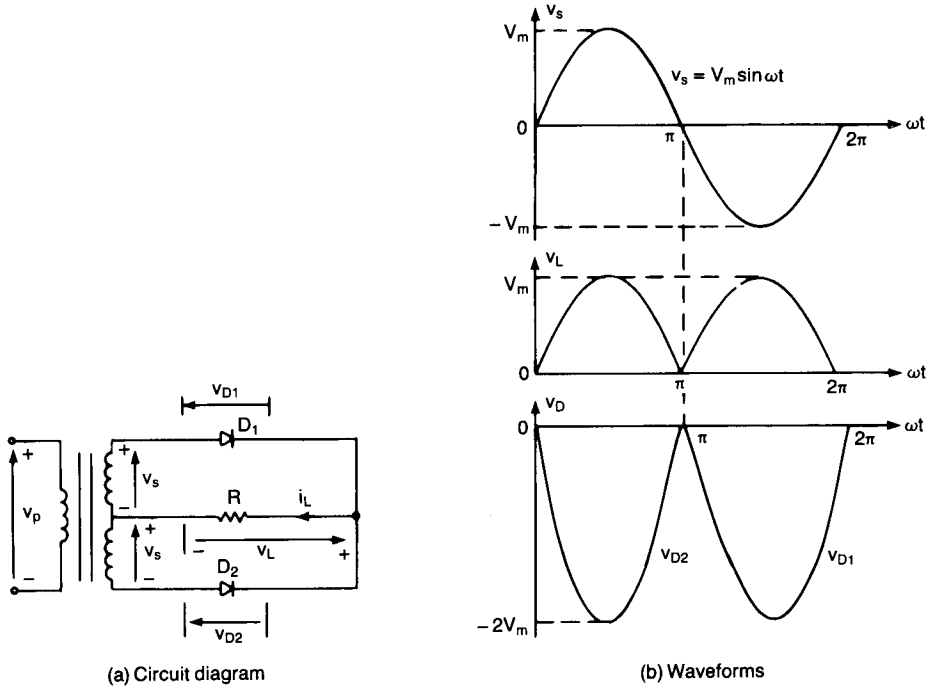
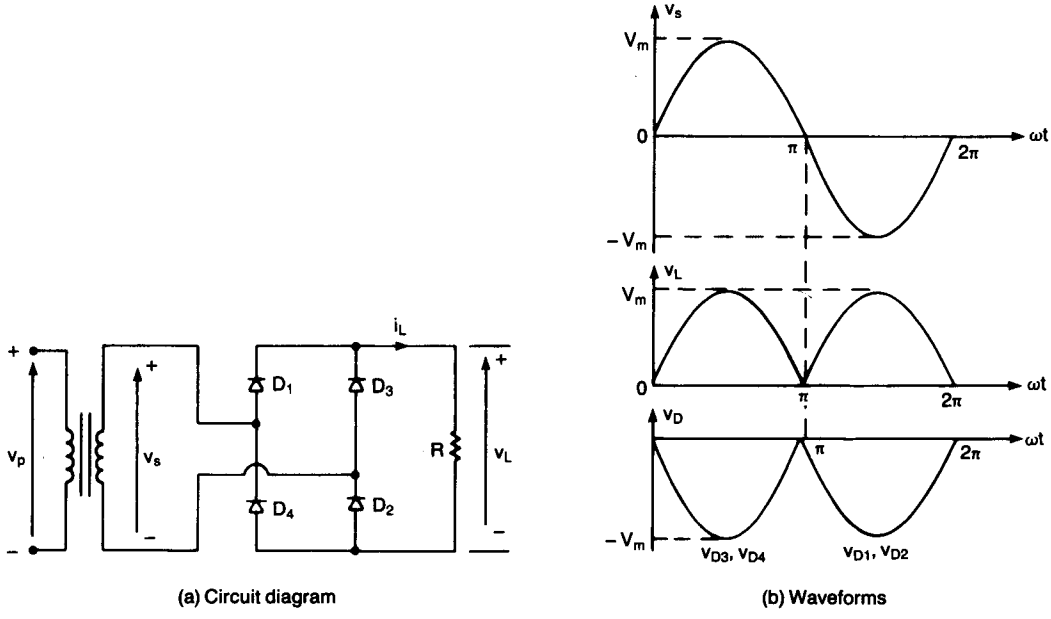


Figure 2-14 Full-wave rectifier with center-tapped transformer.



(a) Circuit diagram

(b) Waveforms

Figure 2-15 Full-wave bridge rectifier.

Example 2-8

The rectifier in Fig. 2-14a has an *RL* load. (a) Use the method of Fourier series to obtain expressions for output voltage $v_L(t)$ and load current $i_L(t)$. (b) If $V_m = 170$ V, $f = 60$ Hz, and $R = 500\ \Omega$, determine the value of series inductance L to limit ripple current to 5% of I_{dc}.

Solution (a) The rectifier output voltage may be described by a Fourier series (which is reviewed in Appendix E) as

$$v_L(t) = V_{dc} + \sum_{n=1,2,\ldots}^{\infty} (a_n \cos n\omega t + b_n \sin n\omega t) \tag{2-62}$$

where

$$V_{dc} = \frac{1}{2\pi}\int_0^{2\pi} v_L(t)\, d(\omega t) = \frac{2}{2\pi}\int_0^{\pi} V_m \sin \omega t\, d(\omega t) = \frac{2V_m}{\pi}$$

$$a_n = \frac{1}{\pi}\int_0^{2\pi} v_L \cos n\omega t\, d(\omega t) = \frac{2}{\pi}\int_0^{\pi} V_m \sin \omega t \cos n\omega t\, d(\omega t)$$

$$b_n = \frac{1}{\pi}\int_0^{2\pi} v_L \sin n\omega t\, d(\omega t) = \frac{2}{\pi}\int_0^{\pi} V_m \sin \omega t \sin n\omega t\, d(\omega t) = 0$$

$$= \frac{4V_m}{\pi} \sum_{n=2,4,\ldots}^{\infty} \frac{1}{(n-1)(n+1)}$$

Substituting the values of a_n and b_n, the expression for the output voltage is

$$v_L(t) = \frac{2V_m}{\pi} - \frac{4V_m}{3\pi}\cos 2\omega t - \frac{4V_m}{15\pi}\cos 4\omega t - \frac{4V_m}{35\pi}\cos 6\omega t - \cdots \quad (2\text{-}63)$$

The load impedance

$$Z = R + j(n\omega L) = \sqrt{R^2 + (n\omega L)^2}\ \angle\theta_n \quad (2\text{-}64)$$

and

$$\theta_n = \tan^{-1}\frac{n\omega L}{R} \quad (2\text{-}65)$$

and the instantaneous current is

$$i_L(t) = I_{dc} - \frac{4V_m}{\pi\sqrt{R^2 + (n\omega L)^2}}\left[\frac{1}{3}\cos(2\omega t - \theta_2) - \frac{1}{15}\cos(4\omega t - \theta_4)\cdots\right] \quad (2\text{-}66)$$

where

$$I_{dc} = \frac{V_{dc}}{R} = \frac{2V_m}{\pi R}$$

(b) Equation (2-66) gives the rms value of the ripple current as

$$I_{ac}^2 = \frac{(4V_m)^2}{2\pi^2[R^2 + (2\omega L)^2]}\left(\frac{1}{3}\right)^2 + \frac{(4V_m)^2}{2\pi^2[R^2 + (4\omega L)^2]}\left(\frac{1}{15}\right)^2 + \cdots$$

Considering only the lowest-order harmonic ($n = 2$), we have

$$I_{ac} = \frac{4V_m \times 0.34}{\sqrt{2}\pi\sqrt{R^2 + (2\omega L)^2}}$$

Using the value of I_{dc} and after simplification, the ripple factor is

$$\text{RF} = \frac{I_{ac}}{I_{dc}} = \frac{0.481}{\sqrt{1 + (2\omega L/R)^2}} = 0.05$$

For $R = 500\ \Omega$ and $f = 60$ Hz, the inductance value is obtained as $0.481^2 = 0.05^2[1 + (4 \times 60 \times \pi L/500)^2]$ and this gives $L = 6.34$ H.

Note. The output of a full-wave rectifier contains only even harmonics and the second harmonic is the most dominant one and its frequency is $2f$ ($= 120$ Hz). The output voltage in Eq. (2-63) can be derived by spectrum multiplication of switching function, and this is explained in Appendix C.

We can notice from Eq. (2-66) that an inductance in the load offers a high impedance for the harmonic currents and acts like a filter in reducing the harmonics. However, this inductance introduces a time delay of the load current with respect to the input voltage; and in the case of the single-phase half-wave rectifier, a freewheeling diode is required to provide a path for this inductive current.

Example 2-9

A single-phase bridge rectifier that supplies a dc motor is shown in Fig. 2-16a. The turns ratio of the transformer is unity. The load is such that the motor draws a ripple-

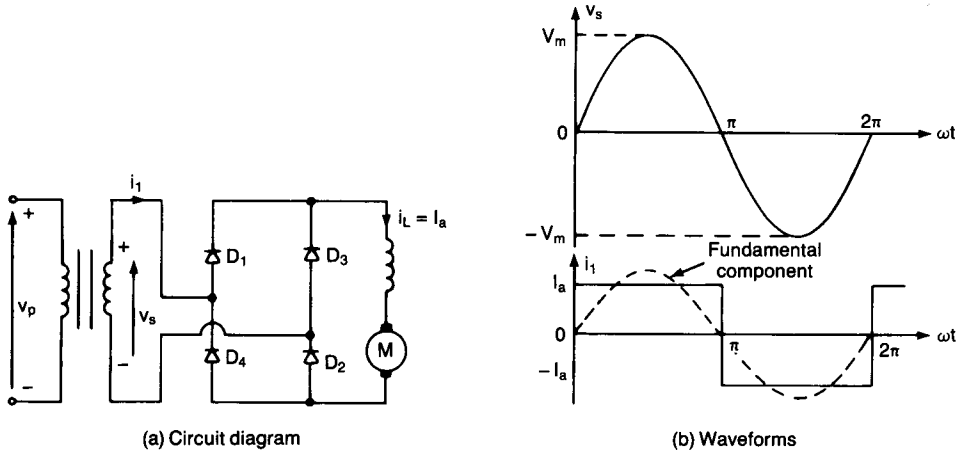


Figure 2-16 Full-wave bridge rectifier with dc motor load.

free armature current of I_a. Determine the (a) harmonic factor of input current, HF; and (b) input power factor of the rectifier, PF.

Solution Normally, a dc motor is highly inductive and acts like a filter in reducing the ripple current of the load.

(a) The waveforms for the input current and input voltage of the rectifier are shown in Fig. 2-16b. The input current can be expressed in a Fourier series as

$$i_1(t) = I_{dc} + \sum_{n=1}^{\infty} (a_n \cos n\omega t + b_n \sin n\omega t) \tag{2-67}$$

where

$$I_{dc} = \frac{1}{2\pi}\int_0^{2\pi} i_1(t)\, d(\omega t) = \frac{1}{2\pi}\int_0^{2\pi} I_a\, d(\omega t) = 0$$

$$a_n = \frac{1}{\pi}\int_0^{2\pi} i_1(t) \cos n\omega t\, d(\omega t) = \frac{2}{\pi}\int_0^{\pi} I_a \cos n\omega t\, d(\omega t) = 0$$

$$b_n = \frac{1}{\pi}\int_0^{2\pi} i_1(t) \sin n\omega t\, d(\omega t) = \frac{2}{\pi}\int_0^{\pi} I_a \sin n\omega t\, d(\omega t) = \frac{4I_a}{n\pi}$$

Substituting the values of a_n and b_n, the expression for the input current is

$$i_1(t) = \frac{4I_a}{\pi}\left(\frac{\sin \omega t}{1} + \frac{\sin 3\omega t}{3} + \frac{\sin 5\omega t}{5} + \cdots\right) \tag{2-68}$$

The rms value of the fundamental component of input current is

$$I_1 = \frac{4I_a}{\pi\sqrt{2}} = 0.90I_a$$

The rms value of the input current is

$$I_s = \frac{4}{\pi\sqrt{2}} I_a\left[1 + \left(\frac{1}{3}\right)^2 + \left(\frac{1}{5}\right)^2 + \left(\frac{1}{7}\right)^2 + \left(\frac{1}{9}\right)^2 + \cdots\right]^{1/2} = I_a$$

From Eq. (2-51),

$$\text{HF} = \left[\left(\frac{1}{0.90}\right)^2 - 1\right]^{1/2} = 0.4843 \quad \text{or} \quad 48.43\%$$

(b) The displacement angle, $\phi = 0$ and displacement factor, $\text{DF} = \cos\phi = 1$. From Eq. (2-52), the power factor, PF = 0.90 (lagging).

2-9 MULTIPHASE STAR RECTIFIERS

We have seen in Eq. (2-59) that the average output voltage which could be obtained from single-phase full-wave rectifiers is $0.6366V_m$ and these rectifiers are used in applications up to the 15-kW power level. For larger power output, *three-phase* and *multiphase* rectifiers are used. The Fourier series of the output voltage given by Eq. (2-63) indicates that the output contains harmonics and the frequency of the *fundamental component* is two times the source frequency ($2f$). In practice, a filter is normally used to reduce the level of harmonics in the load; and the size of the filter decreases with the frequency of the harmonics. In addition to the larger power output of multiphase rectifiers, the fundamental frequency of the harmonics is also increased and is q times the source frequency (qf).

The rectifier circuit of Fig. 2-14(a) can be extended to multiple phases by having multiphase windings on the transformer secondary as shown in Fig. 2-17a. This circuit may be considered as q single-phase half-wave rectifiers and can be considered as a half-wave type. The kth diode will conduct during the period when the voltage of kth phase is higher than that of other phases. The waveforms for the voltages and currents are shown in Fig. 2-17b. The conduction period of each diode is $2\pi/q$.

It can be noticed from Fig. 2-17b that the current flowing through the secondary winding is unidirectional and contains a dc component. Only one secondary winding carries current at a particular time, and as a result the primary must be connected in delta in order to eliminate the dc component in the input side of the transformer.

The average output voltage for a q-phase rectifier is given by

$$V_{\text{dc}} = \frac{2}{2\pi/q}\int_0^{\pi/q} V_m \cos\omega t\, d(\omega t) = V_m \frac{q}{\pi}\sin\frac{\pi}{q} \tag{2-69}$$

$$V_{\text{rms}} = \left[\frac{2}{2\pi/q}\int_0^{\pi/q} V_m^2 \cos^2\omega t\, d\,(\omega t)\right]^{1/2}$$

$$= V_m\left[\frac{q}{2\pi}\left(\frac{\pi}{q} + \frac{1}{2}\sin\frac{2\pi}{q}\right)\right]^{1/2} \tag{2-70}$$

If the load is purely resistive, the peak current through a diode is $I_m = V_m/R$ and we can find the rms value of a diode current (or transformer secondary current)

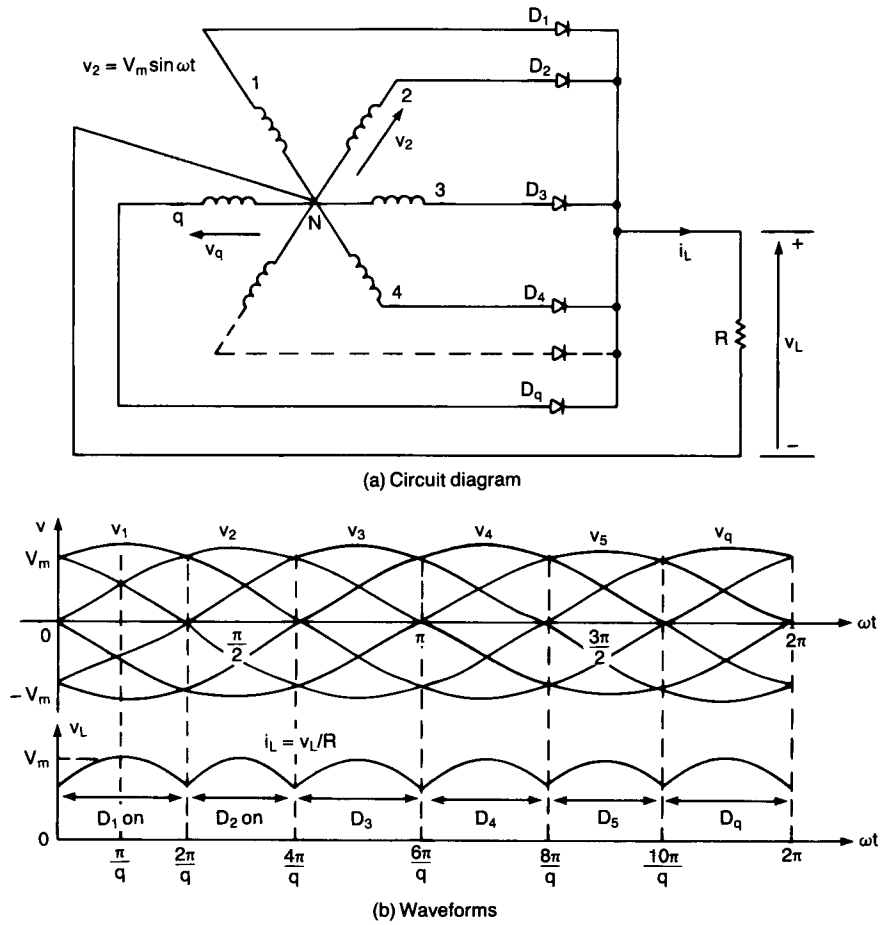


Figure 2-17 Multiphase rectifiers.

as

$$I_s = \left[\frac{2}{2\pi}\int_0^{\pi/q} I_m^2 \cos^2 \omega t \, d\,(\omega t)\right]^{1/2}$$

$$= I_m \left[\frac{1}{2\pi}\left(\frac{\pi}{q} + \frac{1}{2}\sin\frac{2\pi}{q}\right)\right]^{1/2} \tag{2-71}$$

Example 2-10

A three-phase star rectifier has a purely resistive load with R ohms. Determine the (a) efficiency; (b) form factor; (c) ripple factor; (d) transformer utilization factor; (e) peak inverse voltage (PIV) of each diode; and (f) peak current through a diode if the rectifier delivers $I_{dc} = 30$ A at a output voltage of $V_{dc} = 140$ V.

Solution For a three-phase rectifier $q = 3$ in Eqs. (2-69), (2-70), and (2-71).

(a) From Eq. (2-69), $V_{dc} = 0.827V_m$ and $I_{dc} = 0.827V_m/R$. From Eq. (2-70), $V_{rms} = 0.84068V_m$ and $I_{rms} = 0.84068V_m/R$. From Eq. (2-42), $P_{dc} = (0.827V_m)^2/R$, from Eq. (2-43), $P_{ac} = (0.84068V_m)^2/R$, and from Eq. (2-44), the efficiency,

$$\eta = \frac{(0.827V_m)^2}{(0.84068V_m)^2} = 96.77\%$$

(b) From Eq. (2-46), the form factor, FF = 0.84068/0.827 = 1.0165 or 101.65%.

(c) From Eq. (2-48), the ripple factor, RF = $\sqrt{1.0165^2 - 1}$ = 0.1824 = 18.24%.

(d) From Eq. (2-57), the rms voltage of the transformer secondary, $V_s = 0.707V_m$. From Eq. (2-71), the rms current of the transformer secondary,

$$I_s = 0.4854I_m = \frac{0.4854V_m}{R}$$

The volt-ampere rating (VA) of the transformer is

$$VA = 3V_sI_s = 3 \times 0.707V_m \times \frac{0.4854V_m}{R}$$

From Eq. (2-49),

$$TUF = \frac{0.827^2}{3 \times 0.707 \times 0.4854} = 0.6643$$

(e) The peak inverse voltage of each diode is equal to the peak value of the secondary line-to-line voltage. Three-phase circuits are reviewed in Appendix A. The line-to-line voltage is $\sqrt{3}$ times the phase voltage and thus PIV = $\sqrt{3}V_m$.

(f) The average current through each diode is

$$I_d = \frac{2}{2\pi}\int_0^{\pi/q} I_m \cos \omega t \, d(\omega t) = I_m \frac{1}{\pi} \sin \frac{\pi}{q} \tag{2-72}$$

For $q = 3$, $I_d = 0.2757I_m$. The average current through each diode is $I_d = 30/3 = 10$ A and this gives the peak current as $I_m = 10/0.2757 = 36.27$ A.

Example 2-11

(a) Express the output voltage of a q-phase rectifier in Fig. 2-17a in Fourier series. (b) If $q = 6$, $V_m = 170$ V and the supply frequency is $f = 60$ Hz, determine the rms value of the dominant harmonic and its frequency.

Solution (a) The waveforms for q-pulses are shown in Fig. 2-17b and the frequency of the output is q times the fundamental component (qf). To find the constants of the Fourier series, we integrate from $-\pi/q$ to π/q and the constants are

$$b_n = 0$$

$$a_n = \frac{1}{\pi/q}\int_{-\pi/q}^{\pi/q} V_m \cos \omega t \cos n\omega t \, d(\omega t)$$

$$= \frac{qV_m}{\pi}\left\{\frac{\sin [(n-1)\pi/q]}{n-1} + \frac{\sin [(n+1)\pi/q]}{n+1}\right\}$$

$$= \frac{qV_m}{\pi}\frac{(n+1)\sin [(n-1)\pi/q] + (n-1)\sin [(n+1)\pi/q]}{n^2-1}$$

After simplification and then using trigonometric relationships

$$\sin (A + B) = \sin A \cos B + \cos A \sin B$$

and

$$\sin (A - B) = \sin A \cos B - \cos A \sin B$$

we get

$$a_n = \frac{2qV_m}{\pi(n^2 - 1)} \left(n \sin \frac{n\pi}{q} \cos \frac{\pi}{q} - \cos \frac{n\pi}{q} \sin \frac{\pi}{q} \right) \tag{2-73}$$

For a rectifier with q pulses per cycle, the harmonics of the output voltage are: qth, $2q$th, $3q$th, $4q$th and Eq. (2-73) is valid for $n = 0, 1q, 2q, 3q$. The term $\sin (n\pi/q) = \sin \pi = 0$ and Eq. (2-73) becomes

$$a_n = \frac{-2qV_m}{\pi(n^2 - 1)} \left(\cos \frac{n\pi}{q} \sin \frac{\pi}{q} \right)$$

The dc component is found by letting $n = 0$ and is

$$V_{dc} = \frac{a_0}{2} = V_m \frac{q}{\pi} \sin \frac{\pi}{q} \tag{2-74}$$

which is the same as Eq. (2-69). The Fourier series of the output voltage is expressed as

$$v_L(t) = \frac{a_0}{2} + \sum_{n=q,2q,\ldots}^{\infty} a_n \cos n\omega t$$

Substituting the value of a_n, we obtain

$$v_L = V_m \frac{q}{\pi} \sin \frac{\pi}{q} \left(1 - \sum_{n=q,2q,\ldots}^{\infty} \frac{2}{n^2 - 1} \cos \frac{n\pi}{q} \cos n\omega t \right) \tag{2-75}$$

(b) For $q = 6$, the output voltage is expressed as

$$v_L(t) = 0.9549V_m \left(1 + \frac{2}{35} \cos 6\omega t - \frac{2}{143} \cos 12\omega t + \cdots \right) \tag{2-76}$$

The sixth harmonic is the dominant one. The rms value of a sinusoidal voltage is $1/\sqrt{2}$ times its peak magnitude, and the rms of the sixth harmonic is $V_6 = V_m \times 2 \times 0.9549/(35 \times \sqrt{2}) = 6.56$ A and its frequency is $f_6 = 6f = 360$ Hz.

2-10 THREE-PHASE BRIDGE RECTIFIERS

The three-phase bridge rectifier is very common in high-power applications and is shown in Fig. 2-18. This is a *full-wave rectifier*. It can operate with or without a transformer and gives six-pulse ripples on the output voltage. The diodes are numbered in order of conduction sequences and each one conducts for 120°. The conduction sequence for diodes is 12, 23, 34, 45, 56, and 61. The pair of diodes which are connected between that pair of supply lines having the highest amount of instantaneous line-to-line voltage will conduct. The line-to-line voltage is $\sqrt{3}$

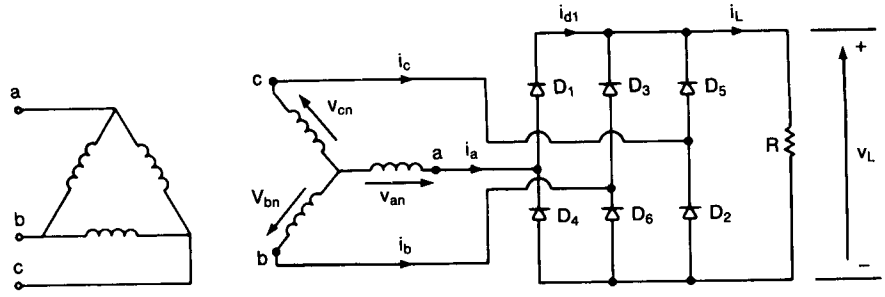


Figure 2-18 Three-phase bridge rectifier.

times the phase voltage of a three-phase Y-connected source. The waveforms and conduction times of diodes are shown in Fig. 2-19.

The average output voltage is found from

$$V_{dc} = \frac{2}{2\pi/6}\int_0^{\pi/6} \sqrt{3}\, V_m \cos \omega t\, d(\omega t) = \frac{3\sqrt{3}}{\pi} V_m = 1.6542 V_m \tag{2-77}$$

where V_m is the peak phase voltage.

$$V_{rms} = \left[\frac{2}{2\pi/6}\int_0^{\pi/6} 3V_m^2 \cos^2 \omega t\, d(\omega t)\right]^{1/2} = \left(\frac{3}{2} + \frac{9\sqrt{3}}{4\pi}\right)^{1/2} V_m = 1.6554 V_m \tag{2-78}$$

If the load is purely resistive, the peak current through a diode is $I_m = \sqrt{3}\, V_m/R$ and the rms value of the diode current is

$$I_d = \left[\frac{4}{2\pi}\int_0^{\pi/6} I_m^2 \cos^2 \omega t\, d\,(\omega t)\right]^{1/2} = I_m\left[\frac{1}{\pi}\left(\frac{\pi}{6} + \frac{1}{2}\sin\frac{2\pi}{6}\right)\right]^{1/2} = 0.5518 I_m \tag{2-79}$$

and the rms value of the transformer secondary current,

$$I_s = \left[\frac{8}{2\pi}\int_0^{\pi/6} I_m^2 \cos^2 \omega t\, d(\omega t)\right]^{1/2} = I_m\left[\frac{2}{\pi}\left(\frac{\pi}{6} + \frac{1}{2}\sin\frac{2\pi}{6}\right)\right]^{1/2} = 0.7804 I_m \tag{2-78}$$

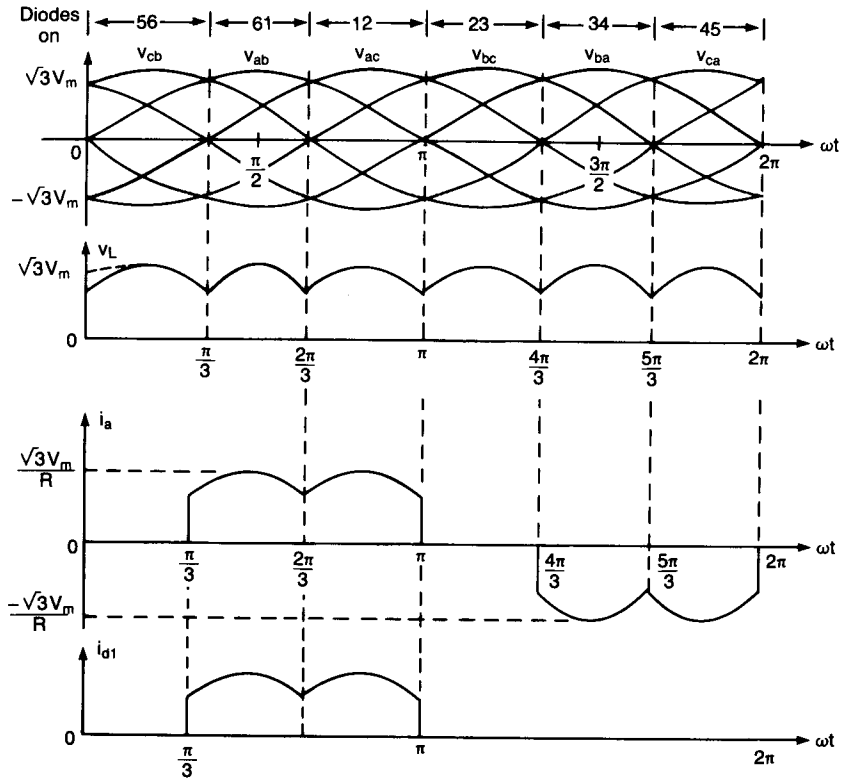


Figure 2-19 Waveforms and conduction times of diodes.

Example 2-12

A three-phase bridge rectifier has a purely resistive load of R. Determine the (a) efficiency; (b) form factor; (c) ripple factor; (d) transformer utilization factor; (e) peak inverse (or reverse) voltage (PIV) of each diode; and (f) peak current through a diode. The rectifier delivers $I_{dc} = 60$ A at an output voltage of $V_{dc} = 280.7$ V and the frequency of the source is 60 Hz.

Solution (a) From Eq. (2-77), $V_{dc} = 1.6542V_m$ and $I_{dc} = 1.6542V_m/R$. From Eq. (2-78), $V_{rms} = 1.6554V_m$ and $I_{rms} = 1.6554V_m/R$. From Eq. (2-42), $P_{dc} = (1.6542V_m)^2/R$, from Eq. (2-43), $P_{ac} = (1.6554V_m)^2/R$, and from Eq. (2-44) the efficiency,

$$\eta = \frac{(1.6542V_m)^2}{(1.6554V_m)^2} = 99.86\%$$

(b) From Eq. (2-46), the form factor, FF = 1.6554/1.6542 = 1.0007 = 100.07%.

(c) From Eq. (2-48), the ripple factor, RF = $\sqrt{1.0007^2 - 1}$ = 0.0374 = 3.74%.

(d) From Eq. (2-57), the rms voltage of the transformer secondary, $V_s = 0.707V_m$.

From Eq. (2-80), the rms current of the transfromer secondary,

$$I_s = 0.7804I_m = 0.7804 \times \sqrt{3}\frac{V_m}{R}$$

The volt-ampere rating of the transfromer,

$$\text{VA} = 3V_sI_s = 3 \times 0.707V_m \times 0.7804 \times \sqrt{3}\frac{V_m}{R}$$

From Eq. (2-49),

$$\text{TUF} = \frac{1.6542^2}{3 \times \sqrt{3} \times 0.707 \times 0.7804} = 0.9545$$

(e) From Eq. (2-77), the peak line-neutral voltage is $V_m = 280.7/1.6542 = 169.7$ V. The peak inverse voltage of each diode is equal to the peak value of the secondary line-to-line voltage, PIV $= \sqrt{3}\,V_m = \sqrt{3} \times 169.7 = 293.9$ V.

(f) The average current through each diode is

$$I_d = \frac{4}{2\pi}\int_0^{\pi/6} I_m \cos \omega t\, d(\omega t) = I_m \frac{2}{\pi} \sin \frac{\pi}{6} = 0.3184I_m$$

The average current through each diode is $I_d = 60/3 = 20$ A and the peak current is $I_m = 20/0.3184 = 62.81$ A.

Note. This rectifier has improved performances considerably compared to that of the multiphase rectifier in Fig. 2-17 with six pulses.

2-11 RECTIFIER CIRCUIT DESIGN

The design of a rectifier involves determining the ratings of semiconductor diodes. The ratings of diodes are normally specified in terms of the average current, rms current, peak current, and peak inverse voltage. There are no standard procedures for the design, but it is required to determine the shapes of the diode currents and voltages.

We have noticed in Eqs. (2-63), (2-66), and (2-76) that the output of the rectifiers contain harmonics. In addition, Eq. (2-66) indicates that the ripple current can be reduced by connecting an inductor in series with the load. Filters can be used to smooth out the dc output voltage of the rectifier and these are known as *dc filters*. The dc filters are usually of L, C, and LC type, as shown in Fig. 2-20. Due to the rectification action, the input current of the rectifier also

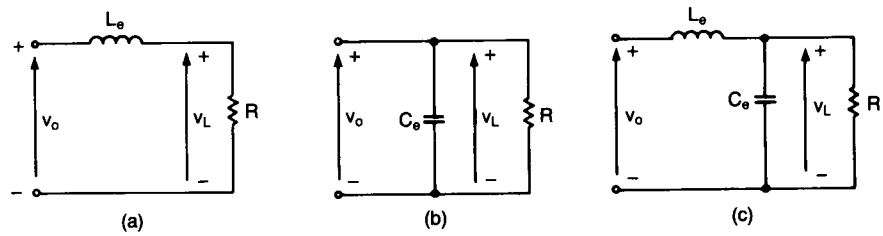
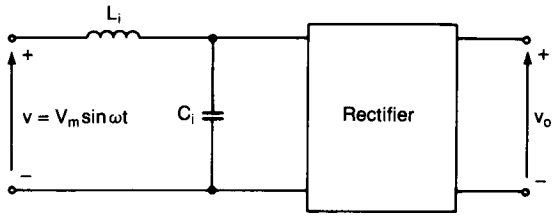


Figure 2-20 Dc filters.



;ure 2-21 Ac filters.

contains harmonics and an *ac filter* is used to filter out some of the harmonics from the supply system. The ac filter is normally of *LC* type, as shown in Fig. 2-21. Normally, the filter design requires determining the magnitudes and frequencies of the harmonics. The steps involved in designing rectifiers and filters are explained by examples.

Example 2-13

A three-phase bridge rectifier supplies a highly inductive load such that the average load current is $I_{dc} = 60$ A and the ripple content is negligible. Determine the ratings of the diodes if the line-to-neutral voltage of the supply is 120 V at 60 Hz.

Solution The currents through the diodes are shown in Fig. 2-22. The average current of a diode, $I_d = 60/3 = 20$ A. The rms current is

$$I_r = \left[\frac{1}{2\pi}\int_{\pi/6}^{5\pi/6} I_{dc}^2 \, d(\omega t)\right]^{1/2} = \frac{I_{dc}}{\sqrt{3}} = 46.19 \text{ A}$$

The peak inverse voltage, PIV $= \sqrt{3}\, V_m = \sqrt{3} \times \sqrt{2} \times 120 = 294$ V.

Note. The factor of $\sqrt{2}$ is used to convert rms to peak value.

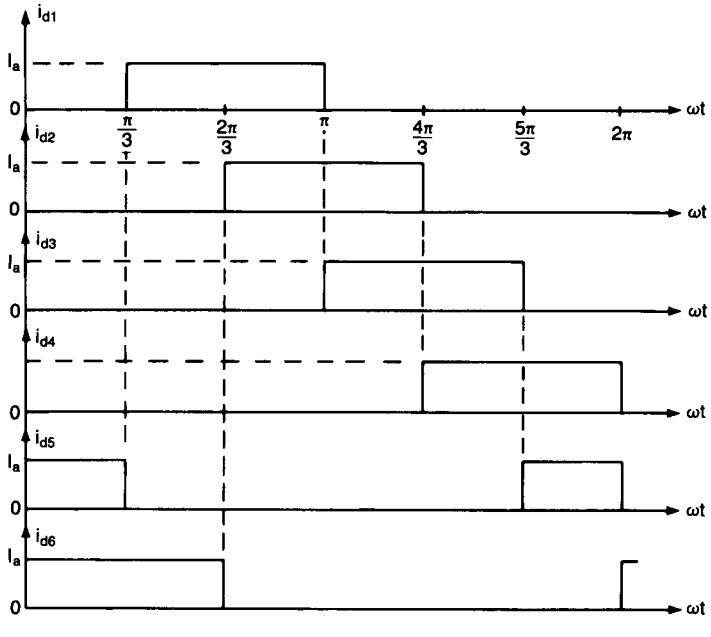


Figure 2-22 Current through diodes.

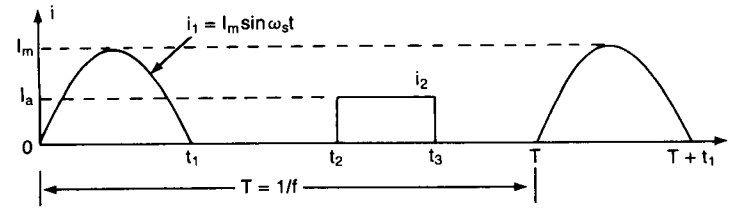


Figure 2-23 Current waveform.

Example 2-14

The current through a diode is shown in Fig. 2-23. Determine the (a) rms current, and (b) average diode current if $t_1 = 100$ μs, $t_2 = 350$ μs, $t_3 = 500$ μs, $f = 250$ Hz, $f_s = 5$ kHz, $I_m = 450$ A, and $I_a = 150$ A.

Solution (a) The rms value is defined as

$$I = \left[\frac{1}{T}\int_0^{t_1} (I_m \sin \omega_s t)^2 \, dt + \frac{1}{T}\int_{t_2}^{t_3} I_a^2 \, dt\right]^{1/2} \tag{2-81}$$

$$= (I_{r1}^2 + I_{r2}^2)^{1/2} \tag{2-82}$$

where $\omega_s = 2\pi f_s = 31{,}415.93$ rad/s, $t_1 = \pi/\omega_s = 100$ μs, and $T = 1/f$.

$$I_{r1} = \left[\frac{1}{T}\int_0^{t_1} (I_m \sin \omega_s t)^2 \, dt\right]^{1/2} = I_m \sqrt{\frac{ft_1}{2}} \tag{2-83}$$

$$= 50.31 \text{ A}$$

and

$$I_{r2} = \left(\frac{1}{T}\int_{t_2}^{t_3} I_a \, dt\right)^2 = I_a \sqrt{f(t_3 - t_2)} \tag{2-84}$$

$$= 29.05 \text{ A}$$

Substituting Eqs. (2-83) and (2-84) in Eq. (2-82), the rms value is

$$I = \left[\frac{I_m^2 f t_1}{2} + I_a^2 f(t_3 - t_2)\right]^{1/2} \tag{2-85}$$
$$= (50.31^2 + 29.05^2)^{1/2} = 58.09 \text{ A}$$

(b) The average current is found from

$$I_{dc} = \left[\frac{1}{T}\int_0^{t_1} (I_m \sin \omega_s t) \, dt + \frac{1}{T}\int_{t_2}^{t_3} I_a \, dt\right] \tag{2-86}$$

$$= I_{d1} + I_{d2} \tag{2-87}$$

where

$$I_{d1} = \frac{1}{T}\int_0^{t_1} (I_m \sin \omega_s t) \, dt = \frac{I_m f}{\pi f_s} \tag{2-88}$$

$$I_{d2} = \frac{1}{T}\int_{t_2}^{t_3} I_a \, dt = I_a f(t_3 - t_2) \tag{2-89}$$

Therefore, the average current becomes

$$I_{dc} = \frac{I_m f}{\pi f_s} + I_a f(t_3 - t_2) = 7.16 + 5.63 = 12.79 \text{ A}$$

Example 2-15

A LC filter as shown in Fig. 2-20c is used to reduce the ripple content of the output voltage for a single-phase full-wave rectifier. The load resistance, $R = 40\ \Omega$, load inductance, $L = 10$ mH, and source frequency is 60 Hz (or 377 rad/s). Determine the values of L_e and C_e so that the ripple factor of the output voltage is 10%.

Solution The equivalent circuit for the harmonics is shown in Fig. 2-24. To make it easier for the nth harmonic ripple current to pass through the filter capacitor, the load impedance must be greater than that of the capacitor:

$$\sqrt{R^2 + (n\omega L)^2} >> \frac{1}{n\omega C_e}$$

This condition is generally satisfied by the relation

$$\sqrt{R^2 + (n\omega L)^2} = \frac{10}{n\omega C_e} \tag{2-90}$$

and under this condition, the effect of the load will be negligible. The rms value of the nth harmonic component appearing on the output can be found by using the voltage-divider rule and is expressed as

$$V_{on} = \frac{1/(n\omega C_e)}{(n\omega L_e) - 1/(n\omega C_e)} V_n = \frac{1}{(n\omega)^2 L_e C_e - 1} V_n \tag{2-91}$$

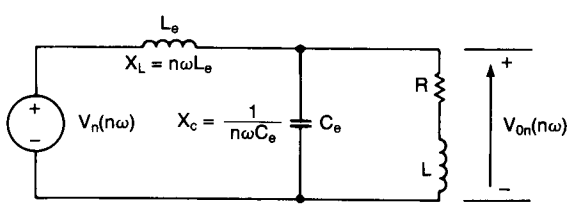
The total amount of ripple voltage due to all harmonics is

$$V_{ac} = \left(\sum_{n=2,4,6\ldots}^{\infty} V_{on}^2 \right)^{1/2} \tag{2-92}$$

For a specified value of V_{ac} and with the value of C_e from Eq. (2-90), the value of L_e can be computed. We can simplify the computation by considering only the dominant harmonic. From Eq. (2-63) we find that the second harmonic is the dominant one and its rms value is $V_2 = 4V_m/(3\sqrt{2}\,\pi)$ and the dc value, $V_{dc} = 2V_m/\pi$.

For $n = 2$ Eqs. (2-91) and (2-92) give

$$V_{ac} = V_{o2} = \frac{1}{(2\omega)^2 L_e C_e - 1} V_2$$



POWEREN.IR

Figure 2-24 Equivalent circuit for harmonics.

The value of the filter capacitor is calculated as

$$\sqrt{R^2 + (2\omega L)^2} = \frac{10}{2\omega C_e}$$

or

$$C_e = \frac{10}{4\pi f\sqrt{R^2 + (4\pi fL)^2}} = 326\ \mu\text{F}$$

From Eq. (2-47) the ripple factor is defined as

$$\text{RF} = \frac{V_{ac}}{V_{dc}} = \frac{V_{o2}}{V_{dc}} = \frac{V_2}{V_{dc}}\frac{1}{(4\pi f)^2 L_e C_e - 1} = \frac{\sqrt{2}}{3}\frac{1}{[(4\pi f)^2 L_e C_e - 1]} = 0.1$$

or $(4\pi f)^2 L_e C_e - 1 = 4.714$ and $L_e = 30.83$ mH.

Example 2-16

An *LC* input filter as shown in Fig. 2-21 is used to reduce the input current harmonics in a single-phase full-wave rectifier of Fig. 2-16a. The load current is riple free and its average value is I_a. If the supply frequency is $f = 60$ Hz (or 377 rad/s), determine the resonant frequency of the filter so that the total input harmonic current is reduced to 1% of the fundamental component.

Solution The equivalent circuit for the nth harmonic component is shown in Fig. 2-25. The rms value of the nth harmonic current appearing in the supply is obtained by using the current-divider rule,

$$I_{sn} = \frac{1/(n\omega C_i)}{(n\omega L_i) - 1/(n\omega C_i)} I_n = \frac{1}{(n\omega)^2 L_i C_i - 1} I_n \tag{2-93}$$

where I_n is the rms value of the nth harmonic current. The total amount of harmonic current is

$$I_h = \left(\sum_{n=2,3,\ldots}^{\infty} I_{sn}^2\right)^{1/2} \tag{2-94}$$

and the harmonic factor of input current (with the filter) is

$$r = \frac{I_h}{I_{s1}} = \left[\sum_{n=2,3,\ldots}^{\infty}\left(\frac{I_{sn}}{I_1}\right)^2\right]^{1/2} \tag{2-95}$$

From Eq. (2-68), $I_1 = 4I_a/\sqrt{2}\,\pi$ and $I_n = 4I_a/(\sqrt{2}\,n\pi)$ for $n = 3, 5, 7, \ldots$. From Eqs. (2-93) and (2-95) we get

$$r^2 = \sum_{n=3,5,7,\ldots}^{\infty}\left(\frac{I_{sn}}{I_1}\right)^2 = \sum_{n=3,5,7,\ldots}^{\infty}\frac{1}{n^2[(n\omega)^2 L_i C_i - 1]^2}$$

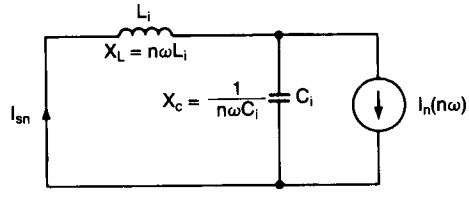


Figure 2-25 Equivalent circuit for harmonic current.

This can be solved for the value of L_iC_i. To simplify the calculations, if we consider only the third harmonic, $3[(3 \times 2 \times \pi \times 60)^2 L_iC_i - 1] = 1/0.01 = 100$ or $L_iC_i = 26.84 \times 10^{-6}$ and the filter frequency is $1/\sqrt{L_iC_i} = 193.02$ rad/s.

Note. The ac filter is generally tuned to the harmonic frequency involved, but it requires a careful design to avoid the possibility of resonance with the power system. The resonant frequency of the third harmonic current is $377 \times 3 = 1131$ rad/s.

2-12 EFFECTS OF SOURCE AND LOAD INDUCTANCES

In the derivations of the output voltages and the performance criteria of rectifiers, it was assumed that the source has no inductances and resistances. But in a practical transformer and supply, these are always present and the performances of rectifiers are slightly changed. The effect of the source inductance, which is more significant than that of resistance, can be explained with reference to Fig. 2-26a.

The diode with the most positive voltage will conduct. Let us consider the point $\omega t = \pi$ where voltages v_{ac} and v_{bc} are equal as shown in Fig. 2-26b. The current I_{dc} is still flowing through the diode D_1. Due to the inductance L_1, the current cannot fall to zero immediately and the transfer of current cannot be on an instantaneous basis. The current i_{d1} decreases, resulting in an induced voltage across L_1 of $+v_{L1}$ and the output voltage becomes $v_L = v_{ac} + v_{L1}$. At the same time the current through D_3, i_{d3} increases from zero, inducing an equal voltage across L_2 of $-v_{L2}$ and the output voltage becomes $v_L = v_{bc} - v_{L2}$. The result is that the anode voltages of diodes D_1 and D_3 are equal; and both diodes conduct for a certain period which is called *commutation (or overlap) angle*, α. This transfer of current from one diode to another is called *commutation*. The reactance corresponding to the inductance is known as *commutating reactance*.

The effect of this overlap is to reduce the average output voltage of converters. The voltage across L_2 is

$$v_{L2} = L_2 \frac{di}{dt} \tag{2-96}$$

Assuming a linear rise of the current from 0 to I_{dc} (or a constant di/dt), we can write Eq. (2-96) as

$$v_{L2}\,\Delta t = L_2\,\Delta i \tag{2-97}$$

and this is repeated six times for a three-phase bridge rectifier. Using Eq. (2-97), the average voltage reduction due to the commutating inductances is

$$\begin{aligned} V_x &= \frac{1}{T} 2(v_{L1} + v_{L2} + v_{L3})\,\Delta t = 2f(L_1 + L_2 + L_3)\,\Delta i \\ &= 2f(L_1 + L_2 + L_3)I_{dc} \end{aligned} \tag{2-98}$$

If all the inductances are equal and $L_c = L_1 = L_2 = L_3$, Eq. (2-98) becomes

$$V_x = 6fL_cI_{dc} \tag{2-99}$$

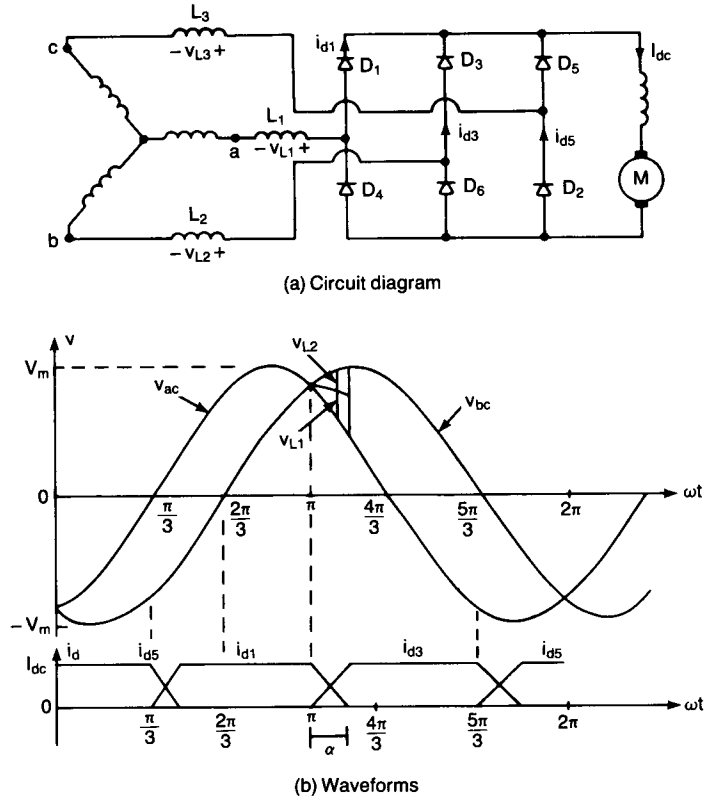


Figure 2-26 Three-phase bridge rectifier with source inductances.

Example 2-17

A three-phase bridge rectifier is supplied from a Y-connected 208-V 60-Hz supply. The average output voltage is 170 V. The load current is 60 A and has negligible ripple. Calculate the percentage reduction of output voltage due to commutation if the line inductance per phase is 0.5 mH.

Solution $L_c = 0.5$ mH, $V_s = 208/\sqrt{3} = 120$ V, $f = 60$ Hz, $I_{dc} = 60$ A, and $V_m = \sqrt{2} \times 120 = 169.7$ V. From Eq. (2-77), $V_{dc} = 1.6542 \times 169.7 = 280.7$ V. Equation (2-99) gives the output voltage reduction,

$$V_x = 6 \times 60 \times 0.5 \times 10^{-3} = 10.8 \text{ V or } 10.8 \times \frac{100}{280.7} = 3.85\%$$

and the effective output voltage is $(280.7 - 10.8) = 266.9$ V.

SUMMARY

In this chapter we have seen the applications of power semiconductor diodes in freewheeling action, recovering energy from inductive loads and in conversion of signal from ac to dc. There are different types of rectifiers depending on the

connections of diodes and input transformer. The performance parameters of rectifiers are defined and it has been shown that the performances of rectifiers vary with their types. The rectifiers generate harmonics into the load and the supply line; and these harmonics can be reduced by filters. The performances of the rectifiers are also influenced by the source and load inductances.

REFERENCES

1. J. Schaefer, *Rectifier Circuits—Theory and Design*, New York: John Wiley & Sons, Inc., 1975.
2. R. W. Lee, *Power Converter Handbook—Theory Design and Application*, Peterborough, Ont.: Canadian General Electric, 1979.

REVIEW QUESTIONS

2–1. What is the time constant of an *RL* circuit?
2–2. What is the time constant of an *RC* circuit?
2–3. What is the resonant frequency of an *LC* circuit?
2–4. What is the damping factor of an *RLC* circuit?
2–5. What is the difference between the resonant frequency and the ringing frequency of an *RLC* circuit?
2–6. What is a freewheeling diode, and what is its purpose?
2–7. What is the trapped energy of an inductor?
2–8. How is the trapped energy recovered by a diode?
2–9. What is the turns ratio of a transformer?
2–10. What is a rectifier? What is the difference between a rectifier and a converter?
2–11. What is the blocking condition of a diode?
2–12. What are the performance parameters of a rectifier?
2–13. What is the significance of the form factor of a rectifier?
2–14. What is the significance of the ripple factor of a rectifier?
2–15. What is the efficiency of rectification?
2–16. What is the significance of the transformer utilization factor?
2–17. What is the displacement factor?
2–18. What is the input power factor?
2–19. What is the harmonic factor?
2–20. What is the difference between a half-wave and a full-wave rectifier?
2–21. What is the dc output voltage of a single-phase half-wave rectifier?
2–22. What is the dc output voltage of a single-phase full-wave rectifier?
2–23. What is the fundamental frequency of the output voltage of a single-phase full-wave rectifier?

2–24. What are the advantages of a three-phase rectifier over a single-phase rectifier?
2–25. What are the disadvantages of a multiphase half-wave rectifier?
2–26. What are the advantages of a three-phase bridge rectifier over a six-phase star rectifier?
2–27. What are the purposes of filters in rectifier circuits?
2–28. What are the differences between ac and dc filters?
2–29. What are the effects of source inductances on the output voltage of a rectifier?
2–30. What are the effects of load inductances on the rectifier output?
2–31. What is a commutation?
2–32. What is the commutation angle of a rectifier?

PROBLEMS

2–1. The current waveforms of a capacitor are shown in Fig. P2-1. Determine the average, rms, and peak current ratings of the capacitor.

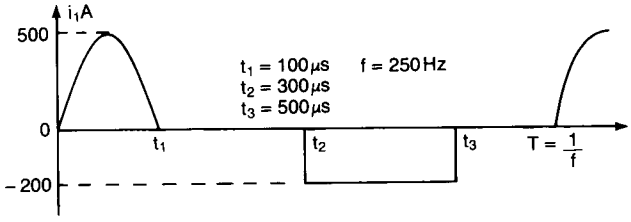


Figure P2-1

2–2. The waveforms of the current flowing through a diode are shown in Fig. P2-2. Determine the average, rms, and peak current ratings of the diode.

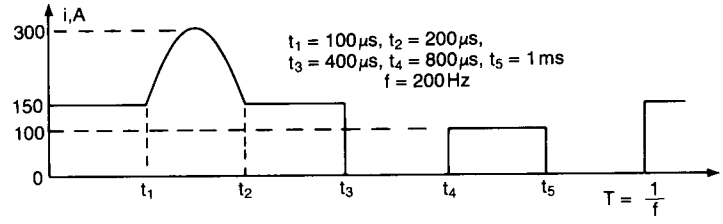


Figure P2-2

2–3. A diode circuit is shown in Fig. P2-3 and $R = 22\ \Omega$ and $C = 10\ \mu$F. If the switch S_1 is closed at $t = 0$, determine the expression for the voltage across the capacitor and the energy lost in the circuit.

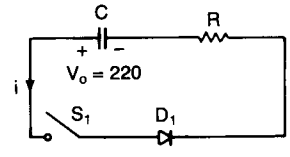
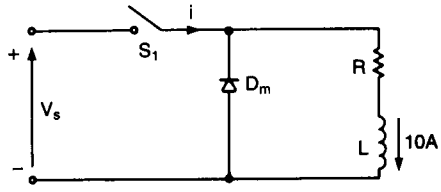


Figure P2-3

2–4. A diode circuit is shown in Fig. P2-4 with $R = 10\ \Omega$, $L = 5$ mH, and $V_s = 220$ V. If a load current of 10 A is flowing through the freewheeling diode D_m and the switch S_1 is closed at $t = 0$, determine the expression for the current through the switch.



re P2-4

2–5. If the inductor of the circuit in Fig. 2-4 has an initial current of I_0, determine the expression for the voltage across the capacitor.

2–6. If the switch S_1 of Fig. P2-6 is closed at $t = 0$, determine the expression for (**a**) current flowing through the switch, $i(t)$; and (**b**) the rate of rise of the current, di/dt. (**c**) Draw sketches of $i(t)$ and di/dt. (**d**) What is the value of initial di/dt? For Fig. P2-6d, find the initial di/dt only.

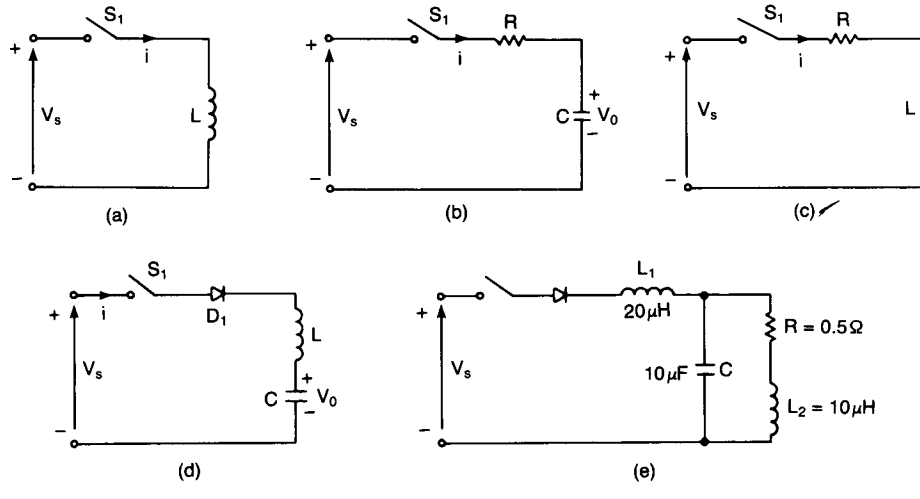


Figure P2-6

2–7. In the second-order circuit of Fig. 2-6, the source voltage, $V_s = 220$ V, inductance, $L = 5$ mH, capacitance, $C = 10\ \mu$F, and resistance, $R = 22\ \Omega$. The initial voltage of the capacitor is $V_0 = 50$ V. If the switch is closed at $t = 0$, determine (**a**) an expression for the current; and (**b**) the conduction time of the diode. (**c**) Draw a sketch of $i(t)$.

2–8. For the energy recovery circuit of Fig. 2-10a, the magnetizing inductance of the transformer is $L_m = 150\ \mu$H, $N_1 = 10$, and $N_2 = 200$. The leakage inductances and resistances of the transformer are negligible. The source voltage is $V_s = 200$ V and there is no initial current in the circuit. If switch S_1 is closed for a time $t_1 = 100\ \mu$s and is then opened, (**a**) determine the reverse voltage of diode D_1; (**b**) calculate the peak value of the primary current; (**c**) calculate the peak value of secondary current;

(**d**) determine the time for which diode D_1 conducts; and (**e**) determine the energy supplied by the source.

2–9. A single-phase bridge rectifier has a purely resistive load, $R = 10\ \Omega$, the peak value of the supply voltage, $V_m = 170$ V, and the supply frequency, $f = 60$ Hz. Determine the average output voltage of the rectifier if the source inductance is negligible.

2–10. Repeat Prob. 2-9 if the source inductance per phase (including transformer leakage inductance) is $L_c = 0.5$ mH.

2–11. A six-phase star rectifier has a purely resistive load of $R = 10\ \Omega$, the peak value of the supply voltage, $V_m = 170$ V, and the supply frequency $f = 60$ Hz. Determine the average output voltage of the rectifier if the source inductance is neglibile.

2–12. Repeat Prob. 2-11 if the source inductance per phase (including the transformer leakage inductance) is $L_c = 0.5$ mH.

2–13. A three-phase bridge rectifier has a purely resistive load of $R = 100\ \Omega$ and is supplied from a 280-V 60-Hz supply. The primary and secondary of the input transformer are connected in wye. Determine the average output voltage of the rectifier if the source inductances are negligible.

2–14. Repeat Prob. 2-13 if the source inductance per phase (including transformer leakage inductance) is $L_c = 0.5$ mH.

2–15. The single-phase bridge rectifier of Fig. 2-15 is required to supply an average voltage of $V_{dc} = 400$ V to a resistive load of $R = 10\ \Omega$. Determine the voltage and current ratings of diodes and transformer.

2–16. A three-phase bridge rectifier is required to supply an average voltage of $V_{dc} = 750$ V at a ripple-free current of $I_{dc} = 9000$ A. The primary and secondary of the transformer are connected in wye. Determine the voltage and current ratings of diodes and transformer.

2–17. The single-phase rectifier of Fig. 2-14a has an RL load. If the peak value of the input voltage is $V_m = 170$ V, the supply frequency, $f = 60$ Hz, and the load resistance, $R = 15\ \Omega$, determine the value of load inductance, L, to limit the load current harmonic to 4% of the average value, I_{dc}.

2–18. The three-phase star rectifier of Fig. 2-17a has an RL load. If the secondary peak voltage per phase is $V_m = 170$ V at 60 Hz, and the load resistance is $R = 15\ \Omega$, determine the value of load inductance, L, to limit the load current harmonics to 2% of the average value, I_{dc}.

2–19. The single-phase rectifier of Fig. 2-14a has a resistive load of R, and a capacitor C is connected across the load. The average value of the load current is I_{dc}. Assuming that the charging time of the capacitor is negligible compared to the discharging time, determine the rms value of the output voltage harmonics, V_{ac}.

2–20. The LC filter shown in Fig. 2-20c is used to reduce the ripple content of the output voltage for a six-phase star rectifier. The load resistance, $R = 20\ \Omega$, load inductance, $L = 5$ mH, and source frequency is 60 Hz. Determine the values of the filter parameters L_1 and C so that the ripple factor of the output voltage is 5%.

2–21. The three-phase bridge rectifier of Fig. 2-18a has an RL load and is supplied from a Y-connected supply. (**a**) Use the method of Fourier series to obtain expressions for the output voltage, $v_L(t)$, and load current, $i_L(t)$. (**b**) If peak phase voltage, $V_m = 170$ V at 60 Hz and the load resistance, $R = 200\ \Omega$, determine the value of load inductance, L, to limit the ripple current to 2% of the average value, I_{dc}.

2–22. The single-phase half-wave rectifier of Fig. 2-13a has a freewheeling diode and a

ripple-free average load current of I_a. (**a**) Draw the waveforms for the currents in D_1, D_m, and the transformer prmary; (**b**) express the primary current in Fourier series; and (**c**) determine the input power factor, PF, and harmonic factor of the input current, HF, at the rectifier input. Assume a transformer turns ratio of unity.

2–23. The single-phase full-wave rectifier of Fig. 2-14a has a ripple-free average load current of I_a. (**a**) Draw the waveforms for currents in D_1, D_2, and transformer primary; (**b**) express the primary current in Fourier series; and (**c**) determine the input power factor, PF, and harmonic factor of the input current, HF, at the rectifier input. Assume a transformer turns ratio of unity.

2–24. The multiphase star rectifier of Fig. 2-17a has three pulses and supplies a ripple-free average load current of I_a. The primary and secondary of the transformer are connected in wye. Assume a transformer turns ratio of unity. (**a**) Draw the waveforms for currents in D_1, D_2, D_3, and transformer primary; (**b**) express the primary current in Fourier series; and (**c**) determine the input power factor, PF, and harmonic factor of input current, HF.

2–25. Repeat Prob. 2-24 if the primary of the transformer is connected in delta and secondary in wye.

2–26. The multiphase star rectifier of Fig. 2-17a has six pulses and supplies a ripple-free average load current of I_a. The primary of the transformer is connected in delta and secondary in wye. Assume a transformer turns ratio of unity. (**a**) Draw the waveforms for currents in D_1, D_2, D_3, and transformer primary; (**b**) express the primary current in Fourier series; and (**c**) determine the input power factor, PF, and harmonic factor of the input current, HF.

2–27. The three-phase bridge rectifier of Fig. 2-18a supplies a ripple-free load current of I_a. The primary and secondary of the transformer are connected in wye. Assume a transformer turns ratio of unity. (**a**) Draw the waveforms for currents in D_1, D_3, D_5 and the secondary phase current of the transformer; (**b**) express the secondary phase current in Fourier series; and (**c**) determine the input power factor, PF, and harmonic factor of the input current, HF.

2–28. Repeat Prob. 2-27 if the primary of the transformer is connected in delta and secondary in wye.

2–29. Repeat Prob. 2-27 if the primary and secondary of the transformer are connected in delta.

2–30. A typical diode circuit is shown in Fig. P2-30, where the load current is flowing through diode D_m. If switch S_1 is closed at a time $t = 0$, determine the (**a**) expressions for $v_c(t)$, $i_c(t)$, and $i_d(t)$; (**b**) time t_1 when the diode D_1 stops conducting; (**c**) time t_q when the voltage across the capacitor becomes zero; and (**d**) time required for capacitor to recharge to the supply voltage, V_s.

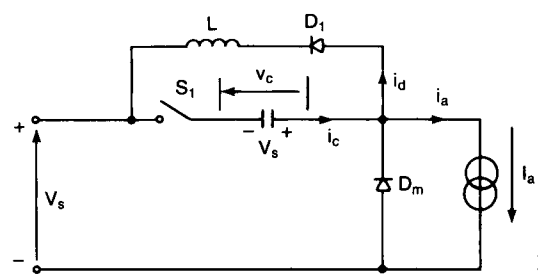


Figure P2-30

3

Thyristor Commutation Techniques

3-1 INTRODUCTION

A thyristor is normally switched on by applying a pulse of gate signal. When a thyristor is in a conduction mode, its voltage drop is small, ranging from 0.25 to 2 V, and is neglected in this chapter. Once the thyristor is turned on and the output requirements are satisfied, it is usually necessary to turn it off. The turn-off means that the forward conduction of the thyristor has ceased and the reapplication of a positive voltage to the anode will not cause current flow without applying the gate signal. *Commutation* is the process of turning off a thyristor, and it normally causes transfer of current flow to other parts of the circuit. A commutation circuit normally uses additional components to accomplish the turn-off. With the developments of thyristors, many commutation circuits have been developed and the objective of all the circuits is to reduce the turn-off process of the thyristors.

There are many techniques to commutate a thyristor. However, these can be broadly classified into two types:

1. Natural commutation
2. Forced commutation

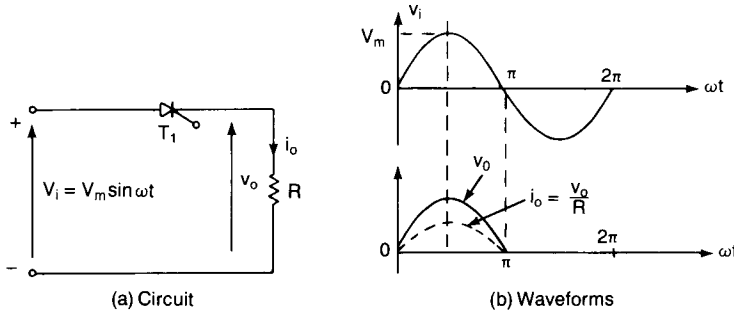


Figure 3-1 Thyristor with natural commutation.

3-2 NATURAL COMMUTATION

If the source (or input) voltage is ac, the thyristor current goes through a natural zero, and a reverse voltage appears across the thyristor. The device is then automatically turned off due to the natural behavior of the source voltage. This is known as *natural commutation* or *line commutation*. In practice, the thyristor is triggered synchronously with the zero crossing of the positive input voltage in every cycle in order to provide a continuous control of power. This type of commutation is applied in ac voltage controllers, phase-controlled rectifiers, and cycloconverters. Figure 3-1a shows the circuit arrangement for natural commutation and Fig. 3-1b shows the voltage and current waveforms with a delay angle, $\alpha = 0$. The *delay angle* α is defined as the angle between the zero crossing of the input voltage and the instant the thyristor is fired.

3-3 FORCED COMMUTATION

In some thyristor circuits, the input voltage is dc and the forward current of the thyristor is forced to zero by an additional circuitry called *commutation circuit* to turn off the thyristor. This technique is called *forced commutation* and normally applied in dc–dc converters (choppers) and dc–ac converters (inverters). The forced commutation of a thyristor can be achieved by seven ways and can be classified as:

1. Self-commutation
2. Impulse commutation
3. Resonant pulse commutation
4. Complementary commutation
5. External pulse commutation
6. Load-side commutation
7. Line-side commutation

This classification of forced commutations is based on the arrangement of the commutation circuit components and the manner in which the current of a thyristor is forced to zero. The commutation circuit normally consists of a capacitor, an inductor, and one or more thyristor(s) and/or diode(s).

3.3.1 Self-Commutation

In this type of commutation, a thyristor is turned off due to the natural characteristics of the circuit. Let us consider the circuit in Fig. 3-2a with the assumption that the capacitor is initially uncharged. When thyristor T_1 is switched on, the capacitor charging current is given by

$$V_s = v_L + v_c = L\frac{di}{dt} + \frac{1}{C}\int i\,dt + v_c\,(t = 0) \tag{3-1}$$

With initial condition $v_c(t = 0) = 0$ and $i(t = 0) = 0$, the solution of Eq. (3-1) (which is derived in Appendix D.3) gives the charging current as

$$i(t) = V_s\sqrt{\frac{C}{L}}\sin \omega_m t \tag{3-2}$$

and the capacitor voltage as

$$v_c(t) = V_s(1 - \cos \omega_m t) \tag{3-3}$$

where $\omega_m = 1\sqrt{LC}$. After time $t = t_0 = \sqrt{LC}$, the charging current becomes zero and thyristor T_1 is switched off itself. Once thyristor T_1 is fired, there is a delay of t_0 seconds before T_1 is turned off and t_0 may be called as the *commutation time* of the circuit. This method of turning off a thyristor is called *self-commutation* and thyristor T_1 is said to be self-commutated. When the circuit current falls to zero, the capacitor is charged to $2V_s$. The waveforms are shown in Fig. 3-2b.

Figure 3-3a shows a typical circuit where the capacitor has an initial voltage of V_0. When thyristor T_1 is fired, the current that will flow through the circuit is given by

$$L\frac{di}{dt} + \frac{1}{C}\int i\,dt + v_c(t = 0) = 0 \tag{3-4}$$

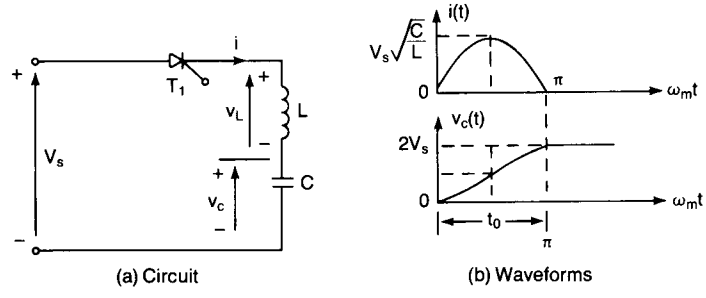


Figure 3-2 Self-commutation circuit.

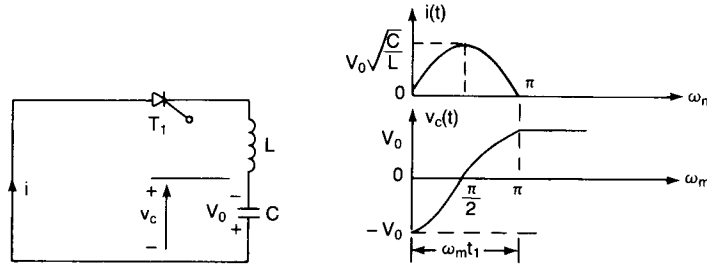


Figure 3-3 Self-commutation circuit.

With initial voltage $v_c\,(t = 0) = -V_0$ and $i(t = 0) = 0$, Eq. (3-4) gives the capacitor current as

$$i(t) = V_0 \sqrt{\frac{C}{L}} \sin \omega_m t \tag{3-5}$$

and the capacitor voltage as

$$v_c(t) = -V_0 \cos \omega_m t \tag{3-6}$$

After time $t = t_r = t_0 = \pi \sqrt{LC}$, the current becomes zero and the capacitor voltage is reversed to V_0. t_r is called the *reversing time*. The waveforms are shown in Fig. 3-3b.

Example 3-1

A typical thyristor circuit is shown in Fig. 3-4. If thyristor T_1 is switched on at $t = 0$, determine the conduction time of thyristor T_1 and the capacitor voltage after T_1 is turned off. The circuit parameters are $L = 10$ μH, $C = 50$ μF, and $V_s = 200$ V. The inductor carries an initial current of $I_m = 250$ A.

Solution The capacitor current is expressed as

$$L \frac{di}{dt} + \frac{1}{C} \int i\, dt + v_c\,(t = 0) = V_s$$

with initial current $i\,(t = 0) = I_m$ and $v_c\,(t = 0) = V_0 = V_s$. The voltage and current of the capacitor (from Appendix D) are

$$i(t) = I_m \cos \omega_m t$$

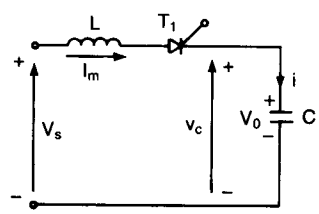


Figure 3-4 Self-commutated thyristor circuit.

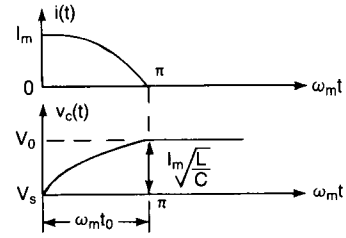


Figure 3-5 Current and voltage waveforms.

and

$$v_c(t) = I_m \sqrt{\frac{L}{C}} \sin \omega_m t + V_s$$

At $t = t_0 = 0.5 \times \pi\sqrt{LC}$, the commutation period ends and the capacitor voltage becomes

$$\begin{aligned} v_c\,(t = t_0) &= V_0 = V_s + I_m \sqrt{\frac{L}{C}} \\ &= V_s + \Delta V \end{aligned} \tag{3-7}$$

where ΔV is the overvoltage of the capacitor and depends on the initial current of the inductor, I_m, which is, in most cases, the load current. Figure 3-4 shows a typical equivalent circuit during the commutation process. For $C = 50$ μF, $L = 10$ μH, $V_s = 200$ V, and $I_m = 250$ A, $\Delta V = 111.8$ V, $V_0 = 200 + 111.8 = 311.8$ V, and $t_0 = 35.12$ μs. The current and voltage waveforms are shown in Fig. 3-5.

3-2.2 Impulse Commutation

An impulse-commutated circuit is shown in Fig. 3-6. It is assumed that the capacitor is initially charged to a voltage of $-V_0$ with the polarity shown.

Let us assume that thyristor T_1 is initially conducting and carrying a load current of I_m. When the auxiliary thyristor T_2 is fired, thyristor T_1 is reversed biased by the capacitor voltage. The current thorugh thyristor T_1 will cease to flow and the capacitor would carry the load current. The capacitor will discharge from $-V_0$ to zero and then charge to the dc input voltage, V_s, when the capacitor

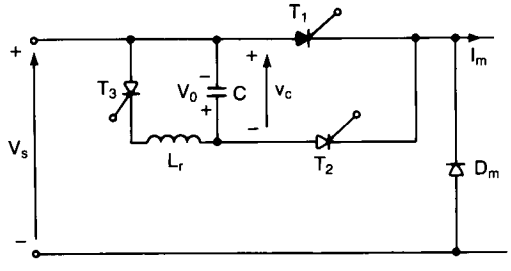


Figure 3-6 Impulse-commutated circuit.

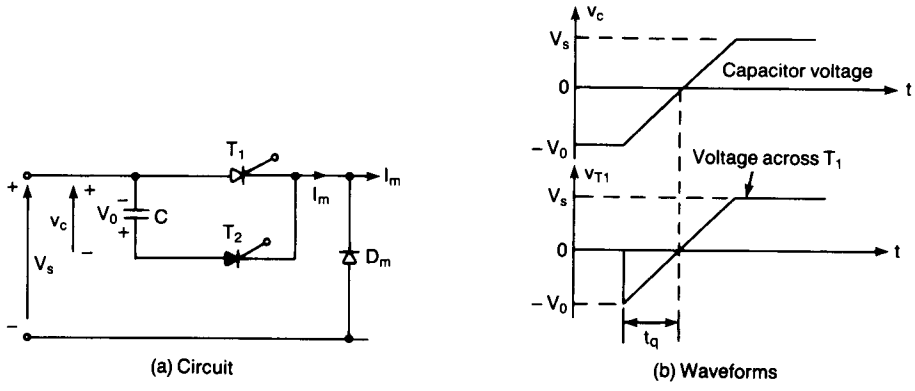


Figure 3-7 Equivalent circuit and waveforms.

current falls to zero and thyristor T_2 turns off. The charge reversal of the capacitor from V_0 ($= V_s$) to $-V_0$ is then done by firing thyristor T_3. Thyristor T_3 is self-commutated similar to the circuit in Fig. 3-3.

The equivalent circuit during the commutation period is shown in Fig. 3-7a. The thyristor and capacitor voltages are shown in Fig. 3-7b. The time required for the capacitor to discharge from $-V_0$ to zero is called the *circuit turn-off time*, t_q, and must be greater than the turn-off time of the thyristor, t_{off}. t_q is also called the *available turn-off time*. The discharging time will depend on the load current and assuming a constant load current of I_m, t_q is given by

$$V_0 = \frac{1}{C}\int_0^{t_q} I_m\, dt = \frac{I_m t_q}{C}$$

or

$$t_q = \frac{V_0 C}{I_m} \tag{3-8}$$

Since a reverse voltage of V_0 is applied across thyristor T_1 immediately after firing of thyristor T_2, this is known as *voltage commutation*. Due to the use of auxiliary thyristor T_2, this type of commutation is also called *auxiliary commutation*. Thyristor T_1 is sometimes known as the *main thyristor* because it carries the load current.

It can be noticed from Eq. (3-8) that the circuit turn-off time is inversely proportional to the load current; and at a very light load (or low load current) the turn-off time will be large. On the other hand, at a high load current the turn-off time will be small. In an ideal commutation circuit, the turn-off time should be independent of the load current in order to guarantee the commutation of thyristor T_1. The discharging of the capacitor can be accelerated by connecting a diode D_1 and an inductor L_1 across the main thyristor as shown in Fig. 3-8; and this is illustrated in Example 3-3.

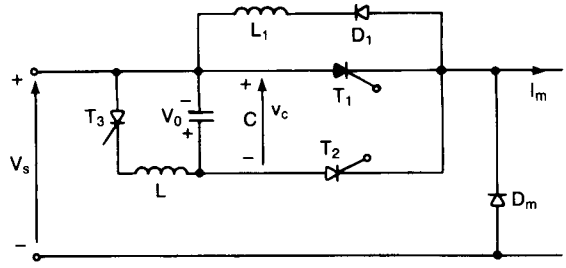


Figure 3-8 Impulse-commutated circuit with accelerated recharging.

Example 3-2

An impulse-commutated thyristor circuit is shown in Fig. 3-9. Determine the available turn-off time of the circuit if $V_s = 200$ V, $R = 10\ \Omega$, $C = 5\ \mu$F, and $V_0 = V_s$.

Solution The equivalent circuit during the commutation period is shown in Fig. 3-10. The voltage across the commutation capacitor is given by

$$v_c = \frac{1}{C}\int i\,dt + v_c\,(t = 0)$$

$$V_s = v_c + Ri$$

The solution of these equations with initial voltage $v_c\,(t = 0) = -V_0 = -V_s$ give the capacitor voltage as

$$v_c(t) = V_s(1 - 2e^{-t/RC})$$

The turn-off time, t_q, which can be found if the condition $v_c\,(t = t_q) = 0$ is satisfied, is solved as

$$t_q = RC \ln (2)$$

For $R = 10\ \Omega$ and $C = 5\ \mu$F, $t_q = 34.7\ \mu$s.

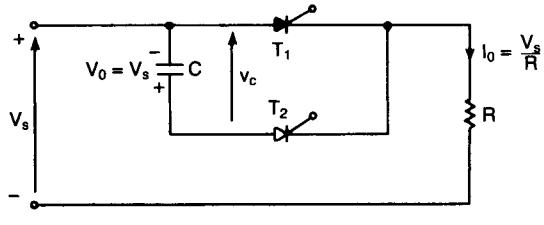


Figure 3-9 Impulse-commutated circuit with resistive load.

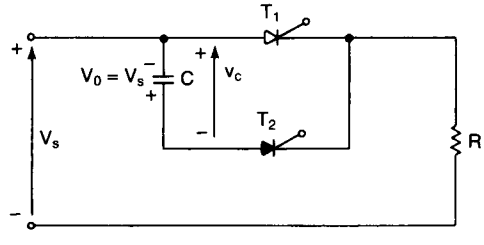


Figure 3-10 Equivalent circuit for Example 3-2.

Example 3-3

The commutation circuit in Fig. 3-8 has a capacitance $C = 20\ \mu F$ and recharging inductor $L_1 = 25\ \mu H$. The initial capacitor voltage is equal to the input voltage, $V_0 = V_s = 200$ V. If the load current, I_m, varries between 50 and 200 A, determine the variations of the circuit turn-off time, t_q.

Solution The equivalent circuit during the commutation period is shown in Fig. 3-11. The defining equations are

$$i_c = i + I_m$$

$$v_c = \frac{1}{C}\int i_c\, dt + v_c\,(t = 0)$$

$$= -L_1 \frac{di_1}{dt} = -L_1 \frac{di_c}{dt}$$

The initial conditions $i_c\,(t = 0) = I_m$ and $v_c\,(t = 0) = -V_o = -V_s$. The solutions of these equations yield the capacitor current (from Appendix D) as

$$i_c(t) = V_0 \sqrt{\frac{C}{L_1}} \sin \omega_1 t + I_m \cos \omega_1 t$$

The voltage across the capacitor is expressed as

$$v_c(t) = I_m \sqrt{\frac{L_1}{C}} \sin \omega_1 t - V_0 \cos \omega_1 t$$

where $\omega_1 = 1/\sqrt{L_1 C}$. The available turn-off time or circuit turn-off time is obtained from the condition $v_c\,(t = t_q) = 0$ and is solved as

$$t_q = \sqrt{CL_1} \tan^{-1}\left(\frac{V_0}{I_m}\sqrt{\frac{C}{L_1}}\right) \tag{3-9}$$

For $C = 20\ \mu F$, $L_1 = 25\ \mu H$, $V_0 = 200$ V, and $I_m = 50$ A, $t_q = 29.0\ \mu s$. For $C = 20\ \mu F$, $L_1 = 25\ \mu H$, $V_0 = 200$ V, and $I_m = 100$ A, $t_q = 23.7.\ \mu s$. For $C = 20\ \mu F$, $L_1 = 25\ \mu H$, $V_0 = 200$ V, and $I_m = 200$ A, $t_q = 16.3\ \mu s$.

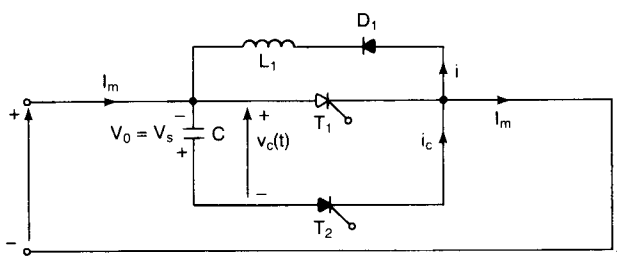


Figure 3-11 Equivalent circuit for Example 3-3.

Note. As the load current increases from 50 A to 200 A, the turn-off time decreases from 29 μs to 16.3 μs. The use of an extra diode makes the turn-off time less dependent on the load.

3-3.3 Resonant Pulse Commutation

The resonant pulse commutation can be explained with Fig. 3-12a. Figure 3-12b shows the waveforms for the capacitor current and voltage. The capacitor is initially charged with the polarity as shown and thyristor T_1 is in the conduction mode carrying a load current of I_m.

When commutation thyristor T_2 is fired, a resonant circuit is formed by L, C, T_1 and T_2. The resonant current can be derived as

$$\begin{aligned} i(t) &= V_0 \sqrt{\frac{C}{L}} \sin \omega_m t \\ &= I_p \sin \omega_m t \end{aligned} \tag{3-10}$$

and the capacitor voltage is

$$v_c(t) = -V_0 \cos \omega_m t \tag{3-12}$$

where I_p is the peak permissible value of resonant current.

Due to the resonant current, the forward current of thyristor T_1 is reduced to zero at $t = t_1$, when the resonant current equals the load current, I_m. The time t_1 must satisfy the condition $i\ (t = t_1) = I_m$ and is found as

$$t_1 = \sqrt{LC} \sin^{-1} \left(\frac{I_m}{V_0} \sqrt{\frac{L}{C}} \right) \tag{3-13}$$

The corresponding value of the capacitor voltage is

$$v_c\ (t = t_1) = -V_1 = -V_0 \cos \omega_m t_1 \tag{3-14}$$

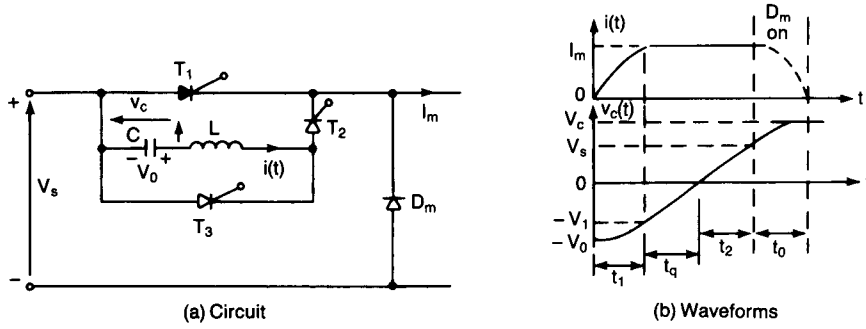


Figure 3-12 Resonant pulse commutation.

The current through thyristor T_1 will cease to flow and the capacitor will recharge at a rate determined by the load current I_m. The capacitor will discharge from $-V_1$ to zero and its voltage will then rise to the dc source voltage V_s, in which case diode D_m starts conducting and a situation similar to the circuit in Fig. 3-4 exists with a time duration of t_0. This is shown in Fig. 3-12b. The energy stored in inductor L due to the load current I_m is transferred to the capacitor, causing it to be overcharged, and the capacitor voltage V_0 can be calculated from Eq. (3-7). The capacitor voltage is reversed from V_c ($= V_0$) to $-V_0$ by firing T_3. T_3 is self-commutated similar to the circuit in Fig. 3-3.

The equivalent circuit for the charging period is similar to the one in Fig. 3-7a. From Eq. (3-8), the circuit turn-off time is

$$t_q = \frac{CV_1}{I_m} \tag{3-15}$$

Let us define a parameter x which is the ratio of the peak resonant current to the load current. Then

$$x = \frac{I_p}{I_m} = \frac{V_0}{I_m}\sqrt{\frac{C}{L}} \tag{3-16}$$

To reduce the forward current of T_1 to zero, the value of x must be greater than 1.0. In practice, the value of L and C are chosen such that $x = 1.5$. The value of t_1 in Eq. (3-13) is normally small and $V_1 \approx V_0$. The value of t_q obtained from Eq. (3-15) should be approximately equal to that obtained from Eq. (3-8).

Due to the fact that a resonant pulse of current is used to reduce the forward current of thyristor T_1 to zero, this type of commutation is also known as *current commutation*. It can be noticed from Eq. (3-15) that the circuit turn-off time is also dependent on the load current. The discharging of the capacitor voltage can be accelerated by connecting a diode D_2 as shown in Fig. 3-13a. However, once the current of thyristor T_1 is reduced to zero, the reverse voltage appearing across T_1 is the forward voltage drop of diode D_2, which is small. This will make the

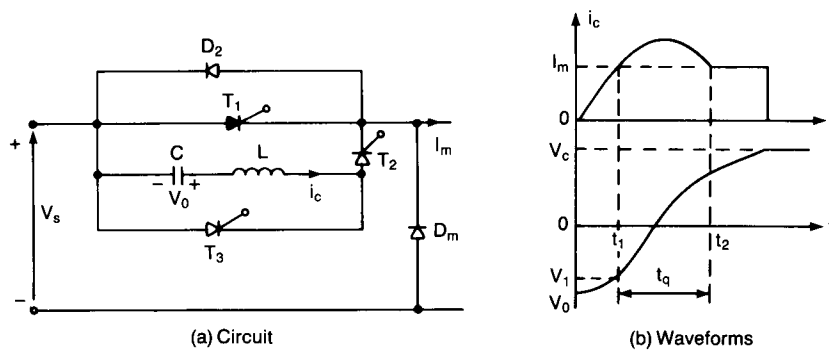


Figure 3-13 Resonant pulse commutation with an accelerating diode.

thyristor's recovery process slow and it would be necessary to provide longer reverse bias time than that if the diode D_2 were not present. The capacitor current, $i_c(t)$, and the capacitor voltage, $v_c(t)$, are shown in Fig. 3-13b.

Example 3-4

The resonant pulse commutation circuit in Fig. 3-12a has capacitance, $C = 30\ \mu F$ and inductance, $L = 4\ \mu H$. The initial capacitor voltage is $V_0 = 200$ V. Determine the circuit turn-off time, t_q, if the load current, I_m, is (a) 250 A, and (b) 50 A.

Solution (a) $I_m = 250$ A. From Eq. (3-13),

$$t_1 = \sqrt{4 \times 30}\ \sin^{-1}\left(\frac{250}{200}\sqrt{\frac{4}{30}}\right) = 5.192\ \mu s$$

$$\omega_m = \frac{1}{\sqrt{LC}} = 91{,}287.1\ \text{rad/s} \quad \text{and} \quad \omega_m t_1 = 0.474\ \text{rad}$$

From Eq. (3-14), $V_1 = 200 \cos(0.474) = 177.95$ V and from Eq. (3-15),

$$t_q = 177.95 \times \frac{30}{250} = 21.35\ \mu s$$

(b) $I_m = 50$ A.

$$t_1 = \sqrt{4 \times 30}\ \sin^{-1}\left(\frac{50}{200}\sqrt{\frac{4}{30}}\right) = 1.0095\ \mu s$$

$$\omega_m = \frac{1}{\sqrt{LC}} = 91{,}287.1\ \text{rad/s} \quad \text{and} \quad \omega_m t_1 = 0.0914\ \text{rad}$$

$$V_1 = 200 \cos(0.0914) = 199.16\ \text{V}$$

$$t_q = 199.16 \times \frac{30}{250} = 119.5\ \mu s$$

Example 3-5

Repeat Example 3-4 if an antiparallel diode D_2 is connected across thyristor T_1 as shown in Fig. 3-13a.

Solution (a) $I_m = 250$ A. When thyristor T_2 is fired, a resonant pulse of current flows through the capacitor and the forward current of thyristor T_1 is reduced to zero at time $t = t_1 = 5.192\ \mu s$. The capacitor current $i_c(t)$ at this time is equal to the load current $I_m = 250$ A. After the current of T_1 is reduced to zero, the resonant oscillation continues through diode D_2 until the resonant current falls back to the load current level at time t_2. This is shown in Fig. 3-13b.

$$t_2 = \pi\sqrt{LC} - t_1 = \pi\sqrt{4 \times 30} - 5.192 = 29.22\ \mu s$$

$$\omega_m = 91{,}287.1\ \text{rad/s} \quad \text{and} \quad \omega_m t_2 = 2.667\ \text{rad}$$

From Eq. (3-14) the capacitor voltage at $t = t_2$ is

$$V_2 = -200 \cos(2.667) = -177.9\ \text{V}$$

The reverse bias time of thyristor T_1 is

$$t_q = t_2 - t_1 = 29.22 - 5.192 = 24.03 \ \mu s$$

(b) $I_m = 50$ A.

$$t_1 = 1.0095 \ \mu s$$

$$t_2 = \pi \sqrt{LC} - t_1 = \pi \sqrt{4 \times 30} - 1.0095 = 33.41 \ \mu s$$

$$\omega_m = 91{,}287.1 \text{ rad/s} \quad \text{and} \quad \omega_m t_2 = 3.05 \text{ rad}$$

The capacitor voltage at $t = t_2$ is

$$V_2 = 200 \cos (3.05) = -199.1 \text{ V}$$

The reverse bias time of thyristor T_1 is

$$t_q = t_2 - t_1 = 33.41 - 1.0095 = 32.41 \ \mu s$$

Note. It can be noticed by comparing the reverse bias times with those of Example 3-4 that the addition of a diode makes t_q less dependent on the load current variations. However, for a higher load current (e.g., $I_m = 250$ A), t_q in Example 3-4 is less that of Example 3-5.

3-3.4 Complementary Commutation

A complementary commutation is used to transfer current between two loads and such an arrangement is shown in Fig. 3-14. The firing of one thyristor commutates the other one.

When thyristor T_1 is fired, the load with R_1 is connected to the supply voltage, V_s, and at the same time the capacitor C is charged to V_s through the other load with R_2. The polarity of capacitor C is as shown in Fig. 3-14. When thyristor T_2 is fired, the capacitor is then placed across thyristor T_1 and the load with R_2 is connected to the supply voltage, V_s. T_1 is reverse biased and is turned off by impulse commutation. Once thyristor T_1 is switched off, the capacitor voltage is reversed to $-V_s$ through R_1, T_2, and the supply. If thyristor T_1 is fired again, thyristor T_2 is turned off and the cycle is repeated. Normally, the two thryristors conduct with equal time intervals. The waveforms for voltages and currents are shown in Fig. 3-15 for $R_1 = R_2 = R$. Since each thyristor is switched off due to impulse commutation, this type of commutation is sometimes known as *complementary impulse commutation*.

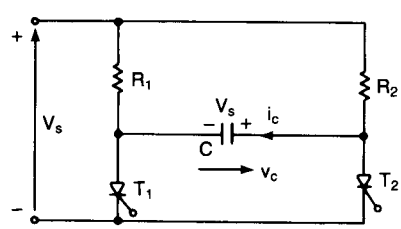


Figure 3-14 Complementary commutation circuit.

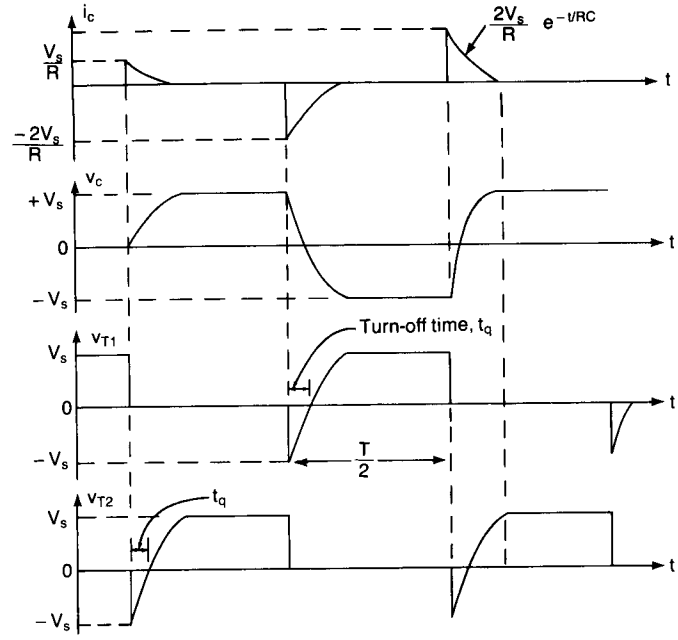


Figure 3-15 Waveforms for the circuit of Fig. 3-14.

Example 3-6

The circuit in Fig. 3-14, has load resistances of $R_1 = R_2 = R = 5\ \Omega$, capacitance, $C = 10\ \mu F$, and supply voltage, $V_s = 100$ V. Determine the circuit turn-off time, t_q.

Solution Assuming that the capacitor is charged to supply voltage V_s in the previous commutation of a complementary thyristor, the equivalent circuit during the commutation period is similar to Fig. 3-10. The current through the capacitor is given by

$$V_s = \frac{1}{C}\int i\,dt + v_c\,(t = 0) + Ri$$

With $v_c\,(t = 0) = -V_0 = V_s$, the solution of this equation gives the capacitor current as

$$i(t) = \frac{2V_s}{R}\,e^{-t/RC}$$

The capacitor voltage is obtained as

$$v_c(t) = V_s\,(1 - 2e^{-t/RC})$$

The turn-off time t_q can be found if the condition $v_c\,(t = t_q) = 0$ is satisfied and is solved as

$$t_q = RC \ln (2)$$

For $R = 5\ \Omega$ and $C = 10\ \mu F$, $t_q = 34.7\ \mu s$.

3-3.5 External Pulse Commutation

A pulse of current is obtained from an external voltage to turn off a conducting thyristor. Figure 3-16 shows a thyristor circuit using an external pulse commutation and two supply sources. V_s is the voltage of the main supply and V is the voltage of the auxiliary source.

If thyristor T_3 is fired, the capacitor will charge from the auxiliary source. Assuming that the capacitor is initially uncharged, a resonant current pulse of peak $V\sqrt{C/L}$, which is similar to the circuit in Fig. 3-2, will flow through T_3 and the capacitor is charged to 2V. If thyristor T_1 is conducting and a load current is supplied from the main source V_s, firing of thyristor T_2 will apply a reverse voltage of $V_s - 2V$ across thyristor T_1 and T_1 will be turned off. Once thyristor T_1 is turned off, the capacitor will discharge through the load at a rate determined by the magnitude of the load current.

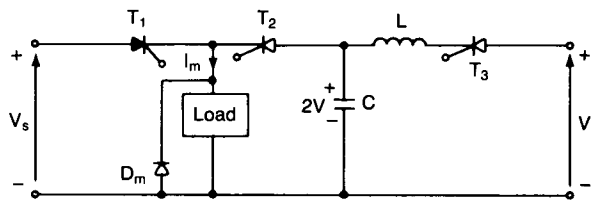


Figure 3-16 External pulse commutation.

3-3.6 Load-Side Commutation

In load-side commutation, the load forms a series circuit with the capacitor; and the discharging and recharging of the capacitor are done through the load. The performance of load-side commutation circuits depends on the load and in addition the commutation circuits cannot be tested without connecting the load. Figures 3-6, 3-8, 3-12, and 3-13 are examples of load-side commutation.

3-3.7 Line-Side Commutation

In this type of commutation, the discharging and recharging of the capacitor are not accomplished through the load and the commutation circuit can be tested without connecting the load. Figure 3-17a shows such a circuit.

When thyristor T_2 is fired, capacitor C is charged to $2V_s$ and T_2 is self-commutated similar to the circuit in Fig. 3-2. Thyristor T_3 is fired to reverse the voltage of capacitor to $-2V_s$ and T_3 is also self-commutated. Assuming that thyristor T_1 is conducting and carries a load current of I_m, thyristor T_2 is fired to turn off T_1. The firing of thyristor T_2 will forward bias the diode D_m and apply a reverse voltage of $2V_s$ across T_1; and T_1 will be turned off. The discharging and recharging of the capacitor will be done through the supply. The connection of the load is not required to test the commutation circuit.

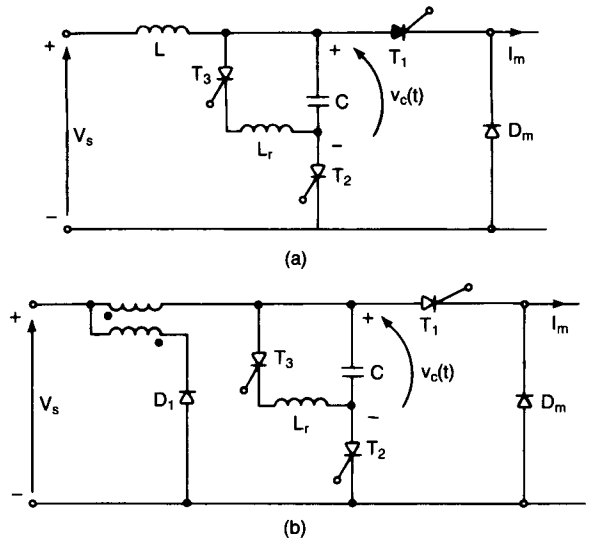


Figure 3-17 Line-side commutated circuit.

The inductor L carries the load current I_m and the equivalent circuit during the commutation period is shown in Fig. 3-18. The capacitor current is expressed (from Appendix D) as

$$V_s = L\frac{di}{dt} + \frac{1}{C}\int i\,dt + v_c\,(t = 0) \tag{3-17}$$

with initial conditions $i\,(t = 0) = I_m$ and $v_c\,(t = 0) = -2V_s$. The solution of Eq. (3-17) gives the capacitor current and voltage as

$$i(t) = I_m \cos \omega_m t + 3V_s \sqrt{\frac{C}{L}} \sin \omega_m t \tag{3-18}$$

and (3-19)

$$v_c(t) = I_m \sqrt{\frac{L}{C}} \sin \omega_m t - 3V_s \cos \omega_m t + V_s$$

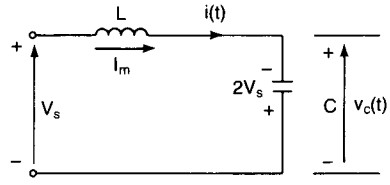


Figure 3-18 Equivalent circuit during commutation period.

where

$$\omega_m = 1/\sqrt{LC}$$

The circuit turn-off time, t_q, is obtained from the condition $v_c\ (t = t_q) = 0$ of Eq. (3-19) and solved after simplification as

$$t_q = \sqrt{LC}\left(\tan^{-1} 3x - \sin^{-1}\frac{x}{9x^2 + 1}\right) \tag{3-20}$$

where

$$x = \frac{V_s}{I_m}\sqrt{\frac{C}{L}} \tag{3-21}$$

The conduction time of thyristor T_2, which can be found from the condition $i\ (t = t_1) = 0$ of Eq. (3-18),

$$t_1 = \sqrt{LC}\tan^{-1}\frac{-1}{3x} \tag{3-22}$$

Under no-load conditions, $I_m = 0$ and x is infinite. t_q becomes

$$t_q = \sqrt{LC}\,(\pi - \sin^{-1}\tfrac{1}{3}) = 1.231\sqrt{LC}$$

and (3-23)

$$t_1 = \pi\sqrt{LC}$$

Note. If $I_m = 0$ and $t_1 = \pi\sqrt{LC}$, the capacitor voltage in Eq. (3-19) becomes $v_c\ (t = t_1) = V_0 = 4V_s$ and there will be continuous buildup of the capacitor voltage. To limit the overcharging of the capacitor, the inductor L is normally replaced by a energy recovery transformer and diode as shown in Fig. 3-17b.

3-4 COMMUTATION CIRCUIT DESIGN

The design of commutation circuits requires determining the values of capacitor C and inductor L. For the impulse commutation circuit in Fig. 3-6, the value of capacitor C is calculated from Eq. (3-8) and the reversal inductor L_r is determined from the peak permissible reversal current of Eq. (3-5). For the circuit in Fig. 3-8, the turn-off-time requirement t_q of Eq. (3-9) can be satisfied by choosing either C or L_1.

For the resonant pulse commutation circuit in Fig. 3-12, the values of L and C can be calculated from Eqs. (3-15) and (3-16). In Eqs. (3-14) and (3-15) V_0 and V_1 also depend on L and C as in Eq. (3-17).

Example 3-7

For the circuit in Fig. 3-6, determine the values of capacitor C and reversing inductor L_r if the supply voltage, V_s = 200 V, load current, I_m = 100 A, the turn-off time, t_q = 20 μs, and the peak reversal current is limited to 140% of I_m.

Solution $V_c = V_s$ = 200 V. From Eq. (3-8), $C = 100 \times 20/200 = 10$ μF. From Eq. (3-5), the peak resonant current is $1.4 \times 100 = 140 = 200\sqrt{10/L_r}$ and L_r = 20.4 μH.

Example 3-8

For the resonant commutation circuit in Fig. 3-13, determine the optimum values of C and L so that the minimum energy losses would occur during the commutation period if I_m = 350 A, V_0 = 200 V, and t_q = 20 μs.

Solution Substituting Eq. (3-16) into Eq. (3-13), the time required for the capacitor current to rise to the level of peak load current I_m is given by

$$t_1 = \sqrt{LC}\sin^{-1}\frac{1}{x}$$

where $x = I_p/I_m = (V_0/I_m)\sqrt{C/L}$. From Fig. 3-13b, the available reverse bias time or turn-off time is

$$t_q = t_2 - t_1 = \pi\sqrt{LC} - 2t_1 = \sqrt{LC}\left(\pi - 2\sin^{-1}\frac{1}{x}\right) \tag{3-25}$$

From Eq. (3-11), the peak resonant current is

$$I_p = V_0\sqrt{\frac{C}{L}} \tag{3-26}$$

Let us define a function $F_1(x)$ such that

$$F_1(x) = \frac{t_q}{\sqrt{LC}} = \pi - 2\sin^{-1}\frac{1}{x} \tag{3-27}$$

The commutation energy can be expressed as

$$W = 0.5CV_0^2 = 0.5LI_p^2 \tag{3-28}$$

Substituting the value of I_p from Eq. (3-26), gives us

$$W = 0.5\sqrt{LC}\,V_0 I_p$$

Substituting the value of $\sqrt{LC}$ from Eq. (3-27), we have

$$W = 0.5V_0 I_m\frac{xt_q}{F_1(x)} = \frac{x}{2[\pi - 2\sin(1/x)]} \tag{3-29}$$

Let us define an another function $F_2(x)$ such that

$$F_2(x) = \frac{W}{V_0 I_m t_q} = \frac{x}{2F_1(x)} \tag{3-30}$$

It can be shown mathematically or by plotting $F_2(x)$ against x that $F_2(x)$ is minimum when $x = 1.5$. Table 3-1 shows the values of $F_2(x)$ against x. For $x = 1.5$, Table 3-1 gives $F_1(x) = 1.68214$ and $F_2(x) = 0.44586$.

TABLE 3-1 $F_2(x)$ AGAINST x

x	$F_2(x)$
1.2	0.5122202
1.3	0.4688672
1.4	0.4515002
1.5	0.4458613
1.6	0.4465956
1.7	0.4512053
1.8	0.4583579

Substituting $x = 1.5$ in Eqs. (3-25) and (3-16), we obtain

$$t_q = 1.682\sqrt{LC}$$

and

$$1.5 = \frac{V_0}{I_m}\sqrt{\frac{C}{L}}$$

Solving these, the optimum values of L and C are

$$L = 0.398\frac{t_q V_0}{I_m} \tag{3-31}$$

$$C = 0.8917\frac{t_q I_m}{V_0} \tag{3-32}$$

For $I_m = 350$ A, $V_0 = 200$ V, and $t_q = 20$ μs,

$$L = 0.398 \times 20 \times \frac{200}{350} = 4.6\ \mu\text{H}$$

and

$$C = 0.8917 \times 20 \times \frac{350}{200} = 31.2\ \mu\text{F}$$

Note. Due to the freewheeling diode across the load as shown in Figs. 3-12a and 3.13a, the capacitor will get overcharged by the energy stored in inductor L. The capacitor voltage V_0 ($= V_c$), which will depend on the values of L and C, can be determined from Eq. (3-7). In this case, Eqs. (3-31) and (3-32) should be solved for the values of L and C.

Example 3-9

A diode is connected across the output as shown in Fig. 3-12a and the capacitor gets overcharged due to the energy stored in inductor L. Determine the values of L and C. The particulars are: $V_s = 200$ V, $I_m = 350$ A, $t_q = 20$ μs, and $x = 1.5$.

Solution Substituting Eq. (3-7) into Eq. (3-16), $x = (V_s/I_m)\sqrt{C/L} + 1$. Substituting Eqs. (3-7), (3-13), and (3-14), into Eq. (3-15),

$$t_q = \left[\frac{V_s C}{I_m} + \sqrt{LC}\right] \cos\left(\sin^{-1}\frac{1}{x}\right)$$

The values of C and L can be found from these two equations. The results are $L = 20.4$ μH and $C = 15.65$ μF.

Example 3-10

Repeat Example 3-9 for the circuit in Fig. 3-13.

Solution From Eq. (3-25), $t_q = \sqrt{LC}\,[\pi - 2\sin^{-1}(1/x)]$. From Eqs. (3-7) and (3-16), $x = (V_s/I_m)\sqrt{C/L} + 1$. The values of L and C are found as $C = 10.4$ μF and $L = 13.59$ μH.

3-5 COMMUTATION CAPACITORS

If the switching frequencies are below 1 kHz, the thyristor commutation time can be considered short compared with the switching period. Although the peak current through the capacitor is high, the average current could be relatively low. If the switching frequencies are above 5 kHz, the capacitor carries for a significant part of the switching period and the capacitor must therefore be chosen for a continuous current rating.

In selecting a commutation capacitor, the specifications of peak, rms, and average current and peak-to-peak voltage must be satisfied.

SUMMARY

We have seen in this chapter that a conducting thyristor can be turned off by a natural or forced commutation. In the natural commutation, the thyristor current is reduced to zero due to the natural characteristics of the input voltage. In the forced commutation, the thyristor current is reduced to zero by an additional circuitry called a commutation circuit, and the turn-off process depends on the load current. To guarantee the turn-off of a thyristor, the circuit (or available) turn-off must be greater than the turn-off time of a thyristor, which is normally specified by the thyristor manufacturer.

REFERENCES

1. M. H. Rashid, "Commutation limits of dc chopper on output voltage control." *Electronic Engineering*, Vol. 51, No. 620 (April) 1979, pp. 103–105.

2. M. H. Rashid, "A thyristor chopper with minimum limits on voltage control of dc drives." *International Journal of Electronics*, Vol. 53, No. 1 (July) 1982, pp. 71–89.
3. W. McMurry, "Thyristor commutation in dc chopper—a comparative study." *IEEE Industry Applications Society Conference Record*, October 2–6, 1977, pp. 385–397.

REVIEW QUESTIONS

3-1. What are the two general types of commutation?
3-2. What are the types of forced commutation?
3-3. What is the difference between self- and natural commutation?
3-4. What is the principle of self-commutation?
3-5. What is the principle of impulse commutation?
3-6. What is the principle of resonant pulse commutation?
3-7. What is the principle of complementary commutation?
3-8. What is the principle of external pulse commutation?
3-9. What are the differences between load-side and line-side commutation?
3-10. What are the differences between voltage and current commutation?
3-11. What are the purposes of a commutation circuit?
3-12. Why should the available reverse bias time be greater than the turn-off time of a thyristor?
3-13. What is the purpose of connecting an antiparallel diode across the main thyristor with or without a series inductor?
3-14. What is the ratio of peak resonant to load current for resonant pulse commutation that would minimize the commutation losses?
3-15. What are the expressions for the optimum value of commutation capacitor and inductor in a resonant pulse commutation?
3-16. Why does the commutation capacitor in a resonant pulse commutation get over-charged?
3-17. How is the voltage of the commutation capacitor reversed in a commutation circuit?
3-18. What type of capacitor is normally used in high switching frequencies?

PROBLEMS

3-1. In Fig. 3-3a, the initial capacitor voltage, $V_0 = 600$ V, capacitance, $C = 40$ μF, and inductance, $L = 10$ μH. Determine the peak value of resonant current and the conduction time of thyristor T_1.
3-2. Repeat Prob. 3-1 if the inductor in the resonant reversal circuit has a resistance, $R = 0.015\ \Omega$. (*Hint:* Determine the roots of a second-order system and then find the solution.)
3-3. The circuit in Fig. 3-4 has $V_s = 600$ V, $V_0 = 0$ V, $L = 20$ μH, $C = 50$ μF, and I_m

= 350 A. Determine (**a**) the peak capacitor voltage and current; and (**b**) the conduction time of thyristor T_1.

3-4. In the commutation circuit in Fig. 3-6, capacitance, $C = 20$ μF, input voltage, V_s, varies between 180 and 220 V, and load current, I_m, varies between 50 and 200 A. Determine the minimum and maximum values of available turn-off time, t_q.

3-5. For the circuit in Fig. 3-6, determine the values of capacitor C and reversing inductor L_r if the supply voltage, $V_s = 220$ V, load current, $I_m = 150$ A, turn-off time, $t_q = 15$ μs, and the reversal current is limited to 150% of I_m.

3-6. The circuit in Fig. 3.8 has $V_s = 220$ V, $C = 20$ μF, and $I_m = 150$ A. Determine the value of recharging inductance, L_1, which will provide turn-off time, $t_q = 15$ μs.

3-7. For the circuit in Fig. 3-8, determine the values of L_1 and C. The supply voltage, $V_s = 200$ V, load current, $I_m = 350$ A, turn-off time, $t_q = 20$ μs, and the peak current through diode D_1 is limited to 2.5 times I_m.

3-8. For the impulse commutation circuit in Fig. 3-9, the supply voltage, $V_s = 220$ V, capacitance, $C = 20$ μF, and load current, $R = 10\ \Omega$. Determine the turn-off time, t_q.

3-9. In the resonant pulse circuit in Fig. 3-12a, supply voltage, $V_s = 200$ V, load current, $I_m = 150$ A, commutation inductance, $L = 4$ μH, and commutation capacitance, $C = 20$ μF. Determine the peak resonant reversing current of thyristor T_3, I_k, and the turn-off time, t_q.

3-10. Repeat Prob. 3-9 if an antiparallel diode is connected across thyristor T_1 as shown in Fig. 3-13a.

3-11. If a diode is connected across thyristor T_1 in Fig. 3-12a and the capacitor gets overcharged, determine the values of L and C. The supply voltage, $V_s = 200$ V, load current, $I_m = 350$ A, turn-off time, $t_q = 20$ μs, and the ratio of peak resonant to load current, $x = 1.5$.

3-12. Repeat Prob. 3-11 for the circuit in Fig. 3-13a.

3-13. In the circuit in Fig. 3-13a, load current, $I_m = 200$ A, capacitor voltage, $V_0 = 220$ V, and turn-off time, $t_q = 15$ μs. Determine the optimum values of C and L so that the minimum energy losses would occur during the commutation period.

3-14. In the circuit in Fig. 3-18, the supply voltage, $V_s = 220$ V, capacitance, $C = 30$ μF, commutation inductance, $L = 10$ μH, and load current, $I_m = 100$ A. Determine the turn-off time, t_q, of the circuit.

3-15. Explain the operation of the circuit in Fig. 3-17a and identify the types of commutation involved in this circuit.

4

Controlled Rectifiers

4-1 INTRODUCTION

We have seen in Chapter 2 that diode rectifiers provide a fixed output voltage only. To obtain controlled output voltages, phase control thyristors are used instead of diodes. The output voltage of thyristor rectifiers is varied by controlling the delay or firing angle of thyristors. A phase-control thyristor is turned on by applying a short pulse to its gate and turned off due to *natural or line commutation*; and in case of a highly inductive load, it is turned off by firing another thyristor of the rectifier during the negative half-cycle of input voltage.

These phase-controlled rectifiers are simple and less expensive; and the efficiency of these rectifiers are, in general, above 95%. Since these rectifiers convert from ac to dc, these controlled rectifiers are also called *ac–dc converters* and are used extensively in industrial applications, especially in variable-speed drives, ranging from fractional horsepower to megawatt power level.

The phase-control converters can be classified into two types depending on the input supply: (1) single-phase converters, and (2) three-phase converters. Each type can be subdivided into (a) semiconverter, (b) full converter, and (c) dual converter. A *semiconverter* is a one-quadrant converter and it has one polarity of output voltage and current. A *full converter* is a two-quadrant converter and the polarity of its output voltage can be either positive or negative. However, the

output current of full converter has one polarity only. A *dual converter* can operate in four quadrants; and both the output voltage and current can be either positive or negative. In some applications, converters are connected in series to operate at higher voltages and to improve the input power factor.

The method of Fourier series similar to that of diode rectifiers can be applied to analyze the performances of phase-controlled converters with *RL* loads. However, to simplify the analysis, it is assumed in this chapter that the load inductance is sufficiently high; and the load current is continuous and has negligible ripple.

4-2 PRINCIPLE OF PHASE-CONTROLLED CONVERTER OPERATION

Let us consider the circuit in Fig. 4-1a with a resistive load. During the positive half-cycle of input voltage, the thyristor anode is positive with respect to its cathode and the thyristor is said to be *forward biased*. When thyristor T_1 is fired at $\omega t = \alpha$, thyristor T_1 conducts and the input voltage appears across the load. When the input voltage starts to be negative at $\omega t = \pi$, the thyristor anode is negative with respect to its cathode and thyristor T_1 is said to be *reverse biased*; and it is turned

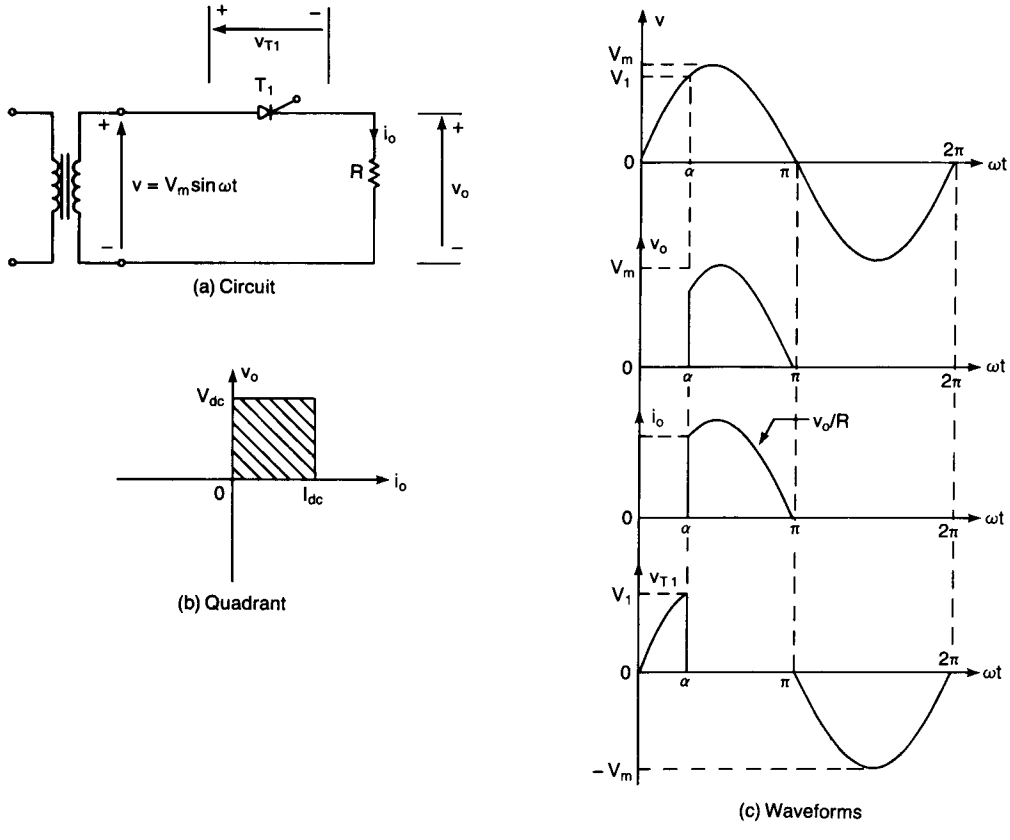


Figure 4-1 Single-phase thyristor converter with a resistive load.

off. The time after the input voltage starts to go positive until the thyristor is fired at $\omega t = \alpha$ is called the *delay or firing angle*, α.

Figure 4-1b shows the region of converter operation, where the output voltage and current have one polarity. Figure 4-1c shows the waveforms for input voltage, output voltage, load current, and voltage across T_1. This converter is not normally used in industrial applications because it has high ripple content and low ripple frequency. If f_s is the frequency of input supply, the lowest frequency of output ripple voltage is f_s.

If V_m is the peak input voltage, the average output voltage can be found from

$$V_{dc} = \frac{1}{2\pi}\int_{\alpha}^{\pi} V_m \sin \omega t \, d(\omega t) = \frac{V_m}{2\pi}[-\cos \omega t]_{\alpha}^{\pi}$$
$$= \frac{V_m}{2\pi}(1 + \cos \alpha) \tag{4-1}$$

and V_{dc} can be varied from V_m/π to 0 by varying α from 0 to π. The average output voltage becoms maximum when $\alpha = 0$ and the maximum voltage, V_{dm}, is

$$V_{dm} = \frac{V_m}{\pi} \tag{4-2}$$

Normalizing the output voltage with respect to V_{dm}, the normalized voltage,

$$V_n = \frac{V_{dc}}{V_{dm}} = 0.5(1 + \cos \alpha) \tag{4-3}$$

The rms output voltage is given by

$$V_{rms} = \left[\frac{1}{2\pi}\int_{\alpha}^{\pi} V_m^2 \sin^2 \omega t \, d(\omega t)\right]^{1/2} = \left[\frac{V_m^2}{4\pi}\int_{\alpha}^{\pi}(1 - \cos 2\omega t)\, d(\omega t)\right]^{1/2}$$
$$= \frac{V_m}{2}\left[\frac{1}{\pi}\left(\pi - \alpha + \frac{\sin 2\alpha}{2}\right)\right]^{1/2} \tag{4-4}$$

Example 4-1

If the converter of Figure 4-1a has a purely resistive load of R and the delay angle is $\alpha = \pi/2$, determine the (a) rectification efficiency; (b) form factor, FF; (c) ripple factor, RF; (d) transformer utilization factor, TUF; and (e) peak inverse voltage, PIV, of thyristor T_1.

Solution The delay angle, $\alpha = \pi/2$. From Eq. (4-1), $V_{dc} = 0.1592V_m$ and $I_{dc} = 0.1592V_m/R$. From Eq. (4-3), $V_n = 0.5$ pu. From Eq. (4-4), $V_{rms} = 0.3536V_m$ and $I_{rms} = 0.3536V_m/R$. From Eq. (2-42), $P_{dc} = V_{dc}I_{dc} = (0.1592V_m)^2/R$ and from Eq. (2-43), $P_{ac} = V_{rms}I_{rms} = (0.3536V_m)^2/R$.

(a) From Eq. (2-44) the rectification efficiency,

$$\eta = \frac{(0.1592V_m)^2}{(0.3536V_m)^2} = 20.27\%$$

(b) From Eq. (2-46), the form factor

$$FF = \frac{0.3536V_m}{0.1592V_m} = 2.221 \text{ or } 222.1\%$$

(c) From Eq. (2-48), the ripple factor, RF = $(2.221^2 - 1)^{1/2} = 1.983$ or 198.3%.

(d) The rms voltage of transformer secondary, $V_s = V_m/\sqrt{2} = 0.707V_m$. The rms value of the transformer secondary current is the same as that of the load, $I_s = 0.3536V_m/R$. The volt-ampere rating (VA) of the transformer, VA = $V_s I_s = 0.707V_m \times 0.3536V_m/R$. From Eq. (2-49),

$$\text{TUF} = \frac{0.1592^2}{0.707 \times 0.3536} = 0.1014 \quad \text{and} \quad \frac{1}{\text{TUF}} = 9.86$$

(e) The peak inverse voltage, PIV = V_m.

Note. The performance of the converter is degraded at the lower range of delay angle, α.

4-3 SINGLE-PHASE SEMICONVERTERS

The circuit arrangement of a single-phase semiconverter is shown in Fig. 4-2a with a highly inductive load. The load current is assumed continuous. During the positive half-cycle, thyristor T_1 is forward biased. When thyristor T_1 is fired at $\omega t = \alpha$, the load is connected to the input supply through T_1 and D_2 during the period $\alpha \leq \omega t \leq \pi$. During the period from $\pi \leq \omega t \leq (\pi + \alpha)$, the input voltage is negative and the freewheeling diode D_m is forward biased. D_m conducts to provide the continuity of current in the inductive load. The load current is transferred from T_1 and D_2 to D_m; and thyristor T_1 and diode D_2 are turned off. During the negative half-cycle of input voltage, thyristor T_2 is forward biased, and firing of thyristor T_2 at $\omega t = \pi + \alpha$ will reverse bias D_m. The diode D_m is turned off and the load is connected to the supply through T_2 and D_1.

Figure 4-2b shows the region of converter operation, where the output voltage and current have positive polarity. Figure 4-2c shows the waveforms for the input voltage, output voltage, input current, and currents through T_1, T_2, D_1, and D_2. This converter has a better power factor due to the freewheeling diode and is commonly used in applications up to 15 kW, where one-quadrant operation is acceptable.

The average output voltage can be found from

$$V_{dc} = \frac{2}{2\pi}\int_{\alpha}^{\pi} V_m \sin \omega t \, d(\omega t) = \frac{2V_m}{2\pi}[-\cos \omega t]_{\alpha}^{\pi}$$
$$= \frac{V_m}{\pi}(1 + \cos \alpha) \tag{4-5}$$

and V_{dc} can be varied from $2V_m/\pi$ to 0 by varying α from 0 to π. The maximum average output voltage is $V_{dm} = 2V_m/\pi$ and the normalized average output voltage is

$$V_n = \frac{V_{dc}}{V_{dm}} = 0.5(1 + \cos \alpha) \tag{4-6}$$

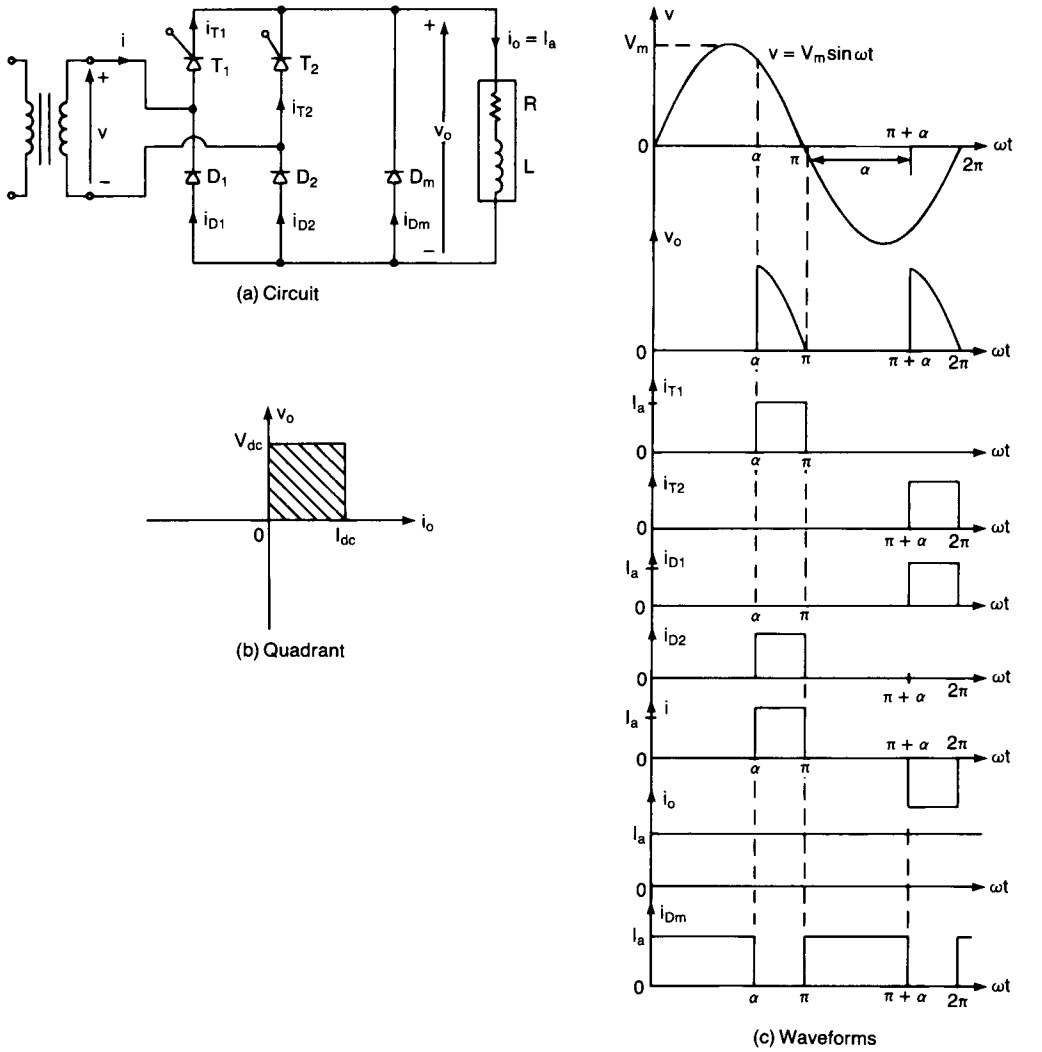


Figure 4-2 Single-phase semiconverter.

The rms output voltage is found from

$$V_{\text{rms}} = \left[\frac{2}{2\pi}\int_{\alpha}^{\pi} V_m^2 \sin^2 \omega t \, d(\omega t)\right]^{1/2} = \left[\frac{V_m^2}{2\pi}\int_{\alpha}^{\pi} (1 - \cos 2\omega t)\, d(\omega t)\right]^{1/2}$$

$$= \frac{V_m}{\sqrt{2}}\left[\frac{1}{\pi}\left(\pi - \alpha + \frac{\sin 2\alpha}{2}\right)\right]^{1/2} \tag{4-7}$$

Example 4-2

The semiconverter in Fig. 4-2a is connected to a 120-V 60-Hz supply. The load current, I_a, can be assumed to be continuous and its ripple content is negligible. The turns ratio of the transformer is unity. (a) Express the input current in a Fourier series; determine the harmonic factor of input current, HF; displacement factor, DF; and input power factor, PF. (b) If delay angle is $\alpha = \pi/2$, calculate V_{dc}, V_n, V_{rms}, HF, DF, and PF.

Solution (a) The waveform for input current is shown in Fig. 4-2c and the instantaneous input current can be expressed in a Fourier series as

$$i(t) = I_{dc} + \sum_{n=1,2,\ldots}^{\infty} (a_n \cos n\omega t + b_n \sin n\omega t) \tag{4-8}$$

where

$$I_{dc} = \frac{1}{2\pi}\int_{\alpha}^{2\pi} i(t)\, d(\omega t) = \frac{1}{2\pi}\left[\int_{\alpha}^{\pi} I_a\, d(\omega t) - \int_{\pi+\alpha}^{2\pi} I_a\, d(\omega t)\right] = 0$$

$$a_n = \frac{1}{\pi}\int_{\alpha}^{2\pi} i(t) \cos n\omega t\, d(\omega t)$$

$$= \frac{1}{\pi}\left[\int_{\alpha}^{\pi} I_a \cos n\omega t\, d(\omega t) - \int_{\pi+\alpha}^{2\pi} I_a \cos n\omega t\, d(\omega t)\right]$$

$$= -\frac{2I_a}{n\pi}\sin n\alpha \qquad \text{for } n = 1, 3, 5, \ldots$$

$$= 0 \qquad \text{for } n = 2, 4, 6, \ldots$$

$$b_n = \frac{1}{\pi}\int_{\alpha}^{2\pi} i(t) \sin n\omega t\, d(\omega t)$$

$$= \frac{1}{\pi}\left[\int_{\alpha}^{\pi} I_a \sin n\omega t\, d(\omega t) - \int_{\pi+\alpha}^{2\pi} I_a \sin n\omega t\, d(\omega t)\right]$$

$$= \frac{2I_a}{n\pi}(1 + \cos n\alpha) \qquad \text{for } n = 1, 3, 5, \ldots$$

$$= 0 \qquad \text{for } n = 2, 4, 6, \ldots$$

Since $I_{dc} = 0$, Eq. (4-8) can be written as

$$i(t) = \sum_{n=1,2,\ldots}^{\infty} \sqrt{2}\, I_n \sin(n\omega t + \phi_n) \tag{4-9}$$

where

$$\phi_n = \tan^{-1}\frac{a_n}{b_n} = -\frac{n\alpha}{2} \tag{4-10}$$

The rms value of the nth harmonic component of the input current is derived as

$$I_n = \frac{1}{\sqrt{2}}(a_n^2 + b_n^2)^{1/2} = \frac{2\sqrt{2}\, I_a}{n\pi}\cos\frac{n\alpha}{2} \tag{4-11}$$

From Eq. (4-11), the rms value of the fundamental current is

$$I_1 = \frac{2\sqrt{2}\, I_a}{\pi} \cos\frac{\alpha}{2} \tag{4-12}$$

The rms input current can be calculated from Eq. (4-11) as

$$I_s = \left(\sum_{n=1,2,\ldots}^{\infty} I_n^2 \right)^{1/2}$$

I_s can also be determined directly from

$$I_s = \left[\frac{2}{2\pi} \int_{\alpha}^{\pi} I_a^2 \, d(\omega t) \right]^{1/2} = I_a \left(1 - \frac{\alpha}{\pi} \right)^{1/2} \tag{4-13}$$

From Eq. (2-51), HF = $[(I_s/I_1)^2 - 1]^{1/2}$ or

$$\text{HF} = \left[\frac{\pi(\pi - \alpha)}{4(1 + \cos\alpha)} - 1 \right]^{1/2} \tag{4-14}$$

From Eqs. (2-50) and (4-10),

$$\text{DF} = \cos\phi_1 = \cos -\frac{\alpha}{2} \tag{4-15}$$

From Eq. (2-52),

$$\text{PF} = \frac{I_1}{I_s} \cos\frac{\alpha}{2} = \frac{\sqrt{2}\,(1 + \cos\alpha)}{[\pi(\pi - \alpha)]^{1/2}} \tag{4-16}$$

(b) $\alpha = \pi/2$ and $V_m = \sqrt{2} \times 120 = 169.83$ V. From Eq. (4-5), $V_{dc} = (V_m/\pi)(1 + \cos\alpha) = 51.57$ V, from Eq. (4-6), $V_n = 0.5$ pu, and from Eq. (4-7),

$$V_{\text{rms}} = \frac{V_m}{\sqrt{2}} \left[\frac{1}{\pi} \left(\pi - \alpha + \frac{\sin 2\alpha}{2} \right) \right]^{1/2} = 81 \text{ V}$$

$$I_1 = \frac{2\sqrt{2}\, I_a}{\pi} \cos\frac{\pi}{4} = 0.6366 I_a$$

$$I_s = I_a \left(1 - \frac{\alpha}{\pi} \right)^{1/2} = 0.7071 I_a$$

$$\text{HF} = \left[\left(\frac{I_s}{I_1} \right)^2 - 1 \right]^{1/2} = 0.4835 \text{ or } 48.35\%$$

$$\phi_1 = -\frac{\pi}{4} \quad \text{and} \quad \text{DF} = \cos -\frac{\pi}{4} = 0.7071$$

$$\text{PF} = \frac{I_1}{I_s} \cos\frac{\alpha}{2} = 0.6366 \text{ (lagging)}$$

Note. The performance parameters of the converter depend on the delay angle, α.

4-4 SINGLE-PHASE FULL CONVERTERS

The circuit arrangement of a single-phase full converter is shown in Fig. 4-3a with a highly inductive load. During the positive half-cycle, thyristors T_1 and T_2 are forward biased; and when these two thyristors are fired simultaneously at $\omega t = \alpha$, the load is connected to the input supply through T_1 and T_2. Due to the inductive load, thyristors T_1 and T_2 will continue to conduct beyond $\omega t = \pi$, even though the input voltage is already negative. During the negative half-cycle of the input voltage, thyristors T_3 and T_4 are forward biased; and firing of thyristors T_3 and T_4 will apply the supply voltage across thyristors T_1 and T_2 as reverse blocking voltage. T_1 and T_2 will be turned off due to *line* or *natural commutation* and the load current will be transferred from T_1 and T_2 to T_3 and T_4. Figure 4-3b shows the regions of converter operation and Fig. 4-3c shows the waveforms for input voltage, output voltage, and input and output currents.

During the period from α to π, the input voltage, v, and input current, i, are positive; and the power flows from the supply to the load. The converter is said to be operated in *rectification* mode. During the period from π to $\pi + \alpha$, the

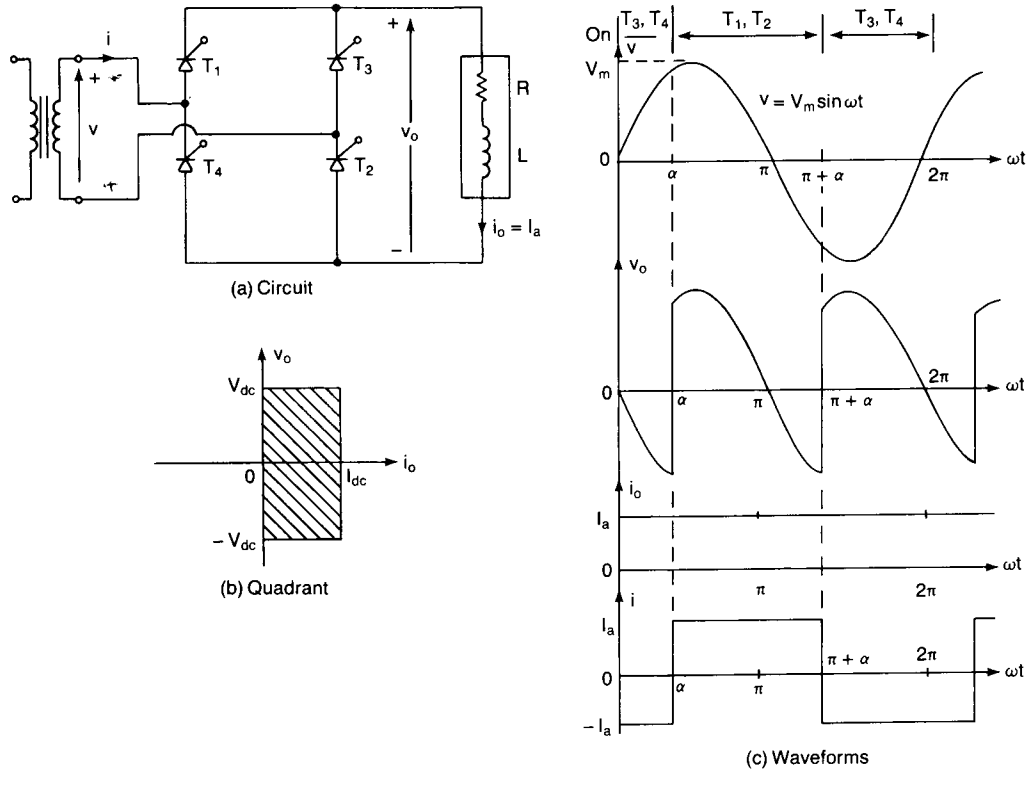


Figure 4-3 Single-phase full converter.

input voltage, v, is negative and the input current is positive; and there will be reverse power flow from the load to the supply. The converter is operated in *inversion mode*. This converter is extensively used in industrial applications up to 15 kW. Depending on the value of α, the average output voltage could be either positive or negative and it provides two-quadrant operation.

The average output voltage can be found from

$$V_{dc} = \frac{2}{2\pi}\int_{\alpha}^{\pi+\alpha} V_m \sin \omega t \, d(\omega t) = \frac{2V_m}{2\pi}[-\cos \omega t]_{\alpha}^{\pi+\alpha}$$
$$= \frac{2V_m}{\pi}\cos \alpha \tag{4-17}$$

and V_{dc} can be varied from $2V_m/\pi$ to $-2V_m/\pi$ by varying α from 0 to π. The maximum average output voltage is $V_{dm} = 2V_m/\pi$ and the normalized average output voltage is

$$V_n = \frac{V_{dc}}{V_{dm}} = \cos \alpha \tag{4-18}$$

The rms value of the output voltage is given by

$$V_{rms} = \left[\frac{2}{2\pi}\int_{\alpha}^{\pi+\alpha} V_m^2 \sin^2 \omega t \, d(\omega t)\right]^{1/2} = \left[\frac{V_m^2}{2\pi}\int_{\alpha}^{\pi+\alpha}(1-\cos 2\omega t)\, d(\omega t)\right]^{1/2}$$
$$= \frac{V_m}{\sqrt{2}} = V_s \tag{4-19}$$

Example 4-3

For a delay angle of $\alpha = \pi/3$, repeat Example 4-2 for the single-phase full converter in Fig. 4-3a.

Solution (a) The waveform for input current is shown in Fig. 4-3c and the instantaneous input current can be expressed in a Fourier series as

$$i(t) = I_{dc} + \sum_{n=1,2,\ldots}^{\infty} (a_n \cos n\omega t + b_n \sin n\omega t) \tag{4-20}$$

where

$$I_{dc} = \frac{1}{2\pi}\int_{\alpha}^{2\pi+\alpha} i(t)\, d(\omega t) = \frac{1}{\pi}\left[\int_{\alpha}^{\pi+\alpha} I_a \, d(\omega t) - \int_{\pi+\alpha}^{2\pi+\alpha} I_a \, d(\omega t)\right] = 0$$

$$a_n = \frac{1}{\pi}\int_{\alpha}^{2\pi+\alpha} i(t) \cos n\omega t \, d(\omega t)$$
$$= \frac{1}{\pi}\left[\int_{\alpha}^{\pi+\alpha} I_a \cos n\omega t \, d(\omega t) - \int_{\pi+\alpha}^{2\pi+\alpha} I_a \cos n\omega t \, d(\omega t)\right] \tag{4-21}$$
$$= -\frac{4I_a}{n\pi}\sin n\alpha \qquad \text{for } n = 1, 3, 5, \ldots$$
$$= 0 \qquad \text{for } n = 2, 4, \ldots$$

$$b_n = \frac{1}{\pi}\int_{\alpha}^{2\pi+\alpha} i(t)\sin n\omega t\, d(\omega t)$$

$$= \frac{1}{\pi}\left[\int_{\alpha}^{\pi+\alpha} I_a \sin n\omega t\, d(\omega t) - \int_{\pi+\alpha}^{2\pi+\alpha} I_a \sin n\omega t\, d(\omega t)\right] \tag{4-22}$$

$$= \frac{4I_a}{n\pi}\cos n\alpha \qquad \text{for } n = 1, 3, 5, \ldots$$

$$= 0 \qquad \text{for } n = 2, 4, \ldots$$

Since $I_{dc} = 0$, Eq. (4-20) can be written as

$$i(t) = \sum_{n=1,2,\ldots}^{\infty} \sqrt{2}\, I_n \sin(\omega t + \phi_n) \tag{4-23}$$

where

$$\phi_n = \tan^{-1}\frac{a_n}{b_n} = -n\alpha \tag{4-24}$$

and ϕ_n is the displacement angle of the nth harmonic current. The rms value of the nth harmonic input current is

$$I_n = \frac{1}{\sqrt{2}}(a_n^2 + b_n^2)^{1/2} = \frac{4I_a}{\sqrt{2}\,n\pi} = \frac{2\sqrt{2}\,I_a}{n\pi} \tag{4-25}$$

and the rms value of the fundamental current is

$$I_1 = \frac{2\sqrt{2}\,I_a}{\pi} \tag{4-26}$$

The rms value of the input current can be calculated from Eq. (4-25) as

$$I_s = \left(\sum_{n=1,2,\ldots}^{\infty} I_n^2\right)^{1/2} \tag{4-27}$$

I_s can also be determined directly from

$$I_s = \left[\frac{2}{2\pi}\int_{\alpha}^{\pi+\alpha} I_a^2\, d(\omega t)\right]^{1/2} = I_a \tag{4-28}$$

From Eq. (2-51) the harmonic factor is found as

$$\text{HF} = \left[\left(\frac{I_s}{I_1}\right)^2 - 1\right]^{1/2} = 0.4834 \text{ or } 48.24\%$$

From Eqs. (2-50) and (4-24), the displacement factor,

$$\text{DF} = \cos\phi_1 = \cos -\alpha \tag{4-29}$$

From Eq. (2-52) the power factor is found as

$$\text{PF} = \frac{I_1}{I_s}\cos -\alpha = \frac{2\sqrt{2}}{\pi}\cos\alpha \tag{4-30}$$

(b) $\alpha = \pi/3$.

$$V_{dc} = \frac{2V_m}{\pi}\cos\alpha = 54.02 \text{ V} \quad \text{and} \quad V_n = 0.5 \text{ pu}$$

$$V_{rms} = \frac{V_m}{\sqrt{2}} = V_s = 120 \text{ V}$$

$$I_1 = \left(2\sqrt{2}\frac{I_a}{\pi}\right) = 0.90032I_a \quad \text{and} \quad I_s = I_a$$

$$\text{HF} = \left[\left(\frac{I_s}{I_1}\right)^2 - 1\right]^{1/2} = 0.4834 \text{ or } 48.34\%$$

$$\phi_1 = -\alpha \quad \text{and} \quad \text{DF} = \cos -\alpha = \cos\frac{-\pi}{3} = 0.5$$

$$\text{PF} = \frac{I_1}{I_s}\cos -\alpha = 0.45 \text{ (lagging)}$$

Note. The fundamental component of input current is always 90.03% of I_a and the harmonic factor remains constant at 48.34%.

4-5 SINGLE-PHASE DUAL CONVERTERS

We have seen in Section 4-4 that single-phase full converters allow only two-quadrant operation. If two of these full converters are connected back to back as shown in Fig. 4-4a, both the output voltage and the load current can be reversed. The system will provide four-quadrant operation and is called a *dual converter*. Dual converters are normally used in high-power variable-speed drives. If α_1 and α_2 are the delay angles of converters 1 and 2, respectively, the corresponding average output voltages are V_{dc1} and V_{dc2}. The delay angles are controlled such that one converter operates as a rectifier and the other converter operates as an inverter; but both converters produce the same average output voltage. Figure 4-4b shows the output waveforms for two converters, where the two output voltages are the same. Figure 4-4c shows the v–i characteristics of a dual converter.

From Eq. (4-17) the average output voltages are

$$V_{dc1} = \frac{2V_m}{\pi}\cos\alpha_1 \tag{4-31}$$

and

$$V_{dc2} = \frac{2V_m}{\pi}\cos\alpha_2 \tag{4-32}$$

Since one converter is rectifying and the other one is inverting,

$$V_{dc1} = -V_{dc2} \quad \text{or} \quad \cos\alpha_2 = -\cos\alpha_1 = \cos(\pi - \alpha_1)$$

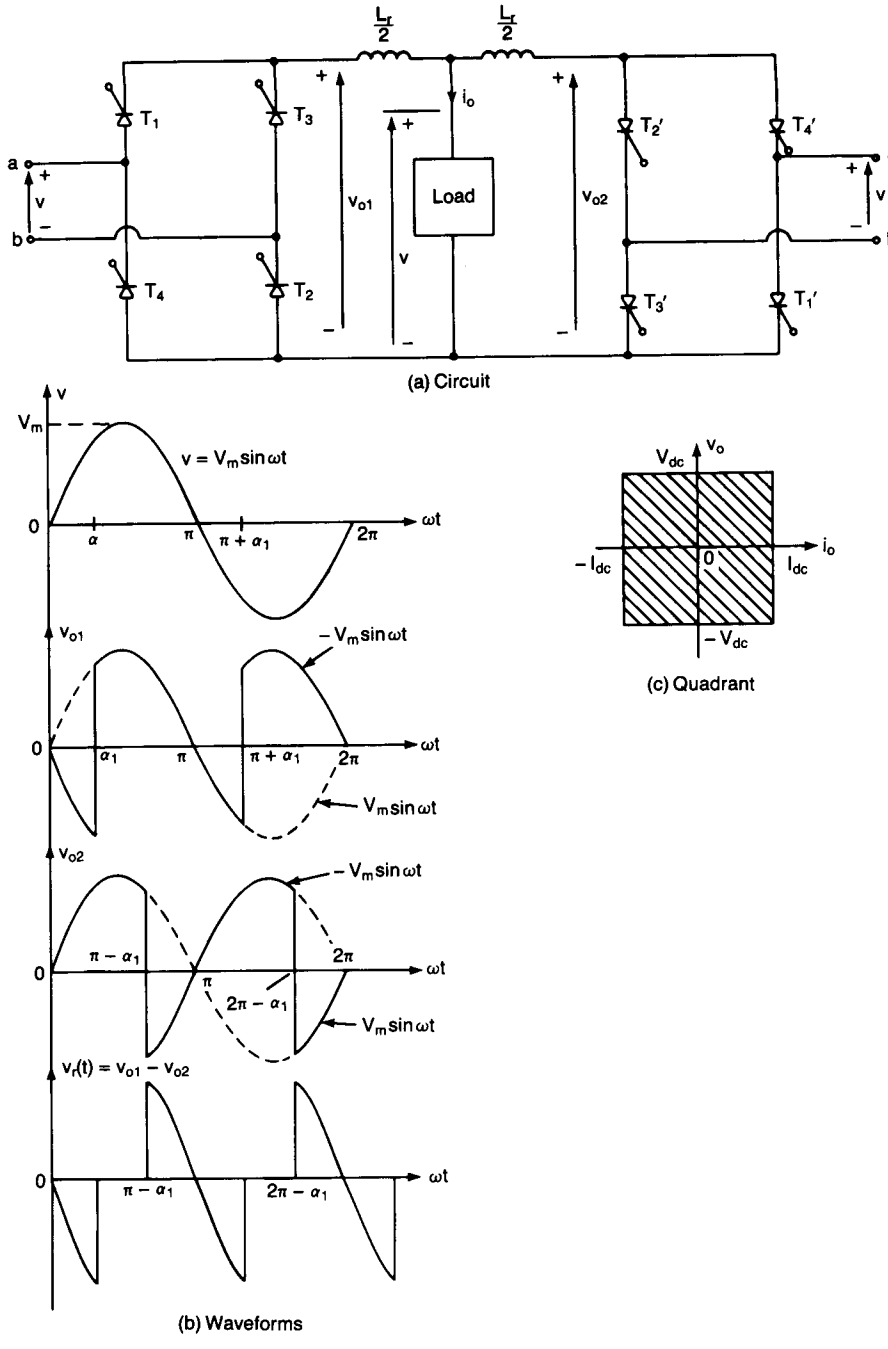


Figure 4-4 Single-phase dual converter.

Therefore,

$$\alpha_2 = \pi - \alpha_1 \tag{4-33}$$

Since the instantaneous output voltages of the two converters are out of phase, there will be an instantaneous voltage difference and this will result in circulating current between the two converters. This circulating current will not flow through the load and is normally limited by a *circulating current reactor* L_r as shown in Fig. 4-4a.

If v_{o1} and v_{o2} are the instantaneous output voltages of converters 1 and 2, respectively, the circulating current can be found by integrating the instantaneous voltage difference starting from $\omega t = 2\pi - \alpha_1$. Since the two output voltages during the interval $\omega t = \pi + \alpha_1$ to $2\pi - \alpha_1$ are equal, their contributions to the instantaneous circulating current i_r is zero.

$$\begin{aligned} i_r &= \frac{1}{\omega L_r}\int_{2\pi-\alpha_1}^{\omega t} v_r\, d(\omega t) = \frac{1}{\omega L_r}\int_{2\pi-\alpha_1}^{\omega t} (v_{o1} - v_{o2})\, d(\omega t) \\ &= \frac{V_m}{\omega L_r}\left[\int_{2\pi-\alpha_1}^{\omega t} - \sin \omega t\, d(\omega t) - \int_{2\pi-\alpha_1}^{\omega t} \sin \omega t\, d(\omega t)\right] \\ &= \frac{2V_m}{\omega L_r}(\cos \omega t - \cos \alpha_1) \end{aligned} \tag{4-34}$$

The circulating current depends on the delay angle and becomes maximum when $\alpha_1 = \pi$, $\omega t = n\pi$, $n = 0, 2, 4, \ldots$, and minimum at $\alpha_1 = 0$, $\omega t = n\pi$, $n = 1, 3, \ldots$. If the peak load current is I_p, one of the converters that controls the power flow may carry a peak current of $(I_p + 4V_m/\omega L_r)$.

The dual converters can be operated with or without a circulating current. In case of operation without circulating current, only one converter operates at a time and carries the load current; and the other converter is completely blocked by inhibited gate pulses. However, the operation with circulating current has the following advantages:

1. The circulating current maintains continuous conduction of both converters over the whole control range, independent of the load.

2. Since one converter always operates as a rectifier and the other converter operates as an inverter, the power flow in either direction at any time is possible.

3. Since both converters are in continuous conduction, the time response for changing from one quadrant operation to another is faster.

Example 4-4

The single-phase dual converter in Fig. 4-4a is operated from a 120-V 60-Hz supply and the load resistance is $R = 10\ \Omega$. The circulating inductance is $L_c = 40$ mH; delay angles are $\alpha_1 = 60°$ and $\alpha_2 = 120°$. Calculate the peak circulating current and the peak current of converter 1.

Solution $\omega = 2\pi \times 60 = 377$ rad/s, $\alpha_1 = 60°$, $V_m = \sqrt{2} \times 120 = 169.7$ V, $f = 60$ Hz, and $L_r = 40$ mH. For $\omega t = 2\pi$ and $\alpha_1 = \pi/3$, Eq. (4-34) gives the peak

circulating current

$$I_r(\max) = \frac{2V_m}{\omega L_r}(1 - \cos \alpha_1) = \frac{169.7}{377 \times 0.04} = 11.25 \text{ A}$$

The peak load current, $I_p = 169.71/10 = 16.97$ A. The peak current of converter 1 is $(16.97 + 11.25) = 28.22$ A.

4-6 SINGLE-PHASE SERIES CONVERTERS

For high-voltage applications, two or more converters can be connected in series to share the voltage and also to improve the power factor. Figure 4-5a shows two semiconverters that are connected in series. Each secondary has the same number of turns, and the turns ratio between the primary and secondary is $N_p/N_s = 2$. If α_1 and α_2 are the delay angles of converter 1 and converter 2, respectively, the maximum output voltage V_{dm} is obtained when $\alpha_1 = \alpha_2 = 0$.

In two-converter systems, one converter is operated to obtain output voltage from 0 to $V_{dm}/2$ and the other converter is bypassed through its freewheeling diode. To obtain output voltage from $V_{dm}/2$ to V_{dm}, one converter is fully turned on (delay angle, $\alpha_1 = 0$) and the delay angle of other converter, α_2, is varied. Figure 4-5b shows the output voltage, input currents to converters, and the input current from the supply when both the converters are operating.

From Eq. (4-5), the average output voltages of two semiconverters are

$$V_{dc1} = \frac{V_m}{\pi}(1 + \cos \alpha_1)$$

$$V_{dc2} = \frac{V_m}{\pi}(1 + \cos \alpha_2)$$

The resultant output voltage of converters is

$$V_{dc} = V_{dc1} + V_{dc2} = \frac{V_m}{\pi}(2 + \cos \alpha_1 + \cos \alpha_2) \tag{4-35}$$

The maximum average output voltage for $\alpha_1 = \alpha_2 = 0$ is $V_{dm} = 4V_m/\pi$. If converter 1 is operating: $0 \le \alpha_1 \le \pi$ and $\alpha_2 = \pi$, then

$$V_{dc} = V_{dc1} + V_{dc2} = \frac{V_m}{\pi}(1 + \cos \alpha_1) \tag{4-36}$$

and the normalized average output voltage is

$$V_n = \frac{V_{dc}}{V_{dm}} = 0.25(1 + \cos \alpha_1) \tag{4-37}$$

If both converters are operating: $\alpha_1 = 0$ and $0 \le \alpha_2 \le \pi$, then

$$V_{dc} = V_{dc1} + V_{dc2} = \frac{V_m}{\pi}(3 + \cos \alpha_2) \tag{4-38}$$

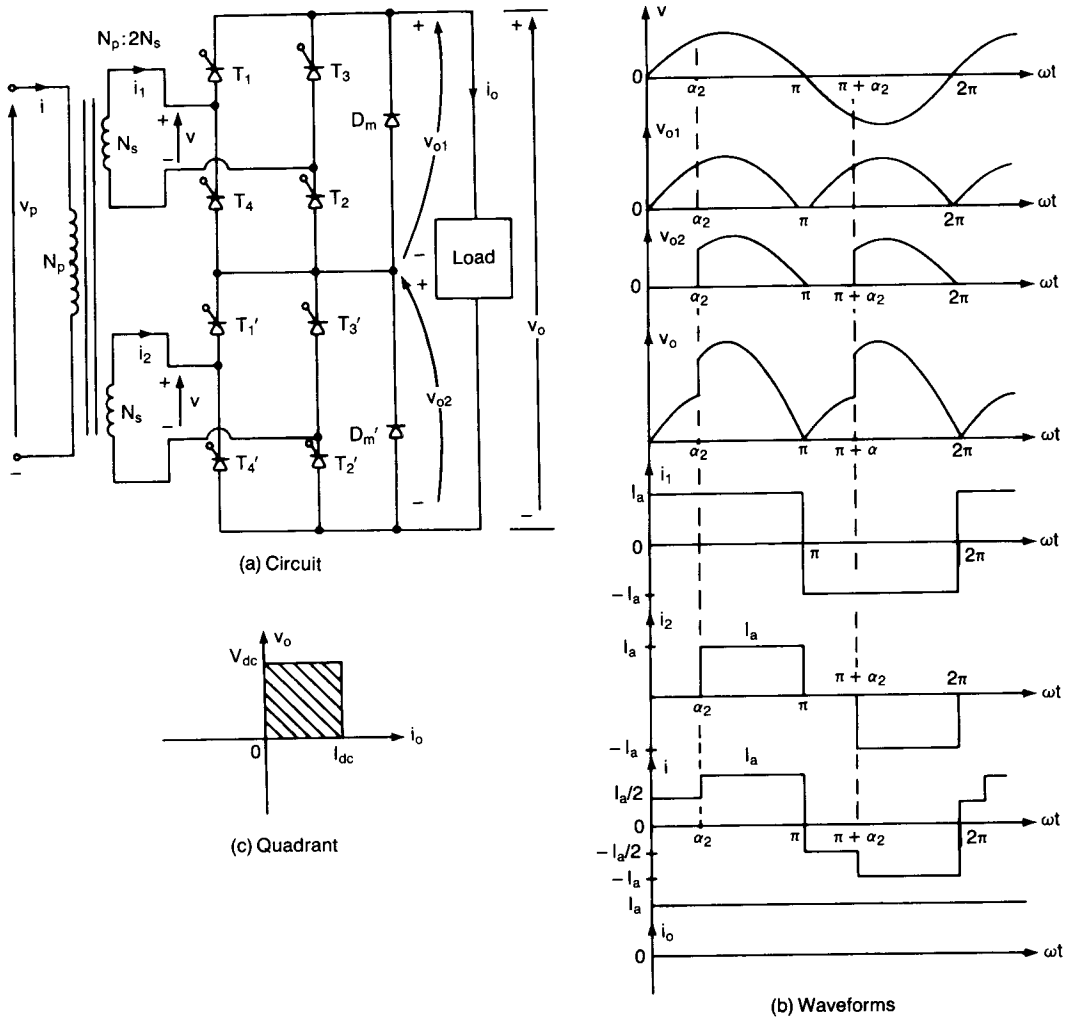


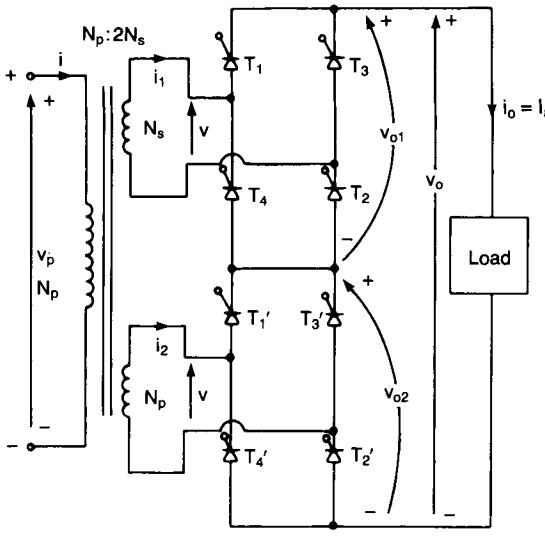
Figure 4-5 Single-phase series semiconverters.

and the normalized average output voltage is

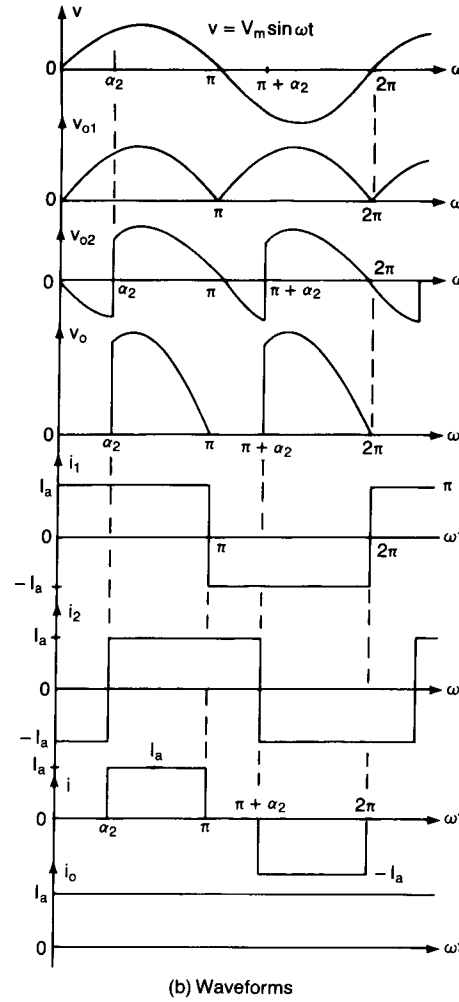
$$V_n = \frac{V_{dc}}{V_{dm}} = 0.25(3 + \cos \alpha_2) \tag{4-39}$$

Figure 4-6a shows two full converters that are connected in series and the turns ratio between the primary and secondary is $N_p/N_s = 2$. Due to the fact that there are no freewheeling diodes, one of the converters cannot be bypassed and both converters must operate at the same time.

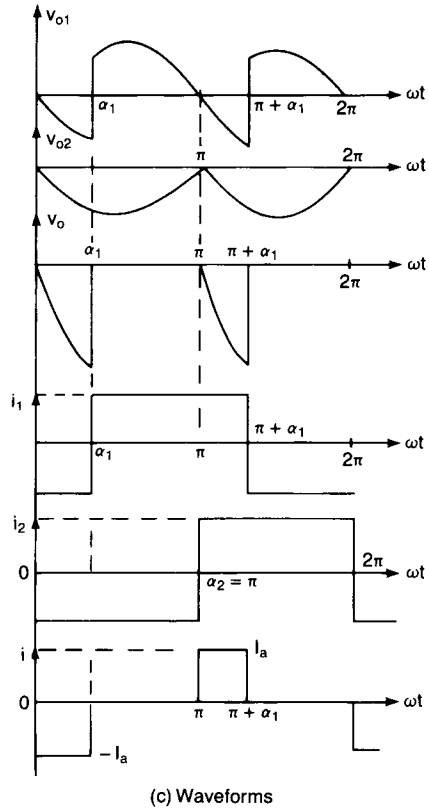
In rectification mode, one converter is fully advanced ($\alpha_1 = 0$) and the delay angle of the other converter, α_2, is varied from 0 to π to control the dc output



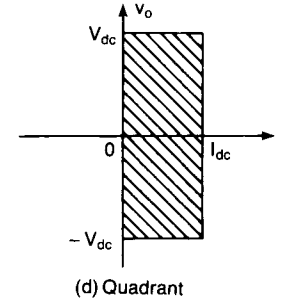
(a) Circuit



(b) Waveforms



(c) Waveforms



(d) Quadrant

Figure 4-6 Single-phase full converters.

voltage. Figure 4-6b shows the input voltage, output voltages, input currents to the converters, and input supply current. Comparing Fig. 4-6b with Fig. 4-2b, we can notice that the input current from the supply is similar to that of semiconverter, and as a result the power factor of this converter is improved, but the power factor is less than that of series semiconverters.

In inversion mode, one converter is fully retarded, $\alpha_2 = \pi$, and the delay angle of the other converter, α_1, is varied from 0 to π to control the average output voltage. Figure 4-6d shows the v–i characteristics of series full converters.

From Eq. (4-17), the average output voltages of two full converters are

$$V_{dc1} = \frac{2V_m}{\pi} \cos \alpha_1$$

$$V_{dc2} = \frac{2V_m}{\pi} \cos \alpha_2$$

The resultant output voltage is

$$V_{dc} = V_{dc1} + V_{dc2} = \frac{2V_m}{\pi} (\cos \alpha_1 + \cos \alpha_2) \tag{4-40}$$

The maximum average output voltage for $\alpha_1 = \alpha_2 = 0$ is $V_{dm} = 4V_m/\pi$. In the rectification mode, $\alpha_1 = 0$ and $0 \leq \alpha_2 \leq \pi$; then

$$V_{dc} = V_{dc1} + V_{dc2} = \frac{2V_m}{\pi} (1 + \cos \alpha_2) \tag{4-41}$$

and the normalized dc output voltage is

$$V_n = \frac{V_{dc}}{V_{dm}} = 0.5(1 + \cos \alpha_2) \tag{4-42}$$

In the inversion mode, $0 \leq \alpha_1 \leq \pi$ and $\alpha_2 = \pi$; then

$$V_{dc} = V_{dc1} + V_{dc2} = \frac{2V_m}{\pi} (\cos \alpha_1 - 1) \tag{4-43}$$

and the normalized average output voltage is

$$V_n = \frac{V_{dc}}{V_{dm}} = 0.5(\cos \alpha_1 - 1) \tag{4-44}$$

Example 4-5

The load current (with an average value of I_a) of series full converters in Fig. 4-6a is continuous and the ripple content is negligible. The turns ratio of the transformer is $N_p/N_s = 2$. The converters operate in rectification mode such that $\alpha_1 = 0$ and α_2 varies from 0 to π. (a) Express the input supply current in Fourier series, determine the harmonic factor of input current, HF; displacement factor, DF; and input power factor, PF. (b) If the delay angle is $\alpha_2 = \pi/2$ and the peak input voltage is $V_m = 162$ V, calculate V_{dc}, V_n, V_{rms}, HF, DF, and PF.

Solution (a) The waveform for input current is shown in Fig. 4-6b and the instantaneous input supply current can be expressed in a Fourier series as

$$i(t) = \sum_{n=1,2,\ldots}^{\infty} \sqrt{2}\, I_n \sin(n\omega t + \phi_n)$$

where $\phi_n = -n\alpha_2/2$. Equation (4.11) gives the rms value of the nth harmonic input current

$$I_n = \frac{4I_a}{\sqrt{2}\, n\pi} \cos\frac{n\alpha_2}{2} = \frac{2\sqrt{2}\, I_a}{n\pi} \cos\frac{n\alpha_2}{2} \tag{4-45}$$

The rms value of fundamental current is

$$I_1 = \frac{2\sqrt{2}\, I_a}{\pi} \cos\frac{\alpha_2}{2} \tag{4-46}$$

The rms input current is found as

$$I_s = I_a \left(1 - \frac{\alpha_2}{\pi}\right)^{1/2} \tag{4-47}$$

From Eq. (2-51),

$$\text{HF} = \left[\frac{\pi(\pi - \alpha_2)}{4(1 + \cos\alpha_2)} - 1\right]^{1/2} \tag{4-48}$$

From Eqs. (2-50),

$$\text{DF} = \cos\phi_1 = \cos - \frac{\alpha_2}{2} \tag{4-49}$$

From Eq. (2-52),

$$\text{PF} = \frac{I_1}{I_s} \cos\frac{\alpha}{2} = \frac{\sqrt{2}\,(1 + \cos\alpha_2)}{[\pi(\pi - \alpha_2)]^{1/2}} \tag{4-50}$$

(b) $\alpha_1 = 0$ and $\alpha_2 = \pi/2$. From Eq. (4-41),

$$V_{dc} = \left(2 \times \frac{162}{\pi}\right)\left(1 + \cos\frac{\pi}{2}\right) = 103.13 \text{ V}$$

From Eq. (4-42), $V_n = 0.5$ pu and

$$V_{rms}^2 = \frac{2}{2\pi}\int_{\alpha_2}^{\pi} (2V_m)^2 \sin\omega t\, d(\omega t)$$

$$V_{rms} = \sqrt{2}\, V_m \left[\frac{1}{\pi}\left(\pi - \alpha_2 + \frac{\sin 2\alpha_2}{2}\right)\right]^{1/2} = V_m = 162\text{V}$$

$$I_1 = I_a \frac{2\sqrt{2}}{\pi} \cos\frac{\pi}{4} = 0.6366 I_a \quad \text{and} \quad I_s = 0.7071 I_a$$

$$\text{HF} = \left[\left(\frac{I_s}{I_1}\right)^2 - 1\right]^{1/2} = 0.4835 \quad \text{or} \quad 48.35\%$$

$$\phi_1 = -\frac{\pi}{4} \quad \text{and} \quad \text{DF} = \cos -\frac{\pi}{4} = 0.7071$$

$$\text{PF} = \frac{I_1}{I_s}\cos(-\phi_1) = 0.6366\,(\text{lagging})$$

Note. The performance of series full converters is similar to that of single-phase semiconverters.

4-7 THREE-PHASE HALF-WAVE CONVERTERS

Three-phase converters provide higher average output voltage, and in addition the frequency of the ripples on the output voltage is higher compared to that of single-phase converters. As a result, the filtering requirements for smoothing out the load current is simpler. For these reasons, three-phase converters are used extensively in high-power variable-speed drives. Three single-phase half-wave converters in Fig. 4-1a can be connected to form a three-phase half-wave converter, as shown in Fig. 4-7a.

When thyristor T_1 is fired at $\omega t = \pi/6 + \alpha$, the phase voltage v_{an} appears across the load until thyristor T_2 is fired at $\omega t = 5\pi/6 + \alpha$. When thyristor T_2 is fired, thyristor T_1 is reverse biased, because the line-to-line voltage, v_{ab} ($= v_{an} - v_{bn}$), is negative and T_1 is turned off. The phase voltage v_{bn} appears across the load until thyristor T_3 is fired at $\omega t = 3\pi/2 + \alpha$. When thyristor T_3 is fired, T_2 is turned off and v_{cn} appears across the load until T_1 is fired again at the beginning of next cycle. Figure 4-7b shows the $v - i$ characteristics of the load and this is a one-quadrant converter. Figure 4-7c shows the input voltages, output voltage, and the current through thyristor T_1 for a highly inductive load. For a resistive load and $\alpha > \pi/6$, the load current would be discontinuous and each thyristor is self-commutated when the polarity of its phase voltage is reversed. The frequency of output ripple voltage is $3f_s$. This converter is not normally used in practical systems, because the supply currents contain dc components.

If the phase voltage is $v_{an} = V_m \sin \omega t$, the average output voltage for a continuous load current is

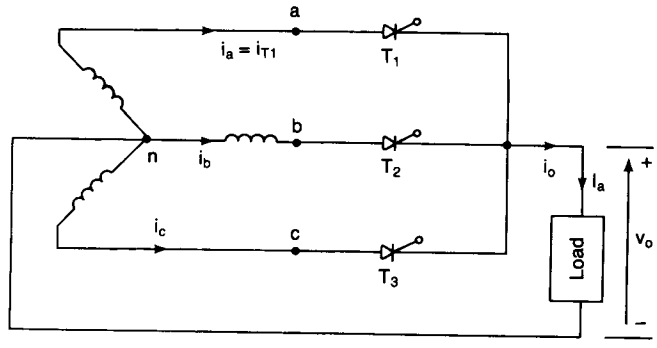
$$V_{\text{dc}} = \frac{3}{2\pi}\int_{\pi/6+\alpha}^{5\pi/6+\alpha} V_m \sin \omega t \, d(\omega t) = \frac{3\sqrt{3}\,V_m}{2\pi}\cos\alpha \qquad (4\text{-}51)$$

where V_m is the peak phase voltage. The maximum average output voltage that occurs at delay angle, $\alpha = 0$ is

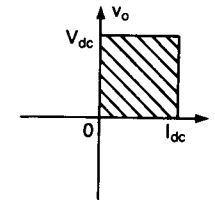
$$V_{dm} = \frac{3\sqrt{3}\,V_m}{2\pi}$$

and the normalized average output voltage is

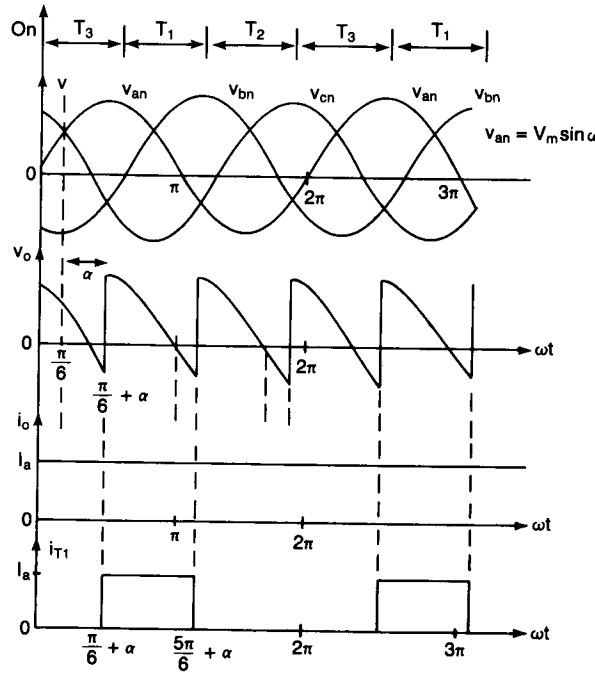
$$V_n = \frac{V_{\text{dc}}}{V_{dm}} = \cos\alpha \qquad (4\text{-}52)$$



(a) Circuit



(b) Quadrant



(c) For inductive load

Figure 4-7 Three-phase half-wave converter.

The rms output voltage is found from

$$V_{\text{rms}} = \left[\frac{3}{2\pi}\left[\int_{\pi/6+\alpha}^{5\pi/6+\alpha} V_m^2 \sin^2 \omega t \, d(\omega t)\right]\right]^{1/2}$$
$$= \sqrt{3}\, V_m \left(\frac{1}{6} + \frac{\sqrt{3}}{8\pi}\cos 2\alpha\right)^{1/2} \tag{4-53}$$

For a resistive load and $\alpha \geq \pi/6$:

$$V_{dc} = \frac{3}{2\pi}\int_{\pi/6+\alpha}^{\pi} V_m \sin\omega t\, d(\omega t) = \frac{3V_m}{2\pi}\left[1 + \cos\left(\frac{\pi}{6} + \alpha\right)\right] \tag{4-51a}$$

$$V_n = \frac{V_{dc}}{V_{dm}} = \frac{1}{\sqrt{3}}\left[1 + \cos\left(\frac{\pi}{6} + \alpha\right)\right] \tag{4-52a}$$

$$V_{rms} = \frac{3}{2\pi}\left[\int_{\pi/6+\alpha}^{\pi} V_m^2 \sin^2\omega t\, d(\omega t)\right]^{1/2}$$

$$= \sqrt{3}V_m\left[\frac{5}{24} - \frac{\alpha}{4\pi} + \frac{1}{8\pi}\sin\left(\frac{\pi}{3} + 2\alpha\right)\right]^{1/2} \tag{4-53a}$$

Example 4-6

A three-phase half-wave converter in Fig. 4-7a is operated from a three-phase Y-connected 208-V 60-Hz supply and the load resistance is $R = 10\ \Omega$. If it is required to obtain an average output voltage of 50% of the maximum possible output voltage, calculate the (a) delay angle α; (b) rms and average output currents; (c) average and rms thyristor currents; (d) rectification efficiency; (e) transformer utilization factor, TUF; and (f) input power factor, PF.

Solution The phase voltage is $V_s = 208/\sqrt{3} = 120.1$ V, $V_m = \sqrt{2}\,V_s = 169.83$ V, $V_n = 0.5$, and $R = 10\ \Omega$. The maximum output voltage is

$$V_{dm} = \frac{3\sqrt{3}\,V_m}{2\pi} = 3\sqrt{3} \times \frac{169.83}{2\pi} = 140.45 \text{ V}$$

The average output voltage, $V_{dc} = 0.5 \times 140.45 = 70.23$ V.

(a) For a resistive load, the load current is continuous if $\alpha \leq \pi/6$ and Eq. (4-52) gives $V_n \geq \cos(\pi/6) = 86.6\%$. With a resistive load and 50% output, the load current is discontinuous. From Eq. (4-52a), $0.5 = (1/\sqrt{3})[1 + \cos(\pi/6 + \alpha)]$ and the delay angle is $\alpha = 67.7°$.

(b) The average output current, $I_{dc} = V_{dc}/R = 70.23/10 = 7.02$ A. From Eq. (4-53a), $V_{rms} = 94.74$ V and the rms load current, $I_{rms} = 94.74/10 = 9.47$ A.

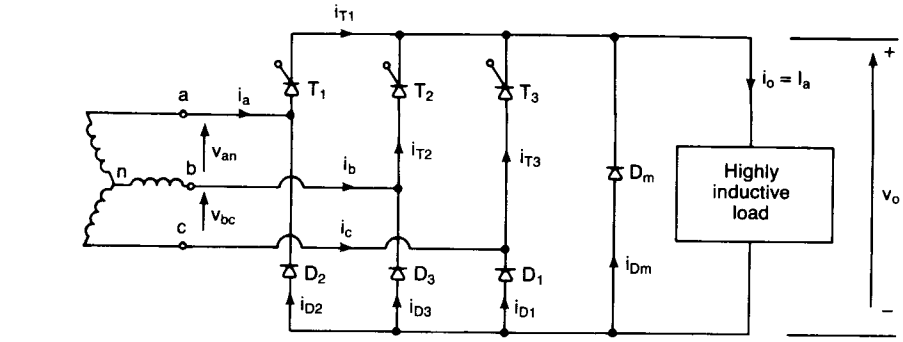
(c) The average current of a thyristor, $I_{DT} = I_{dc}/3 = 7.02/3 = 2.34$ A and the rms current of a thyristor, $I_{RT} = I_{rms}/\sqrt{3} = 9.47/\sqrt{3} = 5.47$ A.

(d) From Eq. (2-44) the rectification efficiency is $= 70.23 \times 7.02/(94.74 \times 9.47) = 54.95\%$.

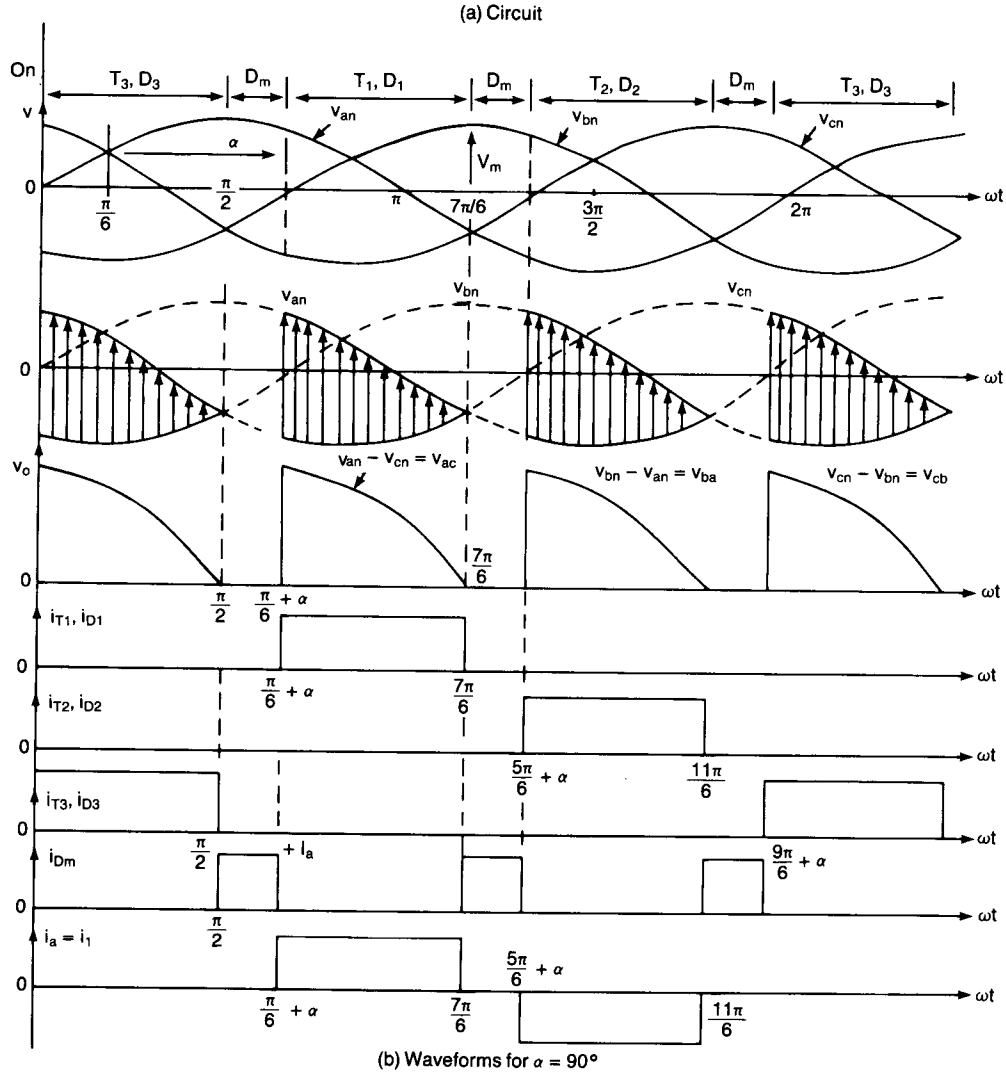
(e) The rms input line current is the same as the thyristor rms current, and the input volt-ampere rating, $VI = 3V_sI_s = 3 \times 120.1 \times 5.47 = 1970.84$ W. From Eq. (2-49), TUF $= 70.23 \times 7.02/1970.84 = 0.25$ or 25%.

(f) The output power, $P_o = I_{rms}^2 R = 9.47^2 \times 10 = 896.81$ W. The input power factor, PF $= 896.81/1970.84 = 0.455$ (lagging).

Note. Due to the delay angle, α, the fundamental component of input line current is also delayed with respect to the input phase voltage.



(a) Circuit



(b) Waveforms for $\alpha = 90°$

Figure 4-8 Three-phase semiconverter.

4-8 THREE-PHASE SEMICONVERTERS

Three-phase semiconverters are used in industrial applications up to the 120-kW level, where one-quadrant operation is required. The power factor of this converter decreases as the delay angle increases, but it is better than that of three-phase half-wave converter. Figure 4-8a shows a three-phase semiconverter with a highly inductive load and the load current has a negligible ripple content.

Figure 4-8b shows the waveforms for input voltages, output voltage, input current, and the current through thyristors and diodes. The frequency of output voltage is $3f_s$. The delay angle, α, can be varied from 0 to π. During the period $\pi/6 \leq \omega t < 7\pi/6$, thyristor T_1 is forward biased. If T_1 is fired at $\omega t = (\pi/6 + \alpha)$, T_1 and D_1 conduct and the line-to-line voltage v_{ac} appears across the load. At $\omega t = 7\pi/6$, v_{ac} starts to be negative and the freewheeling diode D_m conducts. The load current continues to flow through D_m; and T_1 and D_1 are turned off.

If there was no freewheeling diode, T_1 would continue to conduct until thyristor T_2 is fired at $\omega t = 5\pi/6 + \alpha$ and the freewheeling action would be accomplished through T_1 and D_2. If $\alpha \leq \pi/3$, each thyristor conducts for $2\pi/3$ and the freewheeling diode D_m does not conduct.

If we define the three line-neutral voltages as follows:

$$v_{an} = V_m \sin \omega t$$

$$v_{bn} = V_m \sin\left(\omega t - \frac{2\pi}{3}\right)$$

$$v_{cn} = V_m \sin\left(\omega t + \frac{2\pi}{3}\right),$$

the corresponding line-to-line voltages are

$$v_{ac} = v_{an} - v_{cn} = \sqrt{3}\, V_m \sin\left(\omega t - \frac{\pi}{6}\right)$$

$$v_{ba} = v_{bn} - v_{an} = \sqrt{3}\, V_m \sin\left(\omega t - \frac{5\pi}{6}\right)$$

$$v_{cb} = v_{cn} - v_{bn} = \sqrt{3}\, V_m \sin\left(\omega t + \frac{\pi}{2}\right)$$

where V_m is the peak phase voltage of a wye-connected source.

For $\alpha \geq \pi/3$, and discontinuous output voltage: the average output voltage is found from

$$V_{dc} = \frac{3}{2\pi}\int_{\pi/6+\alpha}^{7\pi/6} v_{ac}\, d(\omega t) = \frac{3}{2\pi}\int_{\pi/6+\alpha}^{7\pi/6} \sqrt{3}\, V_m \sin\left(\omega t - \frac{\pi}{6}\right) d(\omega t)$$

$$= \frac{3\sqrt{3}\, V_m}{2\pi}(1 + \cos\alpha) \qquad (4\text{-}54)$$

The maximum average output voltage that occurs at a delay angle of $\alpha = 0$ is $V_{dm} = 3\sqrt{3}\,V_m/\pi$ and the normalized average output voltage is

$$V_n = \frac{V_{dc}}{V_{dm}} = 0.5(1 + \cos\alpha) \tag{4-55}$$

The rms output voltage is found from

$$V_{rms} = \left[\frac{3}{2\pi}\int_{\pi/6+\alpha}^{7\pi/6} 3V_m^2 \sin^2\left(\omega t - \frac{\pi}{6}\right) d(\omega t)\right]^{1/2}$$

$$= \sqrt{3}\,V_m\left[\frac{3}{4\pi}\left(\pi - \alpha + \frac{1}{2}\sin 2\alpha\right)\right]^{1/2} \tag{4-56}$$

For $\alpha \leq \pi/3$, and continuous output voltage:

$$V_{dc} = \frac{3}{2\pi}\int_{\pi/6+\alpha}^{5\pi/6+\alpha} v_{ac}\, d(\omega t) = \frac{3\sqrt{3}\,V_m}{2\pi}(1 + \cos\alpha) \tag{4-54a}$$

$$V_n = \frac{V_{dc}}{V_{dm}} = 0.5(1 + \cos\alpha) \tag{4-55a}$$

$$V_{rms} = \left[\frac{3}{2\pi}\int_{\pi/6+\alpha}^{5\pi/6+\alpha} 3V_m^2 \sin^2\left(\omega t - \frac{\pi}{6}\right) d(\omega t)\right]^{1/2}$$

$$= \sqrt{3}\,V_m\left[\frac{3}{4\pi}\left(\pi - \alpha + \frac{1}{2}\sin 2\alpha\right)\right]^{1/2}$$

Example 4-7

Repeat Example 4-6 for the three-phase semiconductor in Fig. 4-8a.

Solution The phase voltage is $V_s = 208/\sqrt{3} = 120.1$ V, $V_m = \sqrt{2}\,V_s = 169.83$, $V_n = 0.5$, and $R = 10\ \Omega$. The maximum output voltage is

$$V_{dm} = \frac{3\sqrt{3}\,V_m}{\pi} = 3\sqrt{3} \times \frac{169.83}{\pi} = 280.9\ \text{V}$$

The average output voltage, $V_{dc} = 0.5 \times 280.9 = 140.45$ V.

(a) For $\alpha \geq \pi/3$ and Eq. (4-55) gives $V_n \leq (1 + \cos\pi/3)/2 = 75\%$. With a resistive load and 50% output, the output voltage is discontinuous. From Eq. (4-55), $0.5 = 0.5(1 + \cos\alpha)$, which gives the delay angle, $\alpha = 90°$.

(b) The average output current, $I_{dc} = V_{dc}/R = 140.45/10 = 14.05$ A. From Eq. (4-56),

$$V_{rms} = \sqrt{3} \times 169.83\left[\frac{3}{4\pi}\left(\pi - \frac{\pi}{2} + 0.5\sin 2 \times 90°\right)\right]^{1/2} = 180.13\ \text{V}$$

and the rms load current, $I_{rms} = 180.13/10 = 18.01$ A.

(c) The average current of a thyristor, $I_{DT} = I_{dc}/3 = 14.05/3 = 4.68$ A and the rms current of a thyristor, $I_{RT} = I_{rms}/\sqrt{3} = 18.01\sqrt{3} = 10.4$ A.

(d) From Eq. (2-44) the rectification efficiency is

$$\eta = \frac{140.45 \times 14.05}{180.13 \times 18.01} = 0.688 \text{ or } 68.8\%$$

(e) The rms input line current is $I_s = I_{rms}\sqrt{(2/3)} = 14.71$ A. The input volt-ampere rating, $VI = 3V_sI_s = 3 \times 120.1 \times 14.71 = 5300$. From Eq. (2-49), TUF = 140.45 × 14.05/5300 = 0.372.

(f) The output power, $P_o = I_{rms}^2R = 18.01^2 \times 10 = 3243.6$ W. The power factor is PF = 3243.6/5300 = 0.612 (lagging).

Note. The power factor is better than that of three-phase half-wave converters.

4-9 THREE-PHASE FULL CONVERTERS

Three-phase converters are extensively used in industrial applications up to the 120-kW level, where two-quadrant operation is required. Figure 4-9a shows a full-converter circuit with a highly inductive load. The thyristors are fired at an interval of $\pi/3$. The frequency of output ripple voltage is $6f_s$ and the filtering requirement is less than that of three-phase semi- and half-wave converters. At $\omega t = \pi/6 + \alpha$, thyristor T_6 is already conducting and thyristor T_1 is turned on. During interval $(\pi/6 + \alpha) \leq \omega t \leq (\pi/2 + \alpha)$, thyristors T_1 and T_6 conduct and the line-to-line voltage, v_{ab} $(= v_{an} - v_{bn})$ appears across the load. At $\omega t = \pi/2 + \alpha$, thyristor T_2 is fired and thyristor T_6 is reversed biased immediately. T_6 is turned off due to natural commutation. During interval $(\pi/2 + \alpha) \leq \omega t \leq (5\pi/6 + \alpha)$, thyristors T_1 and T_2 conduct and the line-to-line voltage, v_{ac} appears across the load. If the thyristors are numbered as shown in Fig. 4-9a, the firing sequence is 12, 23, 34, 45, 56, and 61. Figure 4-9b shows the waveforms for input voltage, output voltage, input current, and currents through thyristors.

If the line-neutral voltages are defined as

$$v_{an} = V_m \sin \omega t$$

$$v_{bn} = V_m \sin\left(\omega t - \frac{2\pi}{3}\right)$$

$$v_{cn} = V_m \sin\left(\omega t + \frac{2\pi}{3}\right),$$

the corresponding line-to-line voltages are

$$v_{ab} = v_{an} - v_{bn} = \sqrt{3}\, V_m \sin\left(\omega t + \frac{\pi}{6}\right)$$

$$v_{bc} = v_{bn} - v_{cn} = \sqrt{3}\, V_m \sin\left(\omega t - \frac{\pi}{2}\right)$$

$$v_{ca} = v_{cn} - v_{an} = \sqrt{3}\, V_m \sin\left(\omega t + \frac{\pi}{2}\right)$$

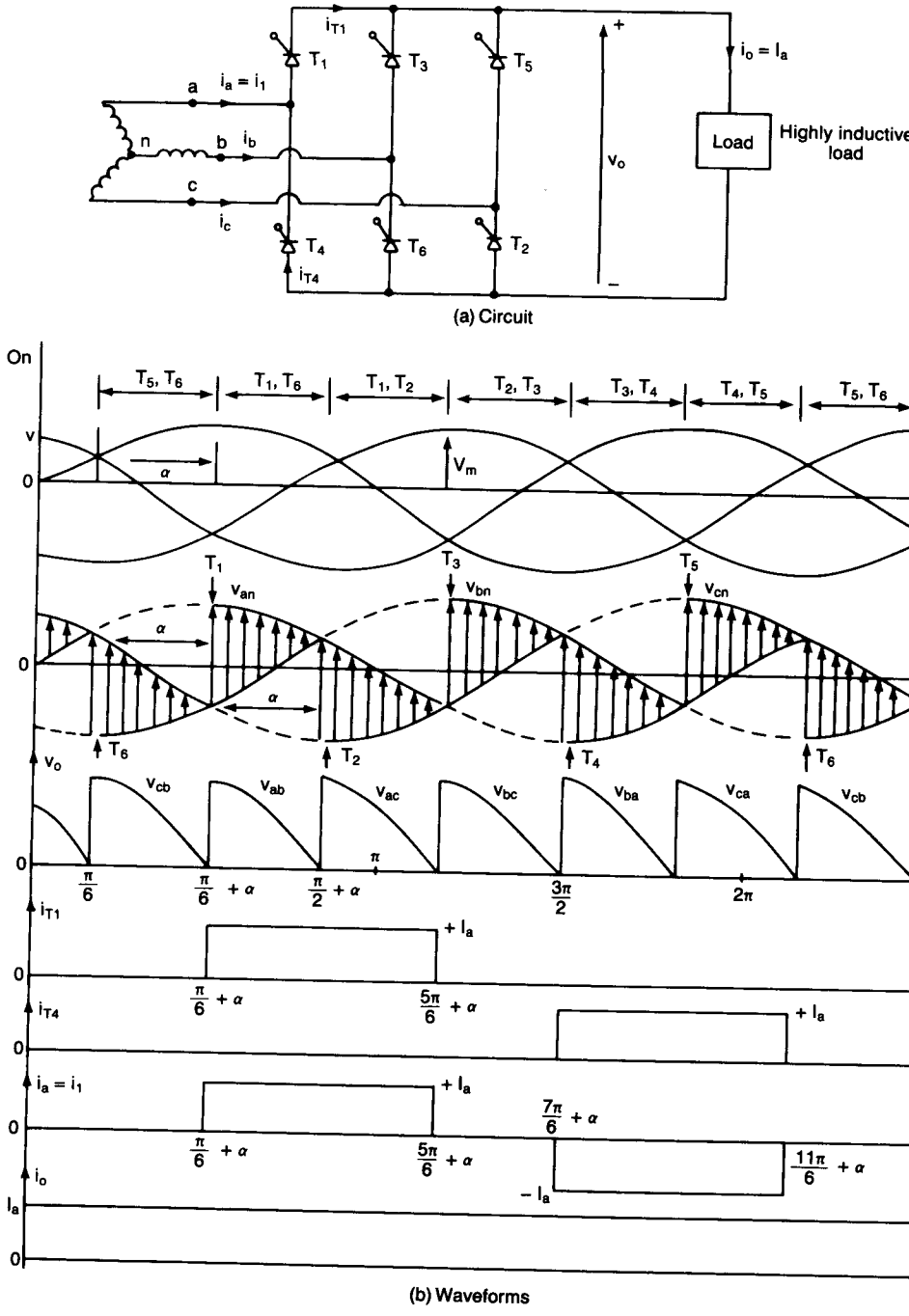


Figure 4-9 Three-phase full converter.

The average output voltage is found from

$$V_{dc} = \frac{3}{\pi}\int_{\pi/6+\alpha}^{\pi/2+\alpha} v_{ab}\, d(\omega t) = \frac{3}{\pi}\int_{\pi/6+\alpha}^{\pi/2+\alpha} \sqrt{3}\, V_m \sin\left(\omega t + \frac{\pi}{6}\right) d(\omega t) \qquad (4\text{-}57)$$

$$= \frac{3\sqrt{3}\, V_m}{\pi}\cos\alpha$$

The maximum average output voltage for delay angle, $\alpha = 0$ is

$$V_{dm} = 3\sqrt{3}\, V_m/\pi.$$

and the normalized average output voltage is

$$V_n = \frac{V_{dc}}{V_{dm}} = \cos\alpha \qquad (4\text{-}58)$$

The rms value of the output voltage is found from

$$V_{rms} = \left[\frac{3}{\pi}\int_{\pi/6+\alpha}^{\pi/2+\alpha} 3V_m^2 \sin^2\left(\omega t + \frac{\pi}{6}\right) d(\omega t)\right]^{1/2} \qquad (4\text{-}59)$$

$$= \sqrt{6}\, V_m \left(\frac{1}{4} + \frac{3\sqrt{3}}{8\pi}\cos 2\alpha\right)^{1/2}$$

Example 4-8

Repeat Example 4-6 for the three-phase full converter in Fig. 4-9a.

Solution The phase voltage, $V_s = 208/\sqrt{3} = 120.1$ V, $V_m = \sqrt{2}\, V_s = 169.83$, $V_n = 0.5$, and $R = 10\ \Omega$. The maximum output voltage, $V_{dm} = 3\sqrt{3}\, V_m/\pi = 3\sqrt{3} \times 169.83/\pi = 280.9$ V. The average output voltage, $V_{dc} = 0.5 \times 280.9 = 140.45$ V.

(a) From Eq. (4-58), $0.5 = \cos\alpha$, and the delay angle, $\alpha = 60°$.

(b) The average output current, $I_{dc} = V_{dc}/R = 140.45/10 = 14.05$ A. From Eq. (4-59),

$$V_{rms} = \sqrt{6} \times 169.83\left[\frac{1}{4} + \frac{3\sqrt{3}}{8\pi}\cos(2 \times 60°)\right]^{1/2} = 159.29 \text{ V},$$

and the rms current, $I_{rms} = 159.29/10 = 15.93$ A.

(c) The average current of a thyristor, $I_{DT} = I_{dc}/3 = 14.05/3 = 4.68$ A, and the rms current of a thyristor, $I_{RT} = I_{rms}\sqrt{2/6} = 15.93\sqrt{2/6} = 9.2$ A.

(d) From Eq. (2-44) the rectification efficiency is

$$\eta = \frac{140.45 \times 14.05}{159.29 \times 15.93} = 0.778 \text{ or } 77.8\%$$

(e) The rms input line current, $I_s = I_{rms}\sqrt{4/6} = 13$ A and the input volt-ampere rating, $VI = 3V_sI_s = 3 \times 120.1 \times 13 = 4683.9$ W. From Eq. (2-49), TUF $= 140.45 \times 14.05/4683.9 = 0.421$.

(f) The output power, $P_o = I_{rms}^2 R = 15.93^2 \times 10 = 2537.6$ W. The power factor, PF $= 2537.6/4683.9 = 0.542$ (lagging).

Note. The power factor is less than that of three-phase semiconverters, but higher than that of three-phase half-wave converters.

Example 4-9

The load current of a three-phase full converter in Fig. 4-9a is continuous with a negligible ripple content. (a) Express the input current in Fourier series, and determine the harmonic factor of input current, HF; displacement factor, DF; and the input power factor, PF. (b) If the delay angle, $\alpha = \pi/3$ and the peak input phase voltage, $V_m = 169.83$ V, calculate V_n, HF, DF, and PF.

Solution (a) The waveform for input current is shown in Fig. 4-9b and the instantaneous input current of a phase can be expressed in a Fourier series as

$$i_1(t) = I_{dc} + \sum_{n=1,2,\ldots}^{\infty} (a_n \cos n\omega t + b_n \sin n\omega t) \tag{4-60}$$

where

$$I_{dc} = \frac{1}{2\pi}\int_0^{2\pi} i_1(t)\, d(\omega t) = 0$$

$$a_n = \frac{1}{\pi}\int_0^{2\pi} i_1(t) \cos n\omega t\, d(\omega t)$$

$$= \frac{1}{\pi}\left[\int_{\pi/6+\alpha}^{5\pi/6+\alpha} I_a \cos n\omega t\, d(\omega t) - \int_{7\pi/6+\alpha}^{11\pi/6+\alpha} I_a \cos n\omega t\, d(\omega t)\right]$$

$$= -\frac{4I_a}{n\pi}\sin\frac{n\pi}{3}\sin n\alpha \qquad \text{for } n = 1, 3, 5, \ldots$$

$$= 0 \qquad \text{for } n = 2, 4, 6, \ldots$$

$$b_n = \frac{1}{\pi}\int_0^{2\pi} i_1(t) \sin n\omega t\, d(\omega t)$$

$$= \frac{1}{\pi}\left[\int_{\pi/6+\alpha}^{5\pi/6+\alpha} I_a \sin n\omega t\, d(\omega t) - \int_{7\pi/6+\alpha}^{11\pi/6+\alpha} I_a \sin n\omega t\, d(\omega t)\right]$$

$$= \frac{4I_a}{n\pi}\sin\frac{n\pi}{3}\cos n\alpha \qquad \text{for } n = 1, 3, 5, \ldots$$

$$= 0 \qquad \text{for } n = 2, 4, 6, \ldots$$

Since $I_{dc} = 0$, Eq. (4-60) can be written as

$$i_1(t) = \sum_{n=1,2,\ldots}^{\infty} \sqrt{2}\, I_n \sin(n\omega t + \phi_n)$$

where

$$\phi_n = \tan^{-1}\frac{a_n}{b_n} = -n\alpha \tag{4-61}$$

The rms value of the nth harmonic input current is given by

$$I_n = \frac{1}{\sqrt{2}}(a_n^2 + b_n^2)^{1/2} = \frac{2\sqrt{2}\, I_a}{n\pi}\sin\frac{n\pi}{3} \tag{4-62}$$

The rms value of the fundamental current is

$$I_1 = \frac{\sqrt{6}}{\pi} I_a = 0.7797 I_a$$

The rms input current,

$$I_s = \left[\frac{2}{2\pi}\int_{\pi/6+\alpha}^{5\pi/6+\alpha} I_a^2 \, d(\omega t)\right]^{1/2} = I_a\sqrt{\frac{2}{3}} = 0.8165 I_a$$

$$\text{HF} = \left[\left(\frac{I_s}{I_1}\right)^2 - 1\right]^{1/2} = \left[\left(\frac{\pi}{3}\right)^2 - 1\right]^{1/2} = 0.3108 \quad \text{or} \quad 31.08\%$$

$$\text{DF} = \cos \phi_1 = \cos -\alpha$$

$$\text{PF} = \frac{I_1}{I_s}\cos -\alpha = \frac{3}{\pi}\cos \alpha = 0.9549 \text{ DF}$$

(b) For $\alpha = \pi/3$, $V_n = \cos(\pi/3) = 0.5$ pu, HF = 31.08%, DF = $\cos 60° = 0.5$, and PF = 0.478 (lagging).

Note. If we compare the power factor with that of Example 4-8, where the load is purely resistive, we can notice that the input power factor depends on the power factor of the load.

4-10 THREE-PHASE DUAL CONVERTERS

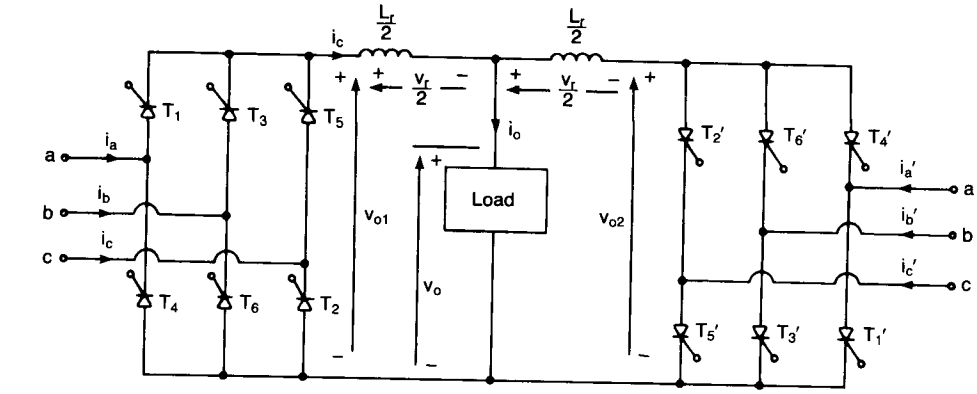
In many variable-speed drives, the four-quadrant operation is required and three-phase dual converters are extensively used in applications up to the 2000-kW level. Figure 4-10a shows three-phase dual converters where two three-phase converters are connected back to back. We have seen in Section 4-5 that due to the instantaneous voltage differences between the output voltages of converters, a circulating current flows through the converters. The circulating current is normally limited by circulating reactor, L_r as shown in Fig. 4-10a. The two converters are controlled in such a way that if α_1 is the delay angle of converter 1, the delay angle of converter 2 is $\alpha_2 = \pi - \alpha_1$. Figure 4-10b shows the waveforms for input voltages, output voltages, and the voltage across inductor L_r. The operation of each converter is exactly similar to that of three-phase full converter. During the interval $(\pi/6 + \alpha_1) \leq \omega t \leq (\pi/2 + \alpha_1)$, the line-to-line voltage v_{ab} appears across the output of converter 1 and v_{bc} appears across converter 2.

If the line-neutral voltages are defined as

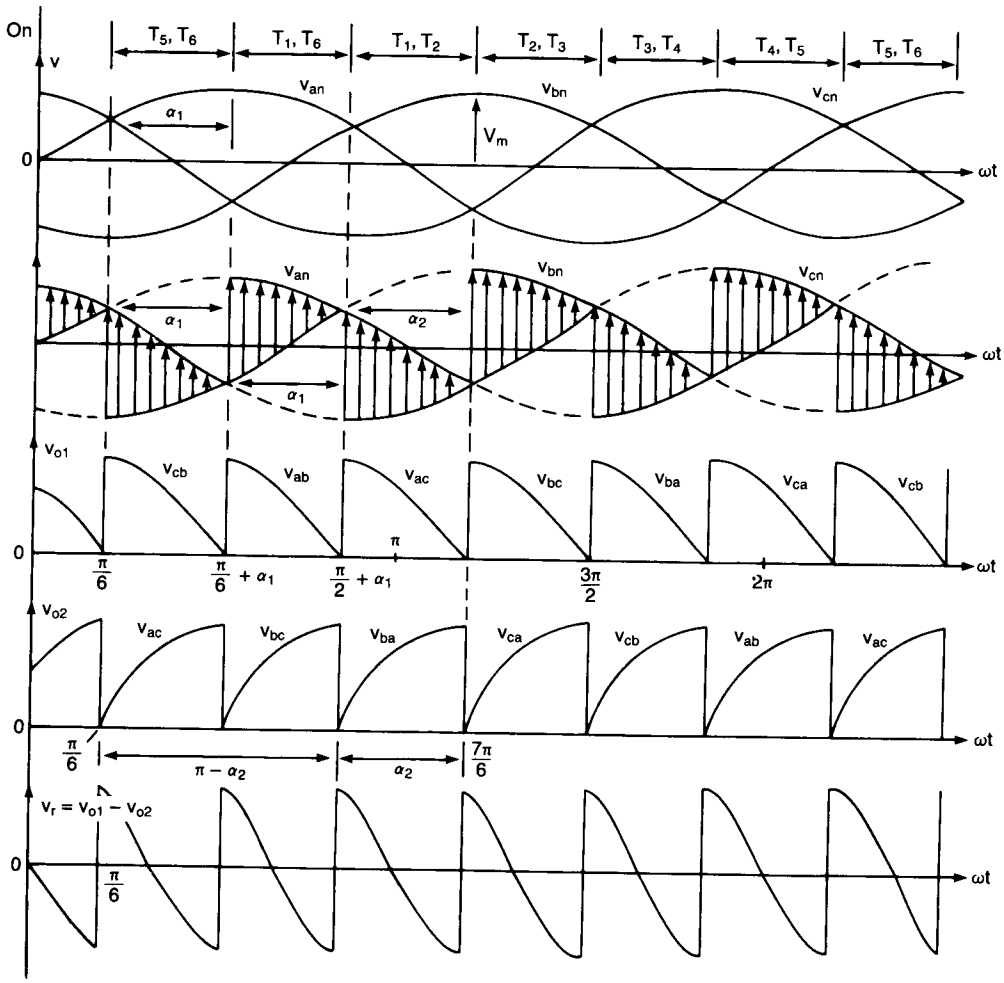
$$v_{an} = V_m \sin \omega t$$

$$v_{bn} = V_m \sin\left(\omega t - \frac{2\pi}{3}\right)$$

$$v_{cn} = V_m \sin\left(\omega t + \frac{2\pi}{3}\right)$$



(a) Circuit



(b) Waveforms

Figure 4-10 Three-phase dual converter.

the corresponding line-to-line voltages are

$$v_{ab} = v_{an} - v_{bn} = \sqrt{3}\, V_m \sin\left(\omega t + \frac{\pi}{6}\right)$$

$$v_{bc} = v_{bn} - v_{cn} = \sqrt{3}\, V_m \sin\left(\omega t - \frac{\pi}{2}\right)$$

$$v_{ca} = v_{cn} - v_{an} = \sqrt{3}\, V_m \sin\left(\omega t + \frac{\pi}{2}\right)$$

If v_{o1} and v_{o2} are the output voltages of converters 1 and 2, the instantaneous voltage across the inductor during interval $(\pi/6 + \alpha_1) \leq \omega t \leq (\pi/2 + \alpha_1)$ is

$$\begin{aligned} v_r &= v_{o1} - v_{o2} = v_{ab} - v_{bc} \\ &= \sqrt{3}V_m \left[\sin\left(\omega t + \frac{\pi}{6}\right) - \sin\left(\omega t - \frac{\pi}{2}\right)\right] \\ &= 3V_m \cos\left(\omega t - \frac{\pi}{6}\right) \end{aligned} \tag{4-63}$$

The circulating current can be found from

$$\begin{aligned} i_r(t) &= \frac{1}{\omega L_r}\int_{\pi/6+\alpha_1}^{\omega t} v_r\, d(\omega t) = \frac{1}{\omega L_r}\int_{\pi/6+\alpha_1}^{\omega t} 3V_m \cos\left(\omega t - \frac{\pi}{6}\right) d(\omega t) \\ &= \frac{3V_m}{\omega L_r}\left[\sin\left(\omega t - \frac{\pi}{6}\right) - \sin\alpha_1\right] \end{aligned} \tag{4-64}$$

The circulating current depends on delay angle and on inductance, L_r. This current becomes maximum when $\omega t = 2\pi/3$ and $\alpha_1 = 0$. Even without any external load, the converters would be continuously running due to the circulating current as a result of ripple voltage across the inductor. This allows smooth reversal of load current during the change over from one quadrant operation to another and provides fast dynamic responses, especially for electrical motor drives.

4-11 POWER FACTOR IMPROVEMENTS

The power factor of phase-controlled converters depends on delay angle α, and is in general low, especially at the low output voltage range. These converters generate harmonics into the supply. Forced commutations can improve the input power factor and reduce the harmonics levels. These forced-commutation techniques are becoming attractive to ac–dc conversion. With the advancement of power semiconductor devices (e.g., gate-turn-off thyristors), the forced commutation can be implemented in practical systems. In this section the basic techniques of forced commutation for ac–dc converters are discussed and can be classified as follows:

1. Extinction angle control

2. Symmetrical angle control
3. Pulse-width modulation
4. Sinusoidal pulse-width modulation

4-11.1 Extinction Angle Control

Figure 4-11a shows a single-phase semiconverter, where thyristors T_1 and T_2 are replaced by switches S_1 and S_2. The switching actions of S_1 and S_2 can be performed by gate-turn-off thyristors (GTOs). The characteristics of GTOs are such that GTOs can be turned on by applying a short positive pulse to its gate as in the case of normal thyristors and turned off by applying a short negative pulse to its gate.

In an extinction angle control, the switch S_1 is turned on at $\omega t = 0$ and is turned off by forced commutation at $\omega t = \pi - \beta$. The switch S_2 is turned on at $\omega t = \pi$ and is turned off at $\omega t = (2\pi - \beta)$. The output voltage is controlled by varying the extinction angle, β. Figure 4-11b shows the waveforms for input voltage, output voltage, input current, and the current through thyristor switches. The fundamental component of input current leads the input voltage, and the displacement factor (and power factor) is leading. In some applications, this feature may be desirable to simulate a capacitive load and to compensate for line voltage drops.

POWEREN.IR

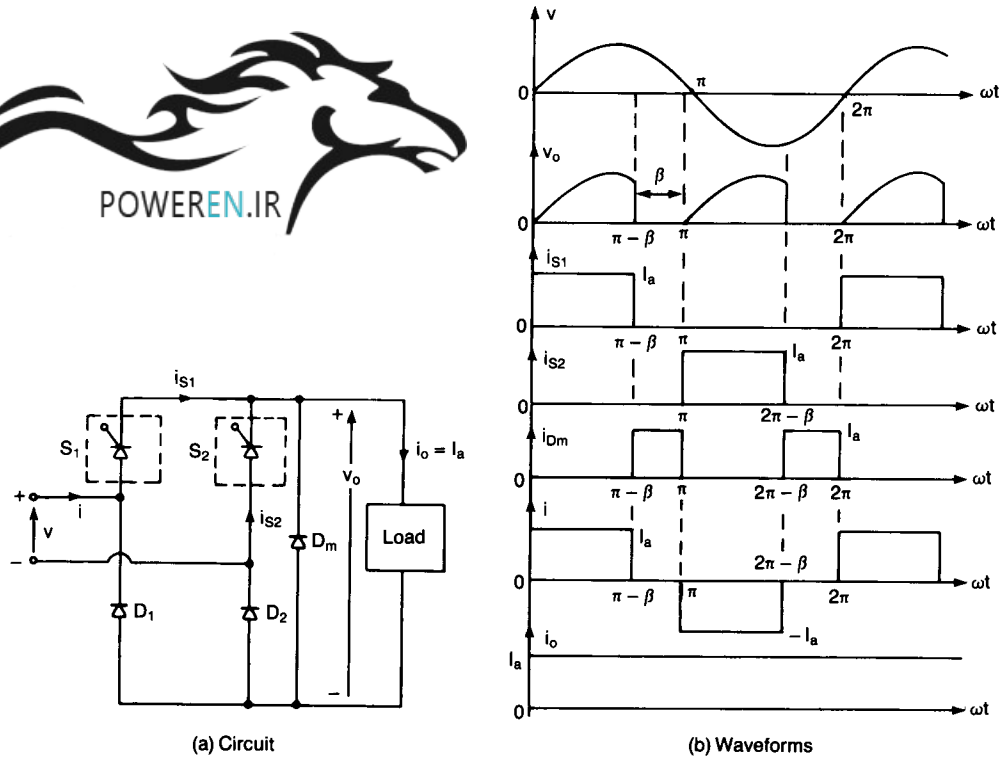


Figure 4-11 Single-phase forced-commutated semiconverter.

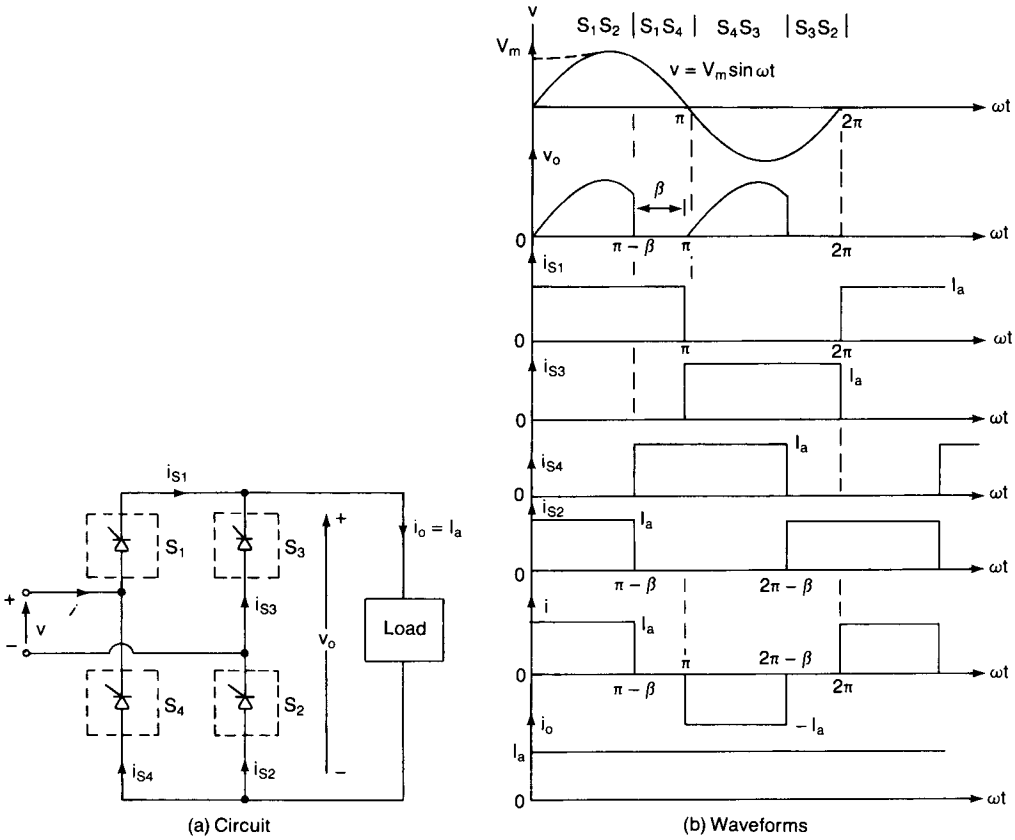


Figure 4-12 Single-phase forced-commutated full converter.

The average output voltage is found from

$$V_{dc} = \frac{2}{2\pi}\int_0^{\pi-\beta} V_m \sin \omega t \, d(\omega t) = \frac{V_m}{\pi}(1 + \cos \beta) \tag{4-65}$$

and V_{dc} can be varied from $2V_m/\pi$ to 0 by varying β from 0 to π. The rms output voltage is given by

$$\begin{aligned} V_{rms} &= \left[\frac{2}{2\pi}\int_0^{\pi-\beta} V_m^2 \sin^2 \omega t \, d(\omega t)\right]^{1/2} \\ &= \frac{V_m}{\sqrt{2}}\left[\frac{1}{\pi}\left(\pi - \beta + \frac{\sin 2\beta}{2}\right)\right]^{1/2} \end{aligned} \tag{4-66}$$

Figure 4-12a shows a single-phase full converter, where thyristors T_1, T_2, T_3, and T_4 are replaced by forced-commutated switches S_1, S_2, S_3, and S_4. The switches S_1 and S_2 are turned on simultaneously at $\omega t = 0$ and are turned off at $\omega t = \pi - \beta$. The switches S_3 and S_4 are turned on at $\omega t = \pi$ and are turned off at $\omega t = 2\pi - \beta$. For an inductive load, the freewheeling path must be provided by switches S_1S_4 or S_3S_2. The firing sequence would be 12, 14, 43, and 32. Figure 4-12b

shows the waveforms for input voltage, output voltage, input current, and the current through switches. Each switch conducts for 180° and this converter is operated as a semiconverter. The freewheeling action is accomplished through two switches of the same arm. The average and rms output voltage are expressed by Eq. (4-65) and Eq. (4-66), respectively.

The performance of semi- and full converters with extinction angle control are similar to that with phase-angle control, except the power factor is leading. With phase-angle control, the power factor is lagging.

4-11.2 Symmetrical Angle Control

The symmetrical angle control allows one-quadrant operation and Fig. 4-11a shows a single-phase semiconverter with forced-commutated switches S_1 and S_2. The switch S_1 is turned on at $\omega t = (\pi = \beta)/2$ and is turned off at $\omega t = (\pi + \beta)/2$. The switch S_2 is turned on at $\omega t = (3\pi - \beta)/2$ and off at $\omega t = (3\pi + \beta)/2$. The output voltage is controlled by varying conduction angle, β. Figure 4-13 shows the waveforms for input voltage, output voltage, input current, and the current through switches. The fundamental component of input current is in phase with the input voltage and the displacement factor is unity. Therefore, the power factor is improved.

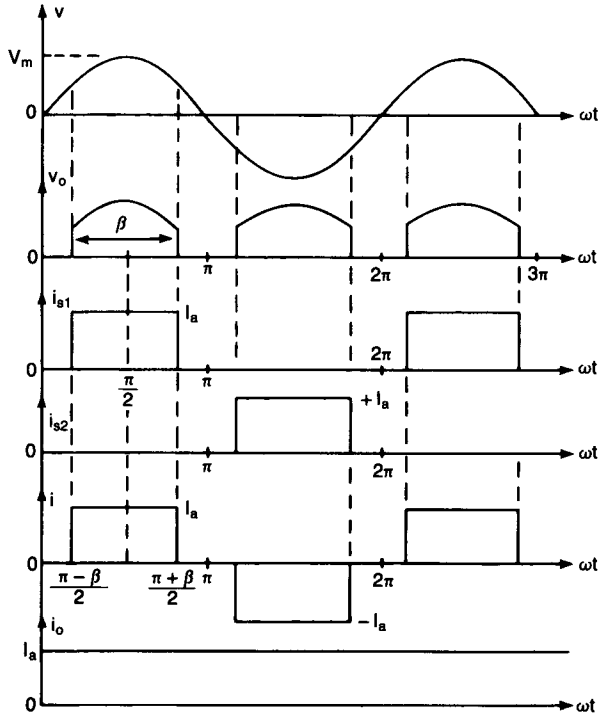


Figure 4-13 Symmetrical angle control.

The average output voltage is found from

$$V_{dc} = \frac{2}{2\pi}\int_{(\pi-\beta)/2}^{(\pi+\beta)/2} V_m \sin \omega t \, d(\omega t) = \frac{2V_m}{\pi}\sin\frac{\beta}{2} \tag{4-67}$$

and V_{dc} can be varied from $2V_m/\pi$ to 0 by varying β from 0 to π. The rms output voltage is given by

$$\begin{aligned} V_{rms} &= \left[\frac{2}{2\pi}\int_{(\pi-\beta)/2}^{(\pi+\beta)/2} V_m^2 \sin^2 \omega t \, d(\omega t)\right]^{1/2} \\ &= \frac{V_m}{\sqrt{2}}\left[\frac{1}{\pi}(\beta + \sin\beta)\right]^{1/2} \end{aligned} \tag{4-68}$$

Example 4-10

The single-phase full converter in Fig. 4-12a is operated with symmetrical angle control. The load current with an average value of I_a, is continuous, where the ripple content is negligible. (a) Express the input current of converter in Fourier series, determine the harmonic factor of input current, HF; displacement factor, DF; and input power factor, PF. (b) If the conduction angle is $\beta = \pi/3$ and the peak input voltage is $V_m = 169.83$ V, calculate V_{dc}, V_{rms}, HF, DF, and PF.

Solution (a) The waveform for input current is shown in Fig. 4-13 and the instantaneous input current can be expressed in Fourier series as

$$i(t) = I_{dc} + \sum_{n=1,2,\ldots}^{\infty} (a_n \cos n\omega t + b_n \sin n\omega t) \tag{4-69}$$

where

$$I_{dc} = \frac{1}{2\pi}\left[\int_{(\pi-\beta)/2}^{(\pi+\beta)/2} I_a \, d(\omega t) - \int_{(3\pi-\beta)/2}^{(3\pi+\beta)/2} I_a \, d(\omega t)\right] = 0$$

$$a_n = \frac{1}{\pi}\int_0^{2\pi} i(t)\cos n\omega t \, d(\omega t) = 0$$

$$b_n = \frac{1}{\pi}\int_0^{2\pi} i(t)\sin n\omega t \, d(\omega t) = \frac{4I_a}{n\pi}\sin\frac{n\beta}{2} \qquad \text{for } n = 1, 3, \ldots$$

$$= 0 \qquad \text{for } n = 2, 4, \ldots$$

Since $I_{dc} = 0$, Eq. (4-69) can be written as

$$i(t) = \sum_{n=1,2,\ldots}^{\infty} \sqrt{2}\, I_n \sin(n\omega t + \phi_n) \tag{4-70}$$

where

$$\phi_n = \tan^{-1}\frac{a_n}{b_n} = 0 \tag{4-71}$$

The rms value of the nth harmonic input current is given as

$$I_n = \frac{1}{\sqrt{2}}(a_n^2 + b_n^2)^{1/2} = \frac{2\sqrt{2}\, I_a}{n\pi}\sin\frac{n\beta}{2} \tag{4-72}$$

The rms value of the fundamental current is

$$I_1 = \frac{2\sqrt{2}\,I_a}{\pi}\sin\frac{\beta}{2} \tag{4-73}$$

The rms input current is found as

$$I_s = I_a\sqrt{\frac{\beta}{\pi}} \tag{4-74}$$

$$\text{HF} = \left[\left(\frac{I_s}{I_2}\right)^2 - 1\right]^{1/2} = \left[\frac{\pi\beta}{4(1-\cos\beta)} - 1\right]^{1/2} \tag{4-75}$$

$$\text{DF} = \cos\phi_1 = 1 \tag{4-76}$$

$$\text{PF} = \left(\frac{I_1}{I_s}\right)\text{DF} = \frac{2\sqrt{2}}{\sqrt{\beta\pi}}\sin\frac{\beta}{2} \tag{4-77}$$

(b) $\beta = \pi/3$ and DF = 1.0. From Eq. (4-67),

$$V_{dc} = \left(2 \times \frac{169.83}{\pi}\right)\sin\frac{\pi}{6} = 54.06 \text{ V}$$

From Eq. (4-68),

$$V_{rms} = \frac{169.83}{\sqrt{2}}\left[\frac{\beta + \sin\beta}{\pi}\right]^{1/2} = 93.72 \text{ V}$$

$$I_1 = I_a\left(\frac{2\sqrt{2}}{\pi}\right)\sin\frac{\pi}{6} = 0.4502I_a$$

$$I_s = I_a\sqrt{\frac{\beta}{\pi}} = 0.5774I_a$$

$$\text{HF} = \left[\left(\frac{I_s}{I_1}\right)^2 - 1\right]^{1/2} = 0.803 \text{ or } 80.3\%$$

$$\text{PF} = \frac{I_1}{I_s} = 0.7797 \text{ (lagging)}$$

Note. The power factor is improved significantly, even higher than that of the single-phase series full converter in Fig. 4-6a. However, the harmonic factor is increased.

4-11.3 Pulse-Width-Modulation Control

If the output voltage of single-phase semi- or full converters is controlled by varying the delay angle, extinction angle, or symmetrical angle, there is only one pulse per half-cycle in the input current of the converter, and as a result the lowest-order harmonic is the third. It is difficult to filter out the lower-order harmonics. In pulse-width-modulation (PWM) control, the converter switches are turned on and off several times during a half-cycle and the output voltage is controlled by varying

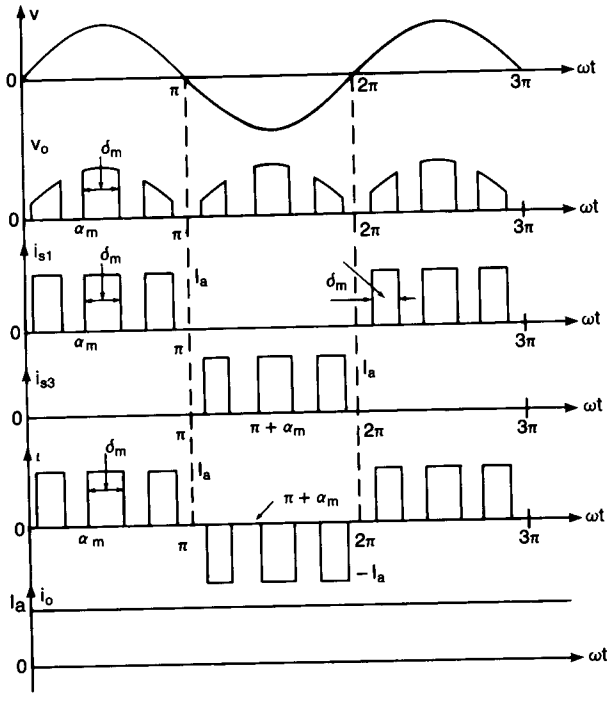


Figure 4-14 Pulse-width-modulation control.

the width of pulses. Figure 4-14 shows the input voltage, output voltage, and input current. The lower-order harmonics can be eliminated or reduced by selecting the number of pulses per half-cycle. However increasing the number of pulses would increase the magnitude of higher-order harmonics, which could easily be filtered out.

The output voltage and the performance parameters of the converter can be determined in two steps: (1) by considering only one pair of pulses such that if one pulse starts at $\omega t = \alpha_1$ and ends at $\omega t = \alpha_1 + \delta_1$, the other pulse starts at $\omega t = \pi + \alpha_1$ and ends at $\omega t = (\pi + \alpha_1 + \delta_1)$, and (2) by combining the effects of all pairs. If mth pulse starts at $\omega t = \alpha_m$ and its width is δ_m, the average output voltage due to p number of pulses is found from

$$V_{dc} = \sum_{m=1}^{p} \left[\frac{2}{2\pi} \int_{\alpha_m}^{\alpha_m + \delta_m} V_m \sin \omega t \, d(\omega t) \right]$$
$$= \frac{V_m}{\pi} \sum_{m=1}^{p} [\cos \alpha_m - \cos (\alpha_m + \delta_m)] \tag{4-78}$$

If the load current with an average value of I_a is continuous and has negligible ripple, the instantaneous input current can be expressed in a Fourier series as

$$i(t) = I_{dc} + \sum_{n=1,3,\ldots}^{\infty} (a_n \cos n\omega t + b_n \sin n\omega t) \tag{4-79}$$

Due to symmetry of the input current waveform, there will be no even harmonics and I_{dc} should be zero and the coefficients of Eq. (4-79) are:

$$a_n = \frac{1}{\pi}\int_0^{2\pi} i(t)\cos n\omega t\, d(\omega t)$$

$$= \sum_{m=1}^{p}\left[\frac{1}{\pi}\int_{\alpha_m}^{\alpha_m+\delta_m} I_a \cos n\omega t\, d(\omega t) - \frac{1}{\pi}\int_{\pi+\alpha_m}^{\pi+\alpha_m+\delta_m} I_a \cos n\omega t\, d(\omega t)\right] = 0$$

$$b_n = \frac{1}{\pi}\int_0^{2\pi} i(t)\sin n\omega t\, d(\omega t) \tag{4-80}$$

$$= \sum_{m=1}^{p}\left[\frac{1}{\pi}\int_{\alpha_m}^{\alpha_m+\delta_m} I_a \sin n\omega t\, d(\omega t) - \frac{1}{\pi}\int_{\pi+\alpha_m}^{\pi+\alpha_m+\delta_m} I_a \sin n\omega t\, d(\omega t)\right]$$

$$= \frac{2I_a}{n\pi}\sum_{m=1}^{p}[\cos n\alpha_m - \cos n(\alpha_m + \delta_m)]$$

Equation (4-79) can be rewritten as

$$i(t) = \sum_{n=1,3,\ldots}^{\infty} \sqrt{2}\, I_n \sin(n\omega t + \phi_n) \tag{4-81}$$

where $\phi_n = \tan^{-1}(a_n/b_n)$ and $I_n = (a_n^2 + b_n^2)^{1/2}/\sqrt{2}$.

4-11.4 Sinusoidal Pulse-Width Modulation

The widths of pulses are varied to control the output voltage. If there are p pulses per half-cycle of the same width, the maximum width of a pulse is π/p. The widths of pulses could be different. It is possible to choose the widths of pulses in such a way that certain harmonics could be eliminated. There are different methods of varying the widths of pulses and the most common one is the sinusoidal pulse-width modulation (SPWM). In sinusoidal PWM control as shown in Fig. 4-15, the pulse widths are generated by comparing a triangular voltage v_r of amplitude A_r and frequency f_r with a half-sinusoidal voltage v_c of variable amplitude A_c and frequency $2f_s$. The sinusoidal voltage, v_c, is in phase with the input phase voltage and has twice the supply frequency, f_s. The widths of the pulses (and the output voltage) are varied by changing the amplitude A_c or the modulation index, M from 0 to 1. The *modulation index* is defined as

$$M = \frac{A_c}{A_r} \tag{4-82}$$

In a sinusoidal PWM control, the displacement factor is unity and the power factor is improved. The lower-order harmonics are eliminated or reduced. For example, with four pulses per half-cycle the lowest-order harmonic is the fifth; and with six pulses per half-cycle, the lowest-order harmonic is the seventh. Computer programs, named PROG-1 and PROG-2, which are listed in Appendix F, can be used to evaluate the performances of uniform PWM and sinusoidal PWM control, respectively.

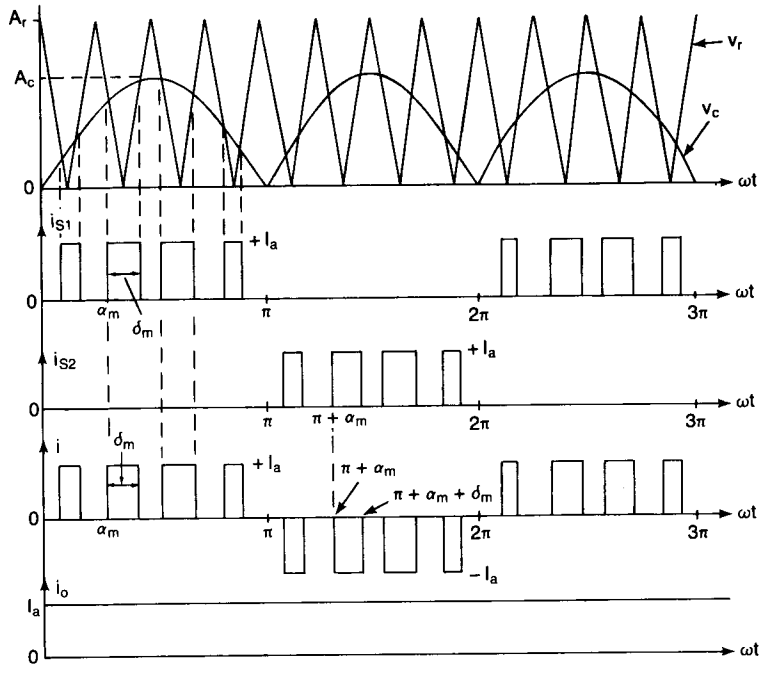


Figure 4-15 Sinusoidal pulse-width control.

4-12 DESIGN OF CONVERTER CIRCUITS

The design of converter circuits requires determining the ratings of thyristors and diodes. The thyristors and diodes are specified by the average current, rms current, peak current, and peak inverse voltage. In the case of controlled rectifiers, the current ratings of devices depend on the delay (or control) angle. The ratings of power devices must be designed under the worst-case condition and this occurs when the converter delivers the maximum average output voltage V_{dm}.

The output of converters contains harmonics that depend on the control (or delay) angle and the worst-case condition prevails under the minimum output voltage. The input and output filters must be designed under the minimum output voltage condition. The steps involved in designing the converters and filters are similar to that of rectifier circuit design in Section 2-11.

Example 4-11

A three-phase full converter is operated from a three-phase 230-V 60-Hz supply. The load is highly inductive and the average current is I_a = 150 A with negligible ripple content. If the delay angle is $\alpha = \pi/3$, determine the ratings of thyristors.

Solution The waveforms for thyristor currents are shown in Fig. 4-9b. $V_s = 230/\sqrt{3} = 132.79$ V, $V_m = 187.79$ V, and $\alpha = \pi/3$. From Eq. (4-57), $V_{dc} = 3(\sqrt{3}/\pi) \times 187.79 \times \cos(\pi/3) = 155.3$ V. The output power, $P_o = 155.3 \times 150 = 23{,}295$ W. The average current through a thyristor, $I_{DT} = 150/3 = 50$ A. The rms current through a thyristor, $I_{RT} = 150\sqrt{2/6} = 86.6$ A. The peak current through

a thyristor, I_{PT} = 150 A. The peak inverse voltage is the peak amplitude of line-to-line voltage, PIV = $\sqrt{3}\,V_m = \sqrt{3} \times 187.79 = 325.27$ V.

Example 4-12

A single-phase full converter as shown in Fig. 4-16 uses delay-angle control and is supplied from a 120-V 60-Hz supply. (a) Use the method of Fourier series to obtain expressions for output voltage, $v_L(t)$, and load current, $i_L(t)$, as a function of decay angle, α. (b) If $\alpha = \pi/3$, E = 10 V, L = 20 mH, and R = 10 Ω, determine the rms value of lowest-order harmonic current in the load. (c) If in part (b), a filter capacitor is connected across the load, determine the capacitor value to reduce the lowest-order harmonic to 10%.

Solution (a) The waveform for output voltage is shown in Fig. 4-3c. The frequency of output voltage is twice that of the main supply. The instantaneous output voltage can be expressed in a Fourier series as

$$v_L(t) = V_{dc} + \sum_{n=2,4,\ldots}^{\infty} (a_n \cos n\omega t + b_n \sin n\omega t) \tag{4-83}$$

where

$$V_{dc} = \frac{1}{2\pi}\int_{\alpha}^{2\pi+\alpha} V_m \sin \omega t\, d(\omega t) = \frac{2V_m}{\pi}\cos\alpha$$

$$a_n = \frac{2}{\pi}\int_{\alpha}^{\pi+\alpha} V_m \sin \omega t \cos n\omega t\, d(\omega t) = \frac{2V_m}{\pi}\left[\frac{\cos(n+1)\alpha}{n+1} - \frac{\cos(n-1)\alpha}{n-1}\right]$$

$$b_n = \frac{2}{\pi}\int_{\alpha}^{\pi+\alpha} V_m \sin \omega t \sin n\omega t\, d(\omega t) = \frac{2V_m}{\pi}\left[\frac{\sin(n+1)\alpha}{n+1} - \frac{\sin(n-1)\alpha}{n-1}\right]$$

The load impedance

$$Z = R + j(n\omega L) = [R^2 + (n\omega L)^2]^{1/2} \angle\theta_n$$

and $\theta_n = \tan^{-1}(n\omega L/R)$. Dividing $v_L(t)$ of Eq. (4-83) by load impedance Z and simplifying the sine and cosine terms give the instantaneous load current as

$$i_L(t) = I_{dc} + \sum_{n=2,4,\ldots}^{\infty} \sqrt{2}\, I_n \sin(n\omega t + \phi_n - \theta_n) \tag{4-84}$$

where $I_{dc} = (V_{dc} - E)/R$, $\phi_n = \tan^{-1}(a_n/b_n)$, and

$$I_n = \frac{1}{\sqrt{2}}\frac{(a_n^2 + b_n^2)^{1/2}}{\sqrt{R^2 + (n\omega L)^2}}$$

(b) If $\alpha = \pi/3$, E = 10 V, L = 20 mH, R = 10 Ω, $\omega = 2\pi \times 60$ rad/s, $V_m = \sqrt{2} \times 120 = 169.71$ V, and V_{dc} = 54.04 V.

$$I_{dc} = \frac{54.04 - 10}{10} = 4.40 \text{ A}$$

$$a_1 = -0.833, \quad b_1 = -0.866, \quad \phi_1 = 223.9°, \quad \theta_1 = 56.45°$$

$$a_2 = 0.433, \quad b_2 = -0.173, \quad \phi_2 = 111.79°, \quad \theta_2 = 71.65°$$

$$a_3 = -0.029, \quad b_3 = 0.297, \quad \phi_3 = -5.5°, \quad \theta_3 = 77.53°$$

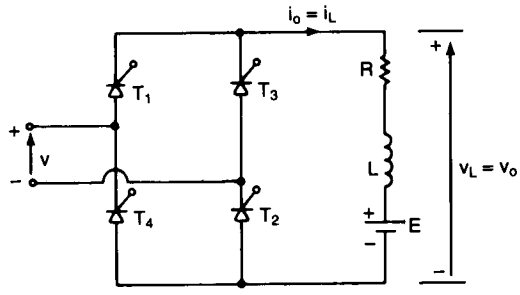


Figure 4-16 Single-phase full converter with *RL* load.

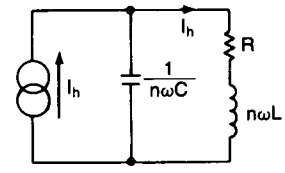


Figure 4-17 Equivalent circuit for harmonics.

$$i_L(t) = 4.4 + \frac{2V_m}{\pi[R^2 + (n\omega L)^2]^{1/2}}[1.2\sin(2\omega t + 223.9° - 56.45°) + 0.47\sin(4\omega t + 111.79° - 71.65°) + 0.3\sin(6\omega t - 5.5° - 77.53°) + \cdots]$$

$$= 4.4 + \frac{2 \times 169.71}{\pi[10^2 + (7.54n)^2]^{1/2}}[1.2\sin(2\omega t + 167.47°) + 0.47\sin(4\omega t + 40.14°) + 0.3\sin(6\omega t - 80.03°) + \cdots] \quad (4\text{-}85)$$

The second harmonic is the lowest one and its rms value is

$$I_2 = \frac{2 \times 169.71}{\pi[10^2 + (7.54 \times 2)^2]^{1/2}}\left(\frac{1.2}{\sqrt{2}}\right) = 5.07 \text{ A}$$

(c) Figure 4-17 shows the equivalent circuit for the harmonics. Using the current-divider rule, the harmonic current through the load is given by

$$\frac{I_h}{I_n} = \frac{1/(n\omega C)}{\{R^2 + [n\omega L - 1/(n\omega C)]^2\}^{1/2}}$$

For $n = 2$ and $\omega = 377$,

$$\frac{I_h}{I_n} = \frac{1/(2 \times 377C)}{\{10^2 + [2 \times 7.54 - 1/(2 \times 377C)]^2\}^{1/2}} = 0.1$$

and this gives $C = -670$ μF or 793 μF. Thus $C = 793$ μF.

4-13 EFFECTS OF LOAD AND SOURCE INDUCTANCES

We can notice from Eq. (4-85) that the load current harmonics depend on load inductances. The input power factor is calculated in Example 4-8 for a purely resistive load and in the Example 4-9 for a highly inductive load. We can also notice that the input power factor depends on the load power factor.

In the derivations of output voltages and the performance criteria of converters, we have assumed that the source has no inductances and resistances. Normally, the values of line resistances are small and can be neglected. The amount of voltage drop due to source inductances is the same as that of rectifiers

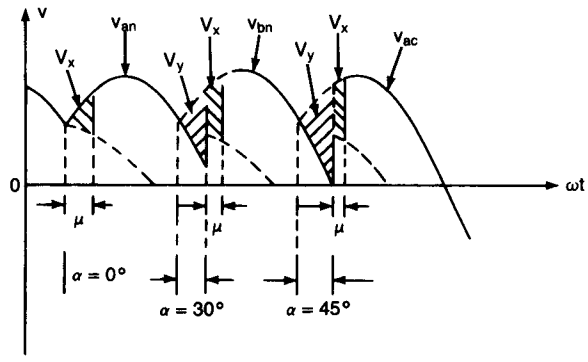


Figure 4-18 Relationship between the delay angle and overlap angle.

and does not change due to the phase control. Equation (2-96) can be applied to calculate the voltage drop due to the commutating reactance L_c. If all the line inductances are equal, Eq. (2-99) gives the voltage drop as $V_x = 6fL_cI_{dc}$ for a three-phase full converter.

The voltage drop is not dependent on delay angle, α_1, under normal operation. However, the commutation (or overlap) angle, μ, will vary with the delay angle. As the delay angle is increased, the overlap angle becomes smaller. This is illustrated in Fig. 4-18. The volt-time integral as shown by crosshatched areas is equal to $I_{dc}L_c$ and is independent of voltages. As the commutating phase voltage increases, the time required to commutate gets smaller, but the "volt-seconds" remain the same.

If V_x is the average voltage drop per commutation due to overlap and V_y is the average voltage reduction due to phase-angle control, the average output voltage for a delay angle of α is

$$V_{dc}(\alpha) = V_{dc}(\alpha = 0) - V_y = V_{dm} - V_y \tag{4-86}$$

and

$$V_y = V_{dm} - V_{dc}(\alpha) \tag{4-87}$$

The average output voltage with overlap angle μ and two commutations is

$$V_{dc}(\alpha + \mu) = V_{dc}(\alpha = 0) - 2V_x - V_y = V_{dm} - 2V_x - V_y \tag{4-88}$$

Substituting V_y from Eq. (4-87) into Eq. (4-88) we can write the voltage drop due to overlap as

$$2V_x = 2fI_{dc}L_c = V_{dc}(\alpha) - V_{dc}(\alpha + \mu) \tag{4-89}$$

The overlap angle, μ, can be determined from Eq. (4-89) for known values of load current, I_{dc}; commutating inductance, L_c; and delay angle, α. It should be noted that Eq. (4-89) is applicable to single-phase full converter.

Example 4-13

A three-phase full converter is supplied from a three-phase 230-V 60-Hz supply. The load current is continuous and has negligible ripple. If the average load current, I_{dc}

= 150 A and the commutating inductance, L_c = 0.1 mH, determine the overlap angle when (a) $\alpha = 10°$, (b) $\alpha = 30°$, and (c) $\alpha = 60°$.

Solution $V_m = \sqrt{2} \times 230/\sqrt{3} = 187.79$ V and $V_{dm} = 310.6$ V. From Eq. (4-57), $V_{dc}(\alpha) = 310.6 \cos \alpha$ and

$$V_{dc}(\alpha + \mu) = 310.6 \cos (\alpha + \mu)$$

For a three-phase converter, Eq. (4-89) can be modified to

$$6V_x = 6fI_{dc}L_c = V_{dc}(\alpha) - V_{dc}(\alpha + \mu) \tag{4-90}$$

$$6 \times 60 \times 150 \times 0.1 \times 10^{-3} = 310.6[\cos \alpha - \cos (\alpha + \mu)]$$

(a) For $\alpha = 10°$, $\mu = 4.66°$.
(b) For $\alpha = 30°$, $\mu = 1.94°$.
(c) For $\alpha = 60°$, $\mu = 1.14°$.

Regulators only:-

SUMMARY

In this chapter we have seen that average output voltage (and output power) of ac–dc converters can be controlled by varying the conduction time of thyristors. Depending on the types of supply, the converters could be single-phase or three-phase. For each type of supply, they can be half-wave, semi-, or full converters. The semi- and full converters are used extensively in practical applications. Although semiconverters provide better input power factor than that of full converters, these converters are only suitable for one-quadrant operation. Full converters and dual converters allow two-quadrant and four-quadrant operations, respectively. Three-phase converters are normally used in high-power applications and the frequency of output ripples is higher.

The input power factor, which is dependent on the load, can be improved and the voltage rating can be increased by series connection of converters. With forced commutations, the power factor can be further improved and certain lower-order harmonics can be reduced or eliminated.

The load current could be continuous or discontinuous depending on the load-time constant and delay angle. For the analysis of converters, the method of Fourier series is used. However, other techniques (e.g., transfer function approach or spectrum multiplication of switching function) can be used for the analysis of power switching circuits. The delay-angle control does not affect the voltage drop due to commutating inductances, and this drop is the same as that of normal diode rectifiers.

REFERENCES

1. P. C. Sen, *Thyristor DC Drives*. New York: Wiley-Interscience, 1981.
2. P. C., Sen and S. R. Doradla, "Evaluation of control schemes for thyristor controlled dc motors." *IEEE Transactions on Industrial Electronics and Control Instrumentation*, Vol. IECI25, No. 3 (August) 1978, pp. 247–255.

3. P. D. Ziogas, "Optimum voltage and harmonic control PWM techniques for 3-phase static UPS systems." *IEEE Transactions on Industry Applications*, Vol. 1A16, No. 4. (July) 1980, pp. 542–546.
4. M. H. Rashid, and M. Aboudina, "Analysis of forced-commutated techniques for ac-dc converters." *1st European Conference on Power Electronics and Applications*, Brussels, October 16–18, 1985, pp. 2.263–2.266.
5. P. D. Ziogas, and P. Photiadis, "An exact output current analysis of ideal static PWM inverters." *IEEE Transactions on Industry Applications*, Vol. 1A119, No. 2 (March–April) 1983, pp. 281–295.
6. M. H. Rashid and A. I. Maswood, "Analysis of 3-phase ac-dc converters under unbalanced supply conditions." *IEEE Industry Applications Conference Record*, 1985, pp. 1190–1194.

REVIEW QUESTIONS

4-1. What is a natural or line commutation?
4-2. What is a controlled rectifier?
4-3. What is a converter?
4-4. What is delay-angle control of converters?
4-5. What is a semiconverter? Draw two semiconverter circuits.
4-6. What is a full converter? Draw two full-converter circuits.
4-7. What is a dual converter? Draw two dual-converter circuits.
4-8. What is the principle of phase control?
4-9. What are the effects of removing the freewheeling diode in single-phase semiconverters?
4-10. Why is the power factor of semiconverters better than that of full converters?
4-11. What is the cause of circulating current in dual converters?
4-12. Why is a circulating current inductor required in dual converters?
4-13. What are the advantages and disadvantages of series converters?
4-14. How is the delay angle of one converter related to the delay angle of the other converter in a dual-converter system?
4-15. What is the inversion mode of converters?
4-16. What is the rectification mode of converters?
4-17. What is the frequency of the lowest-order harmonic in three-phase semiconverters?
4-18. What is the frequency of the lowest-order harmonic in three-phase full converters?
4-19. What is the frequency of the lowest-order harmonic in a single-phase semiconverter?
4-20. How are gate-turn-off thyristors turned on and off?
4-21. How is a phase-control thyristor turned on and off?
4-22. What is a forced commutation? What are the advantages of forced commutation for ac–dc converters?
4-23. What is extinction-angle control of converters?
4-24. What is symmetrical-angle control of converters?
4-25. What is pulse-width-modulation control of converters?

4-26. What is sinusoidal pulse-width-modulation control of a converter?

4-27. What is the modulation index?

4-28. How is the output voltage of a phase-control converter varied?

4-29. How is the output voltage of a sinusoidal PWM control converter varied?

4-30. Does the commutation angle depend on the delay angle of converters?

4-31. Does the voltage drop due to commutating inductances depend on the delay angle of converters?

4-32. Does the input power factor of converters depend on the load power factor?

4-33. Do the output ripple voltages of converters depend on the delay angle?

PROBLEMS

4-1. A single-phase half-wave converter in Fig. 4-1a is operated from a 120-V 60-Hz supply. If the load resistive load is $R = 10\ \Omega$ and the delay angle is $\alpha = \pi/3$, determine the (**a**) efficiency; (**b**) form factor; (**c**) ripple factor; (**d**) transformer utilization factor; and (**e**) peak inverse voltage (PIV) of thyristor T_1.

4-2. A single-phase half-wave converter in Fig. 4-1a is operated from a 120-V 60-Hz supply and the load resistive load is $R = 10\ \Omega$. If the average output voltage is 25% of the maximum possible average output voltage, calculate the (**a**) delay angle; (**b**) rms and average output currents; (**c**) average and rms thyristor currents; and (**d**) input power factor.

4-3. A single-phase half-converter in Fig. 4-1a is supplied from a 120-V 60-Hz supply and a freewheeling diode is connected across the load. The load consists of series-connected resistance, $R = 10\ \Omega$, inductance, $L = 5$ mH, and battery voltage, $E = 20$ V. (**a**) Express the instantaneous output voltage in a Fourier series, and (**b**) determine the rms value of the lowest-order output harmonic current.

4-4. A single-phase semiconverter in Fig. 4-2a is operated from a 120-V 60-Hz supply. The load current with an average value of I_a is continuous with negligible ripple content. The turns ratio of the transformer is unity. If the delay angle is $\alpha = \pi/3$, calculate the (**a**) harmonic factor of input current; (**b**) displacement factor; and (**c**) input power factor.

4-5. Repeat Prob. 4-2 for the single-phase semiconverter in Fig. 4-2a.

4-6. The single-phase semiconverter in Fig. 4-2a is operated from a 120-V 60-Hz supply. The load consists of series-connected resistance, $R = 10\ \Omega$, inductance, $L = 5$ mH, and battery voltage, $E = 20$ V. (**a**) Express the output voltage in a Fourier series, and (**b**) determine the rms value of the lowest-order output harmonic current.

4-7. Repeat Prob. 4-4 for the single-phase full converter in Fig. 4-3a.

4-8. Repeat Prob. 4-2 for the single-phase full converter in Fig. 4-3a.

4-9. Repeat Prob. 4-6 for the single-phase full converter in Fig. 4-3a.

4-10. The dual converter in Fig. 4-4a is operated from a 120-V 60-Hz supply and delivers ripple-free average current of $I_{dc} = 20$ A. The circulating inductance, $L_r = 5$ mH, and the delay angles are $\alpha_1 = 30°$ and $\alpha_2 = 150°$. Calculate the peak circulating current and the peak current of converter 1.

4-11. A single-phase series semiconverter in Fig. 4-5a is operated from a 120-V 60-Hz supply

and the load resistance, $R = 10\ \Omega$. If the average output voltage is 75% of the maximum possible average output voltage, calculate the (**a**) delay angles of converters, (**b**) rms and average output currents, (**c**) average and rms thyristor currents, and (**d**) input power factor.

4-12. A single-phase series semiconverter in Fig. 4-5a is operated from a 120-V 60-Hz supply. The load current with an average value of I_a is continuous and the ripple content is negligible. The turns ratio of the transformer is $N_p/N_s = 2$. If delay angles are $\alpha_1 = 0$ and $\alpha_2 = \pi/3$, calculate the (**a**) harmonic factor of input current; (**b**) displacement factor; and (**c**) input power factor.

4-13. Repeat Prob. 4-11 for the single-phase series full converter in Fig. 4-6a.

4-14. Repeat Prob. 4-12 for the single-phase series full converter in Fig. 4-6a.

4-15. The three-phase half-wave converter in Fig. 4-7a is operated from a three-phase Y-connected 220-V 60-Hz supply and a freewheeling diode is connected across the load. The load current with an average value of I_a is continuous and the ripple content is negligible. If the delay angle, $\alpha = \pi/3$, calculate the (**a**) harmonic factor of input current; (**b**) displacement factor; and (**c**) input power factor.

4-16. The three-phase half-wave converter in Fig. 4-7a is operated from a three-phase Y-connected 220-V 60-Hz supply and the load resistance is $R = 10\ \Omega$. If the average output voltage is 25% of the maximum possible average output voltage, calculate the (**a**) delay angle; (**b**) rms and average output currents; (**c**) average and rms thyristor currents; (**d**) rectification efficiency; (**e**) transformer utilization factor; and (**f**) input power factor.

4-17. The three-phase half-wave converter in Fig. 4-7a is operated from a three-phase Y-connected 220-V 60-Hz supply and a freewheeling diode is connected across the load. The load consists of series-connected resistance, $R = 10\ \Omega$, inductance, $L = 5$ mH, and battery voltage, $E = 20$ V. (**a**) Express the instantaneous output voltage in a Fourier series, and (**b**) determine the rms value of the lowest-order harmonic on the output current.

4-18. The three-phase semiconverter in Fig. 4-8a is operated from a three-phase Y-connected 220-V 60-Hz supply. The load current with an average value of I_a is continuous with negligible ripple content. The turns ratio of the transformer is unity. If the delay angle is $\alpha = 2\pi/3$, calculate the (**a**) harmonic factor of input current; (**b**) displacement factor; and (**c**) input power factor.

4-19. Repeat Prob. 4-16 for the three-phase semiconverter in Fig. 4-8a.

4-20. Repeat Prob. 4-19 if the average output voltage is 90% of the maximum possible output voltage.

4-21. Repeat Prob. 4-17 for the three-phase semiconverter in Fig. 4-8a.

4-22. Repeat Prob. 4–18 for the three-phase full converter in Fig. 4-9a.

4-23. Repeat Prob. 4-16 for the three-phase full converter in Fig. 4-9a.

4-24. Repeat Prob. 4-17 for the three-phase full converter in Fig. 4-9a.

4-25. The three-phase dual converter in Fig. 4-10a is operated from a three-phase Y-connected 220-V 60-Hz supply and the load resistance, $R = 10\ \Omega$. The circulating inductance, $L_r = 5$ mH, and the delay angles are $\alpha_1 = 60°$ and $\alpha_2 = 120°$. Calculate the peak circulating current and the peak current of converters.

4-26. The single-phase semiconverter in Fig. 4-11a is operated from a 120-V 60-Hz supply and uses an extinction angle control. The load current with an average value of I_a is continuous and has negligible ripple content. If the extinction angle is $\beta = \pi/3$,

calculate the (**a**) output V_{dc} and V_{rms}; (**b**) harmonic factor of input current; (**c**) displacement factor; and (**d**) input power factor.

4-27. Repeat Prob. 4-26 for the single-phase full converter in Fig. 4-12a.

4-28. Repeat Prob. 4-18 if symmetrical-angle control is used.

4-29. Repeat Prob. 4-18 if extincction-angle control is used.

4-30. The single-phase semiconverter in Fig. 4-11a is operated with a sinusoidal PWM control and is supplied from a 120-V 60-Hz supply. The load current with an average value of I_a is continuous with negligible ripple content. There are five pulses per half-cycle and the pulses are $\alpha_1 = 7.93°$, $\delta_1 = 5.82°$; $\alpha_2 = 30°$, $\delta_2 = 16.25°$; $\alpha_3 = 52.07°$, $\delta_3 = 127.93°$; $\alpha_4 = 133.75°$, $\delta_4 = 16.25°$; and $\alpha_5 = 166.25°$, $\delta_5 = 5.82°$. Calculate the (**a**) V_{dc} and V_{rms}; (**b**) harmonic factor of input current; (**c**) displacement factor; and (**d**) input power factor.

4-31. Repeat Prob. 4-30 for five pulses per half-cycle with equal pulse width, $M = 0.8$.

4-32. A three-phase semiconverter is operated from a three-phase Y-connected 220-V 60-Hz supply. The load current is continuous and has negligible ripple. The average load current is $I_{dc} = 150$ A and commutating inductance per phase is $L_c = 0.5$ mH. Determine the overlap angle if (**a**) $\alpha = \pi/6$, and (**b**) $\alpha = \pi/3$.

5

Static Switches

5-1 INTRODUCTION

Thyristors that can be turned on and off within a few microseconds may be operated as fast-acting switches to replace mechanical and electromechanical circuit breakers. For low-power dc applications, power transistors can also be used as switches. The static switches have many advantages (e.g., very high switching speeds, no moving parts, and no contact bounce upon closing).

In addition to normal applications as static switches, the thyristor (or transistor) circuits can be designed to provide time-delay, latching, over- and undercurrent, and voltage detections. The transducers for detecting mechanical, electrical, position, proximity, and so on, signals can provide the gating or control signals for the thyristors (or transistors).

The static switches can be classified into two types: (1) ac switches, and (2) dc switches. The ac switches can be subdivided into (a) single-phase, and (b) three-phase. In the case of ac switches, the thyristors are line or natural commutated and the switching speed is limited by the frequency of the ac supply and the turn-off time of thyristors. The dc switches are forced commutated and the switching speed depends on the commutation circuitry and the turn-off time of fast thyristors.

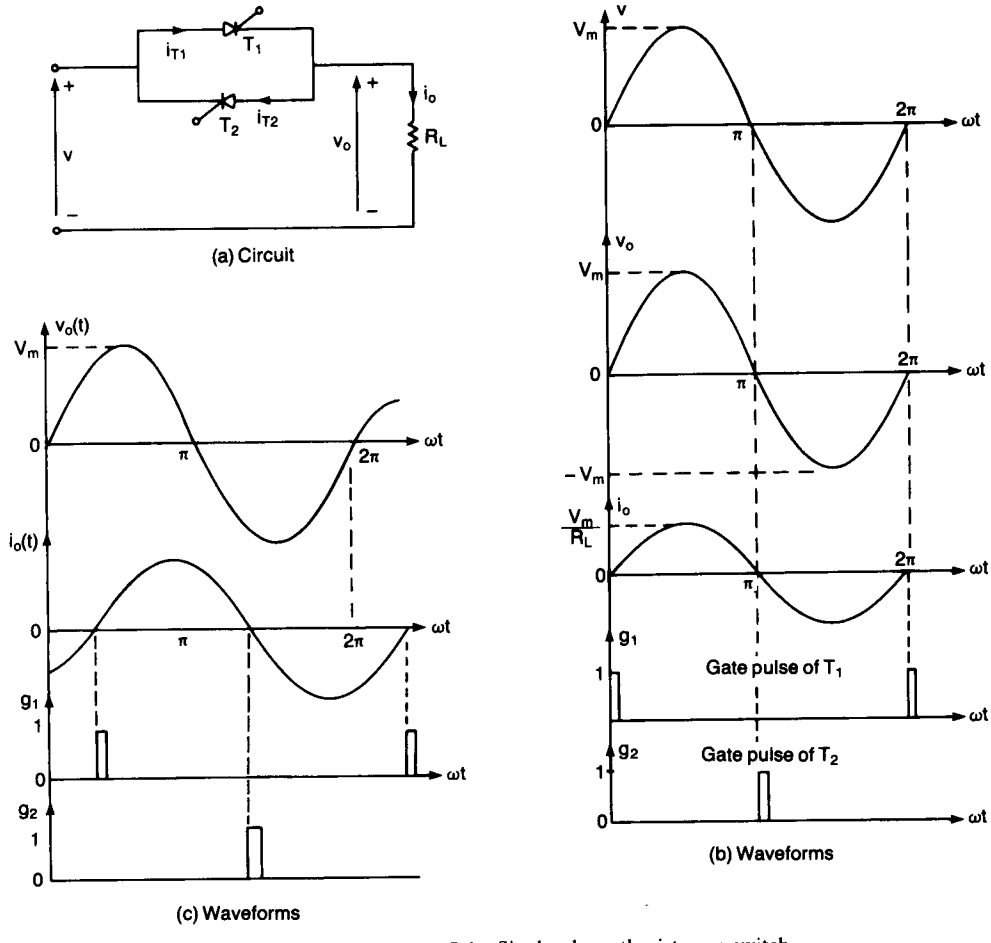


Figure 5-1 Single-phase thyristor ac switch.

5-2 SINGLE-PHASE AC SWITCHES

The circuit diagram of a single-phase full-wave switch is shown in Fig. 5-1a, where the two thyristors are connected in inverse parallel. Thyristor T_1 is fired at $\omega t = 0$ and thyristor T_2 is fired at $\omega t = \pi$. The output voltage is the same as the input voltage. The thyristors act like switches and are line commutated. The waveforms for the input voltage, output voltage, and output current are shown in Fig. 5-1b.

With an inductive load, thyristor T_1 should be fired when the current passes through the zero crossing during the positive half-cycle of input voltage and thyristor T_2 should be fired when the current passes through the zero crossing during the negative half-cycle of input voltage. The triggering pulses for T_1 and T_2 are shown in Fig. 5-1c. A TRIAC may be used instead of two thyristors as shown in Fig. 5-2.

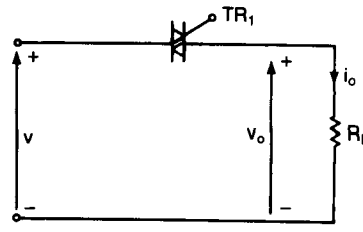


Figure 5-2 Single-phase TRIAC ac switch.

If the instantaneous line current is $i(t) = I_m \sin \omega t$, the rms line current is

$$I_s = \left[\frac{2}{2\pi}\int_0^{\pi} I_m^2 \sin^2 \omega t \, d(\omega t)\right]^{1/2} = \frac{I_m}{\sqrt{2}} \tag{5-1}$$

Since each thyristor carries current for only one-half cycle, the average current through each thyristor is

$$I_{av} = \frac{1}{2\pi}\int_0^{\pi} I_m \sin \omega t \, d(\omega t) = \frac{I_m}{\pi} \tag{5-2}$$

and the rms current of each thyristor is

$$I_{rms} = \left[\frac{1}{2\pi}\int_0^{\pi} I_m^2 \sin^2 \omega t \, d(\omega t)\right]^{1/2} = \frac{I_m}{2} \tag{5-3}$$

The circuit in Fig. 5-1a can be modified as shown in Fig. 5-3a, where the two thyristors have a common cathode and the gating signals have a common terminal. Thyristor T_1 and diode D_1 conduct for one half-cycle and thyristor T_2 and diode D_2 conduct for the other half-cycle.

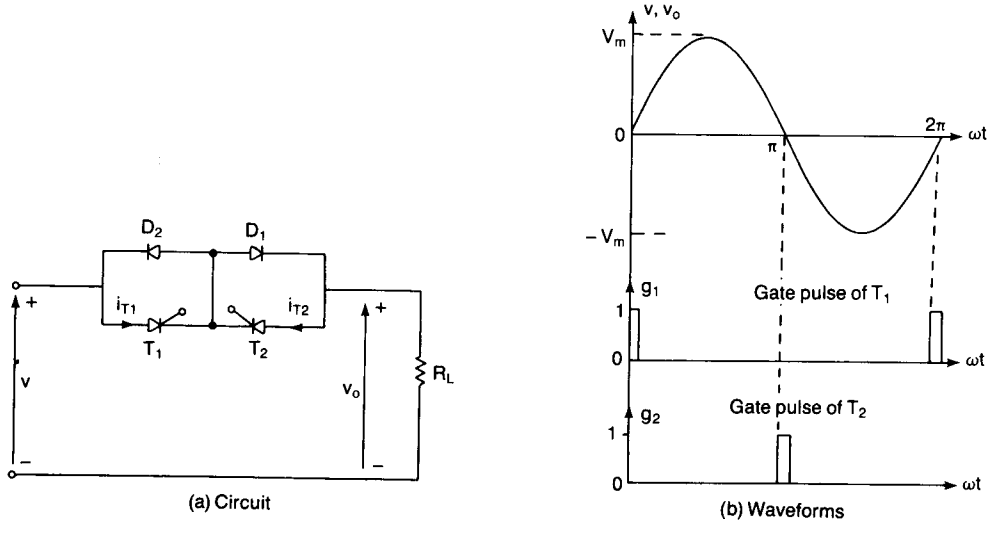


Figure 5-3 Single-phase bridge diode and thyristor ac switch.

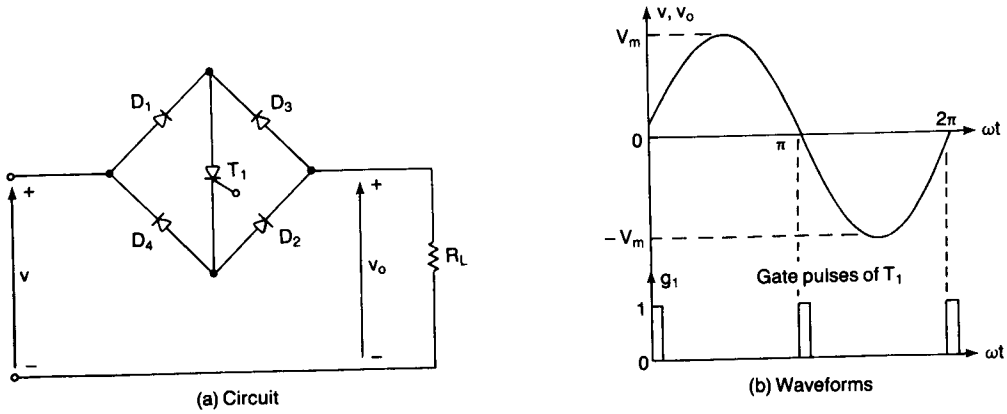


Figure 5-4 Single-phase bridge rectifier and thyristor ac switch.

A diode bridge rectifier and a thyristor T_1 as shown in Fig. 5-4a can perform the same function as that of Fig. 5-1a. The current though the load is ac and that through thyristor T_1 is dc. A transistor can replace thyristor T_1. The unit comprising of the transistor (or thyristor) and bridge rectifier is known as a *bidirectional switch*.

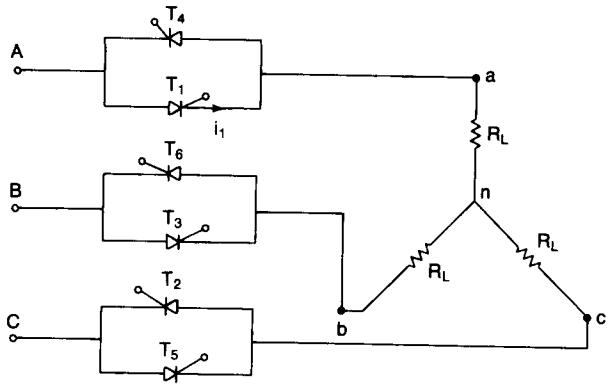
5-3 THREE-PHASE AC SWITCHES

The concept of single-phase ac switching can be extended to three-phase applications. Three single-phase switches in Fig. 5-1a can be connected to form a three-phase switch as shown in Fig. 5-5a. The gating signals for thyristors and the current through T_1 are shown in Fig. 5-5b. The load could be connected in either wye or delta.

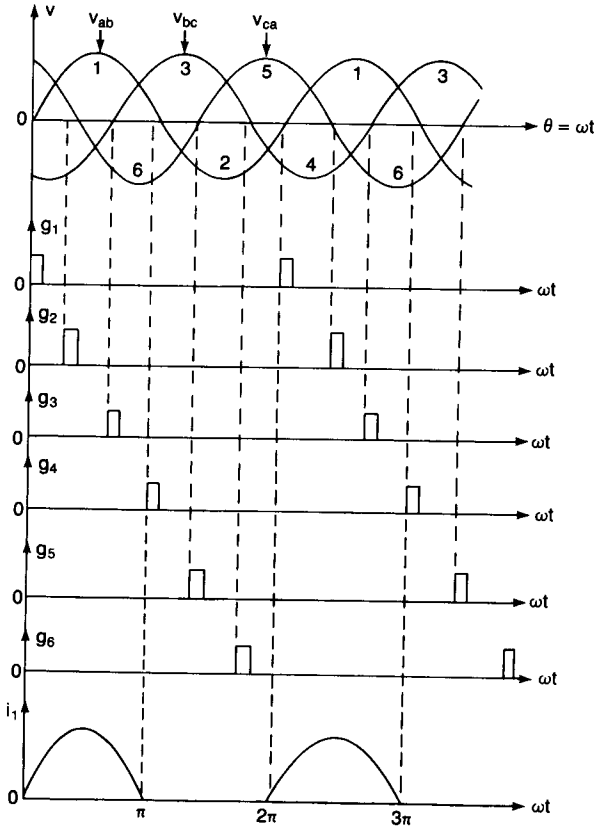
To reduce the number of thyristors and costs, the circuit with a diode and a thyristor similar to that in Fig. 5-3a can also be used to form a three-phase switch as shown in Fig. 5-6. In case of two thyristors connected in back to back, there is the possibility to stop the current flow in every half-cycle. But with a diode and a thyristor, the current flow can only be stopped in every cycle of input voltage and the reaction time becomes slow.

5-4 THREE-PHASE REVERSING SWITCHES

The reversal of three-phase power supplied to a load can be achieved by extending the three-phase switch in Fig. 5-5a with two more single-phase switches, as shown in Fig. 5-7. Under normal operation, thyristors T_7 through T_{10} are turned off by gate pulse inhibiting (or suppression) and thyristors T_1 through T_6 are turned on. Line A feeds terminal a, line B feeds terminal b, and line C feeds terminal c.



(a) Circuit



(b) Waveforms

Figure 5-5 Three-phase thyristor ac switch.

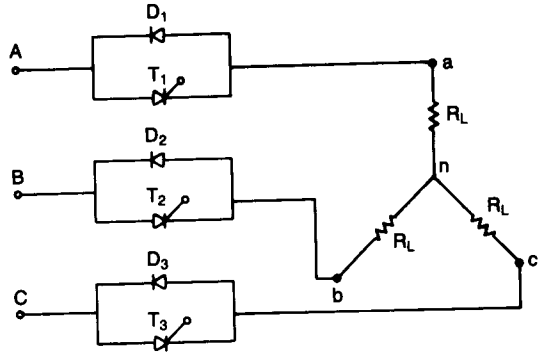


Figure 5-6 Three-phase diode and thyristor ac switch.

Under phase-reversing operation, thyristors T_2, T_3, T_5, and T_6 are turned off by gate pulse and thyristors T_7 through T_{10} are operative. Line B feeds terminal c and line C feeds terminal b, resulting in a phase reversal of the voltage applied to the load. To obtain phase reversal, all the devices must be thyristors. A combination of thyristors and diodes as shown in Fig. 5-6 cannot be used; otherwise, phase-to-phase short circuits would occur.

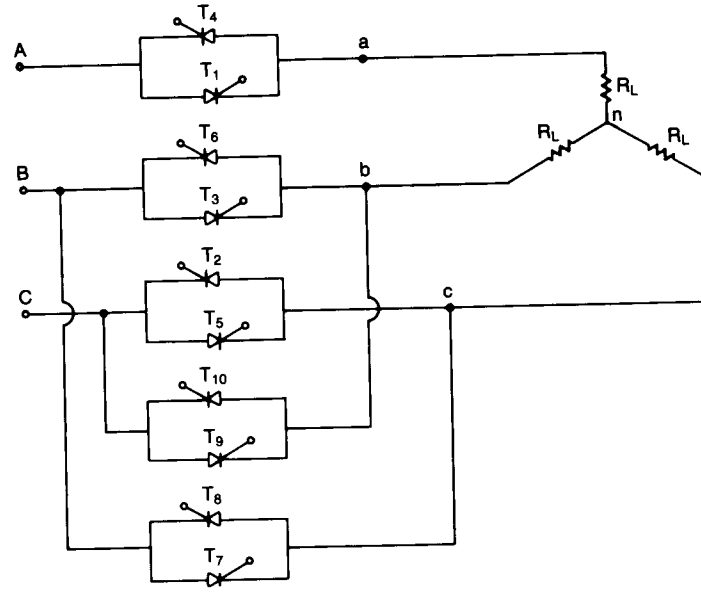


Figure 5-7 Three-phase reversing thyristor ac switch.

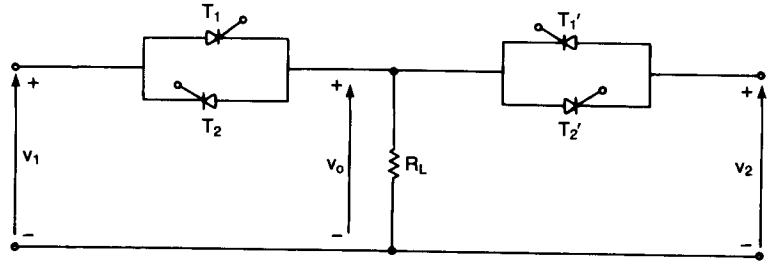


Figure 5-8 Single-phase bus transfer.

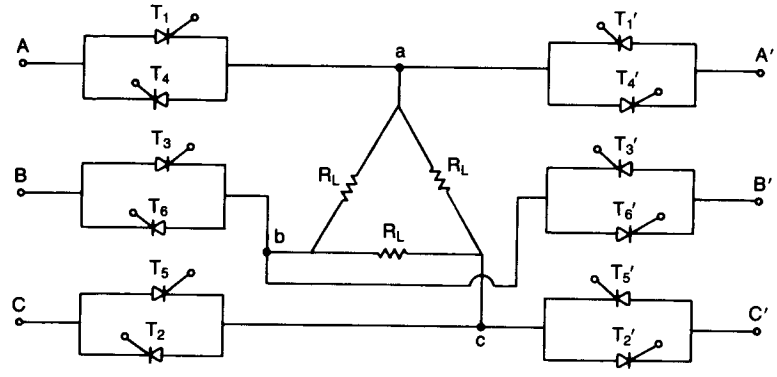


Figure 5-9 Three-phase bus transfer.

5-5 AC SWITCHES FOR BUS TRANSFER

The static switches can be used for bus transfer from one source to another. In a practical supply system, it is sometimes required to switch the load from the normal source to an alternative source in case of (1) unavailability of normal source, and (2) undervoltage or overvoltage condition of normal source. Figure 5-8 shows a single-phase bus transfer switch. When thyristors T_1 and T_2 are operative, the load is connected to the normal source; and for transfer to an alternative source, thyristors T_1' and T_2' are operative, while T_1 and T_2 are turned off by gate signal inhibiting. The extension of single-phase bus transfer to three-phase transfer is shown in Fig. 5-9.

5-6 DC SWITCHES

In the case of dc switches, the input voltage is dc and power transistors or fast-switching thyristors can be used. Once a thyristor is turned on, it must be turned off by forced commutation and the techniques for forced commutation are discussed

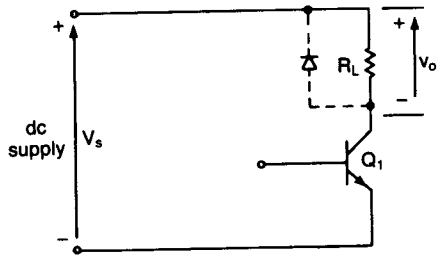


Figure 5-10 Single-pole transistor dc switch.

in Chapter 3. A single-pole transistor switch is shown in Fig. 5-10, with a resistive load; and in case of an inductive load, a diode (as shown by dashed lines) must be connected across the load to protect the transistor during switch-off. The single-pole switches can also be extended to bus transfer from one source to another.

If forced commutated thyristors are used, the commutation circuit is an integral part of the switch and a typical dc switch for high-power applications is shown in Fig. 5-11. If thyristor T_3 is fired, the capacitor C is charged through the supply, L and T_3. From Eqs. (3-2) and (3-3), the charging current and the capacitor voltage are expressed as

$$i(t) = V_s \sqrt{\frac{C}{L}} \sin \omega t \tag{5-4}$$

and

$$v_c(t) = V_s(1 - \cos \omega t) \tag{5-5}$$

where $\omega = 1/\sqrt{LC}$.

After time $t = t_0 = \pi \sqrt{LC}$, the charging current becomes zero and the capacitor is charged to $2V_s$. If thyristor T_1 is conducting to supply power to the load, thyristor T_2 is fired to switch T_1 off. Firing T_2 causes a resonant pulse of current through capacitor C, inductor L, and thyristor T_2. As the resonant current increases, the current through thyristor T_1 reduces. When the resonant current rises to the load current, I_L, the current of thyristor T_1 falls to zero and thyristor T_1 is turned off.

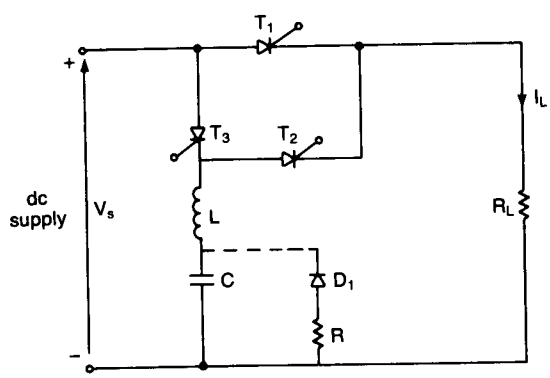


Figure 5-11 Single-pole thyristor dc switch.

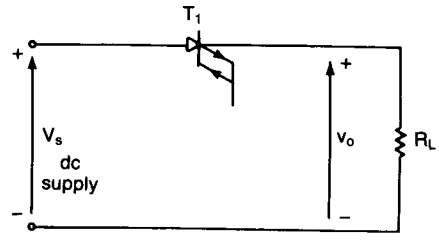


Figure 5-12 Single-pole GTO dc switch.

The capacitor discharges through the load resistance, R_L. A freewheeling diode, D_m, across the load is necessary for an inductive load. The capacitor must be discharged completely in every switching action; and a negative voltage on the capacitor can be prevented by connecting a resistor and a diode as shown in Fig. 5-11 by dashed lines.

The dc switches can be applied for the control of power flow in very high voltage and high current applications (e.g., fusion reactor) [1] and these can also be used as fast-acting current breaker [2]. Instead of transistors, gate-turn-off thyristors (GTOs) can be used. A GTO is turned on by the application of a short positive pulse to its gate similar to the normal thyristors; however, a GTO can be turned off by applying a short negative pulse to its gate and it does not require any commutation circuitry. A single-pole GTO switch is shown in Fig. 5-12.

5-7 SOLID-STATE RELAYS

The static switches can be used as solid-state relays (SSRs), which are used for the control of ac and dc power. SSRs find many applications in industrial control (e.g., control of motor loads, transformers, resistance heating, etc.) to replace electromechanical relays. For ac applications, thyristors or TRIACs can be used; and for dc applications, transistors are used. The SSRs are normally isolated electrically between the control circuit and the load circuit by reed relay, transformer, or optocoupler.

Figure 5-13 shows two basic circuits for dc SSRs, one with reed relay isolation and the other with an optocoupler. Although the single-phase circuit in Fig. 5-1a can be used to operate as an SSR, the circuit in Fig. 5-2 with a TRIAC is normally

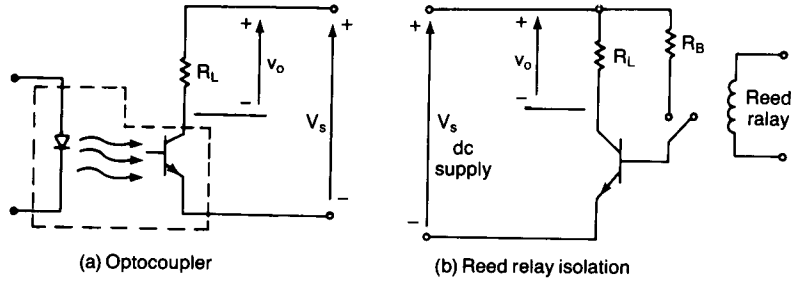


Figure 5-13 Dc solid-state relays.

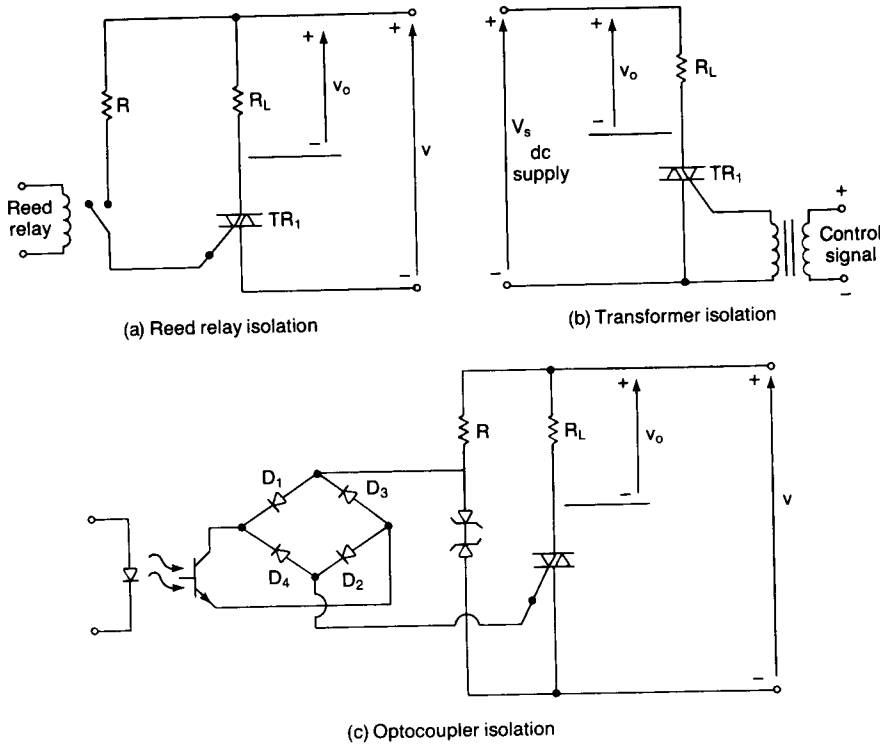


Figure 5-14 Ac solid-state relays.

used for ac power, because of the requirement of only one gating circuit for a TRIAC. Figure 5-14 shows SSRs with reed relay, a transformer isolation, and an optocoupler. If the application requirements demand thyristors for high power levels, the circuit in Fig. 5-1a can also be used to operate as an SSR even though the complexity of the gating circuit would increase.

5-8 DESIGN OF STATIC SWITCHES

The solid-state switches are available commercially with limited voltage and current ratings ranging from 1 A to 50 A and up to 440 V. If it is necessary to design SSRs to meet specific requirements, the design is simple and requires determining the voltage and current ratings of power semiconductor devices. The design procedures can be illustrated by examples.

Example 5-1

A single-phase ac switch with configuration in Fig. 5-1a is used between a 120-V 60-Hz supply and an inductive load. The load power is 5 kW at a power factor of 0.88 lagging. Determine the (a) voltage and current ratings of thyristors; and (b) firing angles of thyristors.

Solution P_o = 5000 W, PF = 0.88, and V_s = 120 V.

(a) The peak load current, $I_m = \sqrt{2} \times 5000/(120 \times 0.88) = 66.96$ A. From Eq. (5-2) the average current, $I_{av} = 66.96/\pi = 21.31$ A and from Eq. (5-3) the rms current, $I_{rms} = 66.96/2 = 33.48$ A. The peak inverse voltage, PIV = $\sqrt{2} \times 120 = 169.7$ V.

(b) $\cos \theta = 0.88$ or $\theta = 28.36°$. Thus the firing angle of T_1 is $\alpha_1 = 28.36°$ and for thyristor T_2, $\alpha_2 = 180° + 28.36° = 208.36°$.

Example 5-2

A three-phase ac switch with configuration in Fig. 5-5a is used between a three-phase 440-V 60-Hz supply and a three-phase wye-connected load. The load power is 20 kW at a power factor of 0.707 lagging. Determine the voltage and current ratings of thyristors.

Solution P_o = 20,000 W, PF = 0.707, V_L = 440 V, and $V_s = 440/\sqrt{3} = 254.03$ V. The line current is calculated from the power as

$$I_s = \frac{20{,}000}{\sqrt{3} \times 440 \times 0.707} = 37.119 \text{ A}$$

The peak current of a thyristor, $I_m = \sqrt{2} \times 37.119 = 52.494$ A. The average current of a thyristor, $I_{av} = 52.494/\pi = 16.71$ A. The rms current of a thyristor, $I_{rms} = 52.474/2 = 26.247$ A. The peak inverse voltage of a thyristor, PIV = $\sqrt{2} \times 440 = 762.1$ V.

SUMMARY

Solid-state ac and dc switches have a number of advantages over conventional electromechanical switches and relays. With the developments of power semiconductor devices and integrated circuits, static switches can find a wide range of applications in industrial control. Static switches can be interfaced with digital or computer control systems.

REFERENCES

1. W. F. Praeg, "Detailed design of a 13-kA, 13-kV DC solid state turn-off switch." *IEEE Industry Applications Conference Record*, 1985, pp. 1221–1226.
2. P. F. Dawson, L. E. Lansing, and S. B. Dewan, "A fast dc current breaker." *IEEE Transactions on Industry Applications*, Vol. IA21, No. 5, 1985, pp. 1176–1181.

REVIEW QUESTIONS

5-1. What is a static switch?

5-2. What are the differences between ac and dc switches?

5-3. What are the advantages of static switches over mechanical or electromechanical switches?

5-4. What are the advantages and disadvantages of inverse-parallel thyristor ac switches?

5-5. What are the advantages and disadvantages of TRIAC ac switches?

5-6. What are the advantages and disadvantages of diode and thyristor ac switches?

5-7. What are the advantages and disadvantages of bridge rectifier and thyristor ac switches?

5-8. What are the effects of load inductance on the gating requirements of ac switches?

5-9. What is the principle of operation of SSRs?

5-10. What are the methods of isolating the control circuit from the load circuit of SSRs?

5-11. What are the factors involved in the design of dc switches?

5-12. What are the factors involved in the design of ac switches?

5-13. What type of commutation is required for dc switches?

5-14. What type of commutation is required for ac switches?

PROBLEMS

5-1. A single-phase ac switch with configuration in Fig. 5-1a is used between a 120-V 60-Hz main supply and an inductive load. The load power is 15 kW at a power factor of 0.90 lagging. Determine the voltage and current ratings of the thyristors.

5-2. Determine the firing angles of thyristors T_1 and T_2 in Prob. 5-1.

5-3. A single-phase ac switch with configuration in Fig. 5-3a is used between a 120-V 60-Hz main supply and an inductive load. The load power is 15 kW at a power factor of 0.90 lagging. Determine the voltage and current ratings of diodes and thyristors.

5-4. A single-phase ac switch with configuration in Fig. 5-4a is used between a 120-V 60-Hz main supply and an inductive load. The load power is 15 kW at a power factor of 0.90 lagging. Determine the voltage and current ratings of the thyristor and diodes in the bridge rectifier.

5-5. Determine the firing angles of thyristors T_1 in Prob. 5-4.

5-6. A three-phase ac switch with configuration in Fig. 5-5a is used between a three-phase 440-V 60-Hz supply and a three-phase wye-connected load. The load power is 20 kW at a power factor of 0.86 lagging. Determine the voltage and current ratings of thyristors.

5-7. Determine the firing angles of thyristors in Prob. 5-6.

5-8. Repeat Prob. 5-6 for a delta-connected load.

5-9. A three-phase ac switch with configuration in Fig. 5-6 has a three-phase 440-V 60-Hz input and a three-phase wye-connected load. The load power is 20 kW at a power factor of 0.86 lagging. Determine the voltage and current ratings of diodes and thyristors.

5-10. A thyristor dc switch in Fig. 5-11 has a load resistance, $R_L = 5\ \Omega$; dc supply voltage, $V_s = 220$ V; inductance, $L = 40\ \mu$H; and capacitance, $C = 40\ \mu$F. Determine the **(a)** peak current through thyristor T_3, and **(b)** time required to reduce the current of thyristor T_1 from the steady-state value to zero.

5-11. For Prob. 5-10, determine the time required for the capacitor to discharge from $2V_s$ to zero after the firing of thyristor T_2.

5-12. A thyristor dc switch in Fig. 5-11 has a load resistance, $R_L = 0.5\ \Omega$; supply voltage, $V_s = 220$ V; inductance, $L = 40\ \mu$H; and capacitance, $C = 80\ \mu$F. If the switch is operated at a frequency of 60 Hz, determine the **(a)** peak, rms, and average currents of thyristors T_1, T_2, and T_3; and **(b)** rms current rating of capacitor.

5-13. For Prob. 5-12, determine the time required for the capacitor to discharge from $2V_s$ to zero after the firing of thyristor T_2.

6

AC Voltage Controllers

6-1 INTRODUCTION

We have seen in Chapter 5 that thyristors can be operated as switches. If a thyristor switch is connected between ac supply and load, the power flow can be controlled by varying the rms value of ac voltage applied to the load; and this type of power circuit is known as an *ac voltage controller*. The most common applications of ac voltage controllers are: industrial heating, on-load transformer tap changing, light controls, speed control of polyphase induction motors, and ac magnet controls. For power transfer, two types of control are normally used:

1. On–off control
2. Phase-angle control

In on–off control, thyristor switches connect the load to the ac source for a few cycles of input voltage and then disconnect it for another few cycles. In phase control, thyristor switches connect the load to ac source for a portion of each cycle of input voltage.

The ac voltage controllers can be classified into two types: (1) single-phase controllers and (2) three-phase controllers. Each type can be subdivided into (a) unidirectional or half-wave control and (b) bidirectional or full-wave control. There

are various configurations of three-phase controllers depending on the connections of thyristor switches.

Since the input voltage is ac, thyristors are line commutated; and phase-control thyristors, which are relatively inexpensive and slower than fast-switching thyristors, are normally used. For applications up to 400 Hz, if TRIACs are available to meet the voltage and current ratings of a particular application, TRIACs are more commonly used.

Due to line or natural commutation, there is no need of extra commutation circuitry and the circuits for ac voltage controllers are very simple. Due to the nature of output waveforms, the analysis for the derivations of explicit expressions for the performance parameters of circuits are not simple, especially for phase-angle-controlled converters with *RL* loads. For the sake of simplicity, resistive loads are considered in this chapter to compare the performances of various configurations.

6-2 PRINCIPLE OF ON–OFF CONTROL

The principle of on–off control can be explained with a single-phase full-wave controller as shown in Fig. 6-1a. The thyristor switch connects the ac supply to load for a time t_n; the switch is turned off by a gate pulse inhibiting for time t_0. The on-time, t_n, usually consists of an integral number of cycles. The thyristors are turned on at the zero-voltage crossings of ac input voltage. The gate pulses for thyristors T_1 and T_2 and the waveforms for input and output voltages are shown in Fig. 6-1b.

This type of control is applied in applications, which have a high mechanical inertia and high thermal time constant (e.g., industrial heating and speed control of motors). Due to zero voltage switching of thyristors, the harmonics generated by switching actions are reduced.

For a sinusoidal input voltage, $v_s = V_m \sin \omega t = \sqrt{2}\, V_s \sin \omega t$. If the input voltage is connected to load for n cycles and is disconnected for m cycles, the rms output (or load) voltage can be found from

$$V_o = \left[\frac{n}{2\pi(n+m)} \int_0^{2\pi} 2V_s^2 \sin^2 \omega t \, d(\omega t)\right]^{1/2} = V_s \sqrt{\frac{n}{m+n}} = V_s \sqrt{k} \tag{6-1}$$

where $k = n/(m + n)$ and k is called the *duty cycle*. V_s is the rms phase voltage. The circuit configurations for on–off control are similar to those of phase control and the performance analysis is also similar. For these reasons, the phase-control techniques are only discussed and analyzed in this chapter.

Example 6-1

A ac voltage controller in Fig. 6-1a has a resistive load of $R = 10\ \Omega$ and the rms input voltage is $V_s = 120$ V, 60 Hz. The thyristors switch is on for $n = 25$ cycles

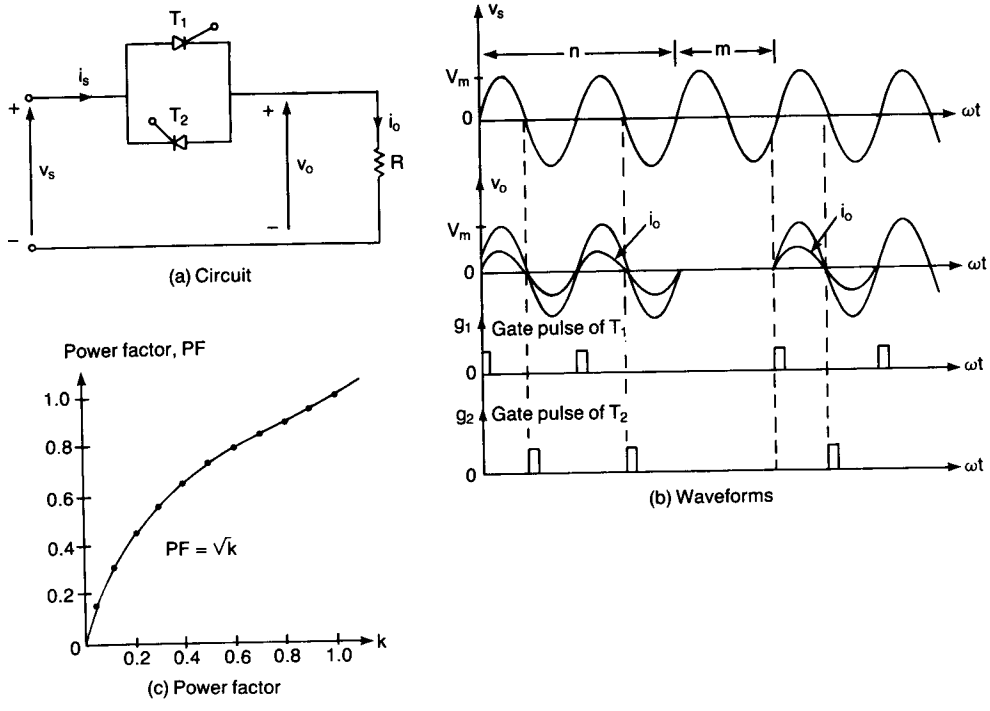


Figure 6-1 On-off control.

and is off for $m = 75$ cycles. Determine the (a) rms output voltage, V_o; (b) input power factor, PF; and (c) average and rms current of thyristors.

Solution $R = 10\ \Omega$, $V_s = 120$ V, $V_m = \sqrt{2} \times 120 = 169.7$ V, and $k = n/(n + m) = 25/100 = 0.25$.

(a) From Eq. (6-1), the rms value of output voltage is

$$V_o = V_s\sqrt{k} = V_s\sqrt{\frac{n}{m+n}} = 120\sqrt{\frac{25}{100}} = 60\text{ V}$$

and the rms load current is $I_o = V_o/R = 60/10 = 6.0$ A.

(b) The load power is $P_o = I_o^2 R = 6^2 \times 10 = 360$ W. Since the input current is the same as the load current, the input volt-amperes is

$$\text{VA} = V_s I_s = V_s I_o = 120 \times 6 = 720\text{ W}$$

The input power factor is

$$\text{PF} = \frac{P_o}{\text{VA}} = \frac{n}{m+n} = \sqrt{k} \qquad (6\text{-}2)$$
$$= \sqrt{0.25} = \frac{360}{720} = 0.5\ \text{(lagging)}$$

(c) The peak thyristor current is $I_m = V_m/R = 169.7/10 = 16.97$ A. The

average current of thyristors is

$$I_A = \frac{n}{2\pi(m+n)}\int_0^{\pi} I_m \sin \omega t \, d(\omega t) = \frac{I_m n}{\pi(m+n)} = \frac{kI_m}{\pi} \qquad ((6\text{-}3)$$
$$= \frac{16.97}{\pi} \times 0.25 = 1.35 \text{ A}$$

The rms current of thyristors is

$$I_R = \left[\frac{n}{2\pi(m+n)}\int_0^{\pi} I_m^2 \sin^2 \omega t \, d(\omega t)\right]^{1/2} = \frac{I_m}{2}\sqrt{\frac{n}{m+n}} = \frac{I_m\sqrt{k}}{2} \qquad (6\text{-}4)$$
$$= \frac{16.97}{2} \times \sqrt{0.25} = 4.24 \text{ A}$$

Note. The power factor and output voltage vary with the square root of the duty cycle. The power factor is poor at the low value of duty the cycle, k, and is shown in Fig. 6-1c.

6-3 PRINCIPLE OF PHASE CONTROL

The principle of phase control can be explained with reference to Fig. 6-2a. The power flow to the load is controlled by delaying the firing angle of thyristor T_1. Figure 6-2b illustrates the gate pulses of thyristor T_1 and the waveforms for the input and output voltages. Due to the presence of diode D_1, the control range is limited and the effective rms output voltage can only be varied between 70.7 and 100%. The output voltage and input current are asymmetrical and contain a dc component. If there is an input transformer, it may be saturated. This circuit is a single-phase half-wave controller and is suitable only for low-power resistive loads, such as heating and lighting. Since the power flow is controlled during the positive half-cycle of input voltage, this type of controller is also known as a *unidirectional controller*.

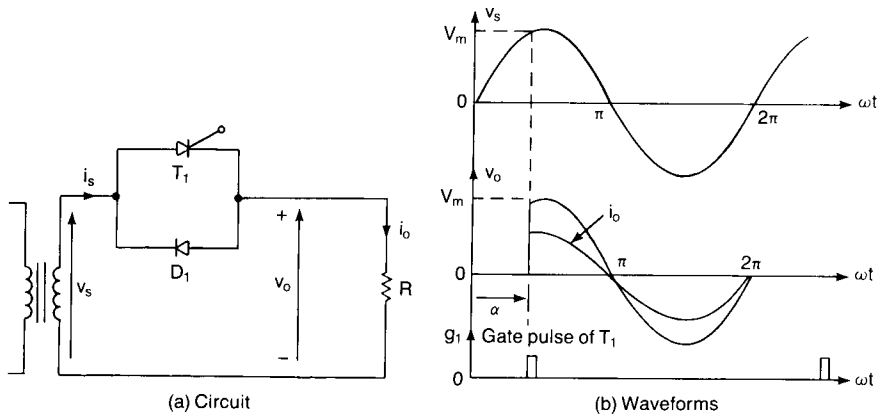


Figure 6-2 Single-phase angle control.

If $v_s = V_m \sin \omega t = \sqrt{2}\, V_s \sin \omega t$ is the input voltage and the delay angle of thyristor T_1 is $\omega t = \alpha$, the rms output voltage is found from

$$V_o = \left\{\frac{1}{2\pi}\left[\int_{\alpha}^{\pi} 2V_s^2 \sin^2 \omega t\, d(\omega t) + \int_{\pi}^{2\pi} 2V_s^2 \sin^2 \omega t\, d(\omega t)\right]\right\}^{1/2}$$

$$= \left\{\frac{2V_s^2}{4\pi}\left[\int_{\alpha}^{\pi} (1 - \cos 2\omega t)\, d(\omega t) + \int_{\pi}^{2\pi} (1 - \cos 2\omega t)\, d(\omega t)\right]\right\}^{1/2} \qquad (6\text{-}5)$$

$$= V_s\left[\frac{1}{2\pi}\left(2\pi - \alpha + \frac{\sin 2\alpha}{2}\right)\right]^{1/2}$$

The average value of output voltage is

$$V_{dc} = \frac{1}{2\pi}\left[\int_{\alpha}^{\pi} \sqrt{2}\, V_s \sin \omega t\, d(\omega t) + \int_{\pi}^{2\pi} \sqrt{2}\, V_s \sin \omega t\, d(\omega t)\right] \qquad (6\text{-}6)$$

$$= \frac{\sqrt{2}\, V_s}{2\pi}(\cos \alpha - 1)$$

If α is varied from 0 to π, V_o varies from V_s to $V_s/\sqrt{2}$ and V_{dc} varied from 0 to $-\sqrt{2}\, V_s/\pi$.

Example 6-2

A single-phase ac voltage controller in Fig. 6-2a has a resistive load of $R = 10\ \Omega$ and the input voltage is $V_s = 120$ V, 60 Hz. The delay angle of thyristor T_1 is $\alpha = \pi/2$. Determine the (a) rms value of output voltage, V_o; (b) input power factor, PF; and (c) average input current.

Solution $R = 10\ \Omega$, $V_s = 120$ V, $\alpha = \pi/2$, and $V_m = \sqrt{2} \times 120 = 169.7$ V.

(a) From Eq. (6-5), the rms value of the output voltage,

$$V_o = 120\sqrt{\frac{3}{4}} = 103.92 \text{ V}$$

(b) The rms load current,

$$I_o = \frac{V_o}{R} = \frac{103.92}{10} = 10.392 \text{ A}$$

The load power,

$$P_o = I_o^2 R = 10.392^2 \times 10 = 1079.94 \text{ W}$$

Since the input current is the same as the load current, the input volt-ampere rating is

$$\text{VA} = V_s I_s = V_s I_o = 120 \times 10.392 = 1247.04 \text{ VA}$$

The input power factor,

$$\text{PF} = \frac{P_o}{\text{VA}} = \frac{V_o}{V_s} = \left[\frac{1}{2\pi}\left(2\pi - \alpha + \frac{\sin 2\alpha}{2}\right)\right]^{1/2} \qquad (6\text{-}7)$$

$$= \sqrt{\frac{3}{4}} = \frac{1079.94}{1247.04} = 0.866 \text{ (lagging)}$$

(c) From Eq. (6-6), the average output voltage,

$$V_{dc} = -120 \times \frac{\sqrt{2}}{2\pi} = -27 \text{ V}$$

and the average input current,

$$I_D = \frac{V_{dc}}{R} = -\frac{27}{10} = -2.7 \text{ A}$$

Note. The negative sign of I_D signifies that the input current during the positive half-cycle is less than that during the negative half-cycle. If there is an input transformer, the transformer core may be saturated. The unidirectional control is not normally used in practice.

6-4 SINGLE-PHASE BIDIRECTIONAL CONTROLLERS WITH RESISTIVE LOADS

The problem of dc input current can be prevented by using bidirectional (or full-wave) control, and a single-phase full-wave controller with a resistive load is shown in Fig. 6-3a. During the positive half-cycle of input voltage, the power flow is controlled by varying the delay angle of thyristor T_1; and thyristor T_2 controls the power flow during the negative half-cycle of input voltage. The firing pulses of T_1 and T_2 are kept 180° apart. The waveforms for the input voltage, output voltage, and gating signals for T_1 and T_2 are shown in Fig. 6-3b.

If $v_s = \sqrt{2}\, V_s \sin \omega t$ is the input voltage and the delay angles of thyristors T_1 and T_2 are equal $\alpha_1 = \alpha_2 = \alpha$, the rms output voltage can be found from

$$\begin{aligned} V_o &= \left[\frac{2}{2\pi}\int_{\alpha}^{\pi} 2V_s^2 \sin^2 \omega t \, d(\omega t)\right]^{1/2} \\ &= \left[\frac{4V_s^2}{4\pi}\int_{\alpha}^{\pi} (1 - \cos 2\omega t) \, d(\omega t)\right]^{1/2} \\ &= V_s\left[\frac{1}{\pi}\left(\pi - \alpha + \frac{\sin 2\alpha}{2}\right)\right]^{1/2} \end{aligned} \tag{6-8}$$

By varying α from 0 to π, V_o can be varied from V_s to 0.

In Fig. 6-3a, the gating circuits for thyristors T_1 and T_2 must be isolated. It is possible to have a common cathode for T_1 and T_2 by adding two diodes as shown in Fig. 6-4. Thyristor T_1 and diode D_1 conduct together during the positive half-cycle; and thyristor T_2 and diode D_2 conduct during the negative half-cycle. Since this circuit can have a common terminal for gating signals of T_1 and T_2, only one isolation circuit is required, but at the expense of two power diodes. Due to two power devices conducting at the same time, the conduction losses of devices would increase and efficiency would be reduced.

A single-phase full-wave controller can also be implemented with one thyristor and four diodes as shown in Fig. 6-5a. The four diodes act as a bridge rectifier. The voltage across thyristor T_1, and its current, are always unidirectional. With

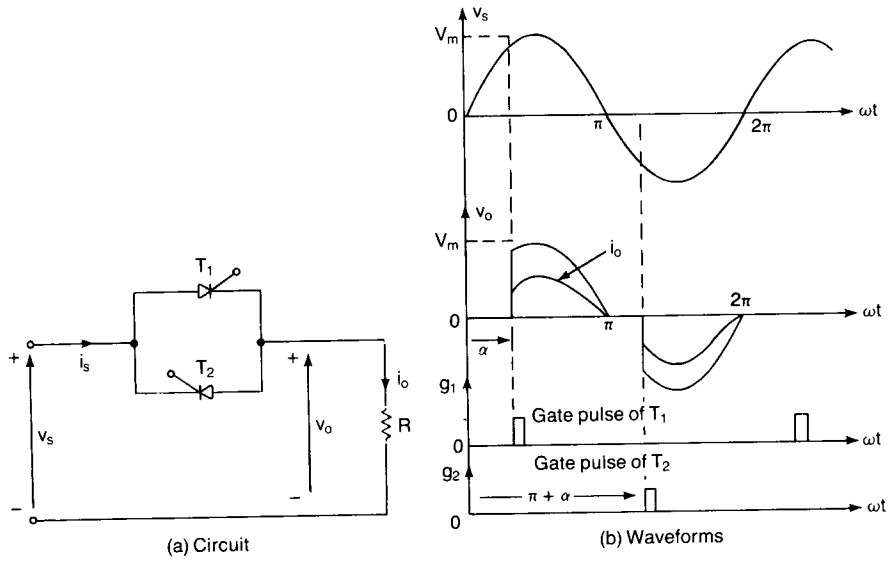


Figure 6-3 Single-phase full-wave controller.

a resistive load, the thyristor current would fall to zero due to natural commutation in every half-cycle, as shown in Fig. 6-5b. However, if there is a large inductance in the circuit, thyristor T_1 may not be turned off in every half-cycle of input voltage, and this may result in a loss of control. Three power devices conduct at the same time and the efficiency is also reduced. The bridge rectifier and thyristor (or transistor) act as a *bidirectional switch*, which is commercially available as a single device with a relatively low on-state conduction loss.

Example 6-3

A single-phase full-wave ac voltage controller in Fig. 6-3a has a resistive load of $R = 10\ \Omega$ and the input voltage is $V_s = 120$ V, 60 Hz. The delay angles of thyristors T_1 and T_2 are equal: $\alpha_1 = \alpha_2 = \alpha = \pi/2$. Determine the (a) rms output voltage, V_o; (b) input power factor, PF; (c) average current of thyristors, I_A; and (d) rms current of thyristors, I_R.

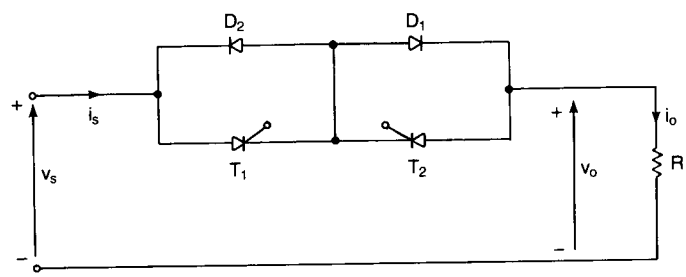


Figure 6-4 Single-phase full-wave controller with common cathode.

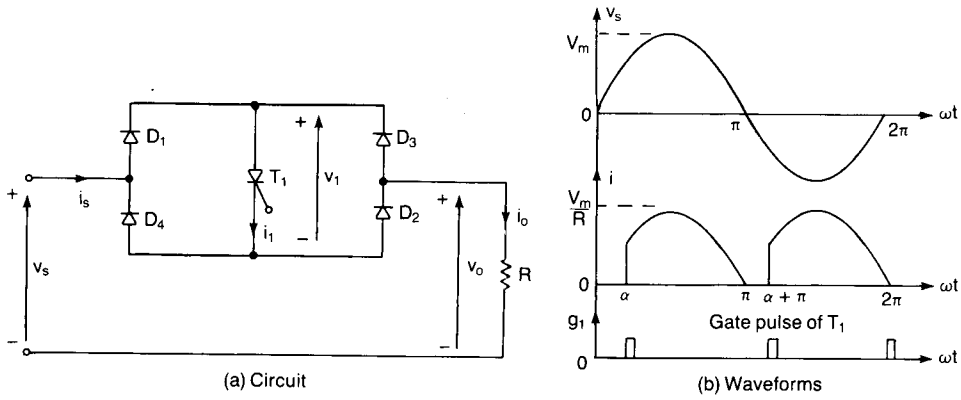


Figure 6-5 Single-phase full-wave controller with one thyristor.

Solution $R = 10\ \Omega$, $V_s = 120$ V, $\alpha = \pi/2$, and $V_m = \sqrt{2} \times 120 = 169.7$ V.

(a) From Eq. (6-8), the rms output voltage,

$$V_o = \frac{120}{\sqrt{2}} = 84.85 \text{ V}$$

(b) The rms value of load current, $I_o = V_o/R = 84.85/10 = 8.485$ A and the load power, $P_o = I_o^2 R = 8.485^2 \times 10 = 719.95$ W. Since the input current is the same as the load current, the input volt-ampere rating,

$$\text{VA} = V_s I_s = V_s I_o = 120 \times 8.485 = 1018.2 \text{ W}$$

The input power factor,

$$\text{PF} = \frac{P_o}{\text{VA}} = \frac{V_o}{V_s} = \left[\frac{1}{\pi}\left(\pi - \alpha + \frac{\sin 2\alpha}{2}\right)\right]^{1/2} \tag{6-9}$$

$$= \frac{1}{\sqrt{2}} = \frac{719.95}{1018.2} = 0.707 \text{ (lagging)}$$

(c) The average thyristor current,

$$I_A = \frac{1}{2\pi R}\int_{\alpha}^{\pi} \sqrt{2}\, V_s \sin \omega t\, d(\omega t)$$

$$= \frac{\sqrt{2}\, V_s}{2\pi R}(\cos \alpha + 1) \tag{6-10}$$

$$= \sqrt{2} \times \frac{120}{2\pi \times 10} = 2.7 \text{ A}$$

(d) The rms value of the thyristor current,

$$I_R = \left[\frac{1}{2\pi R^2}\int_{\alpha}^{\pi} 2V_s^2 \sin^2 \omega t\, d(\omega t)\right]^{1/2}$$

$$= \left[\frac{2V_s^2}{4\pi R^2}\int_{\alpha}^{\pi} (1 - \cos 2\omega t)\, d(\omega t)\right]^{1/2}$$

$$= \frac{V_s}{\sqrt{2}\,R}\left[\frac{1}{\pi}\left(\pi - \alpha + \frac{\sin 2\alpha}{2}\right)\right]^{1/2} \tag{6-11}$$

$$= \frac{120}{2 \times 10} = 6\text{A}$$

6-5 SINGLE-PHASE CONTROLLERS WITH INDUCTIVE LOADS

Section 6-4 deals with the single-phase controllers with resistive loads. In practice, most loads are inductive to a certain extent. A full-wave controller with an *RL* load is shown in Fig. 6-6a. Let us assume that thyristor T_1 is fired during the positive half-cycle and carries the load current. Due to inductance in the circuit, the current of thyristor T_1 may not fall to zero at $\omega t = \pi$, when the input voltage starts to be negative. Thyristor T_1 will continue to conduct until its current i_1 falls to zero at $\omega t = \beta$. The conduction angle of thyristor T_1 is $\delta = \beta - \alpha$ and depends

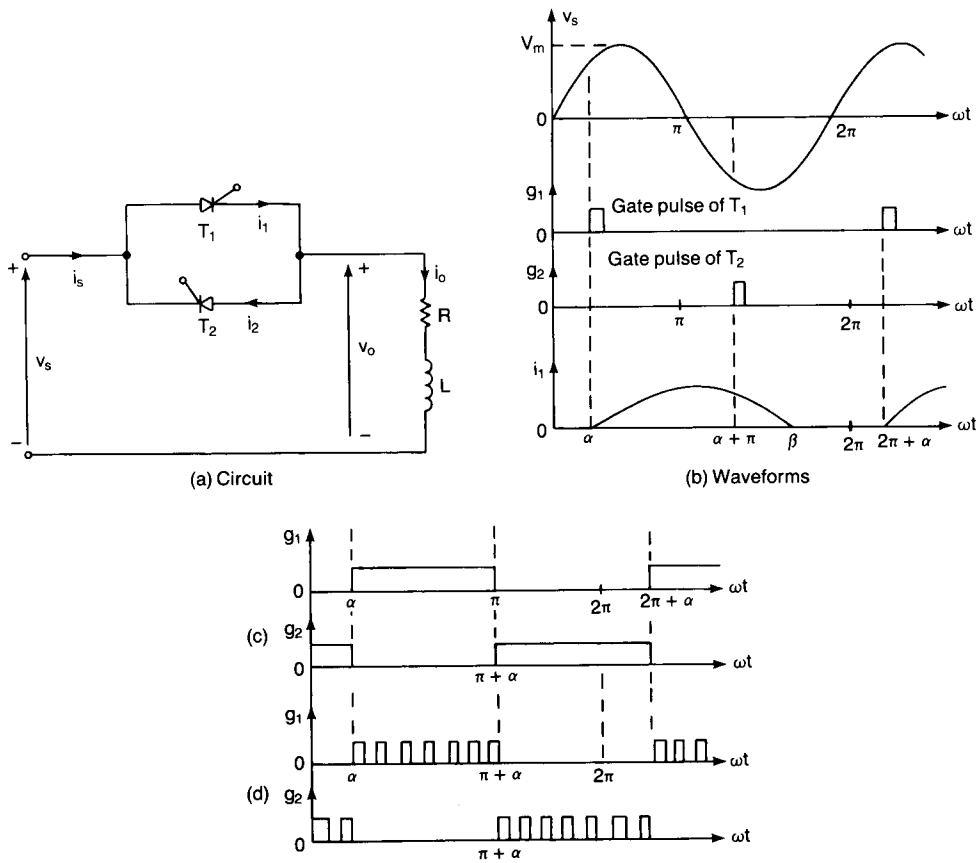


Figure 6-6 Single-phase full-wave controller with *RL* load.

on the delay angle, α, and the power factor angle of load, θ. The waveforms for the thyristor current, gating pulses, and input voltage are shown in Fig. 6-6b.

If $v_s = \sqrt{2}\, V_s \sin \omega t$ is the instantaneous input voltage and the delay angle of thyristor T_1 is α, thyristor current i_1 can be found from

$$L \frac{di_1}{dt} + Ri_1 = \sqrt{2}\, V_s \sin \omega t \tag{6-12}$$

The solution of Eq. (6-12) is of the form

$$i_1 = \frac{\sqrt{2}\, V_s}{Z} \sin (\omega t - \theta) + A_1 e^{-(R/L)t} \tag{6-13}$$

where load impedance, $Z = [R^2 + (\omega L)^2]^{1/2}$ and load angle, $\theta = \tan^{-1} (\omega L/R)$.

The constant A_1 can be determined from the initial condition: at $\omega t = \alpha$, $i_1 = 0$. From Eq. (6-10) A_1 is found as

$$A_1 = -\frac{\sqrt{2}\, V_s}{Z} \sin (\alpha - \theta) e^{(R/L)(\alpha/\omega)} \tag{6-14}$$

Substitution of A_1 from Eq. (6-14) in Eq. (6-13) yields

$$i_1 = \frac{\sqrt{2}\, V_s}{Z} [\sin (\omega t - \theta) - \sin (\alpha - \theta) e^{(R/L)(\alpha/\omega - t)}] \tag{6-15}$$

The angle β, when current i_1 falls to zero and thyristor T_1 is turned off, can be found from the condition: $i_1(\omega t = \beta) = 0$ in Eq. (6-15) and is given by the relation

$$\sin (\beta - \theta) = \sin (\alpha - \theta) e^{(R/L)(\alpha - \beta)/\omega} \tag{6-16}$$

The angle β, which is also known as an *extinction angle*, can be determined from this transcendental equation and it requires an iterative method of solution. Once β is known, the conduction angle (δ) of thyristor T_1 can be found from

$$\delta = \beta - \alpha \tag{6-17}$$

The rms output voltage,

$$\begin{aligned} V_o &= \left[\frac{2}{2\pi} \int_\alpha^\beta 2V_s^2 \sin^2 \omega t \, d(\omega t)\right]^{1/2} \\ &= \left[\frac{4V_s^2}{4\pi} \int_\alpha^\beta (1 - \cos 2\omega t) \, d(\omega t)\right]^{1/2} \\ &= V_s \left[\frac{1}{\pi} \left(\beta - \alpha + \frac{\sin 2\alpha}{2} - \frac{\sin 2\beta}{2}\right)\right]^{1/2} \end{aligned} \tag{6-18}$$

The rms thyristor current can be found from Eq. (6-15) as

$$\begin{aligned} I_R &= \left[\frac{1}{2\pi} \int_\alpha^\beta i_1^2 \, d(\omega t)\right]^{1/2} \\ &= \frac{V_s}{Z} \left[\frac{1}{\pi} \int_\alpha^\beta \{\sin (\omega t - \theta) - \sin (\alpha - \theta) e^{(R/L)(\alpha/\omega - t)}\}^2 \, d(\omega t)\right]^{1/2} \end{aligned} \tag{6-19}$$

and the rms output current can then be determined by combining the rms current of each thyristor as

$$I_o = (I_R^2 + I_R^2)^{1/2} = \sqrt{2}\, I_R \tag{6-20}$$

The average value of thyristor current can also be found from Eq. (6-15) as

$$\begin{aligned} I_A &= \frac{1}{2\pi}\int_{\alpha}^{\beta} i_1\, d(\omega t) \\ &= \frac{\sqrt{2}\, V_s}{2\pi Z}\int_{\alpha}^{\beta} [\sin(\omega t - \theta) - \sin(\alpha - \theta)e^{(R/L)(\alpha/\omega - t)}]\, d(\omega t) \end{aligned} \tag{6-21}$$

The gating signals of thyristors could be short pulses for a controller with resistive loads. However, such short pulses are not suitable for inductive loads. This can be explained with reference to Fig. 6-6b. When thyristor T_2 is fired at $\omega t = \pi + \alpha$, thyristor T_1 is still conducting due to load inductance. By the time the current of thyristor T_1 falls to zero and T_1 is turned off at $\omega t = \beta = \alpha + \delta$, the gate pulse of thyristor T_2 has already ceased and consequently, T_2 will not be turned on. As a result, only thyristor T_1 will operate, causing asymmetrical waveforms of output voltage and current. This difficulty can be resolved by using continuous gate signals with a duration of $(\pi - \alpha)$ as shown in Fig. 6-6c. As soon as the current of T_1 falls to zero, thyristor T_2 (with gate pulses as shown in Fig. 6-6c) would be turned on. However, a continuous gate pulse increases the switching loss of thyristors and requires a larger isolating transformer for the gating circuit. In practice, a train of pulses with short durations as shown in Fig. 6-6d are normally used to overcome these problems.

Equation (6-15) indicates that the load voltage (and current) will be sinusoidal if the delay angle, α, is less than the load angle, θ. If α is greater than θ, the load current would be discontinuous and nonsinusoidal.

Notes

1. If $\alpha = \theta$, from Eq. (6-16),

$$\sin(\beta - \theta) = \sin(\beta - \alpha) = 0 \tag{6-22}$$

and

$$\beta - \alpha = \delta = \pi \tag{6-23}$$

2. Since the conduction angle, δ cannot exceed π, the delay angle, α, may not be less than θ and the control range of delay angle is

$$\theta \leq \alpha \leq \pi \tag{6-24}$$

3. If $\alpha \leq \theta$ and the gate pulses of thyristors are of long duration, the load current would not change with α, and both thyristors would conduct. Thyristor T_1 would turn on at $\omega t = \theta$ and thyristor T_2 would turn on at $\omega t = \pi + \theta$.

Example 6-4

The single-phase full-wave controller in Fig. 6-6a supplies an RL load. The input rms voltage is $V_s = 120$ V at 60 Hz. The load is such that $L = 6.5$ mH and $R = 2.5\ \Omega$. The delay angles of thyristors are equal: $\alpha_1 = \alpha_2 = \pi/2$. Determine the (a)

conduction angle of thyristor T_1, δ; (b) rms output voltage, V_o; (c) rms thyristor current, I_R; (d) rms output current, I_o; (e) the average current of a thyristor, I_A; and (f) input power factor, PF.

Solution $R = 2.5\ \Omega$, $L = 6.5$ mH, $f = 60$ Hz, $\omega = 2\pi \times 60 = 377$ rad/s, $V_s = 120$ V, $\alpha = 90°$, and $\theta = \tan^{-1}(\omega L/R) = 44.43°$.

(a) The extinction angle can be determined from the solution of Eq. (6-16) and an iterative solution yields $\beta = 220.35°$. The conduction angle is $\delta = \beta - \alpha = 220.43 - 90 = 130.43°$.

(b) From Eq. (6-18), the rms output voltage is $V_o = 68.09$ V.

(c) Numerical integration of Eq. (6-19) between the limits $\omega t = \alpha$ to β gives the rms thyristor current as $I_R = 15.07$ A.

(d) From Eq. (6.20), $I_o = \sqrt{2} \times 15.07 = 21.3$ A.

(e) Numerical integration of Eq. (6-21) yields the average thyristor current as $I_A = 8.23$ A.

(f) The output power, $P_o = 21.3^2 \times 2.5 = 1134.2$ W, and the input volt-ampere rating, VA $= 120 \times 21.3 = 2556$ W; therefore,

$$\text{PF} = \frac{P_o}{\text{VA}} = \frac{1134.200}{2556} = 0.444 \text{ (lagging)}$$

Note. The switching action of thyristors makes the equations for currents nonlinear. A numerical method of solution for the thyristor conduction angle and currents is more efficient than classical techniques. A computer program named PROG-3 is used to solve this example and the program is listed in Appendix F. Students are encouraged to verify the results of this example and to appreciate the usefulness of a numerical solution, especially in solving nonlinear equations of thyristor circuits.

6-6 THREE-PHASE HALF-WAVE CONTROLLERS

The circuit diagram of a three-phase half-wave (or unidirectional) controller is shown in Fig. 6-7 with a wye-connected resistive load. The current flow to the load is controlled by thyristors T_1, T_3, and T_5; and the diodes provide the return

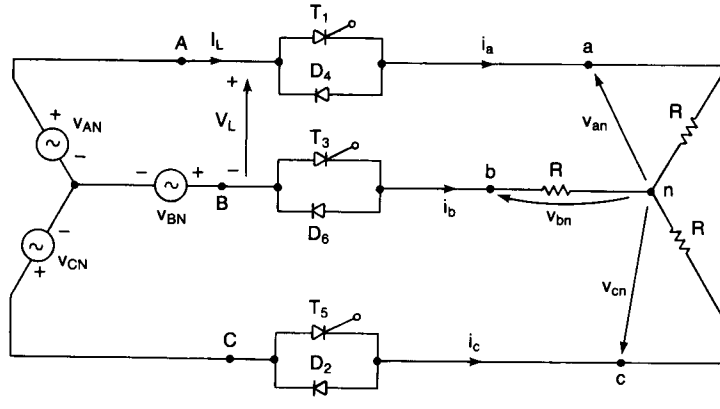


Figure 6-7 Three-phase unidirectional controller.

current path. The firing sequence of thyristors is T_1, T_3, T_5. For the current to flow through the power controller, at least one thyristor must conduct. If all the devices were diodes, three diodes would conduct at the same time and the conduction angle of each diode would be 180°. We may recall that a thyristor will conduct if its anode voltage is higher than that of its cathode and it is fired. Once a thyristor starts conducting, it would be turned off only when its current falls to zero.

If V_s is the rms value of input phase voltage and we define the instantaneous input phase voltages as

$$v_{AN} = \sqrt{2}\, V_s \sin \omega t$$

$$v_{BN} = \sqrt{2}\, V_s \sin\left(\omega t - \frac{2\pi}{3}\right)$$

$$v_{CN} = \sqrt{2}\, V_s \sin\left(\omega t - \frac{4\pi}{3}\right)$$

then the input line voltages are

$$v_{AB} = \sqrt{6}\, V_s \sin\left(\omega t + \frac{\pi}{6}\right)$$

$$v_{BC} = \sqrt{6}\, V_s \sin\left(\omega t - \frac{\pi}{2}\right)$$

$$v_{CA} = \sqrt{6}\, V_s \sin\left(\omega t - \frac{7\pi}{6}\right)$$

The waveforms for input voltages, conduction angles of devices, and output voltages are shown in Fig. 6-8 for $\alpha = 60°$ and $\alpha = 150°$. For $0 \leq \alpha < 60°$, either two or three devices can conduct at the same time and the possible combinations are (1) two thyristors and one diode, (2) one thyristor and one diode, and (3) one thyristor and two diodes. If three devices conduct, a normal three-phase operation occurs as shown in Fig. 6-9a and the output voltage of a phase is the same as the input phase voltage, for example,

$$v_{an} = v_{AN} = \sqrt{2}\, V_s \sin \omega t \tag{6-25}$$

On the other hand, if two devices conduct at the same time, the current flows only through two lines and the third line can be considered open circuited. The line-to-line voltage would appear across two terminals of the load as shown in Fig. 6-9b and the output phase voltage would be one-half of the line voltage (e.g., with terminal c being open circuited),

$$v_{an} = \frac{v_{AB}}{2} = \frac{\sqrt{3}\,\sqrt{2}\, V_s}{2} \sin\left(\omega t + \frac{\pi}{6}\right) \tag{6-26}$$

The waveform for an output phase voltage (e.g., v_{an}) can be drawn directly from the input phase and line voltages by noting that v_{an} would correspond to v_{AN} if three devices conduct, to $v_{AB}/2$ (or $v_{AC}/2$) if two devices conduct, and to zero if

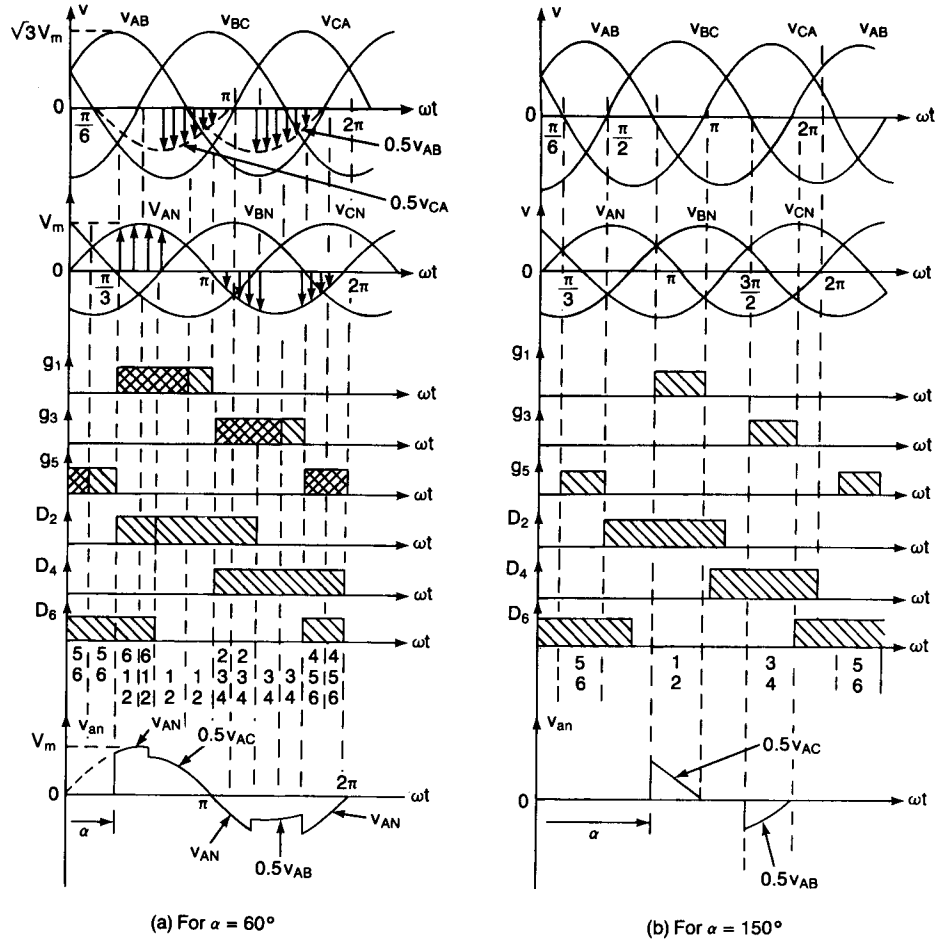


Figure 6-8 Waveforms for three-phase unidirectional controller.

terminal a is open circuited. For $60° \leq \alpha < 120°$, at any time only one thyristor is conducting and the return path is shared by one or two diodes. For $120° \leq \alpha < 210°$, only one thyristor and one diode conduct at the same time.

The extinction angle, β, of a thyristor can be delayed beyond 180° (e.g., β of T_1 is 210°). This is due to the fact that an output phase voltage may depend on the input line-to-line voltage. When v_{AB} becomes zero at $\omega t = 150°$, the current of thyristor T_1 can continue to flow until v_{CA} becomes zero at $\omega t = 210°$ and a delay angle of $\alpha = 210°$ gives zero output voltage (and power).

The gating pulses of thyristors should be continuous, and for example, the pulse of T_1 should end at $\omega t = 210°$. In practice, the gate pulses consist of two parts. The first pulse of T_1 starts anywhere between 0 and 150° and ends at $\omega t = 150°$, the second pulse, which can start at $\omega t = 150°$, always ends at $\omega t = 210°$. This allows the current to flow through thyristor T_1 during the period $150° \leq \omega t$

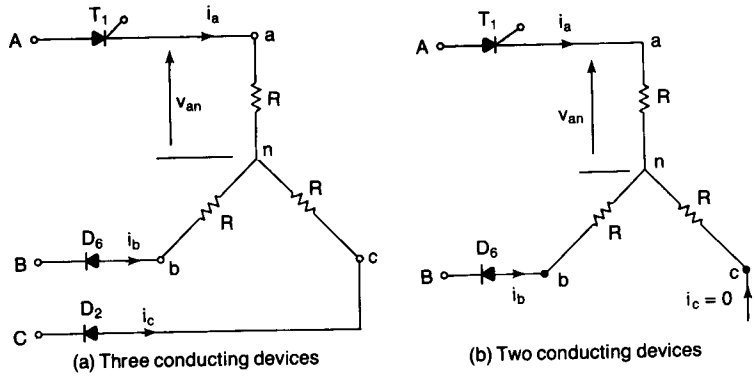


Figure 6-9 Wye-connected resistive load.

$\leq 210°$ and increases the control range of output voltage. The range of delay is

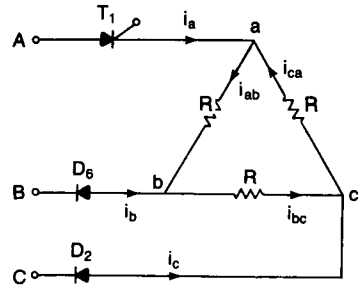
$$0 \leq \alpha \leq 210° \tag{6-27}$$

The expression for the rms output phase voltage depends on the range of delay angle. The rms output voltage for a wye-connected load can be found as follows. For $0 \leq \alpha < 90°$:

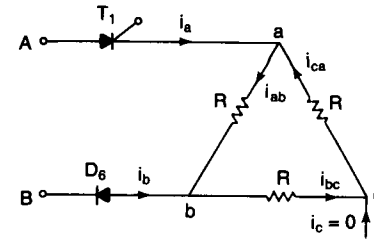
$$\begin{aligned} V_o &= \left[\frac{1}{2\pi}\int_0^{2\pi} v_{an}^2\, d(\omega t)\right]^{1/2} \\ &= \sqrt{6}\, V_s \left\{\frac{1}{2\pi}\left[\int_0^{2\pi/3} \frac{\sin^2 \omega t}{3}\, d(\omega t) + \int_{\pi/2}^{\pi/2+\alpha} \frac{\sin^2 \omega t}{4}\, d(\omega t)\right.\right. \\ &\quad + \int_{2\pi/3+\alpha}^{4\pi/3} \frac{\sin^2 \omega t}{3}\, d(\omega t) + \int_{3\pi/2}^{3\pi/2+\alpha} \frac{\sin^2 \omega t}{4}\, d(\omega t) \\ &\quad \left.\left. + \int_{4\pi/3+\alpha}^{2\pi} \frac{\sin^2 \omega t}{3}\, d(\omega t)\right]\right\}^{1/2} \\ &= \sqrt{3}\, V_s \left[\frac{1}{\pi}\left(\frac{\pi}{3} - \frac{\alpha}{4} + \frac{\sin 2\alpha}{8}\right)\right]^{1/2} \end{aligned} \tag{6-28}$$

For $90° \leq \alpha < 120°$:

$$\begin{aligned} V_o &= \sqrt{6}\, V_s \left\{\frac{1}{2\pi}\left[\int_\alpha^{2\pi/3} \frac{\sin^2 \omega t}{3}\, d(\omega t) + \int_{\pi/2}^{\pi} \frac{\sin^2 \omega t}{4}\, d(\omega t)\right.\right. \\ &\quad + \int_{2\pi/3+\alpha}^{4\pi/3} \frac{\sin^2 \omega t}{3}\, d(\omega t) + \int_{3\pi/2}^{2\pi} \frac{\sin^2 \omega t}{4}\, d(\omega t) \\ &\quad \left.\left. + \int_{4\pi/3+\alpha}^{2\pi} \frac{\sin^2 \omega t}{3}\, d(\omega t)\right]\right\}^{1/2} \\ &= \sqrt{3}\, V_s \left[\frac{1}{\pi}\left(\frac{11\,\pi}{24} - \frac{\alpha}{2}\right)\right]^{1/2} \end{aligned} \tag{6-29}$$



(a) Three conducting devices



(b) Two conducting devices

For $120° \leq \alpha < 210°$:

$$V_o = \sqrt{6}\, V_s \left\{ \frac{1}{2\pi} \left[\int_{\pi/2 - 2\pi/3 + \alpha}^{\pi} \frac{\sin^2 \omega t}{3}\, d(\omega t) + \int_{3\pi/2 - 2\pi/3 + \alpha}^{2\pi} \frac{\sin^2 \omega t}{4}\, d(\omega t) \right\} \right]^{1/2} \tag{6-30}$$

$$= \sqrt{3}\, V_s \left[\frac{1}{\pi} \left(\frac{7\pi}{24} - \frac{\alpha}{4} + \frac{\sin 2\alpha}{16} - \frac{\sqrt{3} \cos 2\alpha}{16} \right) \right]^{1/2}$$

In the case of delta-connected load, the output phase voltage would be the same as the line-to-line voltage. However, the line current of the load would depend on the number of devices conducting at the same time. If three devices conduct, the line and phase currents would follow the normal relationship of a three-phase system, as shown in Fig. 6-10a. If the current in phase a is $i_{ab} = I_m \sin \omega t$, the line current will be $i_a = i_{ab} - i_{ca} = \sqrt{3}\, I_m \sin (\omega t - \pi/6)$. If two devices conduct at the same time, one terminal of load can be considered open-circuited as shown in Fig. 6-10b and $i_{ca} = i_{bc} = -i_{ab}/2$. The line current of load would be $i_a = i_{ab} - i_{ca} = (3I_m/2) \sin \omega t = 1.5 I_m \sin \omega t$.

The power devices can be connected together as shown in Fig. 6-11. This arrangement, which permits assembly as a compact unit, is possible only if the neutral of load is accessible.

Example 6-5

The three-phase unidirectional controller in Fig. 6-7 supplies a wye-connected resistive load of $R = 10\ \Omega$ and the line-to-line input voltage is 208 V, 60 Hz. The delay is $\alpha = \pi/3$. Determine the (a) rms output phase voltage, V_o; (b) input power factor, PF; and (c) expressions for the instantaneous output voltage of phase a.

Solution $V_L = 208$ V, $V_s = V_L/\sqrt{3} = 208/\sqrt{3} = 120$ V, $\alpha = \pi/3$, and $R = 10\ \Omega$.

(a) From (6-28) the rms output phase voltage is $V_o = 110.86$ V.

(b) The rms phase current of the load, $I_a = 110.86/10 = 11.086$ A and the

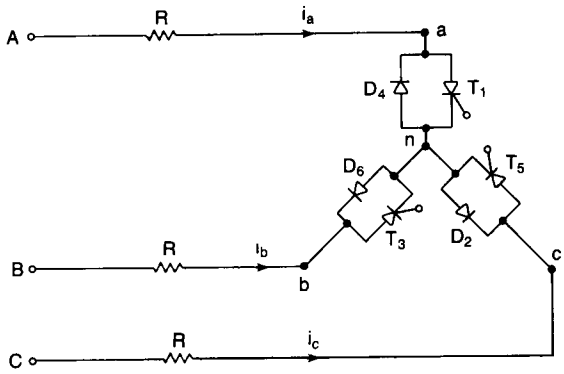


Figure 6-11 Alternative arrangement of three-phase unidirectional controller.

output power,

$$P_o = 3I_a^2R = 3 \times 11.086^2 \times 10 = 3686.98 \text{ W}$$

Since the load is connected in wye, the phase current is equal to the line current, $I_L = I_a = 11.086$ A. The input volt-ampere rating,

$$\text{VA} = 3V_sI_L = 3 \times 120 \times 11.086 = 3990.96 \text{ VA}$$

The power factor,

$$\text{PF} = \frac{P_o}{\text{VA}} = \frac{3686.98}{3990.96} = 0.924 \text{ (lagging)}$$

(c) If the input phase voltage is taken as the reference and is $v_{AN} = 120\sqrt{2} \sin \omega t = 169.7 \sin \omega t$, the instantaneous input line voltages are

$$v_{AB} = 208\sqrt{2} \sin\left(\omega t + \frac{\pi}{6}\right) = 294.2 \sin\left(\omega t + \frac{\pi}{6}\right)$$

$$v_{BC} = 294.2 \sin\left(\omega t - \frac{\pi}{2}\right)$$

$$v_{CA} = 294.2 \sin\left(\omega t - \frac{7\pi}{6}\right)$$

The instantaneous output phase voltage, v_{an}, which depends on the number of conducting devices, can be determined from Fig. 6-8a as follows:

For $0 \le \omega t < \pi/3$: $v_{an} = 0$
For $\pi/3 \le \omega t < 4\pi/6$: $v_{an} = v_{AN} = 169.7 \sin \omega t$
For $4\pi/6 \le \omega t < \pi$: $v_{an} = v_{AC}/2 = -v_{CA}/2 = 147.1 \sin(\omega t - 7\pi/6 - \pi)$
For $\pi \le \omega t < 3\pi/2$: $v_{an} = v_{AN} = 169.7 \sin \omega t$
For $3\pi/2 \le \omega t < 5\pi/3$: $v_{an} = v_{AB}/2 = 147.1 \sin(\omega t + \pi/6)$
For $5\pi/3 \le \omega t < 2\pi$: $v_{an} = v_{AN} = 169.7 \sin \omega t$

Note. The power factor of this power controller depends on the delay angle, α.

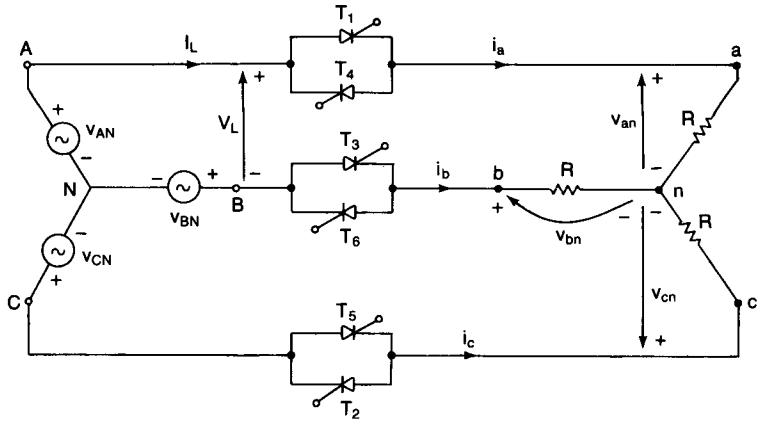


Figure 6-12 Three-phase bidirectional controller.

6-7 THREE-PHASE FULL-WAVE CONTROLLERS

The unidirectional controllers, which contain dc input current and higher harmonic content due to the asymmetrical nature of the output voltage waveform, are not normally used in ac motor drives; a three-phase bidirectional control is commonly used. The circuit diagram of a three-phase full-wave (or bidirectional) controller is shown in Fig. 6-12 with a wye-connected resistive load. The operation of this controller is similar to that of a half-wave controller, except that the return current path is provided by thyristors T_2, T_4, and T_6 instead of diodes. The firing sequence of thyristors is T_1, T_2, T_3, T_4, T_5, T_6.

If we define the instantaneous input phase voltages as

$$v_{AN} = \sqrt{2}V_s \sin \omega t$$

$$v_{BN} = \sqrt{2}V_s \sin\left(\omega t - \frac{2\pi}{3}\right)$$

$$v_{CN} = \sqrt{2}V_s \sin\left(\omega t - \frac{4\pi}{3}\right)$$

the instantaneous input line voltages are

$$v_{AB} = \sqrt{6}\, V_s \sin\left(\omega t + \frac{\pi}{6}\right)$$

$$v_{BC} = \sqrt{6}\, V_s \sin\left(\omega t - \frac{\pi}{2}\right)$$

$$v_{CA} = \sqrt{6}\, V_s \sin\left(\omega t - \frac{7\pi}{6}\right)$$

The waveforms for the input voltages, conduction angles of thyristors, and

output phase voltages are shown in Fig. 6-13 for $\alpha = 60°$ and $\alpha = 120°$. For $0 \leq \alpha < 60°$, immediately before the firing of T_1, two thyristors conduct. Once T_1 is fired, three thyristors conduct. A thyristor turns off when its current attempts to reverse. The conditions alternate between two and three conducting thyristors.

For $60° \leq \alpha < 90°$, only two thyristors conduct at any time. For $90° \leq \alpha < 150°$, although two thyristors conduct at any time, there are periods when no thyristors are on. For $\alpha \geq 150°$, there is no period for two conducting thyristors and the output voltage becomes zero at $\alpha = 150°$. The range of delay angle is

$$0 \leq \alpha \leq 150° \tag{6-31}$$

Similar to half-wave controllers, the expression for the rms output phase

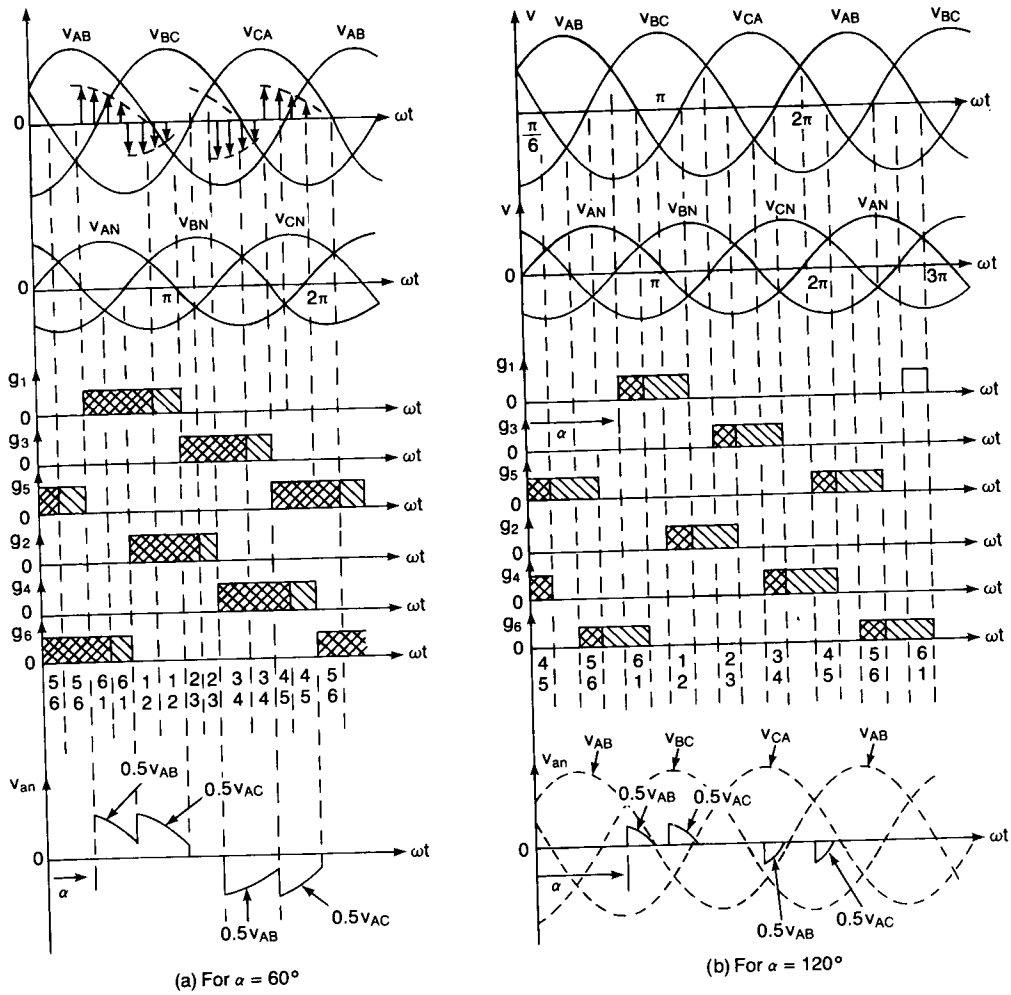


Figure 6-13 Waveforms for three-phase bidirectional controller.

voltage depends on the range of delay angles. The rms output voltage for a wye-connected load can be found as follows. For $0 \le \alpha < 60°$:

$$\begin{aligned} V_o &= \left[\frac{1}{2\pi}\int_0^{2\pi} v_{an}^2\, d(\omega t)\right]^{1/2} \\ &= \sqrt{6}\, V_s \left\{\frac{2}{2\pi}\left[\int_\alpha^{\pi/3} \frac{\sin^2 \omega t}{3}\, d(\omega t) + \int_{\pi/2}^{\pi/2+\alpha} \frac{\sin^2 \omega t}{4}\, d(\omega t)\right.\right. \\ &\quad + \int_{\pi/3+\alpha}^{2\pi/3} \frac{\sin^2 \omega t}{3}\, d(\omega t) + \int_{\pi/2}^{\pi/2+\alpha} \frac{\sin^2 \omega t}{4}\, d(\omega t) \\ &\quad \left.\left. + \int_{2\pi/3+\alpha}^{\pi} \frac{\sin^2 \omega t}{3}\, d(\omega t)\right]\right\}^{1/2} \\ &= \sqrt{6}\, V_s \left[\frac{1}{\pi}\left(\frac{\pi}{6} - \frac{\alpha}{4} + \frac{\sin 2\alpha}{8}\right)\right]^{1/2} \end{aligned} \tag{6-32}$$

For $60° \le \alpha$ $90°$:

$$\begin{aligned} V_o &= \sqrt{6}V_s\left[\frac{2}{2\pi}\left\{\int_{\pi 2-\pi/3+\alpha}^{5\pi/6-\pi/3+\alpha} \frac{\sin^2\omega t}{4} d(\omega t) + \int_{\pi/2-\pi/3+\alpha}^{5\pi/6-\pi/3+\alpha} \frac{\sin^2\omega t}{4} d(\omega t)\right\}\right]^{1/2} \\ &= \sqrt{6}V_s\left[\frac{1}{\pi}\left(\frac{\pi}{12} + \frac{3\sin 2\alpha}{16} + \frac{\sqrt{3}\cos 2\alpha}{16}\right)\right]^{1/2} \end{aligned} \tag{6-33}$$

For $90° \le \alpha \le 150°$:

$$\begin{aligned} V_0 &= \sqrt{6}V_s\left\{\frac{2}{2\pi}\left[\int_{\pi/2-\pi/3+\alpha}^{\pi} \frac{\sin^2\omega t}{4} d(\omega t) + \int_{\pi/2-\pi/3+\alpha}^{\pi} \frac{\sin^2\omega t}{4} d(\omega t)\right]\right\}^{1/2} \\ &= \sqrt{6}V_s\left[\frac{1}{\pi}\left(\frac{5\pi}{24} - \frac{\alpha}{4} + \frac{\sin 2\alpha}{16} + \frac{\sqrt{3}\cos 2\alpha}{16}\right)\right]^{1/2} \end{aligned} \tag{6-34}$$

The power devices of a three-phase bidirectional controller can be connected together as shown in Fig. 6-14. This arrangement is also known as *tie control* and allows assembly of all thyristors as one unit.

Example 6-6

Repeat Example 6-5 for the three-phase bidirectional controller in Fig. 6-12.

Solution $V_L = 208$ V, $V_s = V_L/\sqrt{3} = 208/\sqrt{3} = 120$ V, $\alpha = \pi/3$, and $R = 10\ \Omega$.

(a) From (6-32) the rms output phase voltage is $V_o = 100.9$ V.

(b) The rms phase current of the load is $I_a = 100.9/10 = 10.09$ A and the output power is

$$P_o = 3I_a^2R = 3 \times 10.09^2 \times 10 = 3054.24 \text{ W}$$

Since the load is connected in wye, the phase current is equal to the line current, $I_L = I_a = 10.09$ A. The input volt-ampere,

$$\text{VA} = 3V_sI_L = 3 \times 120 \times 10.09 = 3632.4 \text{ VA}$$

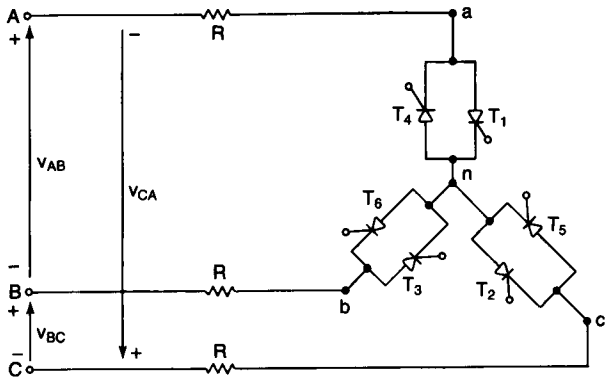


Figure 6-14 Arrangement for three-phase bidirectional tie control.

The power factor,

$$\text{PF} = \frac{P_o}{\text{VA}} = \frac{3054.24}{3632.4} = 0.84 \text{ (lagging)}$$

(c) If the input phase voltage is taken as the reference and is $v_{AN} = 120\sqrt{2} \sin \omega t = 169.7 \sin \omega t$, the instantaneous input line voltages are

$$v_{AB} = 208\sqrt{2} \sin\left(\omega t + \frac{\pi}{6}\right) = 294.2 \sin\left(\omega t + \frac{\pi}{6}\right)$$

$$v_{BC} = 294.2 \sin\left(\omega t - \frac{\pi}{2}\right)$$

$$v_{CA} = 294.2 \sin\left(\omega t - \frac{7\pi}{6}\right)$$

The instantaneous output phase voltage, v_{an}, which depends on the number of conducting devices, can be determined from Fig. 6-13a as follows:

For $0 \le \omega t < \pi/3$: $v_{an} = 0$
For $\pi/3 \le \omega t < 2\pi/3$: $v_{an} = v_{AB}/2 = 147.1 \sin(\omega t + \pi/6)$
For $2\pi/3 \le \omega t < \pi$: $v_{an} = v_{AC}/2 = -v_{CA}/2 = -147.1 \sin(\omega t - 7\pi/6 - \pi)$
For $\pi \le \omega t < 4\pi/3$: $v_{an} = 0$
For $4\pi/3 \le \omega t < 5\pi/3$: $v_{an} = v_{AB}/2 = 147.1 \sin(\omega t + \pi/6)$
For $5\pi/3 \le \omega t < 2\pi$: $v_{an} = v_{AC}/2 = 147.1 \sin(\omega t - 7\pi/6 - \pi)$

Note. The power factor, which depends on the delay angle, α, is in general poor compared to that of the half-wave controller.

6-8 THREE-PHASE BIDIRECTIONAL DELTA-CONNECTED CONTROLLERS

If the terminals of a three-phase system are accessible, the control elements (or power devices) and load may be connected in delta as shown in Fig. 6-15. Since the phase current in a normal three-phase system is only $1/\sqrt{3}$ of the line current,

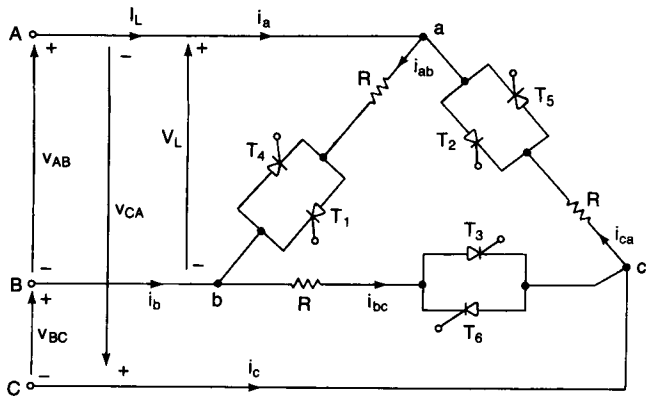


Figure 6-15 Delta-connected three-phase controller.

the current ratings of thyristors would be less than that if thyristors (or control elements) were placed in the line.

Let us assume that the instantaneous line-to-line voltages are:

$$v_{AB} = v_{ab} = \sqrt{2}V_s \sin \omega t$$

$$v_{BC} = v_{bc} = \sqrt{2}V_s \sin\left(\omega t - \frac{2\pi}{3}\right)$$

$$v_{CA} = v_{ca} = \sqrt{2}V_s \sin\left(\omega t - \frac{4\pi}{3}\right)$$

The input line voltages, phase and line currents, and thyristor gating signals are shown in Fig. 6-16 for $\alpha = 120°$ and resistive load.

For resistive loads, the rms output phase voltage can be determined from

$$V_o = \left[\frac{1}{2\pi}\int_{\alpha}^{2\pi} v_{ab}^2 \, d(\omega t)\right]^{1/2} = \left[\frac{2}{2\pi}\int_{\alpha}^{\pi} 2\,V_s^2 \sin \omega t \, d(\omega t)\right]^{1/2}$$

$$= V_s\left[\frac{1}{\pi}\left(\pi - \alpha + \frac{\sin 2\alpha}{2}\right)\right]^{1/2} \tag{6-35}$$

The maximum output voltage would be obtained when $\alpha = 0$ and the control range of delay angle is

$$0 \le \alpha \le \pi \tag{6-36}$$

The line currents, which can be determined from the phase currents, are

$$\begin{aligned} i_a &= i_{ab} - i_{ca} \\ i_b &= i_{bc} - i_{ab} \\ i_c &= i_{ca} - i_{bc} \end{aligned} \tag{6-37}$$

We can notice from Fig. 6-16 that the line currents depend on the delay angle and

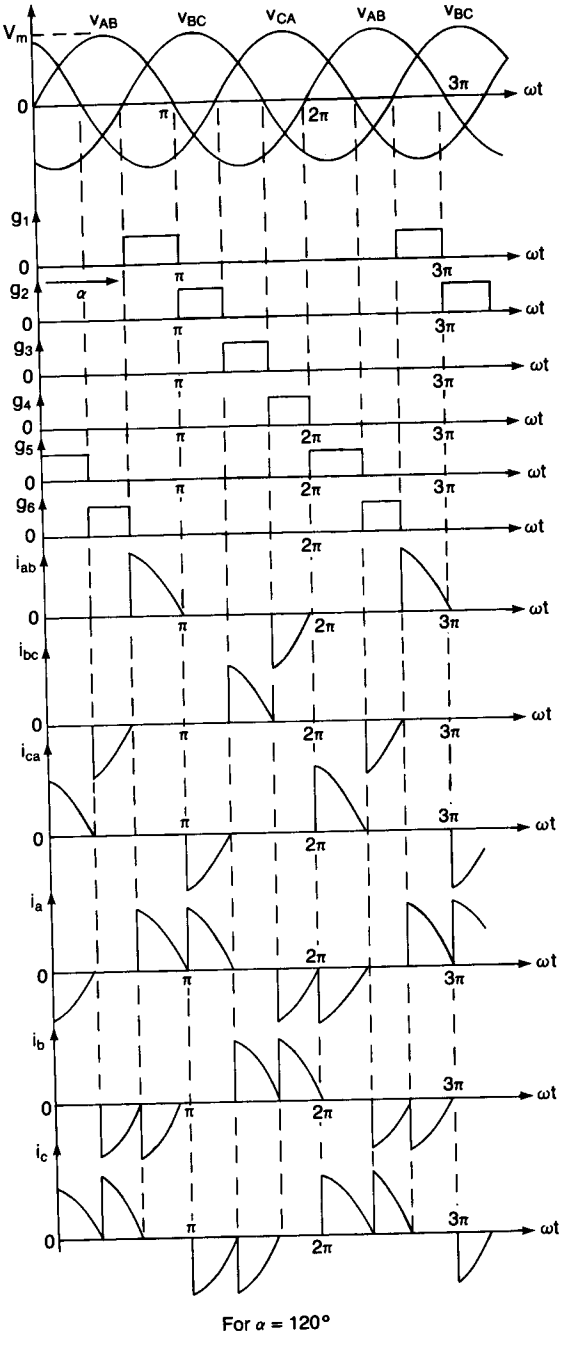


Figure 6-16 Waveforms for delta-connected controller.

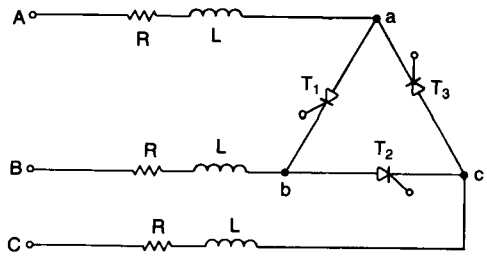


Figure 6-17 Three-phase three-thyristors controller.

may be discontinuous. The rms value of line and phase currents for the load circuits can be determined by numerical solution or Fourier analysis. If I_n is the rms value of the nth harmonic component of a phase current, the rms value of phase current can be found from

$$I_{ab} = (I_1^2 + I_3^2 + I_5^2 + I_7^2 + I_9^2 + I_{11}^2 + \cdots)^{1/2} \tag{6-38}$$

Due to the delta connection, the triplen harmonic components (i.e., those of order $n = 3m$, where m is an odd integer) of the phase currents would flow around the delta and would not appear in the line. This is due to the fact that the zero-sequence harmonics are in phase in all three phases of load. The rms line current becomes

$$I_a = \sqrt{3}\,(I_1^2 + I_5^2 + I_7^2 + I_{11}^2 + \cdots)^{1/2} \tag{6-39}$$

As a result, the rms value of line current would not follow the normal relationship of a three-phase system such that

$$I_a < \sqrt{3}\, I_{ab} \tag{6-40}$$

An alternative form of delta-connected controllers which requires only three thyristors and simplifies the control circuitry is shown in Fig. 6-17. This arrangement is also known as a *polygon-connected controller.*

Example 6-7

The three-phase bidirectional delta-connected controller in Fig. 6-15 has a resistive load of $R = 10\ \Omega$. If the line-to-line voltage is $V_s = 208$ V, 60 Hz, and the delay angle $\alpha = 2\pi/3$, determine the (a) rms output phase voltage, V_o; (b) expressions for instantaneous currents i_a, i_{ab}, and i_{ca}; (c) rms output phase current, I_{ab}, and rms line current, I_a; (d) input power factor, PF; and (e) rms current of a thyristor, I_R.

Solution $V_L = V_s = 208$ V, $\alpha = 2\pi/3$, $R = 10\ \Omega$, and peak value of phase current, $I_m = \sqrt{2} \times 208/10 = 29.4$ A.

(a) From Eq. (6-35), $V_o = 92$ V.

(b) Assuming i_{ab} as the reference phasor and $i_{ab} = I_m \sin \omega t$, the instantaneous currents are:

For $0 \le \omega t < \pi/3$: $i_{ab} = 0$

$$i_{ca} = I_m \sin(\omega t - 4\pi/3)$$

$$i_a = i_{ab} - i_{ca} = -I_m \sin(\omega t - 4\pi/3)$$

For $\pi/3 < \omega t < 2\pi/3$: $i_{ab} = i_{ca} = i_a = 0$

For $2\pi/3 < \omega t < \pi$: $i_{ab} = I_m \sin \omega t$

$i_{ca} = 0$

$i_a = i_{ab} - i_{ca} = I_m \sin \omega t$

For $\pi < \omega t < 4\pi/3$: $i_{ab} = 0$

$i_{ca} = I_m \sin (\omega t - 4\pi/3)$

$i_a = i_{ab} - i_{ca} = -I_m \sin (\omega t - 4\pi/3)$

For $4\pi/3 < \omega t < 5\pi/3$: $i_{ab} = i_{ca} = i_a = 0$

For $5\pi/3 < \omega t < 2\pi$: $i_{ab} = I_m \sin \omega t$

$i_{ca} = 0$

$i_a = i_{ab} - i_{ca} = I_m \sin \omega t$

(c) The rms values of i_{ab} and i_a are determined by numerical integration using a computer program named PROG-4, which is given in Appendix F. Students are encouraged to verify the results.

$$I_{ab} = 9.32 \text{ A} \qquad I_L = I_a = 13.18 \text{ A} \qquad \frac{I_a}{I_{ab}} = \frac{13.18}{9.32} = 1.1414 \neq \sqrt{3}$$

(d) The output power,

$$P_o = 3I_{ab}^2 R = 3 \times 9.32^2 \times 10 = 2605.9$$

The volt-amperes,

$$\text{VA} = 3V_s I_L = 3 \times 208 \times 9.32 = 5815.7$$

The power factor,

$$\text{PF} = \frac{P_o}{\text{VA}} = \frac{2605.900}{5815.7} = 0.448 \text{ (lagging)}$$

(e) The thyristor current can be determined from the phase current,

$$I_R = \frac{I_{ab}}{\sqrt{2}} = \frac{9.32}{\sqrt{2}} = 6.59 \text{ A}$$

Note. $V_o = I_{ab}R = 9.32 \times 10 = 93.2$ V, whereas Eq. (6-35) gives 92 V. The difference is due to rounding off in the numerical solution.

6-9 SINGLE-PHASE TRANSFORMER TAP CHANGERS

Thyristors can be used as static switches for on-load tap changing of transformers. The static tap changers have the advantage of very fast switching action. The changeover can be controlled to cope with load conditions and is smooth. The circuit diagram of a single-phase transformer tap changer is shown in Fig. 6-18. Although a transformer may have multiple secondary windings, only two secondary windings are shown, for the sake of simplicity.

The turn ratio of input transformer are such that if the primary instantaneous voltage is

$$v_p = \sqrt{2}\, V_s \sin \omega t = \sqrt{2}\, V_p \sin \omega t$$

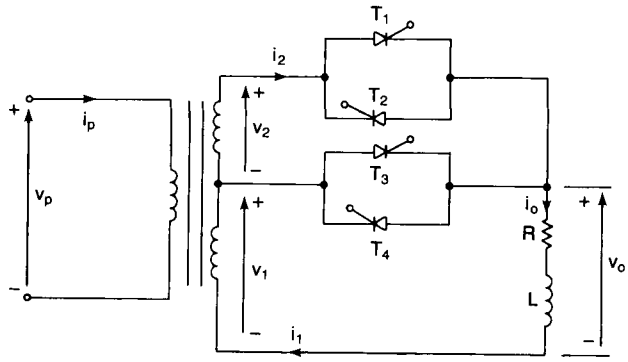


Figure 6-18 Single-phase transformer tap changer.

the secondary instantaneous voltages are

$$v_1 = \sqrt{2}\, V_1 \sin \omega t$$

and

$$v_2 = \sqrt{2}\, V_2 \sin \omega t$$

A tap changer is most commonly used for resistive heating loads. When only thyristors T_3 and T_4 are alternately fired with a delay angle of $\alpha = 0$, the load voltage is held at a reduced level of $V_o = V_1$. If full output voltage is required, only thyristors T_1 and T_2 are alternately fired with a delay angle of $\alpha = 0$ and the full voltage is $V_o = V_1$ and V_2.
The gating pulses of thyristors can be controlled to vary the load voltage. The rms value of load voltage, V_o, can be varied within three possible ranges:

$$0 < V_o < V_1$$

$$0 < V_o < (V_1 + V_2)$$

and

$$V_1 < V_o < (V_1 + V_2)$$

Control range 1: $0 \le V_o \le V_1$. To vary the load voltage within this range, thyristors T_1 and T_2 are turned off. Thyristors T_3 and T_4 can operate as a single-phase voltage controller. The instantaneous load voltage v_0 and current i_0 are shown in Fig. 6-19c for a resistive load. The rms load voltage which can be determined from Eq. 6-8) load is

$$V_o = V_1 \left[\frac{1}{\pi} \left(\pi - \alpha + \frac{\sin 2\alpha}{2} \right) \right]^{1/2} \tag{6-41}$$

and the range of delay angle is $0 \le \alpha \le \pi$.

Control range 2: $0 \le V_o \le (V_1 + V_2)$. Thyristors T_3 and T_4 are turned off. Thyristors T_1 and T_2 operate as a single-phase voltage controller. Figure

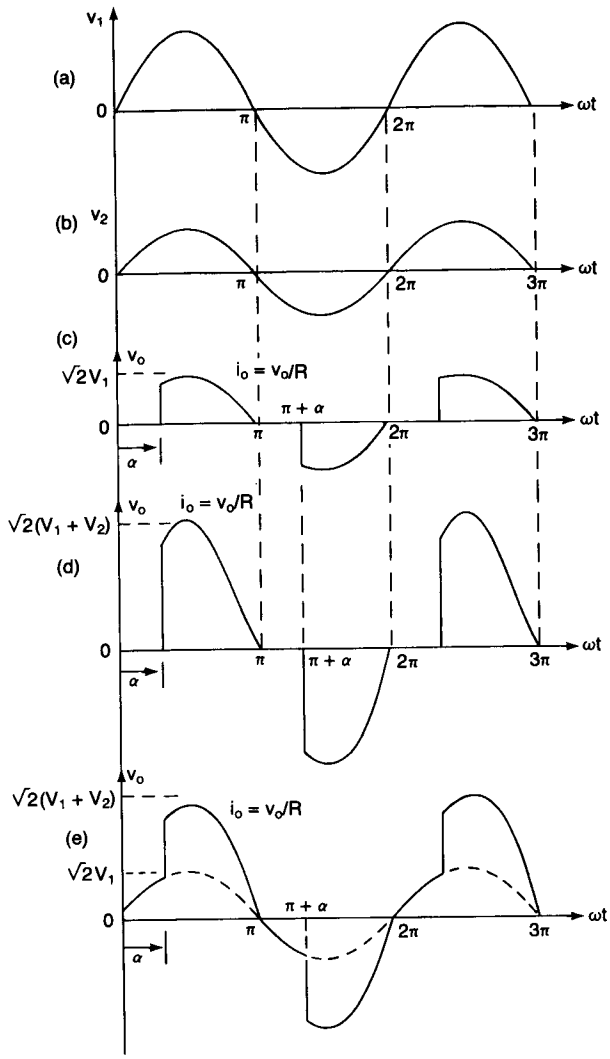


Figure 6-19 Waveforms for transformer tap changer.

6-19d shows the load voltage v_0 and current i_0 for a resistive load. The rms load voltage can be found from

$$V_o = (V_1 + V_2)\left[\frac{1}{\pi}\left(\pi - \alpha + \frac{\sin 2\alpha}{2}\right)\right]^{1/2} \tag{6-42}$$

and the range of delay angle is $0 \leq \alpha \leq \pi$.

Control range 3: $V_1 < V_o < (V_1 + V_2)$. Thyristor T_3 is turned on at $\omega t = 0$ and the secondary voltage, v_1, appears across the load. If thyristor T_1 is turned on at $\omega t = \alpha$, thyristor T_3 is reverse biased due to secondary voltage v_2, and T_3 is turned off. The voltage appearing across the load is $(v_1 + v_2)$. At ωt

$= \pi$, T_1 is self-commutated and T_4 is turned on. The secondary voltage v_1 appears across the load until T_2 is fired at $\omega t = \pi + \alpha$. When T_2 is turned on at $\omega t = \pi + \alpha$, T_4 is turned off due to reverse voltage v_2 and the load voltage is $(v_1 + v_2)$. At $\omega t = 2\pi$, T_2 is self-commutated, T_3 is turned on again and the cycle is repeated. The instantaneous load voltage v_0 and current i_0 are shown in Fig. 6-19e for a resistive load.

A tap changer with this type of control is also known as a *synchronous tap changer*. It uses two-step control. A part of secondary voltage v_2 is superimposed on a sinusoidal voltage v_1. As a result the harmonic contents are less that which would be obtained by a normal phase delay as discussed above for control range 2. The rms load voltage can be found from

$$\begin{aligned} V_o &= \left[\frac{1}{2\pi}\int_0^{2\pi} v_0^2 d(\omega t)\right]^{1/2} \\ &= \left\{\frac{2}{2\pi}\left[\int_0^{\alpha} 2V_1^2 \sin^2\omega t\, d(\omega t) + \int_{\alpha}^{\pi} 2(V_1 + V_2)^2 \sin^2\omega t\, d(\omega t)\right]\right\}^{1/2} \\ &= \left[\frac{V_1^2}{\pi}\left(\alpha - \frac{\sin 2\alpha}{2}\right) + \frac{(V_1 + V_2)^2}{\pi}\left(\pi - \alpha + \frac{\sin 2\alpha}{2}\right)\right]^{1/2} \end{aligned} \tag{6-43}$$

With RL loads, the gating circuit of a synchronous tap changer requires a careful design. Let us assume that thyristors T_1 and T_2 are turned off, while thyristors T_3 and T_4 are turned on during the alternate half-cycle. The load current would then be

$$i_o = \frac{\sqrt{2}\, V_1}{Z} \sin(\omega t - \theta)$$

where $Z = [R^2 + (\omega L)^2]^{1/2}$ and $\theta = \tan^{-1}(\omega L/R)$.

The instantaneous load current i_0 is shown in Fig. 6-20a. If T_1 is then turned on at $\omega t = \alpha$, where $\alpha < \theta$, the second winding of transformer would be short circuited because thyristor T_4 is still conducting and carrying current due to the inductive load. Therefore, the control circuit should be designed so that T_1 is not turned on until T_4 turns off and $i_0 \geq 0$. Similarly, T_2 should not be turned on until T_3 turns off and $i_0 \leq 0$. The waveforms of load voltage v_0 and load current i_0 are shown in Fig. 6-20b for $\alpha > \theta$.

Example 6-8

The circuit in Fig. 6-18 is controlled as a synchronous tap changer. The primary voltage is 240 V, 60 Hz. The secondary voltages are $V_1 = 120$ V and $V_2 = 120$ V. If the load resistance is $R = 10\ \Omega$ and the rms load voltage is 180 V, determine the (a) delay angle of thyristors T_1 and T_2; (b) rms current of thyristors T_1 and T_2; (c) rms current of thyristors T_3 and T_4; and (d) input power factor, PF.

Solution $V_o = 180$ V, $V_p = 240$ V, $V_1 = 120$ V, $V_2 = 120$ V, and $R = 10\ \Omega$.

(a) The required value of delay angle α for $V_o = 180$ V can be found from Eq. (6-43) in two ways (1) plot V_o against α and find the required value of α, or (2) use an iterative method of solution. A computer program is used to solve Eq. (6-43) for α by iteration and this gives $\alpha = 98°$.

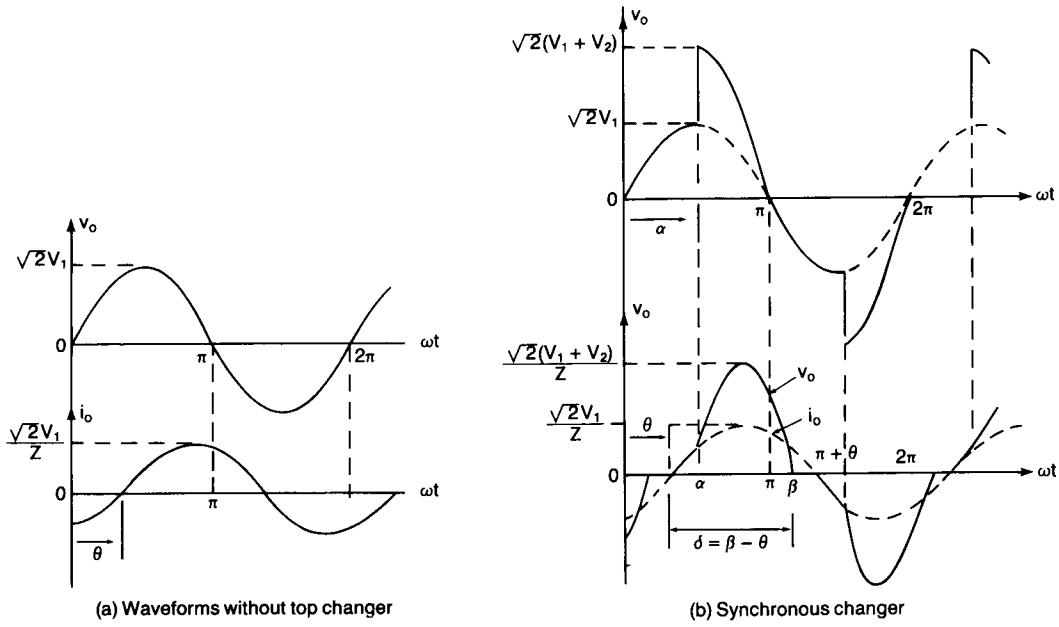


Figure 6-20 Voltage and current waveforms for *RL* load.

(b) The rms current of thyristors T_1 and T_2 can be found from

$$I_{R1} = \left[\frac{1}{2\pi R^2}\int_{\alpha}^{\pi} 2(V_1 + V_2)^2 \sin^2 \omega t \, d(\omega t)\right]^{1/2}$$

$$= \frac{V_1 + V_2}{\sqrt{2}R}\left[\frac{1}{\pi}\left(\pi - \alpha + \frac{\sin 2\alpha}{2}\right)\right]^{1/2} \tag{6-44}$$

$$= 10.9 \text{ A}$$

(c) The rms current of thryistors T_3 and T_4 is found from

$$I_{R3} = \left[\frac{1}{2\pi R^2}\int_{0}^{\alpha} 2V_1^2 \sin^2 \omega t \, d(\omega t)\right]^{1/2}$$

$$= \frac{V_1}{\sqrt{2}R}\left[\frac{1}{\pi}\left(\alpha - \frac{\sin 2\alpha}{2}\right)\right]^{1/2} \tag{6-45}$$

$$= 6.5 \text{ A}$$

(d) The rms current of a second secondary winding is $I_2 = \sqrt{2}\, I_{R1} = 15.4$ A. The rms current of the first secondary winding, which is the total rms current of thyristors T_1, T_2, T_3, and T_4, is

$$I_1 = [(\sqrt{2}\, I_{R1})^2 + (\sqrt{2}\, I_{R3})^2]^{1/2} = 17.94 \text{ A}$$

The volt-ampere rating of primary or secondary, VA $= V_1 I_1 + V_2 I_2 = 4000.8$. The load power, $P_o = V_0^2/R = 3240$ W, and the power factor,

$$\text{PF} = \frac{P_o}{\text{VA}} = \frac{3240}{4000.8} = 0.8098 \text{ (lagging)}$$

6-10 CYCLOCONVERTERS

The ac voltage controllers provide a variable output voltage, but the frequency of output voltage is fixed and in addition the harmonic content is high, especially at a low output voltage range. A variable output voltage at variable frequency can be obtained from two-stage conversions: fixed ac to variable dc (e.g., controlled rectifiers) and variable dc to variable ac at variable frequency (e.g., inverters, which are discussed in Chapter 8). However, cycloconverters can eliminate the need of one or more intermediate converters. A cycloconverter is a direct-frequency changer that converts ac power at one frequency to ac power at another frequency by ac–ac conversion, without an intermediate conversion link.

The majority of cycloconverters are naturally commutated and the maximum output frequency is limited to a value that is only a fraction of the source frequency. As a result the major applications of cycloconverters are low speed, ac motor drives in the range up to 15 000 kW with frequencies from 0 to 20 Hz. Ac drives are discussed in Chapter 11.

With the development of power conversion techniques and modern control methods, inverter-fed ac motor drives are taking over cycloconverter-fed drives. However, recent advancements in fast-switching power devices and microprocessors permit synthesizing and implementing advanced conversion strategies for forced-commutated direct-frequency changers (FDFCs) to optimize the efficiency and reduce the harmonic contents [1,2]. The switching functions of FCDFCs can be programmed to combine the switching functions of ac–dc and dc–ac converters. Due to the nature of derivations involved in FCDFCs, forced-commutated cycloconverters will not be discussed further.

6-10.1 Single-Phase Cycloconverters

The principle of operation of single-phase/single-phase cycloconverters can be explained with the help of Fig. 6-21a. The two single-phase controlled converters are operated as bridge rectifiers. However, their delay angles are such that the output voltage of one converter is equal and opposite to that of the other converter. If converter P is operating alone, the average output voltage is positive and if converter N is operating, the output voltage is negative. Figure 6-21b shows the waveforms for the output voltage and gating signals of positive and negative converters, with the positive converter on for time $T_0/2$ and the negative converter on for time $T_0/2$. The frequency of the output voltage is $f_o = 1/T_0$.

If α_p is the delay angle of positive converter, the delay angle of negative converter is $\alpha_n = \pi - \alpha_p$. The average output voltage of the positive converter is equal and opposite that of the negative converter.

$$v_{o2} = -V_{o1} \tag{6-46}$$

Similar to dual converters in Sections 4-5 and 4-10, the instantaneous values of two output voltages may not be equal. It is possible for large harmonic currents to circulate within the converters.

The circulating current can be eliminated by suppressing the gate pulses to

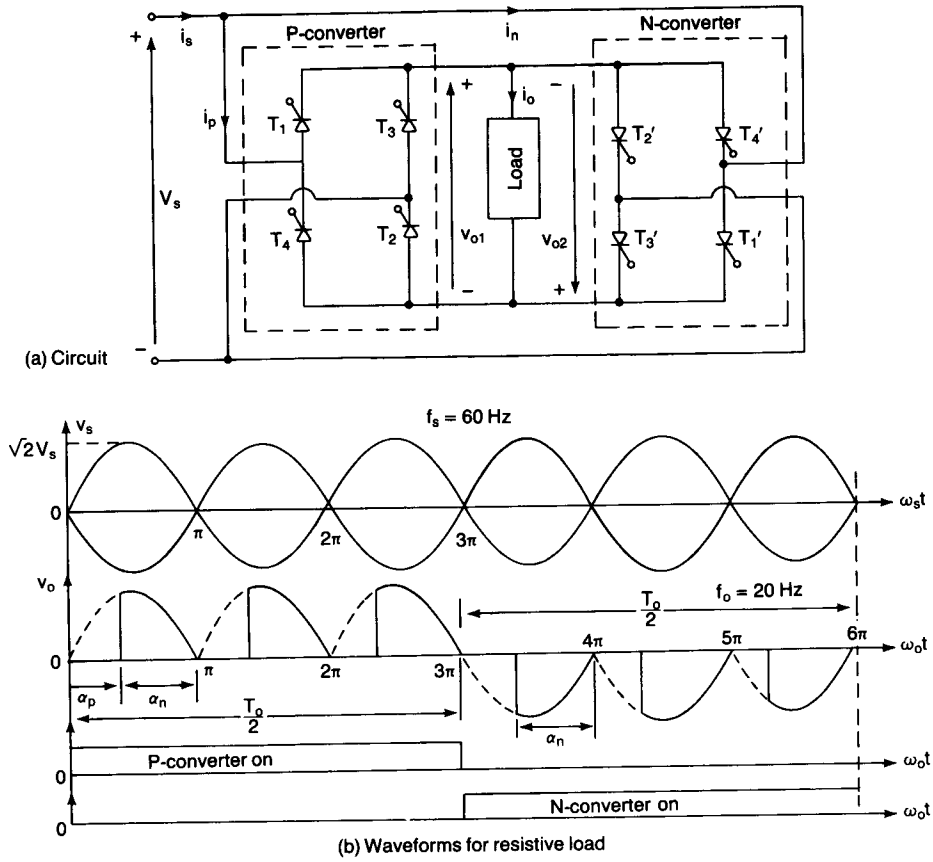
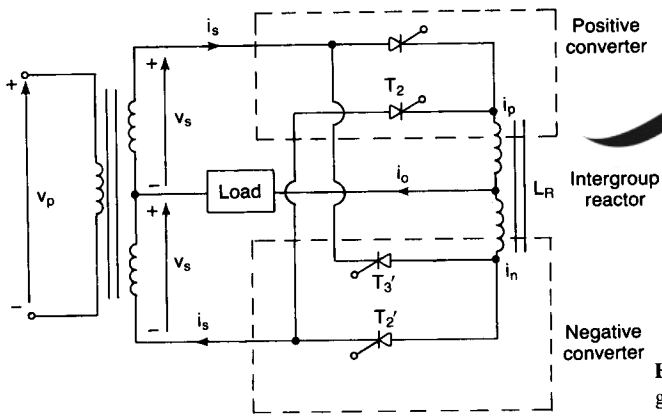


Figure 6-21 Single-phase/single-phase cycloconverter.

the converter not delivering load current. A single-phase converter with center-tap transformer as shown in Fig. 6-22 has an intergroup reactor, which maintains a continuous current flow and also limits the circulating current.



POWEREN.IR

Figure 6-22 Cycloconverter with intergroup reactor.

Example 6-9

The input voltage to the cycloconverter in Fig. 6-21a is 120 V, 60 Hz. The load resistance is 5 Ω and the load inductance is L = 40 mH. The frequency of the output voltage is 20 Hz. If the converters are operated as semiconverters such that $0 \leq \alpha \leq \pi$ and the delay angle is $\alpha_p = 2\pi/3$, determine the (a) rms value of output voltage, V_o, (b) rms current of each thyristor, I_R; and (c) input power factor, PF.

Solution V_s = 120 V, f_s = 60 Hz, f_o = 20 Hz, R = 5 Ω, L = 40 mH, $\alpha_p = 2\pi/3$, $\omega_0 = 2\pi \times 20 = 125.66$ rad/s, and $X_L = \omega_0 L = 5.027$ Ω.

(a) For $0 \leq \alpha \leq \pi$, Eq. (6-8) gives the rms output voltage

$$V_o = V_s \left[\frac{1}{\pi}\left(\pi - \alpha + \frac{\sin 2\alpha}{2}\right)\right]^{1/2} = 53 \text{ V} \tag{6-47}$$

(b) $Z = [R^2 + (\omega_0 L)^2]^{1/2} = 7.09$ Ω and $\theta = \tan^{-1}(\omega_0 L/R) = 45.2°$. The rms load current, $I_o = V_o/Z = 53/7.09 = 7.48$ A. The rms current through each converter, $I_p = I_N = I_o/\sqrt{2} = 5.29$ A and the rms current through each thryistor, $I_R = I_p/\sqrt{2} = 3.74$ A.

(c) The rms input current, $I_s = I_0 = 7.48$ A, the volt-ampere rating VA $= V_s I_s = 897.6$ VA, and the output power, $P_o = V_o I_o \cos\theta = 279.65$ W. From Eq. (6-8), the input power factor,

$$\text{PF} = \frac{P_o}{V_s I_s} = \frac{V_o \cos\theta}{V_s} = \cos\theta \left[\frac{1}{\pi}\left(\pi - \alpha + \frac{\sin 2\alpha}{2}\right)\right]^{1/2} = \frac{279.65}{897.6} = 0.312 \text{ (lagging)} \tag{6-48}$$

Note. Equation (6-48) does not include the harmonic content on the output voltage and gives the approximate value of power factor. The actual value will be less than that given by Eq. (6-48). Equations (6-47) and (6-48) are also valid for resistive loads.

6-10.2 Three-Phase Cycloconverters

The circuit diagram of a three-phase/single-phase cycloconverter is shown in Fig. 6-23a. The two ac–dc converters are three-phase controlled rectifiers. The synthesis of output waveform for an output frequency of 12 Hz is shown in Fig. 6-23b. The positive converter operates for half the period of output frequency and the negative converter operates for the other half-period. The analysis of this cycloconverter is similar to that of single-phase/single-phase cycloconverters.

The control of ac motors requires a three-phase voltage at variable frequency. The cycloconverter in Fig. 6-23a can be extended to provide three-phase output by having six three-phase converters as shown in Fig. 6-24a. Each phase consists of six thyristors as shown in Fig. 6-24b, and a total of 18 thyristors are required. If six full-wave three-phase rectifiers are used, 36 thyristors would be required.

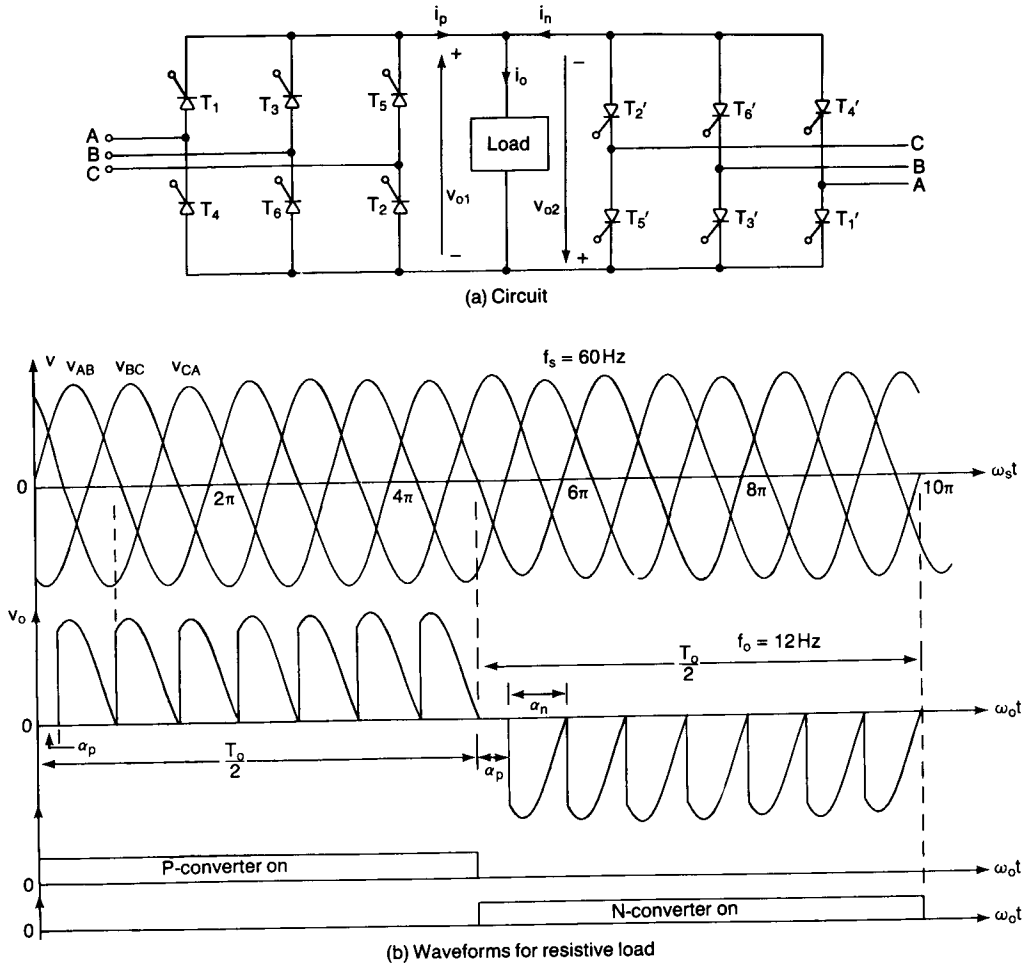


Figure 6-23 Three-phase/single-phase cycloconverter.

6-10.3 Reduction of Output Harmonics

We can notice from Figs. 6-21b and 6-23b that the output voltage is not purely sinusoidal, and as a result the output voltage contains harmonics. Equation (6-48) shows that the input power factor depends on the delay angle of thyristors and is poor, especially at the low output voltage range.

The output voltage of cycloconverters is basically made up of segments of input voltage(s) and the average value of a segment depends on the delay angle for that segment. If the delay angles of segments were varied in such a way that the average values of segments correspond as closely as possible to the variations of desired sinusoidal output voltage, the harmonics on the output voltage can be minimized. Since the average output voltage of a segment is a cosine function of

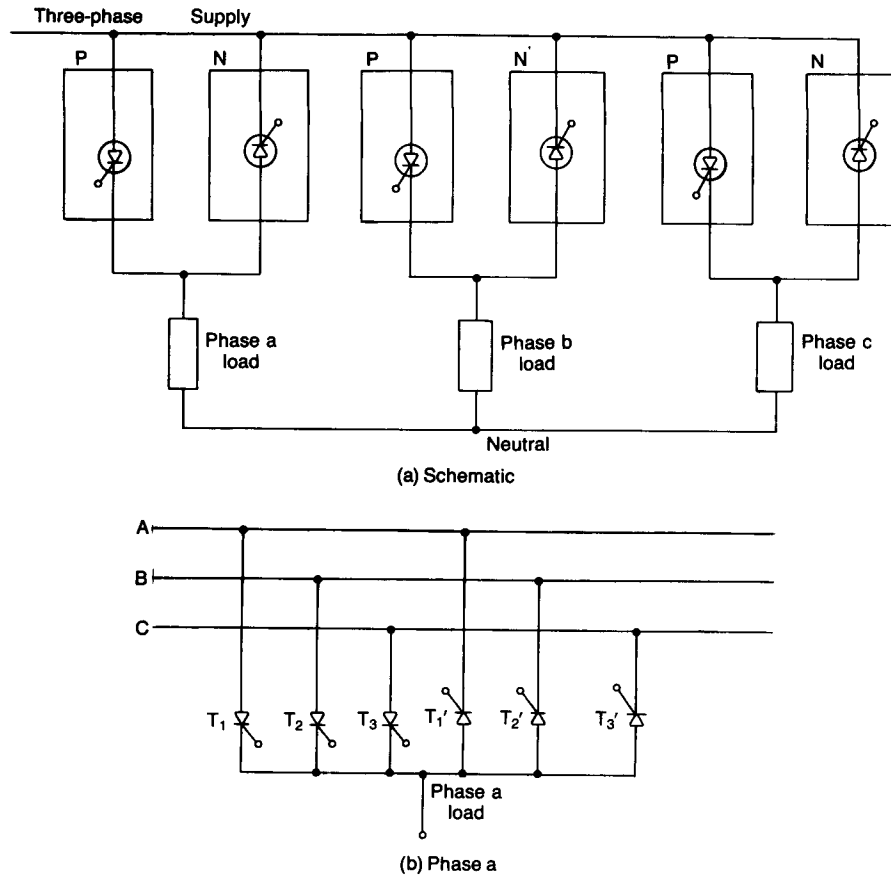


Figure 6-24 Three-phase/three-phase cycloconverter.

delay angle, the delay angles for segments can be generated by comparing a cosine signal at source frequency ($v_c = \sqrt{2}\, V_s \cos \omega_s t$) with an ideal sinusoidal output voltage at the output frequency ($v_r = \sqrt{2}\, V_r \sin \omega_0 t$). Figure 6-25 shows the generation of gating signals for the thyristors of the cycloconverter in Fig. 6-23a.

The maximum average voltage of a segment (which occurs for $\alpha_p = 0$) should be equal to the peak value of output voltage, for example,

$$V_p = \frac{2\sqrt{2}\, V_s}{\pi} = \sqrt{2}\, V_o \tag{6-49}$$

and Eq. (6-49) gives the rms value of output voltage as

$$V_o = \frac{\sqrt{2}\, V_s}{\pi} \tag{6-50}$$

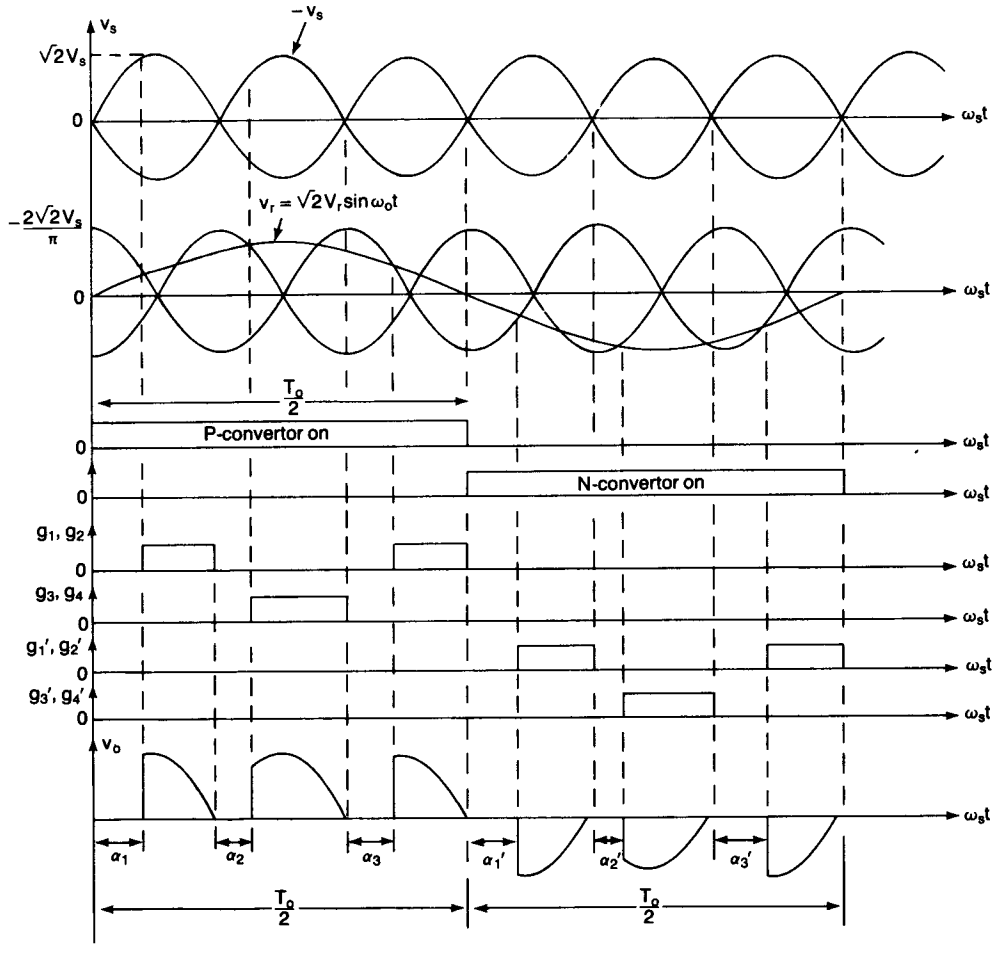


Figure 6-25 Generation of thyristor gating signals.

Example 6-10

Repeat Example 6-9 if the delay angles of the cycloconverter are generated by comparing a cosine signal at the source frequency with a sinusoidal signal at the output frequency as shown in Fig. 6-25.

Solution $V_s = 120$ V, $f_s = 60$ Hz, $f_o = 20$ Hz, $R = 5\ \Omega$, $L = 40$ mH, $\alpha_p = 2\pi/3$, $\omega_0 = 2\pi \times 20 = 125.66$ rad/s, and $X_L = \omega_0 L = 5.027\ \Omega$.

(a) From Eq. (6-50), the rms value of the output voltage,

$$V_o = \frac{\sqrt{2}\,V_s}{\pi} = 0.6366V_s = 0.6366 \times 120 = 76.39 \text{ V}$$

(b) $Z = [R^2 + (\omega_0 L)^2]^{1/2} = 7.09\ \Omega$ and $\theta = \tan^{-1}(\omega_0 L/R) = 45.2°$. The rms

load current, $I_o = V_o/Z = 76.39/7 = 10.77$ A. The rms current through each converter, $I_p = I_N = I_L/\sqrt{2} = 7.62$ A, and the rms current through each thyristor, $I_R = I_p/\sqrt{2} = 5.39$ A.

(c) The rms input current, $I_s = I_o = 10.77$ A, the volt-ampere rating, VA = $V_s I_s = 1292.4$ VA, and the output power,

$$P_o = V_o I_o \cos\theta = 0.6366 V_s I_o \cos\theta = 580.25 \text{ W}.$$

The input power factor,

$$\begin{aligned} \text{PF} &= 0.6366 \cos\theta \\ &= \frac{580.25}{1292.4} = 0.449 \text{ (lagging)} \end{aligned} \tag{6-51}$$

Note. Equation (6-51) shows that the input power factor is independent of delay angle, α and depends only on the load angle θ. But for normal phase angle control, the input power factor is dependent on both delay angle, α, and load angle, θ. If we compare Eq. (6-48) with Eq. (6-51), there is a critical value of delay angle α_c, which is given by

$$\left[\frac{1}{\pi}\left(\pi - \alpha_c + \frac{\sin 2\alpha_c}{2}\right)\right]^{1/2} = 0.6366 \tag{6-52}$$

For $\alpha < \alpha_c$, the normal delay-angle control would exhibit a better power factor and the solution of Eq. (6-52) yields $\alpha_c = 98.59°$.

6-11 DESIGN OF AC VOLTAGE-CONTROLLER CIRCUITS

The ratings of power devices must be designed for the worst-case condition, which occurs when the converter delivers the maximum rms value of output voltage V_o. The input and output filters must also be designed for worst-case conditions. The output of a power controller contains harmonics, and the delay angle for the worst-case condition of a particular circuit arrangement should be determined. The steps involved in designing the power circuits and filters are similar to that of rectifier circuit design in Section 2-11.

Example 6-11

A single-phase full-wave ac voltage controller in Fig. 6-3a controls power flow from a 230-V 60-Hz ac source into a resistive load. The maximum desired output power is 10 kW. Calculate the (a) maximum rms current rating of thyristors, I_{RM}; (b) maximum average current rating of thyristors, I_{AM}; (c) peak current of thyristors, I_p; and (d) peak value of thyristor voltage, V_p.

Solution $P_o = 10{,}000$ W, $V_s = 230$ V, and $V_m = \sqrt{2} \times 230 = 325.3$ V. The maximum power will be delivered when the delay angle is $\alpha = 0$. From Eq. (6-8), the rms value of output voltage $V_o = V_s = 230$ V, $P_o = V_0^2/R = 230^2/R = 10{,}000$, and load resistance is $R = 5.29\ \Omega$.

(a) The maximum rms value of load current, $I_{oM} = V_o/R = 230/5.29 = 43.48$ A and the maximum rms value of thyristor current, $I_{RM} = I_{oM}/\sqrt{2} = 30.75$ A.

(b) From Eq. (6-10), the maximum average current of thyristors,

$$I_{AM} = \frac{\sqrt{2} \times 230}{\pi \times 5.29} = 19.57 \text{ A}$$

(c) The peak current of thyristors, $I_p = V_m/R = 325.3/5.29 = 61.5$ A.
(d) The peak thyristor voltage, $V_p = V_m = 325.3$ V.

Example 6-12

A single-phase full-wave controller in Fig. 6-6a controls power to a RL load and the source voltage is 120 V, 60 Hz. (a) Use the method of Fourier series to obtain expressions for output voltage $v_o(t)$ and load current $i_o(t)$ as a function of delay angle α. (b) Determine the delay angle for the maximum amount of lowest-order harmonic current in the load. (c) If $R = 5\ \Omega$, $L = 10$ mH, and $\alpha = \pi/2$, determine the rms value of third harmonic current. (d) If a capacitor is connected across the load (Fig. 6-26), calculate the value of capacitance to reduce the third harmonic current in the load to 10% of the load current.

Solution (a) The waveform for the output voltage is shown in Fig. 6-6b. The instantaneous output voltage can be expressed in Fourier series as

$$v_o(t) = V_{dc} + \sum_{n=1,2,\ldots}^{\infty} a_n \cos n\omega t + \sum_{n=1,2,\ldots}^{\infty} b_n \sin n\omega t \tag{6-53}$$

where

$$V_{dc} = \frac{1}{2\pi}\int_0^{2\pi} V_m \sin \omega t\, d(\omega t) = 0$$

$$a_n = \frac{2}{\pi}\int_\alpha^\pi \sqrt{2} V_s \sin \omega t \cos n\omega t\, d(\omega t)$$

$$= \frac{\sqrt{2}V_s}{\pi}\left[\frac{\cos(n+1)\alpha - \cos(n+1)\pi}{n+1} - \frac{\cos(n-1)\alpha - \cos(n-1)\pi}{n-1}\right]$$

$$\text{for } n = 3,5,\ldots \tag{6-54}$$

$$= 0 \qquad \text{for } n = 2,4,\ldots$$

$$b_n = \frac{2}{\pi}\int_\alpha^\pi \sqrt{2} V_s \sin \omega t \sin n\omega t\, d(\omega t)$$

$$= \frac{\sqrt{2}V_s}{\pi}\left[\frac{\sin(n+1)\alpha}{n+1} - \frac{\sin(n-1)\alpha}{n-1}\right] \qquad \text{for } n = 3,5,\ldots \tag{6-55}$$

$$= 0 \qquad \text{for } n = 2,4,\ldots$$

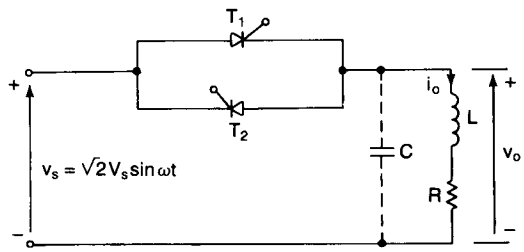


Figure 6-26 Single-phase full converter with RL load.

$$a_1 = \frac{2}{\pi}\int_{\alpha}^{\pi} \sqrt{2}\, V_s \sin \omega t \cos \omega t\, d(\omega t) = -\frac{\sqrt{2}\, V_s}{\pi} \sin^2 \alpha \tag{6-56}$$

$$b_1 = \frac{2}{\pi}\int_{\alpha}^{\pi} \sqrt{2}\, V_s \sin \omega t \sin \omega t\, d(\omega t)$$

$$= \sqrt{2}\, V_s \left[\frac{1}{\pi}\left(\pi - \alpha + \frac{\sin 2\alpha}{2}\right)\right] \tag{6-57}$$

The load impedance,

$$Z = R + j(n\omega L) = [R^2 + (n\omega L)^2]^{1/2} \angle \underline{\theta_n}$$

and $\theta_n = \tan^{-1}(n\omega L/R)$. Dividing $v_o(t)$ in Eq. (6-53) by load impedance Z and simplifying the sine and cosine terms give the load current as

$$i_o(t) = \sum_{n=2,4,\ldots}^{\infty} \sqrt{2}\, I_n \sin(n\omega t - \theta_n + \phi_n) \tag{6-58}$$

where $\phi_n = \tan^{-1}(a_n/b_n)$ and

$$I_n = \frac{1}{\sqrt{2}} \frac{(a_n^2 + b_n^2)^{1/2}}{[R^2 + (n\omega L)^2]^{1/2}}$$

(b) The third harmonic is the lowest-order harmonic. The calculation of third harmonic for various values of delay angle shows that it becomes maximum for $\alpha = \pi/2$.

(c) For $\alpha = \pi/2$, $L = 10$ mH, $R = 5\ \Omega$, $\omega = 2\pi \times 60 = 377$ rad/s and $V_s = 120$ V,

$$i_0(t) = [16.06 \sin(\omega t - 32.48° - 37°) + 4.37 \sin(3\omega t + 90° - 66.15°)$$
$$+ 0.923 \sin(5\omega t - 90° - 75.14°) + 0.67 \sin(7\omega t + 90° - 79.27°)$$
$$+ 0.315 \sin(9\omega t - 90° - 81.62°) + \cdots]$$

The rms value of third harmonic current is

$$I_3 = \frac{4.37}{\sqrt{2}} = 3.09 \text{ A}$$

(c) Figure 6-27 shows the equivalent circuit for harmonic current. Using the current-divider rule, the harmonic current through load is given by

$$\frac{I_h}{I_n} = \frac{X_c}{[R^2 + (n\omega L - X_c)^2]^{1/2}}$$

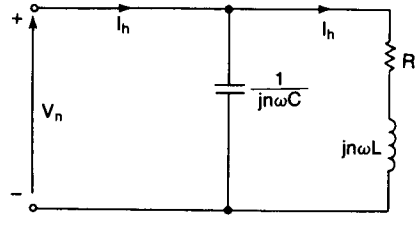


Figure 6-27 Equivalent circuit for harmonic current.

where $X_c = 1/(n\omega C)$. For $n = 3$ and $\omega = 377$,

$$\frac{I_h}{I_n} = \frac{X_c}{[5^2 + (3 \times 3.77 - X_c)^2]^{1/2}} = 0.1$$

which yields $X_c = -1.362$ or 1.134. Since X_c cannot be negative, $X_c = 1.134 = 1/(3 \times 377C)$ or $C = 779.85\ \mu F$.

6-12 EFFECTS OF SOURCE AND LOAD INDUCTANCES

In the derivations of output voltages, we have assumed that the source has no inductance. The effect of any source inductance would be to delay the turn-off of thyristors. Thyristors would not turn off at the zero crossing of input voltage as shown in Fig. 6-28b, and gate pulses of short duration may not be suitable. The harmonic contents on the output voltage would also increase.

We have seen in Section 6-5 that the load inductance plays a significant part on the performance of power controllers. Although the output voltage is a pulsed waveform, the load inductance tries to maintain a continuous current flow as shown in Figs. 6-6b and 6-28b. We can also notice from Eqs. (6-48) and (6-52) that the input power factor of power converter depends on the load power factor. Due to the switching characteristics of thyristors, any inductance in the circuit makes the analysis more complex.

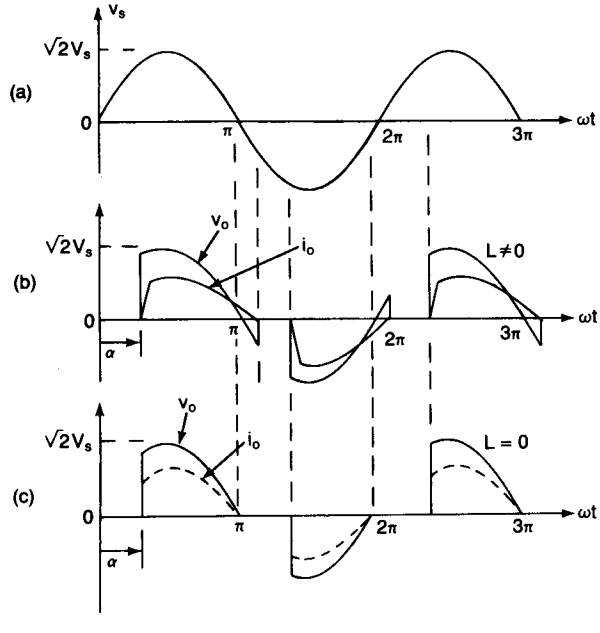


Figure 6-28 Effects of load inductance on load current and voltage.

SUMMARY

The ac voltage controller can use on–off control or phase-angle control. The on–off control is more suitable for systems having a high time constant. Due to the dc component on the output of unidirectional controllers, bidirectional controllers are normally used in industrial applications. Due to the switching characteristics of thyristors, an inductive load makes the solutions of equations describing the performance of controllers more complex and an iterative method of solution is more convenient. The input power factor of controllers, which varies with delay angle, is generally poor, especially at the low output range. The ac voltage controllers can be used as transformer static tap changers.

The voltage controllers provide an output voltage at a fixed frequency. Two phase-controlled rectifiers connected as dual converters can be operated as direct-frequency changers known as *cycloconverters*. With the development of fast-switching power devices, the forced commutation of cycloconverters is possible; however, it requires synthesizing the switching functions for power devices [1,2].

REFERENCES

1. P. D. Ziogas, S. I. Khan, and M. H. Rashid, "Some improved forced commutated cycloconverter structures." *IEEE Transactions on Industry Applications*, Vol. 1A121, No. 5 (September–October) 1985, pp. 1242–1253.
2. M. Venturi, "A new sine wave in sine wave out conversion technique eliminates reactive elements." *Proceedings Powercon 7*, 1980, pp. E3-1–E3-13.
3. L. Gyugi, and B. R. Pelly, *Static Power Frequency Changes—Theory, Performance, and Applications*, New York: Wiley-Interscience, 1976.
4. B. R. Pelly, *Thyristor-Phase Controlled Converters and Cycloconverters*. New York: Wiley-Interscience, 1971.
5. "IEEE standard definition and requirements for thyristor ac power controllers," *IEEE Standard*, No. 428-1981, 1981.

REVIEW QUESTIONS

6-1. What are the advantages and disadvantages of on–off control?

6-2. What are the advantages and disadvantages of phase-angle control?

6-3. What are the effects of load inductance on the performance of ac voltage controllers?

6-4. What is the extinction angle?

6-5. What are the advantages and disadvantages of unidirectional controllers?

6-6. What are the advantages and disadvantages of bidirectional controllers?

6-7. What is a tie control arrangement?

6-8. What are the steps involved in determining the output voltage waveforms of three-phase unidirectional controllers?

6-9. What are the steps involved in determining the output voltage waveforms of three-phase bidirectional controllers?

6-10. What are the advantages and disadvantages of delta-connected controllers?

6-11. What is the control range of the delay angle for single-phase unidirectional controllers?

6-12. What is the control range of the delay angle for single-phase bidirectional controllers?

6-13. What is the control range of the delay angle for three-phase unidirectional controllers?

6-14. What is the control range of the delay angle for three-phase bidirectional controllers?

6-15. What are the advantages and disadvantages of transformer tap changers?

6-16. What are the methods for output voltage control of transformer tap changers?

6-17. What is a synchronous tap changer?

6-18. What is a cycloconverter?

6-19. What are the advantages and disadvantages of cycloconverters?

6-20. What are the advantages and disadvantages of ac voltage controllers?

6-21. What is the principle of operation of cycloconverters?

6-22. What are the effects of load inductance on the performance of cycloconverters?

6-23. What are the three possible arrangements for a single-phase full-wave ac voltage controller?

6-24. What are the advantages of sinusoidal harmonic reduction techniques for cycloconverters?

6-25. What are the gate signal requirements of thyristors for voltage controllers with *RL* loads?

6-26. What are the effects of source and load inductances?

6-27. What are the conditions for the worst-case design of power devices for ac voltage controllers?

6-28. What are the conditions for the worst-case design of load filters for ac voltage controllers?

PROBLEMS

6-1. The ac voltage controller in Fig. 6-1a is used for heating a resistive load of $R = 5\ \Omega$ and the input voltage is $V_s = 120$ V, 60 Hz. The thyristor switch is on for $n = 125$ cycles and is off for $m = 75$ cycles. Determine the **(a)** rms output voltage, V_o; **(b)** input power factor, PF; and **(c)** average and rms current of thyristors.

6-2. The ac voltage controller in Fig. 6-1a uses on–off control for heating a resistive load of $R = 4\ \Omega$ and the input voltage is $V_s = 208$ V, 60 Hz. If the desired output power is $P_o = 3$ kW, determine the **(a)** duty cycle, k; and **(b)** input power factor, PF.

6-3. The single-phase half-wave ac voltage controller in Fig. 6-2a has a resistive load of $R = 5\ \Omega$ and the input voltage is $V_s = 120$ V, 60 Hz. The delay angle of thyristor T_1 is $\alpha = \pi/3$. Determine the **(a)** rms output voltage, V_o; **(b)** input power factor, PF; and **(c)** average input current.

6-4. The single-phase half-wave ac voltage controller in Fig. 6-2a has a resistive load of $R = 5\ \Omega$ and the input voltage is $V_s = 208$ V, 60 Hz. If the desired output power is $P_o = 2$ kW, calculate the **(a)** delay angle, α; and **(b)** input power factor, PF.

6-5. The single-phase full-wave ac voltage controller in Fig. 6-3a has a resistive load of $R = 5\ \Omega$ and the input voltage is $V_s = 120$ V, 60 Hz. The delay angles of thyristors T_1 and T_2 are equal: $\alpha_1 = \alpha_2 = \alpha = 2\pi/3$. Determine the **(a)** rms output voltage, V_o; ((**b**) input power factor, PF; **(c)** average current of thyristors, I_A; and **(d)** rms current of thyristors, I_R.

6-6. The single-phase full-wave ac voltage controller in Fig. 6-3a has a resistive load of $R = 1.5\ \Omega$ and the input voltage is $V_s = 120$ V, 60 Hz. If the desired output power is $P_o = 7.5$ kW, determine the **(a)** delay angles of thyristors T_1 and T_2; **(b)** rms output voltage, V_o; **(c)** input power factor, PF; **(d)** average current of thyristors, I_A; and **(e)** rms current of thyristors, I_R.

6-7. The load of an ac voltage controller is resistive, with $R = 1.5\ \Omega$. The input voltage is $V_s = 120$ V, 60 Hz. Plot the power factor against the delay angle for single-phase half-wave and full-wave controllers.

6-8. The single-phase full-wave controller in Fig. 6-6a supplies an RL load. The input voltage is $V_s = 120$ V at 60 Hz. The load is such that $L = 5$ mH and $R = 5\ \Omega$. The delay angles of thyristor T_1 and thyristor T_2 are equal, where $\alpha = \pi/3$. Determine the **(a)** conduction angle of thyristor T_1, δ; **(b)** rms output voltage, V_o; **(c)** rms thyristor current, I_R; **(d)** rms output current, I_o; **(e)** average current of a thyristor, I_A; and **(f)** input power factor, PF.

6-9. The single-phase full-wave controller in Fig. 6-6a supplies an RL load. The input voltage is $V_s = 120$ V at 60 Hz. Plot the power factor, PF, against the delay angle, α, for **(a)** $L = 5$ mH and $R = 5\ \Omega$, and **(b)** $R = 5\ \Omega$ and $L = 0$.

6-10. The three-phase unidirectional controller in Fig. 6-7 supplies a wye-connected resistive load with $R = 5\ \Omega$ and the line-to-line input voltage is 208 V, 60 Hz. The delay angle is $\alpha = \pi/6$. Determine the **(a)** rms output phase voltage, V_o; **(b)** input power; and **(c)** expressions for the instantaneous output voltage of phase a.

6-11. The three-phase unidirectional controller in Fig. 6-7 supplies a wye-connected resistive load with $R = 2.5\ \Omega$ and the line-to-line input voltage is 208 V, 60 Hz. If the desired output power is $P_o = 12$ kW, calculate the **(a)** delay angle, α; **(b)** rms output phase voltage, V_o; and **(c)** input power factor, PF.

6-12. The three-phase unidirectional controller in Fig. 6-7 supplies a wye-connected resistive load with $R = 5\ \Omega$ and the line-to-line input voltage is 208 V, 60 Hz. The delay angle is $\alpha = 2\pi/3$. Determine the **(a)** rms output phase voltage, V_o; **(b)** input power factor, PF; and **(c)** expressions for the instantaneous output voltage of phase a.

6-13. Repeat Prob. 6-10 for the three-phase bidirectional controller in Fig. 6-12.

6-14. Repeat Prob. 6-11 for the three-phase bidirectional controller in Fig. 6-12.

6-15. Repeat Prob. 6-12 for the three-phase bidirectional controller in Fig. 6-12.

6-16. The three-phase bidirectional controller in Fig. 6-12 supplies a wye-connected load of $R = 5\ \Omega$ and $L = 10$ mH. The line-to-line input voltage is 208 V, 60 Hz. The delay angle is $\alpha = \pi/2$. Plot the line current for the first cycle after the controller is switched on.

6-17. A three-phase ac voltage controller supplies a wye-connected resistive load of $R = 5\ \Omega$ and the line-to-line input voltage is $V_s = 208$ V at 60 Hz. Plot the power factor, PF, against the delay angle, α, for the **(a)** half-wave controller in Fig. 6-7, and **(b)** full-wave controller in Fig. 6-12.

6-18. A three-phase bidirectional delta-connected controller in Fig. 6-15 has a resistive load of $R = 5\ \Omega$. If the line-to-line voltage is $V_s = 208$ V, 60 Hz and the delay angle $\alpha = \pi/3$, determine the **(a)** rms output phase voltage, V_o; **(b)** expressions for instanta-

neous currents i_a, i_{ab}, and i_{ca}; **(c)** rms output phase current, I_{ab}, and rms output line current, I_a; **(d)** input power factor, PF; and **(e)** rms current of thyristors, I_R.

6-19. The circuit in Fig. 6-18 is controlled as a synchronous tap changer. The primary voltage is 208 V, 60 Hz. The secondary voltages are $V_1 = 120$ V and $V_2 = 88$ V. If the load resistance is $R = 5\ \Omega$ and the rms load voltage is 180 V, determine the **(a)** delay angles of thyristors T_1 and T_2; **(b)** rms current of thyristors T_1 and T_2; **(c)** rms current of thyristors T_3 and T_4; and **(d)** input power factor, PF.

6-20. The input voltage to the single-phase/single-phase cycloconverter in Fig. 6-21a is 120 V, 60 Hz. The load resistance is 2.5 Ω and load inductance is $L = 40$ mH. The frequency of output voltage is 20 Hz. If the delay angle of thyristors is $\alpha_p = 2\pi/4$, determine the **(a)** rms output voltage; **(b)** rms current of each thyristor; and **(c)** input power factor, PF.

6-21. Repeat Prob. 6-20 if $L = 0$.

6-22. For Prob. 6-20, plot the power factor against the delay angle, α.

6-23. Repeat Prob. 6-20 for the three-phase/single-phase cycloconverter in Fig. 6-23a, $L = 0$.

6-24. Repeat Prob. 6-20 if the delay angles are generated by comparing a cosine signal at source frequency with a sinusoidal signal at output frequency as shown in Fig. 6-25.

6-25. For Prob. 6-24, plot the input power factor against the delay angle.

6-26. The single-phase full-wave ac voltage controller in Fig. 6-5a controls the power from a 208-V 60-Hz ac source into a resistive load. The maximum desired output power is 10 kW. Calculate the **(a)** maximum rms current rating of thyristor; **(b)** maximum average current rating of thyristor; and **(c)** the peak thyristor voltage.

6-27. The three-phase full-wave ac voltage controller in Fig. 6-12 is used to control the power from a 2300-V 60-Hz ac source into a delta-connected resistive load. The maximum desired output power is 100 kW. Calculate the **(a)** maximum rms current rating of thyristors, I_{RM}; **(b)** maximum average current rating of thyristors, I_{AM}; and **(c)** the peak value of thyristor voltage, V_p.

6-28. The single-phase full-wave controller in Fig. 6-6a controls power to a RL load and the source voltage is 208 V, 60 Hz. The load is $R = 5\ \Omega$ and $L = 10$ mH. **(a)** Determine the rms value of third harmonic current. **(b)** If a capacitor is connected across the load, calculate the value of capacitance to reduce the third harmonic current in the load to 5% of the load current, $\alpha = \pi/3$.

7

DC Choppers

7-1 INTRODUCTION

In many industrial applications, it is required to convert a fixed-voltage dc source into a variable-voltage dc source. A dc chopper converts directly from dc to dc and is also known as a *dc-to-dc converter*. A chopper can be considered as dc equivalent to an ac transformer with a continuously variable turns ratio. Like a transformer, it could be used to step-down or step-up a dc voltage source.

Choppers are widely used for traction motor control in electric automobiles, trolley cars, marine hoists, forklift trucks, and mine haulers. They provide smooth acceleration control, high efficiency, and fast dynamic response. Choppers can be used in regenerative braking of dc motors to return energy back into the supply, and this feature results in energy savings for transportation systems with frequent stops. Choppers are also used in dc voltage regulators.

7-2 PRINCIPLE OF STEP-DOWN OPERATION

The principle of operation can be explained by Fig. 7-1a. When switch SW is closed for a time t_1, the input voltage V_s appears across the load. If the switch remains off for a time t_2, the voltage across the load is zero. The waveforms for

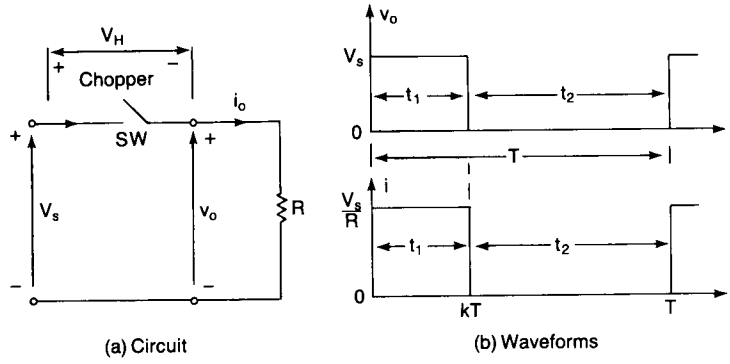


Figure 7-1 Step-down chopper with resistive load.

the output voltage and load current are also shown in Fig. 7-1b. The chopper switch can be implemented by using a (1) power BJT, (2) power MOSFET, (3) GTO, or (4) forced-commutated thyristor. The practical devices have a finite voltage drop ranging from 0.5 to 2 V, and for the sake of simplicity the voltage drops of these power semiconductor devices are neglected.

The average output voltage is given by

$$V_a = \frac{1}{T}\int_0^{t_1} v_0\, dt = \frac{t_1}{T} V_s = f t_1 V_s = k V_s \tag{7-1}$$

and the average load current, $I_a = V_a/R = kV_s/R$, where T is the chopping period, $k = t_1/T$ is the duty cycle of chopper, and f is the chopping frequency. The rms value of output voltage is found from

$$V_o = \left(\frac{1}{T}\int_0^{kT} v_0^2\, dt\right)^{1/2} = \sqrt{k}\, V_s \tag{7-2}$$

Assuming a lossless chopper, the input power to the chopper is the same as the output power and is given by

$$P_i = \frac{1}{T}\int_0^{kT} v_0 i\, dt = \frac{1}{T}\int_0^{kT} \frac{v_0^2}{R}\, dt = k\frac{V_s^2}{R} \tag{7-3}$$

The effective input resistance seen by the source is

$$R_i = \frac{V_s}{I_a} = \frac{V_s}{kV_s/R} = \frac{R}{k} \tag{7-4}$$

The duty cycle, k, can be varied from 0 to 1 by varying t_1, T, or f. Therefore, the output voltage V_o can be varied from 0 to V_s by controlling k and the power flow can be controlled.

1. *Constant-frequency operation.* The chopping frequency, f (or chopping period T), is kept constant and the on-time, t_1, is varied. The width of the pulse is varied and this type of control is known as *pulse-width-modulation* (PWM) control.

2. *Variable-frequency operation.* The chopping frequency, f, is varied. Either on-time, t_1, or off-time, t_2, is kept constant. This is called *frequency modulation.* The frequency has to be varied over a wide range to obtain the full output voltage range. This type of control would generate harmonics at unpredictable frequencies and the filter design would be difficult.

Example 7-1

The dc chopper in Fig. 7-1a has a resistive load of $R = 10\ \Omega$ and the input voltage is $V_s = 220$ V. When the chopper switch remains on, its voltage drop is $v_{ch} = 2$ V and the chopping frequency is $f = 1$ kHz. If the duty cycle is 50%, determine the (a) average output voltage, V_a; (b) rms output voltage, V_o; (c) chopper efficiency; (d) effective input resistance of the chopper, R_i; and (e) rms value of the fundamental component of output harmonic voltage.

Solution $V_s = 220$ V, $k = 0.5$, $R = 10\ \Omega$, and $v_{ch} = 2$ V.

(a) From Eq. (7-1), $V_a = 0.5 \times (220 - 2) = 109$ V.

(b) From Eq. (7-2), $V_o = \sqrt{0.5} \times (220 - 2) = 154.15$ V.

(c) The output power can be found from

$$P_o = \frac{1}{T}\int_0^{kT} \frac{v_0^2}{R}\,dt = \frac{1}{T}\int_0^{kT} \frac{(V_s - v_{ch})^2}{R}\,dt = k\,\frac{(V_s - v_{ch})^2}{R}$$
$$= 0.5 \times \frac{(220 - 2)^2}{10} = 2376.2\ \text{W} \tag{7-5}$$

The input power to the chopper can be found from

$$P_i = \frac{1}{T}\int_0^{kT} V_s i\,dt = \frac{1}{T}\int_0^{kT} \frac{V_s(V_s - v_{ch})}{R}\,dt = k\,\frac{V_s(V_s - v_{ch})}{R}$$
$$= 0.5 \times 220 \times \frac{220 - 2}{10} = 2398\ \text{W} \tag{7-6}$$

The chopper efficiency is

$$\frac{P_o}{P_i} = \frac{2376.2}{2398} = 99.09\%$$

(d) From Eq. (7-4), $R_i = 10/0.5 = 20\ \Omega$.

(e) The output voltage as shown in Fig. 7-1b can be expressed in a Fourier series as

$$v_o(t) = kV_s + \frac{V_s}{n\pi}\sum_{n=1}^{\infty} \sin 2n\pi k \cos 2n\pi ft + \frac{V_s}{n\pi}\sum_{n=1}^{\infty} (1 - \cos 2n\pi k)\sin 2n\pi ft \tag{7-7}$$

The fundamental component (for $n = 1$) of output voltage harmonic can be determined from Eq. (7-7) as

$$v_1(t) = \frac{V_s}{\pi}[\sin 2\pi k \cos 2\pi ft + (1 - \cos 2\pi k)\sin 2\pi ft]$$
$$= \frac{220 \times 2}{\pi}\sin(2\pi \times 1000t) = 140.06 \sin(6283.2t) \tag{7-8}$$

and its rms value is $V_1 = 140.06/\sqrt{2} = 99.04$ V.

Note. The efficiency calculation, which includes the conduction loss of the chopper, does not take into account the switching loss due to turn-on and turn-off of the chopper.

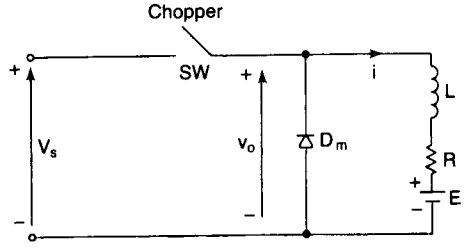


Figure 7-2 Chopper with RL loads.

7-3 STEP-DOWN CHOPPER WITH *RL* LOAD

A chopper with an *RL* load is shown in Fig. 7-2. The operation of the chopper can be divided into two modes. During mode 1, the chopper is switched on and the current flows from the supply to the load. During mode 2, the chopper is switched off and the load current continues to flow through freewheeling diode D_m. The equivalent circuits for these modes are shown in Fig. 7-3a. The load current and output voltage waveforms are shown in Fig. 7-3b.

The load current for mode 1 can be found from

$$V_s = Ri_1 + L\frac{di_1}{dt} + E \tag{7-9}$$

The solution of Eq. (7-9) with initial current $i_1(t = 0) = I_1$ gives the load current as

$$i_1(t) = I_1 e^{-tR/L} + \frac{V_s - E}{R}(1 - e^{-tR/L}) \tag{7-10}$$

This mode is valid $0 \le t \le t_1 (= kT)$; and at the end of this mode, the load current becomes

$$i_1 (t = t_1 = kT) = I_2 \tag{7-11}$$

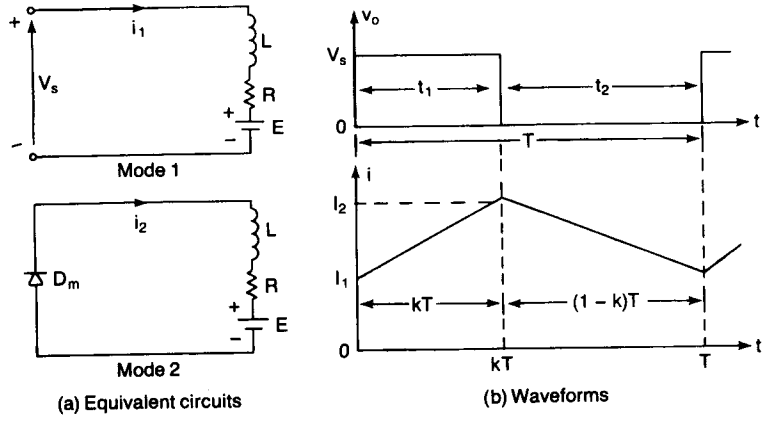


Figure 7-3 Equilvalent circuits and waveforms for RL loads.

The load current for mode 2 can be found from

$$0 = Ri_2 + L\frac{di_2}{dt} + E \tag{7-12}$$

With initial current $i_2(t = 0) = I_2$ and redefining the time origin at the beginning of mode 2, we have

$$i_2(t) = I_2 e^{-tR/L} - \frac{E}{R}(1 - e^{-tR/L}) \tag{7-13}$$

This mode is valid for $0 \leq t \leq t_2$ [$= (1 - k)T$]. At the end of this mode, the load current becomes

$$i_2(t = t_2) = I_3 \tag{7-14}$$

At the end of mode 2, the chopper is turned on again in the next cycle after time, $T = 1/f = t_1 + t_2$.

Under steady-state conditions, $I_1 = I_3$. The peak-to-peak load ripple current can be determined from Eqs. (7-10), (7-11), (7-13), and (7-14). From Eqs. (7-10) and (7-11), I_2 is given by

$$I_2 = I_1 e^{-kTR/L} + \frac{V_s - E}{R}(1 - e^{-kTR/L}) \tag{7-15}$$

From Eqs. (7-13) and (7-14), I_3 is given by

$$I_3 = I_1 = I_2 e^{-(1-k)TR/L} - \frac{E}{R}(1 - e^{-(1-k)TR/L}) \tag{7-16}$$

The peak-to-peak ripple current is

$$\Delta I = I_2 - I_1$$

which after simplifications becomes

$$\Delta I = \frac{V_s}{R}\frac{1 - e^{-kTR/L} + e^{-TR/L} - e^{-(1-k)TR/L}}{1 - e^{-TR/L}} \tag{7-17}$$

The condition for maximum ripple,

$$\frac{d(\Delta I)}{dk} = 0 \tag{7-18}$$

gives $e^{-kTR/L} - e^{-(1-k)TR/L} = 0$ or $-k = -(1 - k)$ or $k = 0.5$. The maximum peak-to-peak ripple current (at $k = 0.5$) is

$$\Delta I_{max} = \frac{V_s}{R}\tanh\frac{R}{4fL} \tag{7-19}$$

For $4fL >> R$, $\tanh\theta \approx \theta$ and the maximum ripple current can be approximated to

$$\Delta I_{max} = \frac{V_s}{4fL} \tag{7-20}$$

Note. Equations (7-9) to (7-20) are valid only for continuous curent flow. For a large off-time, particularly at low frequency and low output voltage, the load current may be discontinuous. The load current would be continuous if $L/R >> T$ or $Lf >> R$. In case of discontinuous load current, $I_1 = 0$ and Eq. (7-10) becomes

$$i_1(t) = \frac{V_s - E}{R}(1 - e^{-tR/L})$$

and Eq. (7-13) is valid for $0 \le t \le t_2$ such that $i_2(t = t_2) = I_3 = I_1 = 0$.

Example 7-2

A chopper is feeding an *RL* load as shown in Fig. 7-2 with $V_s = 220$ V, $R = 5\ \Omega$, $L = 7.5$ mH, $f = 1$ kHz, and $E = 0$ V. Calculate the (a) minimum instantaneous load curent, I_1; (b) peak instantaneous load current, I_2; (c) maximum peak-to-peak load ripple current; (d) average value of load current, I_a; (e) rms load current, I_o; (f) effective input resistance seen by the source, R_i; and (g) rms chopper current, I_R.

Solution $V_s = 220$ V, $R = 5\ \Omega$, $L = 7.5$ mH, $E = 0$ V, $k = 0.5$, and $f = 1000$ Hz. From Eq. (7-15), $I_2 = 0.7165I_1 + 12.473$ and from Eq. (7-16), $I_1 = 0.7165I_2 + 0$.

(a) Solving these two equations yields $I_1 = 18.37$ A.

(b) $I_2 = 25.63$ A.

(c) $\Delta I = I_2 - I_1 = 25.63 - 18.37 = 7.26$ A. From Eq. (7-19), $\Delta I_{max} = 7.26$ A and Eq. (7-20) gives the approximately value, $\Delta I_{max} = 7.33$ A.

(d) The average load current is, approximately,

$$I_a = \frac{I_2 + I_1}{2} = \frac{25.63 + 18.37}{2} = 22 \text{ A}$$

(e) Assuming that the load current rises linearly from I_1 to I_2, the instantaneous load current can be expressed as

$$i_1 = I_1 + \frac{\Delta I\, t}{kT} \qquad \text{for } 0 < t < kT$$

The rms value of load current can be found from

$$I_o = \left(\frac{1}{kT}\int_0^{kT} i_1^2\, dt\right)^{1/2} = \left[I_1^2 + \frac{(I_2 - I_1)^2}{3} + I_1(I_2 - I_1)\right]^{1/2} \qquad (7\text{-}21)$$
$$= 22.1 \text{ A}$$

(f) The average source current,

$$I_s = kI_a = 0.5 \times 22 = 11 \text{ A}$$

and the input resistance, $R_i = V_s/I_s = 220/11 = 20\ \Omega$.

(g) The rms chopper current can be found from

$$I_R = \left(\frac{1}{T}\int_0^{kT} i_1^2 dt\right)^{1/2} = \sqrt{k}\left[I_1^2 + \frac{(I_2 - I_1)^2}{3} + I_1(I_2 - I_1)\right]^{1/2} \qquad (7\text{-}22)$$
$$= \sqrt{k}\, I_o = \sqrt{0.5} \times 22.1 = 15.63 \text{ A}$$

Example 7-3

The chopper in Fig. 7-2 has a load resistance, $R = 0.25\ \Omega$, input voltage, $V_s = 550$ V, and battery voltage, $E = 0$ V. The average load current, $I_a = 200$ A, and chopping frequency, $f = 250$ Hz. Use the average output voltage to calculate the load inductance, L, which would limit the maximum load ripple current to 10% of I_a.

Solution $V_s = 550$ V, $R = 0.25\ \Omega$, $E = 0$ V, $f = 250$ Hz, $T = 1/f = 0.004$ s, and $\Delta i = 200 \times 0.1 = 20$ A. The average output voltage, $V_a = kV_s = RI_a$. The voltage across the inductor is given by

$$L\frac{di}{dt} = V_s - RI_a = V_s - kV_s = V_s(1 - k)$$

If the load current is assumed to rise linearly, $dt = t_1 = kT$ and $di = \Delta i$:

$$\Delta i = \frac{V_s(1 - k)}{L} kT$$

For the worst-case ripple conditions,

$$\frac{d(\Delta i)}{dk} = 0$$

and this gives $k = 0.5$ and

$$\Delta i\, L = 20 \times L = 550(1 - 0.5)0.5 \times 0.004$$

and the required value of inductance is $L = 27.5$ mH.

7-4 PRINCIPLE OF STEP-UP OPERATION

A chopper can be used to step up a dc voltage and an arrangement for step-up operation is shown in Fig. 7-4a. When switch SW is closed for time t_1, the inductor current rises and energy is stored in the inductor. If the switch is opened for time t_2, the energy stored in the inductor is transferred to load through diode D_1 and the inductor current falls. Assuming a continuous current flow, the waveform for the inductor current is shown in Fig. 7-4b.

When the chopper is turned on, the voltage across the inductor is

$$v_L = L\frac{di}{dt}$$

and this gives the peak-to-peak ripple current in the inductor as

$$\Delta I = \frac{V_s}{L} t_1 \tag{7-23}$$

The instantaneous output voltage is

$$v_o = V_s + L\frac{\Delta I}{t_2} = V_s\left(1 + \frac{t_1}{t_2}\right) = V_s\frac{\Delta I}{1 - k} \tag{7-24}$$

If a large capacitor, C_L, is connected across the load as shown by dashed lines

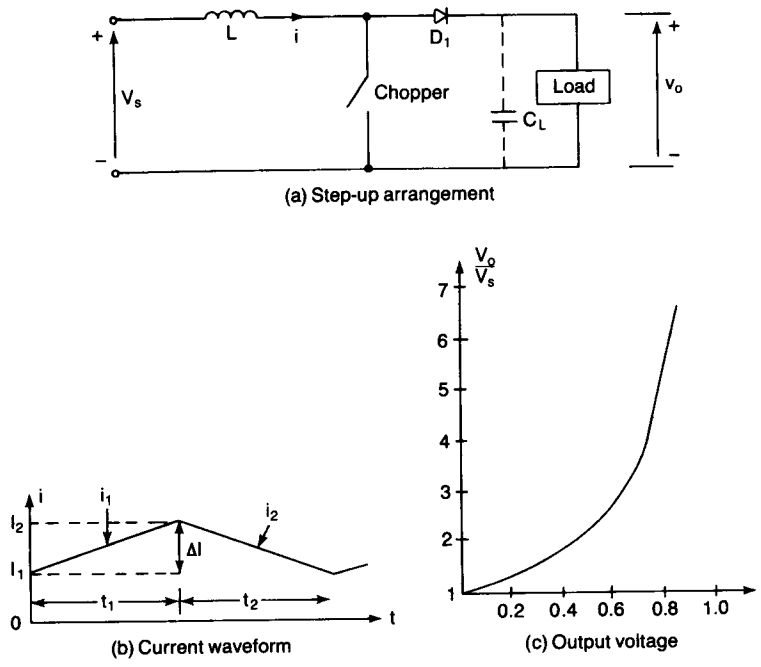


Figure 7-4 Arrangement for step-up operation.

in Fig. 7-4a, the output voltage will be continuous and v_o would become the average value V_a. We can notice from Eq. (7-24) that the voltage across the load can be stepped up by varying the duty cycle, k, and the minimum output voltage is V_s when $k = 0$. However, the chopper cannot be switched on continuously such that $k = 1$. For values of k tending to unity, the output voltage becomes very large and is very sensitive to changes in k, as shown in Fig. 7-4c.

This principle can be applied to transfer energy from one voltage source to another as shown in Fig. 7-5a. The equivalent circuits for the modes of operation are shown in Fig. 7-5b and the current waveforms in Fig. 7-5c. The inductor current for mode 1 is given by

$$V_s = L \frac{di_1}{dt}$$

and is expressed as

$$i_1(t) = \frac{V_s}{L} t + I_1 \tag{7-25}$$

where I_1 is the initial current for mode 1. During mode 1, the current must rise and the necessary condition,

$$\frac{di_1}{dt} > 0 \quad \text{or} \quad V_s > 0 \tag{7-26}$$

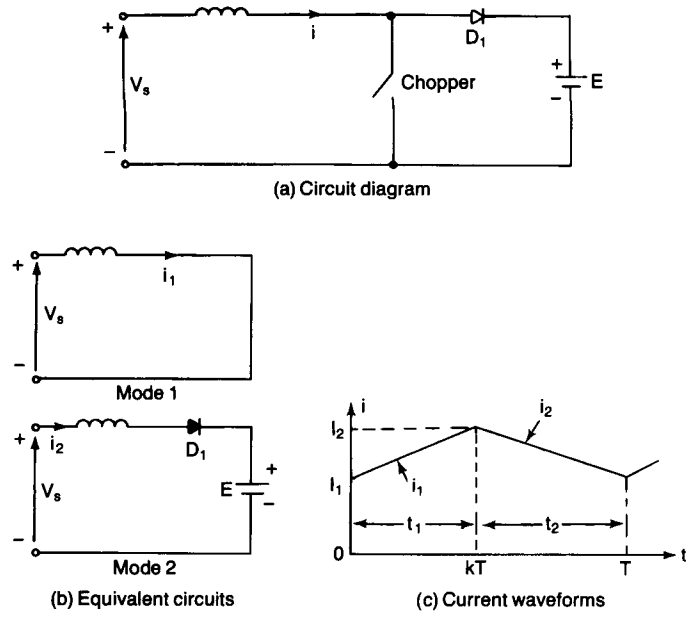


Figure 7-5 Arrangement for transfer of energy.

The current for mode 2 is given by

$$V_s = L\frac{di_2}{dt} + E$$

and is solved as

$$i_2(t) = \frac{V_s - E}{L}t + I_2 \tag{7-27}$$

where I_2 is initial current for mode 2. For a stable system, the current must fall and the condition is

$$\frac{di_2}{dt} < 0 \qquad \text{or} \qquad V_s < E \tag{7-28}$$

If the condition of Eq. (7-28) is not satisfied, the inductor current would continue to rise and an unstable situation would occur. Therefore, the conditions for permissible potentials of the two voltages are

$$0 < V_s < E \tag{7-29}$$

Equation (7-29) indicates that the source voltage V_s must be less than the voltage E to permit transfer of power from a fixed (or variable) source to a fixed dc voltage. In electric braking of dc motors, where the motors operate as dc generators, the chopper permits transfer of power to a fixed dc source or a rheostat.

7-5 PERFORMANCE PARAMETERS

The power semiconductor devices require a minimum time to turn on and turn off. Therefore, the duty cycle, k, can only be controlled between a minimum value k_{min} and a maximum value k_{max}, thereby limiting the minimum and maximum value of output voltage. The switching frequency of the chopper is also limited. It could be noticed from Eq. (7-20) that the load ripple current depends inversely on the chopping frequency. The frequency should be as high as possible to reduce the load ripple current and to minimize the size of any additional series inductor in the load circuit.

7-6 SWITCHING-MODE REGULATORS

The dc choppers can be used as switching-mode regulators to convert a dc voltage, normally unregulated, to a regulated dc output voltage. The regulation is normally achieved by pulse-width modulation at a fixed frequency and the switching device is normally a power BJT or MOSFET. The elements of switching-mode regulators are shown in Fig. 7-6. We can notice from Fig. 7-1b that the output of dc choppers with resistive load is discontinuous and contains harmonics. The ripple content is normally reduced by an LC filter.

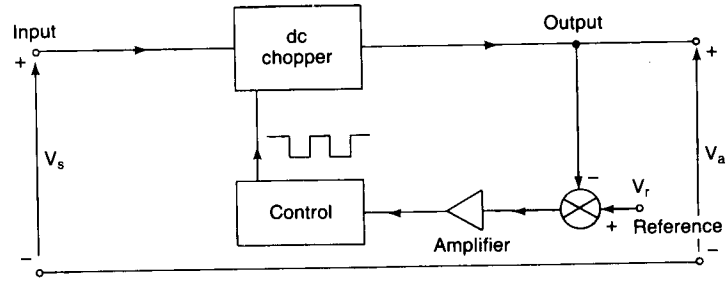


Figure 7-6 Elements of switching-mode regulators.

Switching regulators are commercially available as integrated circuits. The designer can select the switching frequency by choosing the values of R and C of frequency oscillator. As a rule of thumb, to maximize efficiency, the minimum oscillator period should be about 100 times longer than the transistor switching time; for example, if a transistor has a switching time of 0.5 μs, the oscillator period would be 50 μs, which gives the maximum oscillator frequency of 20 kHz. This is due to the switching loss in the transistor. The transistor switching loss increases with the switching frequency and the efficiency decreases. In addition, the core loss of inductors limits the high-frequency operation. There are four basic topologies of switching regulators:

1. Buck regulators
2. Boost regulators

3. Buck-boost regulators
4. Cúk regulators

7-6.1 Buck Regulators

In a Buck regulator, the average output voltage V_a, is less than the input voltage, V_s—hence the name "buck," a very popular regulator. The circuit diagram of a buck regulator using a power BJT is shown in Fig. 7-7a, and this is like a step-down chopper. The circuit operation can be divided into two modes. Mode 1 begins when transistor Q_1 is switched on at $t = 0$. The input current, which rises, flows through filter inductor L, filter capacitor C, and load resistor R. Mode 2 begins when transistor Q_1 is switched off at $t = t_1$. The freewheeling diode D_m conducts due to energy stored in the inductor and the inductor current continues to flow through L, C, load, and diode D_m. The inductor current falls until transistor Q_1 is switched on again in the next cycle. The equivalent circuits for the modes of operation are shown in Fig. 7-7b. The waveforms for the voltages and currents are shown in Fig. 7-7c for a continuous current flow in the inductor L. Depending on the switching frequency, filter inductance, and capacitance, the inductor current could be discontinuous.

The voltage across the inductor, L, is, in general,

$$e_L = L\frac{di}{dt}$$

Assuming that the inductor current rises linearly from I_1 to I_2 in time t_1,

$$V_s - V_a = L\frac{I_2 - I_1}{t_1} = L\frac{\Delta I}{t_1} \tag{7-30}$$

or

$$t_1 = \frac{\Delta I\, L}{V_s - V_a} \tag{7-31}$$

and the inductor current falls linearly from I_2 to I_1 in time t_2,

$$V_a = L\frac{\Delta I}{t_2} \tag{7-32}$$

or

$$t_2 = \frac{\Delta I\, L}{V_a} \tag{7-33}$$

where ΔI is the peak-to-peak ripple current of the inductor, L. Equating the value of ΔI in Eqs. (7-30) and (7-32) gives

$$\Delta I = \frac{(V_s - V_a)t_1}{L} = \frac{V_a t_2}{L}$$

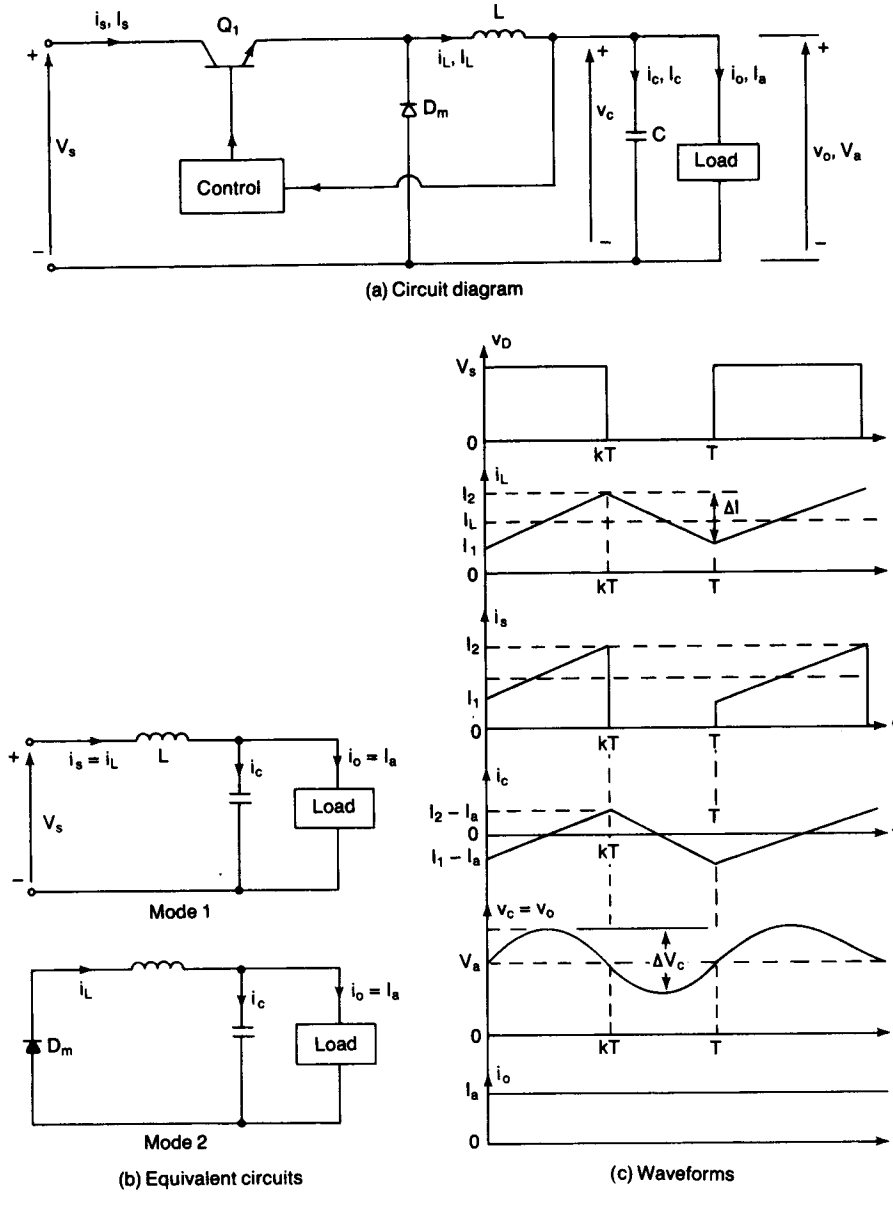


Figure 7-7 Buck regulator.

Substituting $t_1 = kT$ and $t_2 = (1 - k)T$ yields the average output voltage as

$$V_a = kV_s \tag{7-34}$$

Assuming a lossless transistor switch, $V_sI_s = V_aI_a = kV_sI_a$ and the average input current,

$$I_s = kI_a \tag{7-35}$$

The switching period T can be expressed as

$$T = \frac{1}{f} = t_1 + t_2 = \frac{\Delta I\, L}{V_s - V_a} + \frac{\Delta I\, L}{V_a} = \frac{\Delta I\, LV_s}{V_a(V_s - V_a)} \tag{7-36}$$

which gives the peak-to-peak ripple current as

$$\Delta I = \frac{V_a(V_s - V_a)}{fLV_s} \tag{7-37}$$

or

$$\Delta I = \frac{V_sk(1 - k)}{fL} \tag{7-38}$$

Using Kirchhoff's current law, we can write the load current as

$$i_L = i_c + i_o$$

If we assume that the load ripple current, Δi_o, is very small and negligible, $\Delta i_L = \Delta i_c$. The average capacitor current, which flows for $t_1/2 + t_2/2 = T/2$, is

$$I_c = \frac{\Delta I}{4}$$

The capacitor voltage is expressed as

$$v_c = \frac{1}{C}\int i_c\, dt + v_c\,(t = 0)$$

and the peak-to-peak ripple voltage of the capacitor is

$$\Delta V_c = v_c - v_c\,(t = 0) = \frac{1}{C}\int_0^{T/2} \frac{\Delta I}{4}\, dt = \frac{\Delta I\, T}{8C} = \frac{\Delta I}{8fC} \tag{7-39}$$

Substituting the value of ΔI from Eq. (7-37) or (7-38) in Eq. (7-39) yields

$$\Delta V_c = \frac{V_a(V_s - V_a)}{8LCf^2V_s} \tag{7-40}$$

or

$$\Delta V_c = \frac{V_sk(1 - k)}{8LCf^2} \tag{7-41}$$

The buck regulator requires only one transistor, is simple, and has high

efficiency. The *di/dt* of the load current is limited by inductor L. However, the input current is discontinuous and a smoothing input filter is normally required. It provides one polarity of output voltage and unidirectional output current. It requires a protection circuit in case of possible short circuit of the diode path.

Example 7-4

The buck regulator in Fig. 7-7a has an input voltage of V_s = 12 V. The required average output voltage is V_a = 5 V and the peak-to-peak output voltage is 20 mV. The switching frequency is 25 kHz. If the peak-to-peak ripple current of inductor is limited to 0.8 A, determine the (a) duty cycle, k; (b) filter inductance, L; and (c) filter capacitor, C.

Solution V_s = 12 V, ΔV_c = 20 mV, ΔI = 0.8 A, f = 25 kHz, and V_a = 5 V.
(a) From Eq. (7-34), $V_a = kV_s$ and $k = V_a/V_s = 5/12 = 0.4167$.
(b) From Eq. (7-37),

$$L = \frac{5(12 - 5)}{0.8 \times 25{,}000 \times 12} = 145.84\ \mu\text{H}$$

(c) From Eq. (7-39),

$$C = \frac{0.8}{8 \times 20 \times 10^{-3} \times 25{,}000} = 200\ \mu\text{F}$$

7-6.2 Boost Regulators

In a boost regulator, the output voltage is greater than the input voltage—hence the name "boost." A boost regulator using a power MOSFET is shown in Fig. 7-8a, and this is similar to a step-up chopper. The circuit operation can be divided into two modes. Mode 1 begins when transistor Q_1 is switched on at $t = 0$. The input current, which rises, flows through inductor L and transistor Q_1. Mode 2 begins when transistor Q_1 is switched off at $t = t_1$. The current which was flowing through the transistor would now flow through L, C, load, and diode D_m. The inductor current falls until transistor Q_1 is turned on again in the next cycle. The energy stored in inductor L is transferred to the load. The equivalent circuits for the modes of operation are shown in Fig. 7-8b. The waveforms for voltages and currents are shown in Fig. 7-8c for continuous load current.

Assuming that the inductor current rises linearly from I_1 to I_2 in time t_1,

$$V_s = L\frac{I_2 - I_1}{t_1} = L\frac{\Delta I}{t_1} \tag{7-42}$$

or

$$t_1 = \frac{\Delta I\, L}{V_s} \tag{7-43}$$

and the inductor current falls linearly from I_2 to I_1 in time t_2,

$$V_a - V_s = L\frac{\Delta I}{t_2} \tag{7-44}$$

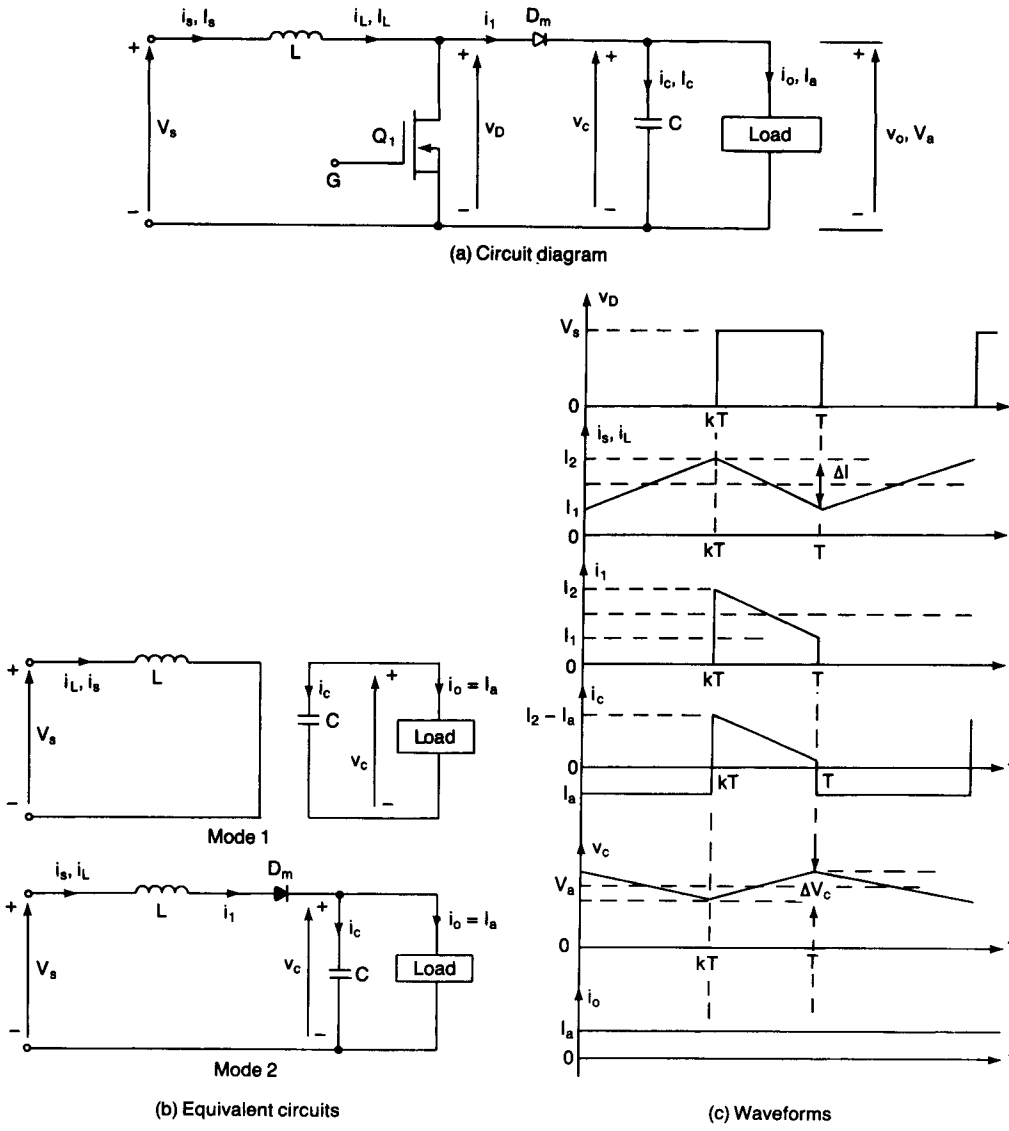


Figure 7-8 Boost regulator.

or

$$t_2 = \frac{\Delta I\, L}{V_a - V_s} \tag{7-45}$$

where ΔI is the peak-to-peak ripple current of inductor L. From Eqs. (7-42) and (7-44),

$$\Delta I = \frac{V_s t_1}{L} = \frac{(V_a - V_s)t_2}{L}$$

Substituting $t_1 = kT$ and $t_2 = (1 - k)T$ yields the average output voltage,

$$V_a = \frac{V_s}{1 - k} \tag{7-46}$$

Assuming a lossless transistor, $V_s I_s = V_a I_a = V_s I_a/(1 - k)$ and the average input current is

$$I_s = \frac{I_a}{1 - k} \tag{7-47}$$

The switching period T can be found from

$$T = \frac{1}{f} = t_1 + t_2 = \frac{\Delta I\, L}{V_s} + \frac{\Delta I\, L}{V_a - V_s} = \frac{\Delta I\, L V_a}{V_s(V_a - V_s)} \tag{7-48}$$

and this gives the peak-to-peak ripple current,

$$\Delta I = \frac{V_s(V_a - V_s)}{fLV_a} \tag{7-49}$$

or

$$\Delta I = \frac{V_s k}{fL} \tag{7-50}$$

When the transistor is on, the capacitor supplies the load current for $t = t_1$. The average capacitor current is $I_c = I_a$ and the peak-to-peak ripple voltage of the capacitor is

$$\Delta V_c = v_c - v_c\,(t = 0) = \frac{1}{C}\int_0^{t_1} I_c\, dt = \frac{1}{C}\int_0^{t_1} I_a = \frac{I_a t_1}{C} \tag{7-51}$$

Equation (7-46) gives $t_1 = (V_a - V_s)/(V_a f)$ and substituting t_1 in Eq. (7-51) gives

$$\Delta V_c = \frac{I_a(V_a - V_s)}{V_a f C} \tag{7-52}$$

or

$$\Delta V_c = \frac{I_a k}{fC} \tag{7-53}$$

A boost regulator can step up the output voltage without a transformer. Due to single transistor, it has high efficiency. The input current is continuous. However, a high peak current has to flow through the power transistor. The output voltage is very sensitive to changes in the duty cycle k and it might be difficult to stabilize the regulator. Since the transistor is in shunt with the load circuit, it might also be difficult to protect the output circuit in case of short circuit. The average output current is less than the average inductor current by a factor of $(1 - k)$, and a much higher rms current would flow through the filter capacitor, resulting in the use of a larger filter capacitor and a larger inductor than those of a buck regulator.

Example 7-5

A buck regulator in Fig. 7-8a has an input voltage of V_s = 5 V. The average output voltage, V_a = 15 V and the average load current, I_a = 0.5 A. The switching frequency is 25 kHz. If L = 150 μH and C = 220 μF, determine the (a) duty cycle, k; (b) ripple current of inductor, ΔI; (c) peak current of inductor, I_2; and (d) ripple voltage of filter capacitor, V_c.

Solution V_s = 5 V, V_a = 15 V, f = 25 kHz, L = 150 μH, and C = 220 μF.

(a) From Eq. (7-46), 15 = 5/(1 − k) or k = 2/3 = 0.6667 = 66.67%.

(b) From Eq. (7-49),

$$\Delta L = \frac{5 \times (15 - 5)}{25{,}000 \times 150 \times 10^{-6} \times 15} = 0.89 \text{ A}$$

(c) From Eq. (7-47), I_s = 0.5/(1 − 0.667) = 1.5 A and peak inductor current,

$$I_2 = I_s + \frac{\Delta I}{2} = 1.5 + \frac{0.89}{2} = 1.945 \text{ A}$$

(d) From Eq. (7-53),

$$\Delta V_c = \frac{0.5 \times 0.6667}{25{,}000 \times 220 \times 10^{-6}} = 60.61 \text{ mV}$$

7-6.3 Buck–Boost Regulators

A buck–boost regulator provides an output voltage which may be less than or greater than the input voltage—hence the name "buck–boost"; the output voltage polarity is opposite to that of the input voltage. This regulator is also known as an *inverting or flyback regulator*. The circuit arrangement of a buck–boost regulator is shown in Fig. 7-9a.

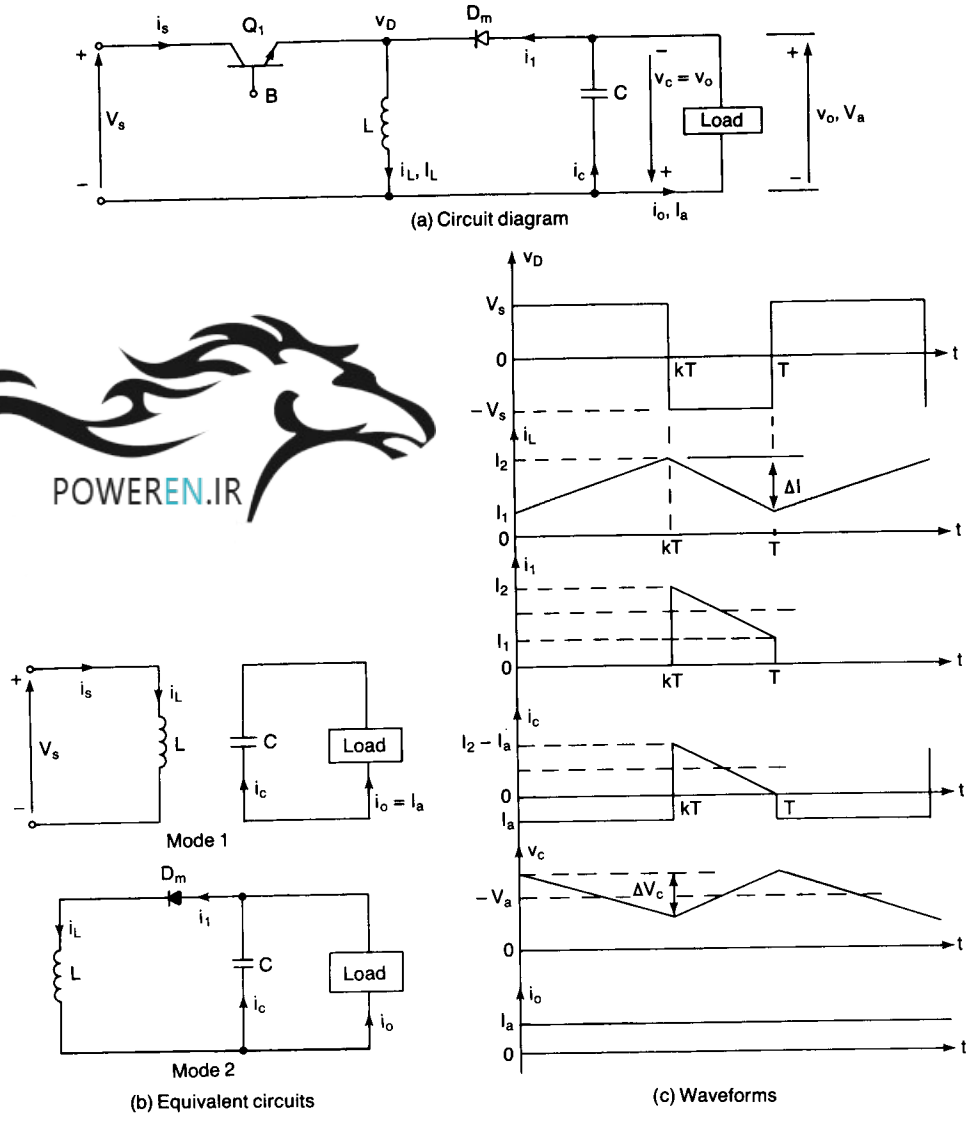
The circuit operation can be divided into two modes. During mode 1, transistor Q_1 is turned on and diode D_m is reversed biased. The input current, which rises, flows through inductor L and transistor Q_1. During mode 2, transistor Q_1 is switched off and the current, which was flowing through inductor L, would now flow through L, C, D_m, and the load. The energy stored in inductor L would be transferred to the load and the inductor current would fall until transistor Q_1 is switched on again in the next cycle. The equivalent circuits for the modes are shown in Fig. 7-9b. The waveforms for steady-state voltages and currents of the buck–boost regulator are shown in Fig. 7-9c for continuous load current.

Assuming that the inductor current rises linearly from I_1 to I_2 in time t_1,

$$V_s = L \frac{I_2 - I_1}{t_1} = L \frac{\Delta I}{t_1} \tag{7-54}$$

or

$$t_1 = \frac{\Delta I \, L}{V_s} \tag{7-55}$$



POWEREN.IR

Figure 7-9 Buck–Boost regulator.

and the inductor current falls linearly from I_2 to I_1 in time t_2,

$$V_a = -L\frac{\Delta I}{t_2} \tag{7-56}$$

or

$$t_2 = \frac{-\Delta I\, L}{V_a} \tag{7-57}$$

where ΔI is the peak-to-peak ripple current of inductor L. From Eqs. (7-54) and (7-56),

$$\Delta I = \frac{V_s t_1}{L} = \frac{-V_a t_2}{L}$$

Substituting $t_1 = kT$ and $t_2 = (1 - k)T$, the average output voltage is

$$V_a = -\frac{V_s k}{1 - k} \tag{7-58}$$

Assuming a lossless circuit, $V_s I_s = V_a I_a = V_s I_a k/(1 - k)$ and the average input current, I_s, is related to the average output current, I_a, by

$$I_s = \frac{I_a k}{1 - k} \tag{7-59}$$

The switching period, T, can be found from

$$T = \frac{1}{f} = t_1 + t_2 = \frac{\Delta I\, L}{V_s} - \frac{\Delta I\, L}{V_a} = \frac{\Delta I\, L(V_a - V_s)}{V_s V_a} \tag{7-60}$$

and this gives the peak-to-peak ripple current,

$$\Delta I = \frac{V_s V_a}{fL(V_a - V_s)} \tag{7-61}$$

or

$$\Delta I = \frac{V_s k}{fL} \tag{7-62}$$

When transistor Q_1 is on, the filter capacitor supplies the load current for $t = t_1$. The average discharging current of the capacitor is $I_c = I_a$ and the peak-to-peak ripple voltage of the capacitor is

$$\Delta V_c = \frac{1}{C}\int_0^{t_1} I_c\, dt = \frac{1}{C}\int_0^{t_1} I_a\, dt = \frac{I_a t_1}{C} \tag{7-63}$$

Equation (7-58) gives $t_1 = V_a/[V_a - V_s)f]$ and Eq. (7-63) becomes

$$\Delta V_c = \frac{I_a V_a}{(V_a - V_s)fC} \tag{7-64}$$

or

$$\Delta V_c \doteq \frac{I_a k}{fC} \tag{7-65}$$

A buck–boost regulator provides output voltage polarity reversal without a transformer. It has high efficiency. Under a fault condition of the transistor, the di/dt of the fault current would be V_s/L and is limited by the inductor L. Output

short-circuit protection would be easy to implement. However, the input current is discontinuous and and a high peak current flows through transistor Q_1.

Example 7-6

The buck–boost regulator in Fig. 7-9a has an input voltage of V_s = 12 V. The duty cycle, k = 0.25 and the switching frequency is 25 kHz. The inductance, L = 150 μH and filter capacitance, C = 220 μF. The average load current, I_a = 1.25 A. Determine the (a) average output voltage, V_a; (b) peak-to-peak output voltage ripple, ΔV_c: (c) peak-to-peak ripple current of inductor, ΔI; and (d) peak current of the transistor, I_p.

Solution V_s = 12 V, k = 0.25, I_a = 1.25 A, f = 25 kHz, L = 150 μH, and C = 220 μF.

(a) From Eq. (7-58), $V_a = -12 \times 0.25/(1 - 0.25) = -4\text{V}$.

(b) From Eq. (7-65), the peak-to-peak output ripple voltage is

$$\Delta V_c = \frac{1.25 \times 0.25}{25{,}000 \times 220 \times 10^{-6}} = 56.8 \text{ mV}$$

(c) From Eq. (7-62), the peak-to-peak inductor ripple is

$$\Delta I = \frac{12 \times 0.25}{25{,}000 \times 150 \times 10^{-6}} = 0.8 \text{ A}$$

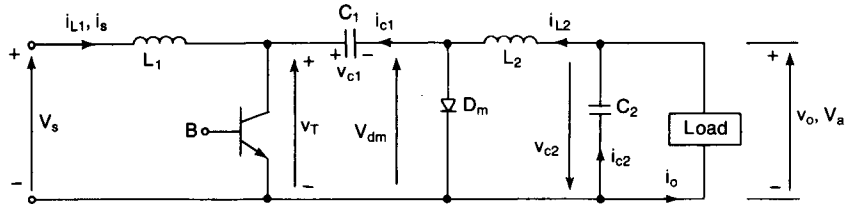
(d) From Eq. (7-59), $I_s = 1.25 \times 0.25/(1 - 0.25) = 0.4167$ A. Since I_s is the average of duration kT, the peak-to-peak current of the transistor,

$$I_p = \frac{I_s}{k} + \frac{\Delta I}{2} = \frac{0.4167}{0.25} + \frac{0.8}{2} = 2.067 \text{ A}$$

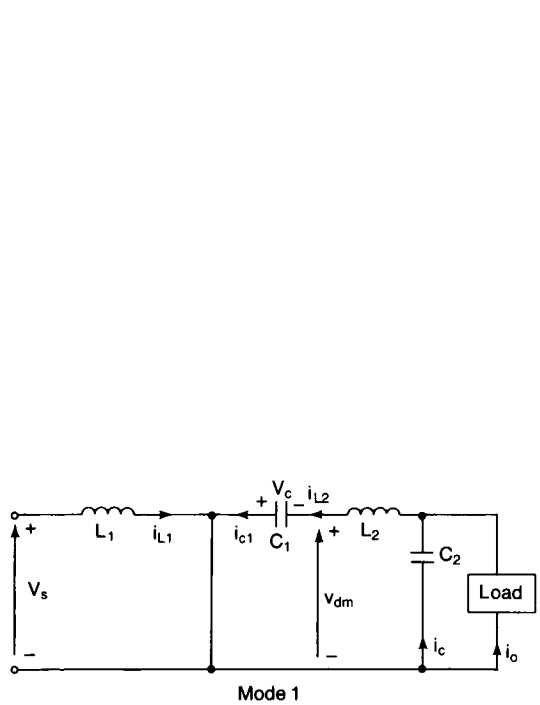
7-6.4 Cúk Regulators

The circuit arrangement of the Cuk regulator using a power BJT is shown in Fig. 7-10a. Similar to the buck–boost regulator, the Cuk regulator provides an output voltage which is less than or greater than the input voltage and the output voltage polarity is also opposite to that of the input voltage. It is named after its inventor [1]. When the input voltage is turned on and transistor Q_1 is switched off, diode D_m is forward biased and capacitor C_1 is charged through L_1, D_m, and the input supply, V_s.

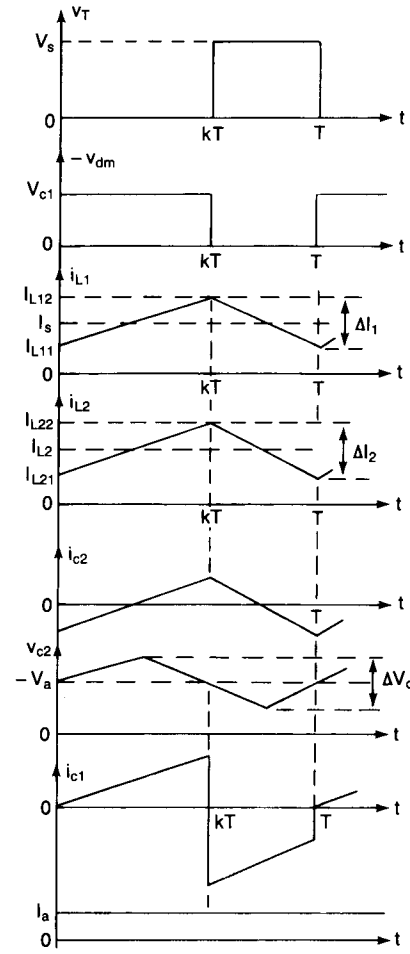
The circuit operation can be divided into two modes. Mode 1 begins when transistor Q_1 is turned on at t = 0. The current through inductor L_1 rises. At the same time, the voltage of capacitor C_1 reverse biases diode D_m and turns it off. The capacitor C_1 discharges its energy to the circuit formed by C_1, C_2, the load, and L_2. Mode 2 begins when transistor Q_1 is turned off at $t = t_1$. The capacitor C_1 is charged from the input supply and the energy stored in the inductor L_2 is transferred to the load. The diode D_m and transistor Q_1 provide a synchronous switching action. The equivalent circuits for the modes are shown in Fig. 7-10b and the waveforms for steady-state voltages and currents are shown in Fig. 7-10c for continuous load current.



(a) Circuit diagram



(b) Equivalent circuits



(c) Waveforms

Figure 7-10 Cúk regulator.

Assuming that the current of inductor L_1 rises linearly from I_{L11} to I_{L12} in time t_1,

$$V_s = L_1 \frac{I_{L12} - I_{L11}}{t_1} = L_1 \frac{\Delta I_1}{t_1} \tag{7-66}$$

or

$$t_1 = \frac{\Delta I_1 L_1}{V_s} \tag{7-67}$$

and due to the charged capacitor C_1, the current of inductor L_1 falls linearly from I_{L12} to I_{L11} in time t_2,

$$V_s - V_{c1} = L_1 \frac{\Delta I_1}{t_2} \tag{7-68}$$

or

$$t_2 = \frac{\Delta I_1 L_1}{V_s - V_{c1}} \tag{7-69}$$

where V_{c1} is the average voltage of capacitor C_1. From Eqs. (7-66) and (7-68),

$$\Delta I_1 = \frac{V_s t_1}{L_1} = \frac{(V_s - V_{c1})t_2}{L_1}$$

Substituting $t_1 = kT$ and $t_2 = (1 - k)T$, the average voltage of capacitor C_1 is

$$V_{c1} = \frac{V_s(1 - 2k)}{1 - k} \tag{7-70}$$

Assuming that the current of filter inductor L_2 rises linearly from I_{L21} to I_{L22} in time t_1,

$$V_{c1} - V_a = L_2 \frac{I_{L22} - I_{L21}}{t_1} = L_2 \frac{\Delta I_2}{t_1} \tag{7-71}$$

or

$$t_1 = \frac{\Delta I_2 L_2}{V_{c1} - V_a} \tag{7-72}$$

and the current of inductor L_2 falls linearly from I_{L22} to I_{L21} in time t_2,

$$V_a = -L_2 \frac{\Delta I_2}{t_2} \tag{7-73}$$

or

$$t_2 = -\frac{\Delta I_2 L_2}{V_a} \tag{7-74}$$

From Eqs. (7-71) and (7-73),

$$\Delta I_2 = \frac{(V_{c1} - V_a)t_1}{L_2} = -\frac{V_a t_2}{L_2}$$

Substituting $t_1 = kT$ and $t_2 = (1 - k)T$, the average voltage of capacitor C_1 is

$$V_{c1} = -\frac{V_a(1 - 2k)}{k} \tag{7-75}$$

Equating Eq. (7-70) to Eq. (7-75), we can find the average output voltage as

$$V_a = -\frac{kV_s}{1 - k} \tag{7-76}$$

Assuming a lossless circuit, $V_s I_s = V_a I_a = V_s I_a k/(1 - k)$ and the average input current,

$$I_s = \frac{kI_a}{1 - k} \tag{7-77}$$

The switching period T can be found from Eqs. (7-67) and (7-69):

$$T = \frac{1}{f} = t_1 + t_2 = \frac{\Delta I_1 L_1}{V_s} + \frac{\Delta I_1 L_1}{V_s - V_{c1}} = \frac{\Delta I_1 L_1(2V_s - V_{c1})}{V_s(V_s - V_{c1})} \tag{7-78}$$

which gives the peak-to-peak ripple current of inductor L_1 as

$$\Delta I_1 = \frac{V_s(V_s - V_{c1})}{fL_1(2V_s - V_{c1})} \tag{7-79}$$

or

$$\Delta I_1 = \frac{V_s k}{fL_1} \tag{7-80}$$

The switching period T can also be found from Eqs. (7-72) and (7-74):

$$T = \frac{1}{f} = t_1 + t_2 = \frac{\Delta I_2 L_2}{V_{c1} - V_a} - \frac{\Delta I_2 L_2}{V_a} = \frac{\Delta I_2 L_2(2V_a - V_{c1})}{V_a(V_{c1} - V_a)} \tag{7-81}$$

and this gives the peak-to-peak ripple current of inductor L_2 as

$$\Delta I_2 = \frac{V_a(V_{c1} - V_s)}{fL_2(2V_a - V_{c1})} \tag{7-82}$$

or

$$\Delta I_2 = -\frac{V_a(1 - k)}{fL_2} = \frac{kV_s}{fL_2} \tag{7-83}$$

When transistor Q_1 is off, the energy transfer capacitor C_1 is charged by the input current for $t = t_2$. The average charging current for C_1 is $I_{c1} = I_s$ and the peak-

to-peak ripple voltage of the capacitor C_1 is

$$\Delta V_{c1} = \frac{1}{C_1}\int_0^{t_2} I_{c1}\,dt = \frac{1}{C_1}\int_0^{t_2} I_s = \frac{I_s t_2}{C_1} \tag{7-84}$$

Equation (7-76) gives $t_2 = V_s/[(V_s - V_a)f]$ and Eq. (7-84) becomes

$$\Delta V_{c1} = \frac{I_s V_s}{(V_s - V_a)fC_1} \tag{7-85}$$

or

$$\Delta V_{c1} = \frac{I_s(1 - k)}{fC_1} \tag{7-86}$$

If we assume that the load current ripple, Δi_o, is negligible, $\Delta i_{L2} = \Delta i_{c2}$. The average charging current of C_2, which flows for time $T/2$, is $I_{c2} = \Delta I_2/4$ and the peak-to-peak ripple voltage of capacitor C_2 is

$$\Delta V_{c2} = \frac{1}{C_2}\int_0^{T/2} I_{c2}\,dt = \frac{1}{C_2}\int_0^{T/2} \frac{\Delta I_2}{4} = \frac{\Delta I_2}{8fC_2} \tag{7-87}$$

or

$$\Delta V_{c2} = -\frac{V_a(1 - k)}{8C_2L_2f^2} = \frac{kV_s}{8C_2L_2f^2} \tag{7-88}$$

The Cúk regulator is based on the capacitive energy transfer and as a result, the input current is continuous. The circuit has low switching losses and has high efficiency. When transistor Q_1 is turned on, it has to carry the currents of inductors L_1 and L_2. As a result a high peak current flows through transistor Q_1. Since the capacitor provides the energy transfer, the ripple current of the capacitor C_1 is also high.

Example 7-7

The input voltage of a Cúk converter in Fig. 7-10a, $V_s = 12$ V. The duty cycle, $k = 0.25$ and the switching frequency is 25 kHz. The filter inductance, $L_2 = 150$ μH and filter capacitance is $C_2 = 220$ μF. The energy transfer capacitance is $C_1 = 200$ μF and inductance $L_1 = 200$ μH. The average load current is $I_a = 1.12$ A. Determine the (a) average output voltage, V_a; (b) average input current, I_s; (c) peak-to-peak ripple current of inductor L_1, ΔI_1; (d) peak-to-peak ripple voltage of capacitor C_1, ΔV_{c1}; (e) peak-to-peak ripple current of inductor L_2, ΔI_2; (f) peak-to-peak ripple voltage of capacitor C_2, ΔV_{c2}; and (g) peak current of the transistor, I_p.

Solution $V_s = 12$ V, $k = 0.25$, $I_a = 1.25$ A, $f = 25$ kHz, $L_1 = 180$ μH, $C_1 = 200$ μF, $L_2 = 150$ μH, and $C_2 = 220$ μF.

(a) From Eq. (7-76), $V_a = -0.25 \times 12/(1 - 0.25) = -4$V.
(b) From Eq. (7-77), $I_s = 1.25 \times 0.25/(1 - 0.25) = 0.42$ A.
(c) From Eq. (7-80), $\Delta I_1 = 12 \times 0.25/(25{,}000 \times 180 \times 10^{-6}) = 0.67$ A.
(d) From Eq. (7-86), $\Delta V_{c1} = 0.42(1 - 0.25)/(25{,}000 \times 200 \times 10^{-6}) = 63$ mV.
(e) From Eq. (7-83), $\Delta I_2 = 0.25 \times 12/(25{,}000 \times 150 \times 10^{-6}) = 0.8$ A.
(f) From Eq. (7-87), $\Delta V_{c2} = 0.8/(8 \times 25{,}000 \times 220 \times 10^{-6}) = 18.18$ mV.

(g) The average voltage across the diode can be found from

$$V_{dm} = kV_{c1} = -V_a k \frac{(1 - 2k)}{k} = -V_a(1 - 2k) \tag{7-89}$$

For a lossless circuit, $I_{L2}V_{dm} = V_a I_a$ and the average value of the current in inductor L_2 is

$$I_{L2} = \frac{I_a}{1 - 2k} = \frac{1.25}{1 - 2 \times 0.25} = 2.5 \text{ A} \tag{7-90}$$

Therefore, the peak current of transistor is

$$I_p = I_s + \frac{\Delta I_1}{2} + I_{L2} + \frac{\Delta I_2}{2} = 0.42 + \frac{0.67}{2} + 2.5 + \frac{0.8}{2} = 3.655 \text{ A}$$

7-6.5 Limitations of Single-Stage Conversion

These four regulators use only one transistor, employing only one stage conversion, and require inductors or capacitors for energy transfer. Due to the current-handling limitation of a single transistor, the output power of these regulators is small, typically tens of watts. At higher current, the size of these components increases, with increased component losses, and the efficiency deceases. In addition, there is no isolation between the input and output voltage, which is a highly desirable criterion in most applications. For high power, multistage conversions are used, where a dc voltage is converted to ac by an inverter. The ac output is isolated by a transformer and then converted to dc by rectifiers. The multistage conversions are discussed in Section 9-4.

7-7 THYRISTOR CHOPPER CIRCUITS

A thyristor chopper circuit, which uses a fast turn-off thyristor as a switch, requires commutation circuitry to turn it off. There are various techniques by which a thyristor can be turned off and these are described in detail in Chapter 3. During the early stage of fast-turn-off thyristors, a number of chopper circuits have been published. The various circuits are the outcome of meeting certain criteria: (1) reduction of minimum on-time limit, (2) high frequency of operation, and (3)

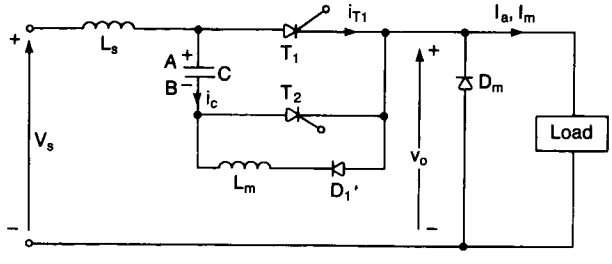


Figure 7-11 Impulse-commutated chopper.

reliable operation. However, with the development of alternative switching devices (e.g, power transistors, GTOs), the applications of thyristor chopper circuits are limited to high power levels and especially, to traction motor control. Some of the chopper circuits used by traction equipment manufacturers are discussed in this section.

7-7.1 Impulse-Commutated Choppers

The impulse-commutated chopper is a very common circuit with two thyristors as shown in Fig. 7-11 and is also known as a *classical chopper*. At the beginning of the operation, thyristor T_2 is fired and this causes the commutation capacitor C to charge through the load to voltage V_c, which should be the supply voltage, V_s, in the first cycle. The plate A becomes positive with respect to plate B. The circuit operation can be divided into five modes, and the equivalent circuits under steady-state conditions are shown in Fig. 7-12.

Mode 1 begins when T_1 is fired. The load is connected to the supply. The commutation capacitor C reverses its charge through the resonant reversing circuit formed by T_1, D_1, and L_m. The resonant current is given by

$$i_r = V_c \sqrt{\frac{C}{L_m}} \sin \omega_m t \tag{7-91}$$

The peak value of resonant reversal current is

$$I_p = V_c \sqrt{\frac{C}{L_m}} \tag{7-92}$$

The capacitor voltage is found from

$$v_c(t) = V_c \cos \omega_m t \tag{7-93}$$

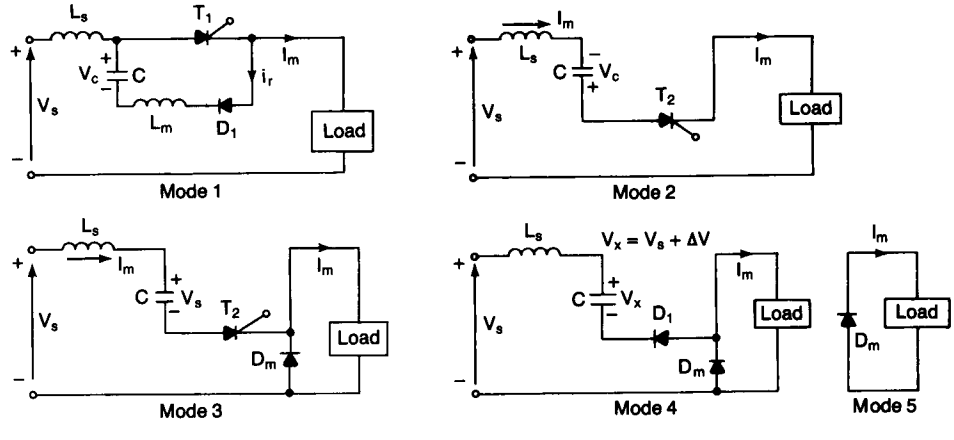


Figure 7-12 Mode equivalent circuits.

where $\omega_m = 1/\sqrt{L_m C}$. After time $t = t_r = \pi\sqrt{L_m C}$, the capacitor voltage is reversed to $-V_c$. This is sometimes called *commutation readiness*.

Mode 2 begins when the commutation thyristor T_2 is fired. A reverse voltage is applied across the main thyristor T_1 and it is turned off. The capacitor C discharges through the load from $-V_c$ to zero and this discharging time, which is also called the *circuit (or available) turn-off time*, is given by

$$t_q = \frac{V_c C}{I_m} \tag{7-94}$$

where I_m is the peak load current. The circuit turn-off time, t_q, must be greater than the turn-off time of the thyristor, t_{off}. t_q varies with the load current and must be designed for the worst-case condition, which occurs at the maximum value of load current and the minimum value of capacitor voltage.

The time required for the capacitor to recharge back to the supply voltage is called the *recharging time* and is given by

$$t_c = \frac{V_s C}{I_m} \tag{7-95}$$

Thus the total time necessary for the capacitor to discharge and recharge is called the *commutation time*, which is

$$t_d = t_q + t_c \tag{7-96}$$

This mode ends at $t = t_d$ when the commutation capacitor C recharges to V_s and the freewheeling diode D_m starts conducting.

Mode 3 begins when the freewheeling diode D_m starts conducting and the load current decays. The energy stored in the source inductance L_s (plus any stray inductance in the circuit) is transferred into the capacitor and the current is

$$i_s(t) = I_m \cos \omega_s t \tag{7-97}$$

and the instantaneous capacitor voltage is

$$v_c(t) = V_s + I_m \sqrt{\frac{L_s}{C}} \sin \omega_s t \tag{7-98}$$

where $\omega_s = 1/\pi\sqrt{L_s C}$. After time $t = t_s = 0.5\pi\sqrt{L_s C}$, the overcharging current becomes zero and the capacitor is recharged to

$$V_x = V_s + \Delta V \tag{7-99}$$

where ΔV and V_x are the overvoltage and peak voltage of commutation capacitor, respectively. Equation (7-98) gives the overcharging voltage as

$$\Delta V = I_m \sqrt{\frac{L_s}{C}}. \tag{7-100}$$

Mode 4 begins when the overcharging is complete and the load current continues to decay. It is important to note that this mode exists due to diode D_1,

because it allows the resonant oscillation to continue through the circuit formed by D_m, D_1, C, and the supply. This will undercharge the commutation capacitator C and the undercharging current through the capacitor is given by

$$i_c(t) = -\Delta V \sqrt{\frac{C}{(L_s + L_m)}} \sin \omega_u t \tag{7-101}$$

The commutation capacitor voltage is

$$v_c(t) = V_x - \Delta V(1 - \cos \omega_u t) \tag{7-102}$$

where $\omega_u = 1/\pi \sqrt{C(L_s + L_m)}$. After time $t = t_u = \pi \sqrt{C(L_s + L_m)}$, the undercharging current becomes zero and the diode D_1 stops conducting. Equation (7-102) gives the available commutation voltage of the capacitor as

$$V_c = V_x - 2\Delta V = V_s - \Delta V \tag{7-103}$$

If there is no overcharge, there will not be any undercharge.

Mode 5 begins when the commutation process is complete and the load current continues to decay through diode D_m. This mode ends when the main thyristor is refired at the beginning of next cycle. The different waveforms for the currents and voltages are shown in Fig. 7-13.

The average output voltage of the chopper is

$$V_o = \frac{1}{T}\left[V_s kT + t_d \frac{1}{2}(V_c + V_s)\right] \tag{7-104}$$

It could be noticed from Eq. (7-104) that even at $k = 0$, the output voltage becomes

$$V_o(k = 0) = 0.5 f t_d (V_c + V_s) \tag{7-105}$$

This limits the minimum output voltage of the chopper. However, the thyristor T_1 must be on for a minimum time of $t_r = \pi\sqrt{L_m C}$ to allow the charge reversal of the capacitor and t_r is fixed for a particular circuit design. Therefore, the minimum duty cycle and minimum output voltage are also set.

$$t_r = k_{\min} T = \pi \sqrt{L_m C} \tag{7-106}$$

The minimum duty cycle,

$$k_{\min} = t_r f = \pi f \sqrt{L_m C} \tag{7-107}$$

The minimum average output voltage,

$$\begin{aligned} V_{o(\min)} &= k_{\min} V_s + 0.5 t_d (V_c + V_s) f \\ &= f[V_s t_r + 0.5 t_d (V_c + V_s)] \end{aligned} \tag{7-108}$$

The minimum output voltage, $V_{o(\min)}$, can be varied by controlling the chopping frequency. Normally, $V_{o(\min)}$ is fixed by the design requirement to a permissible value.

The maximum value of the duty cycle is also limited to allow the commutation capacitor to discharge and recharge. The maximum value of this duty cycle is

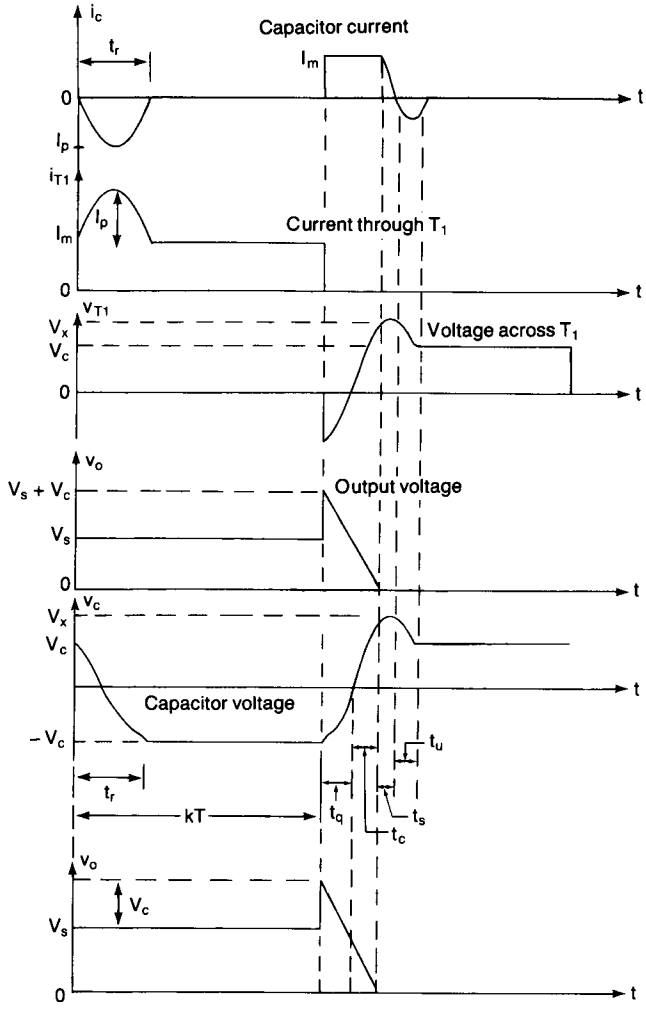


Figure 7-13 Waveforms for impulse-commutated chopper.

given by

$$k_{\max} T = T - t_d - t_s - t_u \tag{7-109}$$

and

$$k_{\max} = 1 - \frac{t_d + t_s + t_u}{T}$$

The maximum output voltage,

$$V_{o(\max)} = k_{\max} V_s + 0.5 t_d (V_c + V_s) f \tag{7-110}$$

An ideal thyristor chopper should have no limit on the (1) minimum on-time, (2) maximum on-time, (3) maximum output voltage, and (4) maximum chopping frequency. The turn-off time, t_q, should be independent of the load current. At

higher frequency, the load ripple currents and the supply harmonic current become smaller. In addition, the size of the input filter is reduced.

This chopper circuit is very simple and requires two thyristors and one diode. However, the main thyristor T_1 has to carry the resonant reversal current, thereby increasing its peak current rating and limiting the minium output voltage. The discharging and charging time of commutation capacitor are dependent on the load current and this limits the high-frequency operation, especially at a low load current. This chopper cannot be tested without connecting the load. This circuit has many disadvantages. However, it points out the problems of thyristor commutation.

Example 7-8

An inductive load controlled by the chopper in Fig. 7-11 requires an average current of I_a = 425 A with peak current of I_m = 450 A. The input supply voltage is V_s = 220 V. The chopping frequency is f = 400 Hz and the turn-off time of the main thyristor is t_{off} = 18 μs. If the peak current through the main thyristor is limited to 180% of I_m and the source inductance (including the stray inductance) is negligible (L_s = 0), determine the (a) commutation capacitance, C; (b) inductance, L_m; and (c) minimum and maximum output voltage.

Solution I_a = 425 A, I_m = 450 A, $V_c = V_s$ = 220 V, f = 400 Hz, t_{off} = 18 μs, and L_s = 0.

(a) From Eqs. (7-99), (7-100), and (7-103), the overvoltage is ΔV = 0 and $V_c = V_x = V_s$ = 220 V. From Eq. (7-94), the turn-off requirement gives

$$\frac{V_c C}{I_m} = t_q > t_{off}$$

and $C > (450 \times 18/220) = 36.8$ μF. Let C = 40 μF.

(b) From Eq. (7-92), the peak resonant current

$$I_p = 1.8 \times 450 - 450 = 220\sqrt{\frac{40}{L_m}}$$

which gives inductance, L_m = 14.94 μH.

(c) From Eq. (7-94), discharging time, $t_q = (220 \times 40)/450 = 19.56$ μs, from Eq. (7-95), recharging time, $t_c = (220 \times 40)/450 = 19.56$ μs, and from Eq. (7-96), total time, $t_d = 19.56 \times 2 = 39.12$ μs. From Eq. (7-106), resonant reversal time,

$$t_r = \pi[(14.94 \times 40) \times 10^{-6}]^{1/2} = 76.8\ \mu s$$

From Eq. (7-107), the minimum duty cycle, $k_{min} = t_r f = 0.0307$. From Eq. (7-108), the minimum output voltage,

$$V_{o(min)} = 0.0307 \times 220 + 0.5 \times 39.12 \times 10^{-6} \times 2 \times 220 \times 400 = 6.75 + 3.44 = 10.19\ V$$

Since there is no overcharging, there will be no overcharging period, and the overcharging and undercharging time, $t_u = t_s = 0$. From Eq. (7-109), the maximum duty cycle, $k_{max} = 1 - (t_d + t_u + t_s)f = 0.984$, and from Eq. (7-110), the maximum output voltage,

$$V_{o(max)} = 0.984 \times 220 + 0.5 \times 39.12 \times 10^{-6} \times 2 \times 220 \times 400 = 216.48 + 3.44 = 219.92\ V$$

7-7.2 Effects of Source and Load Inductance

The source inductance plays a significant role on the operation of the chopper, and this inductance should be as small as possible to limit the transient voltage within an acceptable level. It is evident from Eq. (7-100) that the commutation capacitor is overcharged due to the source inductance L_s, and the semiconductor devices would be subjected to this capacitor voltage. If the minimum value of the source inductance cannot be guaranteed, an input filter is required. In practical systems, the stray inductance always exists and its value depends on the type of wiring and the layout of the components. Therefore, L_s in Eq. (7-100) has a finite value and the capacitor gets overcharged.

Due to inductance L_s and diode D_1 in Fig. 7-11, the capacitor also gets undercharged and this may cause commutation problem of the chopper. Equation (7-20) indicates that the load ripple current is an inverse function of load inductance and chopping frequency. Hence the peak load current is dependent on the load inductance. Therefore, the performances of the chopper are also influenced by the load inductance. A smoothing choke is normally used in series with the load to limit the load ripple current.

Example 7-9

If the supply in Example 7-8 has an inductance of $L_s = 4$ μH, determine the (a) peak capacitor voltage, V_x; (b) available turn-off time, t_q; and (c) total commutation time, t_d.

Solution $I_a = 425$ A, $I_m = 450$ A, $V_s = 220$ V, $f = 400$ Hz, $t_{off} = 18$ μs, $L_s = 4$ μH, and $C = 40$ μF.

(a) From Eq. (7-100), overvoltage, $\Delta V = 450 \times \sqrt{4/40} = 142.3$ V. From Eq. (7-99), peak capacitor, $V_x = 220 + 142.3 = 362.3$ V and from Eq. (7-103), available commutation voltage, $V_c = 220 - 142.3 = 77.7$.

(b) From Eq. (7-94), available turn-off time, $t_q = (77.7 \times 40)/450 = 6.9$ μs.

(c) From Eq. (7-95), recharging time, $t_c = (220 \times 40)/450 = 19.56$ μs and from Eq. (7-96), commutation time, $t_d = 6.0 + 19.56 = 26.46$ μs.

Note. The turn-off requirement of the main thyristor is 19 μs, whereas the available turn-off time is only 6.9 μs. Therefore, a commutation failure would occur.

7-7.3 Impulse-Commutated Three-Thyristor Choppers

This problem of undercharging can be remedied by replacing diode D_1 with thyristor T_3, as shown in Fig. 7-14. The available turn-off time, t_q, commutation time, t_d, and the overvoltage depend on the peak value of the load current rather than the average value. In a good chopper, the commutation time, t_d, should ideally be independent of the load current. t_d could be made less dependent on the load current by adding an antiparallel diode D_1 across the main thyristor as shown in Fig. 7-14 by dashed lines. A modified version of the circuit is shown in Fig. 7-15, where the charge reversal of the capacitor is done independently of main thyristor

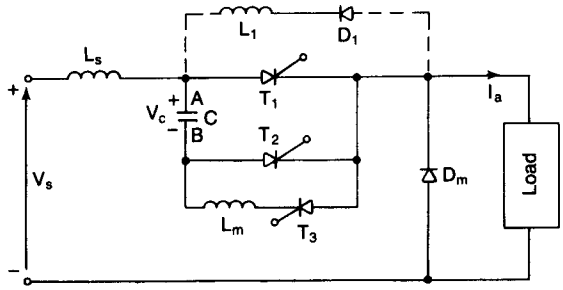


Figure 7-14 Impulse-commutated three thyristors chopper.

T_1 by firing thyristor T_3. There are four possible modes and their equivalent circuits are shown in Fig. 7-16.

Mode 1 begins when the main thyristor T_1 is fired and the load is connected to the supply. Thyristor T_3 may be fired at the same time as T_1 to reverse the charge on capacitor C. If this charge reversal is done independently, the minimum output voltage would not be limited due to the resonant reversal as in the case of classical chopper in Fig. 7-11.

Mode 2 begins when commutation thyristor T_2 is fired and capacitor C discharges and recharges through the load at a rate determined by the load current.

Mode 3 begins when the capacitor is recharged to the supply voltage and the freewheeling diode D_m starts conducting. During this mode the capacitor overcharges due to the energy stored in the source inductance, L_s, and the load current decays through D_m. This mode ends when the overcharging current reduces to zero.

Mode 4 begins when the thyristor T_2 stops conducting. The freewheeling diode D_m continues to conduct and the load current decays.

All the equations for the classical chopper except Eqs. (7-101), (7-102), and (7-103) are valid for this chopper, and mode 4 of the classical chopper is not applicable. The available commutation voltage

$$V_c = V_x = V_s + \Delta V \tag{7-111}$$

The resonant reversal is independent of the main thyristor and the minimum on-time of the chopper is not limited. However, the commutation time is dependent on the load and the high-frequency operation is limited. The chopper circuit cannot be tested without connecting the load.

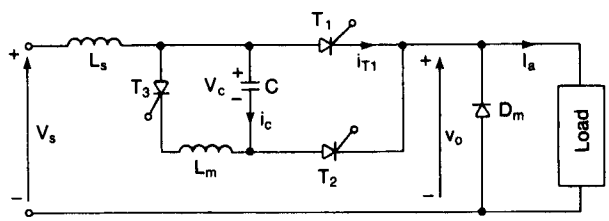


Figure 7-15 Impulse-commutated chopper with independent charge reversal.

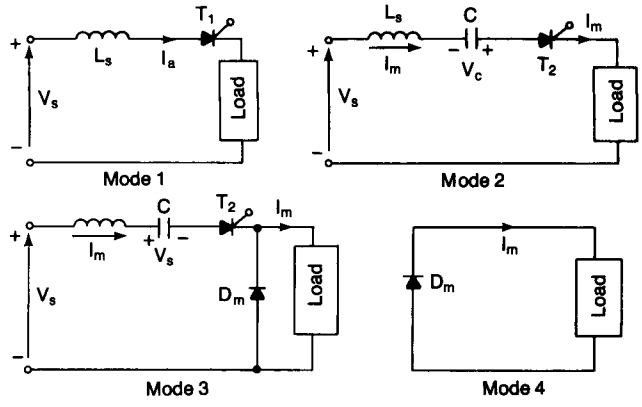


Figure 7-16 Equivalent circuits.

7-7.4 Resonant Pulse Choppers

A resonant pulse chopper is shown in Fig. 7-17. As soon as the supply is switched on, the capacitor is charged to a voltage V_c through L_m, D_1, and load. The circuit operation can be divided into five modes and the equivalent circuits are shown in Fig. 7-18. The waveforms for currents and voltages are shown in Fig. 7-19.

Mode 1 begins when main thyristor T_1 is fired and the supply is connected to the load. This mode is valid for $t = kT$.

Mode 2 begins when commutation thyristor T_2 is fired. The commutation capacitor reverses its charge through C, L_m, and T_2. The reversal current is given by

$$i_r = -i_c = V_c \sqrt{\frac{C}{L_m}} \sin \omega_m t = I_p \sin \omega_m t \tag{7-112}$$

and the capacitor voltage is

$$v_c(t) = V_c \cos \omega_m t \tag{7-113}$$

where $\omega_m = 1\sqrt{L_m C}$. After time, $t = t_r = \pi\sqrt{L_m c}$, the capacitor voltage is reversed to $-V_c$. However, the resonant oscillation continues through diode D_1. The peak resonant current, I_p, must be greater than load current I_m and the circuit is normally designed for a ratio of $I_p/I_m = 1.5$.

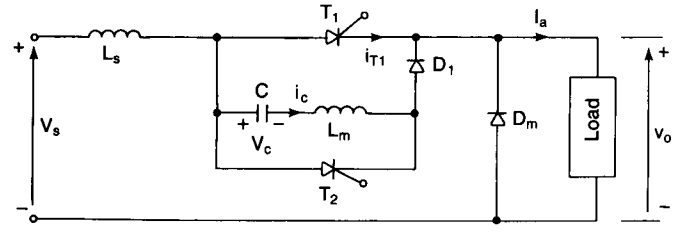


Figure 7-17 Resonant pulse chopper.

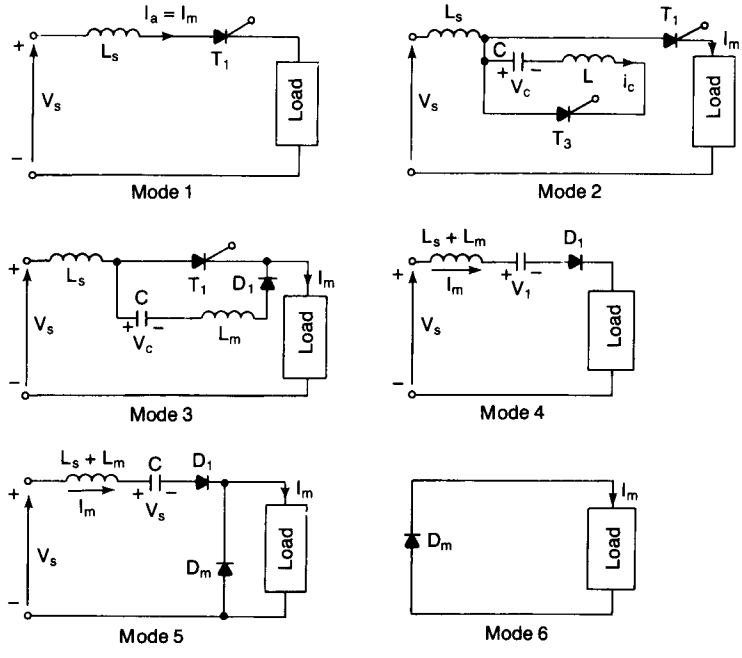


Figure 7-18 Equivalent circuits for modes.

Mode 3 begins when T_2 is self-commutated and the capacitor discharges due to resonant oscillation through diode D_1. This mode ends when the capacitor current rises to the level of I_m. Assuming that the capacitor current rises linearly from 0 to I_m and that the current of thyristor T_1 falls from I_m to 0 in time t_x, the time duration for this mode is

$$t_x = \frac{L_m I_m}{V_c} \tag{7-114}$$

and the capacitor voltage falls to

$$V_1 = V_c - \frac{t_x I_m}{2C} = V_c - \frac{L_m I_m^2}{2CV_c} \tag{7-115}$$

Mode 4 begins when the current through T_1 falls to zero. The capacitor continues to discharge through the load at a rate determined by the peak load current. The available turn-off time,

$$t_q = \frac{V_1 C}{I_m} \tag{7-116}$$

The time required for the capacitor to recharge to the supply voltage,

$$t_c = \frac{V_s C}{I_m} \tag{7-117}$$

The total time to discharge and recharge to the supply V_s is $t_d = t_q + t_c$.

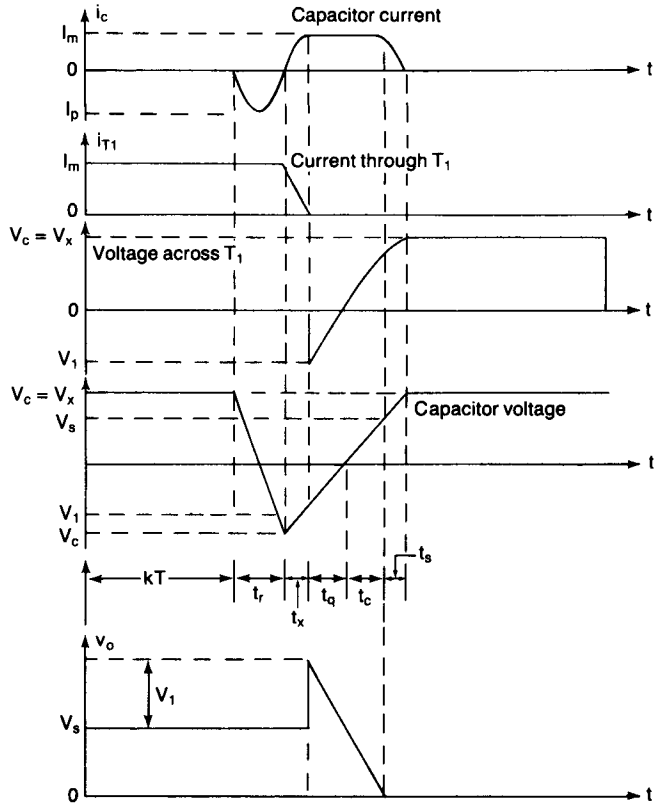


Figure 7-19 Chopper waveforms.

Mode 5 begins when the freewheeling diode D_m starts conducting and the load current decays through D_m. The energy stored in commutation inductance L_m and source inductance L_s is transferred to capacitor C. After time, $t_s = \pi\sqrt{(L_s + L_m)C}$, the overcharging current becomes zero and the capacitor is recharged to

$$V_x = V_s + \Delta V \tag{7-118}$$

and

$$\Delta V = I_m \sqrt{\frac{L_m + L_s}{C}} \tag{7-119}$$

Mode 6 begins when the overcharging is complete. Diode D_1 turns off. The load current continues to decay until the main thyristor is refired in the next cycle. In the steady-state condition $V_c = V_x$. The average output voltage is given by

$$\begin{aligned} V_o &= \frac{1}{T}[V_s kT + V_s(t_r + t_x) + 0.5t_d(V_1 + V_s)] \\ &= V_s k + f[(t_r + t_x)V_s + 0.5t_d(V_1 + V_s)] \end{aligned} \tag{7-120}$$

Although the circuit does not have any constraint on the minimum value of duty

cycle k, in practice the value of k cannot be zero. The maximum value of k is

$$k_{\max} = 1 - (t_r + t_x + t_d)f \tag{7-121}$$

Due to commutation by a resonant pulse, the reverse *di/dt* of thyristor T_1 is limited by inductor L_m, and this is also known as *soft commutation*. The resonant reversal is independent of thyristor T_1. However, the inductance, L_m, overcharges capacitor C and this would increase the voltage ratings of the components. After thyristor T_2 is fired, the capacitor has to reverse its charge before turning off thyristor T_1. There is an inherent delay in commutation and this limits the minimum on-time of the chopper. The commutation time is dependent on the load.

Example 7-10

An inductive load that is controlled by the chopper in Fig. 7-17 requires an average current, $I_a = 425$ A with a peak current, $I_m = 450$ A. The supply voltage, $V_s = 220$ V. The chopping frequency, $f = 400$ Hz, commutation inductance, $L_m = 8$ μH, and commutation capacitance, $C = 40$ μF. If the source inductance (including the stray inductance) is $L_s = 4$ μH, determine the (a) peak resonant current, I_p; (b) peak load voltage, V_x; (c) turn-off time, t_q; and (d) minimum and maximum output voltage.

Solution The reversing time, $t_r = \pi\sqrt{8 \times 4} = 56.2$ μs. From Eq. (7-119), overvoltage, $\Delta V = 450\sqrt{(8 + 4)/40} = 246.5$ V and from Eq. (7-118), peak capacitor voltage, $V_c = V_x = 220 + 246.5 = 466.5$ V.

(a) From Eq. (7-112), $I_p = 466.5\sqrt{40/8} = 1043.1$ A.

(b) From Eq. (7-114), $t_x = 8 \times 450/466.5 = 7.72$ μs and from Eq. (7-115), the peak load voltage,

$$V_1 = 466.5 - \frac{8 \times 450 \times 450}{2 \times 40 \times 466.5} = 423.1 \text{ V}$$

(c) From Eq. (7-116), the turn-off time, $t_q = 423.1 \times 40/450 = 37.6$ μs.

(d) From Eq. (7-117), $t_c = 220 \times 40/450 = 19.6$ μs and $t_d = 37.6 + 19.6 = 57.2$ μs. From Eq. (7-121), the maximum duty cycle,

$$k_{\max} = 1 - (57.2 + 7.72 + 56.2) \times 400 \times 10^{-6} = 0.952$$

For $k = k_{\max}$, Eq. (7-120) gives the maximum output voltage,

$$V_{o(\max)} = 220 \times 0.952 + 400[(56.2 + 7.72) \times 220 + 0.5 \times 57.2 \times (423.1 + 220)] \times 10^{-6} = 209.4 + 12.98 = 223.4 \text{ V}$$

The minimum output voltage (for $k = 0$), $V_{o(\min)} = 12.98$ V.

7-8 CHOPPER CIRCUIT DESIGN

The main requirement for the design of commutation circuit is to provide an adequate turn-off time to switch the main thyristor off. The analyses of the mode equations for the classical chopper in Section 7-7.1 and resonant pulse chopper in Section 7-7.4 show that the turn-off time depends on the voltage of commutation capacitor V_c.

It is much simpler to design the commutation circuit if the source inductance

can be neglected or the load current is not high. But in the case of higher load current, stray inductances, which are always present in practical systems, play a significant part in the design of the commutation circuit because the energy stored in the circuit inductance increases as the square of the peak load current. The source inductance makes the design equations nonlinear and an iterative method of solution is required to determine the commutation components. The voltage stresses on the power devices depend on the source inductance and load current.

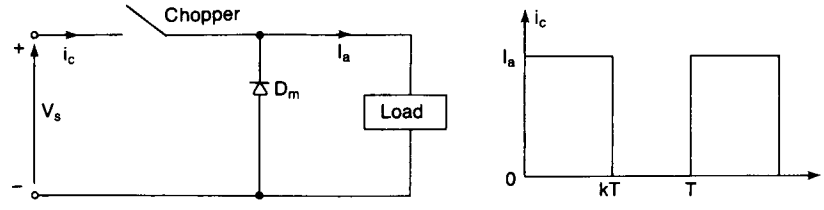
There are no fixed rules for the design of a chopper circuit and the design varies with the types of circuits used. The designer has a wide range of choice and the values of L_mC components are influenced by the designer's choice of thyristors, peak resonant reversal current, and peak allowable voltage of the circuit. The voltage and current ratings of the L_mC components and devices give the minimum limits, but the actual selection of components and devices is left to the designer based on the considerations of price, availability, and safety margin. In general, the following steps are involved in the design:

1. Identify the modes of operation for the chopper circuit.
2. Determine the equivalent circuits for the modes.
3. Determine the currents and voltages for the modes and their waveforms.
4. Evaluate the values of commutation components L_mC that would satisfy the design limits.
5. Determine the voltage and current rating requirements of all components and devices.

We can notice from Eq. (7-7) that the output voltage contains harmonics. An output filter of C, LC, L type may be connected to the output in order to reduce the output harmonics. The techniques for filter design are similar to that of Examples 2-15 and 4-12.

A chopper with a highly inductive load is shown in Fig. 7-20a. The load current ripple is negligible ($\Delta I = 0$). If the average load current is I_a, the peak load current is $I_m = I_a + \Delta I = I_a$. The input current, which is of pulsed shape as shown in Fig. 7-20b, contains harmonics and can be expressed in Fourier series as

$$i_c(t) = kI_a + \frac{I_a}{n\pi}\sum_{n=1}^{\infty} \sin 2n\pi k \cos 2n\pi ft + \frac{I_a}{n\pi}\sum_{n=1}^{\infty}(1 - \cos 2n\pi k)\sin 2n\pi ft \qquad (7\text{-}122)$$



(a) Circuit diagram (b) Chopper current

Figure 7-20 Input current waveform of chopper.

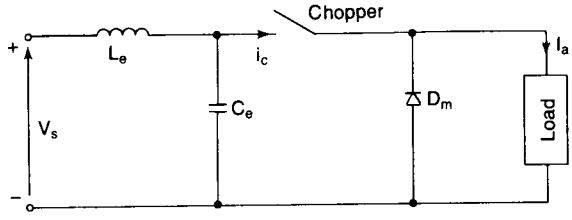


Figure 7-21 Chopper with an input filter.

The fundamental component ($n = 1$) of the chopper-generated harmonic current into the supply is given by

$$i_{1c}(t) = \frac{I_a}{\pi} \sin 2\pi k \cos 2\pi ft + \frac{I_a}{\pi}(1 - \cos 2\pi k) \sin 2\pi ft \qquad (7\text{-}123)$$

In practice, an input filter as shown in Fig. 7-21 is normally connected to filter out the chopper generated harmonics from the supply source. The equivalent circuit for the chopper-generated harmonic currents is shown in Fig. 7-22, and the rms value of the nth harmonic component in the supply is calculated as

$$I_{ns} = \frac{1}{1 + (2n\pi f)^2 L_e C_e} I_{nc} = \frac{1}{1 + (nf/f_0)^2} I_{nc} \qquad (7\text{-}124)$$

where f is the chopping frequency and f_0 [$= 1/(2\pi \sqrt{L_e C_e})$] is the filter resonant frequency. If $(f/f_0) >> 1$, the nth harmonic current in the supply becomes

$$I_{ns} = I_{nc} \left(\frac{f_0}{nf}\right)^2 \qquad (7\text{-}125)$$

A high chopping frequency reduces the sizes of input filter elements. But the frequencies of chopper-generated harmonics in the supply line are also increased, and this may cause interference problems with the control and communication signals.

If the source has some inductances, L_s, and the chopper switch as in Fig. 7-1a is turned on, a certain amount of energy would be stored in the source inductance. If an attempt is made to turn off the chopper switch, the power semiconductor devices might be damaged due to the induced voltage resulting from this stored energy. The LC input filter provides a low-impedance source for the chopper action.

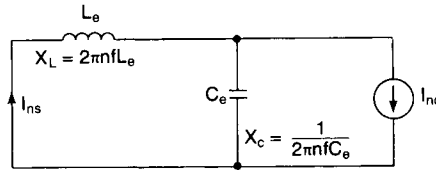


Figure 7-22 Equivalent circuit for harmonic currents.

Example 7-11

It is required to design the impulse-commutated chopper in the circuit of Fig. 7-14 to operate from a supply voltage of $V_s = 220$ V and the peak load current is $I_m = 440$ A.

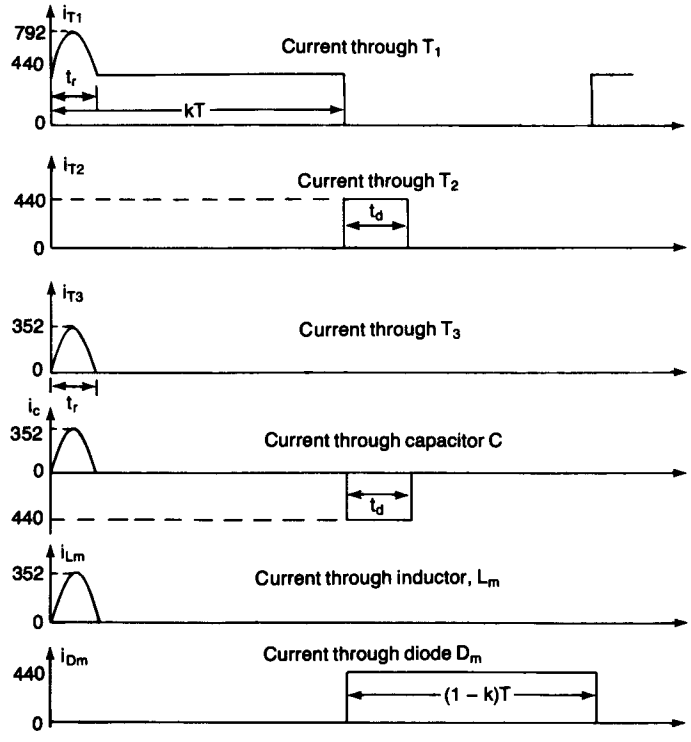


Figure 7-23 Waveforms for Example 7-11.

The minimum output voltage should be less than 5% of V_s, the peak resonant current should be limited to 80% of I_m, the turn-off time requirement is $t_q = 25$ μs, and the source inductance is $L_s = 4$ μH. Determine the (a) values of L_mC components; (b) maximum allowable chopping frequency; and (c) ratings of components and devices.

Solution $V_s = 220$ V, $I_m = 440$ A, $t_q = 25$ μs, $L_s = 4$ μH, and $V_{o(\min)} = 0.05 \times 220 = 11$ V. The waveforms for the various currents and capacitor voltage are shown in Fig. 7-23.

(a) From Eqs. (7-94), (7-99), and (7-100), the turn-off time is

$$t_q = \frac{V_cC}{I_m} = \left[V_s + I_m\sqrt{\frac{L_s}{C}}\right]\frac{C}{I_m} = \frac{V_sC}{I_m} + \sqrt{L_sC}$$

or

$$\left[t_q - \frac{V_sC}{I_m}\right]^2 = t_q^2 + \left(\frac{V_sC}{I_m}\right)^2 - \frac{2V_sCt_q}{I_m} = L_sC$$

Substituting the numerical values, $0.25C^2 - 29C + 625 = 0$ and $C = 87.4$ μF or 28.6 μF. Choose the lowest value, $C = 28.6$ μF, and let $C = 30$ μF.

(b) From Eq. (7-100), the overvoltage is $\Delta V = 440\sqrt{4/30} = 160$ V, and from Eq. (7-99), the capacitor voltage, $V_c = V_x = 220 + 160 = 380$ V. From Eq.

(7-92), the peak resonant current,

$$I_p = 380\sqrt{\frac{30}{L_m}} = 0.8 \times 440 = 352 \quad \text{or} \quad L_m = 34.96\ \mu\text{H}$$

Let $L_m = 35\ \mu$H; then the reversing time, $t_r = \pi\sqrt{35 \times 30} = 101.8\ \mu$s. From Eq. (7-94), the turn-off time, $t_q = 380 \times 30/440 = 25.9\ \mu$s, from Eq. (7-95), $t_c = 220 \times 30/440 = 15\ \mu$s, and from Eq. (7-96), the commutation time, $t_d = 25.9 + 15 = 40.9\ \mu$s. The chopping frequency can be determined from the condition of minimum voltage to satisfy Eq. (7-108):

$$11 = f[220 \times 101.8 + 0.5 \times 40.9\,(380 + 220)] \times 10^{-6} \text{ or } f = 317\ \text{Hz}$$

The maximum chopping frequency is $f = 317$ Hz; let $f = 300$ Hz.

(c) At this stage, we have all the particulars to determine the ratings.

T_1: The average current, $I_{av} = 440$ A.
The peak current, $I_p = 440 + 0.8 \times 440 = 792$ A.
The maximum rms current due to the load, $I_{r1} = 440$ A.
The rms current due to resonant reversal,

$$I_{r2} = 0.8 \times 440\sqrt{t_r f/2} = 0.352\sqrt{101.8 \times 300/2} = 43.5\ \text{A}$$

The effective rms current, $I_{rms} = (440^2 + 43.5)^{1/2} = 442.14$ A.

T_2: The peak current, $I_p = 440$ A.
The rms current, $I_{rms} = 440\sqrt{ft_d} = 0.44\sqrt{300 \times 40.9} = 48.7$ A.
The average current, $I_{av} = I_p t_d f = 440 \times 40.9 \times 300 \times 10^{-6} = 5.4$ A.

T_3: The peak current, $I_p = 0.8 \times 440 = 352$ A.
The rms current, $I_{rms} = I_p\sqrt{ft_r} = 0.352\sqrt{101.8 \times 300} = 43.5$ A.
The average current,

$$I_{av} = 2I_p f t_r/\pi = 2 \times 352 \times 300 \times 101.8 \times 10^{-6}/\pi = 6.84\ \text{A}$$

C: The value of capacitance, $C = 30\ \mu$F.
The peak-to-peak voltage, $V_{pp} = 2 \times 380 = 760$ V.
The peak current, $I_p = 440$ A.
The rms current, $I_{rms} = (48.7^2 + 43.5^2)^{1/2} = 65$ A.

L_m: The peak current, $I_p = 352$ A.
The rms current, $I_{rms} = 43.5$ A.

D_m: The average current, $I_{av} = 440$ A.
The rms current, $I_{rms} = 440$ A.
The peak current, $I_p = 440$ A.

Note. Due to resonant reversal through the main thyristor, its current ratings and losses are increased. The main thyristor could be avoided in the reversal process as in Fig. 7-15. If V_s varies between $V_{s(min)}$ and $V_{s(max)}$ and L_s varies between $L_{s(min)}$ and $L_{s(max)}$, then $V_{s(min)}$ and $L_{s(min)}$ should be used to calculate the values of L_m and C. $V_{s(max)}$ and $L_{s(max)}$ should be used to determine the ratings of components and devices.

Example 7-12

It is required to design the resonant pulse chopper circuit in Fig. 7-17 to operate from a supply voltage of $V_s = 220$ V and a peak load current, $I_m = 440$ A. The peak resonant current should be limitd to 150% of I_m; the turn-off time requirement,

t_q = 25 μs, and the source inductance, L_s = 4 μH. Determine the (a) values of L_mC components; (b) overcharged voltage, ΔV; and (c) available commutation voltage, V_c.

Solution I_m = 440 A, I_p = 1.5 × 440 = 660 A, L_s = 4 μH, t_q = 25 μs, and V_s = 220 V. From Eqs. (7-115) and (7-116), the turn-off time is given as

$$t_q = \frac{V_c C}{I_m} - \frac{L_m I_m}{2V_c}$$

From Eq. (7-112), the peak resonant current, $I_p = V_c\sqrt{C/L_m}$. From Eqs. (7-118) and (7-119), the capacitor voltage,

$$V_c = V_x = V_s + I_m\sqrt{\frac{L_s + L_m}{C}}$$

Find the values of L_m and C that would satisfy the conditions of t_q and I_p. An iterative method of solution yields:

(a) L_m = 25.29 μH, C = 18.17 μF.

(b) ΔV = 558.67 V.

(c) V_c = 220 + 558.67 = 778.68 V, and Eq. (7-115) gives V_1 = 605.63 V.

Note. For L_s = 0, L_m = 21.43 μH, C = 21.43 μF, ΔV = 440 V, V_c = 660 V, and V_1 = 513.33 V.

Example 7-13

A highly inductive load is controlled by a chopper. The average load current is I_a = 100 A and the load ripple current can be considered negligible (ΔI = 0). A simple LC input filter with L_e = 0.3 mH and C_e = 4500 μF is used. If the chopper is operated at a frequency of 350 Hz and a duty cycle of 0.5, determine the maximum rms value of the fundamental component of chopper-generated harmonic current.

Solution For I_a = 100 A, f = 350 Hz, k = 0.50, C_e = 4500 μF, and L_e = 0.3 mH, $f_0 = 1/(2\pi\sqrt{C_eL_e})$ = 136.98 Hz. Equation (7-123) can be written as

$$I_{1c}(t) = A_1 \sin 2\pi ft + B_1 \cos 2\pi ft$$

where $A_1 = (I_a/\pi)\sin 2\pi k$ and $B_1 = (I_a/\pi)(1 - \cos 2\pi k)$. The peak magnitude of this current is calculated from

$$I_{pc} = (A_1^2 + B_1^2)^{1/2} = \frac{\sqrt{2I_a}}{\pi}(1 - \cos 2\pi k)^{1/2}$$

The rms value of this current is

$$I_{1c} = \frac{I_a}{\pi}(1 - \cos 2\pi k)^{1/2} = 45.02 \text{ A}$$

and this becomes maximum at k = 0.5. The fundamental component of chopper-generated harmonic current in the supply can be calculated from Eq. (7-124) and is given by

$$I_{1s} = \frac{1}{1 + (f/f_0)^2} I_{1c} = \frac{45.02}{1 + (350/136.98)^2} = 5.98 \text{ A}$$

If $f/f_0 >> 1$, the harmonic current in the supply becomes

$$I_{1s} = I_{1c}\left(\frac{f_0}{f}\right)^2$$

7-9 MAGNETIC CONSIDERATIONS

Inductances, which are used to create resonant oscillation for voltage reversal of commutation capacitor and turning off thyristors, act as energy storage elements in switched-mode regulators and as filter elements to smooth out the current harmonics. We can notice from Eqs. (B-17) and (B-18) in Appendix B that the magnetic loss increases with the square of frequency. On the other hand, higher frequency reduces the size of inductors for the same value of ripple current and filtering requirement. The design of dc–dc converters requires a compromise among switching frequency, inductor sizes, and switching losses.

SUMMARY

A dc chopper can be used as a dc transformer to step up or step down a fixed dc voltage. The chopper can also be used for switching-mode voltage regulators and for transferring energy between two dc sources. However, harmonics are generated in the input and load side of the chopper and these harmonics can be reduced by input and output filters. A chopper can operate on either constant frequency or variable frequency. A variable-frequency chopper generates harmonics of variable frequencies and a filter design becomes difficult. A fixed-frequency chopper is normally used. To reduce the sizes of filters and to lower the load ripple current, the chopping frequency should be high. Thyristor choppers require extra circuitry to turn off the main thyristor, and as a result the chopping frequency and minimum on-time are limited.

REFERENCES

1. S. Cúk, and R. D. Middlebrook, "Advances in switched mode power conversion." *IEEE Transactions on Industrial Electronics*, Vol. IE30, No. 1, 1983, pp. 10–29.
2. C. E. Band, and D. W. Venemans, "Chopper control on a 1600-V dc traction supply." *IRCA, Cybernatics and Electronics on the Railways*, Vol. 5, No. 12, 1968, pp. 473–478.
3. F. Nouvion, "Use of power semiconductors to control locomotive traction motors in the French National Railways." *Proceedings, IEE*, Vol. 55, No. 3 (August) 1967.
4. Westinghouse Electric, "Choppers for São Paulo metro follow BART pattern." *Railway Gazette International*, Vol. 129, No. 8, 1973, pp.. 309–310.
5. T. Tsuboi, S. Izawa, K. Wajima, T. Ogawa, and T. Katta, "Newly developed thyristor

chopper equipment for electric railcars." *IEEE Transactions on Industry and General Applications*, Vol. IA9, No. 3, 1973.
6. J. Gouthiere, J. Gregoire, and H. Hologne, "Thyristor choppers in electric tractions." *ACEC Review*, No. 2, 1970, pp. 46–47.
7. M. H. Rashid, "A thyristor chopper with minimum limits on voltage control of dc drives." *International Journal of Electronics*, Vol. 53, No. 1, 1982, pp. 71–81.
8. R. P. Severns, and G. E. Bloom, *Modern DC-to-DC Switchmode Power Converter Circuits*. New York: Van Nostrand Reinhold Company, Inc., 1983.
9. Peter Wood, *Switching Power Converters*. New York: Van Nostrand Reinhold Company, Inc., 1981.
10. S. Cúk, "Survey of switched mode power supplies," *IEE International Conference on Power Electronics and Variable Speed Drives*, London, 1985, pp. 83–94.
11. S. A. Chin, D. Y. Chen, and F. C. Lee, "Optimization of the energy storage inductors for dc to dc converters." *IEEE Transactions on Aerospace and Electronic Systems*, Vol. AES19, No. 2, 1983, pp. 203–214.
12. M. Ehsani, R. L. Kustom, and R. E. Fuja, "Microprocessor control of a current source dc-dc converter." *IEEE Transactions on Industry Applications*, Vol. IA19, No. 5, 1983, pp. 690–698.

REVIEW QUESTIONS

7-1. What is meant by a dc chopper or dc–dc converter?
7-2. What is the principle of operation of a step-down chopper?
7-3. What is the principle of operation of a step-up chopper?
7-4. What is pulse-width-modulation control of a chopper?
7-5. What is frequency-modulation control of a chopper?
7-6. What are the advantages and disadvantages of a variable-frequency chopper?
7-7. What is the effect of load inductance on the load ripple current?
7-8. What is the effect of chopping frequency on the load ripple current?
7-9. What are the constraints for transfer of energy between two dc voltage sources?
7-10. What are the performance parameters of a chopper?
7-11. What is a switching-mode regulator?
7-12. What are the four basic types of switching-mode regulators?
7-13. What are the advantages and disadvantages of a buck regulator?
7-14. What are the advantages and disadvantages of a boost regulator?
7-15. What are the advantages and disadvantages of a buck–boost regulator?
7-16. What are the advantages and disadvantages of a Cuk regulator?
7-17. What is the purpose of the commutation circuit of a chopper?
7-18. What is the difference between the circuit turn-off time and the turn-off time of a thyristor?
7-19. Why does the commutation capacitor get overcharged?
7-20. Why is the minimum output voltage of the classical chopper limited?
7-21. What are the advantages and disadvantages of the classical chopper?

7-22. What are the effects of source inductance?

7-23. Why should the resonant reversal be independent of the main thyristor?

7-24. Why should the peak resonant current of the resonant pulse chopper be greater than the peak load current?

7-25. What are the advantages and disadvantages of a resonant pulse chopper?

7-26. At what duty cycle does the load ripple current become maximum?

7-27. Why may the design of commutation circuits require an iterative method of solution?

7-28. What are the general steps for the design of chopper circuits?

7-29. Why is the peak load current rather than the average load current used in the design of thyristor choppers?

7-30. What are the effects of chopping frequency on filter sizes?

PROBLEMS

7-1. The dc chopper in Fig. 7-1a has a resistive load, $R = 20\ \Omega$ and input voltage, $V_s = 220$ V. When the chopper remains on, its voltage drop, $V_{ch} = 1.5$ V and chopping frequency, $f = 10$ kHz. If the duty cycle is 80%, determine the (**a**) average output voltage, V_a; (**b**) rms output voltage, V_o; (**c**) chopper efficiency; (**d**) effective input resistance, R_i; and (**e**) rms value of the fundamental component of harmonics on the output voltage.

7-2. A chopper is feeding an RL load as shown in Fig. 7-2 with $V_s = 220$ V, $R = 10\ \Omega$, $L = 15.5$ mH, $f = 5$ kHz, and $E = 20$ V. Calculate the (**a**) minimum instantaneous load current, I_1; (**b**) peak instantaneous load current, I_2; (**c**) maximum peak-to-peak ripple current in the load; (**d**) average load current, I_a (**e**) rms load current, I_o; (**f**) effective input resistance, R_i; and (**g**) rms value of chopper current, I_R.

7-3. The chopper in Fig. 7-2 has load resistance, $R = 0.2\ \Omega$, input voltage, $V_s = 220$ V, and battery voltage, $E = 10$ V. The average load current, $I_a = 200$ A, and the chopping frequency, $f = 200$ Hz ($T = 5$ ms). Use the average output voltage to calculate the value of load inductance, L, which would limit the maximum load ripple current to 5% of I_a.

7-4. The dc chopper shown in Fig. 7-5a is used to control power flow from a dc voltage, $V_s = 110$ V to a battery voltage, $E = 220$ V. The power transferred to the battery is 30 kW. The current ripple of the inductor is negligible. Determine the (**a**) duty cycle, k; (**b**) effective load resistance, R_{eq}; and (**c**) average input current, I_s.

7-5. For Prob. 7-4, plot the instantaneous inductor current and current through the battery E if inductor L has a finite value of $L = 7.5$ mH, $f = 250$ Hz, and $k = 0.5$.

7-6. An RL load as shown in Fig. 7-2 is controlled by a chopper. If load resistance, $R = 0.25\ \Omega$, inductance, $L = 20$ mH, supply voltage, $V_s = 600$, battery voltage, $E = 150$ V, and chopping frequency, $f = 250$ Hz, determine the minimum and maximum load current, the peak-to-peak load ripple current, and average load current for $k = 0.1$ to 0.9 with a step of 0.1.

7-7. Determine the maximum peak-to-peak ripple current of Prob. 7-6 by using Eqs. (7-19) and (7-20), and compare the results.

7-8. The buck regulator in Fig. 7-7a has an input voltage, $V_s = 15$ V. The required average output voltage, $V_a = 5$ V and the peak-to-peak output ripple voltage is 10 mV. The

switching frequency is 20 kHz. The peak-to-peak ripple current of inductor is limited to 0.5 A. Determine the (**a**) duty cycle, k; (**b**) filter inductance, L; and (**c**) filter capacitor, C.

7-9. The boost regulator in Fig. 7-8a has an input voltage, V_s = 6 V. The average output voltage, V_a = 15 V and average load current, I_a = 0.5 A. The switching frequency is 20 kHz. If L = 250 μH and C = 440 μF, determine the (**a**) duty cycle, k; (**b**) ripple current of inductor, ΔI; (**c**) peak current of inductor, I_2; and (**d**) ripple voltage of filter capacitor, ΔV_c.

7-10. The buck–boost regulator in Fig. 7-9a has an input voltage, V_s = 12 V. The duty cycle, k = 0.6 and the switching frequency is 25 kHz. The inductance, L = 250 μH and filter capacitance, C = 220 μF. The average load current, I_a = 1.5 A. Determine the (**a**) average output voltage, V_a; (**b**) peak-to-peak output ripple voltage, ΔV_c; (**c**) peak-to-peak ripple current of inductor, ΔI; and (**d**) peak current of the transistor, I_p.

7-11. The Cuk regulator in Fig. 7-10a has an input voltage, V_s = 15 V. The duty cycle, k = 0.4 and the switching frequency is 25 kHz. The filter inductance, L_2 = 350 μH and filter capacitance, C_2 = 220 μF. The energy transfer capacitance, C_1 = 400 μF and inductance, L_1 = 250 μH. The average load current, I_a = 1.25 A. Determine the (**a**) average output voltage, V_a; (**b**) average input current, I_s; (**c**) peak-to-peak ripple current of inductor L_1, ΔI_1; (**d**) peak-to-peak ripple voltage of capacitor C_1, ΔV_{c1}, (**e**) peak-to-peak ripple current of inductor L_2, ΔI_2; (**f**) peak-to-peak ripple voltage of capacitor C_2, ΔV_{c2}; and (**g**) peak current of the transistor, I_p.

7-12. An inductive load is controlled by an impulse commutation chopper in Fig. 7-11 and peak load current, I_m = 450 A at a supply voltage of 220 V. The chopping frequency, f = 275 Hz, commutation capacitor, C = 60 μF, and reversing inductance, L_m = 20 μH. The source inductance, L_s = 8 μH. Determine the circuit turn-off time and minimum and maximum output voltage limits.

7-13. Repeat Prob. 7-12 for the case when the source inductance is negligible (L_s = 0).

7-14. An inductive load is controlled by the chopper in Fig. 7-15 and peak load current, I_m = 350 A at a supply voltage, V_s = 750 V. The chopping frequency, f = 250 Hz, commutation capacitance, C = 15 μF, and commutation inductance, L_m = 70 μH. If the source inductance, L_s = 10 μH, determine the turn-off time, t_q; minimum and maximum output voltage; and output voltage for a duty cycle of k = 0.5.

7-15. Repeat Prob. 7-12 for the resonant pulse chopper circuit in Fig. 7-17 if commutation capacitance, C = 30 μF and commutation inductance, L_m = 35 μH.

7-16. Design the values of commutation components L_m and C to provide a turn-off time, t_q = 20 μs for the circuit in Fig. 7-11. The specifications for the circuit are V_s = 600 V, I_m = 350 A, and L_s = 6 μH. The peak current through T_1 is not to exceed $2I_m$.

7-17. Repeat Prob. 7-16 for the chopper circuit in Fig. 7-14 if the peak current of diode D_1 is limited to $2I_m$. Determine C and L_1.

7-18. Repeat Prob. 7-16 for the chopper circuit in Fig. 7-15 if the peak resonant reversal current is limited to I_m.

7-19. Repeat Prob. 7-16 for the circuit in Fig. 7-17 if the resonant reversal current through T_2 is limited to $2I_m$.

7-20. Design the value of the commutation capacitor C to provide a turn-off-time requirement of t_q = 20 μs for the circuit in Fig. P7-20 if V_s = 600 V, I_m = 350 A, and L_s = 8 μH.

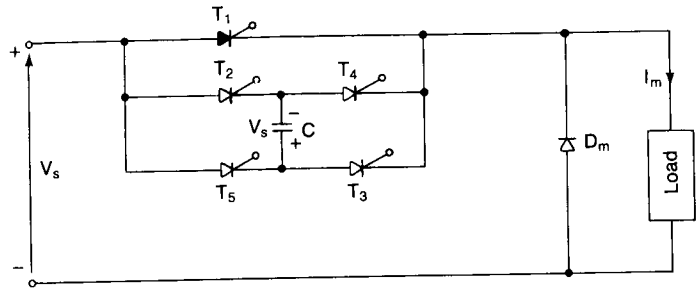


Figure P7-20

7-21. A highly inductive load is controlled by a chopper as shown in Fig. 7-20. The average load current is 250 A, which has negligible ripple current. A simple LC input filter with $L_e = 0.4$ mH and $C_e = 5000$ μF is used. If the chopper is operated at frequency, $f = 250$ Hz, determine the total chopper generated harmonic current in the supply for $k = 0.5$. (*Hint:* Consider up to the seventh harmonic.)

8

Inverters

8-1 INTRODUCTION

Dc-to-ac converters are known as *inverters*. The function of an inverter is to change a dc input voltage to a symmetrical ac output voltage of desired magnitude and frequency. The output voltage could be fixed or variable at a fixed or variable frequency. A variable output voltage can be obtained by varying the input dc voltage and maintaining the gain of the inverter constant. On the other hand, if the dc input voltage is fixed and it is not controllable, a variable output voltage can be obtained by varying the gain of the inverter, which is normally accomplished by pulse-width-modulation (PWM) control within the inverter. The *inverter gain* may be defined as the ratio of the ac output voltage to dc input voltage.

The output voltage waveforms of ideal inverters should be sinusoidal. However, the waveforms of practical inverters are nonsinusoidal and contain certain harmonics. For low- and medium-power applications, square-wave or quasi-square-wave voltages may be acceptable; and for high-power applications, low distorted sinusoidal waveforms are required. With the availability of high-speed power semiconductor devices, the harmonic contents of output voltage can be minimized or reduced significantly by switching techniques.

Inverters are widely used in industrial applications (e.g., variable-speed ac motor drives, induction heating, standby power supplies, uninterruptible power

supplies). The input may be a battery, fuel cell, solar cell, or other dc source. The typical single-phase outputs are (1) 120 V at 60 Hz, (2) 220 V at 50 Hz, and (3) 115 V at 400 Hz. For high-power three-phase systems, typical outputs are (1) 220/380 V at 50 Hz, (2) 120/208 V at 60 Hz, and (3) 115/200 V at 400 Hz.

Inverters can be broadly classified into two types: (1) single-phase inverters, and (2) three-phase inverters. Each type can be subdivided into four categories, depending on the type of thyristor commutations: (a) pulse width modulation (PWM) inverter, (b) resonant inverter, (c) auxiliary commutated inverter, or (d) complementary commutated inverter. An inverter is called a *voltage-fed inverter* (VFI) if the input voltage remains constant, a *current-fed inverter* (CFI) if the input current is maintained constant, and a *variable dc linked inverter* if the input voltage is controllable.

8-2 PRINCIPLE OF OPERATION

The principle of single-phase inverters can be explained with Fig. 8-1a. The inverter circuit consists of two choppers. When only transistor Q_1 is turned on for a time $T_0/2$, the instantaneous voltage across the load v_0 is $V_s/2$. If transistor Q_2 only is turned on for a time $T_0/2$, $-V_s/2$ appears across the load. The logic circuit should be designed such that Q_1 and Q_2 are not turned on at the same time. Figure 8-1b shows the waveforms for the output voltage and transistor currents with a resistive load. This inverter requires a three-wired dc source, and when a transistor

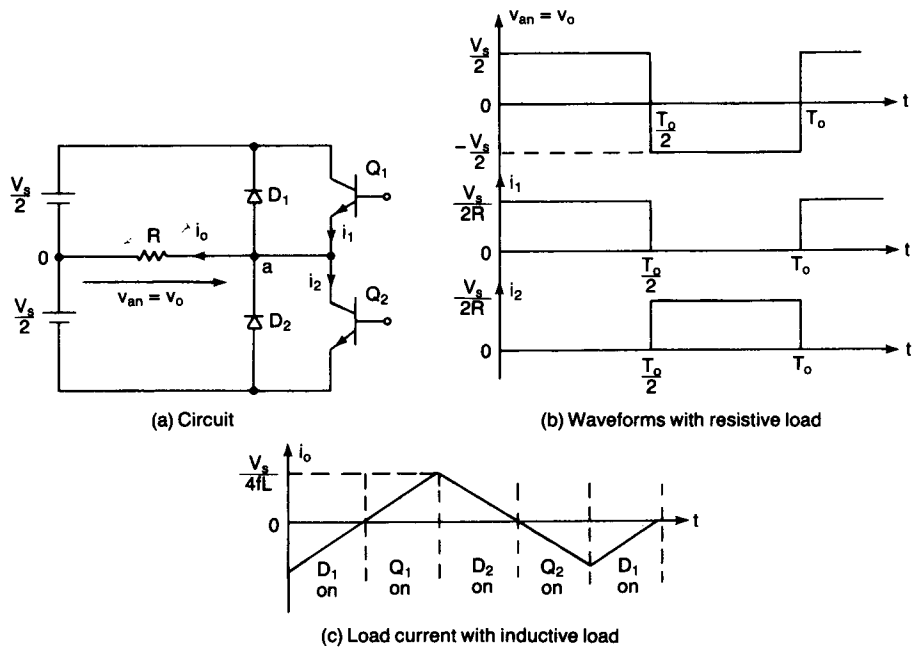


Figure 8-1 Single-phase half-bridge inverter.

is off, its reverse voltage is V_s instead of $V_s/2$. This inverter is known as a *half-bridge inverter.*

The rms output voltage can be found from

$$V_o = \left(\frac{2}{T_0}\int_0^{T_0/2}\frac{V_s^2}{4}\,dt\right)^{1/2} = \frac{V_s}{2} \tag{8-1}$$

The instantaneous output voltage can be expressed in Fourier series as

$$\begin{aligned} v_o &= \sum_{n=1,3,5,\ldots}^{\infty}\frac{2V_s}{n\pi}\sin n\omega t \\ &= 0 \qquad \text{for } n = 2, 4, \ldots \end{aligned} \tag{8-2}$$

where $\omega = 2\pi f_0$ is the frequency of output voltage in rad/s. For $n = 1$, Eq. (8-2) gives the rms value of fundamental components as

$$V_1 = \frac{2V_s}{\sqrt{2}\,\pi} = 0.45V_s \tag{8-3}$$

For an inductive load, the load current cannot change immediately with the output voltage. If Q_1 is turned off at $t = T_0/2$, the load current would continue to flow through D_2, load, and the lower half of the dc source until the current falls to zero. Similarly, when Q_2 is turned off at $t = T_0$, the load current flows through D_1, load, and the upper half of the dc source. When diode D_1 or D_2 conducts, energy is fed back to the dc source and the diode is known as a *feedback diode.* Figure 8-1c shows the load current and conduction intervals of devices for purely inductive loads. It can be noticed that for purely inductive loads, a transistor conducts only for $T_0/2$ (or 90°). Depending on the load power factor, the conduction period of a transistor would vary from 90 to 180°.

The transistors can be replaced by GTOs or forced-commutated thyristors. If t_{off} is the turn-off time of a thyristor, there must be a minimum delay time of t_{off} between the outgoing thyristor and firing of the next incoming thyristor. Otherwise, a short-circuit condition would result through the two thyristors. Therefore, the maximum conduction time of a thyristor would be $T_0/2 - t_{off}$. In practice, even the transistors require a certain turn-on and turn-off time. For successful operation of inverters, the logic circuit should take these into account.

8-3 PERFORMANCE PARAMETERS

The output of practical inverters contain certain harmonics and the quality of an inverter is normally evaluated in terms of the following performance parameters.

Harmonic factor, HF. The harmonic factor (of n^{th} harmonic), which is a measure of individual harmonic contribution, is defined as

$$\text{HF}_n = \frac{V_n}{V_1} \tag{8-4}$$

where V_1 is the rms value of the fundamental component and V_n is the rms value of the nth harmonic component.

Total harmonic distortion, THD. The total harmonic distortion, which is a measure of closeness in shape between a waveform and its fundamental component, is defined as

$$\text{THD} = \frac{1}{V_1}\left(\sum_{n=2,3,\ldots}^{\infty} V_n^2\right)^{1/2} \tag{8-5}$$

Distortion factor, DF. The THD gives the total harmonic content, but it does not indicate the level of each harmonic component. If a filter is used at the output of inverters, the higher-order harmonics would be attenuated more effectively. Therefore, knowledge of both the frequency and magnitude of each harmonic is important. The distortion factor indicates the amount of harmonic distortion that remains in a particular waveform after the harmonics of that waveform have been subjected to a second-order attenuation (i.e., divided by n^2). Thus DF is a measure of effectiveness in reducing unwanted harmonics without having to specify the values of a second-order load filter and is defined as

$$\text{DF} = \frac{1}{V_1}\left[\sum_{n=2,3,\ldots}^{\infty}\left(\frac{V_n}{n^2}\right)^2\right]^{1/2} \tag{8-6}$$

The distortion factor of an individual (or nth) harmonic component is defined as

$$\text{DF}_n = \frac{V_n}{V_1 n^2} \tag{8-7}$$

Lowest-order harmonic, LOH. The lowest-order harmonic is that harmonic component whose frequency is closest to the fundamental one, and its amplitude is greater than or equal to 3% of the fundamental component.

Example 8-1

A single-phase half-bridge inverter in Fig. 8-1a has a resistive load of $R = 2.4\ \Omega$ and the dc input voltage is $V_s = 48$ V. Determine the (a) rms output voltage at the fundamental frequency, V_1; (b) output power, P_o; (c) average and peak currents of each transistor; (d) peak reverse blocking voltage of each transistor, V_B; (e) total harmonic distortion, THD; (f) distortion factor, DF; and (g) harmonic factor and distortion factor of the lowest-order harmonic.

Solution $V_s = 48$ V and $R = 2.4\ \Omega$.

(a) From Eq. (8-3), $V_1 = 0.45 \times 48 = 21.6$ V.

(b) From Eq. (8-1), $V_o = V_s/2 = 48/2 = 24$ V. The output power, $P_o = V_o^2/R = 24^2/2.4 = 240$ W.

(c) The peak transistor current, $I_p = 24/2.4 = 10$ A. Since each transistor conducts for a 50% duty cycle, the average current of each transistor is $I_D = 0.5 \times 10 = 5$ A.

(d) The peak reverse blocking voltage, $V_B = 2 \times 24 = 48$ V.

(e) From Eq. (8-3), $V_1 = 0.45V_s$ and

$$\left(\sum_{n=3,5,7,\ldots}^{\infty} V_n^2\right)^{1/2} = (V_0^2 - V_1^2)^{1/2} = 0.2176V_s$$

From Eq. (8-5), THD $= 0.2176V_s/(0.45V_s) = 48.34\%$.

(f) From Eq. (8-2),

$$\left[\sum_{n=3,5,\ldots}^{\infty}\left(\frac{V_n}{n^2}\right)^2\right]^{1/2} = \left[\left(\frac{V_3}{3}\right)^2 + \left(\frac{V_5}{5}\right)^2 + \left(\frac{V_7}{7}\right)^2 + \cdots\right]^{1/2} = 0.01712V_s$$

From Eq. (8-6), DF $= 0.01712V_s/(0.45V_s) = 3.804\%$.

(g) The lowest-order harmonic is the third, $V_3 = V_1/3$. From Eq. (8-4), $HF_3 = V_3/V_1 = 1/3 = 33.33\%$, and from Eq. (8-7), $DF_3 = (V_3/3^2)/V_1 = 1/27 = 3.704\%$.

8-4 SINGLE-PHASE BRIDGE INVERTERS

A single-phase bridge inverter is shown in Fig. 8-2a. It consists of four choppers. When transistors Q_1 and Q_2 are turned on simultaneously, the input voltage V_s appears across the load. If transistors Q_3 and Q_4 are turned on at the same time, the voltage across the load is reversed and is $-V_s$. The waveform for the output voltage is shown in Fig. 8-2b.

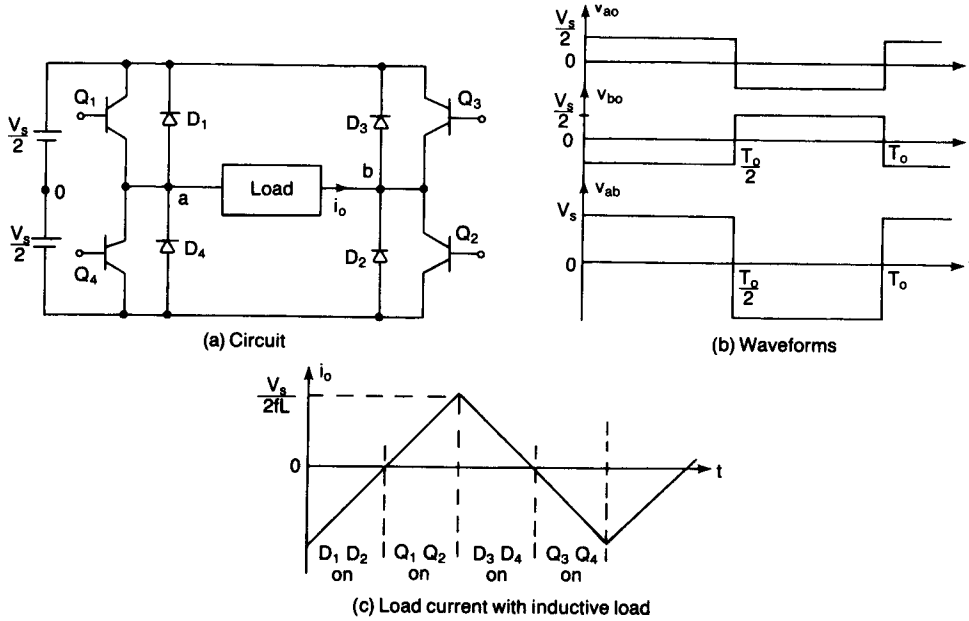


Figure 8-2 Single-phase full-bridge inverter.

The rms output voltage can be found from

$$V_o = \left(\frac{2}{T_0}\int_0^{T_0/2} V_s^2\, dt\right)^{1/2} = V_s \tag{8-8}$$

Equation (8-2) can be extended to express the instantaneous output voltage in a Fourier series as

$$v_o = \sum_{n=1,3,5\ldots}^{\infty} \frac{4V_s}{n\pi} \sin n\omega t \tag{8-9}$$

and for $n = 1$, Eq. (8-9) gives the rms value of fundamental component as

$$V_1 = \frac{4V_s}{\sqrt{2}\,\pi} = 0.90V_s \tag{8-10}$$

When diodes D_1 and D_2 conduct, the energy is fed back to the dc source and they are known as *feedback diodes*. Figure 8-1c shows the waveform of load current for inductive loads.

Example 8-2

Repeat Example 8-1 for a single-phase bridge inverter in Fig. 8-2a.

Solution $V_s = 48$ V and $R = 2.4\ \Omega$.

(a) From Eq. (8-10), $V_1 = 0.90 \times 48 = 43.2$ V.

(b) From Eq. (8-8), $V_o = V_s = 48$ V. The output power, $P_o = V_s^2/R = 48^2/2.4 = 960$ W.

(c) The peak transistor current, $I_p = 48/2.4 = 20$ A. Since each transistor conducts for a 50% duty cycle, the average current of each transistor is $I_D = 0.5 \times 20 = 10$ A.

(d) The peak reverse blocking voltage, $V_B = 48$ V.

(e) From Eq. (8-10), $V_1 = 0.9V_s$

$$\left(\sum_{n=3,5,7\ldots}^{\infty} V_n^2\right)^{1/2} = (V_0^2 - V_1^2)^{1/2} = 0.4352V_s$$

From Eq. (8-5), THD $= 0.4352V_s/(0.9V_s) = 48.34\%$.

(f) $$\left[\sum_{n=3,5,7,\ldots}^{\infty} \left(\frac{V_n}{n^2}\right)^2\right]^{1/2} = 0.03424V_s$$

From Eq. (8-6), DF $= 0.03424V_s/(0.9V_s) = 3.804\%$.

(g) The lowest-order harmonic is the third, $V_3 = V_1/3$. From Eq. (8-4), $HF_3 = V_3/V_1 = 1/3 = 33.33\%$ and from Eq. (8-7), $DF_3 = (V_3/3^2)/V_1 = 1/27 = 3.704\%$.

Note. The peak reverse blocking voltage of each transistor and the quality of output voltage for half-bridge and full-bridge inverters are the same. However, for full-bridge inverters with resistive loads, the output power is four times higher and the fundamental component is twice than that of half-bridge inverters.

Example 8-3

The bridge inverter in Fig. 8-2a has an *RLC* load with $R = 10\ \Omega$, $L = 31.5$ mH, and $C = 112\ \mu$F. The inverter frequency, $f_0 = 60$ Hz and dc input voltage, $V_s = 220$ V. (a) Express the instantaneous load current in Fourier series. Calculate the (b) rms load current at the fundamental frequency, I_1; (c) harmonic factor of load current,

HF; (d) power absorbed by the load, P_0; (e) average current of dc supply; I_s and (f) rms and peak current of each transistor. (g) Draw the waveform of fundamental load current and show the conduction intervals of transistors and diodes. Calculate the conduction time of the (h) transistors, and (i) diodes.

Solution $V_s = 220$ V, $f_0 = 60$ Hz, $R = 10\ \Omega$, $L = 31.5$ mH, $C = 112\ \mu$F, and $\omega = 2\pi \times 60 = 377$ rad/s. The inductive reactance for the nth harmonic voltage is

$$X_L = 2n\pi \times 60 \times 31.5 \times 10^{-3} = j11.87n\ \Omega$$

The capacitive reactance for the nth harmonic voltage is

$$X_c = -\frac{10^6}{2n\pi \times 60 \times 112} = \frac{-j23.68}{n}\ \Omega$$

The impedance for the nth harmonic voltage is

$$Z_n = [10^2 + (11.87n - 23.6/n)^2]^{1/2}$$

and the power factor angle for the nth harmonic voltage is

$$\theta_n = \tan^{-1}\frac{11.87n - 23.6/n}{10} = \tan^{-1}\left(1.187n - \frac{2.346}{n}\right)$$

(a) From Eq. (8-9), the instantaneous output voltage can be expressed as

$$v_o(t) = 280.1 \sin(377t) + 93.4 \sin(3 \times 377t) + 56.02 \sin(5 \times 377t)$$
$$+ 40.02 \sin(7 \times 377t) + 31.12 \sin(9 \times 377t) + \cdots$$

Dividing the output voltage by the load impedance and considering the appropriate delay due to the power factor angles, we can obtain the instantaneous load current as

$$i_o(t) = 18.1 \sin(377t + 49.72°) + 3.17 \sin(3 \times 377t - 70.17°)$$
$$+ \sin(5 \times 377t - 79.63°) + 0.5 \sin(7 \times 377t - 82.85°)$$
$$+ 0.3 \sin(9 \times 377t - 84.52°) + \cdots$$

(b) The rms load current at fundamental frequency, $I_1 = 18.1/\sqrt{2} = 12.8$ A.

(c) Considering up to the ninth harmonic, the peak load current,

$$I_m = (18.1^2 + 3.17^2 + 1.0^2 + 0.5^2 + 0.3^2)^{1/2} = 18.41\ \text{A}$$

The harmonic factor of load current,

$$\text{HF} = \frac{(I_m^2 - I_{m1}^2)^{1/2}}{I_{m1}} = \left[\left(\frac{18.41}{18.1}\right)^2 - 1\right]^{1/2} = 18.59\%$$

(d) The rms load current, $I_o = 18.41/\sqrt{2} = 13.02$ A, and the load power, $P_o = 13.02^2 \times 10 = 1695$ W.

(e) The average supply current, $I_s = 1695/220 = 7.7$ A.

(f) The peak transistor current, $I_p = 18.41$ A. The rms current of each transistor, $I_R = I_o/\sqrt{2} = I_p/2 = 18.41/2 = 9.2$ A.

(g) The waveform for fundamental load current, $i_1(t)$, is shown in Fig. 8.3.

(h) From Fig. 8-3a, the conduction time of each transistor is found from $t_0 = 180 - 49.72 = 130.28°$ or $t_0 = 130.28 \times \pi/(180 \times 377) = 6031\ \mu$s.

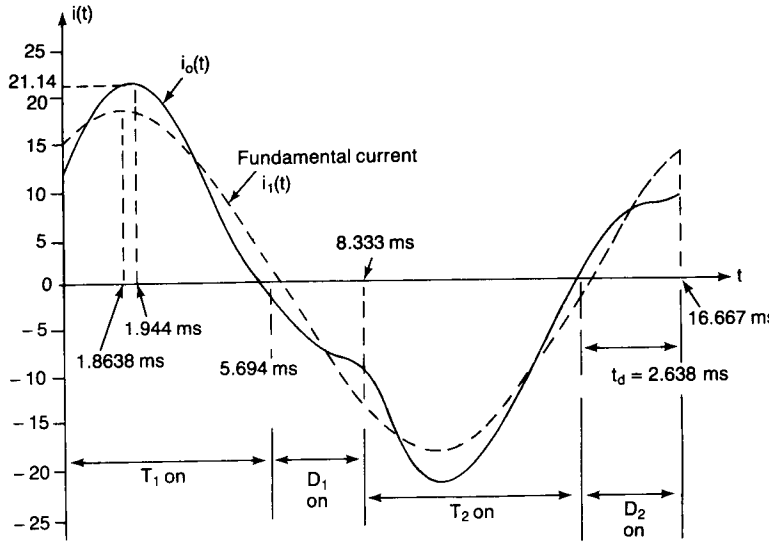


Figure 8-3 Waveforms for Example 8-3.

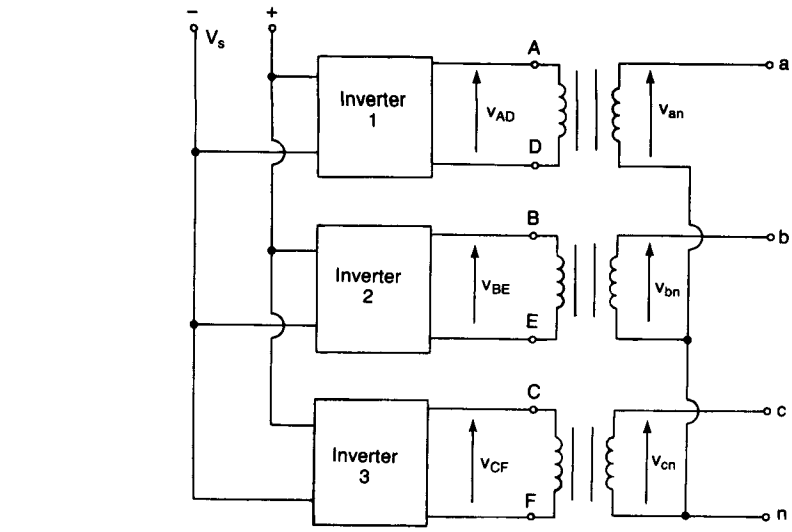
(i) The conduction time of each diode,

$$t_d = (180 - 130.28) \times \frac{\pi}{180 \times 377} = 2302 \ \mu s$$

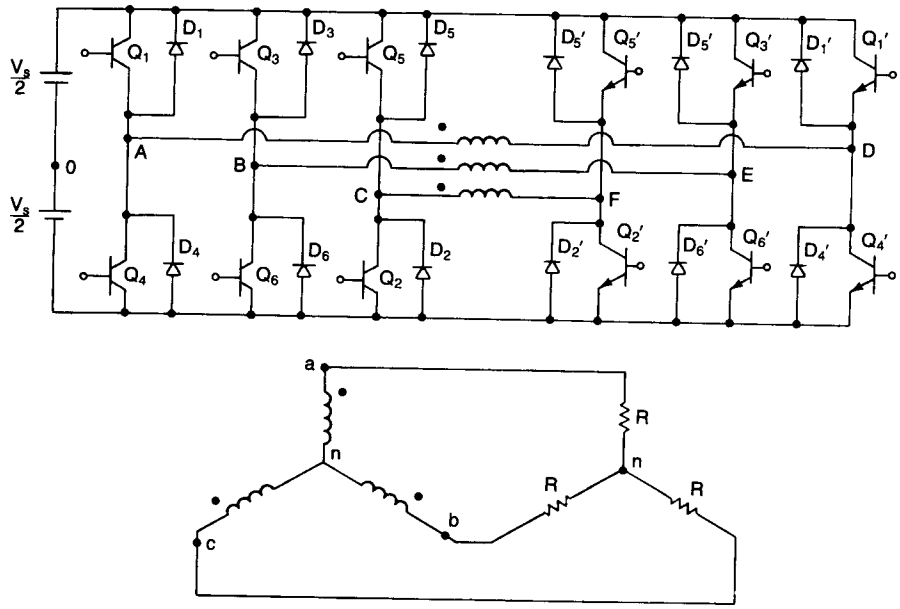
Note. To calculate the exact values of the peak current, the conduction time of transistors and diodes, the instantaneous load current $i_o(t)$ should be plotted as shown in Fig. 8-3. The conduction time of a transistor must satisfy the condition $i_o(t = t_0) = 0$, and a plot of $i_o(t)$ by a computer program gives $I_p = 21.14$ A, $t_0 = 5694$ μs, and $t_d = 2638$ μs.

8-5 THREE-PHASE INVERTERS

Three-phase inverters are normally used for high-power applications. Three single-phase half (or full)-bridge inverters can be connected in parallel as shown in Fig. 8-4a to form the configuration of a three-phase inverter. The gating signals of single-phase inverters should be advanced or delayed by 120° with respect to each other in order to obtain three-phase balanced (fundamental) voltages. The transformer primary windings must be isolated from each other, while the secondary windings may be connected in wye or delta. The transformer secondary is normally connected in wye to eliminate triplen harmonics ($n = 3, 6, 9, \ldots$) appearing on the output voltages and the circuit arrangement is shown in Fig. 8-4b. This arrangement requires three single-phase transformers, 12 transistors (or thyristors), and 12 diodes. If the output voltages of single-phase inverters are not perfectly balanced in magnitudes and phases, the three-phase output voltages will be unbalanced.



(a) Schematic



(b) Circuit diagram

Figure 8-4 Three-phase inverter formed by three single-phase inverters.

A three-phase output can be obtained from a configuration of six transistors and six diodes as shown in Fig. 8-5a. When transistor Q_1 is switched on, terminal a is connected to the positive terminal of the dc input voltage. When transistor Q_4 is switched on, terminal a is brought to the negative terminal of the dc source. There are six modes of operation in a cycle and the duration of each mode is 60°.

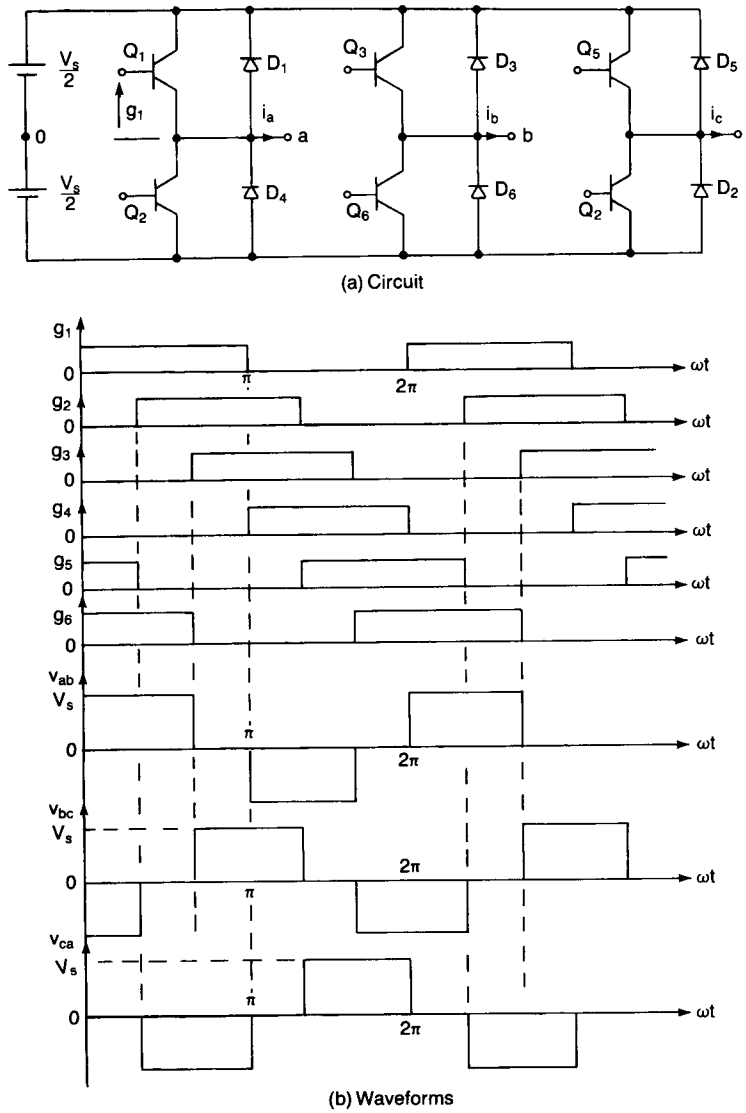


Figure 8-5 Three-phase bridge inverter.

The transistors are numbered in the sequence of gating the transistors (e.g., 123, 234, 345, 456, 561, 612) and each transistor conducts for 180°. The gating signals shown in Fig. 8-5b are shifted from each other by 60° to obtain three-phase balanced (fundamental) voltages.

The load may be connected in wye or delta as shown in Fig. 8-6. For a delta-connected load, the phase currents can be obtained directly from the line-to-line voltages. Once the phase currents are known, the line currents can be determined. For a wye-connected load, the line-to-neutral voltages must be determined to find

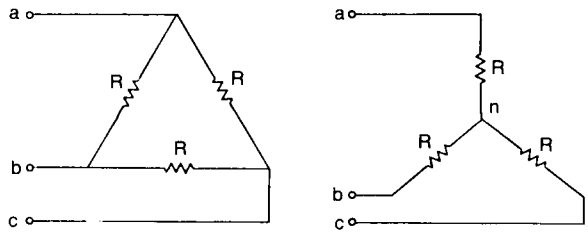


Figure 8-6 Delta/wye-connected load.

the line (or phase) currents. There are three modes of operation in a half-cycle and the equivalent circuits are shown in Fig. 8-7a.

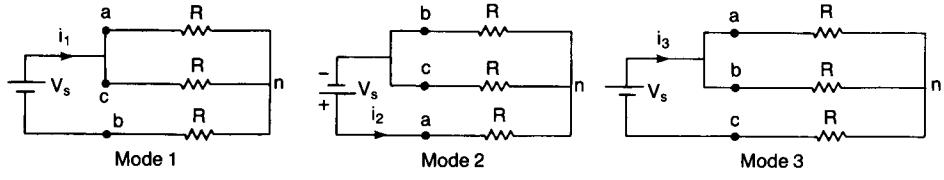
During mode 1 for $0 \leq \omega t < \pi/3$,

$$R_{eq} = R + \frac{R}{2} = \frac{3R}{2}$$

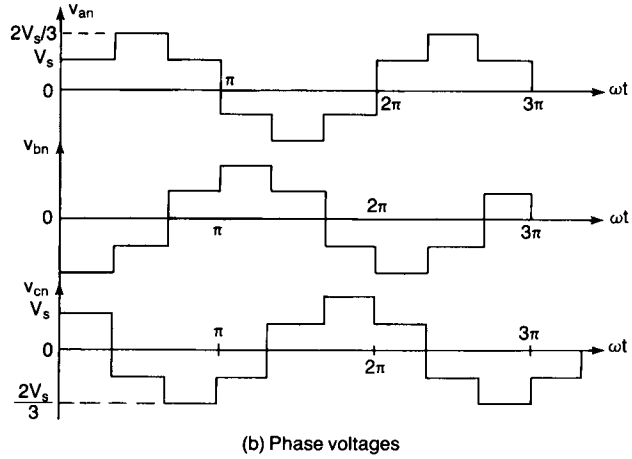
$$i_1 = \frac{V_s}{R_{eq}} = \frac{2V_s}{3R}$$

$$v_{an} = v_{cn} = \frac{i_1 R}{2} = \frac{V_s}{3}$$

$$v_{bn} = -i_1 R = \frac{-2V_s}{3}$$



(a) Equivalent circuits



(b) Phase voltages

Figure 8-7 Equivalent circuits for wye-connected resistive load.

During mode 2 for $\pi/3 \leq \omega t < 2\pi/3$,

$$R_{eq} = R + \frac{R}{2} = \frac{3R}{2}$$

$$i_2 = \frac{V_s}{R_{eq}} = \frac{2V_s}{3R}$$

$$v_{an} = i_2 R = \frac{2V_s}{3}$$

$$v_{bn} = v_{cn} = \frac{-i_2 R}{2} = \frac{-V_s}{3}$$

During mode 3 for $2\pi/3 \leq \omega t < \pi$,

$$R_{eq} = R + \frac{R}{2} = \frac{3R}{2}$$

$$i_3 = \frac{V_s}{R_{eq}} = \frac{2V_s}{3R}$$

$$v_{an} = v_{bn} = \frac{i_3 R}{2} = \frac{V_s}{3}$$

$$v_{cn} = -i_3 R = \frac{-2V_s}{3}$$

The line-to-neutral voltages are shown in Fig. 8-7b. The instantaneous line-to-line voltage, v_{ab}, in Fig. 8-5b can be expressed in a Fourier series, recognizing that v_{ab} is shifted by $\pi/6$ and the even harmonics are zero,

$$v_{ab} = \sum_{n=1,3,5,\ldots}^{\infty} \frac{4V_s}{n\pi} \cos\frac{n\pi}{6} \sin n\left(\omega t + \frac{\pi}{6}\right) \tag{8-11}$$

v_{bc} and v_{ca} can be found from Eq. (8-11) by phase shifting v_{ab} by 120° and 240°, respectively,

$$v_{bc} = \sum_{n=1,3,5,\ldots}^{\infty} \frac{4V_s}{n\pi} \cos\frac{n\pi}{6} \sin n\left(\omega t - \frac{\pi}{2}\right) \tag{8-12}$$

$$v_{ca} = \sum_{n=1,3,5,\ldots}^{\infty} \frac{4V_s}{n\pi} \cos\frac{n\pi}{6} \sin n\left(\omega t - \frac{7\pi}{6}\right) \tag{8-13}$$

We can notice from Eqs. (8-11), (8-12), and (8-13) that the triplen harmonics ($n = 3, 9, 15, \ldots$) would be zero in the line-to-line voltages.

The line-to-line rms voltage can be found from

$$V_L = \left[\frac{2}{2\pi}\int_0^{2\pi/3} V_s^2 \, d(\omega t)\right]^{1/2} = \sqrt{\frac{2}{3}}\, V_s = 0.8165 V_s \tag{8-14}$$

For $n = 1$, the rms value of fundamental component can be found from the peak magnitude in Eq. (8-11):

$$V_{L1} = \frac{4V_s \cos 30°}{\sqrt{2}\,\pi} = 0.7797V_s \tag{8-15}$$

The rms value of line-to-neutral voltages can be found from the phase voltage,

$$V_p = \frac{V_L}{\sqrt{3}} = \frac{\sqrt{2}\,V_s}{3} = 0.4714V_s \tag{8-16}$$

With resistive loads, the diodes across the transistors have no functions. If the load is inductive, the current in each arm of the inverter would be delayed to its voltage as shown in Fig. 8-8. When transistor Q_4 in Fig. 8-5a is off, the only path for the negative line current i_a is through D_1. Hence the load terminal a is connected to the dc source through D_1 until the load current reverses its polarity at $t = t_1$. During the period for $0 \le t \le t_1$, transistor Q_1 will not conduct. Similarly, transistor Q_4 will only start to conduct at $t = t_2$. The transistors (or thyristors) must be continuously gated, since the conduction time of transistors and diodes depends on the load power factor.

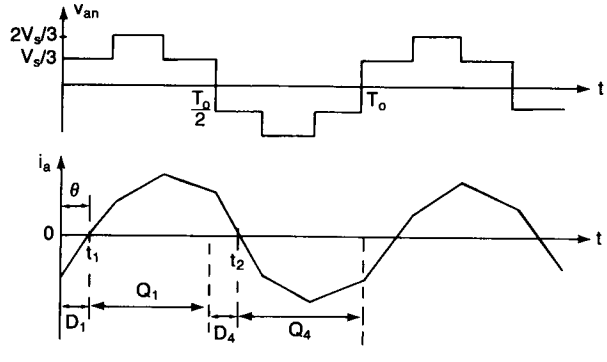


Figure 8-8 Three-phase inverter with *RL* load.

Example 8-4

The three-phase inverter in Fig. 8-5a has a wye-connected resistive load of $R = 10\ \Omega$. The inverter frequency is $f_0 = 60$ Hz and the dc input voltage is $V_s = 220$ V. (a) Express the instantaneous line-to-line voltage, $v_{ab}(t)$, and line current, $i_a(t)$, in a Fourier series. Determine the (b) rms line voltage, V_L; (c) rms phase voltage, V_p; (d) rms line voltage at the fundamental frequency, V_{L1}; (e) rms phase voltage at the fundamental frequency, V_{p1}; (f) total harmonic distortion, THD; (g) distortion factor, DF; (h) harmonic factor and distortion factor of the lowest-order harmonic; (i) load power, P_o; (j) average transistor current, I_D; and (k) rms transistor current, I_R.

Solution $V_s = 220$ V, $R = 10\ \Omega$, $f_0 = 60$ Hz, and $\omega = 2\pi \times 60 = 377$ rad/s.

(a) The instantaneous line-to-line voltage $v_{ab}(t)$ can be written as

$$v_{ab}(t) = 242.58 \sin (377t + 30°) - 48.52 \sin 5(377t + 30°)$$
$$- 34.66 \sin 7(377t + 30°) + 22.05 \sin 11(377t + 30°)$$
$$+ 18.66 \sin 13(377t + 30°) - 14.27 \sin 17(377t + 30°) + \cdots$$

The phase voltage is $v_{an}(t) = V_{ab}(t)/\sqrt{3}$ with a delay of 30°, and dividing the phase voltage by the load resistance ($R = 10\ \Omega$) gives the instantaneous (or phase) current as

$$i_a(t) = 14 \sin (377t) - 2.801 \sin 5(377t) - 2.0 \sin 7(377t) + 1.273 \sin 11(377t) + 1.077 \sin 13(377t) - 0.824 \sin 17(377t) + \cdots$$

(b) From Eq. (8-14), $V_L = 0.8165 \times 220 = 179.63$ V.
(c) From Eq. (8-16), $V_p = 0.4714 \times 220 = 103.7$ V.
(d) From Eq. (8-15), $V_{L1} = 0.7797 \times 220 = 171.53$ V.
(e) $V_{p1} = V_{L1}/\sqrt{3} = 99.03$ V.
(f) From Eq. (8-14), $V_{L1} = 0.7797V_s$

$$\left(\sum_{n=5,7,11,\ldots}^{\infty} V_n^2\right)^{1/2} = (V_L^2 - V_1^2)^{1/2} = 0.24236V_s$$

From Eq. (8-5), THD $= 0.24236V_s/(0.7797V_s) = 31.08\%$.

(g) $$\left[\sum_{n=5,7,11,\ldots}^{\infty} \left(\frac{V_n}{n^2}\right)^2\right]^{1/2} = 0.00668V_s$$

From Eq. (8-6), DF $= 0.00668V_s/(0.7797V_s) = 0.857\%$.

(h) The lowest-order harmonic is the fifth, $V_{L5} = V_{L1}/5$. From Eq. (8-4), $HF_5 = V_{L5}/V_{L1} = 1/5 = 20\%$, and from Eq. (8-7), $DF_5 = (V_{L5}/5^2)/V_{L1} = 1/125 = 0.8\%$.

(i) For wye-connected loads, the line current is the same as the phase current and the rms line current, $I_L = V_p/10 = 103.7/10 = 10.37$ A. The load power,

$$P_o = 3V_pI_p = 3 \times 103.9 \times 10.37 = 3226.4 \text{ W}$$

(j) The average supply current, $I_s = P_o/220 = 3226.4/220 = 14.67$ A and the average transistor current, $I_D = 14.67/3 = 4.89$ A.

(k) Since the line current is shared by two transistors, the rms value of a transistor current is $I_R = I_L/\sqrt{2} = 10.37/\sqrt{2} = 7.33$ A.

8-6 VOLTAGE CONTROL OF SINGLE-PHASE INVERTERS

In many industrial applications, it is often required to control the output voltage of inverters (1) to cope with the variations of dc input voltage, (2) for voltage regulation of inverters, and (3) for the constant volts/frequency control requirement. There are various techniques to vary the inverter gain. The most efficient method of controlling the gain (and output voltage) is to incorporate pulse-width-modulation (PWM) control within the inverters. The commonly used techniques are:

1. Single-pulse-width modulation
2. Multiple-pulse-width modulation
3. Sinusoidal pulse-width modulation
4. Modified sinusoidal pulse-width modulation
5. Phase-displacement control

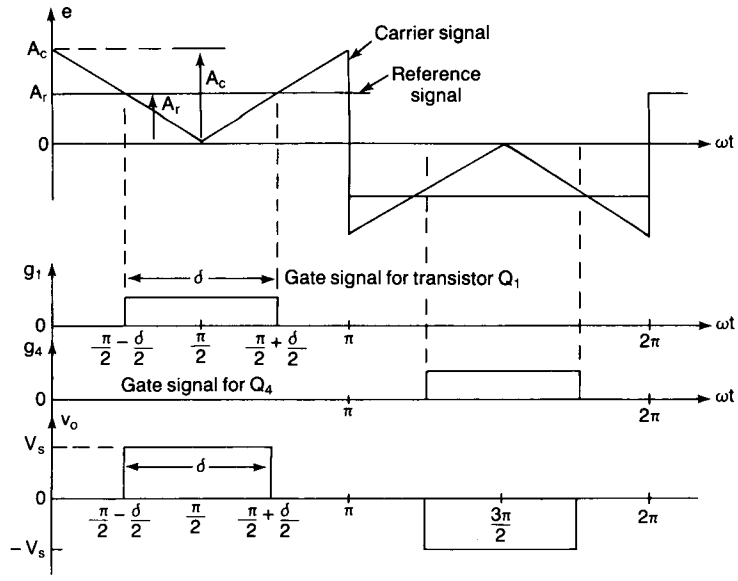


Figure 8-9 Single-pulse-width modulation.

8-6.1 Single-Pulse-Width Modulation

In single-pulse-width modulation control, there is only one pulse per half-cycle and the width of the pulse is varied to control the inverter output voltage. Figure 8-9 shows the generation of gating signals and output voltage of single-phase full-bridge inverters. The gating signals are generated by comparing a rectangular reference signal of amplitude, A_r, with a triangular carrier wave of amplitude, A_c. The frequency of the carrier wave determines the fundamental frequency of output voltage. By varying A_r from 0 to A_c, the pulse width, δ, can be varied from 0 to 180°. The ratio of A_r to A_c is the control variable and defined as the *modulation index*. The modulation index,

$$M = \frac{A_r}{A_c} \tag{8-17}$$

The rms output voltage can be found from

$$V_o = \left[\frac{2}{2\pi}\int_{(\pi-\delta)/2}^{(\pi+\delta)/2} V_s^2\, d(\omega t)\right]^{1/2} = V_s\sqrt{\frac{\delta}{\pi}} \tag{8-18}$$

The Fourier series of output voltage yields

$$v_o(t) = \sum_{n=1,3,5,\ldots}^{\infty} \frac{4V_s}{n\pi} \sin\frac{n\delta}{2} \sin n\omega t \tag{8-19}$$

A computer program named PROG-5 is developed to evaluate the performance of single-pulse modulation for single-phase full-bridge inverters and the pro-

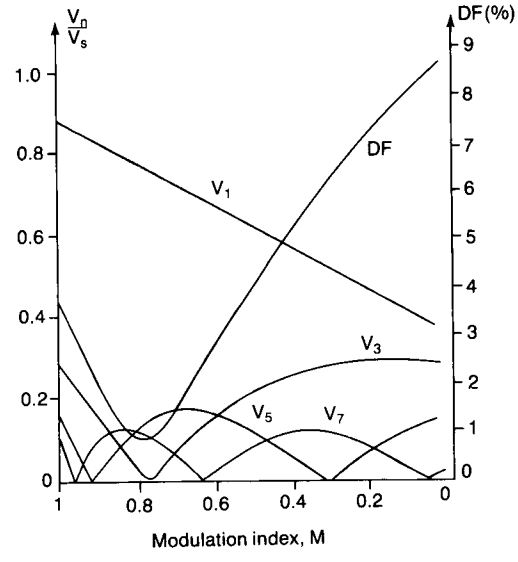


Figure 8-10 Harmonic profile of single-pulse-width modulation.

gram is listed in Appendix F. Figure 8-10 shows the harmonic profile with the variation of modulation index, M. The dominant harmonic is the third, and the distortion factor increases significantly at a low output voltage.

8-6.2 Multiple-Pulse-Width Modulation

The harmonic content can be reduced by using several pulses in each half-cycle of output voltage. The generation of gating signals for turning on and off of transistors is shown in Fig. 8-11a by comparing a reference signal with a triangular carrier wave. The frequency of reference signal sets the output frequency, f_o, and the carrier frequency, f_c, determines the number of pulses per half-cycle, p. The modulation index controls the output voltage. This type of modulation is also known as *uniform pulse-width modulation* (UPWM). The number of pulses per half-cycle is found from

$$N = \frac{f_c}{2f_o} \tag{8-20}$$

The variation of modulation index M from 0 to 1 varies the pulse width from 0 to π/p and the output voltage from 0 to V_s. The output voltage for single-phase bridge inverters is shown in Fig. 8-11b.

If δ is the width of each pulse, the rms output voltage can be found from

$$V_o = \left[\frac{2p}{2\pi}\int_{(\pi/p-\delta)/2}^{(\pi/p+\delta)/2} V_s^2\, d(\omega t)\right]^{1/2} = V_s\sqrt{\frac{p\delta}{\pi}} \tag{8-21}$$

The general form of a Fourier series for the instantaneous output voltage is

$$v_o(t) = \sum_{n=1,3,5,\ldots}^{\infty} (A_n \cos n\omega t + B_n \sin n\omega t) \tag{8-22}$$

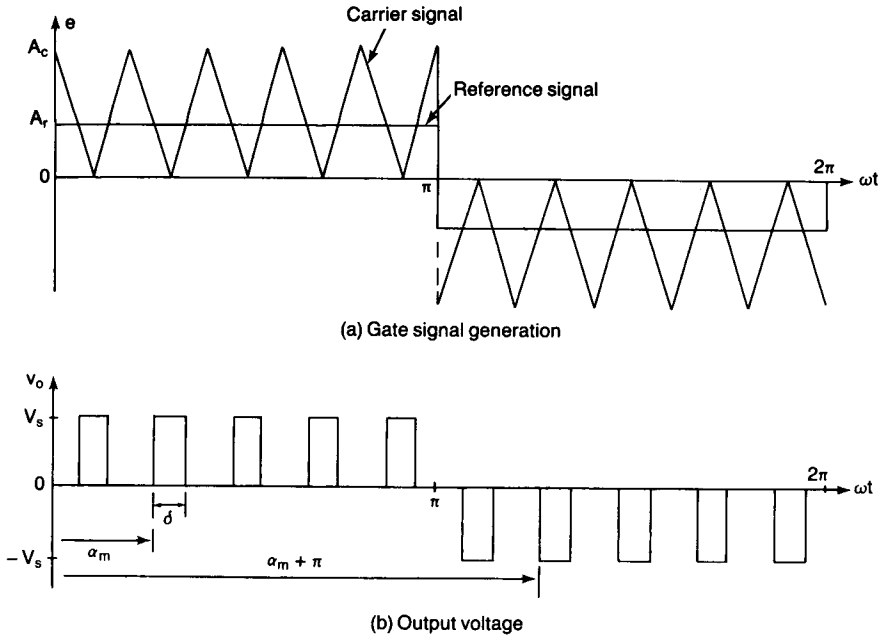


Figure 8-11 Multiple-pulse-width modulation.

The coefficients A_n and B_n in Eq. (8-22) can be determined by considering a pair of pulses such that the positive pulse of duration δ starts at $\omega t = \alpha$ and the negative one of the same width starts at $\omega t = \pi + \alpha$. This is shown in Fig. 8-11b. The effects of all pulses can be combined together to obtain the effective output voltage.

If the positive pulse of mth pair starts at $\omega t = \alpha_m$ and ends at $\omega t = \alpha_m + \pi$, the Fourier coefficients for a pair of pulses are

$$a_n = \frac{2V_s}{\pi}\int_{\alpha_m}^{\alpha_m+\delta} \cos n\omega t\, d(\omega t) = \frac{2V_s}{n\pi}[\sin n(\alpha_m + \delta) - \sin n\alpha_m]$$

$$= \frac{4V_s}{n\pi}\sin\frac{n\delta}{2}\cos n\left(\alpha_m + \frac{\delta}{2}\right) \tag{8-23}$$

$$b_n = \frac{2V_s}{\pi}\int_{\alpha_m}^{\alpha_m+\delta} \sin n\omega t\, d(\omega t) = \frac{2V_s}{n\pi}[\cos n\alpha_m - \cos n(\alpha_m + \delta)]$$

$$= \frac{4V_s}{n\pi}\sin\frac{n\delta}{2}\sin n\left(\alpha_m + \frac{\delta}{2}\right) \tag{8-24}$$

The coefficients of Eq. (8-22) can be found by adding the effects of all pulses,

$$A_n = \sum_{m=1}^{p}\frac{4V_s}{n\pi}\sin\frac{n\delta}{2}\cos n\left(\alpha_m + \frac{\delta}{2}\right) \tag{8-25}$$

$$B_n = \sum_{m=1}^{p}\frac{4V_s}{n\pi}\sin\frac{n\delta}{2}\sin n\left(\alpha_m + \frac{\delta}{2}\right) \tag{8-26}$$

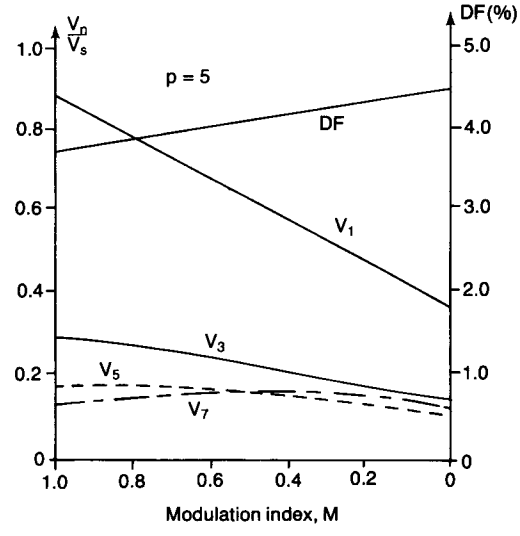


Figure 8-12 Harmonic profile of multiple-pulse-width modulation.

A computer program named PROG-5 is used to evaluate the performance of multiple pulse modulation, and the program is listed in Appendix F. Figure 8-12 shows the harmonic profile against the variation of modulation index for five pulses per half-cycle. The order of harmonics is the same as that of single-pulse modulation. The distortion factor is reduced significantly compared to that of single-pulse modulation. However, due to the larger number of switching on and off processes of power transistors (or thyristors), the switching losses would increase. With larger values of p, the amplitudes of lower-order harmonics would be lower, but the amplitudes of some higher-order harmonics would increase. However, such higher-order harmonics produce negligible ripple or can easily be filtered out.

8-6.3 Sinusoidal Pulse-Width Modulation

Instead of maintaining the width of all pulses the same as in the case of multiple-pulse modulation, the width of each pulse is varied in proportion to the amplitude of a sine wave evaluated at the center of the same pulse. The distortion factor and lower-order harmonics are reduced significantly. The gating signals as shown in Fig. 8-13a are generated by comparing a sinusoidal reference signal with a triangular carrier wave of frequency, f_c. This type of modulation is commonly used in industrial applications and abbreviated as SPWM. The frequency of reference signal, f_r, determines the inverter output frequency, f_o, and its peak amplitude, A_r, controls the modulation index, M, and rms output voltage, V_o. The number of pulses per half-cycle depends on the carrier frequency. Within the constraint that two transistors of the same arm (Q_1 and Q_4) cannot conduct at the same time, the instantaneous output voltage is shown in Fig. 8-13a. The same gating signals can be generated by using unidirectional triangular carrier wave as shown in Fig. 8-13b.

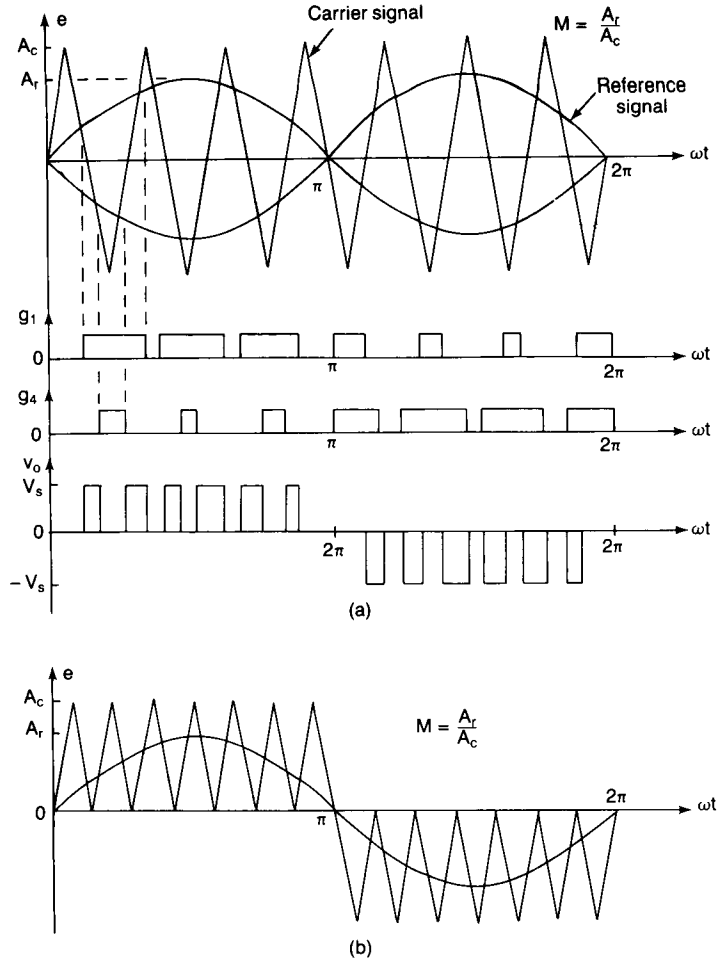


Figure 8-13 Sinusoidal pulse-width modulation.

The rms output voltage can be varied from 0 to V_s by varying the modulation index M from 0 to 1. It can be observed that the area of each pulse corresponds approximately to the area under the sine wave between the adjacent midpoints of off periods on the gating signals. If δ_m is the width of mth pulse, Eq. (8-21) can be extended to find the rms output voltage

$$V_o = V_s \left(\sum_{m=1}^{p} \frac{\delta_m}{\pi} \right)^{1/2} \tag{8-27}$$

Equations (8-25) and (8-26) can also be applied to determine the Fourier coefficients of output voltage as

$$A_n = \sum_{m=1}^{p} \frac{2V_s}{n\pi} [\sin n(\alpha_m + \delta_m) - \sin n\alpha_m] \tag{8-28}$$

$$B_n = \sum_{m=1}^{p} \frac{2V_s}{n\pi} [\cos n\alpha_m - \cos n(\alpha_m + \delta_m)] \tag{8-29}$$

A computer program named PROG-6 is developed to determine the width of pulses and to evaluate the harmonic profile of sinusoidal modulation. The harmonic profile is shown in Fig. 8-14 for five pulses per half-cycle. The distortion factor is significantly reduced compared to that of multiple-pulse modulation. This type of modulation eliminates all harmonics less than or equal to $2p - 1$. For $p = 5$, the lowest-order harmonic is ninth.

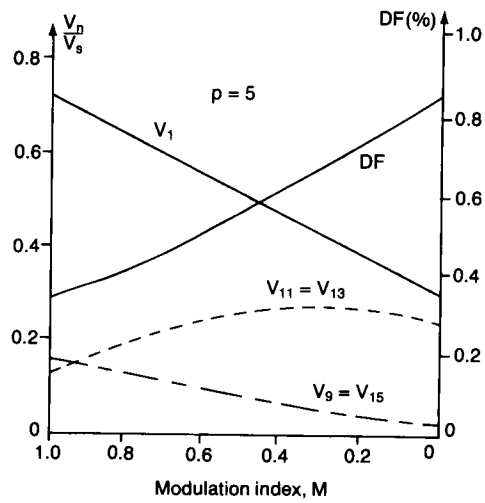


Figure 8-14 Harmonic profile of sinusoidal pulse-width-modulation.

8-6.4 Modified Sinusoidal Pulse-Width Modulation

Figure 8-13 indicates that the widths of pulses that are nearer the peak of the sine wave do not change significantly with the variation of modulation index. This is due to the characteristics of a sine wave, and the SPWM technique can be modified so that the carrier wave is applied during the first and last 60° intervals per half-cycle (e.g., 0 to 60° and 120° to 180°). This type of modulation is known as MSPWM and shown in Fig. 8-15. The fundamental component is increased and its harmonic characteristics are improved. It reduces the number of switching of power devices and also reduces switching losses.

A computer program named PROG-7, which is listed in Appendix F, determines the pulse widths and evaluates the performance of modified SPWM. The number of pulses, q, in the 60° period is normally related to the frequency ratio, particularly in three-phase inverters, by

$$\frac{f_c}{f_o} = 6q + 3 \tag{8-30}$$

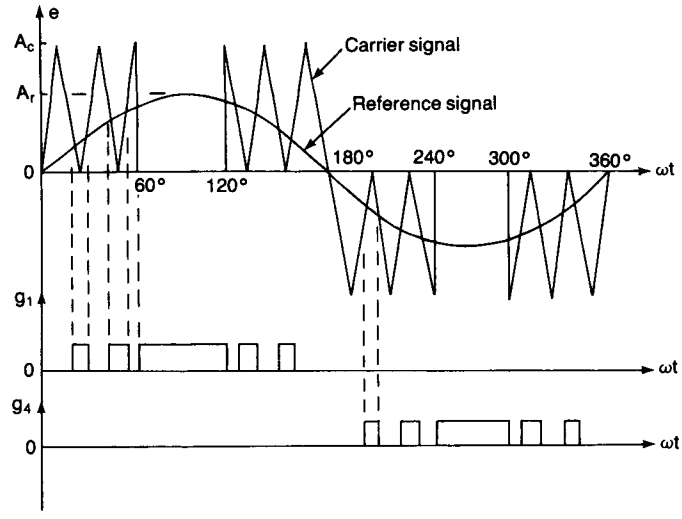


Figure 8-15 Modified sinusoidal pulse-width modulation.

8-6.5 Phase-Displacement Control

Voltage control can be obtained by using multiple inverters and summing the output voltages of individual inverters. A single-phase full-bridge inverter in Fig. 8-2a can be perceived as the sum of two half-bridge inverters in Fig. 8-1a. A 180° phase displacement produces an output voltage as shown in Fig. 8-16c, whereas a delay (or displacement) angle of β produces an output as shown in Fig. 8-16e.

The rms output voltage,

$$V_o = V_s \sqrt{\frac{\beta}{\pi}} \tag{8-31}$$

If

$$v_{ao} = \sum_{n=1,3,5,\ldots}^{\infty} \frac{2V_s}{n\pi} \sin n\omega t$$

then

$$v_{bo} = \sum_{n=1,3,5,\ldots}^{\infty} \frac{2V_s}{n\pi} \sin n(\omega t - \beta)$$

The instantaneous output voltage,

$$v_{ab} = v_{ao} - v_{ob} = \sum_{n=1,3,5,\ldots}^{\infty} \frac{2V_s}{n\pi} [\sin n\omega t - \sin n(\omega t - \beta)] \tag{8-32}$$

since $\sin A - \sin B = 2 \sin [(A + B)/2] \cos [(A - B)/2]$, Eq. (8-32) can be

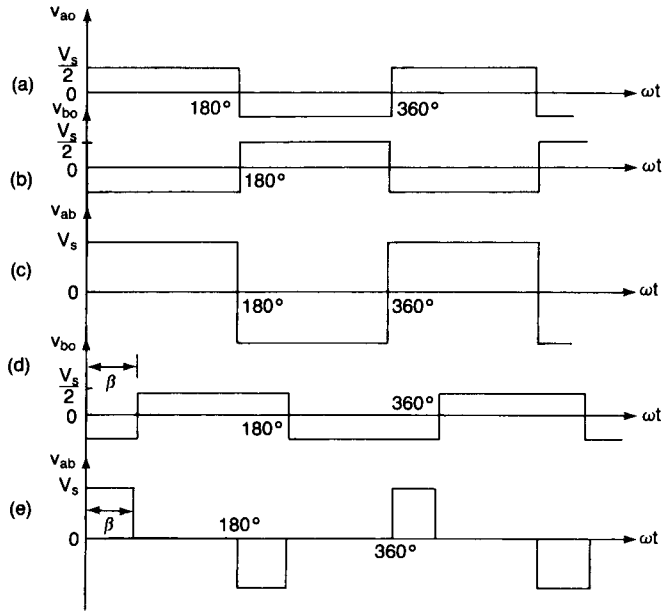


Figure 8-16 Phase-displacement control.

simplified to

$$v_{ab} = \sum_{n=1,3,5,\ldots}^{\infty} \frac{4V_s}{n\pi} \sin\frac{n\beta}{2} \cos n\left(\omega t - \frac{\beta}{2}\right) \tag{8-33}$$

The rms value of the fundamental output voltage is

$$V_1 = \frac{4V_s}{\sqrt{2}\,\pi} \sin\frac{\beta}{2} \tag{8-34}$$

Equation (8-34) indicates that the output voltage can be varied by varying the delay angle. This type of control is especially useful for high-power applications, requiring a large number of transistors (or thyristors) in parallel.

8-7 VOLTAGE CONTROL OF THREE-PHASE INVERTERS

A three-phase inverter may be considered as three single-phase inverters and the output of each single-phase inverter is shifted by 120°. The voltage control techniques discussed in Section 8-6 are applicable to three-phase inverters. As an example, the generations of gating signals with sinusoidal pulse-width modulation are shown in Fig. 8-17. There are three sinusoidal reference waves each shifted by 120°. The carrier wave is compared with the reference signal corresponding to a phase to generate the gating signals for that phase. The output voltage is also shown in Fig. 8-17.

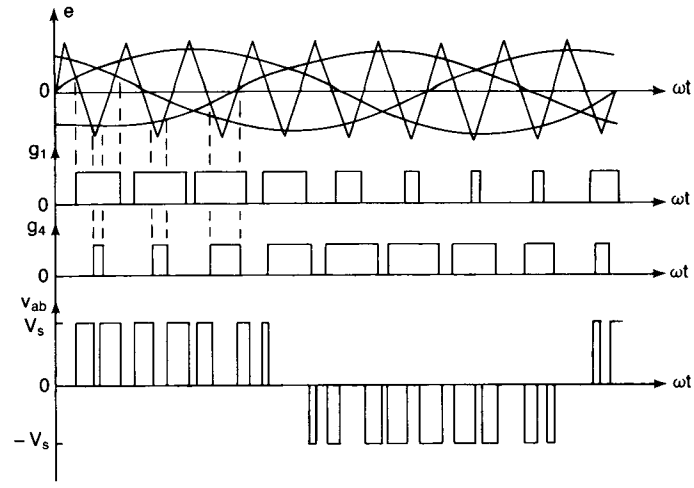


Figure 8-17 Sinusoidal pulse width modulation for three-phase inverter.

Example 8-5

A single-phase full-bridge inverter controls the power in a resistive load. The nominal value of input dc voltage is V_s = 220 V and a uniform pulse-width modulation with five pulses per half-cycle is used. For the required control, the width of each pulse is 30°. (a) Determine the rms voltage of the load. (b) If the dc supply increases by 10%, determine the pulse width to maintain the same load power. (c) If the maximum possible pulse width is 35°, determine the minimum allowable limit of the dc input source.

Solution (a) V_s = 220 V, p = 5, and δ = 30°. From Eq. (8-21), V_o = 220 $\sqrt{5 \times 30/180}$ = 200.8 V.

(b) V_s = 1.1 × 220 = 242 V. Using Eq. (8-21), 242 $\sqrt{5\delta/180}$ = 200.8 and this gives the required value of pulse width, δ = 24.75°.

(c) To maintain the output voltage of 200.8 at the maximum possible pulse width of δ = 35°, the input voltage can be found from 200.8 = $V_s \sqrt{5 \times 35/180}$, and this yields the minimum allowable input voltage, V_s = 203.64 V.

8-8 HARMONIC REDUCTIONS

Equation (8-33) indicates that the nth harmonic can be eliminated by a proper choice of displacement angle, β, if

$$\sin \frac{n\beta}{2} = 0$$

or

$$\beta = \frac{360°}{n} \tag{8-35}$$

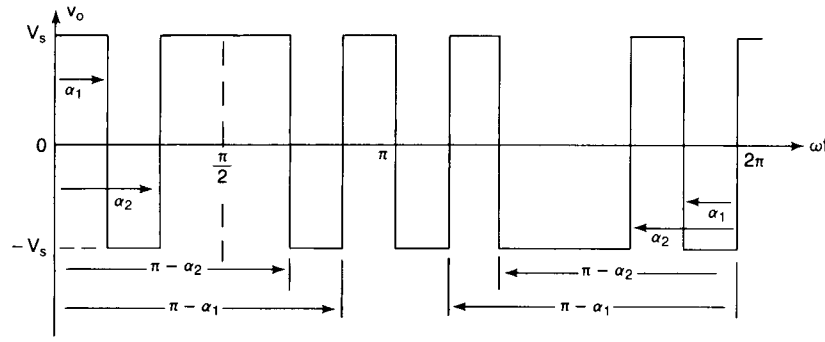


Figure 8-18 Output voltage with two notches per half-wave.

and the third harmonic will be eliminated if $\beta = 360/3 = 120°$. A pair of unwanted harmonics at the output of single-phase inverters can be eliminated by introducing a pair of symmetrically placed voltage *notches* as shown in Fig. 8-18.

The Fourier series of output voltage can be expressed as

$$v_o = \sum_{n=1,3,5,\ldots}^{\infty} A_n \sin n\omega t \tag{8-36}$$

where

$$A_n = \frac{4V_s}{\pi}\left[\int_0^{\alpha_1} \sin n\omega t\, d(\omega t) - \int_{\alpha_1}^{\alpha_2} \sin n\omega t\, d(\omega t) + \int_{\alpha_2}^{\pi/2} \sin n\omega t\, d(\omega t)\right]$$

$$= \frac{4V_s}{\pi}\,\frac{1 - 2\cos n\alpha_1 + 2\cos n\alpha_2}{n} \tag{8-37}$$

The third and fifth harmonics would be eliminated if $A_3 = A_5 = 0$ and Eq. (8-37) gives the necessary equations to be solved.

$$1 - 2\cos 3\alpha_1 + 2\cos 3\alpha_2 = 0 \qquad \text{or} \qquad \alpha_2 = \tfrac{1}{3}\cos^{-1}(\cos 3\alpha_1 - 0.5) \tag{8-38}$$

$$1 - 2\cos 5\alpha_1 + 2\cos 5\alpha_2 = 0 \qquad \text{or} \qquad \alpha_1 = \tfrac{1}{5}\cos^{-1}(\cos 5\alpha_2 + 0.5) \tag{8-39}$$

Equations (8-38) and (8-39) can be solved iteratively by initially assuming that $\alpha_1 = 0$ and repeating the calculations for α_1 and α_2. The result is $\alpha_1 = 23.62°$ and $\alpha_2 = 33.3°$.

The modified sinusoidal pulse-width-modulation techniques can be applied to generate the notches which would eliminate certain harmonics effectively in the output voltage, as shown in Fig. 8-19. Equation (8-37) can be extended to m notches per quarter-wave:

$$A_n = \frac{4V_s}{n\pi}(1 - 2\cos n\alpha_1 + 2\cos n\alpha_2 - 2\cos n\alpha_3 + 2\cos n\alpha_4 - \cdots) \tag{8-40}$$

The output voltages of two or more inverters may be connected in series through a transformer to reduce or eliminate certain unwanted harmonics. The arrangement for combining two inverter output voltages is shown in Fig. 8-20a.

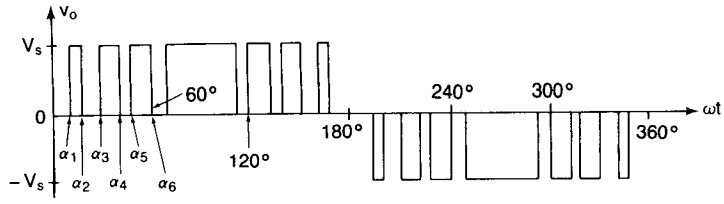


Figure 8-19 Output voltage for modified sinusoidal pulse-width modulation.

The waveforms for the output of each inverter and the resultant output voltage are shown in Fig. 8-20b. The second inverter is phase shifted by $\pi/3$.

From Eq. (8-9), the output of first inverter can be expressed as

$$v_{o1} = A_1 \sin \omega t + A_3 \sin 3\omega t + A_5 \sin 5\omega t + \cdots$$

Since the output of second inverter, v_{o2}, is delayed by $\pi/3$,

$$v_{o2} = A_1 \sin\left(\omega t - \frac{\pi}{3}\right) + A_3 \sin 3\left(\omega t - \frac{\pi}{3}\right) + A_5 \sin 5\left(\omega t - \frac{\pi}{3}\right) + \cdots$$

$$v_o = v_{o1} + v_{o2} = \sqrt{3}\left[A_1 \sin\left(\omega t - \frac{\pi}{6}\right) + A_5 \sin 5\left(\omega t + \frac{\pi}{6}\right) + \cdots\right]$$

Therefore, a phase shifting of $\pi/3$ and combining voltages by transformer connection would eliminate third (and all triplen) harmonics. It should be noted that the resultant fundamental component is $\sqrt{3}/2$ (= 0.866) of that for individual output voltages and the effective output has been reduced by (1 − 0.866 =) 13.4%.

The harmonic elimination techniques, which are only suitable for fixed output

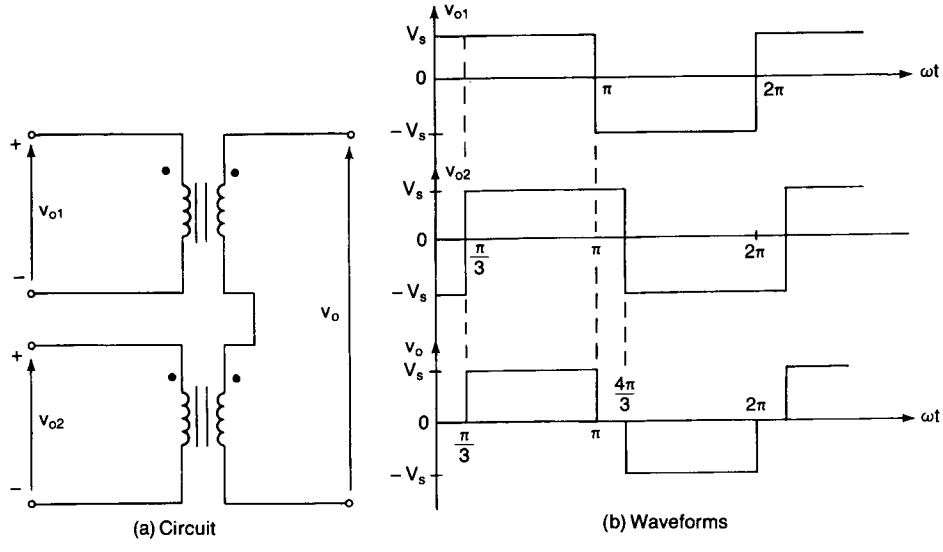


Figure 8-20 Elimination of harmonics by transformer connection.

voltage, increase the order of harmonics and reduce the sizes of output filter. However, this advantage should be weighed against the increased switching losses of power devices and increased iron (or magnetic losses) in the transformer due to higher harmonic frequencies.

Example 8-6

A single-phase full-wave inverter uses multiple notches and is required to eliminate the fifth, seventh, eleventh, and thirteenth harmonics from the output wave. Determine the number of notches and their angles.

Solution For elimination of the fifth, seventh, eleventh, and thirteenth harmonics, $A_5 = A_7 = A_{11} = A_{13} = 0$. Four notches per quarter-wave would be required. Equation (8-40) gives the following set of nonlinear equations to solve for the angles.

$$1 - 2\cos 5\alpha_1 + 2\cos 5\alpha_2 - 2\cos 5\alpha_3 + 2\cos 5\alpha_4 = 0$$

$$1 - 2\cos 7\alpha_1 + 2\cos 7\alpha_2 - 2\cos 7\alpha_3 + 2\cos 7\alpha_4 = 0$$

$$1 - 2\cos 11\alpha_1 + 2\cos 11\alpha_2 - 2\cos 11\alpha_3 + 2\cos 11\alpha_4 = 0$$

$$1 - 2\cos 13\alpha_1 + 2\cos 13\alpha_2 - 2\cos 13\alpha_3 + 2\cos 13\alpha_4 = 0$$

Solution of these equations by iteration yields

$$\alpha_1 = 10.55^\circ \qquad \alpha_2 = 16.09^\circ \qquad \alpha_3 = 30.91^\circ \qquad \alpha_4 = 32.87^\circ$$

Note. It is not always necessary to eliminate the third harmonic (and triplen), which are not normally present in three-phase connections. Therefore, in three-phase inverters, it is preferable to eliminate the fifth, seventh, and eleventh harmonics of output voltages, so that the lowest-order harmonic is the thirteenth.

8-9 SERIES RESONANT INVERTERS

The series resonant inverters are based on resonant current oscillation. The commutating components and switching device are placed in series with the load to form an underdamped circuit. The current through the switching devices falls to zero due to the natural characteristics of the circuit. If the switching element is a thyristor, it is said to be self-commutated. This type of inverter produces an approximately sinusoidal waveform at a high output frequency, ranging from 200 Hz to 100 kHz, and is commonly used in relatively fixed output applications (e.g., induction heating, sonar transmitter, fluorescent lighting, or ultrasonic generators). Due to the high switching frequency, the sizes of commutating components are small.

There are various configurations of series inverters, depending on the connections of the switching devices and load. The series inverters may be classified into two categories:

1. Series resonant inverters with unidirectional switches
2. Series resonant inverters with bidirectional switches

8-9.1 Series Resonant Inverters with Unidirectional Switches

Figure 8-21a shows the circuit diagram of a simple series inverter using two unidirectional thyristor switches. When thyristor T_1 is fired, a resonant pulse of current flows through the load and the current falls to zero at $t = t_{1m}$ and T_1 is self-commutated. Firing of thyristor T_2 causes a reverse resonant current through the load and T_2 is also self-commutated. The circuit operation can be divided into three modes and the equivalent circuits are shown in Fig. 8-21b. The gating signals for thyristors and the waveforms for the load current and capacitor voltage are shown in Fig. 8-21c.

The series resonant circuit formed by L, C, and load (assumed resistive) must be underdamped.

$$R^2 < \frac{4L}{C} \tag{8-41}$$

Mode 1. This mode begins when T_1 is fired and a resonant pulse of current flows through T_1 and the load. The instantaneous load current for this mode is described by

$$L\frac{di_1}{dt} + Ri_1 + \frac{1}{C}\int i_1\,dt + v_{c1}\,(t = 0) = V_s \tag{8-42}$$

with initial conditions $i_1\,(t = 0) = 0$ and $v_{c1}\,(t = 0) = -V_c$. Since the circuit is underdamped, the solution of Eq. (8-42) yields

$$i_1(t) = A_1 e^{-tR/2L} \sin \omega_r t \tag{8-43}$$

where ω_r is the resonant frequency and

$$\omega_r = \left(\frac{1}{LC} - \frac{R^2}{4L^2}\right)^{1/2} \tag{8-44}$$

The constant, A_1, in Eq. (8-43) can be evaluated from the initial condition:

$$\left.\frac{di_1}{dt}\right|_{t=0} = \frac{V_s + V_c}{\omega_r L} = A_1$$

and

$$i_1(t) = \frac{V_s + V_c}{\omega_r L} e^{-\alpha t} \sin \omega_r t \tag{8-45}$$

where

$$\alpha = \frac{R}{2L} \tag{8-46}$$

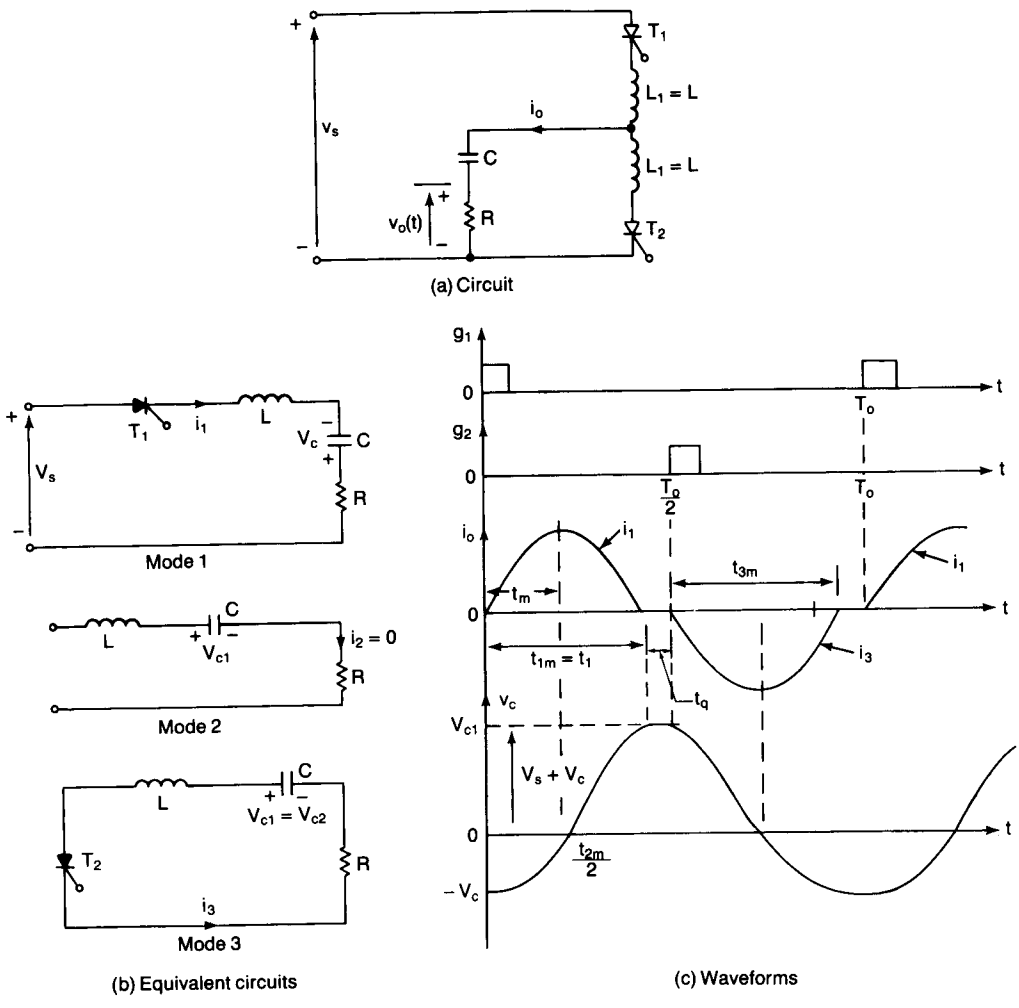


Figure 8-21 Basic series resonant inverter.

The time t_m when the current $i_1(t)$ becomes maximum can be found from the condition

$$\frac{di_1}{dt} = 0 \qquad \text{or} \qquad \omega_r e^{-\alpha t_m} \cos \omega_r t_m - \alpha e^{-\alpha t_m} \sin \omega_r t_m = 0$$

and this gives

$$t_m = \frac{1}{\omega_r} \tan^{-1} \frac{\omega_r}{\alpha} \tag{8-47}$$

The capacitor voltage can be found from

$$\begin{aligned} v_{c1}(t) &= \frac{1}{C}\int_0^t i_1(t) - V_c \\ &= -(V_s + V_c)e^{-\alpha t}(\alpha \sin \omega_r t + \omega_r \cos \omega_r t)/\omega r + V_s \end{aligned} \tag{8-48}$$

This mode is valid for $0 \le t \le t_{1m} = \pi/\omega_r$ and ends when $i_1(t)$ becomes zero at t_{1m}. At the end of this mode,

$$i_1\,(t = t_{1m}) = 0$$

and

$$v_{c1}\,(t = t_{1m}) = v_{c1} = (V_s + V_c)e^{-\alpha\pi/\omega_r} + V_s \tag{8-49}$$

Mode 2. During this mode, thyristors T_1 and T_2 are off. This mode is valid for $0 \le t \le t_{2m}$.

$$i_2(t) = 0, \qquad v_{c2}(t) = V_{c1} \qquad v_{c2}\,(t = t_{2m}) = V_{c2} = V_{c1}$$

Mode 3. This mode begins when T_2 is switched on and a reverse resonant current flows through the load. The load current can be found from

$$L\frac{di_3}{dt} + Ri_3 + \frac{1}{C}\int i_3\,dt + v_{c3}\,(t = 0) = 0 \tag{8-50}$$

with initial conditions $i_3\,(t = 0) = 0$ and $v_{c3}\,(t = 0) = -V_{c2} = -V_{c1}$. The solution of Eq. (8-50) gives

$$i_3(t) = \frac{V_{c1}}{\omega_r L}e^{-\alpha t}\sin \omega_r t \tag{8-51}$$

The capacitor voltage can be found from

$$\begin{aligned} v_{c3}(t) &= \frac{1}{C}\int_0^t i_3(t) - V_{c1} \\ &= V_{c1}e^{-\alpha t}(\alpha \sin \omega_r t + \omega_r \cos \omega_r t)/\omega r \end{aligned} \tag{8-52}$$

This mode is valid for $0 \le t \le t_{3m} = \pi/\omega_r$ and ends when $i_3(t)$ becomes zero. At the end of this mode,

$$i_3\,(t = t_{3m}) = 0$$

and in the steady state,

$$v_{c3}\,(t = t_{3m}) = V_{c3} = V_c = V_{c1}e^{-\alpha\pi/\omega_r} \tag{8-53}$$

Equations (8-49) and (8-53) yield

$$V_c = V_s\frac{1 + e^{-z}}{e^z - e^{-z}} = V_s\frac{e^z + 1}{e^{2z} - 1} = \frac{V_s}{e^z - 1} \tag{8-54}$$

$$V_{c1} = V_s \frac{1 + e^z}{e^z - e^{-z}} = V_s \frac{e^z(1 + e^z)}{e^{2z} - 1} = \frac{V_s e^z}{e^z - 1} \tag{8-55}$$

where $z = \alpha\pi/\omega_r$. Adding V_c from Eq. (8-54) to V_s gives

$$V_s + V_c = V_{c1} \tag{8-56}$$

Equation (8-56) indicates that under steady-state conditions, the peak value of positive current and of negative current through the load is the same.

The load current $i_1(t)$ must be zero and T_1 must be turned off before T_2 is fired. Otherwise, a short-circuit condition will result through the thyristors and dc supply. Therefore, the available off-time t_{2m} ($= t_q$), known as the *dead zone*, must be greater than the turn-off time of thyristors, t_{off}.

$$\frac{\pi}{\omega_o} - \frac{\pi}{\omega_r} = t_q > t_{\text{off}} \tag{8-57}$$

where ω_o is the frequency of output voltage in rad/s. Equation (8-57) indicates that the maximum possible output frequency is limited to

$$f_o \leq f_{\max} = \frac{1}{2(t_{\text{off}} + \pi/\omega_r)} \tag{8-58}$$

The resonant inverter circuit in Fig. 8-21a is very simple. However, the power flow from the dc supply is discontinuous. The dc supply will have a high peak current and would contain harmonics. An improvement of the basic inverter in Fig. 8-21a can be made if inductors are closely coupled, as shown in Fig. 8-22. When T_1 is fired and current $i_1(t)$ begins to rise, the voltage across L_1 will be positive with polarity as shown. The induced voltage on L_2 will now add to the voltage of C in reverse biasing T_2; and T_2 will be turned off. The result is that firing of one thyristor will turn off the other, even before the load current reaches to zero.

The drawback of high pulsed current from the dc supply is overcome in a half-bridge configuration as shown in Fig. 8-23, where $L_1 = L_2$ and $C_1 = C_2$. The power is drawn from the dc source during both half-cycles of output voltage. One-

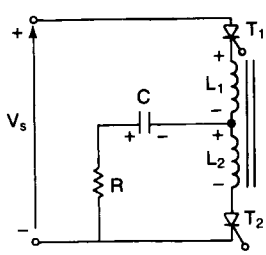


Figure 8-22 Series resonant inverter with coupled inductors.

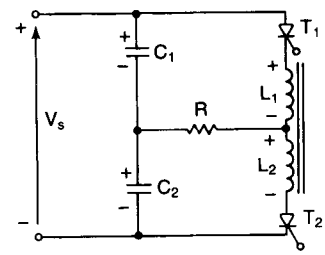


Figure 8-23 Half-bridge series resonant inverter.

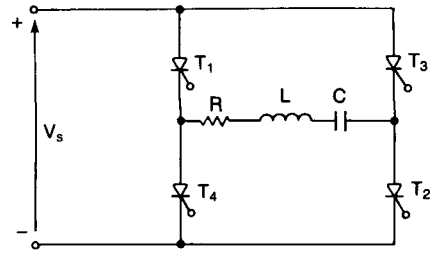


Figure 8-24 Full-bridge series resonant inverter.

half of the load current is supplied by capacitor C_1 or C_2 and the other-half by the dc source.

A full-bridge inverter, which allows higher output power, is shown in Fig. 8-24. When T_1 and T_2 are fired, a positive resonant current flows through the load; and when T_3 and T_4 are fired, a negative load current flows. The supply current is continuous.

The resonant frequency and available dead-zone depend on the load and for this reason, resonant inverters are most suitable for fixed-load applications. The inverter load (or resistor R) could also be connected in parallel with the capacitor.

Example 8-7

The series resonant inverter in Fig. 8-22 has $L_1 = L_2 = L = 50$ μH, $C = 6$ μF, and $R = 2\ \Omega$. The dc input voltage is $V_s = 220$ V and the frequency of output voltage is $f_o = 7$ kHz. The turn-off time of thyristors is $t_{off} = 10$ μs. Determine the (a) available (or circuit) turn-off time, t_q; (b) maximum permissible frequency, f_{max}; (c) peak-to-peak capacitor voltage, V_{pp}; and (d) peak load current, I_p. (e) Sketch the instantaneous load current, $i_o(t)$; capacitor voltage, $v_c(t)$; and dc supply current $i_s(t)$. Calculate the (f) rms load current, I_o; (g) output power, P_o; (h) average supply current, I_s; and (i) average, peak, and rms current of thyristors.

Solution $V_s = 220$ V, $C = 6$ μF, $L = 50$ μH, $R = 2\ \Omega$, $f_o = 7$ kHz, $t_{off} = 10$ μs, and $\omega_o = 2\pi \times 7000 = 43{,}982$ rad/s. From Eq. (8-44),

$$\omega_r = \left(\frac{1}{LC} - \frac{R^2}{4L^2}\right)^{1/2} = \left(\frac{10^{12}}{50 \times 6} - \frac{2^2 \times 10^{12}}{4 \times 50^2}\right]^{1/2} = 54{,}160 \text{ rad/s}$$

The resonant frequency is $f_r = \omega_r/2\pi = 8619.8$ rad/s, $T_r = 1/f_r = 116$ μs. From Eq. (8-46), $\alpha = 2/(2 \times 50 \times 10^{-6}) = 20{,}000$.

(a) From Eq. (8-57),

$$t_q = \frac{\pi}{43{,}982} - \frac{\pi}{54{,}160} = 13.42\ \mu\text{s}$$

(b) From Eq. (8-58), the maximum possible frequency is

$$f_{max} = \frac{1}{2(10 \times 10^{-6} + \pi/54{,}160)} = 7352 \text{ Hz}$$

(c) From Eq. (8-54),

$$V_c = \frac{V_s}{e^{\alpha\pi/\omega_r} - 1} = \frac{220}{e^{20\pi/54.16} - 1} = 100.4 \text{ V}$$

From Eq. (8-56), $V_{c1} = 220 + 100.4 = 320.4$ V. The peak-to-peak capacitor voltage is $V_{pp} = 100.4 + 320.4 = 420.8$ V.

(d) From Eq. (8-47), the peak load current, which is the same as the peak supply current, occurs at

$$t_m = \frac{1}{\omega_r}\tan^{-1}\frac{\omega_r}{\alpha} = \frac{1}{54{,}160}\tan^{-1}\frac{54.16}{20} = 22.47\ \mu s$$

and Eq. (8-45) gives the peak load current as

$$i_1(t = t_m) = I_p = \frac{320.4}{0.05416 \times 50}e^{-0.02\times 22.47}\sin(54{,}160 \times 22.47 \times 10^{-6}) = 70.82\,A$$

(e) The sketches for $i(t)$, $v_c(t)$, and $i_s(t)$ are shown in Fig. 8-25.

(f) The rms load current is found from Eqs. (8-45) and (8-51) by a numerical method and the result is

$$I_o = \left[2f_o\int_0^{T_r/2} i_0^2(t)\,dt\right]^{1/2} = 44.1\ A$$

(g) The output power, $P_o = 44.1^2 \times 2 = 3889$ W.

(h) The average supply current, $I_s = 3889/220 = 17.68$ A.

(i) The average thyristor current,

$$I_A = f_o\int_0^{T_r/2} i_0(t)\,dt = 17.68\ A$$

The peak thyristor current, $I_{pk} = I_p = 70.82$ A, and the rms thyristor current, $I_R = I_o/\sqrt{2} = 44.1/\sqrt{2} = 31.18$ A.

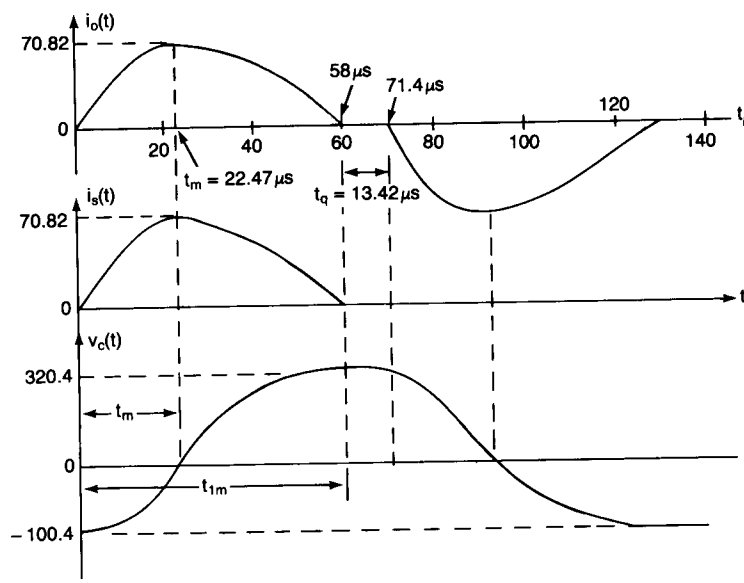


Figure 8-25 Waveforms for Example 8-7.

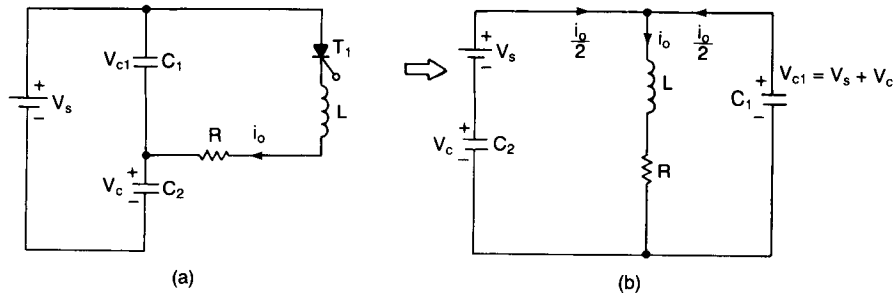


Figure 8-26 Equivalent circuits for Example 8-8.

Example 8-8

The half-bridge resonant inverter in Fig. 8-23 is operated at a frequency, $f_o = 7$ kHz. If $C_1 = C_2 = C = 3$ μF, $L_1 = L_2 = L = 50$ μH, $R = 2\ \Omega$, and $V_s = 220$ V, determine the (a) peak supply current; (b) average thyristor current, I_A; and (c) rms thyristor current, I_R.

Solution $V_s = 220$ V, $C = 3$ μF, $L = 50$ μH, $R = 2\ \Omega$, and $f_o = 7$ kHz. Figure 8-26a shows the equivalent circuit when thyristor T_1 is conducting and T_2 is off. The capacitors C_1 and C_2 would initially be charged to V_{c1} ($= V_s + V_c$) and V_c, respectively, with the polarities as shown, under steady-state conditions. Since $C_1 = C_2$, the load current would be shared equally by C_1 and the dc supply as shown in Fig. 8-26b.

Considering the loop formed by C_2, dc source, L, and load, the instantaneous load current can be described (from Fig. 8-26b) by

$$L\frac{di_o}{dt} + Ri_0 + \frac{1}{2C_2}\int i_o\,dt + v_{c2}\,(t = 0) - V_s = 0 \tag{8-59}$$

with initial conditions $i_0\,(t = 0) = 0$ and $v_{c2}\,(t = 0) = -V_c$. For an underdamped condition and $C_1 = C_2 = C$, Eq. (8-45) is applicable:

$$i_0(t) = \frac{V_s + V_c}{\omega_r L}e^{-\alpha t}\sin\omega_r t \tag{8-60}$$

where the effective capacitance is $C_e = C_1 + C_2 = 2C$ and

$$\omega_r = \left(\frac{1}{2LC_2} - \frac{R^2}{4L^2}\right)^{1/2} = \left(\frac{10^{12}}{2 \times 50 \times 3} - \frac{2^2 \times 10^{12}}{4 \times 50^2}\right)^{1/2} = 54{,}160\ \text{rad/s} \tag{8-61}$$

The voltage across capacitor C_2 can be expressed as

$$\begin{aligned} v_{c2}(t) &= \frac{1}{2C_2}\int_0^t i_0(t)\,dt - V_c \\ &= -(V_s + V_c)e^{-\alpha t}(\alpha\sin\omega_r t + \omega_r\cos\omega_r t)/\omega r + V_s \end{aligned} \tag{8-62}$$

(a) Since the resonant frequency is the same as that of Example 8-7, the results of Example 8-7 are valid, provided that the equivalent capacitance is $C_e = C_1 + C_2 = 6$ μF. From Example 8-7, $V_c = 100.4$ V, $t_m = 22.47$ μs, and $I_o = 44.1$ A. From Eq. (8-60), the peak load current is $I_p = 70.82$ A. The peak supply current, which is half of the peak load current, is $I_{ps} = 70.82/2 = 35.41$ A.

(b) The average thyristor current, $I_A = 17.68$ A.
(c) The rms thyristor current, $I_R = I_o\sqrt{2} = 31.18$ A.

Note. For the same power output and resonant frequency, the capacitances of C_1 and C_2 in Fig. 8-23 should be half that in Figs. 8-21a and 8-22. The peak supply current becomes half. The analysis of full-bridge series inverters is similar to that of the basic series inverter in Fig. 8-21a.

8-9.2 Series Resonant Inverters with Bidirectional Switches

For the resonant inverters with unidirectional switches, the power devices have to be turned on in every half-cycle of output voltage. This limits the inverter frequency and the amount of energy transfer from the source to the load. In addition, the thyristors are subjected to high peak reverse voltage.

The performance of series inverters can be significantly improved by connecting an antiparallel diode across a thyristor as shown in Fig. 8-27a. When thyristor T_1 is fired, a resonant pulse of current flows and T_1 is self-commutated at $t = t_1$. However, the resonant oscillation continues through diode D_1 until the current falls again to zero at the end of a cycle. The waveforms for currents and capacitor voltage are shown in Fig. 8-27b.

The reverse voltage of the thyristor is limited to the forward voltage drop of a diode, typically 1 V. If the conduction time of the diode is greater that the turn-off time of the thyristor, there is no need of a dead zone and the output frequency, f_o, is the same as the resonant frequency, f_r,

$$f_o = f_r = \frac{\omega_r}{2\pi} \tag{8-63}$$

where f_r is the resonant frequency of the series circuit in hertz. If t_{off} is the turn-

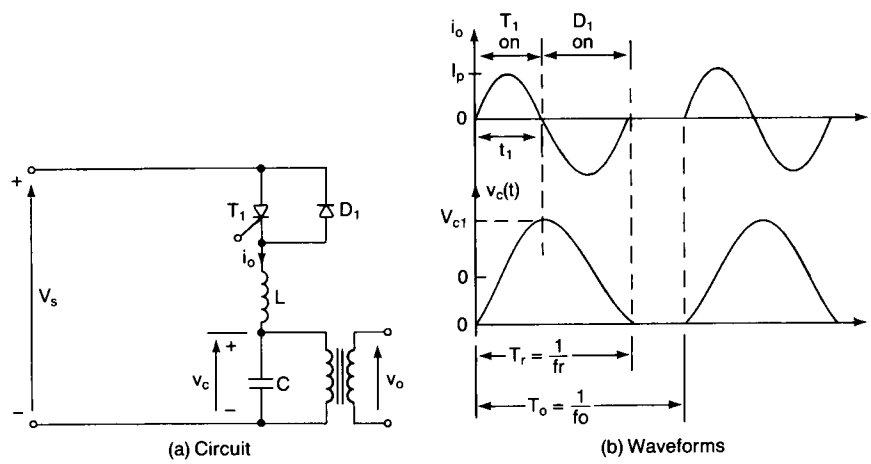


Figure 8-27 Basic series resonant inverter with bidirectional switches.

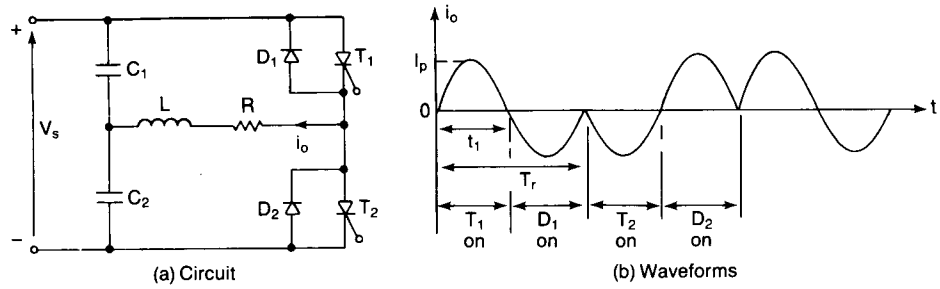


Figure 8-28 Half-bridge series inverters with bidirectional switches.

off time of a thyristor, the maximum inverter frequency is given by

$$f_{\max} = \frac{1}{2t_{\text{off}}} \tag{8-64}$$

and f_o should be less than $f_{\max}$.

The diode D_1 should be connected as close as possible to the thyristor and the connecting leads should be minimum to reduce any stray inductance in the loop formed by T_1 and D_1. As the reverse voltage during the recovery time of thyristor T_1 is already low, typically 1 V, any inductance in the diode path would reduce the net reverse voltage across the terminals of T_1, and thyristor T_1 may not turn off. To overcome this problem, a *reverse conducting thyristor* (RCT) is normally used. A RCT is made by integration of an asymmetrical thyristor and a fast-recovery diode into a single silicon chip and RCTs are ideal for series resonant inverters.

The circuit diagram for the half-bridge version is shown in Fig. 8-28a and the waveform for the load current and the conduction intervals of the power devices are shown in Fig. 8-28b. The full-bridge configuration is shown in Fig. 8-29. The inverters can be operated in two different modes: nonoverlapping and overlapping. In a nonoverlapping mode, the firing of a thyristor is delayed until the last current oscillation through a diode has been completed as in Fig. 8-28b. In an overlapping

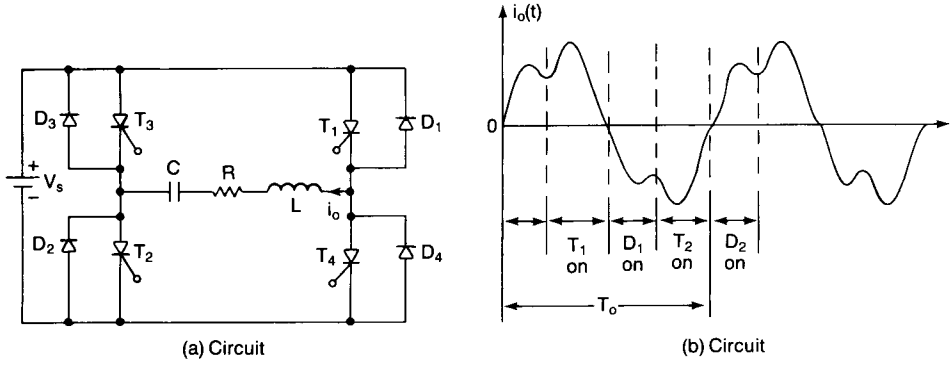


Figure 8-29 Full-bridge series inverters with bidirectional switches.

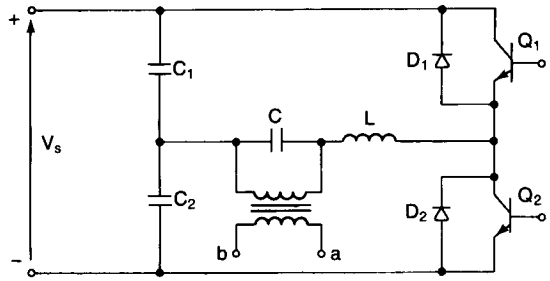


Figure 8-30 Half-bridge transistorized resonant inverter.

mode, a thyristor is fired, while the current in the diode of the other part is still conducting, as shown in Fig. 8-29b. Although overlapping operation reduces the output frequency, the output power is increased.

The maximum frequency of resonant inverters are limited due to the turn-off or commutation requirements of thyristors, typically 12 to 20 μs, whereas transistors, which require only a microsecond or less, can replace the thyristors. The inverter can operate at the resonant frequency. A transistorized half-bridge inverter is shown in Fig. 8-30 with a transformer-connected load. Transistor Q_2 can be turned on almost instantaneously after transistor Q_1 is turned off.

Example 8-9

The resonant inverter in Fig. 8-27a has $C = 2$ μF, $L = 20$ μH, $R = 0$, and $V_s = 220$ V. The turn-off time of the thyristor, $t_{off} = 12$ μs. The output frequency, $f_o = 20$ kHz. Determine the (a) peak supply current, I_{ps}; (b) average thyristor current, I_A; (c) rms thyristor current, I_R; (d) peak-to-peak capacitor voltage, V_{pp}; (e) maximum permissible output frequency, f_{max}; and (f) average supply current, I_s.

Solution When thyristor T_1 is turned on, the current is described by

$$L\frac{di_0}{dt} + \frac{1}{C}\int i_0\,dt + v_c\,(t = 0) = V_s \tag{8-65}$$

with initial conditions $i_0\,(t = 0) = 0$, $v_c\,(t = 0) = V_c = 0$. Solving for the current gives

$$i_0(t) = V_s\sqrt{\frac{C}{L}}\sin\omega_r t \tag{8-66}$$

and the capacitor voltage is

$$v_c(t) = V_s(1 - \cos\omega_r t) \tag{8-67}$$

where $\omega_r = 1/\sqrt{LC}$

$$\omega_r = \frac{10^6}{\sqrt{20 \times 2}} = 158{,}114 \text{ rad/s} \quad \text{and} \quad f_r = \frac{158{,}114}{2\pi} = 25{,}165 \text{ Hz}$$

$$T_r = \frac{1}{f_r} = \frac{1}{25{,}165} = 39.74 \text{ μs} \quad t_1 = \frac{T_r}{2} = \frac{39.74}{2} = 19.87 \text{ μs}$$

At $\omega_r t = \pi$,

$$v_c\,(\omega_r t = \pi) = V_{c1} = 2V_s = 2 \times 220 = 440 \text{ V}$$

(a) $I_p = V_s\sqrt{L/C} = 220\sqrt{20/2} = 695.7$ A.

(b) $I_A = f_o \int_0^{\pi} I_p \sin\theta\, d\theta = I_p f_o/(\pi f_r) = 695.7 \times 20{,}000/(\pi \times 25{,}165) =$ 176 A.

(c) $I_R = I_p\sqrt{f_o t_1/2} = 695.7\sqrt{20{,}000 \times 19.87 \times 10^{-6}/2} = 310.1$ A.

(d) The peak-to-peak capacitor voltage, $V_{pp} = V_{c1} - V_c = 440$ V.

(e) From Eq. (8-64), $f_{max} = 10^6/(2 \times 12) = 41.67$ kHz.

(f) Since there is no power loss in the circuit, $I_s = 0$.

Example 8-10

The half-bridge resonant inverter in Fig. 8-28a is operated at a frequency of $f_o = 3.5$ kHz. If $C_1 = C_2 = C = 3$ μF, $L_1 = L_2 = L = 50$ μH, $R = 2\ \Omega$, and $V_s = 220$ V, determine the (a) peak supply current, I_{ps}; (b) average thyristor current, I_A; (c) rms thyristor current, I_R; (d) rms load current, I_o; and (e) average supply current, I_s.

Solution $V_s = 220$ V, $C_e = C_1 + C_2 = 6$ μF, $L = 50$ μH, $R = 2\ \Omega$, and $f_o = 3500$ Hz. The analysis of this inverter is similar to that of inverter in Fig. 8-23. Instead of two current pulses, there are four pulses in a full cycle of the output voltage with one pulse through each of devices T_1, D_1, T_2, and D_2. Equation (8-60) is applicable. During the positive half-cycle, the current flows through T_1; and during the negative half-cycle the current flows through D_1. In a nonoverlap control, there are two resonant cycles during the entire period of output frequency, f_o. From Eq. (8-61),

$$\omega_r = 54{,}160 \text{ rad/s} \qquad f_r = \frac{54{,}160}{2\pi} = 8619.9 \text{ Hz}$$

$$T_r = \frac{1}{8619.9} = 116\ \mu\text{s} \qquad t_1 = \frac{116}{2} = 58\ \mu\text{s}$$

$$T_0 = \frac{1}{3500} = 285.72\ \mu\text{s}$$

The off-period of load current,

$$t_d = \frac{T_0}{2} - T_r = 142.87 - 58 = 84.87\ \mu\text{s}$$

Since t_d is greater than zero, the inverter would operate in the on-overlap mode. From Eq. (8-54), $V_c = 100.4$ V and $V_{c1} = 220 + 100.4 = 320.4$ V.

(a) From Eq. (8-47),

$$t_m = \frac{1}{54{,}160}\tan^{-1}\frac{54{,}160}{20{,}000} = 22.47\ \mu\text{s}$$

$$i_0(t) = \frac{V_s + V_c}{\omega_r L} e^{-\alpha t} \sin \omega_r t$$

and the peak load current becomes $I_p = i_0\ (t = t_m) = 70.82$ A.

(b) A thyristor conducts from a time of t_1. The average thyristor current can be found from

$$I_A = f_o \int_0^{t_1} i_0(t)\, dt = 8.84 \text{ A}$$

(c) The rms thyristor current is

$$I_R = \left[f_o \int_0^{t_1} i_0^2(t)\, dt \right]^{1/2} = 22.05 \text{ A}$$

(d) The rms load current, $I_o = 2I_R = 2 \times 22.05 = 44.1$ A.

(e) $P_0 = 44.1^2 \times 2 = 3889$ W and the average supply current, $I_s = 3889/220 = 17.68$ A.

Note. With bidirectional switches, the current ratings of the devices are reduced. For the same output power, the average device current is half and the rms current is $1/\sqrt{2}$ of that for an inverter with unidirectional switches.

Example 8-11

The full-bridge resonant inverter in Fig. 8-29a is operated at a frequency, $f_o = 3.5$ kHz. If $C = 6$ μF, $L = 50$ μH, $R = 2\ \Omega$, and $V_s = 220$ V, determine the (a) peak supply current, I_{ps}; (b) average thyristor current, I_A; (c) rms thyristor current, I_R; (d) rms load current, I_o; and (e) average supply current, I_s.

Solution $V_s = 220$ V, $C = 6$ μF, $L = 50$ μH, $R = 2\ \Omega$, and $f_o = 3500$ kHz. From Eq. (8-61), $\omega_r = 54{,}160$ rad/s and $f_r = 54{,}160/(2\pi) = 8619.9$ Hz. $\alpha = 20{,}000$, $T_r = 1/8619.9 = 116$ μs, $t_1 = 116/2 = 58$ μs, and $T_0 = 1/3500 = 285.72$ μs. The off-period of load current is $t_d = T_0/2 - T_r = 142.87 - 58 = 84.87$ μs and the inverter would operate in the non-overlap mode.

Mode 1. This mode begins when T_1 and T_2 are fired. A resonant current flows through T_1, T_2, load, and supply. The instantaneous current is described by

$$L \frac{di_0}{dt} + Ri_0 + \frac{1}{C} \int i_0\, dt + v_c\,(t = 0) = V_s$$

with initial conditions $i_0\,(t = 0) = 0$, $v_{c1}\,(t = 0) = -V_c$ and the solution for the current gives

$$i_0(t) = \frac{V_s + V_c}{\omega_r L} e^{-\alpha t} \sin \omega_r t \tag{8-68}$$

$$v_c(t) = -(V_s + V_c)e^{-\alpha t} (\alpha \sin \omega_r t + \omega_r \cos \omega_r t) + V_s \tag{8-69}$$

Thyristors T_1 and T_2 are turned off at $t_1 = \pi/\omega_r$, when $i_1(t)$ becomes zero.

$$V_{c1} = v_c\,(t = t_1) = (V_s + V_c)e^{-\alpha\pi/\omega_r} + V_s \tag{8-70}$$

Mode 2. This mode begins when T_3 and T_4 are fired. A reverse resonant current flows through T_3, T_4, load, and supply. The instantaneous load current is described by

$$L \frac{di_0}{dt} + Ri_0 + \frac{1}{C} \int i_0\, dt + v_c\,(t = 0) = -V_s$$

with initial conditions $i_2\,(t = 0) = 0$, $v_c\,(t = 0) = V_{c1}$ and the solution for the current gives

$$i_0(t) = -\frac{V_s + V_{c1}}{\omega_r L} e^{-\alpha t} \sin \omega_r t \tag{8-71}$$

$$v_c(t) = (V_s + V_{c1})e^{-\alpha t}(\alpha \sin \omega_r t + \omega_r \cos \omega_r t)/\omega_r - V_s \tag{8-72}$$

Thyristors T_3 and T_4 are turned off at $t_1 = \pi/\omega_r$, when $i_0(t)$ becomes zero.

$$V_c = -v_c(t = t_1) = (V_s + V_{c1})e^{-\alpha\pi/\omega_r} + V_s \tag{8-73}$$

Solving for V_c and V_{c1} from Eqs. (8-70) and (8-73) gives

$$V_c = V_{c1} = V_s \frac{e^z + 1}{e^z - 1} \tag{8-74}$$

where $z = \alpha\pi/\omega_r$. For $z = 20{,}000\pi/54{,}160 = 1.1601$, Eq. (8-74) gives $V_c = V_{c1} = 420.9$ V.

(a) From Eq. (8-47),

$$t_m = \frac{1}{54{,}160} \tan^{-1} \frac{54{,}160}{20{,}000} = 22.47 \ \mu s.$$

From Eq. (8-68), the peak load current, $I_p = i_0(t = t_m) = 141.64$ A.

(b) A thyristor conducts from a time of t_1. The average thyristor current can be found from Eq. (8-68):

$$I_A = f_o \int_0^{t_1} i_0(t)\, dt = 17.68 \text{ A}$$

(c) The rms thyristor current can be found from Eq. (8-68):

$$I_R = \left[f_o \int_0^{t_1} i_0^2(t)\, dt \right]^{1/2} = 44.1 \text{ A}$$

(d) The rms load current is $I_o = 2I_R = 2 \times 44.1 = 88.2$ A.

(e) $P_o = 88.2^2 \times 2 = 15{,}556$ W and the average supply current, $I_s = 15{,}556/220 = 70.71$ A.

Note. For the same circuit parameters, the output power is four times, and the device currents are twice, that for a half-bridge inverter.

8-10 FORCED-COMMUTATED THYRISTOR INVERTERS

Although transistors or GTOs can be employed as switching devices for inverters, they are used mostly in low-power applications. For high-voltage and high-current applications, it is necessary to connect them in series and/or parallel combinations; and this results in an increased complexity of the circuit. Fast-switching thyristors, which are available in high voltage and current ratings, are more suitable for high-power applications. However, thyristors require extra commutation circuits for turn-off and the various techniques for thyristor commutation are discussed in Chapter 3. At the earlier stage of power electronics, many thyristor commutation circuits for inverters were developed. Two types of commutation circuits commonly used in inverter applications are:

1. Auxiliary commutated inverters
2. Complementary commutated inverters

8-10.1 Auxiliary-Commutated Inverters

A single-phase full-bridge thyristor inverter using auxiliary commutation is shown in Fig. 8-31a. The commutation circuit is shared by two thyristors. Let us assume that thyristor T_1 is conducting and supplies the instantaneous load current, I_m; and the capacitor C_m is charged to V_o with polarity as shown. The waveforms for the capacitor voltage and current are shown in Fig. 8-31b. The commutation process of a thyristor can be divided into four modes.

Mode 1. This mode begins when thyristor T_{11} fired to turn off thyristor T_1. Firing of T_{11} causes a resonant current flow through the capacitor and forces the current of T_1 to fall. This can be considered as a reverse current through the circuit formed by L_m, C_m, T_1, and T_{11}. This mode ends when the forward current of T_1 falls to zero and the capacitor current rises to the load current, I_m at $t = t_1$.

Mode 2. This mode begins when diode D_1 starts to conduct and the resonant

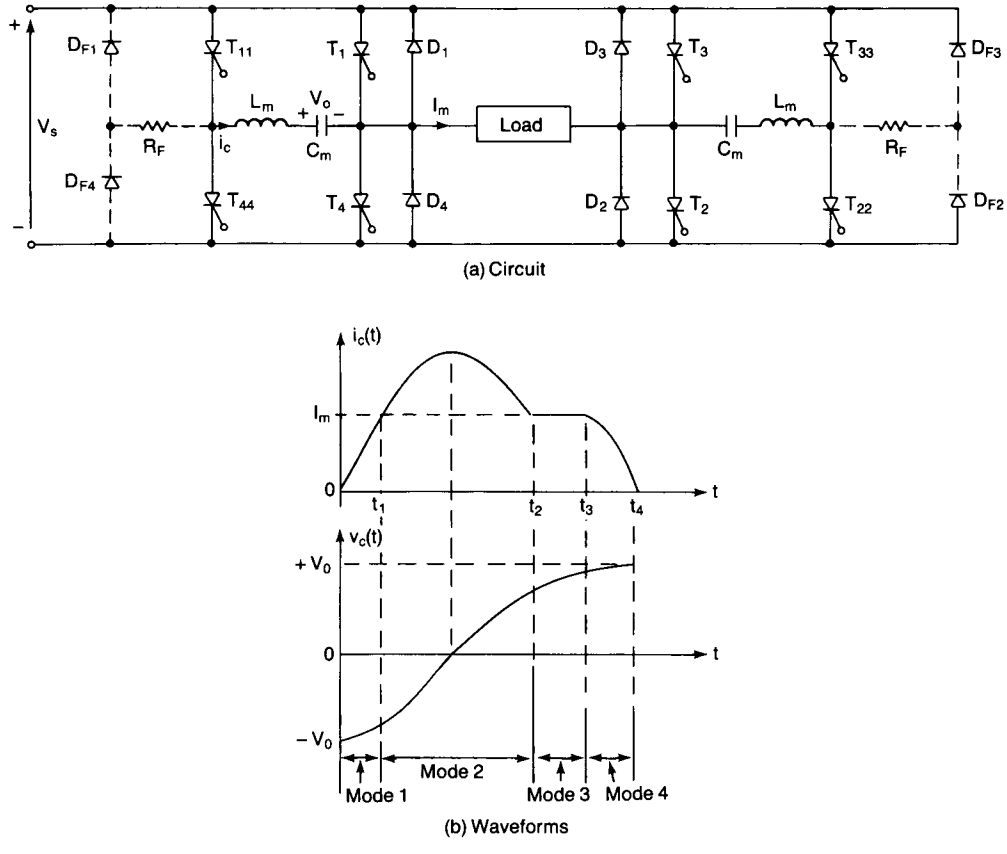


Figure 8-31 Single-phase auxiliary commutated inverter.

oscillation continues through L_m, C_m, D_1, and T_{11}. This mode ends when the capacitor current falls back to the load current at $t = t_2$ and diode D_1 stops conducting.

Mode 3. This mode starts when D_1 stops conducting. The capacitor discharges and recharges through the load at an approximately constant current of I_m. This mode ends when the capacitor voltage becomes equal to the dc supply voltage at $t = t_3$ and tends to overcharge due to the energy stored in inductor L_m.

Mode 4. This mode begins when D_4 is forward biased and the energy stored in inductor L_m is transferred to the capacitor, causing it to be overcharged with respect to supply voltage, V_s. This mode ends when the capacitor current falls again to zero and the capacitor voltage is reversed to that of original polarity. The capacitor is now ready to turn off T_4 if T_{44} is fired.

This inverter is commonly known as the *McMurray inverter*. The circuit operation is similar to that in Fig. 3-13. Equations (3-25) to (3-31) for the available turn-off time and the design conditions are applicable for this inverter circuit. From Eq. (3-25), the available turn-off time or reverse bias time is

$$t_q = \sqrt{L_m C_m}\left(\pi - 2\sin^{-1}\frac{1}{x}\right) \tag{8-75}$$

where

$$x = \frac{V_o}{I_m}\sqrt{\frac{C_m}{L_m}} \tag{8-76}$$

$$V_o = V_s + I_m\sqrt{\frac{L_m}{C_m}} \tag{8-77}$$

In an inverter, the load current varies as a function of time and the commutation circuit should be designed for the peak load current. The capacitor voltage, which depends on the load current at the instant of commutation, increases the voltage and current ratings of devices and components. By connecting diodes, the excess energy can be returned to the dc source as shown in Fig. 8-31a by dashed lines. A part of the energy would be dissipated in resistor R, which may be replaced by a feedback winding.

8-10.2 Complementary-Commutated Inverters

We have seen in Fig. 8-22 that if two inductors are tightly coupled, firing of one thyristor turns off another thyristor in the same arm. This type of commutation is known as *complementary commutation*. This principle can be extended to forced commutated inverter circuits and Fig. 8-32a shows one arm of a single-phase full-bridge inverter. This circuit is also known as a *McMurray–Bedford* inverter. The circuit operation can be divided into three modes and the equivalent circuits for modes are shown in Fig. 8-32b. The waveforms for voltages and currents are

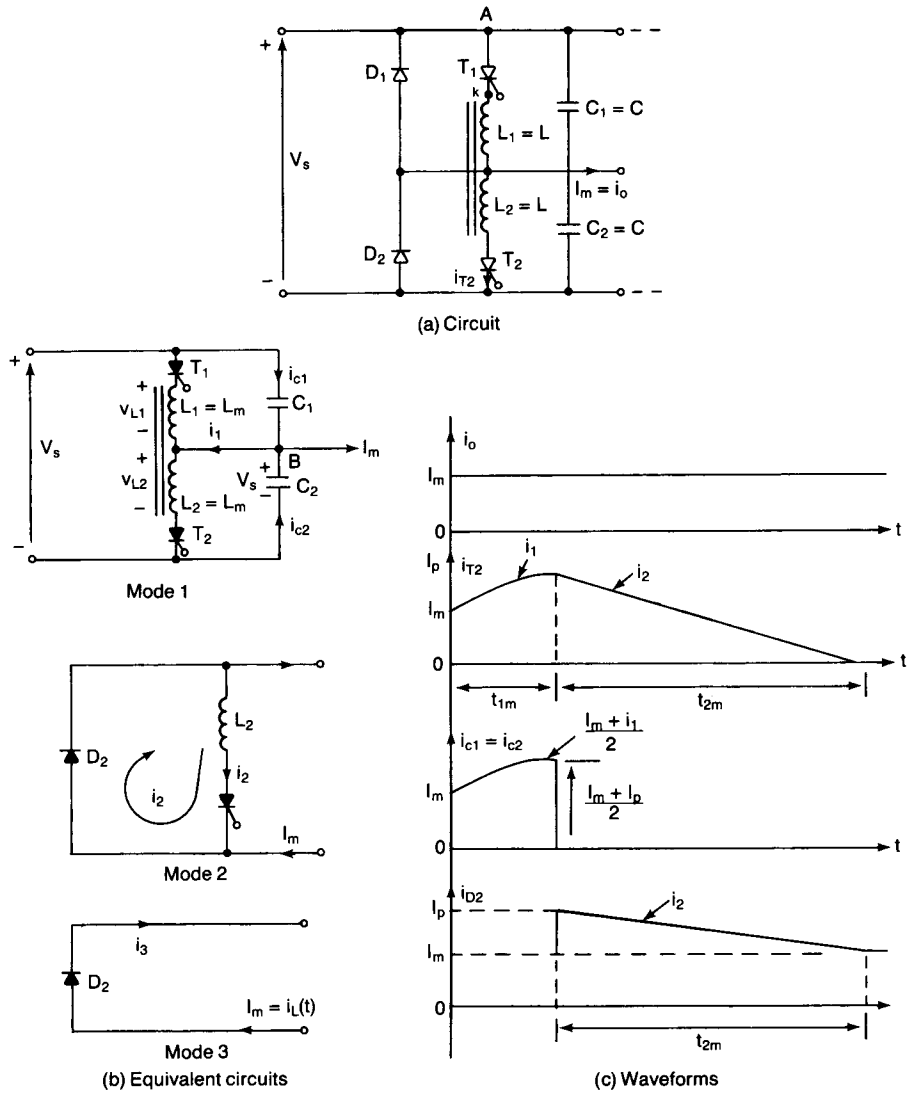


Figure 8-32 Complementary commutation.

shown in Fig. 8-32c under the assumption that the load current remains constant during the commutation period.

Mode 1. This mode begins when T_2 is fired to turn off T_1. The equivalent circuit is shown in Fig. 8-32b. At the start of this mode, capacitor C_2 is charged to V_s. C_1 is shorted by T_1 and has no voltage. The voltage across L_2 is $v_{L2} = V_s$ and the current through L_2 induces a voltage of $v_{L1} = V_s$ across L_1. A reverse voltage of $v_{ak} = V_s - v_{L1} - v_{L2} = -V_s$ is applied across T_1 and the forward

current of T_1 is forced to zero. The current for mode 1, i_1 instantaneously becomes zero and i_2 rises to the level of the instantaneous load current, $i_2 = I_m$.

Assuming that $C_1 = C_2 = C_m$ and by completing the loop around C_1, C_2, and the dc source, the capacitor currents are described by

$$\frac{1}{C_m}\int i_{c1}\,dt + v_{c1}(t = 0) - \frac{1}{C_m}\int i_{c2}\,dt + v_{c2}(t = 0) = V_s \tag{8-78}$$

Since $v_{c1}(t = 0) = 0$ and $v_{c2}(t = 0) = V_s$, Eq. (8-78) yields

$$i_{c1} = i_{c2} \tag{8-79}$$

Using Kirchhoff's current law at the node B,

$$I_m - i_{c1} + i_1 - i_{c2} = 0 \quad \text{or} \quad I_m + i_1 = i_{c1} + i_{c2} = 2i_{c1}$$

or

$$i_{c1} = i_{c2} = \frac{I_m + i_1}{2} \tag{8-80}$$

Assuming that $L_1 = L_2 = L_m$ and completing the loop formed by L_2, T_2, and C_2 gives

$$L_m\frac{di_1}{dt} + \frac{1}{C_m}\int i_{c2}\,dt - v_{c2}(t = 0) = 0 \tag{8-81}$$

with initial conditions $i_1(t = 0) = I_m$ and $v_{c2}(t = 0) = V_s$. The solution of Eq. (8-81) with initial conditions yields

$$i_1(t) = 2I_m\cos\omega t + V_s\sqrt{\frac{2C_m}{L_m}}\sin\omega t - I_m \tag{8-82}$$

where

$$\omega = \frac{1}{\sqrt{2L_mC_m}} \tag{8-83}$$

The voltage across inductor L_2,

$$v_{L2}(t) = v_{L1}(t) = v_{c2}(t) = L_m\frac{di_1}{dt} = V_s\cos\omega t - 2I_m\sqrt{\frac{L_m}{2C_m}}\sin\omega t \tag{8-84}$$

The reverse voltage across T_1 is

$$v_{ak}(t) = V_s - 2v_{L2} = V_s - 2V_s\cos\omega t + 4I_m\sqrt{\frac{L_m}{2C_m}}\sin\omega t \tag{8-85}$$

The available (or circuit) turn-off time can be determined from the condition $v_{ak}(t = t_q) = 0$ in Eq. (8-85), which after simplification gives

$$t_q = \sqrt{2(L_mC_m)}\left[\cos^{-1}\frac{1}{2(1 + x^2)^{1/2}} - \tan^{-1}x\right] \tag{8-86}$$

where

$$x = \frac{I_m}{V_s}\sqrt{\frac{2L_m}{C_m}} \tag{8-87}$$

The circuit turn-off time is dependent on the load current I_m and will be maximum when $I_m = 0$. The maximum value of t_q is

$$t_{q(\max)} = \frac{\pi}{3}\sqrt{2L_mC_m} \tag{8-88}$$

This mode ends when the voltage on capacitor C_2 becomes zero and $v_{c2}(t)$ tends to charge in opposite direction, and the time duration for this mode can be found from the condition $v_{L2}\ (t = t_{1m}) = v_{c2}\ (t = t_{1m}) = 0$, which is also the condition for peak thyristor current. From Eq. (8-84),

$$V_s \cos t_{1m} - 2I_m\sqrt{\frac{L_m}{2C_m}} \sin \omega t_{1m} = 0$$

or

$$t_m = t_{1m} = \sqrt{2L_mC_m}\tan^{-1}\frac{1}{x} \tag{8-89}$$

The thyristor current $i_1(t)$ becomes maximum at $t = t_m = t_{1m}$ and at the end of this mode,

$$i_1\ (t = t_{1m}) = I_1 = I_p \tag{8-90}$$

Mode 2. This mode begins when diode D_2 starts conducting. The equivalent circuit is shown in Fig. 8-32b. The energy stored in inductor L_2 is lost in the circuit formed by T_2, D_2, and L_2. The load current $i_L(t)$ $(= I_m)$ also flows through diode D_2. If V_d is the forward voltage drop of diode D_2 and thyristor T_2, the instantaneous current mode 2, $i_2(t)$, is given by

$$L_m\frac{di_2}{dt} + V_d = 0 \tag{8-91}$$

with initial condition $i_2\ (t = 0) = I_p$ and the solution of Eq. (8-91) is

$$i_2(t) = I_p - \frac{V_d}{L_m}t \tag{8-92}$$

This mode ends when $i_2(t)$ falls to zero and thyristor T_2 is turned off due to self-commutation. The duration of this mode is approximately

$$t_{2m} = \frac{I_pL_m}{V_d} \tag{8-93}$$

Mode 3. This mode begins when T_2 is turned off. The equivalent circuit

is shown in Fig. 8-32b. Diode D_2 continues to carry the load current until the load current falls to zero. The reverse voltage for T_2 is provided by the forward voltage drop of diode D_2.

Example 8-12

The single-phase complementary inverter in Fig. 8-32a has $L_1 = L_2 = L_m = 30$ μH, $C_m = 50$ μF, and the peak load current is $I_m = 175$ A. The dc input voltage is $V_s = 220$ V and the inverter frequency is $f_0 = 60$ Hz. The voltage drop of the circuit formed by thyristor T_2 and diode D_2 is, approximately, $V_d = 2$ V. Determine the (a) circuit turn-off time, t_q; (b) maximum circuit turn-off time, $t_{q(\max)}$ if $I_m = 0$; (c) the peak current of thyristors, I_p; (d) duration of commutation process, $t_c = t_{1m} + t_{2m}$; and (e) energy tapped in inductor L_2 at the end of mode 1.

Solution $V_s = 220$ V, $L_m = 30$ μH, $C_m = 50$ μF, and $I_m = 175$ A.

(a) From Eq. (8-87), $x = (175/220)\sqrt{2 \times 30/50} = 0.8714$. From Eq. (8-86),

$$t_q = \sqrt{2 \times 30 \times 50}\left[\cos^{-1}\frac{1}{2(1 + 0.8714^2)^{1/2}} - \tan^{-1}(0.8714)\right] = 25.6\ \mu s$$

(b) From Eq. (8-88), $t_{q(\max)} = (\pi/3)\sqrt{2 \times 30 \times 50} = 57.36$ μs.

(c) From Eq. (8-89), the time for the peak current is

$$t_m = t_{1m} = \sqrt{2 \times 30 \times 50}\tan^{-1}\frac{1}{0.8714} = 46.78\ \mu s$$

$$\omega = \frac{10^6}{\sqrt{2 \times 30 \times 50}} = 18{,}257\ \text{rad/s}$$

From Eqs. (8-82) and (8-90), the peak thyristor current is

$$I_p = 2 \times 175 \cos(1.8257 \times 0.4678) + 220\sqrt{2 \times \frac{50}{30}}\sin(1.8257 \times 0.4678) - 175 = 357.76\ \text{A}$$

(d) From Eq. (8-93), $t_{2m} = 175 \times 30/2 = 2625$ μs and the commutation time is

$$t_c = t_{1m} + t_{2m} = 46.78 + 2625 = 2671.78\ \mu s$$

(e) At the end of mode 1, the energy stored in inductor L_2 is

$$W = 0.5L_mI_p^2 = 0.5 \times 30 \times 10^{-6} \times 357.76^2 = 1.92\ \text{J}$$

Note. It takes a relatively long time to dissipate the energy and reduces the efficiency and output frequency of the inverter. Due to this energy dissipation in the power devices, there would be thermal problem. This trapped energy can be returned to the source by connecting a feedback transformer and diodes as shown in Fig. 8-33.

Example 8-13

If the turns ratio of feedback transformer in Fig. 8-33 is $N_1/N_2 = a = 0.1$, determine the (a) duration of commutation process, $t_c = t_{1m} + t_{2m}$; (b) energy trapped in inductor L_2 at the end of mode 1; and (c) peak thyristor current.

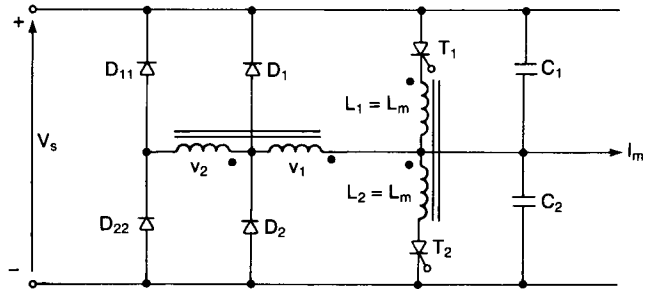


Figure 8-33 Complementary commutation with feedback windings.

Solution $V_s = 220$ V, $L_1 = L_2 = L_m = 30$ μH, $C = 50$ μF, and $I_m = 175$ A. From Eq. (8-87),

$$x = \frac{175}{220}\sqrt{\frac{2 \times 30}{50}} = 0.8714$$

$$\omega = \frac{10^6}{\sqrt{2 \times 30 \times 50}} = 18{,}257 \text{ rad/s}$$

(a) The commutation interval can be divided into two modes. The equivalent circuit for mode 1 is shown in Fig. 8-34a, which is the same as that in Fig. 8-32a. If v_1 and v_2 are the primary and secondary voltage of the feedback transformer, respectively, D_2 and D_{11} would conduct if

$$v_2 \le V_s \quad \text{or} \quad v_1 \le aV_s$$
$$v_1 = av_2 \tag{8-94}$$

where a is the turns ratio of the transformer and $a \le 1$. For D_2 and D_{11} to conduct,

$$v_1 = v_{L1} = v_{L2} = -aV_s \tag{8-95}$$

The duration of mode 1 can be found from Eq. (8-84):

$$v_{L2}(t = t_{1m}) = V_s \cos \omega t_{1m} - 2I_m \sqrt{\frac{L_m}{2C_m}} \sin \omega t_{1m} = -aV_s$$

and solving for t_{1m} yields

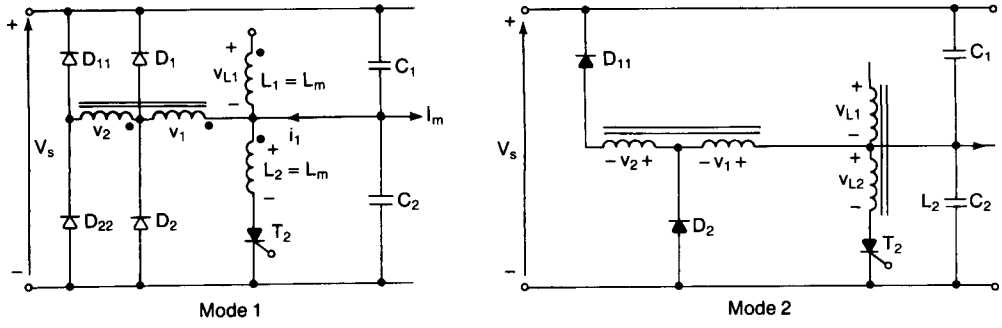
$$t_{1m} = \sqrt{2L_mC_m} \sin^{-1} \frac{a}{(1 + x^2)^{1/2}} + \sqrt{2L_mC_m} \tan^{-1} \frac{1}{x}$$
$$= 50.91 \text{ μs} \tag{8-96}$$

This mode ends when D_2 and D_{11} conducts. At the end of mode 1, Eq. (8-82) gives the current in thyristor T_2:

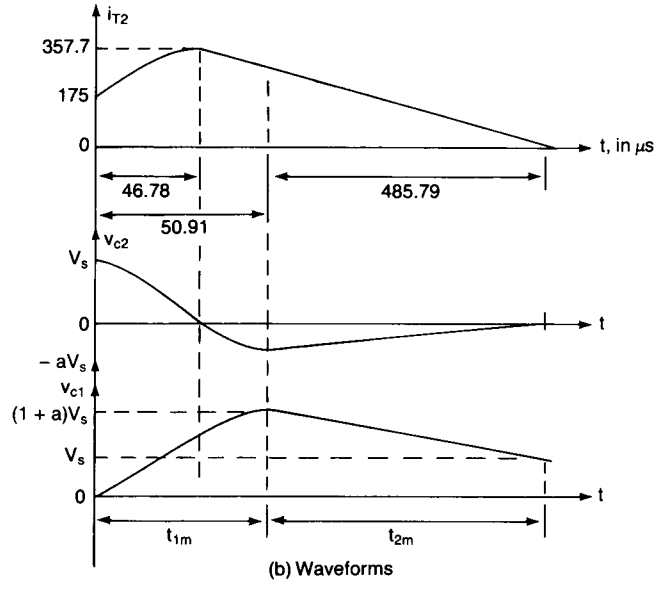
$$i_1(t = t_{1m}) = I_1 \tag{8-97}$$

From Eqs. (8-82) and (8-97),

$$I_1 = 2 \times 175 \cos(1.8257 \times 0.5091) + 220\sqrt{2 \times \frac{50}{30}} \sin(1.8257 \times 0.5091)$$
$$- 175 = 356.24 \text{ A}$$



(a) Equivalent circuits



(b) Waveforms

Figure 8-34 Equivalent circuits and waveforms for Example 8-13.

The voltage on capacitor C_2,

$$\begin{aligned} V_{c2} &= V_{L2} = -aV_s \\ &= -0.1 \times 220 = -22 \text{ V} \end{aligned} \tag{8-98}$$

The voltage on capacitor C_1,

$$\begin{aligned} V_{c1} &= V_s - V_{c2} = (1 + a)V_s \\ &= 1.1 \times 220 = 242 \text{ V} \end{aligned} \tag{8-99}$$

Mode 2 begins when D_2 and D_{11} conduct and the voltage of inductor L_2 is clamped to $-aV_s$. The equivalent circuit is shown in Fig. 8-34b.

$$L_m \frac{di_2}{dt} = -av_2 = -aV_s \tag{8-100}$$

with initial condition $i_2\ (t = 0) = I_1$ and the solution of Eq. (8-100) yields

$$i_2(t) = I_1 - \frac{aV_s}{L_m} t \tag{8-101}$$

Mode 2 ends when $i_2(t)$ becomes zero at $t = t_{2m}$ and

$$\begin{aligned} t_{2m} &= \frac{L_m I_1}{aV_s} \\ &= 30 \times 10^{-6} \times \frac{356.24}{0.1 \times 220} = 485.79\ \mu s \end{aligned} \tag{8-102}$$

The commutation time is

$$t_c = t_{1m} + t_{2m} = 50.91 + 485.79 = 536.7\ \mu s$$

(b) At the end of mode 1, the energy stored in inductor L_2 is

$$W = 0.5 L_m I_1^2 = 0.5 \times 30 \times 10^{-6} \times 356.24^2 = 1.904\ J$$

(c) From Eq. (8-89), $t_m = 46.78\ \mu s$, and from Eq. (8-98), $I_p = 357.76$ A.

Note. The trapped energy is returned to the supply. The commutation time can be reduced by lowering the turns ratio a; this would increase the voltage ratings of feedback diodes.

8-11 CURRENT-SOURCE INVERTERS

In the previous sections the inverters are fed from a voltage source and the load current is forced to fluctuate from positive to negative, and vice versa. To cope with inductive loads, the power switches with a freewheeling diodes are required, whereas in a current-source inverter, the input behaves as a current source. The output current is maintained constant irrespective of load on the inverter and the output voltage is forced to change. The circuit diagram of a single-phase transistorized inverter is shown in Fig. 8-35a. Since there must be a continuous current flow from the source, two switches must always conduct—one from the upper and one from the lower switches. The conduction sequence is 12, 23, 34, and 41. The output current waveform is shown in Fig. 8-35b. The diodes in series with the transistors are required to block the reverse voltages on the transistors.

With a current-source inverter, the commutation circuits for thyristors require only capacitors and are simpler, as shown in Fig. 8-35c. Let us assume that T_1 and T_2 are conducting and capacitors C_1 and C_2 are charged with polarity as shown. Firing of thyristors T_3 and T_4 reverse biases thyristors T_1 and T_2. T_1 and T_2 are turned off. The current now flows through $T_3 C_1 D_1$, load, and $D_2 C_2 T_4$. The capacitors C_1 and C_2 are discharged and recharged at a constant rate determined by load current, $I_m = I_L$. When the current through C_1 and C_2 falls to zero, the load current will be transferred from diode D_1 to D_3 and D_2 to D_4. D_1 and D_2 will be tuned off when the load current is completely reversed. The capacitor is now ready to turn off T_3 and T_4 if thyristors T_1 and T_2 are fired in the next half-

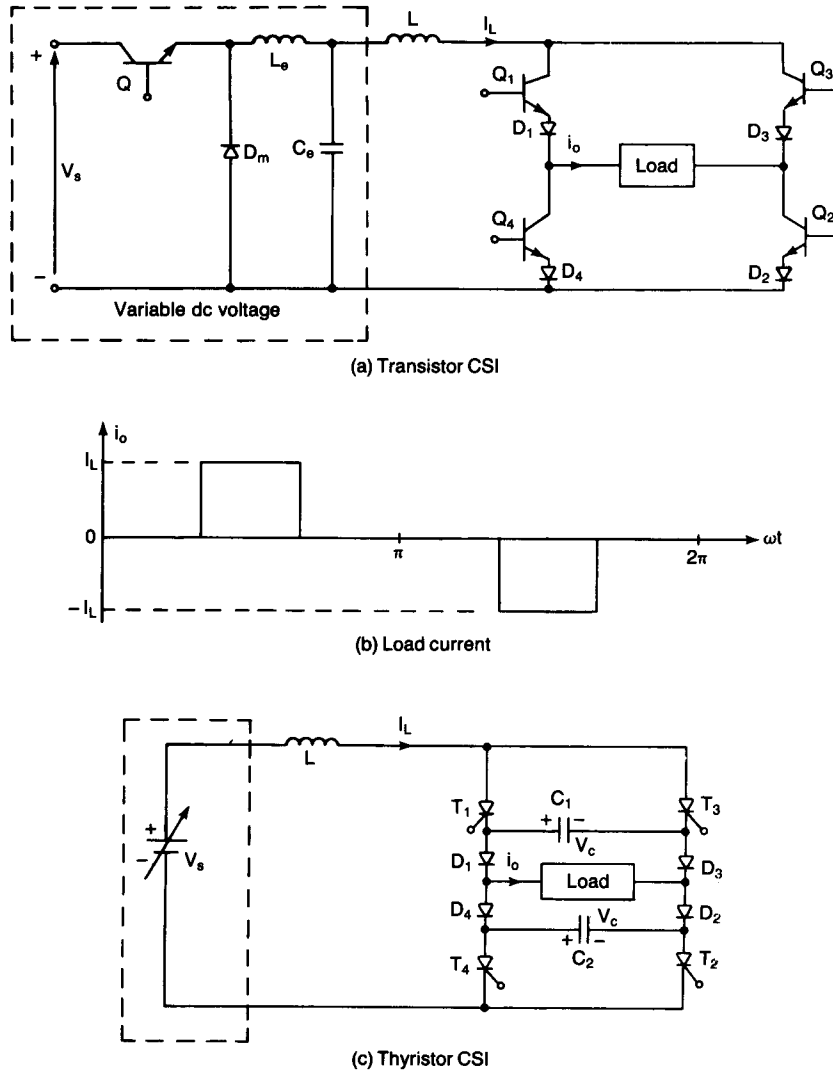
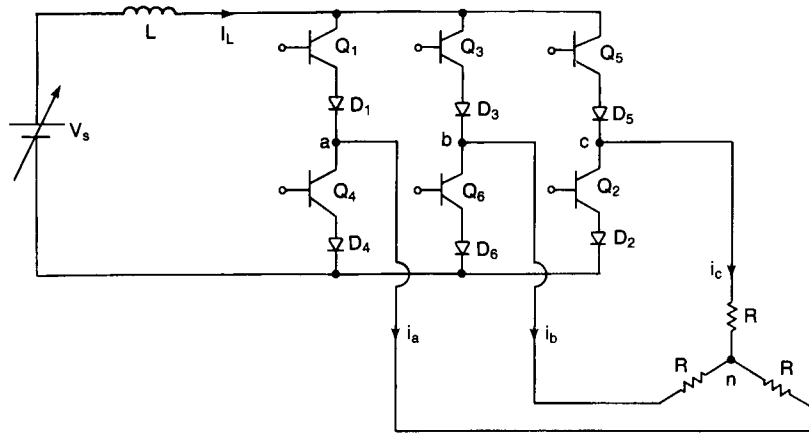


Figure 8-35 Single-phase current source inverter.

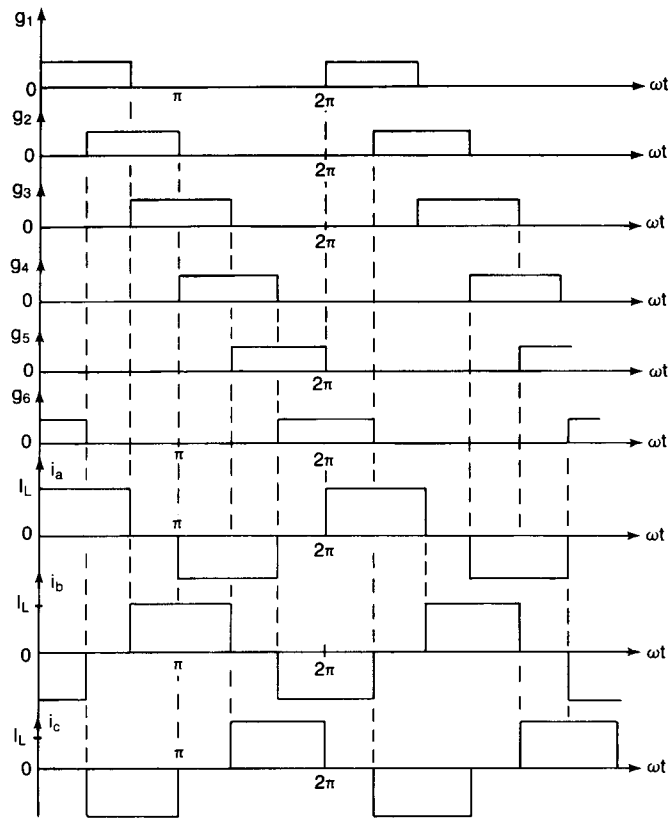
cycle. The commutation time will depend on the load current and load voltage. The diodes in Fig. 8-35c isolate the capacitors from the load voltage.

Figure 8-36a shows the circuit diagram of a three-phase current-source inverter. The waveforms for gating signals and line currents for a wye-connected load are shown in Fig. 8-36b. At any instant, only two thyristors conduct at the same time.

The currrent-source inverter (CSI) is a dual of a voltage-source inverter (VSI). The line-to-line voltage of a VSI is similar in shape to the line current of a CSI. The advantages of the CSI are: (1) since the input dc current is controlled and limited, misfiring of switching devices, or a short circuit, would not be serious



(a) Circuit



(b) Waveforms

Figure 8-36 Three-phase current source transistor inverter.

problems: (2) the peak current of power devices is limited; (3) the commutation circuits for thyristors are simpler; and (4) it has the ability to handle reactive or regenerative load without freewheeling diodes.

A CSI requires a relatively large reactor to exhibit current-source characteristics and an extra converter stage to control the current. The dynamic response is slower. Due to current transfer from one pair of switches to another, an output filter is required to suppress the output voltage spikes.

8-12 VARIABLE DC LINK INVERTER

The output voltage of an inverter can be controlled by varying the modulation index (or pulse widths) and maintaining the dc input voltage constant; but in this type of voltage control, a range of harmonics would be present on the output voltage. The pulse widths can be maintained fixed to eliminate or reduce certain harmonics and the output voltage can be controlled by varying the level of dc input voltage. Such an arrangement as shown in Fig. 8-37 is known as a *variable dc link inverter*. This arrangement requires an additional converter stage; and if it is a chopper, the power cannot be fed back to the dc source.

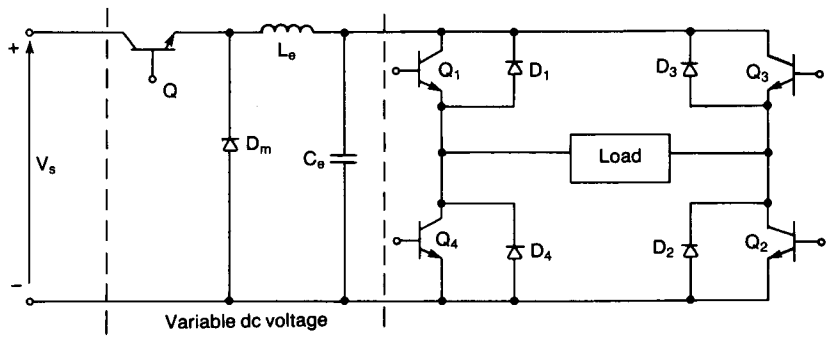


Figure 8-37 Variable dc link inverter.

8-13 INVERTER CIRCUIT DESIGN

The determination of voltage and current ratings of power devices in inverter circuits depends on the types of inverters, load, and methods of voltage and/current control. The design requires (1) deriving the expressions for the instantaneous load current, and (2) plotting the current waveforms for each device and component. Once the current waveform is known, the techniques for calculating the ratings of power devices and commutation components are similar to that in Sections 3-4 and 7-8. The evaluation of voltage ratings requires establishing the reverse voltages of each device.

To reduce the output harmonics, output filters are necessary. Figure 8-38 shows the commonly used output filters. A C-filter is very simple, but it draws

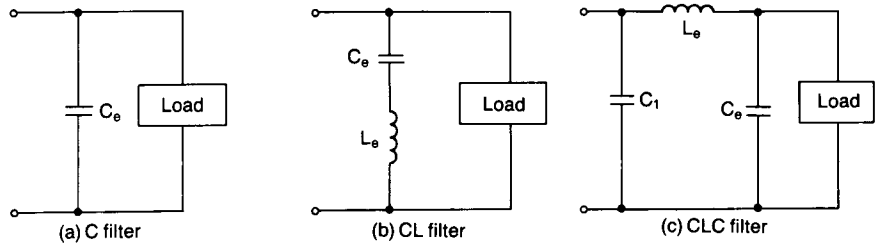


Figure 8-38 Output filters.

more reactive power. An *LC*-tuned filter as in Fig. 8-38b can eliminate only one frequency. A properly designed *CLC* filter as in Fig 8-38c is more effective in reducing harmonics of wide bandwidth and draws less reactive power.

Example 8-14

The single-phase auxiliary-commutated full-bridge inverter in Fig. 8-31a supplies a load of $R = 10\ \Omega$, $L = 31.5$ mH, and $C = 112\ \mu$F. The dc input voltage is $V_s = 220$ V and the inverter frequency is $f_o = 60$ Hz. The turn-off time of thyristors, $t_{off} = 25\ \mu$s. The output voltage has two notches such that third and fifth harmonics are eliminated. Determine the (a) expression for the load current, $i_o(t)$; (b) optimum values of commutation capacitor C_m and inductor L_m to minimize the energy; and (c) peak currents of thyristors T_1 and diode D_1.

Solution The output voltage waveform is shown in Fig. 8-18. $V_s = 220$ V, $f_o = 60$ Hz, $R = 10\ \Omega$, $L = 31.5$ mH, and $C = 112\ \mu$F. Let $t_q = t_{off} = 25\ \mu$s and $\omega = 2\pi \times 60 = 377$ rad/s.

The inductive reactance for the nth harmonic voltage is

$$X_L = j2n\pi \times 60 \times 31.5 \times 10^{-3} = j11.87n\ \Omega$$

The capacitive reactance for the nth harmonic voltage is

$$X_c = -\frac{j10^6}{2n\pi \times 60 \times 112} = -\frac{j23.68}{n}\Omega$$

The impedance for the nth harmonic voltage is

$$Z_n = \left[10^2 + \left(11.87n - \frac{23.6}{n}\right)^2\right]^{1/2}$$

and the power factor angle for the nth harmonic voltage is

$$\theta_n = \tan^{-1}\frac{11.87n - 23.6/n}{10} = \tan^{-1}\left(1.187n - \frac{2.346}{n}\right)$$

(a) Equation (8-37) gives the coefficients of a Fourier series,

$$A_n = \frac{4V_s}{\pi}\frac{1 - 2\cos n\alpha_1 + 2\cos n\alpha_2}{n}$$

For $\alpha_1 = 23.62°$ and $\alpha_2 = 33.3°$, the third and fifth harmonics would be absent. From Eq. (8-36) the instantaneous output voltage can be expressed as

$$v_o(t) = 235.1 \sin 377t + 69.4 \sin (7 \times 377t) + 85.1 \sin (9 \times 377t) + \cdots$$

Dividing the output voltage by the load impedance and considering the appropriate delay due to the power factor angles give the load current as

$$i_o(t) = 15.19 \sin (377t + 49.74°) + 0.86 \sin (7 \times 377t - 82.85°)$$
$$+ 1.09 \sin (9 \times 377t - 84.52°) + 0.66 \sin (11 \times 377t - 85.55°) + \cdots$$

(b) Neglecting the harmonics, the peak load current, $I_m = I_p = 15.19$ A. Equations (3-30) and (3-31) give the optimum values of L_m and C_m.

$$L_m = \frac{0.398 t_q V_o}{I_p} = \frac{0.398 \times 25 \times 10^{-6}}{15.19} V_o$$

$$C_m = \frac{0.8917 t_q I_p}{V_o} = \frac{0.8917 \times 25 \times 10^{-6} \times 15.19}{V_o}$$

From Eq. (8-77),

$$V_o = V_s + I_p \sqrt{\frac{L_m}{C_m}} = 220 + 15.19 \sqrt{\frac{L_m}{C_m}}$$

Solving for C_m and L_m yields $C_m = 0.52$ μF, $L_m = 431.7$ μH, and $V_o = 662.6$ V.

(c) The peak thyristor current, $I_p = 15.19$ A, and the peak resonant current,

$$I_{pk} = V_o \sqrt{\frac{C_m}{L_m}} = 662.6 \sqrt{\frac{0.52}{431.7}} = 22.77 \text{ A}$$

From Fig. 8-31b the peak diode current due to resonant oscillation is

$$I_{pd} = 22.77 - 15.19 = 7.58 \text{ A}.$$

Diode D_1 will carry both the inductive load current and resonant current. Although these two components would determine the rms and average currents of the diode, the peak diode current in this example should be the same as that of thyristor current, namely, 15.19 A.

Example 8-15

In Example 8-14, an output C-filter is used to eliminate seventh and higher-order harmonics. Determine the value of filter capacitor, C_e.

Solution $\omega_0 = 2\pi f = 2\pi \times 60 = 377$ rad/s. The nth and higher-order harmonics would be reduced significantly if the filter impedance is much smaller than that of the load, and a ratio of 1:10 is normally adequate,

$$Z_n = 10X_e$$

where the filter impedance is $X_e = 1/(377nC_e)$ and the load impedance is

$$Z_n = \left[10^2 + \left(11.87n - \frac{23.6}{n}\right)^2\right]^{1/2}$$

The value of filter capacitance C_e can be found from

$$\left[10^2 + \left(11.87n - \frac{23.6}{n}\right)^2\right]^{1/2} = \frac{10}{377nC_e}$$

For the seventh harmonic, $n = 7$ and $C_e = 47.3$ μF.

8-14 MAGNETIC CONSIDERATIONS

Inductors are used in thyristor commutation circuits and for resonant oscillation in resonant inverters. The resonant frequency is usually very very high. The magnetic loss is dependent on the frequency and these inductors should be designed with magnetic cores of very high permeability to reduce the core losses. The output of inverters are normally isolated from the load by an output transformer. The inverter output voltage normally contain harmonics and the transformer losses are increased. A transformer, which is designed to operate at purely sinusoidal voltages, would be subjected to higher losses and it should be derated when it is being operated from the output voltages of inverters. The output voltage should have no dc component; otherwise, the core may be saturated.

SUMMARY

Inverters can provide single-phase and three-phase ac voltages from a fixed or variable dc voltage. There are various voltage control techniques and they produce a range of harmonics on the output voltage. The sinusoidal pulse-width modulation (SPWM) is more effective in reducing the lower-order harmonics. With a proper choice of the switching patterns for power devices, certain harmonics can be eliminated.

The resonant inverters are normally used in high-frequency applications requiring fixed output voltage. The maximum resonant frequency is limited by the turn-off time of thyristors (or transistors). Due to the development of fast-switching power transistors and GTOs, the applications of forced-commutated thyristor inverters are limited to high power.

REFERENCES

1. B. D. Bedford, and R. G. Hoft, *Principle of Inverter Circuits*. New York: John Wiley & Sons, Inc., 1964.
2. H. S. Patel, and R. G. Hoft, "Generalized techniques of harmonic elimination and voltage control in thyristor converter." *IEEE Transactions on Industry Applications*. Vol. IA9, No. 3, 1973, pp. 310–317 and Vol. IA-10, No. 5, 1974, pp. 666–673.
3. T. Ohnishi and H. Okitsu, "A novel PWM technique for three-phase inverter/converter." *International Power Electronics Conference*, 1983, pp. 384–395.
4. M. F. Schlecht, "Novel topologies alternatives to the design of a harmonic-free utility/dc interface." *Power Electronic Specialist Conference*, 1983, pp. 206–216.
5. F. C. Schwarz, "An improved method of resonant current pulse modulation for power converters." *IEEE Transactions on Industrial Electronics and Control Instrumentation*, Vol. IECI23, No. 2, 1976, pp. 133–141.
6. J. Vitnis, A. Schweizer, and J. L. Steiner, "Reverse conducting thyristors for high power series resonant circuits." *IEEE Industry Applications Society Conference Record*, 1985, pp. 715–722.

7. D. M. Divan, "Design considerations for very high frequency resonant mode dc/dc converters." *IEEE Industry Applications Society Conference Record*, 1986, pp. 640–647.
8. A. K. S. Bhat and S. B. Dewan, "A generalized approach for the steady state analysis of resonant inverters." *IEEE Industry Applications Society Conference Record*, 1986, pp. 664–671.
9. P. D. Ziogas, V. T. Ranganathan, and V. R. Stefanovic, "A four-quadrant current regulated converter with a high frequency link." *IEEE Transactions on Industry Applications*, Vol. IA18, No. 5, 1982, pp. 499–505.

REVIEW QUESTIONS

8-1. What is an inverter?
8-2. What is the principle of operation of an inverter?
8-3. What are the types of inverters?
8-4. What are the differences between half-bridge and full-bridge inverters?
8-5. What are the performance parameters of inverters?
8-6. What are the purposes of feedback diodes in inverters?
8-7. What are the arrangments for obtaining three-phase output voltages?
8-8. What are the methods for voltage control within the inverters?
8-9. What are the advantages and disadvantages of displacement-angle control?
8-10. What are the techniques for harmonic reductions?
8-11. What are the effects of eliminating lower-order harmonics?
8-12. What is the principle of series resonant inverters?
8-13. What is the dead zone of a resonant inverter?
8-14. What is the effect of thyristor turn-off time on inverter frequency?
8-15. What are the advantages and disadvantages of resonant inverters with bidirectional switches?
8-16. What are the advantages and disadvantages of resonant inverters with unidirectional switches?
8-17. What is the necessary condition for series resonant oscillation?
8-18. What is the purpose of coupled inductors in half-bridge resonant inverters?
8-19. What are the advantages of reverse-conducting thyristors in resonant inverters?
8-20. What are the advantages and disadvantages of transistorized inverters compared to thyristor inverters?
8-21. What is overlap control of resonant inverters?
8-22. What is nonoverlap control of inverters?
8-23. What is the principle of auxiliary commutated inverters?
8-24. What is the principle of complimentary commutated inverters?
8-25. What is the purpose of feedback transformer in complementary commutated inverters?
8-26. What are the advantages and disadvantages of current-source inverters?
8-27. What are the main differences between voltage-source and current-source inverters?

8-28. What are the main advantages and disadvantages of variable dc link inverters?

8-29. What are the reasons for adding a filter on the inverter output?

8-30. What are the differences between ac and dc filters?

PROBLEMS

8-1. A single-phase half-bridge inverter in Fig. 8-1a has a resistive load of $R = 10\ \Omega$ and the dc input voltage is $V_s = 220$ V. Determine the (**a**) rms output voltage at the fundamental frequency, V_1; (**b**) output power, P_o; (**c**) average, rms, and peak currents of each transistor; (**d**) peak off-state voltage of each transistor, V_B; (**e**) total harmonic distortion, THD; (**f**) distortion factor, DF; and (**g**) harmonic factor and distortion factor of the lowest-order harmonic.

8-2. Repeat Prob. 8-1 for the single-phase full-bridge inverter in Fig. 8-2a.

8-3. The full-bridge inverter in Fig. 8-2a has an *RLC* load with $R = 5\ \Omega$, $L = 10$ mH, and $C = 26\ \mu$F. The inverter frequency, $f_o = 400$ Hz, and the dc input voltage, $V_s = 220$ V. (**a**) Express the instantaneous load current in a Fourier series. Calculate the (**b**) rms load current at the fundamental frequency, I_1; (**c**) harmonic factor of the load current, HF; (**d**) average supply current I_s; and (**e**) average, rms, and peak currents of each transistor.

8-4. Repeat Prob. 8-3 for $f_o = 60$ Hz, $R = 4\ \Omega$, $L = 25$ mH, and $C = 10\ \mu$F.

8-5. Repeat Prob. 8-3 for $f_o = 60$ Hz, $R = 5\ \Omega$, and $L = 20$ mH.

8-6. The three-phase full-bridge inverter in Fig. 8-5a has a wye-connected resistive load of $R = 5\ \Omega$. The inverter frequency is $f_o = 400$ Hz and the dc input voltage is $V_s = 220$ V. Express the instantaneous phase voltages and phase currents in a Fourier series.

8-7. Repeat Prob. 8-6 for the line-to-line voltages and line currents.

8-8. Repeat Prob. 8-6 for a delta-connected load.

8-9. Repeat Prob. 8-7 for a delta-connected load.

8-10. The three-phase full-bridge inverter in Fig. 8-5a has a wye-connected load and each phase consists of $R = 5\ \Omega$, $L = 10$ mH, and $C = 25\ \mu$F. The inverter frequency is $f_o = 60$ Hz and the dc input voltage, $V_s = 220$ V. Determine the rms, average, and peak currents of the transistors.

8-11. The output voltage of a single-phase full-bridge inverter is controlled by pulse-width modulation with one pulse per half-cycle. Determine the required pulse width so that the fundamental component is 70% of dc input voltage.

8-12. A single-phase full-bridge inverter uses a uniform PWM with two pulses per half-cycle for voltage control. Plot the distortion factor, fundamental component, and lower-order harmonics against modulation index.

8-13. A single-phase full-bridge inverter, which uses a uniform PWM with two pulses per half-cycle, has a load of $R = 5\ \Omega$, $L = 15$ mH, and $C = 25\ \mu$F. The dc input voltage is $V_s = 220$ V. Express the instantaneous load current $i_o(t)$ in a Fourier series $M = 0.8$, $f_o = 60$ Hz.

8-14. A single-phase full-bridge inverter uses a uniform PWM with seven pulses per half-cycle for voltage control. Plot the distortion factor, fundamental component, and lower-order harmonics against the modulation index.

8-15. A single-phase full-bridge inverter uses an SPWM with seven pulses per half-cycle for voltage control. Plot the distortion factor, fundamental component, and lower-order harmonics against the modulation index.

8-16. Repeat Prob. 8-15 for the modified SPWM with two pulses per quarter-cycle.

8-17. A single-phase full-bridge inverter uses a uniform PWM with five pulses per half-cycle. Determine the pulse width if the rms output voltage is 80% of the dc input voltage.

8-18. A single-phase full-bridge inverter uses displacement-angle control to vary the output voltage and has one pulse per half-cycle, as shown in Fig. 8-16e. Determine the delay (or displacement) angle if the fundamental component of output voltage is 70% of dc input voltage.

8-19. A single-phase full-bridge inverter uses multiple notches and it is required to eliminate third, fifth, seventh, and eleventh harmonics from the output waveform. Determine the number of notches and their angles.

8-20. Repeat Prob. 8-19 to eliminate third, fifth, seventh, and ninth harmonics.

8-21. The basic series resonant inverter in Fig. 8-21a has $L_1 = L_2 = L = 25\ \mu H$, $C = 2\ \mu F$, and $R = 5\ \Omega$. The dc input voltage, $V_s = 220$ V and the output frequency, $f_o = 6.5$ kHz. The turn-off time of thyristors, $t_{off} = 15\ \mu s$. Determine the (**a**) available (or circuit) turn-off time, t_q; (**b**) maximum permissible frequency, f_{max}; (**c**) peak-to-peak capacitor voltage, V_{pp}; and (**d**) peak load current, I_p. (**e**) Sketch the instantaneous load current $i_0(t)$; capacitor voltage $v_c(t)$; and dc supply current $I_s(t)$. Calculate the (**f**) rms load current, I_o; (**g**) output power, P_o; (**h**) average supply current, I_s; and (**i**) average, peak, and rms currents of the thyristors.

8-22. The half-bridge resonant inverter in Fig. 8-23 uses nonoverlapping control. The inverter frequency is $f_0 = 8.5$ kHz. If $C_1 = C_2 = C = 2\ \mu F$, $L_1 = L_2 = L = 40\ \mu H$, $R = 2\ \Omega$, and $V_s = 220$ V. Determine the (**a**) peak supply current; (**b**) average thyristor current, I_A; and (**c**) rms thyristor current, I_R.

8-23. The resonant inverter in Fig. 8-27a has $C = 2\ \mu F$, $L = 30\ \mu H$, $R = 0$, and $V_s = 220$ V. The turn-off time of thyristor, $t_{off} = 12\ \mu s$. The output frequency, $f_o = 15$ kHz. Determine (**a**) peak supply current, I_{ps}; (**b**) average thyristor current, I_A; (**c**) rms thyristor current, I_R; (**d**) peak-to-peak capacitor voltage, V_c; (**e**) maximum permissible output frequency, f_{max}; and (**f**) average supply current, I_s.

8-24. The half-bridge resonant inverter in Fig. 8-28a is operated at frequency, $f_0 = 3.5$ kHz in the nonoverlap mode. If $C_1 = C_2 = C = 2\ \mu F$, $L_1 = L_2 = L = 20\ \mu H$, $R = 1.5\ \Omega$, and $V_s = 220$ V, determine the (**a**) peak supply current, I_{ps}; (**b**) average thyristor current, I_A; (**c**) rms thyristor current, I_R; (**d**) rms load current, I_o; and (**e**) average supply current, I_s.

8-25. Repeat Prob. 8-24 with an overlapping control so that the firing of T_1 and T_2 are advanced by 50% of the resonant frequency.

8-26. The full-bridge resonant inverter in Fig. 8-29a is operated at a frequency of $f_0 = 3.5$ kHz. If $C = 2\ \mu F$, $L = 20\ \mu H$, $R = 1.5\ \Omega$, and $V_s = 220$ V, determine the (**a**) peak supply current, I_s; (**b**) average thyristor current, I_A; (**c**) rms thyristor current, I_R; (**d**) rms load current, I_o; and (**e**) average supply current, I_s.

8-27. The single-phase full-bridge auxiliary-commutated inverter in Fig. 8-31a has a load of $R = 5\ \Omega$, $L = 10$ mH, and $C = 25\ \mu F$. The input dc voltage is $V_s = 220$ V and the inverter frequency is $f_0 = 60$ Hz. tq = 18 μs. Determine the optimum values of commutation components C_m and L_m.

8-28. Repeat Prob. 8-27 if the peak resonant current of the commutation circuit is limited to two times the peak load current.

8-29. A single-phase full-bridge inverter in Fig. 8-32a, which uses complementary commutation, has $L_1 = L_2 = L_m = 40$ μH and $C_m = 60$ μF. The peak load current is $I_m = 200$ A. The dc input voltage, $V_s = 220$ V and the inverter frequency, $f_0 = 60$ Hz. The voltage drop of the circuit formed by thyristor T_2 and diode D_2 is, approximately, $V_d = 2$ V. Determine the (**a**) circuit turn-off time, t_q; (**b**) maximum available turn-off time, $t_{q(\max)}$ if $I_m = 0$; (**c**) peak current of thyristors; (**d**) duration of commutation process, $t_c = t_{1m} + t_{2m}$; and (**e**) energy trapped in inductor L_2 at the end of mode 1.

8-30. The inverter in Prob. 8-29 has a feedback transformer as shown in Fig. 8-33. The turns ratio of the feedback windings is $N_1/N_2 = a = 0.1$. Determine the (**a**) duration of commutation process, $t_c = t_{1m} + t_{2m}$; (**b**) energy trapped in inductor L_2 at the end of mode 1; and (**c**) peak thyristor current.

8-31. Repeat Prob. 8-30 if $a = 1.0$.

8-32. Repeat Prob. 8-30 if $a = 0.01$.

8-33. A single-phase auxiliary-commutated full-bridge inverter in Fig. 8-31a supplies a load of $R = 5\ \Omega$, $L = 15$ mH, and $C = 30$ μF. The dc input voltage is $V_s = 220$ V and the inverter frequency is $f_0 = 400$ Hz. The turn-off time of thyristors is $t_{\text{off}} = 20$ μs. The output voltage has two notches such that third and fifth harmonics are eliminated. Determine the (**a**) expression for the instantaneous load current, $i_0(t)$; (**b**) optimum values of commutation capacitor C_m and inductor L_m to minimize the energy; and (**c**) average, rms, and peak currents of thyristor T_1 and diode D_1.

8-34. If in Prob. 8-33, a tuned LC filter is used to eliminate the seventh harmonic from the output voltage, determine the suitable values of filter components.

8-35. The single-phase auxiliary-commutated full-bridge inverter in Fig. 8-31a supplies a load of $R = 2\ \Omega$, $L = 25$ mH, and $C = 40$ μF. The dc input voltage is $V_s = 220$ V and the inverter frequency, $f_0 = 60$ Hz. The turn-off time of thyristors, $t_{\text{off}} = 15$ μs. The output voltage has three notches such that the third, fifth, and seventh harmonics are eliminated. Determine the (**a**) expression for the instantaneous load current, $i_0(t)$; and (**b**) values of commutation capacitor C_m and inductor L_m if the peak resonant current is limited to 2.5 times the peak load current.

8-36. If in Prob. 8-35, an output C-filter is used to eliminate ninth and higher-order harmonics, determine the value of filter capacitor, C_e.



9

Power Supplies

9-1 INTRODUCTION

Power supplies, which are used extensively in industrial applications, are often required to meet all or most of the following specifications:

1. Isolation between the source and load
2. High power density for reduction of size and weight
3. Controlled direction of power flow
4. High conversion efficiency
5. Input and output waveforms with a low total harmonic distortion for small filters
6. Controlled power factor if the source is an ac voltage

The single-stage ac–dc or ac–ac or dc–dc or dc–ac converters discussed in Chapters 4, 6, 7, and 8, respectively, do not meet most of these specifications, and multistage conversions are normally required. There are various possible conversion topologies, depending on the permissible complexity and the design requirements. Only the basic topologies are discussed in this chapter. Depending on the type of output voltages, the power supplies can be categorized into two types:

1. Dc power supplies
2. Ac power supplies

9-2 DC POWER SUPPLIES

The ac–dc converters in Chapter 4 can provide the isolation between the input and output through an input transformer, but the harmonic contents are high. The switched-mode regulators in Section 7-6 do not provide the necessary isolation and the output power is low. The common practice is to use two-stage conversions, dc–ac and ac–dc. In case of ac input, it is three-stage conversions, ac–dc, dc–ac, and ac–dc. The isolation is provided by an interstage transformer. The dc–ac conversion can be accomplished by PWM or resonant oscillation. Based on the type of conversion techniques and the direction of power control, the dc power supplies can be subdivided into three types:

1. Switched-mode power supplies
2. Resonant power supplies
3. Bidirectional power supplies

9-2.1 Switched-Mode DC Power Supplies

There are four common configurations with the switched-mode or PWM operation of the inverter (or dc–ac converter) stage: flyback, push-pull, half-bridge, and full-bridge. The output of the inverter, which is varied by a PWM technique, is converted to a dc voltage by a diode rectifier. Since the inverter can operate at a very high frequency, the ripples on the dc output voltage can be filtered out with small filters.

The circuit topology for the *flyback* converter is shown in Fig. 9-1a. When transistor Q_1 is turned on, the supply voltage appears across the transformer primary and a corresponding voltage is induced in the secondary. When Q_1 is off, a voltage of opposite polarity is induced in the primary by the secondary due to the transformer action. The minimum open-circuit voltage of the transistor is $V_{oc} = 2V_s$. If I_s is the average input current with negligible ripple and the duty cycle is $k = 50\%$, the peak transistor current is $I_p = I_s/k = 2I_s$. The input current is pulsating and discontinuous. Without diode D_2, a dc current flows through the transformer. When Q_1 is off, diode D_2 and capacitor C_1 reset the transformer core. C_1 discharges through R_1, when D_2 is off and an energy is lost in every cycle. This circuit is very simple and is restricted to applications below 500 W. This is a forward converter and it requires a voltage control feedback loop.

The transformer core can also be reset by having a reset winding as shown in Fig. 9-1b, where the energy stored in the transformer core is returned to the supply and the efficiency is increased. The open-circuit voltage of the transistor in Fig. 9-1b is

$$V_{oc} = V_s\left(1 + \frac{N_p}{N_r}\right) \tag{9-1}$$

where N_p and N_r are the number of turns on the primary and reset windings, respectively. The reset turns ratio is related to the duty cycle as

$$a_r = \frac{N_r}{N_p} = \frac{1 - k}{k} \tag{9-2}$$

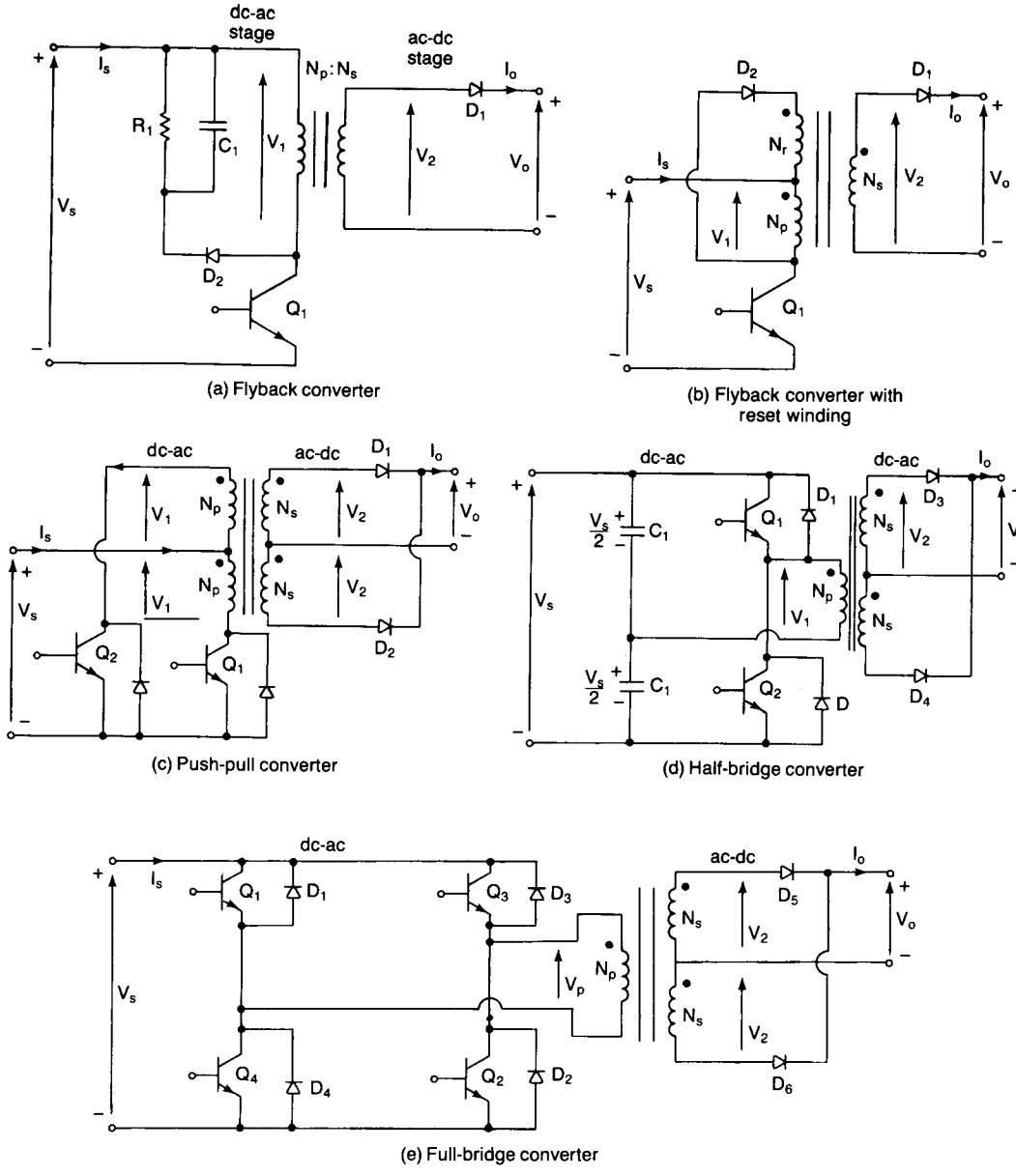


Figure 9-1 Configurations for switched-mode dc power supplies.

For a duty cycle of $k = 0.8$, $N_p/N_r = 0.8/0.2 = 4$ and the open-circuit voltage becomes $V_{oc} = V_s(1 + 4) = 5V_s$. The open-circuit voltage of the transistor is much higher that the supply voltage.

The push-pull configuration is shown in Fig. 9-1c. When Q_1 is turned on, V_s appears across one-half of the primary. When Q_2 is turned on, V_s is applied across the other half of the transformer. The voltage of a primary winding swings from $-V_s$ to V_s. The average current through the transformer should ideally be zero. The average output voltage is

$$V_o = V_2 = \frac{N_s}{N_p} V_1 = aV_1 = aV_s \tag{9-3}$$

Transistors Q_1 and Q_2 operate with a 50% duty cycle. The open-circuit voltage, $V_{oc} = 2V_s$, the average current of a transistor, $I_A = I_s/2$, and the peak transistor current, $I_p = I_s$. Since the open-circuit transistor voltage is twice the supply voltage, this configuration is suitable for low-voltage applications.

The half-bridge circuit is shown in Fig. 9-1d. When Q_1 is on, $V_s/2$ appears across the transformer primary. When Q_2 is on, a reverse voltage of $V_s/2$ appears across the transformer primary. The primary voltage swings from $-V_s/2$ to $V_s/2$. The open-circuit transistor voltage is $V_{oc} = V_s$ and the peak transistor current is $I_p = 2I_s$. The average transistor current is $I_A = I_s$. In high-voltage applications, the half-bridge circuit is preferable to the push-pull circuit. Whereas for low-voltage applications, the push-pull circuit is preferable due to low transistor currents. The average output voltage is

$$V_o = V_2 = \frac{N_s}{N_p} V_1 = aV_1 = 0.5aV_s \tag{9-4}$$

The full-bridge arrangement is shown in Fig. 9-1e. When Q_1 and Q_2 are turned on, V_s appears the primary. When Q_3 and Q_4 are turned on, the primary voltage is reversed to $-V_s$. The average output voltage is

$$V_o = V_2 = \frac{N_s}{N_p} V_1 = aV_1 = aV_s \tag{9-5}$$

The open-circuit transistor voltage is $V_{oc} = V_s$ and the peak transistor current is $I_p = I_s$. The average current of a transistor is only $I_A = I_s/2$. Of all the configurations, this circuit operates with the minimum voltage and current stress of the transistors, and it is very popular for high-power applications above 750 W.

Example 9-1

The average (or dc) output voltage of the push-pull circuit in Fig. 9-1c is $V_o = 24$ V at a resistive load of $R = 0.8\ \Omega$. The on-state voltage drops of transistors and diodes are $V_t = 1.2$ V and $V_d = 0.7$ V, respectively. The turns ratio of the transformer is $a = N_s/N_p = 0.25$. Determine the (a) average input current, I_s; (b) efficiency, η; (c) average transistor current, I_A; (d) peak transistor current, I_p; (e) rms transistor current, I_R; and (f) open-circuit transistor voltage, V_{oc}. Neglect the losses in the transformer, and the ripple current of the load and input supply is negligible.

Solution $a = N_s/N_p = 0.25$ and $I_o = V_o/R = 24/0.8 = 30$ A.

(a) The output power, $P_o = V_oI_o = 24 \times 30 = 720$ W. The secondary voltage, $V_2 = V_o + V_d = 24 + 0.5 = 24.5$ V. The primary voltage, $V_1 = V_2/a = 24.5/0.25 = 98$ V. The input voltage, $V_s = V_1 + V_l = 98 + 1.2$, and the input power,

$$P_i = V_sI_s = 1.2I_A + 1.2I_A + V_dI_o + P_o$$

Substituting $I_A = I_s/2$ gives

$$I_s(99.2 - 1.2) = 0.5 \times 30 + 720$$

$$I_s = \frac{735}{98.0} = 7.44 \text{ A}$$

(b) $P_i = V_sI_s = 100 \times 7.44 = 744$ W. The efficiency, $\eta = 720/744 = 96.7\%$.
(c) $I_A = I_s/2 = 7.44/2 = 3.72$ A.
(d) $I_p = I_s = 7.44$ A.
(e) $I_R = \sqrt{k}\, I_p = \sqrt{0.5} \times 7.44 = 10.52$ A.
(f) $V_{oc} = 2V_s = 2 \times 100 = 200$ V.

9-2.2 Resonant DC Power Supplies

If the variation of the dc output voltage is not wide, resonant pulse inverters can be used. The inverter frequency, which could be the same as the resonant frequency, is very high, and the inverter output voltage is almost sinusoidal. Due to resonant oscillation, the transformer core is always reset and there are no dc saturation problems. The half-bridge and full-bridge configurations of the resonant inverters are shown in Fig. 9-2. The sizes of the transformer and output filter are reduced due to high inverter frequency.

Example 9-2

The average output voltage of the half-bridge circuit in Fig. 9-2a is $V_o = 24$ V at a resistive load of $R = 0.8\ \Omega$. The inverter operates at the resonant frequency. The

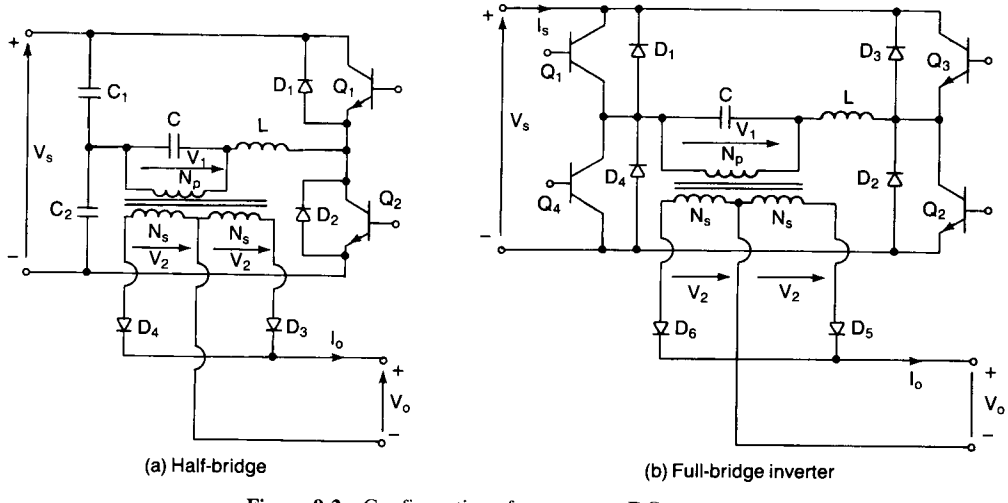


Figure 9-2 Configurations for resonant DC power supplies.

circuit parameters are $C_1 = C_2 = C = 1\ \mu F$, $L = 20\ \mu H$ and $R = 0$. The dc input voltage is $V_s = 100$ V. The on-state voltage drops of transistors and diodes are negligible. The turns ratio of the transformer is $a = N_s/N_p = 0.25$. Determine the (a) average input current, I_s; (b) average transistor current, I_A; (c) peak transistor current, I_p; (d) rms transistor current, I_R; and (e) open-circuit transistor voltage, V_{oc}. Neglect the losses in the transformer, and the effect of the load on the resonant frequency is negligible.

Solution The resonant frequency $\omega_r = 10^6/\sqrt{2 \times 20} = 158{,}113.8$ rad/s or $f_r = 25{,}164.6$ Hz, $a = N_s/N_p = 0.25$, and $I_o = V_o/R = 24/0.8 = 30$ A.

(a) The output power, $P_o = V_o I_o = 24 \times 30 = 720$ W. From Eq. (2-59), the rms secondary voltage, $V_2 = \pi V_o/(2\sqrt{2}) = 1.1107 V_o = 26.66$ V. The average input current, $I_s = 720/100 = 7.2$ A.

(b) The average transistor current, $I_A = I_s = 7.2$ A.

(c) For a sinusoidal pulse of current through the transistor, $I_A = I_p/\pi$ and the peak transistor current, $I_p = 7.2\pi = 22.62$ A.

(d) With a sinusoidal pulse of current with 180° conduction, the rms transistor current, $I_R = I_p/2 = 11.31$ A.

(e) $V_{oc} = V_s = 100$ V.

9-2.3 Bidirectional Power Supplies

In some applications, such as battery charging and discharging, it is desirable to have bidirectional power flow capability. A bidirectional power supply is shown in Fig. 9-3. The direction of the power flow will depend on the values of V_o, V_s, and turns ratio ($a = N_s/N_p$). For power flow from the source to the load, the inverter operates in the inversion mode if

$$V_o < aV_s \tag{9-6}$$

For power flow from the output to the input, the inverter operates as a rectifier if

$$V_o > aV_s \tag{9-7}$$

The bidirectional converters allows the inductive current to flow in either direction and the current flow becomes continuous.

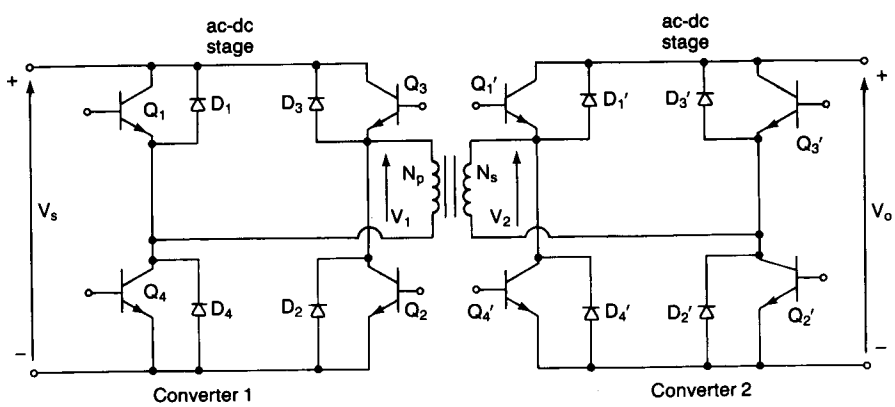


Figure 9-3 Bidirectional dc power supply.

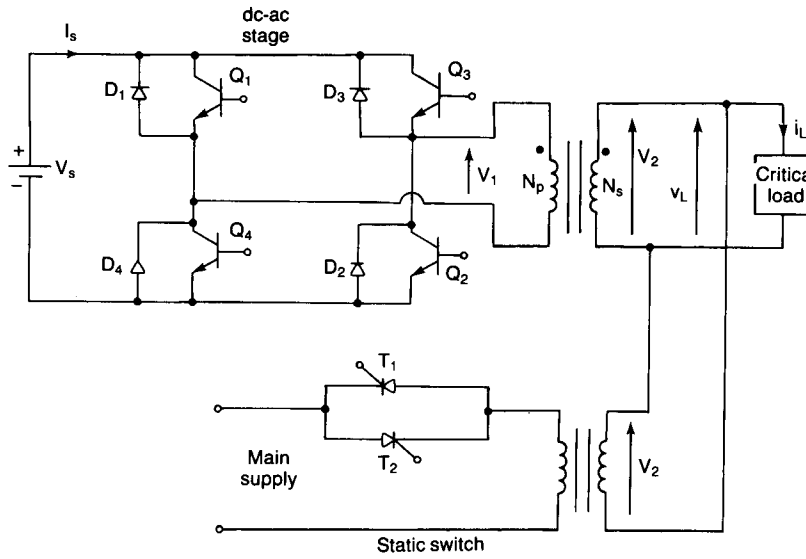


Figure 9-4 Arrangement of UPS systems.

9-3 AC POWER SUPPLIES

The ac power supplies are commonly used as standby sources for critical loads and in applications where normal ac supplies are not available. The standby power supplies are also know as uninterruptible power supply (UPS) systems. An arrangement of an UPS system is shown in Fig. 9-4, which consists of a battery, inverter, and static switch. In case of power failure, the battery supplies the inverter. When the main supply is on, the inverter operates as a rectifier and charges the battery. In this arrangement the inverter has to operate at the fundamental output frequency. Consequently, the high-frequency capability of the inverter is not utilized in reducing the size of the transformer. Similar to the dc power supplies, the ac power supplies can be categorized into three types:

1. Switched-mode ac power supplies
2. Resonant ac power supplies
3. Bidirectional ac power supplies

9-3.1 Switched-Mode AC Power Supplies

The size of the transformer in Fig. 9-4 can be reduced by the addition of a high-frequency dc link as shown in Fig. 9-5. There are two inverters. The input-side inverter operates with PWM at a very high frequency to reduce the size of the transformer and the dc filter at the input of the output-side inverter. The output-side inverter operates at the output frequency.

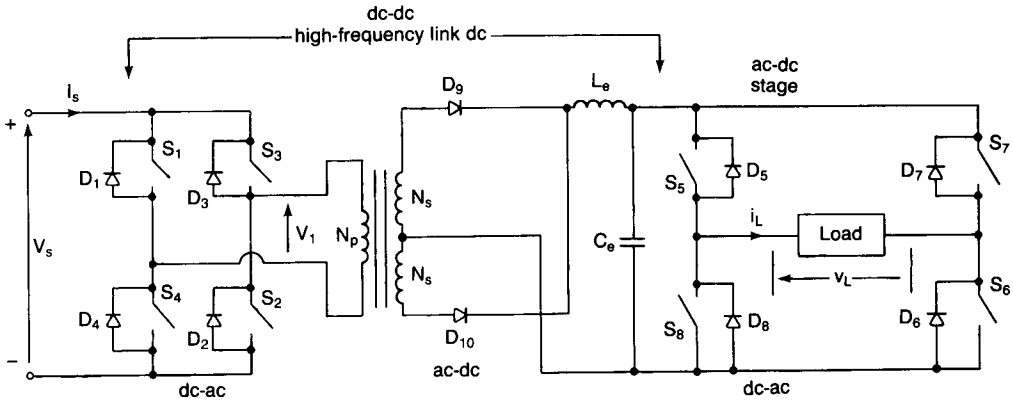


Figure 9-5 Switched-mode ac power supplies.

9-3.2 Resonant AC Power Supplies

The input-stage inverter in Fig. 9-5 can be replaced by a resonant inverter as shown in Fig. 9-6. The output-side inverter operates with PWM at the output frequency.

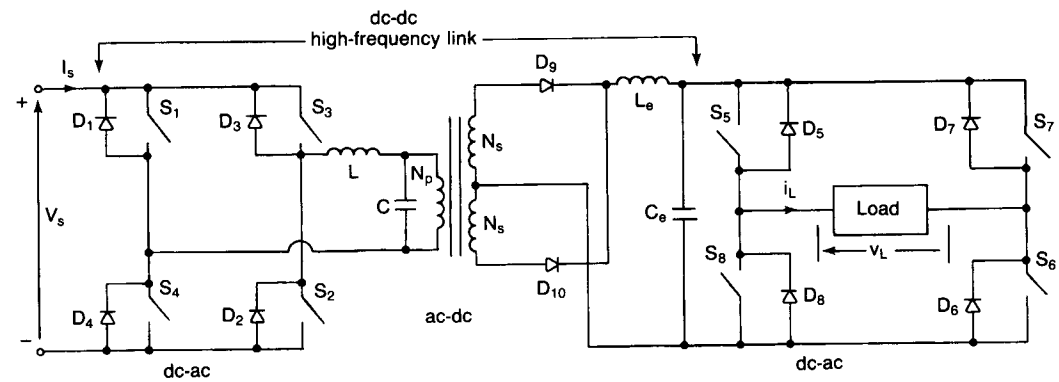


Figure 9-6 Resonant ac power supply.

9-3.3 Bidirectional AC Power Supplies

The diode rectifier and the output inverter can be combined by a cycloconverter with bidirectional switches as shown in Fig. 9-7. The cycloconverter converts the high-frequency ac to a low-frequency ac. The power flow can be controlled in either direction.

Example 9-3

The load resistance of the ac power supplies in Fig. 9-5 is $R = 2.5\ \Omega$. The dc output voltage is $V_s = 100$ V. The input inverter operates at a frequency of 20 kHz with one pulse per half-cycle. The on-state voltage drops of transistor switches and diodes

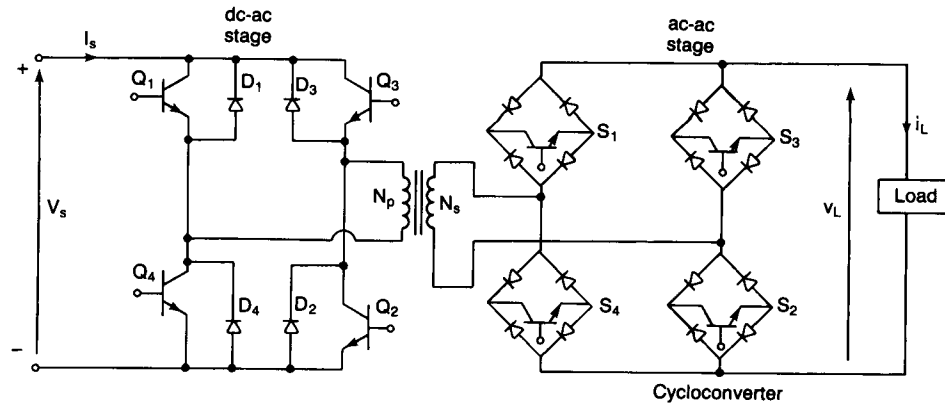


Figure 9-7 Bidirectional ac power supplies.

are negligible. The turns ratio of the transformer is $a = N_s/N_p = 0.5$. The output inverter operates with an uniform PWM of four pulses per half-cycle. The width of each pulse is $\delta = 18°$. Determine the rms load current. The ripple voltage on the output of the rectifier is negligible. Neglect the losses in the transformer, and the effect of the load on the resonant frequency is negligible.

Solution The rms output voltage of the input inverter is $V_1 = V_s = 100$ V. The rms transformer secondary voltage, $V_2 = aV_1 = 0.5 \times 100 = 50$ V. The dc voltage of the rectifier, $V_o = V_2 = 50$ V. With the pulse width of $\delta = 18°$, Eq. (8-18) gives the rms load voltage, $V_L = V_o\sqrt{(p\delta/\pi)} = 50\sqrt{4 \times 18/180} = 31.6$ V. The rms load current, $I_L = V_L/R = 31.6/2.5 = 12.64$ A.

9-4 MULTISTAGE CONVERSIONS

If the input is an ac source, an input-stage rectifier is required as shown in Fig. 9-8 and there are four conversions: ac–dc–ac–dc–ac. The rectifier and inverter pair can be replaced by a converter with bidirectional ac switches as shown in Fig. 9-9. The switching functions of this converter can be synthesized to combine the functions of the rectifier and inverter. This converter, which converts ac–ac di-

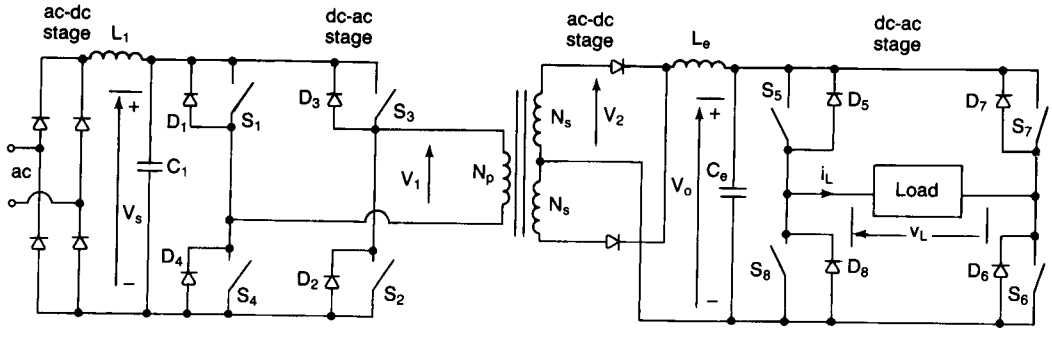


Figure 9-8 Multistage conversions.

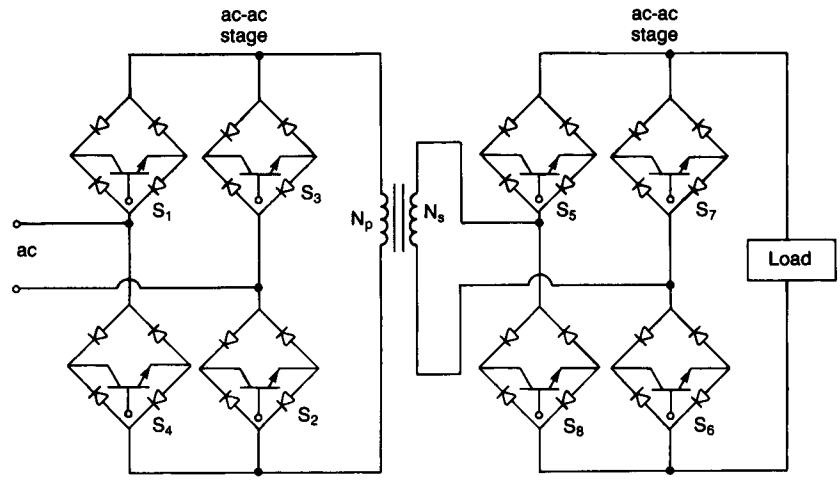


Figure 9-9 Cycloconverters with bilateral switches.

rectly, is called the forced commutated cycloconverter [3]. The ac–dc–ac–dc–ac conversions in Fig. 9-8 can be performed by two forced-commutated cycloconverters as shown in Fig. 9-9.

9-5 MAGNETIC CONSIDERATIONS

If there is any dc imbalance, the transformer core may saturate, resulting in a high magnetizing current. An ideal core should exhibit a very high relative permeability in the normal operating region and under dc imbalance conditions, it should not go into hard saturation. This problem of saturation can be minimized by having two permeability regions in the core, low and high permeability. An air gap may be inserted as shown in a toroid in Fig. 9-10a, where the inner part has high permeability and the outer part has relatively low permeability. Under normal operation the flux flows through the inner part. In case of saturation, the flux has to flow through the outer region, which has a lower permeability due to the air gap, and the core does not go into hard saturation. Two toroids with high and low permeability can be combined as shown in Fig. 9-10b.

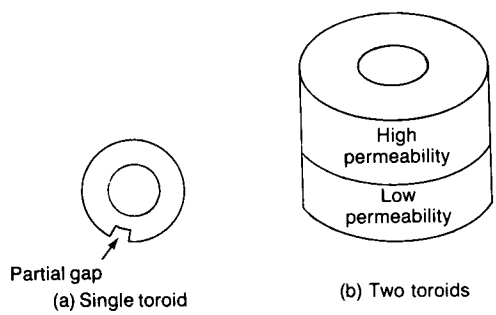


Figure 9-10 Cores with two permeability regions.

SUMMARY

Industrial power supplies are of two types: dc supplies and ac supplies. In a single-stage conversion, the isolating transformer has to operate at the output frequency. To reduce the size of the transformer and meet the industrial specifications, multistage conversions are normally required. There are various power supply topologies, depending on the output power requirement and acceptable complexity. Converters with bidirectional switches, which allow the control of power flow in either directions, require synthesizing the switching functions to obtain the desired output waveforms.

REFERENCES

1. R. E. Hnatek, *Design of Solid-State Power Supplies*. New York: Van Nostrand Reinhold Company, Inc., 1981.
2. S. Manias, and P. D. Ziogas, "A novel sine wave in ac–dc converter with high frequency transformer isolation." *IEEE Transactions on Industrial Electronics*, Vol. IE32, No. 4, 1985, pp. 430–438.
3. K. A. Haddad, T. Krishnan, and V. Rajagopaloan, "Dc to dc converters with high frequency ac link." *IEEE Transactions on Industry Applications*, Vol. IA22, No. 2, 1986, pp. 244–254.
4. P. D. Ziogas, S. I. Khan, and M. H. Rashid, "Analysis and design of cycloconverter structures with improved transfer characteristics." *IEEE Transactions on Industrial Electronics*, Vol. IE33, No. 3, 1986, pp. 271–280.
5. E. D. Weichman, P. D. Ziogas, and V. R. Stefanovic, "A novel bilateral power conversion scheme for variable frequency static power supplies." *IEEE Transactions on Industry Applications*, Vol. IA21, No. 5, 1985, pp. 1226–1233.
6. I. J. Pitel, "Phase-modulated resonant power conversion techniques for high frequency link inverters." *IEEE Industry Applications Society Conference Record*, 1985, pp. 1163–1172.

REVIEW QUESTIONS

9-1. What are the normal specifications of power supplies?
9-2. What the types of power supplies in general?
9-3. Name three types of dc power supplies.
9-4. Name three types of ac power supplies.
9-5. What the advantages and disadvantages of single-stage conversion?
9-6. What are the advantages and disadvantages of switched-mode power supplies?
9-7. What are the advantages and disadvantages of resonant power supplies?
9-8. What are the advantages and disadvantages of bidirectional power supplies?
9-9. What are the advantages and disadvantages of flyback converters?

9-10. What are the advantages and disadvantages of push-pull converters?

9-11. What are the advantages and disadvantages of half-bridge converters?

9-12. What are the various configurations of resonant dc power supplies?

9-13. What are the advantages and disadvantages of high-frequency link power supplies?

9-14. What is the general arrangement of UPS systems?

9-15. What are the problems of the transformer core?

PROBLEMS

9-1. The dc output voltage of the push-pull circuit in Fig. 9-1c, V_o = 24 V at a resistive load of R = 0.4 Ω. The on-state voltage drops of transistors and diodes are V_t = 1.2 V and V_d = 0.7 V, respectively. The turns ratio of the transformer, $a = N_s/N_p$ = 0.5. Determine the **(a)** average input current, I_s; **(b)** efficiency, η; **(c)** average transistor current, I_A; **(d)** peak transistor current, I_p; **(e)** rms transistor current, I_R; and **(f)** open-circuit transistor voltage, V_{oc}. Neglect the losses in the transformer, and the ripple current of the load and input supply is negligible.

9-2. Repeat Prob. 9-1 for the circuit in Fig. 9-1b, for k = 0.5.

9-3. Repeat Prob. 9-1 for the circuit in Fig. 9-1d.

9-4. Repeat Prob. 9-1 for the circuit in Fig. 9-1e.

9-5. The dc output voltage of the half-bridge circuit in Fig. 9-2a, V_o = 24 V at a load resistance of R = 0.8 Ω. The inverter operates at the resonant frequency. The circuit parameters are $C_1 = C_2 = C$ = 2 μF, L = 5 μH, and R = 0. The dc input voltage, V_s = 50 V. The on-state voltage drops of transistors and diodes are negligible. The turns ratio of the transformer, $a = N_s/N_p$ = 0.5. Determine the **(a)** average input current, I_s; **(b)** average transistor current, I_A; **(c)** peak transistor current, I_p; **(d)** rms transistor current, I_R; and **(e)** open-circuit transistor voltage, V_{oc}. Neglect the losses in the transformer, and the effect of the load on the resonant frequency is negligible.

9-6. Repeat Prob. 9-5 for the full-bridge circuit in Fig. 9-2b.

9-7. The load resistance of the ac power supplied in Fig. 9-4 is R = 1.5 Ω. The dc input voltage is V_s = 24 V. The input inverter operates at a frequency of 400 Hz with an uniform PWM of eight pulses per half-cycle and the width of each pulse is δ = 20°. The on-state voltage drops of transistor switches and diodes are negligible. The turns ratio of the transformer, $a = N_s/N_p$ = 4. Determine the rms load current. Neglect the losses in the transformer, and the effect of the load on the resonant frequency is negligible.

9-8. The load resistance of the ac power supplies in Fig. 9-5 is R = 1.5 Ω. The dc input voltage, V_s = 24 V. The input inverter operates at a frequency of 20 kHz with a uniform PWM of four pulses per half-cycle and the width of each pulse is δ_i = 40°. The on-state voltage drops of transistor switches and diodes are negligible. The turns ratio of the transformer, $a = N_s/N_p$ = 0.5. The output inverter operates with uniform PWM of eight pulses per half-cycle and the width of each pulse is δ_0 = 20°. Determine the rms load current. The ripple voltage on the output of the rectifier is negligible. Neglect the losses in the transformer, and the effect of the load on the resonant frequency is negligible.

10

DC Drives

10-1 INTRODUCTION

Direct current (dc) motors have variable characteristics and are used extensively in variable-speed drives. Dc motors can provide a high starting torque and it is also possible to obtain speed control over a wide range. The methods of speed control are normally simpler and less expensive than that of ac drives. Dc motors play a significant role in modern industrial drives. Both series and separately excited dc motors are normally used in variable-speed drives; however, series motors are traditionally employed for traction applications. Due to the commutators, dc motors are not suitable for very high-speed applications and require more maintenance than do ac motors.

Controlled rectifiers provide a variable dc output voltage from a fixed ac voltage, whereas choppers can provide a variable dc voltage from a fixed dc voltage. Due to their ability to supply a continuously variable dc voltage, controlled rectifiers and dc choppers made a revolution in modern industrial control equipment and variable-speed drives, with power levels ranging from fractional horsepower to several megawatts. Dc drives can be classified, in general, into three types:

1. Single-phase drives
2. Three-phase drives
3. Chopper drives

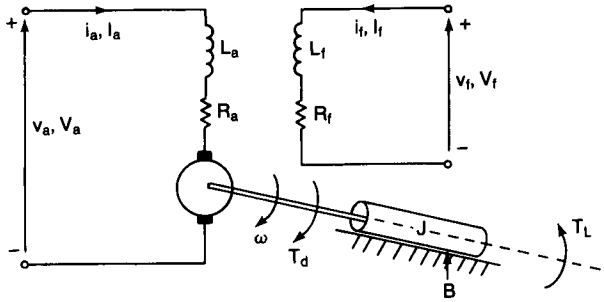


Figure 10-1 Equivalent circuit of separately excited dc motors.

10-2 BASIC CHARACTERISTICS OF DC MOTORS

The equivalent circuit for a separately excited dc motor is shown in Fig. 10-1. When a separately excited motor is excited by a field current of i_f and an armature current of i_a flows in the armature circuit, the motor develops a back emf and a torque to balance the load torque at a particular speed. The field current, i_f, of a separately excited motor is independent of the armature current, i_a, and any change in the armature current has no effect in the field current. The field current is normally much less than the armature current.

The equations describing the characteristics of a separately excited motor can be determined from Fig. 10-1. The instantaneous field current, i_f, is described as

$$v_f = R_f i_f + L_f \frac{di_f}{dt}$$

The instantaneous armature current can be found from

$$v_a = R_a i_a + L_a \frac{di_a}{dt} + e_g$$

The motor back emf, which is also known as *speed voltage*, is expressed as

$$e_g = K_v \omega i_f$$

The torque developed by the motor is

$$T_d = K_t i_f i_a$$

The developed torque must be equal to the load torque:

$$T_d = J \frac{d\omega}{dt} + B\omega + T_L$$

where ω = motor speed, rad/s
B = viscous friction constant, N·m/rad/s
K_v = voltage constant, V/A-rad/s
K_t = K_v = torque constant
L_a = armature circuit inductance, H
L_f = field circuit inductance, H
R_a = armature circuit resistance, Ω

R_f = field circuit resistance, Ω
T_L = load torque, N·m

Under steady-state conditions, the time derivatives in these equations are zero and the steady-state average quantities are

$$V_f = R_f I_f \tag{10-1}$$

$$E_g = K_v \omega I_f \tag{10-2}$$

$$V_a = R_a I_a + E_g$$

$$= R_a I_a + K_v \omega I_f \tag{10-3}$$

$$T_d = K_t I_f I_a \tag{10-4}$$

$$= B\omega + T_L \tag{10-5}$$

The developed power is

$$P_d = T_d \omega \tag{10-6}$$

The relationship between the field current, I_f, and the back emf, E_g, is nonlinear due to magnetic saturation. The relationship, which is shown in Fig. 10-2, is known as *magnetization characteristic* of the motor. From Eq. (10-3), the speed of a separately excited motor can be found from

$$\omega = \frac{V_a - R_a I_a}{K_v I_f} = \frac{V_a - R_a I_a}{K_v V_f / R_f} \tag{10-7}$$

We can notice from Eq. (10-7) that the motor speed can be varied by (1) controlling the armature voltage, V_a, known as *voltage control*; (2) controlling the field current, I_f, known as *field control*; or (3) torque demand, which corresponds to an armature current, I_a, for a fixed field current, I_f. The speed, which corresponds to the rated armature voltage, rated field current and rated armature current, is known as the *base speed*.

In practice, for a speed less than the base speed, the armature current and field currents are maintained constant to meet the torque demand, and the armature voltage, V_a, is varied to control the speed. For speed higher than the base speed, the armature voltage is maintained at the rated value and the field current is varied to control the speed. The power developed by the motor (= torque × speed)

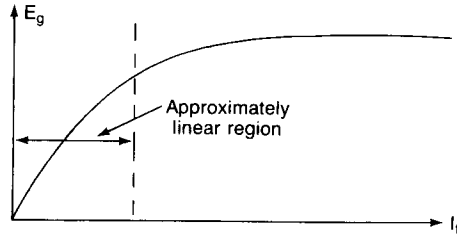


Figure 10-2 Magnetization characteristic.

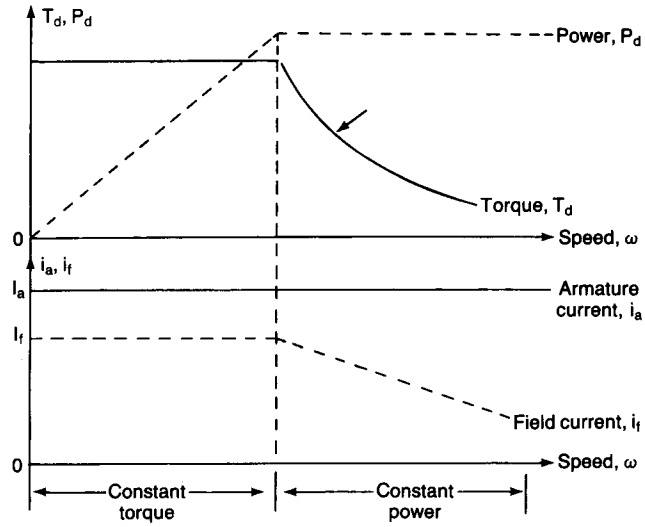


Figure 10-3 Characteristics of separately excited dc motors.

remains constant. Figure 10-3 shows the characteristics of torque, power, armature current, and field current against the speed.

The field of a dc motor may be connected in series with the armature circuit as shown in Fig. 10-4, and this type of motor is called a *series motor*. The field circuit is designed to carry the armature current. The steady-state average quantities are

$$E_g = K_v \omega I_a \tag{10-8}$$

$$V_a = R_a I_a + E_g \tag{10-9}$$

$$= R_a I_a + K_v \omega I_a \tag{10-10}$$

$$T_d = K_t I_a I_a \tag{10-11}$$

$$= B\omega + T_L$$

The speed of a series motor can be determined from Eq. (10-9):

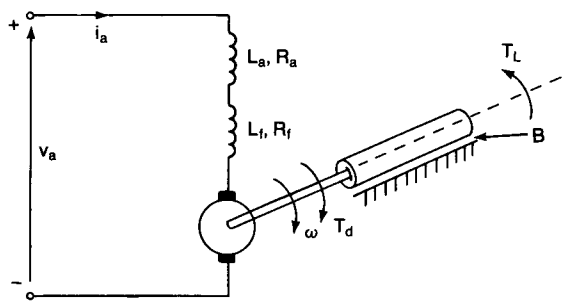


Figure 10-4 Equivalent circuit of dc series motors.

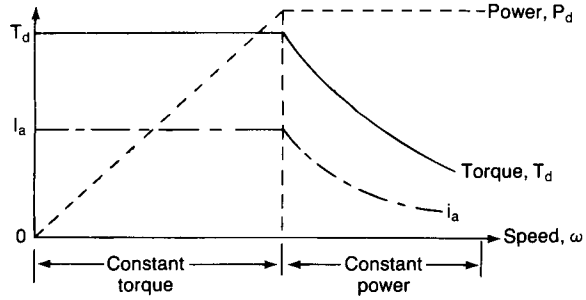


Figure 10-5 Characteristics of dc series motors.

$$\omega = \frac{V_a - R_a I_a}{K_v I_a} \tag{10-12}$$

The speed can be varied by controlling the (1) armature voltage, V_a, or (2) armature current, which is a measure of the torque demand. Equation (10-10) indicates that a series motor can provide a high torque, especially at starting; and for this reason, series motors are commonly used in traction applications.

For a speed up to the base speed, the armature voltage is varied and the torque is maintained constant. Once the rated armature voltage is applied, the speed–torque relationship follows the natural characteristic of the motor and the power (= torque × speed) remains constant. As the torque demand is reduced, the speed increases. At a very light load, the speed could be very high and it is not advisable to run a dc series motor on no-load. Figure 10-5 shows the characteristics of dc series motors.

Example 10-1

A 15-hp 220-V 2000-rpm separately excited dc motor controls a load requiring a torque of $T_L = 45$ N·m at a speed of 1200 rpm. The field circuit resistance is $R_f = 147\ \Omega$, the armature circuit resistance is $R_a = 0.25\ \Omega$, and the voltage constant of the motor is $K_v = 0.7032$ V/A-rad/s. The field voltage is $V_f = 220$ V. The viscous friction and no-load losses are negligible. The armature current may be assumed continuous and ripple free. Determine the (a) back emf, E_g; (b) required armature voltage, V_a; and (c) rated armature current of the motor.

Solution $R_f = 147\ \Omega$, $R_a = 0.25\ \Omega$, $K_v = K_t = 0.7032$ V/A-rad/s, $V_f = 220$ V, $T_d = T_L = 45$ N·m, $\omega = 1200\ \pi/30 = 125.66$ rad/s, and $I_f = 220/147 = 1.497$ A.

(a) From Eq. (10-4), $I_a = 45/(0.7032 \times 1.497) = 42.75$ A. From Eq. (10-2), $E_g = 0.7032 \times 125.66 \times 1.497 = 132.28$ V.

(b) From Eq. (10-3), $V_a = 0.25 \times 42.75 + 132.28 = 142.97$ V.

(c) Since 1 hp is equal to 746 W, $I_{\text{rated}} = 15 \times 746/220 = 50.87$ A.

10-3 SINGLE-PHASE DRIVES

If the armature circuit of a dc motor is connected to the output of a single-phase controlled rectifier, the armature voltage can be varied by varying the delay angle of the converter, α_a. The forced-commutated ac–dc converters can also be used to improve the power factor and to reduce the harmonics. The basic circuit

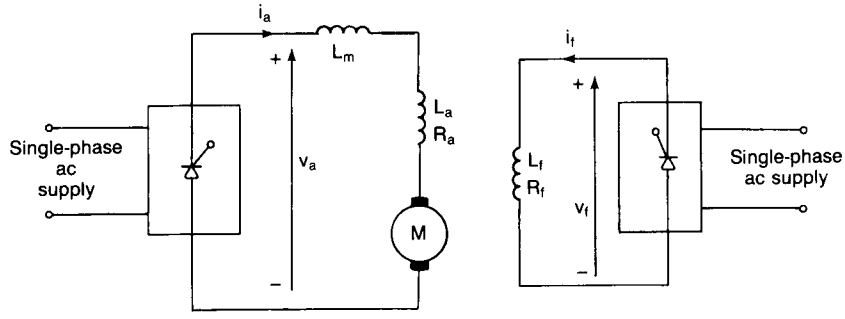


Figure 10-6 Basic circuit arrangement of a single-phase dc drive.

agreement for a single-phase converter-fed separately excited motor is shown in Fig. 10-6. At a low delay angle, the armature current may be discontinuous, and this would increase the losses in the motor. A smoothing inductor, L_m, is normally connected in series with the armature circuit to reduce the ripple current to an acceptable magnitude. A converter is also applied in the field circuit to control the field current by varying the delay angle, α_f. Depending on the type of single-phase converters, single-phase drives may be subdivided into:

1. Single-phase half-wave-converter drives
2. Single-phase semiconverter drives
3. Single-phase full-converter drives
4. Single-phase dual-converter drives

10-3.1 Single-Phase Half-Wave-Converter Drives

A single-phase half-wave converter feeds a dc motor as shown in Fig. 10-7a. The armature current is always discontinuous unless a very large inductor is connected in the armature circuit. A freewheeling diode is always required for a dc motor load and it is a one-quadrant drive, as shown in Fig. 10-7b. The applications of this drive are limited to the $\frac{1}{2}$-kW power level. Figure 10-7c shows the waveforms for a highly inductive load. The converter in the field circuit should be a semiconverter. A half-wave converter in the field circuit would increase the magnetic losses of the motor due to high ripple content on the field excitation current.

With a single-phase half-wave converter in the armature circuit, Eq. (4-1) gives the average armature voltage as

$$V_a = \frac{V_m}{2\pi}(1 + \cos \alpha_a) \qquad \text{for } 0 \leq \alpha_a \leq \pi \tag{10-13}$$

where V_m is the peak voltage of the ac supply. With a semiconverter in the field circuit, Eq. (4-5) gives the average field voltage as

$$V_f = \frac{V_m}{\pi}(1 + \cos \alpha_f) \qquad \text{for } 0 \leq \alpha_f \leq \pi \tag{10-14}$$

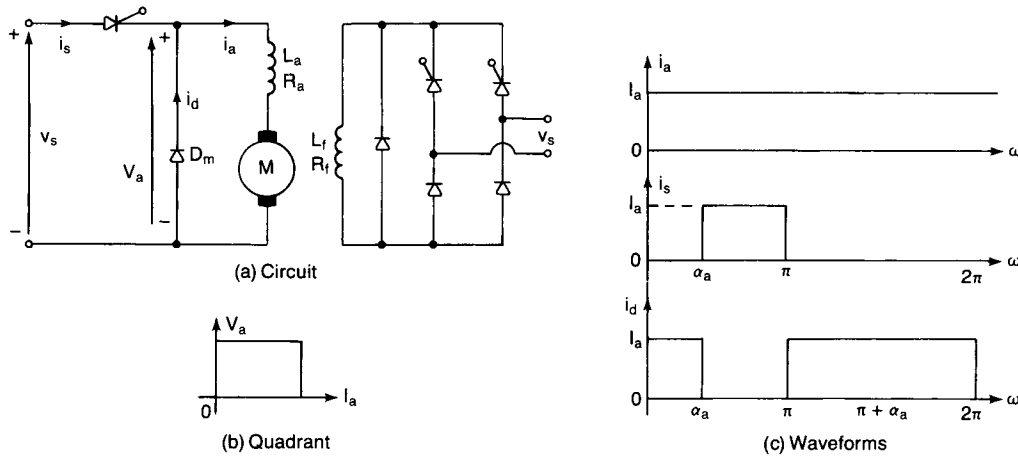


Figure 10-7 Single-phase half-wave converter drive.

10-3.2 Single-Phase Semiconverter Drives

A single-phase semiconverter feeds the armature circuit as shown in Fig. 10-8a. It is a one-quadrant drive as shown in Fig. 10-8b and is limited to applications up to 15 kW. The converter in the field circuit should also be a semiconverter. The current waveforms for a highly inductive load are shown in Fig. 10-8c.

With a single-phase semiconverter in the armature circuit, Eq. (4-5) gives the average armature voltage as

$$V_a = \frac{V_m}{\pi}(1 + \cos \alpha_a) \qquad \text{for } 0 \le \alpha_a \le \pi \tag{10-15}$$

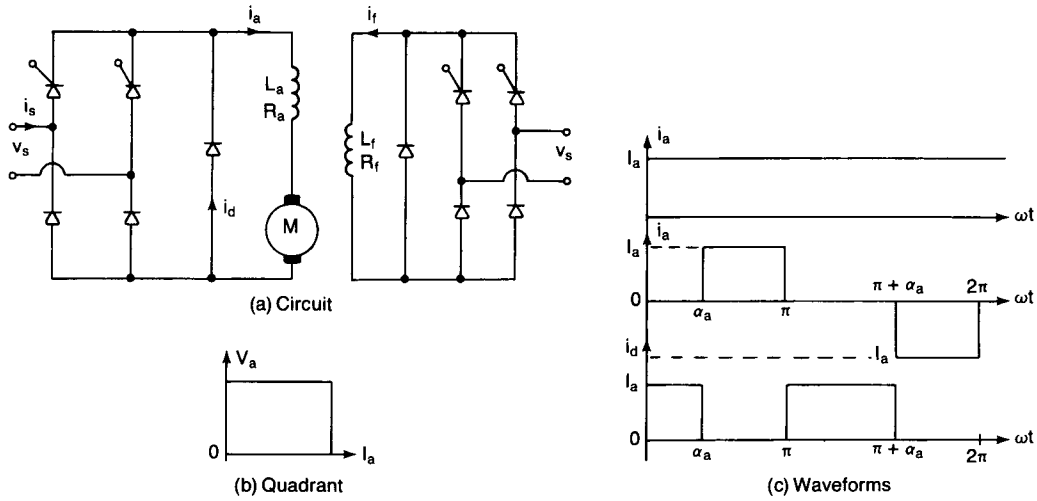


Figure 10-8 Single-phase semiconverter drive.

With a semiconverter in the field circuit, Eq. (4-5) gives the average field voltage as

$$V_f = \frac{V_m}{\pi}(1 + \cos \alpha_f) \qquad \text{for } 0 \le \alpha_f \le \pi \tag{10-16}$$

10-3.3 Single-Phase Full-Converter Drives

The armature voltage is varied by a single-phase full-wave converter as shown in Fig. 10-9a. It is a two-quadrant drive as shown in Fig. 10-9b and is limited to applications up to 15 kW. During regeneration for reversing the direction of power flow, the back emf of the motor is reversed by reversing the field excitation. The converter in the field circuit should be a full-wave converter to reverse the polarity of field current. The current waveforms for a highly inductive load are shown in Fig. 10-9c for powering action. A 9.5-kW 40-A single-phase full-converter drive is shown in Fig. 10-10, where the power stack is on the back of the panel and the control signals are implemented by analog electronics.

With a single-phase full-wave converter in the armature circuit, Eq. (4-17) gives the average armature voltage as

$$V_a = \frac{2v_m}{\pi}\cos \alpha_a \qquad \text{for } 0 \le \alpha_a \le \pi \tag{10-17}$$

With a single-phase full-converter in the field circuit, Eq. (4-17) gives the field voltage as

$$V_f = \frac{2V_m}{\pi}\cos \alpha_f \qquad \text{for } 0 \le \alpha_f \le \pi \tag{10-18}$$

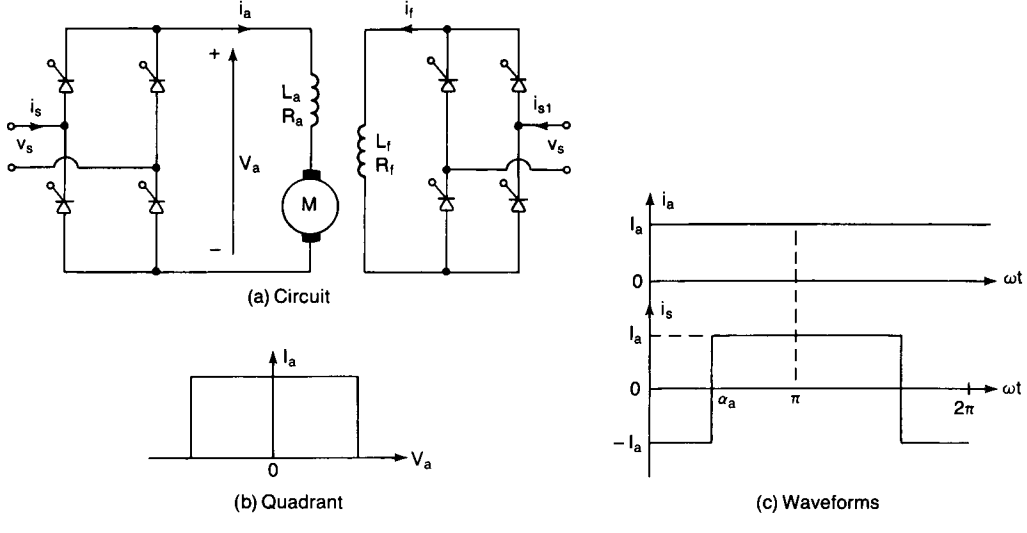


Figure 10-9 Single-phase full-converter drive.

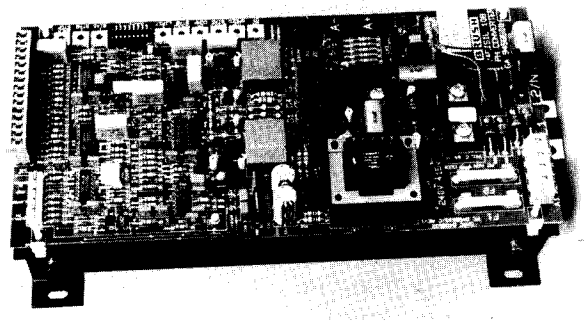


Figure 10-10 A 9.5-kW analog-based single-phase full-wave drive. (*Reproduced by permission of Brush Electrical Machines Ltd., England*)

10-3.4 Single-Phase Dual-Converter Drives

Two single-phase full-wave converters are connected as shown in Fig. 10-11. Either converter 1 operates to supply a positive armature voltage, V_a, or converter 2 operates to supply a negative armature voltage, $-V_a$. It is a four-quadrant drive and permits four modes of operation: forward powering, forward braking (regeneration), reverse powering, and reverse braking (regeneration). It is limited to applications up to 15 kW. The polarity of field current is reversed during forward and reverse regenerations. The field converter should be a full-wave one to allow reversing the direction of field current.

If converter 1 operates with a delay angle of α_{a1}, Eq. (4-31) gives the armature voltage as

$$V_a = \frac{2V_m}{\pi} \cos \alpha_{a1} \qquad \text{for } 0 \leq \alpha_{a1} \leq \pi \tag{10-19}$$

If converter 2 operates with a delay angle of α_{a2}, Eq. (4-32) gives the armature voltage as

$$V_a = \frac{2V_m}{\pi} \cos \alpha_{a2} \qquad \text{for } 0 \leq \alpha_{a2} \leq \pi \tag{10-20}$$

where $\alpha_{a2} = \pi - \alpha_{a1}$. With a full converter in the field circuit, Eq. (4-17) gives the field voltage as

$$V_f = \frac{2V_m}{\pi} \cos \alpha_f \qquad \text{for } 0 \leq \alpha_f \leq \pi \tag{10-21}$$

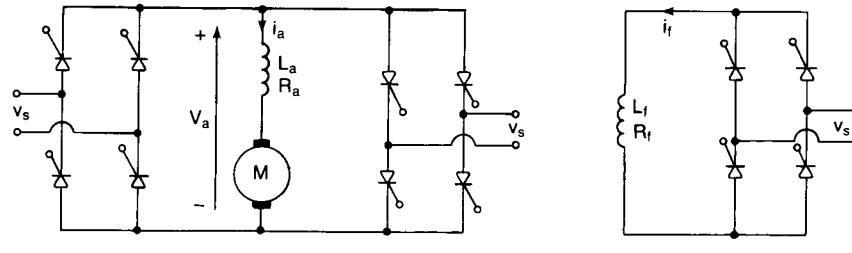


Figure 10-11 Single-phase dual-converter drive.

Example 10-2

The speed of a separately excited motor is controlled by a single-phase semiconverter in Fig. 10-8a. The field current, which is also controlled by a semiconverter, is set to the maximum possible value. The ac supply voltage to the armature and field converters is one-phase, 208 V, 60 Hz. The armature resistance is $R_a = 0.25\ \Omega$, the field resistance is $R_f = 147\ \Omega$, and the motor voltage constant is $K_v = 0.7032$ V/A-rad/s. The load torque is $T_L = 45$ N·m at 1000 rpm. The viscous friction and no-load losses are negligible. The inductances of the armature and field circuits are sufficient enough to make the armature and field currents continuous and ripple-free. Determine the (a) field current, I_f; (b) delay angle of the converter in the armature circuit, α_a; and (c) input power factor of the armature circuit converter, PF.

Solution $V_s = 208$ V, $V_m = \sqrt{2} \times 208 = 294.16$ V, $R_a = 0.25\ \Omega$, $R_f = 147\ \Omega$, $T_d = T_L = 45$ N·m, $K_v = 0.7032$ V/A-rad/s, and $\omega = 1000\ \pi/30 = 104.72$ rad/s.

(a) From Eq. (10-16), the maximum field voltage (and current) is obtained for a delay angle of $\alpha_f = 0$ and

$$V_f = \frac{2V_m}{\pi} = \frac{2 \times 294.16}{\pi} = 187.27 \text{ V}$$

The field current is

$$I_f = \frac{V_f}{R_f} = \frac{187.27}{147} = 1.274 \text{ A}$$

(b) From Eq. (10-4),

$$I_a = \frac{T_L}{K_v I_f} = \frac{45}{0.7032 \times 1.274} = 50.23 \text{ A}$$

From Eq. (10-2),

$$E_g = K_v \omega I_f = 0.7032 \times 104.72 \times 1.274 = 93.82 \text{ V}$$

From Eq. (10-3), the armature voltage is

$$V_a = 93.82 + I_a R_a = 93.82 + 50.23 \times 0.25 = 93.82 + 12.56 = 106.38 \text{ V}$$

From Eq. (10-15), $V_a = 106.38 = (294.16/\pi) \times (1 + \cos \alpha_a)$ and this gives the delay angle as $\alpha_a = 82.2°$.

(c) If the armature current is constant and ripple-free, the output power is $P_o = V_a I_a = 106.38 \times 50.23 = 5343.5$ W. If the losses in the armature converter are neglected, the power from the supply is $P_a = P_o = 5343.5$ W. The rms input current of the armature converter as shown in Fig. 10-8c is

$$I_{sa} = \left(\frac{2}{2\pi} \int_0^{\alpha_a} I_a^2 \, d\theta \right)^{1/2} = I_a \left(\frac{\pi - \alpha_a}{\pi} \right)^{1/2}$$

$$= 50.23 \left(\frac{180 - 82.2}{180} \right)^{1/2} = 37.03 \text{ A}$$

and the input volt-ampere rating, $\text{VI} = V_s I_{sa} = 208 \times 37.03 = 7702.24$. The input power factor,

$$\text{PF} = \frac{P_a}{\text{VI}} = \frac{5343.5}{7702.24} = 0.694 \text{ (lagging)}$$

Example 10-3

The speed of a separately excited dc motor is controlled by a single-phase full-wave converter in Fig. 10-9a. The field circuit is also controlled by a full converter and the field current is set to the maximum possible value. The ac supply voltage to the armature and field converters is one-phase, 440 V, 60 Hz. The armature resistance is $R_a = 0.25\ \Omega$, the field circuit resistance is $R_f = 175\ \Omega$, and the motor voltage constant is $K_v = 1.4$ V/A-rad/s. The armature current corresponding to the load demand is $I_a = 45$ A. The viscous friction and no-load losses are negligible. The inductances of the armature and field circuits are sufficient to make the armature and field currents continuous and ripple-free. If the delay angle of the armature converter is $\alpha_a = 60°$ and the armature current is $I_a = 45$ A, determine the (a) torque developed by the motor, T_d; (b) speed, ω; and (c) input power factor of the drive, PF.

Solution $V_s = 440$ V, $V_m = \sqrt{2} \times 440 = 622.25$ V, $R_a = 0.25\ \Omega$, $R_f = 175\ \Omega$, $\alpha_a = 60°$, and $K_v = 1.4$ V/A-rad/s.

(a) From Eq. (10-16), the maximum field voltage (and current) would be obtained for a delay angle of $\alpha_f = 0$ and

$$V_f = \frac{2V_m}{\pi} = \frac{2 \times 622.25}{\pi} = 396.14 \text{ V}$$

The field current is

$$I_f = \frac{V_f}{R_f} = \frac{396.14}{175} = 2.26 \text{ A}$$

From Eq. (10-4), the developed torque is

$$T_d = T_L = K_v I_f I_a = 1.4 \times 2.26 \times 45 = 142.4 \text{ N·m}$$

From Eq. (10-17), the armature voltage is

$$V_a = \frac{2V_m}{\pi} \cos 60° = \frac{2 \times 622.25}{\pi} \cos 60° = 198.07 \text{ V}$$

The back emf is

$$E_g = V_a - I_a R_a = 198.07 - 45 \times 0.25 = 186.82 \text{ V}$$

From Eq. (10-2), the speed is

$$\omega = \frac{E_g}{K_v I_f} = \frac{186.82}{1.4 \times 2.26} = 59.05 \text{ rad/s or } 564 \text{ rpm}$$

(c) Assuming lossless converters, the total input power from the supply is

$$P_i = V_a I_a + V_f I_f = 198.07 \times 45 + 396.14 \times 2.26 = 9808.4 \text{ W}$$

The input current of the armature converter for a highly inductive load is shown in Fig. 10-9b and its rms value is $I_{sa} = I_a = 45$ A. The rms value of the input current of field converter is $I_{sf} = I_f = 2.26$ A. The effective rms supply current can be found from

$$I_s = (I_{sa}^2 + I_{sf}^2)^{1/2}$$

$$= (45^2 + 2.26^2)^{1/2} = 45.06 \text{ A}$$

and the input volt-ampere rating, VI = $V_s I_s$ = 440 × 45.06 = 19,826.4. The input power factor,

$$\text{PF} = \frac{P_i}{\text{VI}} = \frac{9808.4}{19{,}826.4} = 0.495 \text{ (lagging)}$$

Example 10-4

If the polarity of the motor back emf in Example 10-3 is reversed by reversing the polarity of the field current, determine the (a) delay angle of the field circuit converter, α_f; (b) delay angle of the armature circuit converter, α_a, to maintain the armature current constant at the same value of I_a = 45 A; and (c) power fed back to the supply due to regenerative braking of the motor.

Solution (a) From Eq. (10-18), the polarity of the field current would be reversed if

$$V_f = \frac{2V_m}{\pi} \cos \alpha_f = \frac{2 \times 622.25}{\pi} \cos \alpha_f = -396.14 \text{ V}$$

and this gives the delay angle as α_f = 180°.

(b) From part (b) of Example 10-3, the back emf at the time of polarity reversal is E_g = 186.82 V and after polarity reversal E_g = −186.82 V. From Eq. (10-3),

$$V_a = E_a + I_a R_a = -186.82 + 45 \times 0.25 = -175.57 \text{ V}$$

From Eq. (10-17),

$$V_a = \frac{2V_m}{\pi} \cos \alpha_a = \frac{2 \times 622.25}{\pi} \cos \alpha_a = -175.57 \text{ V}$$

and this yields the delay angle of the armature converter as α_a = 116.38°.

(c) The power fed back to the supply, $P_a = V_a I_a$ = 175.57 × 45 = 7900.7 W.

Note. The speed and back emf of the motor will decrease with time. If the armature current is to be maintained constant at I_a = 45 A during regeneration, the delay angle of the armature converter has to be reduced. This would require a closed-loop control to maintain the armature current constant and to adjust the delay angle continuously.

10-4 THREE-PHASE DRIVES

The armature circuit is connected to the output of a three-phase controlled rectifier or a forced-commutated three-phase ac–dc converter. Three-phase drives are used for high-power applications up to megawatts power level. The ripple frequency of the armature voltage is higher than that of single-phase drives and it requires less inductance in the armature circuit to reduce the armature ripple current. The armature current is mostly continuous, and therefore the motor performance is better compared to that of single-phase drives. Similar to the single-phase drives, three-phase drives may also be subdivided into:

1. Three-phase half-wave-converter drives

2. Three-phase semiconverter drives
3. Three-phase full-converter drives
4. Three-phase dual-converter drives

10-4.1 Three-Phase Half-Wave-Converter Drives

A three-phase half-wave converter-fed dc motor drive is a two-quadrant drive and could be used in applications up to a 40-kW power level. The field converter could be a single-phase or three-phase semiconverter. This drive is not normally used in industrial applications because the ac supply contains dc components.

With a three-phase half-wave converter in the armature circuit, Eq. (4-51) gives the armature voltage as

$$V_a = \frac{3\sqrt{3}\,V_m}{2\pi}\cos\alpha_a \qquad \text{for } 0 \le \alpha_a \le \pi \tag{10-22}$$

where V_m is the peak voltage of a Y-connected three-phase ac supply. With a three-phase semiconverter in the field circuit, Eq. (4-54) gives the field voltage as

$$V_f = \frac{3\sqrt{3}\,V_m}{2\pi}(1 + \cos\alpha_f) \qquad \text{for } 0 \le \alpha_f \le \pi \tag{10-23}$$

10-4.2 Three-Phase Semiconverter Drives

A three-phase semiconverter-fed drive is a one-quadrant drive and is limited to applications up to 115 kW. The field converter should also be a single-phase or three-phase semiconverter.

With a three-phase semiconverter in the armature circuit, Eq. (4-54) gives the armature voltage as

$$V_a = \frac{3\sqrt{3}\,V_m}{2\pi}(1 + \cos\alpha_a) \qquad \text{for } 0 \le \alpha_a \le \pi \tag{10-24}$$

With a three-phase semiconverter in the field circuit, Eq. (4-54) gives the field voltage as

$$V_f = \frac{3\sqrt{3}\,V_m}{2\pi}(1 + \cos\alpha_f) \qquad \text{for } 0 \le \alpha_f \le \pi \tag{10-25}$$

10-4.3 Three-Phase Full-Converter Drives

A three-phase full-wave converter drive is a two-quadrant drive and is limited to applications up to 1500 kW. During regeneration for reversing the direction of power flow, the back emf of the motor is reversed by reversing the field excitation. The converter in the field circuit should be a single- or three-phase full converter to reverse the polarity of field current. A 68-kW 170-A microprocessor-based three-phase full-converter dc drive is shown in Fig. 10-12, where the power semiconductor stacks are at the back of the panel.

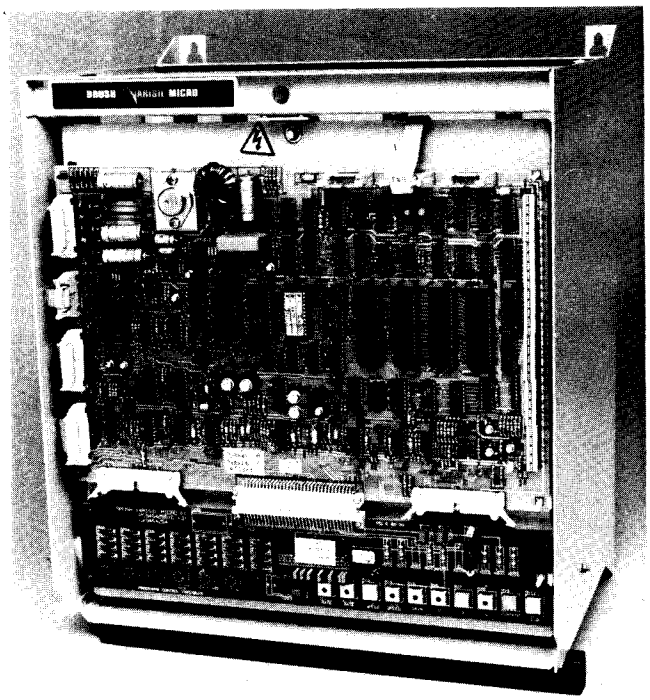


Figure 10-12 A 68-kW microprocessor-based three-phase full converter. (*Reproduced by permission of Brush Electrical Machines Ltd., England*)

With a three-phase full-wave converter in the armature circuit, Eq. (4-57) gives the armature voltage as

$$V_a = \frac{3\sqrt{3}\,V_m}{\pi}\cos\alpha_a \qquad \text{for } 0 \le \alpha_a \le \pi \tag{10-26}$$

With a three-phase full converter in the field circuit, Eq. (4-57) gives the field voltage as

$$V_f = \frac{3\sqrt{3}\,V_m}{\pi}\cos\alpha_f \qquad \text{for } 0 \le \alpha_f \le \pi \tag{10-27}$$

10-4.4 Three-Phase Dual-Converter Drives

Two three-phase full-wave converters are connected as in Fig. 10-14a. Either converter 1 operates to supply a positive armature voltage, V_a, or converter 2 operates to supply a negative armature voltage, $-V_a$. It is a four-quadrant drive and is limited to applications up to 1500 kW. The polarity of field current is reversed during forward and reverse regenerations. Similar to single-phase drives, the field converter should be full-wave to allow reversing the direction of field current.

A 12-pulse ac–dc converter for a 360-kW motor for driving a cement kiln is shown in Fig. 10-13, where the control electronics are mounted on the cubicle door

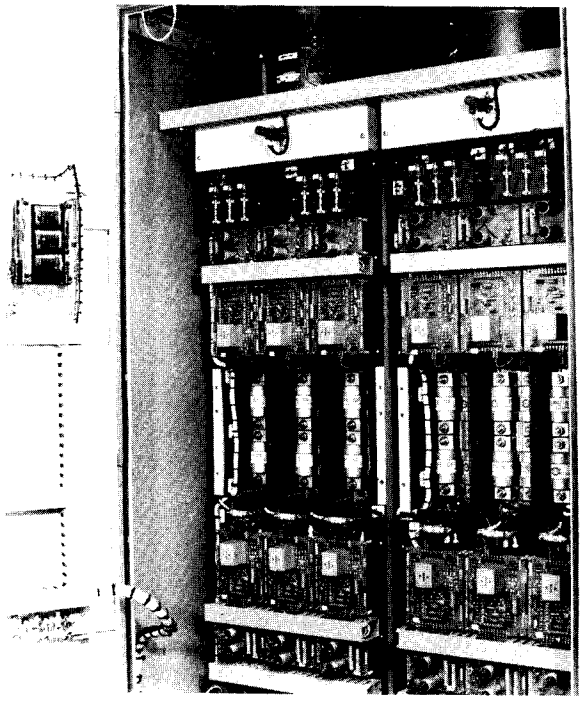


Figure 10-13 A 360-kW 12-pulse ac–dc converter for dc drives. (*Reproduced by permission of Brush Electrical Machines Ltd., England*)

and the pulse drive boards are mounted on the front of the thyristor stacks. The cooling fans are mounted at the top of each stack. If converter 1 operates with a delay angle of α_{a1}, Eq. (4-57) gives the average armature voltage as

$$V_a = \frac{3\sqrt{3}\,V_m}{\pi}\cos\alpha_{a1} \qquad \text{for } 0 \le \alpha_{a1} \le \pi \tag{10-28}$$

If converter 2 operates with a delay angle of α_{a2}, Eq. (4-57) gives the average armature voltage as

$$V_a = \frac{3\sqrt{3}\,V_m}{\pi}\cos\alpha_{a2} \qquad \text{for } 0 \le \alpha_{a2} \le \pi \tag{10-29}$$

With a three-phase full converter in the field circuit, Eq. (4-57) gives the average field voltage as

$$V_f = \frac{3\sqrt{3}\,V_m}{\pi}\cos\alpha_f \qquad \text{for } 0 \le \alpha_f \le \pi \tag{10-30}$$

Example 10-5

The speed of a 20-hp 300-V 1800-rpm separately excited dc motor is controlled by a three-phase full-converter drive. The field current is also controlled by a three-phase full-converter and is set to the maximum possible value. The ac input is a three-

phase Y-connected 208-V 60-Hz supply. The armature resistance is $R_a = 0.25\ \Omega$, the field resistance is $R_f = 245\ \Omega$, and the motor voltage constant is $K_v = 1.2$ V/A-rad/s. The armature and field currents can be assumed to be continuous and ripple-free. The viscous friction is negligible. Determine the (a) delay angle of the armature converter, α_a, if the motor supplies the rated power at the rated speed; (b) no-load speed if the delay angles are the same as in part (a) and the armature current at no-load is 10% of the rated value; and (c) speed regulation.

Solution $R_a = 0.25\ \Omega$, $R_f = 245\ \Omega$, $K_v = 1.2$ V/A-rad/s, $V_L = 208$ V, and $\omega = 1800\ \pi/30 = 188.5$ rad/s. The phase voltage is $V_p = V_L/\sqrt{3} = 208/\sqrt{3} = 120$ V and $V_m = 120 \times \sqrt{2} = 169.7$ V. Since 1 hp is equal to 746 W, the rated armature current is $I_{\text{rated}} = 20 \times 746/300 = 49.73$ A; and for maximum possible field current, $\alpha_f = 0$. From Eq. (10-27),

$$V_f = 3\sqrt{3} \times \frac{169.7}{\pi} = 280.7 \text{ V}$$

$$I_f = \frac{V_f}{R_f} = \frac{280.7}{245} = 1.146 \text{ A}$$

(a) $I_a = I_{\text{rated}} = 49.73$ A and

$$E_g = K_v I_f \omega = 1.2 \times 1.146 \times 188.5 = 259.2 \text{ V}$$

$$V_a = 259.2 + I_a R_a = 259.2 + 49.73 \times 0.25 = 271.63 \text{ V}$$

From Eq. (10-26),

$$V_a = 271.63 = \frac{3\sqrt{3}\, V_m}{\pi} \cos \alpha_a = \frac{3\sqrt{3} \times 169.7}{\pi} \cos \alpha_a$$

and this gives the delay angle as $\alpha_a = 14.59°$.

(b) $I_a = 10\%$ of $49.73 = 4.973$ A and

$$E_g = V_a - R_a I_a = 271.63 - 0.25 \times 4.973 = 270.39 \text{ V}$$

From Eq. (10-2), the no-load speed is

$$\omega_0 = \frac{E_g}{K_v I_f} = \frac{270.39}{1.2 \times 1.146} = 196.62 \text{ rad/s} \quad \text{or} \quad 196.62 \times \frac{30}{\pi} = 1877.58 \text{ rpm.}$$

(c) The speed regulation is defined as

$$\frac{\text{no-load speed} - \text{full-load speed}}{\text{full-load speed}} = \frac{1877.58 - 1800}{1800} = 0.043 \quad \text{or} \quad 4.3\%$$

Example 10-6

The speed of a 20-hp 300-V 900-rpm separately excited dc motor is controlled by a three-phase full converter. The field circuit is also controlled by a three-phase full converter. The ac input to the armature and field converters is three-phase, Y-connected, 208 V, 60 Hz. The armature resistance is $R_a = 0.25\ \Omega$, the field circuit resistance is $R_f = 145\ \Omega$, and the motor voltage constant is $K_v = 1.2$ V/A-rad/s. The viscous friction and no-load losses can be considered negligible. The armature and field currents are continuous and ripple-free. (a) If the field converter is operated at the maximum field current and the developed torque is $T_d = 116$ N·m at 900 rpm,

determine the delay angle of the armature converter, α_a. (b) If the field circuit converter is set for the maximum field current, the developed torque is $T_d = 116$ N·m, and the delay angle of the armature converter is $\alpha_a = 0$, determine the speed of the motor. (c) For the same load demand as in part (b), determine the delay angle of the field converter if the speed has to be increased to 1800 rpm.

Solution $R_a = 0.25\ \Omega$, $R_f = 145\ \Omega$, $K_v = 1.2$ V/A-rad/s, and $V_L = 208$ V. The phase voltage is $V_p = 208/\sqrt{3} = 120$ V and $V_m = \sqrt{2} \times 120 = 169.7$ V.

(a) $T_d = 116$ N·m and $\omega = 900\,\pi/30 = 94.25$ rad/s. For maximum field current, $\alpha_f = 0$. From Eq. (10-27),

$$V_f = \frac{3 \times \sqrt{3} \times 169.7}{\pi} = 280.7 \text{ V}$$

$$I_f = \frac{280.7}{145} = 1.936 \text{ A}$$

From Eq. (10-4),

$$I_a = \frac{T_d}{K_v I_f} = \frac{116}{1.2 \times 1.936} = 49.93 \text{ A}$$

$$E_g = K_v I_f \omega = 1.2 \times 1.936 \times 94.25 = 218.96 \text{ V}$$

$$V_a = E_g + I_a R_a = 218.96 + 49.93 \times 0.25 = 231.44 \text{ V}$$

From Eq. (10-26),

$$V_a = 231.44 = \frac{3 \times \sqrt{3} \times 169.7}{\pi} \cos \alpha_a$$

and the delay angle is $\alpha_a = 34.46°$.

(b) $\alpha_a = 0$ and

$$V_a = \frac{3 \times \sqrt{3} \times 169.7}{\pi} = 280.7 \text{ V}$$

$$E_g = 280.7 - 49.93 \times 0.25 = 268.22 \text{ V}$$

and the speed

$$\omega = \frac{268.22}{1.2 \times 1.936} = 115.36 \text{ rad/s} \quad \text{or} \quad 1101.6 \text{ rpm}$$

(c) $\omega = 1800\,\pi/30 = 188.5$ rad/s

$$E_g = 268.22 \text{ V} = 1.2 \times 188.5 \times I_f \quad \text{or} \quad I_f = 1.186 \text{ A}$$

$$V_f = 1.186 \times 145 = 171.97 \text{ V}$$

From Eq. (10-27),

$$V_f = 171.97 = \frac{3 \times \sqrt{3} \times 169.7}{\pi} \cos \alpha_f$$

and the delay angle is $\alpha_f = 52.2°$.

10-5 CHOPPER DRIVES

Chopper drives are widely used in traction applications all over the world. A dc chopper is connected between a fixed-voltage dc source and a dc motor to vary the armature voltage. In addition to armature voltage control, a dc chopper can provide regenerative braking of the motors and can return energy back to the supply. This energy-saving feature is particularly attractive to transportation systems with frequent stops [e.g., mass rapid transit (MRT)]. Chopper drives are also used in battery electric vehicles (BEVs).

If the supply is nonreceptive during the regenerative braking, the line voltage would increase and regenerative braking may not be possible. In this case, an alternative form of braking is necessary (e.g., rheostatic braking). The possible control modes of a dc chopper drive are:

1. Power (acceleration) control
2. Regenerative brake control
3. Rheostatic brake control
4. Combined regenerative and rheostatic brake control

10-5.1 Principle of Power Control

The chopper is used to control the armature voltage of a dc motor. The circuit arrangement of a chopper-fed dc series motor is shown in Fig. 10-14a. The chopper switch could be a transistor or forced-commutated thyristor chopper, as discussed in Section 7-7. This is a one-quadrant drive, as shown in Fig. 10-14b. The waveforms for the armature voltage, load current, and input current are shown in Fig. 10-14c, assuming a highly inductive load.

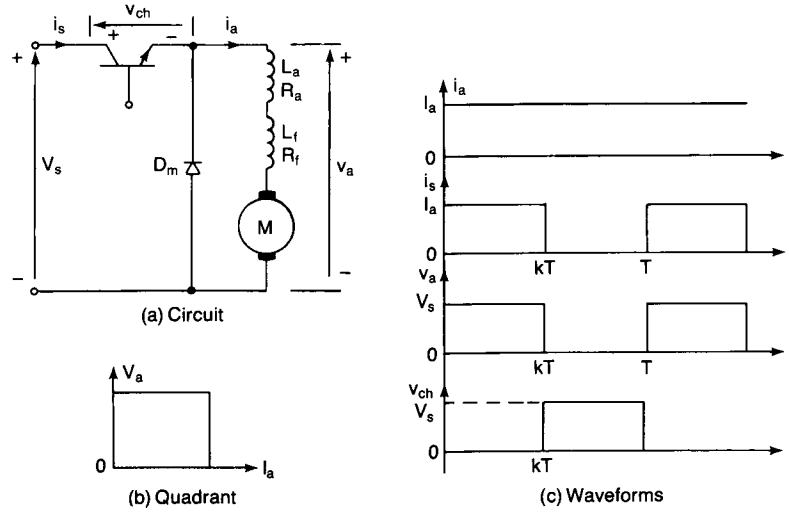


Figure 10-14 Chopper-fed dc drive in power control.

The average armature voltage is

$$V_a = kV_s \tag{10-31}$$

where k is the duty cycle of the chopper. The power supplied to the motor is

$$P_0 = V_a I_a = kV_s I_a \tag{10-32}$$

where I_a is the average armature current of the motor and it is ripple-free. Assuming a lossless chopper, the input power is $P_i = P_0 = kV_s I_s$. The average value of the input current is

$$I_s = kI_a \tag{10-33}$$

The equivalent input of the chopper drive is

$$R_{eq} = \frac{V_s}{I_s} = \frac{V_s}{I_a}\frac{1}{k} \tag{10-34}$$

By varying the duty cycle, k, the power flow to the motor (and speed) can be controlled. For a finite armature circuit inductance, Eq. (7-19) can be applied to find the maximum peak-to-peak ripple current as

$$\Delta I_{max} = \frac{V_s}{R_m} \tanh \frac{R_m}{4fL_m} \tag{10-35}$$

where R_m and L_m are the armature circuit resistance and inductance, respectively.

Example 10-7

The dc series motor is powered by a dc chopper (as shown in Fig. 10-14a) from a 600-V dc source. The armature resistance is $R_a = 0.02\ \Omega$ and the field resistance is $R_f = 0.03\ \Omega$. The back emf constant of the motor is $K_v = 15.27$ mV/A-rad/s. The average armature current is $I_a = 250$ A. The armature current is continuous and has negligible ripple. If the duty cycle of the chopper is 60%, determine the (a) input power from the source; (b) equivalent input resistance of the chopper drive; (c) motor speed; and (d) developed torque.

Solution $V_s = 600$ V, $I_a = 250$ A, and $k = 0.6$. The total armature circuit resistance is $R_m = R_a + R_f = 0.02 + 0.03 = 0.05\ \Omega$.

(a) From Eq. (10-32),

$$P_i = kV_s I_a = 0.6 \times 600 \times 250 = 90\ \text{kW}$$

(b) From Eq. (10-34), $R_{eq} = 600/(250 \times 0.6) = 4\ \Omega$.

(c) From Eq. (10-31), $V_a = 0.6 \times 600 = 360$ V. The back emf is

$$E_g = V_a - R_a I_m = 360 - 0.05 \times 250 = 347.5\ \text{V}$$

From Eq. (10-8), the motor speed is

$$\omega = \frac{347.5}{0.01527 \times 250} = 91.03\ \text{rad/s} \quad \text{or} \quad 91.03 \times \frac{30}{\pi} = 869.3\ \text{rpm}$$

(d) From Eq. (10-10),

$$T_d = 0.01527 \times 250 \times 250 = 954.38\ \text{N·m}$$

10-5.2 Principle of Regenerative Brake Control

In regenerative braking, the motor acts as a generator and the kinetic energy of the motor and load is returned back to the supply. The principle of energy transfer from one dc source to another of higher voltage is discussed in Section 7-4, and this can be applied in regenerative braking of dc motors.

The application of dc choppers in regenerative braking can be explained with Fig. 10-15a. Let us assume that the armature of a series motor is rotating due to the inertia of the motor (and load); and in case of a transportation system, the kinetic energy of the vehicle or train would rotate the armature shaft. Then if the transistor is switched on, the armature current will rise due to the short-circuiting of the motor terminals. If the chopper is turned off, diode D_m would be turned on and the energy stored in the armature circuit inductances would be transferred to the supply, provided that the supply is receptive. It is an one-quadrant drive and operates in the second quadrant as shown in Fig. 10-15b. Figure 10-15c shows the voltage and current waveforms assuming that the armature current is continuous and ripple-free.

The average voltage across the chopper is

$$V_{ch} = (1 - k)V_s \tag{10-36}$$

If I_a is the average armature current, the regenerated power can be found from

$$P_g = I_a V_s(1 - k) \tag{10-37}$$

The voltage generated by the series motor acting as a generator is

$$\begin{aligned} E_g &= K_v I_a \omega \\ &= V_{ch} + R_m I_a = (1 - k)V_s + R_m I_a \end{aligned} \tag{10-38}$$

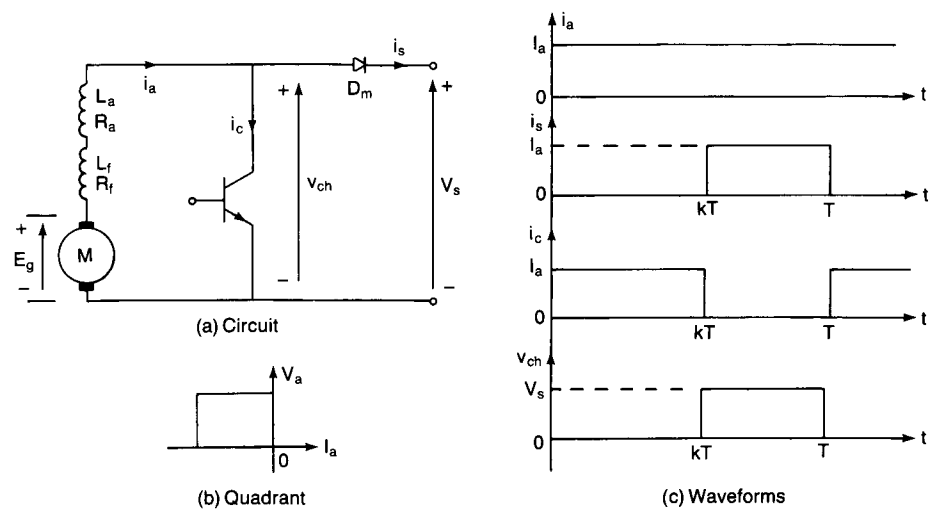


Figure 10-15 Regenerative braking of dc series motors.

where K_v is machine constant and ω is the machine speed in rad/s. Therefore, the equivalent load resistance of the motor acting as a generator is

$$R_{eq} = \frac{V_s}{I_a}(1 - k) + R_m \tag{10-39}$$

By varying the duty cycle, k, the equivalent load resistance seen by the motor can be varied from R_m to $(V_s/I_a + R_m)$ and the regenerative power can be controlled.

From Eq. (7-31), the conditions for permissible potentials and polarity of the two voltages are

$$0 \leq (E_g - R_m I_a) \leq V_s \tag{10-40}$$

which gives the minimum braking speed of a series motor as

$$E_g = K_v \omega_{min} I_a = R_m I_a$$

or

$$\omega_{min} = \frac{R_m}{K_v} \tag{10-41}$$

and $\omega \geq \omega_{min}$. The maximum braking speed of a series motor can be found from Eq. (10-40):

$$K_v \omega_{max} I_a - R_m I_a = V_s$$

or

$$\omega_{max} = \frac{V_s}{K_v I_a} + \frac{R_m}{K_v} \tag{10-42}$$

and $\omega \leq \omega_{max}$.

The regenerative braking would be effective only if the motor speed is between these two speed limits (e.g., $\omega_{min} < \omega < \omega_{max}$). At any speed less than ω_{min}, an alternative braking arrangement would be required.

Although dc series motors are traditionally used for traction applications due to their high starting torque, a series-excited generator is unstable when working into a fixed voltage supply. Thus for running on the traction supply, a separate excitation control is required and such an arrangement of series motor is, normally, sensitive to supply voltage fluctuations and a fast dynamic response is required to provide an adequate brake control. The application of a dc chopper allows the regenerative braking of dc series motors due to its fast dynamic response.

A separately excited dc motor is stable in regenerative braking. The armature and field can be controlled independently to provide the required torque during starting. A chopper-fed series and separately excited dc motors are suitable for traction applications.

Example 10-8

A dc chopper is used in regenerative braking of a dc series motor as shown in Fig. 10-15a. The dc supply voltage is 600 V. The armature resistance is $R_a = 0.02\ \Omega$ and the field resistance is $R_f = 0.03\ \Omega$. The back emf constant is $K_v = 15.27$ mV/

A-rad/s. The average armature current is maintained constant at I_a = 250 A. The armature current is continuous and has negligible ripple. If the duty cycle of the chopper is 60%, determine the (a) average voltage across the chopper, V_{ch}; (b) power regenerated to the dc supply, P_g; (c) equivalent load resistance of the motor acting as a generator, R_{eq}; (d) minimum permissible braking speed, ω_{min}; (e) maximum permissible braking speed, ω_{max}; and (f) motor speed.

Solution V_s = 600 V, I_a = 250 A, K_v = 0.01527 V/A-rad/s, k = 0.6, and $R_m = R_a + R_f$ = 0.02 + 0.03 = 0.05 Ω.

(a) From Eq. (10-36), $V_{ch} = (1 - 0.6) \times 600 = 240$ V.

(b) From Eq. (10-37), $P_g = 250 \times 600 \times (1 - 0.6) = 60$ kW.

(c) From Eq. (10-39), $R_{eq} = (600/250)(1 - 0.6) + 0.05 = 1.01$ Ω.

(d) From Eq. (10-41), the minimum permissible braking speed,

$$\omega_{min} = \frac{0.05}{0.01527} = 3.274 \text{ rad/s} \quad \text{or} \quad 3.274 \times \frac{30}{\pi} = 31.26 \text{ rpm}$$

(e) From Eq. (10-42), the maximum permissible braking speed,

$$\omega_{max} = \frac{600}{0.01527 \times 250} + \frac{0.05}{0.01527} = 160.445 \text{ rad/s} \quad \text{or} \quad 1532.14 \text{ rpm}$$

(f) From Eq. (10-38), $E_g = 240 + 0.05 \times 250 = 252.5$ V and the motor speed,

$$\omega = \frac{252.5}{0.01527 \times 250} = 66.14 \text{ rad/s or } 631.6 \text{ rpm}$$

Note. The motor speed would decrease with time. To maintain the armature current at the same level, the effective load resistance of the series generator should be adjusted by varying the duty cycle of the chopper.

10-5.3 Principle of Rheostatic Brake Control

In a rheostatic braking, the energy is dissipated in a rheostat and it may not be a desirable feature. In mass rapid transit (MRT) systems, the energy may be used in heating the trains. The rheostatic braking is also known as *dynamic braking*. An arrangement for the rheostatic braking of dc series motor is shown in Fig. 10-16a. This is a one-quadrant drive and operates in the second quadrant as shown in Fig. 10-16b. Figure 10-16c shows the waveforms for the current and voltage, assuming that the armature current is continuous and ripple free.

The average current of the braking resistor,

$$I_b = I_a(1 - k) \tag{10-43}$$

and the average voltage across the braking resistor,

$$V_b = R_b I_a(1 - k) \tag{10-44}$$

The equivalent load resistance of the series generator,

$$R_{eq} = \frac{V_b}{I_a} = R_b(1 - k) + R_m \tag{10-45}$$

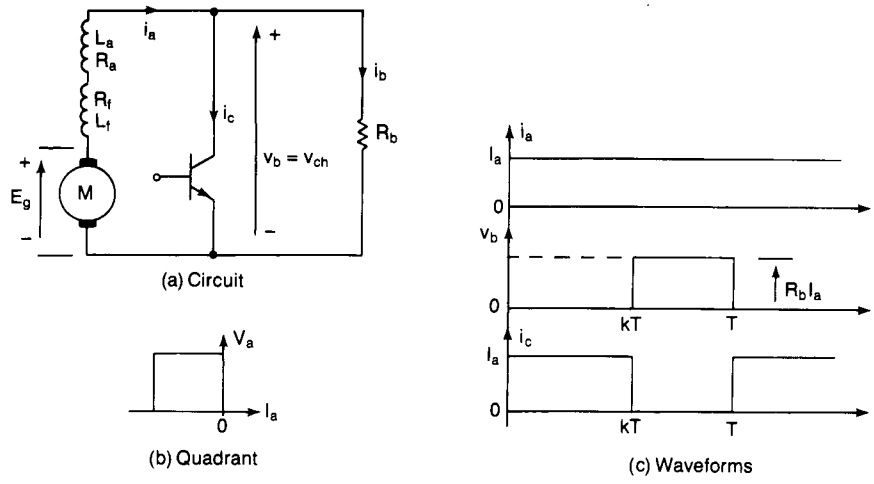


Figure 10-16 Rheostatic braking of dc series motors.

The power dissipated in the resistor, R_b, is

$$P_b = I_a^2 R_b(1 - k) \tag{10-46}$$

By controlling the duty cycle, k, the effective load resistance can be varied from R_m to $R_m + R_b$; and the braking power can be controlled. The braking resistance, R_b, determines the maximum voltage rating of the chopper.

Example 10-9

A dc chopper is used in rheostatic braking of a dc series motor as shown in Fig. 10-16a. The armature resistance is $R_a = 0.02\ \Omega$ and the field resistance is $R_f = 0.03\ \Omega$. The braking resistor, $R_b = 5\ \Omega$. The back emf constant is $K_v = 15.27$ mV/A-rad/s. The average armature current is maintained constant at $I_a = 150$ A. The armature current is continuous and has negligible ripple. If the duty cycle of the chopper is 40%, determine the (a) average voltage across the chopper, V_{ch}; (b) power dissipated in the braking resistor, P_b; (c) equivalent load resistance of the motor acting as a generator, R_{eq}; (d) motor speed; and (e) peak chopper voltage, V_p.

Solution $I_a = 150$ A, $K_v = 0.01527$ V/A-rad/s, $k = 0.4$, and $R_m = R_a + R_f = 0.02 + 0.03 = 0.05\ \Omega$.

(a) From Eq. (10-44), $V_{ch} = V_b = 5 \times 150 \times (1 - 0.4) = 450$ V.

(b) From Eq. (10-46), $P_g = 150 \times 150 \times 5 \times (1 - 0.4) = 13.5$ kW.

(c) From Eq. (10-45), $R_{eq} = 5 \times (1 - 0.4) + 0.05 = 3.01\ \Omega$.

(d) The generated emf, $E_g = 450 + 0.05 \times 150 = 457.5$ V and the braking speed,

$$\omega = \frac{457.5}{0.01527 \times 150} = 199.74 \text{ rad/s} \quad \text{or} \quad 1907.4 \text{ rpm}$$

(e) The peak chopper voltage, $V_p = I_a R_b = 150 \times 5 = 750$ V.

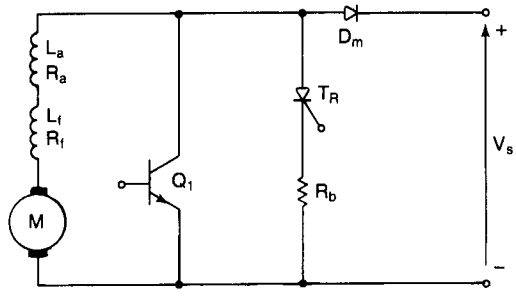


Figure 10-17 Combined regenerative and rheostatic braking.

10-5.4 Principle of Combined Regenerative and Rheostatic Brake Control

Regenerative braking is energy-efficient braking. On the other hand, the energy is dissipated as heat in rheostatic braking. If the supply is partly receptive, which is normally the case in practical traction systems, a combined regenerative and rheostatic brake control would be the most energy efficient. Figure 10-17 shows an arrangement in which rheostatic braking is combined with regenerative braking.

During regenerative brakings, the line voltage is sensed continuously. If it exceeds a certain preset value, normally 20% above the line voltage, the regenerative braking is removed and a rheostatic braking is applied. It allows an almost instantaneous transfer from regenerative to rheostatic braking if the line becomes nonreceptive, even momentarily. In every cycle, the logic circuit determines the receptivity of the supply. If it is nonreceptive, thyristor T_R is turned "on" to divert the motor current to the resistor, R_b. Thyristor T_R is self-commutated when transistor Q_1 is turned "on" in the next cycle.

10-5.5 Two/Four-Quadrant Chopper Drives

During power control, a chopper-fed drive operates in the first quadrant, where the armature voltage and armature current are positive as shown in Fig. 10-14b. In a regenerative braking, the chopper drive operates in the second quadrant, where the armature voltage is positive and the armature current is negative, as shown in Fig. 10-15b.

Two-quadrant operation, as shown in Fig. 10-18a, is required to allow power and regenerative braking control. The circuit arrangement of a transistorized two-quadrant drive is shown in Fig. 10-18b.

Power control. Transistor Q_1 and diode D_1 operate. When Q_1 is turned on, the supply voltage V_s is connected to the motor terminals. When Q_1 is turned off, the armature current which flows through the freewheeling diode D_1 decays.

Regenerative control. Transistor Q_2 and diode D_2 operate. When Q_2 is turned on, the series motor acts as a generator and the armature current rises.

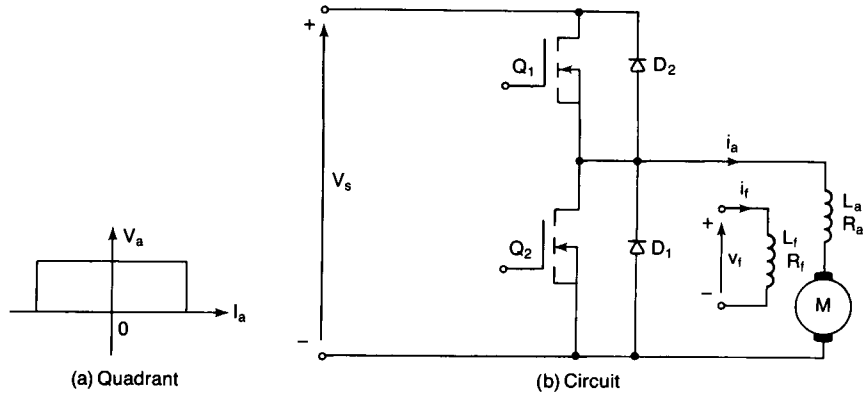


Figure 10-18 Two-quadrant transistorized chopper drive.

When Q_2 is turned off, the motor, acting as a generator, returns energy to the supply through the regenerative diode D_2.

In industrial applications, four-quadrant operation, as shown in Fig. 10-19a, is required. A transistorized four-quadrant drive is shown in Fig. 10-19b.

Forward power control. Transistors Q_1 and Q_2 operate. Transistors Q_3 and Q_4 are off. When Q_1 and Q_2 are turned on together, the supply voltage appears across the motor terminals and the armature current rises. When Q_1 is turned off and Q_2 is still turned on, the armature current decays through Q_2 and D_4.

Forward regeneration. Transistors Q_1, Q_2, and Q_3 are turned off. When transistor Q_4 is turned on, the armature current, which rises, flows through Q_4 and D_2. When Q_4 is turned off, the motor, acting as a generator, returns energy to the supply through D_1 and D_2.

Reverse power control. The field current of the motor is reversed. Transistors Q_3 and Q_4 operate. Transistors Q_1 and Q_2 are off. When Q_3 and Q_4 are

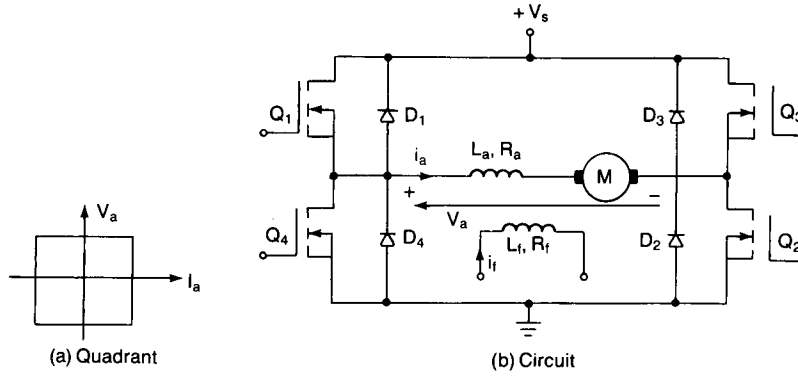


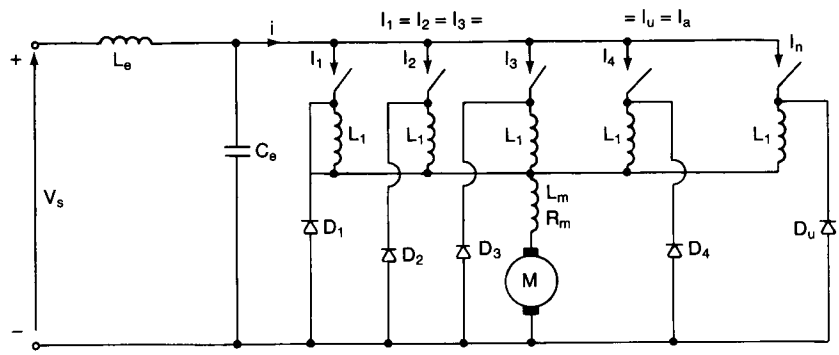
Figure 10-19 Four-quadrant transistorized chopper drive.

turned on together, the armature current rises and flows in the reverse direction. When Q_3 is turned off and Q_4 is turned on, the armature current falls through Q_4 and D_2.

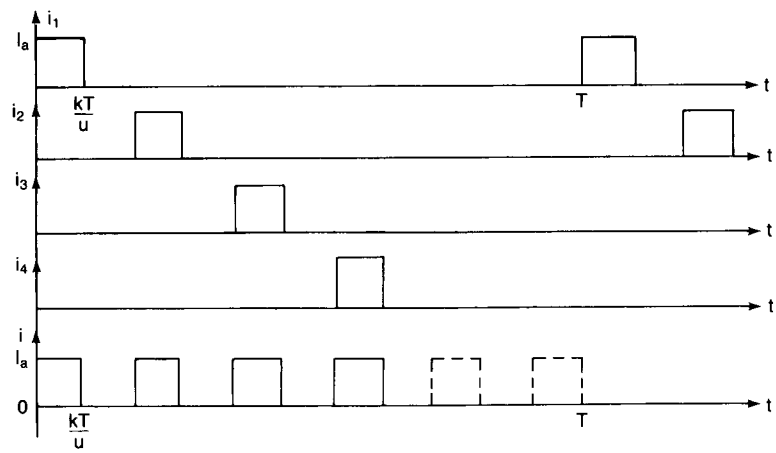
Reverse regeneration. The field current is in the same direction as in reverse power control. Transistors Q_1, Q_3, and Q_4 are off. When Q_2 is turned on, the armature current rises through Q_2 and D_4. When Q_2 is turned off, the armature current falls and the motor returns energy to the supply through D_3 and D_4.

10-5.6 Multiphase Choppers

If two or more choppers are operated in parallel and are phase shifted from each other by π/u as shown in Fig. 10-20a, the amplitude of the load current ripples decreases and the ripple frequency increases. As a result, the chopper-generated harmonic currents in the supply are reduced. The sizes of the input filter are also



(a) Circuit



(b) Waveforms

Figure 10-20 Multiphase choppers.

reduced. The multiphase operation allows the reduction of smoothing chokes, which are normally connected in the armature circuit of dc motors. Separate inductors in each phase are used for current sharing. Figure 10-20b shows the waveforms for the currents with u choppers.

For u choppers in multiphase operation, it can be proved that Eq. (7-19) is satisfied when $k = 1/2u$ and the maximum peak-to-peak load ripple current becomes

$$\Delta I_{\max} = \frac{V_s}{R_m} \tanh \frac{R_m}{4ufL_m} \tag{10-47}$$

where L_m and R_m are the armature inductance and resistance, respectively. For $4ufL_m >> R_m$, the maximum peak-to-peak load ripple current can be approximated to

$$\Delta I_{\max} = \frac{V_s}{4ufL_m} \tag{10-48}$$

If a LC-input filter is used, Eq. (7-124) can be applied to find the rms nth harmonic component of chopper-generated harmonics in the supply

$$\begin{aligned} I_{\text{ns}} &= \frac{1}{1 + (2n\pi uf)^2 L_e C_e} I_{nc} \\ &= \frac{1}{1 + (nuf/f_0)^2} I_{nc} \end{aligned} \tag{10-49}$$

where I_{nc} is the rms value of the nth harmonic component of the chopper current, which is similar to Eq. (7-10), and f_0 [$= 1/2\pi\sqrt{(L_e C_e)}$] is the resonant frequency of the input filter. If $(nuf/f_0) >> 1$, the nth harmonic current in the supply becomes

$$I_{ns} = I_{nc} \left(\frac{f_0}{nuf}\right)^2 \tag{10-50}$$

Multiphase operations are advantageous for large motor drives, especially if the load current requirement is large. However, considering the additional complexity involved in increasing the number of choppers, there is not much reduction in the chopper-generated harmonics in the supply line if more than two choppers are used [7]. In practice, both the magnitude and frequency of the line current harmonics are important factors to determine the level of interferences into the signaling circuits. In many rapid transit systems, the power and signaling lines are very close; in three-line systems, they even share a common line. The signaling circuits are sensitive to particular frequencies and the reduction in the magnitude of harmonics by using a multiphase operation of choppers could generate frequencies within the sensitivity band—which might cause more problems than it solves.

Example 10-10

Two choppers control a dc series motor and they are phase shifted in operation by $\pi/2$. The supply voltage to the chopper drive, $V_s = 220$ V, armature circuit resistance, $R_m = 4\ \Omega$, armature circuit inductance, $L_m = 15$ mH, and the frequency of each chopper, $f = 350$ Hz. Calculate the maximum peak-to-peak load ripple current.

Solution The effective chopping frequency is $f_e = 2 \times 350 = 700$ Hz, $R_m = 4\ \Omega$, $L_m = 15$ mH, $u = 2$, and $V_s = 220$ V. $4ufL_m = 4 \times 2 \times 350 \times 15 \times 10^{-3} = 42$. Since $42 >> 4$, the approximate equation (10-48) can be used, and this gives the maximum peak-to-peak load ripple current, $\Delta I_{max} = 220/42 = 5.24$ A.

Example 10-11

A dc series motor is controlled by two multiphase choppers. The average armature current, $I_a = 100$ A. A simple LC-input filter with $L_e = 0.3$ mH and $C_e = 4500\ \mu$F is used. Each chopper is operated at a frequency of $f = 350$ Hz. Determine the rms fundamental component of the chopper-generated harmonic current in the supply.

Solution $I_a = 100$ A, $u = 2$, $L_e = 0.3$ mH, $C_e = 4500\ \mu$F, and $f_0 = 1/(2\pi\sqrt{L_eC_e}) = 136.98$ Hz. The effective chopper frequency is $f_e = 2 \times 350 = 700$ Hz. From the results of Example 7-13, the rms value of the fundamental component of the chopper current is $I_{1c} = 45.02$ A. From Eq. (10-49), the fundamental component of the chopper-generated harmonic current is

$$I_{1s} = \frac{45.02}{1 + (2 \times 350/136.98)^2} = 1.66 \text{ A}$$

10-6 CLOSED-LOOP CONTROL OF DC DRIVES

The speed of dc motors changes with the load torque. To maintain a constant speed, the armature (and or field) voltage should be varied continuously by varying the delay angle of ac–dc converters or duty cycle of dc choppers. In practical drive systems it is required to operate the drive at a constant torque or constant power; in addition, controlled acceleration and deceleration are required. Most industrial drives operate as closed-loop feedback systems. A closed-loop control system has the advantages of improved accuracy, fast dynamic response, and reduced effects of load disturbances and system nonlinearities.

The block diagram of a closed-loop converter-fed separately excited dc drive is shown in Fig. 10-21. If the speed of the motor decreases due to the application of additional load torque, the speed error V_e increases. The speed controller responses with an increased control signal V_c, changes the delay angle or duty cycle of the converter, and increases the armature voltage of the motor. An increased armature voltage develops more torque to restore the motor speed to the original value. The drive normally passes through a transient period until the developed torque is equal to the load torque.

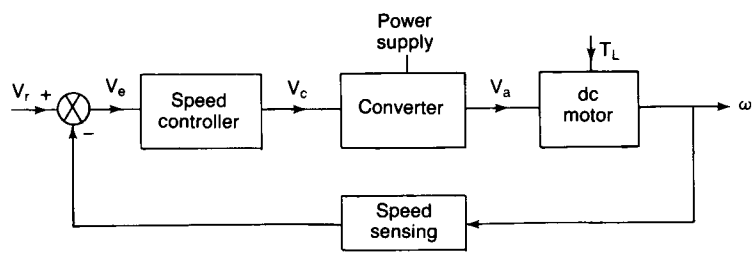


Figure 10-21 Block diagram of a closed-loop converter-fed dc motor drive.

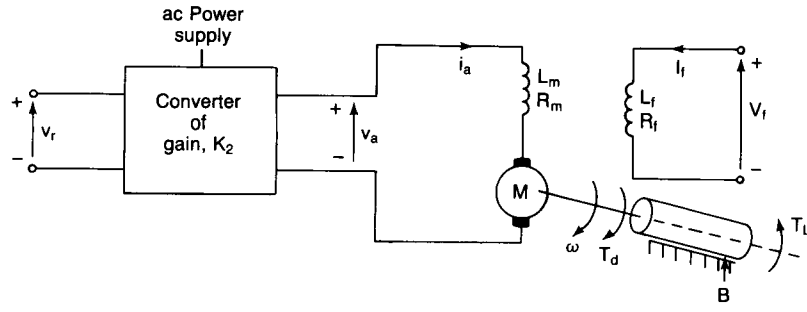


Figure 10-22 Converter-fed separately excited dc motor drive.

10-6.1 Open-Loop Transfer Function

The steady-state characteristics of dc drives, which are discussed in the preceding sections, are of major importance in the selection of dc drives and are not sufficient when the drive is in closed-loop control. Knowledge of the dynamic behavior, which is normally expressed in the form of a transfer function, is also important.

The circuit arrangement of a converter-fed separately excited dc motor drive with open-loop control is shown in Fig. 10-22. The motor speed is adjusted by setting reference (or control) voltage v_r. Assuming a linear power converter of gain K_2, the armature voltage of the motor is

$$v_a = K_2 v_r \tag{10-51}$$

Assuming that the motor field current I_f and the back emf constant remain constant K_v during any transient disturbances, the system equations are

$$e_g = K_v I_f \omega \tag{10-52}$$

$$v_a = R_m i_a + L_m \frac{di_a}{dt} + e_g = R_m i_a + L_m \frac{di_a}{dt} + K_v I_f \omega \tag{10-53}$$

$$T_d = K_t I_f i_a \tag{10-54}$$

$$T_d = K_t I_f i_a = J \frac{d\omega}{dt} + B\omega + T_L \tag{10-55}$$

The transient behavior may be analyzed by changing the system equations into Laplace's transforms with zero initial conditions. Transforming Eqs. (10-51), (10-53), and (10-55) yields

$$V_a(s) = K_1 V_r(s) \tag{10-56}$$

$$V_a(s) = R_m I_a(s) + sL_m I_a(s) + K_v I_f \omega(s) \tag{10-57}$$

$$T_d(s) = K_t I_f I_a(s) = sJ\omega(s) + B\omega(s) + T_L(s) \tag{10-58}$$

From Eq. (10-57), the armature current is

$$I_a(s) = \frac{V_a(s) - K_v I_f \omega(s)}{sL_m + R_m} \tag{10-59}$$

$$= \frac{V_a(s) - K_v I_f \omega(s)}{R_m(s\tau_a + 1)} \tag{10-60}$$

where $\tau_a = L_m/R_m$ is known as the *time constant* of motor armature circuit. From Eq. (10-58), the motor speed is

$$\omega(s) = \frac{T_d(s) - T_L(s)}{sJ + B} \tag{10-61}$$

$$= \frac{T_d(s) - T_L(s)}{B(s\tau_m + 1)} \tag{10-62}$$

where $\tau_m = J/B$ is known as the *mechanical time constant* of the motor. Equations (10-56), (10-60), and (10-62) can be used to draw the open-loop block diagram as shown in Fig. 10-23. Two possible disturbances are control voltage, V_r, and load torque, T_L. The steady-state responses can be determined by combining the individual response due to V_r and T_L.

The response due to a step change in the reference voltage is obtained by setting T_L to zero. From Fig. 10-23, we can obtain the speed response due to reference voltage as

$$\frac{\omega(s)}{V_r(s)} = \frac{K_2 K_v I_f/(R_m B)}{s^2(\tau_a\tau_m) + s(\tau_a + \tau_m) + 1 + (K_v I_f)^2/R_m B} \tag{10-63}$$

The response due to a change in load torque, T_L, can be obtained by setting V_r to zero. The block diagram for a step change in load torque disturbance is shown in Fig. 10-24.

$$\frac{\omega(s)}{T_L(s)} = -\frac{(1/B)(s\tau_a + 1)}{s^2(\tau_a\tau_m) + s(\tau_a + \tau_m) + 1 + (K_v I_f)^2/R_m B} \tag{10-64}$$

Using the final value theorem, the steady-state relationship of a change in speed, $\Delta\omega$, due to a step change in control voltage, ΔV_r, and a step change in load torque,

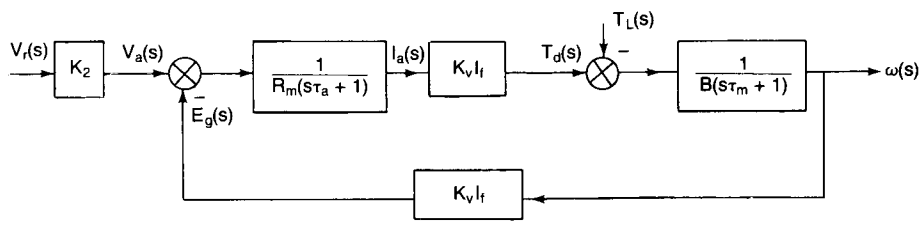


Figure 10-23 Open-loop block diagram of separately excited dc motor drive.

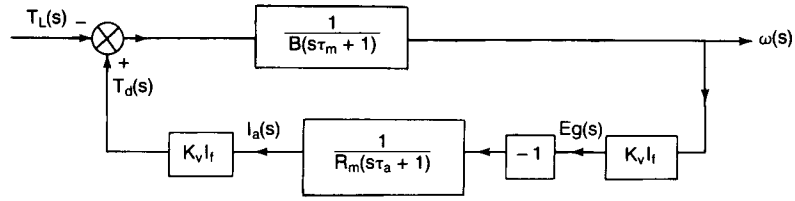


Figure 10-24 Open-loop block diagram for torque disturbance input.

ΔT_L, can be found from Eqs. (10-63) and (10-64), respectively, by substituting $s = 0$.

$$\Delta\omega = \frac{K_2 K_v I_f}{R_m B + (K_v I_f)^2} \Delta V_r \tag{10-65}$$

$$\Delta\omega = -\frac{R_m}{R_m B + (K_v I_f)^2} \Delta T_L \tag{10-66}$$

The dc series motors are used extensively in traction applications where the steady-state speed is determined by the friction and gradient forces. By adjusting the armature voltage, the motor may be operated at a constant torque (or current) up to the base speed, which corresponds to the maximum armature voltage. A chopper-controlled dc series motor drive is shown in Fig. 10-25.

The armature voltage is related to the control (or reference) voltage by a linear gain of the chopper, K_2. Assuming that the back emf constant K_v does not change with the armature current and remains constant, the system equations are

$$v_a = K_2 v_r \tag{10-67}$$

$$e_g = K_v i_a \omega \tag{10-68}$$

$$v_a = R_m i_a + L_m \frac{di_a}{dt} + e_g \tag{10-69}$$

$$T_d = K_t i_a^2 \tag{10-70}$$

$$T_d = J \frac{d\omega}{dt} + B\omega + T_L \tag{10-71}$$

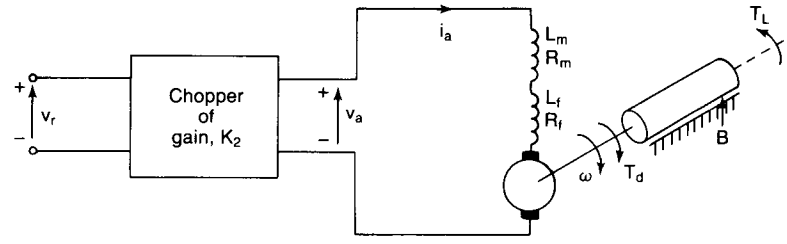


Figure 10-25 Chopper-fed dc series motor drive.

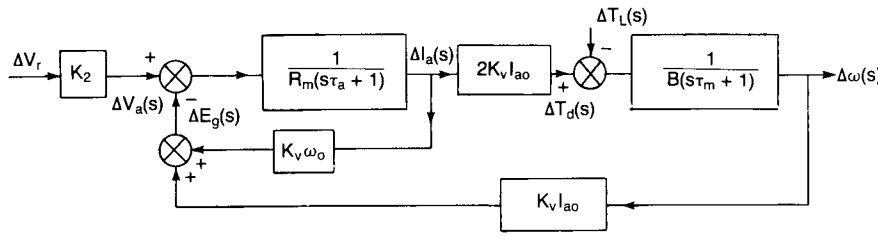


Figure 10-26 Open-loop block diagram of chopper-fed dc series drive.

Equation (10-70) contains a product of variable-type nonlinearities, and as a result the application of transfer function techniques would no longer be valid. However, these equations can be linearized by considering a small perturbation at the operating point. Let us define the system parameters around the operating point as

$$e_g = E_{g0} + \Delta e_g \qquad i_a = I_{a0} + \Delta i_a \qquad v_a = V_{a0} + \Delta v_a \qquad T_d = T_{d0} + \Delta T_d$$

$$\omega = \omega_0 + \Delta\omega \qquad v_r = V_{r0} + \Delta v_r \qquad T_L = T_{L0} + \Delta T_L$$

Recognizing that $\Delta i_a\ \Delta\omega$ and $(\Delta i_a)^2$ are very small, tending to zero, Eqs. (10-67) to (10-71) can be linearized to

$$\Delta v_a = K_2\,\Delta v_r$$

$$\Delta e_g = K_v(I_{a0}\,\Delta\omega + \omega_0\,\Delta i_a)$$

$$\Delta v_a = R_m\,\Delta i_a + L_m\frac{d(\Delta i_a)}{dt} + \Delta e_g$$

$$\Delta T_d = 2K_v I_{a0}\,\Delta i_a$$

$$\Delta T_d = J\frac{d(\Delta\omega)}{dt} + B\,\Delta\omega + \Delta T_L$$

Transforming these equations in Laplace's domain gives us

$$\Delta V_a(s) = K_2\Delta V_r(s) \tag{10-72}$$

$$\Delta E_g(s) = K_v[I_{a0}\,\Delta\omega(s) + \omega_0\,\Delta I_a(s)] \tag{10-73}$$

$$\Delta V_a(s) = R_m\,\Delta I_a(s) + sL_m\,\Delta I_a(s) + \Delta E_g(s) \tag{10-74}$$

$$\Delta T_d(s) = 2K_v I_{a0}\,\Delta I_a(s) \tag{10-75}$$

$$\Delta T_d(s) = sJ\,\Delta\omega(s) + B\,\Delta\omega(s) + \Delta T_L(s) \tag{10-76}$$

These five equations are sufficient to establish the block diagram of a dc series motor drive as shown in Fig. 10-26. It is evident from Fig. 10-26 that any change in either reference voltage or load torque will result in a change of speed. The block diagram for a change in reference voltage is shown in Fig. 10-27a and that for a change in load torque is shown in Fig. 10-27b.

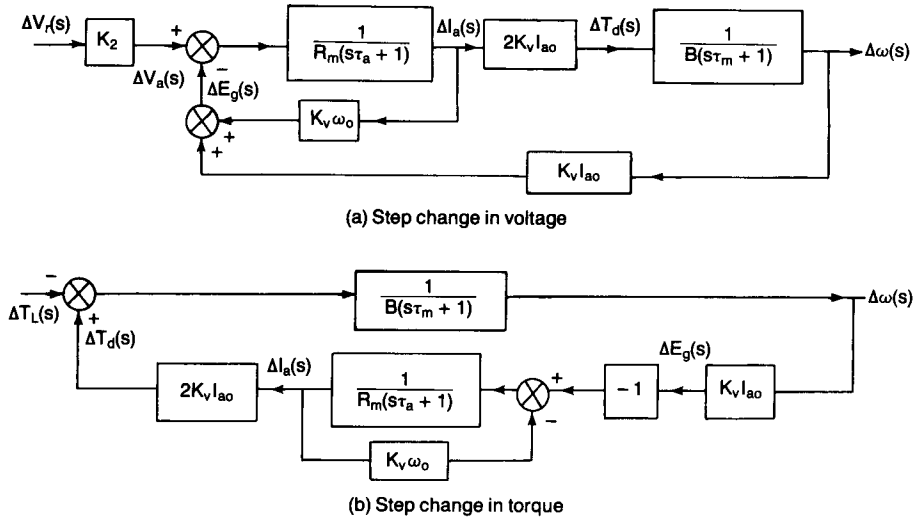


Figure 10-27 Block diagram for reference voltage and load torque disturbances.

10-6.2 Closed-Loop Transfer Function

To change the open-loop arrangement in Fig. 10-22 into a closed-loop system, a speed sensor is connected to the output shaft. The output of the sensor, which is proportional to the speed, is amplified by a factor of K_1 and is compared with the reference voltage V_r to form the error voltage V_e. The complete block diagram is shown in Fig. 10-28.

The closed-loop step response due to a change in reference voltage is found from Fig. 10-28 with $T_L = 0$ as

$$\frac{\omega(s)}{V_r(s)} = \frac{K_2K_vI_f/(R_mB)}{s^2(\tau_a\tau_m) + s(\tau_a + \tau_m) + 1 + [(K_vI_f)^2 + K_1K_2K_vI_f]/R_mB} \tag{10-77}$$

The response due to a change in the load torque T_L can also be obtained from Fig. 10-28 by setting V_r to zero.

$$\frac{\omega(s)}{T_L(s)} = -\frac{(1/B)(s\tau_a + 1)}{s^2(\tau_a\tau_m) + s(\tau_a + \tau_m) + 1 + [(K_vI_f)^2 + K_1K_2K_vI_f]/R_mB} \tag{10-78}$$

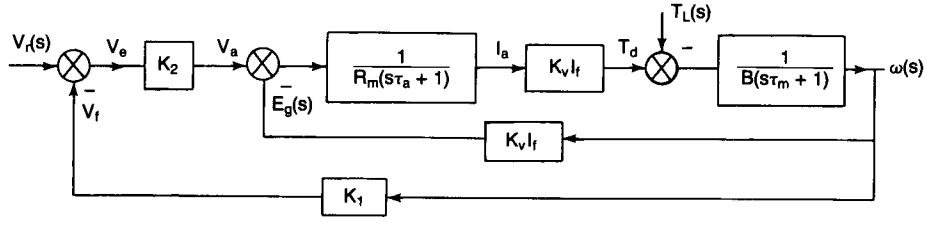


Figure 10-28 Block diagram for closed-loop control of separately excited dc motor.

Using the final value theorem, the steady-state change in speed, $\Delta\omega$, due to a step change in control voltage, ΔV_r, and a step change in load torque, ΔT_L, can be found from Eqs. (10-77) and (10-78), respectively, by substituting $s = 0$.

$$\Delta\omega = \frac{K_2 K_v I_f}{R_m B + (K_v I_f)^2 + K_1 K_2 K_v I_f} \Delta V_r \tag{10-79}$$

$$\Delta\omega = -\frac{R_m}{R_m B + (K_v I_f)^2 + K_1 K_2 K_v I_f} \Delta T_L \tag{10-80}$$

Example 10-12

A 50-kW 240-V 1700-rpm separately excited dc motor is controlled by a converter as shown in the block diagram Fig. 10-28. The field current is maintained constant at $I_f = 1.4$ A and the machine back emf constant is $K_v = 0.91$ V/A-rad/s. The armature resistance is $R_m = 0.1\ \Omega$ and the viscous friction constant is $B = 0.3$ N·m/rad/s. The amplification of the speed sensor is $K_1 = 95$ mV/rad/s and the gain of the power controller is $K_2 = 100$. (a) Determine the rated torque of the motor. (b) Determine the reference voltage V_r to drive the motor at the rated speed. (c) If the reference voltage is kept unchanged, determine the speed when the motor develops the rated torque. (d) If the load torque is increased by 10% of the rated value, determine the motor speed. (e) If the reference voltage is reduced by 10%, determine the motor speed. (f) If the load torque is increased by 10% of the rated value and the reference voltage is reduced by 10%, determine the motor speed. (g) If there was no feedback in an open-loop control, determine the speed regulation for a reference voltage of $V_r = 2.31$ V. (h) Determine the speed regulation with a closed-loop control.

Solution $I_f = 1.4$ A, $K_v = 0.91$ VA-rad/s, $K_1 = 95$ mV/rad/s, $K_2 = 100$, $R_m = 0.1\ \Omega$, $B = 0.3$ N·m/rad/s, and $\omega_{rated} = 1700\ \pi/30 = 178.02$ rad/s.

(a) The rated torque, $T_L = 50{,}000/178.02 = 280.87$ N·m.

(b) Since $V_a = K_2 V_r$, for open-loop control Eq. (10-65) gives

$$\frac{\omega}{V_a} = \frac{\omega}{K_2 V_r} = \frac{K_v I_f}{R_m B + (K_v I_f)^2} = \frac{0.91 \times 1.4}{0.1 \times 0.3 + (0.91 \times 1.4)^2} = 0.7707$$

At rated speed,

$$V_a = \frac{\omega}{0.7707} = \frac{178.02}{0.7707} = 230.98 \text{ V}$$

and feedback voltage,

$$V_b = K_1 \omega = 95 \times 10^{-3} \times 178.02 = 16.912 \text{ V}$$

With closed-loop control, $(V_r - V_b)K_2 = V_a$ or $(V_r - 16.912) \times 100 = 230.98$, which gives the reference voltage, $V_r = 19.222$ V.

(c) $V_r = 19.222$ V, $\Delta T_L = 280.87$ N·m, and Eq. (10-80) gives

$$\Delta\omega = -\frac{0.1 \times 280.86}{0.1 \times 0.3 + (0.91 \times 1.4)^2 + 95 \times 10^{-3} \times 100 \times 0.91 \times 1.4}$$

$$= -2.04 \text{ rad/s}$$

The speed at rated torque,

$$\omega = 178.02 - 2.04 = 175.98 \text{ rad/s} \quad \text{or} \quad 1680.5 \text{ rpm}$$

(d) $\Delta T_L = 1.1 \times 280.86 = 308.87$ N·m and Eq. (10-80) gives

$$\Delta\omega = -\frac{0.1 \times 308.96}{0.1 \times 0.3 + (0.91 \times 1.4)^2 + 95 \times 10^{-3} \times 100 \times 0.91 \times 1.4}$$

$$= -2.246 \text{ rad/s}$$

The motor speed,

$$\omega = 178.02 - 2.246 = 175.774 \text{ rad/s} \quad \text{or} \quad 1678.5 \text{ rpm}$$

(e) $\Delta V_r = -0.1 \times 19.222 = -1.9222$ V and Eq. (10-79) gives the change in speed,

$$\Delta\omega = -\frac{100 \times 0.91 \times 1.4 \times 1.9222}{0.1 \times 0.3 + (0.91 \times 1.4)^2 + 95 \times 10^{-3} \times 100 \times 0.91 \times 1.4}$$

$$= -17.8 \text{ rad/s}$$

The motor speed is

$$\omega = 178.02 - 17.8 = 160.22 \text{ rad/s or } 1530 \text{ rpm}$$

(f) The motor speed can be obtained by using superposition:

$$\omega = 178.02 - 2.246 - 17.8 = 158 \text{ rad/s} \quad \text{or} \quad 1508.5 \text{ rpm}$$

(g) $\Delta V_r = 2.31$ V and Eq. (10-65) gives

$$\Delta\omega = \frac{100 \times 0.91 \times 1.4 \times 2.31}{0.1 \times 0.3 + (0.91 \times 1.4)^2} = 178.02 \text{ rad/s} \quad \text{or} \quad 1700 \text{ rpm}$$

and the no-load speed is $\omega = 178.02$ rad/s or 1700 rpm. For full load, $\Delta T_L = 280.87$ N·m:

$$\Delta\omega = -\frac{0.1 \times 280.87}{0.1 \times 0.3 + (0.91 \times 1.4)^2} = -16.99 \text{ rad/s}$$

and the full-load speed,

$$\omega = 178.02 - 16.99 = 161.03 \text{ rad/s} \quad \text{or} \quad 1537.7 \text{ rpm}$$

The speed regulation with open-loop control is

$$\frac{1700 - 1537.7}{1537.7} = 10.55\%$$

(h) The speed regulation with closed-loop control is

$$\frac{1700 - 1680.5}{1680.5} = 1.16\%$$

Note. By closed-loop control, the speed regulation is reduced by a factor of approximately 10, from 10.55% to 1.16%.

10-6.3 Phase-Locked-Loop Control

For precise speed control of servo systems, closed-loop control is normally used. The speed, which is sensed by analog sensing devices (e.g., tachometer), is com-

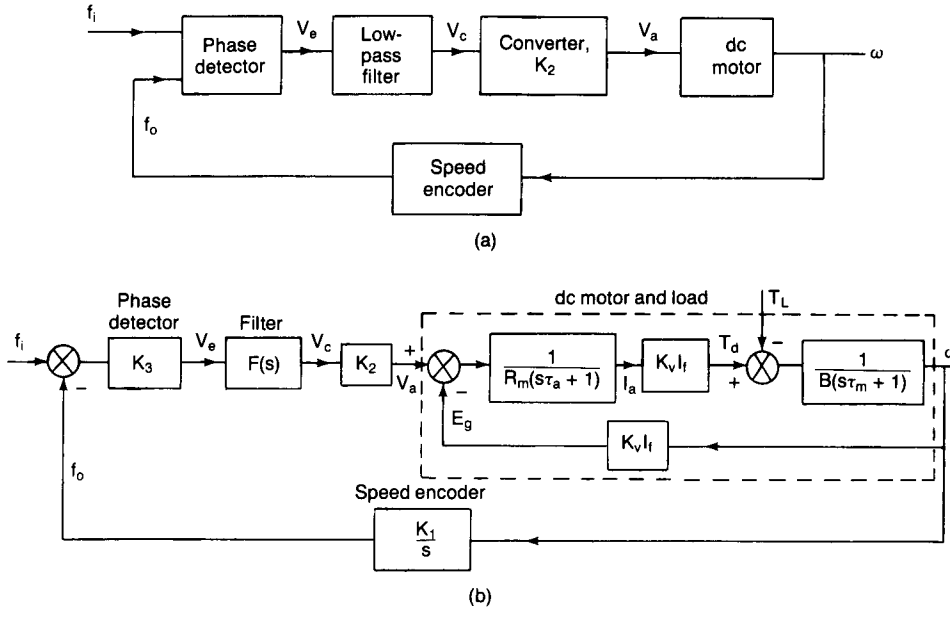


Figure 10-29 Phase-locked-loop control system.

pared with the reference speed to generate the error signal and to vary the armature voltage of the motor. These analog devices for speed sensing and comparing signals are not ideal and the speed regulation is more than 0.2%. The speed regulator can be improved if digital phase-locked-loop (PLL) control is used. The block diagram of a converter-fed dc motor drive with phase-locked-loop control is shown in Fig. 10-29a and the transfer function block diagram is shown in Fig. 10-29b.

In a phase-locked-loop control system, the motor speed is converted to a digital pulse train by using a speed encoder. The output of the encoder acts as the speed feedback signal of frequency f_0. The phase detector compares the reference pulse train (or frequency) f_r with the feedback frequency f_0 and provides a pulse-width-modulated output voltage V_e which is proportional to the difference in phases and frequencies of the reference and feedback pulse trains. The phase detector (or comparator) is available in integrated circuits. A low-pass loop filter converts the pulse train V_e to a continuous dc level V_c which varies the output of the power converter and in turn the motor speed.

When the motor runs at the same speed as the reference pulse train, the two frequencies would be synchronized (or locked) together with a phase difference. The output of the phase detector would be a constant voltage proportional to the phase difference and the steady-state motor speed would be maintained at a fixed value irrespective of the load on the motor. Any disturbances contributing to the speed change would result in a phase difference and the output of the phase detector would respond immediately to vary the speed of the motor in such a direction and magnitude as to retain the locking of the reference and feedback frequencies. The response of the phase detector is very fast. As long as the two frequencies are

locked, the speed regulation should ideally be zero. However, in practice the speed regulation is limited to 0.002%, and this represents a significant improvement over the analog speed control system.

10-6.4 Microcomputer Control of DC Drives

The analog control scheme for a converter-fed dc motor drive can be implemented by hardwired electronics. An analog control scheme has several disadvantages: nonlinearity of speed sensor, temperature dependency, drift, and offset. Once a control circuit is built to meet certain performance criteria, it may require major changes in the hardwired logic circuits to meet other performance requirements.

A microcomputer control reduces the size and costs of hardwired electronics, improving reliability and control performance. This control scheme is implemented in the software and is flexible to change the control strategy to meet different performance characteristics or add extra control features. A microcomputer control system can also perform various desirable functions: on/off of the main power supply, start/stop of the drive, speed control, current control, monitoring the control variables, initiating protection and trip circuit, diagnostics for built-in fault finding, and communication with a supervisory central computer. Figure 10-30 shows a schematic diagram for a microcomputer control of a converter-fed four-quadrant dc drive.

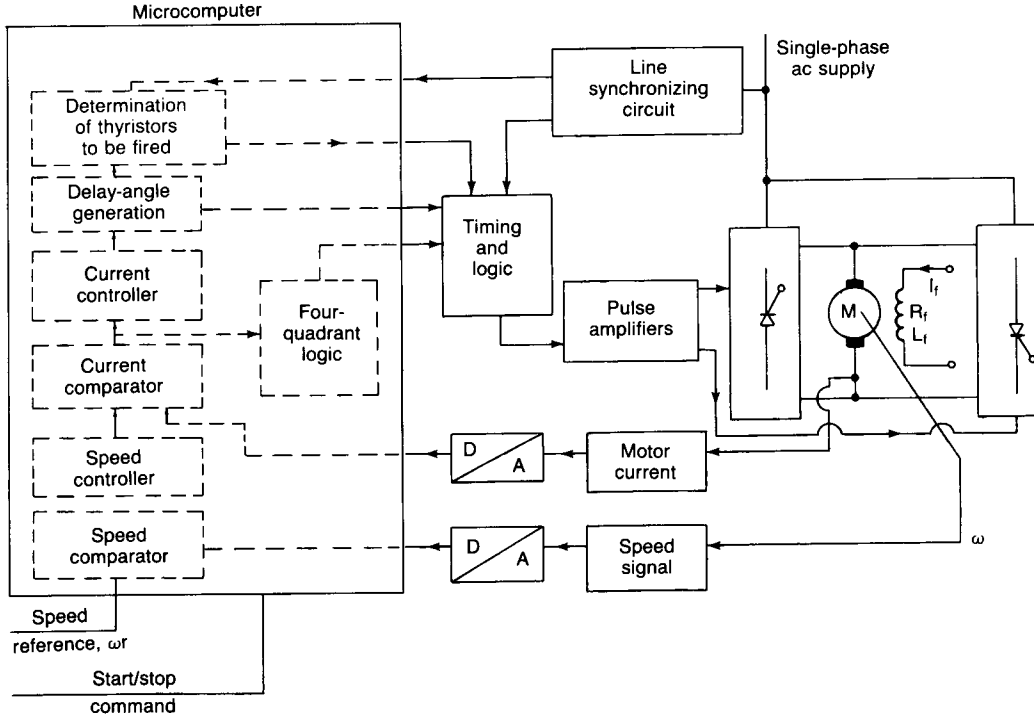


Figure 10-30 Schematic diagram of computer control four-quadrant dc drive.

The speed signal is fed into the microcomputer using an A/D (analog-to-digital) converter. To limit the armature current of the motor, an inner current-control loop is used. The armature current signal can be fed into the microcomputer through an A/D converter or by sampling the armature current. The line synchronizing circuit is required to synchronize the generation of the firing pulses with the supply line frequency. Although the microcomputer can perform the functions of gate pulse generator and logic circuit, these are shown outside the microcomputer. The pulse amplifier provides the necessary isolation and produces gate pulses of required magnitude and duration.

SUMMARY

In dc drives, the armature and field voltages of dc motors are varied by either ac–dc converters or dc choppers. The ac–dc converter-fed drives are normally used in variable-speed applications, whereas chopper-fed drives are more suited for traction applications. Dc series motors are mostly used in traction applications, due to their capability of high starting torque.

Dc drives can be classified broadly into three types depending on the input supply: (1) single-phase drives, (2) three-phase drives, and (3) chopper drives. Again each drive could be subdivided into three types depending on the modes of operation: (a) one-quadrant drives, (b) two-quadrant drives, and (c) four-quadrant drives. The energy-saving feature of chopper-fed drives is very attractive for use in transportation systems requiring frequent stops.

Closed-loop control, which has many advantages, is used in industrial drives. The speed regulation of dc drives can be significantly improved by using phase-locked-loop (PLL) control. The analog control schemes, which are hardwired electronics, are limited in flexibility and have certain disadvantages, whereas microcomputer control drives, which are implemented in software, are more flexible and can perform many desirable functions.

REFERENCES

1. J. F. Lindsay and M. H. Rashid, *Electromechanics and Electrical Machinery*, Englewood Cliffs, N. J. : Prentice-Hall, Inc., 1986.
2. P. C. Sen, *Thyristor DC Drives*. New York: John Wiley & Sons, Inc., 1981.
3. P. C. Sen and M. L. McDonald, "Thyristorized dc drives with regenerative braking and speed reversal." *IEEE Transactions on Industrial Electronics and Control Instrumentation*, Vol. IECI25, No. 4, 1978, pp. 347–354.
4. M. H. Rashid, "Dynamic responses of dc chopper controlled series motor." *IEEE Transactions on Industrial Electronics and Control Instrumentation*, Vol. IECI28, No. 4, 1981, pp. 323–340.
5. M. H. Rashid, "Regenerative characteristics of dc chopper controlled series motor." *IEEE Transactions on Vehicular Technology*, Vol. VT33, No. 1, 1984, pp. 3–13.

6. E. Reimers, "Design analysis of multiphase dc chopper motor drive." *IEEE Transactions on Industry Applications*, Vol. IA8, No. 2, 1972, pp. 136–144.
7. M. H. Rashid, "Design of *LC* input filter for multiphase dc choppers." *Proceedings IEE*, Vol. B130, No. 1, 1983, pp. 310–44.
8. D. F. Geiger, *Phaselock Loops for DC Motor Speed Control.* New York: John Wiley & Sons, Inc., 1981.
9. S. K. Tso and P. T. Ho, "Dedicated microprocessor scheme for thyristor phase control of multiphase converters." *Proceedings IEE*, Vol. B22, 1981, pp. 101–108.
10. J. Best and P. Mutschler, "Control of armature and field current of a chopper-fed dc motor drive by a single chip microcomputer." *3rd IFAC Symposium on Control in Power Electronics and Electrical Drives*, Lausanne, Switzerland, 1983, pp. 515–522.

REVIEW QUESTIONS

10-1. What are the three types of dc drives based on the input supply?
10-2. What is the magnetization characteristic of dc motors?
10-3. What is the purpose of a converter in dc drives?
10-4. What is a base speed of dc motors?
10-5. What are the parameters to be varied for speed control of separately excited dc motors?
10-6. Which are the parameters to be varied for speed control of dc series motors?
10-7. Why are the dc series motors mostly used in traction applications?
10-8. What is a speed regulation of dc drives?
10-9. What is the principle of single-phase full-converter-fed dc motor drives?
10-10. What is the principle of three-phase semiconverter-fed dc motor drives?
10-11. What are the advantages and disadvantages of single-phase full-converter-fed dc motor drives?
10-12. What are the advantages and disadvantages of single-phase semiconverter-fed dc motor drives?
10-13. What are the advantages and disadvantages of three-phase full-converter-fed dc motor drives?
10-14. What are the advantages and disadvantages of three-phase semiconverter-fed dc motor drives?
10-15. What are the advantages and disadvantages of three-phase dual-converter-fed dc motor drives?
10-16. Why is it preferable to use a semiconverter for field control of separately excited motors?
10-17. What is a one-quadrant dc drive?
10-18. What is a two-quadrant dc drive?
10-19. What is a four-quadrant dc drive?
10-20. What is the principle of regenerative braking of dc chopper-fed dc motor drives?
10-21. What is the principle of rheostatic braking of dc chopper-fed dc motor drives?

10-22. What are the advantages of chopper-fed dc drives?

10-23. What are the advantages of multiphase choppers?

10-24. What is the principle of closed-loop control of dc drives.?

10-25. What are the advantages of closed-loop control of dc drives?

10-26. What is the principle of phase-locked-loop control of dc drives?

10-27. What are the advantages of phase-locked-loop control of dc drives?

10-28. What is the principle of microcomputer control of dc drives?

10-29. What are the advantages of microcomputer control of dc drives?

10-30. What is a mechanical time constant of dc motors?

10-31. What is an electrical time constant of dc motors?

PROBLEMS

10-1. A separately excited dc motor is supplied from a dc source of 600 V to control the speed of a mechanical load and the field current is maintained constant. The armature resistance and losses are negligible. (**a**) If the load torque is $T_L = 550$ N·m at 1500 rpm, determine the armature current I_a. (**b**) If the armature current remains the same as that in part (a) and the field current is reduced such that the motor runs at a speed of 2800, determine the load torque.

10-2. Repeat Prob. 10-1 if the armature resistance is $R_a = 0.12\ \Omega$. The viscous friction and the no-load losses are negligible.

10-3. A 30-hp 440-V 2000-rpm separately excited motor dc controls a load requiring a torque of $T_L = 85$ N·m at 1200 rpm. The field circuit resistance is $R_f = 294\ \Omega$, the armature circuit resistance is $R_a = 0.12\ \Omega$, and the motor voltage constant is $K_v = 0.7032$ V/A-rad/s. The field voltage is $V_f = 440$ V. The viscous friction and the no-load losses are negligible. The armature current may be assumed continuous and ripple-free. Determine the (**a**) back emf, E_g; (**b**) required armature voltage, V_a; (**c**) rated armature current of the motor; and (**d**) speed regulation at full load.

10-4. A 120-hp 600-V 1200-rpm dc series motor controls a load requiring a torque of $T_L = 185$ N·m at 1100 rpm. The field circuit resistance, $R_f = 0.06\ \Omega$, the armature circuit resistance, $R_a = 0.04\ \Omega$, and the voltage constant, $K_v = 32$ mV/A-rad/s. The viscous friction and the no-load losses are negligible. The armature current is continuous and ripple-free. Determine the (**a**) back emf, E_g; (**b**) required armature voltage, V_a; (**c**) rated armature current; and (**d**) speed regulation at full speed.

10-5. The speed of a separately excited motor is controlled by a single-phase semiconverter in Fig. 10-8a. The field current is also controlled by a semiconverter and the field current is set to the maximum possible value. The ac supply voltage to the armature and field converter is one-phase, 208 V, 60 Hz. The armature resistance is $R_a = 0.12\ \Omega$, the field resistance is $R_f = 220\ \Omega$, and the motor voltage constant is $K_v = 1.055$ V/A-rad/s. The load torque is $T_L = 75$ N·m at a speed of 700 rpm. The viscous friction and no-load losses are negligible. The armature and field currents are continuous and ripple-free. Determine the (**a**) field current, I_f; (**b**) delay angle of the converter in the armature circuit, α_a; and (**c**) input power factor of the armature circuit.

10-6. The speed of a separately excited dc motor is controlled by a single-phase full-wave converter in Fig. 10-9a. The field circuit is also controlled by a full converter and the field current is set to the maximum possible value. The ac supply voltage to the armature and field converters is one-phase, 208 V, 60 Hz. The armature resistance is $R_a = 0.50\ \Omega$, the field circuit resistance is $R_f = 345\ \Omega$, and the motor voltage constant is $K_v = 0.71$ V/A-rad/s. The viscous friction and no-load losses are negligible. The armature and field currents are continuous and ripple-free. If the delay angle of the armature converter is $\alpha_a = 45°$ and the armature current of the motor is $I_a = 55$ A, determine the (**a**) torque developed by the motor, T_d; (**b**) speed, ω; and (**c**) input power factor of the drive, PF.

10-7. If the polarity of the motor back emf in Prob. 10-6 is reversed by reversing the polarity of the field current, determine the (**a**) delay angle of the field circuit converter, α_f; (**b**) delay angle of the armature circuit converter, α_a, to maintain the armature current constant at the same value of $I_a = 55$ A; and (**c**) power fed back to the supply during regenerative braking of the motor.

10-8. The speed of a 20-hp 300-V 1800-rpm separately excited dc motor is controlled by a three-phase full-converter drive. The field current is also controlled by a three-phase full-converter and is set to the maximum possible value. The ac input is three-phase, Y-connected, 208 V, 60 Hz. The armature resistance, $R_a = 0.35\ \Omega$, the field resistance, $R_f = 250\ \Omega$, and the motor voltage constant motor, $K_v = 1.15$ V/A-rad/s. The armature and field currents is continuous and ripple-free. The viscous friction and no-load losses are negligible. Determine the (**a**) delay angle of the armature converter, α_a, if the motor supplies the rated power at the rated speed; (**b**) no-load speed if the delay angles are the same as in part (a) and the armature current at no-load is 10% of the rated value; and (**c**) speed regulation.

10-9. Repeat Prob. 10-8 if both armature and field circuits are controlled by three-phase semiconverters.

10-10. The speed of a 20-hp 300-V 900-rpm separately excited dc motor is controlled by a three-phase full converter. The field circuit is also controlled by a three-phase full converter. The ac input to armature and field converters is three-phase, Y-connected, 208 V, 60 Hz. The armature resistance, $R_a = 0.15\ \Omega$, the field circuit resistance, $R_f = 145\ \Omega$, and the motor voltage constant, $K_v = 1.15$ V/A-rad/s. The viscous friction and no-load losses are negligible. The armature and field currents are continuous and ripple-free. (**a**) If the field converter is operated at the maximum field current and the developed torque is $T_d = 106$ N·m at 750 rpm, determine the delay angle of the armature converter, α_a. (**b**) If the field circuit converter is set to the maximum field current, the developed torque is $T_d = 108$ N·m, and the delay angle of the armature converter is $\alpha_a = 0$, determine the speed. (**c**) For the same load demand as in part (b), determine the delay angle of the field circuit converter if the speed has to be increased to 1800 rpm.

10-11. Repeat Prob. 10-10 if both the armature and field circuits are controlled by three-phase semiconverters.

10-12. A dc chopper controls the speed of a dc series motor. The armature resistance, $R_a = 0.04\ \Omega$, field circuit resistance, $R_f = 0.06\ \Omega$, and back emf constant, $K_v = 35$ mV/rad/s. The dc input voltage of the chopper, $V_s = 600$ V. If it is required to maintain a constant developed torque of $T_d = 547$ N·m, plot the duty cycle, k, of the chopper against the motor speed.

10-13. A dc series motor is powered by a dc chopper as shown in Fig. 10-14a from a 600-V dc source. The armature resistance is $R_a = 0.03\ \Omega$ and the field resistance is R_f

= 0.05 Ω. The back emf constant of the motor is K_v = 15.27 mV/A-rad/s. The average armature current, I_a = 450 A. The armature current is continuous and has negligible ripple. If the duty cycle of the chopper is 75%, determine the (**a**) input power from the source; (**b**) equivalent input resistance of the chopper drive; (**c**) motor speed; and (**d**) developed torque of the motor.

10-14. The drive in Fig. 10-15a is operated in regenerative braking of a dc series motor. The dc supply voltage is 600 V. The armature resistance, R_a = 0.03 Ω and the field resistance, R_f = 0.05 Ω. The back emf constant of the motor, K_v = 12 mV/A-rad/s. The average armature current is maintained constant at I_a = 350 A. The armature current is continuous and has negligible ripple. If the duty cycle of the chopper is 50%, determine the (**a**) average voltage across the chopper, V_h; (**b**) power regenerated to the dc supply, P_g; (**c**) equivalent load resistance of the motor acting as a generator, R_{eq}; (**d**) minimum permissible braking speed, ω_{min}; (**e**) maximum permissible braking speed, ω_{max}; and (**f**) motor speed.

10-15. A dc chopper is used in rheostatic braking of a dc series motor as shown in Fig. 10-14. The armature resistance, R_a = 0.03 Ω and the field resistance, R_f = 0.05 Ω. The braking resistor, R_b = 5 Ω. The back emf constant, K_v = 14 mV/A-rad/s. The average armature current is maintained constant at I_a = 250 A. The armature current is continuous and has negligible ripple. If the duty cycle of the chopper is 60%, determine the (**a**) average voltage across the chopper, V_{ch}; (**b**) power dissipated in the resistor, P_b; (**c**) equivalent load resistance of the motor acting as a generator, R_{eq}; (**d**) motor speed; and (**e**) peak chopper voltage, V_p.

10-16. Two choppers control a dc series motor as shown in Fig. 10-20a and they are phase shifted in operation by π/m, where m is the number of multiphase choppers. The supply voltage, V_s = 440 V, armature circuit resistance, R_m = 8 Ω, armature circuit inductance, L_m = 12 mH, and the frequency of each chopper, f = 250 Hz. Calculate the maximum value of peak-to-peak load ripple current.

10-17. For Prob. 10-16 plot the maximum value of peak-to-peak load ripple current against the number of multiphase choppers.

10-18. A dc series motor is controlled by two multiphase choppers. The average armature current, I_a = 250 A. A simple LC-input filter with L_e = 0.35 mH and C_e = 5600 μF is used. Each chopper is operated at a frequency, f = 250 Hz. Determine the rms fundamental component of the chopper-generated harmonic current in the supply.

10-19. For Prob. 10-18, plot the rms fundamental component of the chopper-generated harmonic current in the supply against the number of multiphase choppers.

10-20. A 40-hp 230-V 3500-rpm separately excited dc motor is controlled by a linear converter of gain K_2 = 200. The moment of inertia of the motor load, J = 0.156 N·m/rad/s, viscous friction constant is negligible, armature resistance, R_m = 0.045 Ω, and armature inductance, L_m = 730 mH. The back emf constant is K_v = 0.502 V/A-rad/s and the field current is maintained constant at I_f = 1.25 A. (**a**) Obtain the open-loop transfer function $\omega(s)/V_r(s)$ and $\omega(s)/T_L(s)$ for the motor. (**b**) Calculate the motor steady-state speed if the reference voltage is V_r = 1 V and the load torque is 60% of the rated value.

10-21. Repeat Prob. 10-20 with a closed-loop control if the amplification of speed sensor, K_1 = 3 mV/rad/s.

10-22. The motor in Prob. 10-20 is controlled by a linear converter of gain K_2 with a closed-loop control. If the amplification of speed sensor is K_1 = 3 mV/rad/s, determine the gain of the converter K_2 to limit the speed regulation at full load to 1%.

10-23. A 60-hp 230-V 1750-rpm separately excited dc motor is controlled by a converter as shown in the block diagram in Fig. 10-28. The field current is maintained constant at I_f = 1.25 A and the machine back emf constant, K_v = 0.81 V/A-rad/s. The armature resistance, R_a = 0.02 Ω and the viscous friction constant, B = 0.3 N·m/rad/s. The amplification of the speed sensor, K_1 = 96 mV/rad/s and the gain of the power controller, K_2 = 150. (**a**) Determine the rated torque of the motor. (**b**) Determine the reference voltage V_r to drive the motor at the rated speed. (**c**) If the reference voltage is kept unchanged, determine the speed when the motor develops the rated torque.

10-24. Repeat Prob. 10-23. (**a**) If the load torque is increased by 20% of the rated value, determine the motor speed. (**b**) If the reference voltage is reduced by 10%, determine the motor speed. (**c**) If the load torque is reduced by 15% of the rated value and the reference voltage is reduced by 20%, determine the motor speed. (**d**) If there was no feedback, as in an open-loop control, determine the speed regulation for a reference voltage, V_r = 1.24 V. (**e**) Determine the speed regulation with a closed-loop control.

10-25. A 40-hp 230-V 3500-rpm series excited dc motor is controlled by a linear converter of gain K_2 = 200. The moment of inertia of the motor load, J = 0.156 N·m/rad/s, viscous friction constant is negligible, armature resistance, R_m = 0.045 Ω, and armature inductance, L_m = 730 mH. The back emf constant is K_v = 340 mV/A-rad/s. The field resistance, R_f = 0.035 Ω and field inductance, L_f = 450 mH. (**a**) Obtain the open-loop transfer function $\omega(s)/V_r(s)$ and $\omega(s)/T_L(s)$ for the motor. (**b**) Calculate the motor steady-state speed if the reference voltage, V_r = 1 V and the load torque is 60% of the rated value.

10-26. Repeat Prob. 10-25 with closed-loop control if the amplification of speed sensor, K_1 = 3 mV/rad/s.

POWEREN.IR

11

AC Drives

11-1 INTRODUCTION

The control of dc motors requires providing a variable dc voltage which can be obtained from dc choppers or controlled rectifiers. These voltage controllers are simple and less expensive. Dc motors are relatively expensive and require more maintenance, due to the brushes and commutators. However, dc drives are used in many industrial applications.

The ac motors have a number of advantages; they are lightweight (20 to 40% lighter than equivalent dc motors), inexpensive, and of low maintenance compared to dc motors. They require control of frequency, voltage, and current for variable-speed applications. The power converters, inverters and ac voltage controllers, can control the frequency, voltage, and/or current to meet the drive requirements. These power controllers, which are relatively complex and more expensive, require advanced feedback control techniques. However, the advantages of ac drives outweigh the disadvantages. There are two types of ac drives:

1. Induction motor drives
2. Synchronous motor drives

11-2 INDUCTION MOTOR DRIVES

Three-phase induction motors are commonly used in adjustable-speed drives and they have three-phase stator and rotor windings. The stator windings are supplied with balanced three-phase ac voltage, which produce induced voltages in the rotor windings due to transformer action. It is possible to arrange the distribution of stator windings so that there is an effect of multiple poles, producing several cycles of magnetomotive force (mmf) (or field) around the air gap. This field establishes a spatially distributed sinusoidal flux density in the air gap. The speed of rotation of the field is called the *synchronous speed*, which is defined by

$$\omega_s = \frac{2\omega}{p} \tag{11-1}$$

where p is the number of poles and ω is the supply frequency in rad/s.

If a stator phase voltage, $v_s = \sqrt{2}\, V_s \sin \omega t$, produces a flux linkage (in the rotor) given by

$$\phi(t) = \phi_m \cos(\omega_m t + \delta - \omega_s t) \tag{11-2}$$

the induced voltage per phase in the rotor winding is

$$\begin{aligned} e_r &= N_r \frac{d\phi}{dt} = N_r \frac{d}{dt}[\phi_m \cos(\omega_m t + \delta - \omega_s t)] \\ &= -N_r \phi_m (\omega_s - \omega_m) \sin[(\omega_s - \omega_m)t - \delta] \\ &= -sE_m \sin(s\omega_s t - \delta) \\ &= -s\sqrt{2}\, E_r \sin(s\omega_s t - \delta) \end{aligned} \tag{11-3}$$

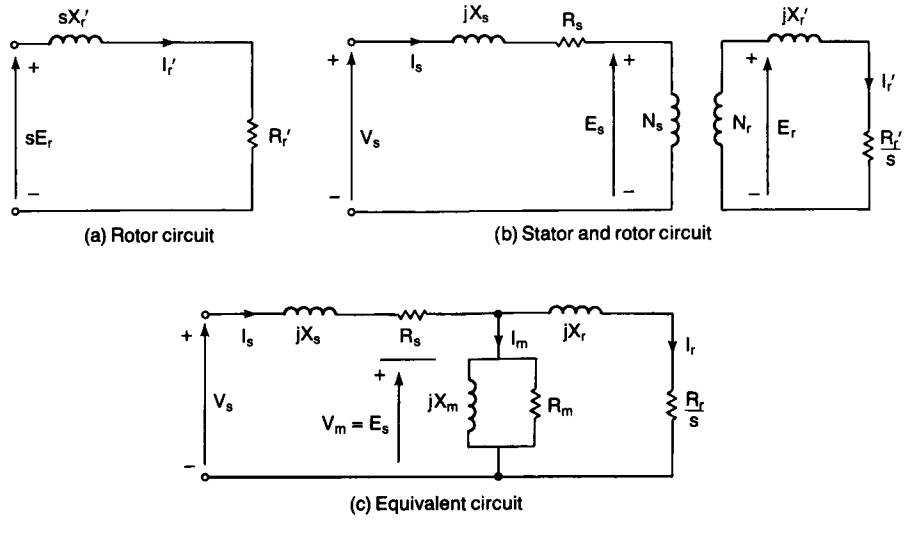


Figure 11-1 Circuit model of induction motors.

where N_r = number of turns on each rotor phase
ω_m = angular speed of the rotor
δ = relative position of the rotor
E_r = rms value of the rotor induced voltage

and s is the slip, defined as

$$s = \frac{\omega_s - \omega_m}{\omega_s} \tag{11-4}$$

The equivalent circuit for one phase of the rotor is shown in Fig. 11-1a, where R'_r is the resistance per phase of the rotor windings, X'_r is the leakage reactance per phase of the rotor at the supply frequency, and E_r represents the induced phase voltage when the speed is zero (or $s = 1$). The rotor current is given by

$$I'_r = \frac{sE_r}{R'_r + jsX'_r} \tag{11-5}$$

$$= \frac{E_r}{R'_r/s + jX'_r} \tag{11-5a}$$

where R'_r and X'_r are referred to the rotor winding.

The per phase circuit model of induction motors is shown in Fig. 11-1b, where R_s and X_s are the per phase resistance and leakage reactance of the stator winding. The complete circuit model with all parameters referred to the stator is shown in Fig. 11-1c, where R_m represents the resistance for excitation (or core) loss and X_m is the magnetizing reactance. There will be stator core loss, when the supply is connected and the rotor core loss depends on the slip. The friction and windage loss, $P_{\text{no load}}$, exists when the machine rotates. The core loss, P_c, may be included as a part of rotational loss, $P_{\text{no load}}$.

11-2.1 Performance Characteristics

The rotor current, I_r, and stator current, I_s, can be found from the circuit model in Fig. 11-1c where R_r and X_r are referred to the stator windings. Once the values of I_r and I_s are known, the performance parameters of the motor can be determined as follows:
Stator copper loss,

$$P_{su} = 3I_s^2R_s \tag{11-6}$$

Rotor copper loss,

$$P_{ru} = 3I_r^2R_r \tag{11-7}$$

Core loss,

$$P_c = \frac{3V_m^2}{R_m} \approx \frac{3V_s^2}{R_m} \tag{11-8}$$

Gap power,

$$P_g = 3I_r^2 \frac{R_r}{\omega_s} \tag{11-9}$$

Developed power,

$$P_d = P_g - P_{ru} = 3I_r^2 \frac{R_r}{s}(1 - s) \tag{11-10}$$

$$= P_g(1 - s) \tag{11-11}$$

Developed torque,

$$T_d = \frac{P_d}{\omega_m} \tag{11-12}$$

$$= \frac{P_g(1 - s)}{\omega_s(1 - s)} = \frac{P_g}{\omega_s} \tag{11-12a}$$

Input power,

$$P_i = 3V_sI_s \cos \theta_m \tag{11-13}$$

$$= P_c + P_{su} + P_g \tag{11-13a}$$

where θ_s is the angle between I_s and V_s. Output power,

$$P_o = P_d - P_{\text{no load}}$$

Efficiency,

$$\eta = \frac{P_o}{P_i} = \frac{P_d - P_{\text{no load}}}{P_c + P_{su} + P_g} \tag{11-14}$$

If $P_g >> (P_c + P_{su})$ and $P_d >> P_{\text{no load}}$, the efficiency becomes

$$\eta \approx \frac{P_d}{P_g} = \frac{P_g(1 - s)}{P_g} = 1 - s \tag{11-14a}$$

The value of X_m is normally large and R_m, which is much larger, can be removed from the circuit model to simplify the calculations. If $X_m^2 >> (R_s^2 + X_s^2)$, then $V_s \approx V_m$, and the magnetizing reactance X_m may be moved to the stator winding to simplify further; this is shown in Fig. 11-2.

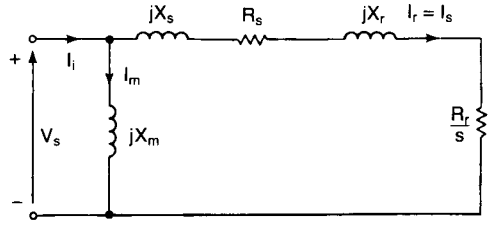


Figure 11-2 Approximate per-phase equivalent circuit.

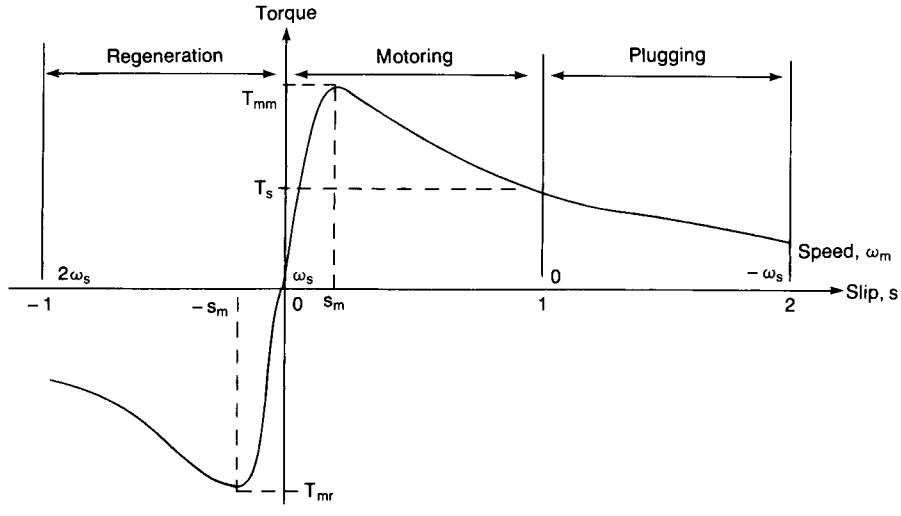


Figure 11-3 Torque–speed characteristics.

The input impedance of the motor,

$$\mathbf{Z}_i = \frac{-X_m(X_s + X_r) + jX_m(R_s + R_r/s)}{R_s + R_r/s + j(X_m + X_s + X_r)} \tag{11-15}$$

and the power factor angle of the motor,

$$\theta_m = \pi - \tan^{-1}\frac{R_s + R_r/s}{X_s + X_r} + \tan^{-1}\frac{X_m + X_s + X_r}{R_s + R_r/s} \tag{11-16}$$

From Fig. (11-2), the rotor current,

$$I_r = \frac{V_s}{[(R_s + R_r/s)^2 + (X_s + X_r)^2]^{1/2}} \tag{11-17}$$

Substituting Eq. (11-17) in Eqs. (11-9) and (11-12a) yields

$$T_d = \frac{3R_rV_s^2}{s\omega_s[(R_s + R_r/s)^2 + (X_s + X_r)^2]} \tag{11-18}$$

If the motor is supplied from a fixed voltage at a constant frequency, the developed torque is a function of the slip and the torque–speed characteristics can be determined from Eq. (11-18). A typical plot of developed torque as a function of slip or speed is shown in Fig. 11-3. There are three regions of operation: (1) motoring or powering, $0 \leq s \leq 1$; (2) regeneration, $s < 0$; and (3) plugging, $1 \leq s \leq 2$. In motoring, the motor rotates in the same direction as the field; and as the slip increases, the torque also increases while the air-gap flux remains constant. Once the torque reaches its maximum value, T_m at $s = s_m$, the torque decreases, with the increase in slip due to reduction of the air-gap flux.

In regeneration, the speed is greater than the synchronous speed, with ω_m and ω_s being in the same direction, and the slip is negative. Therefore, R_r/s is negative. This means that power is being fed back from the shaft into the rotor circuit and the motor operates as a generator. The motor returns power to the supply system. The torque–speed characteristic is similar to that of motoring, but having negative value of torque.

In plugging, the speed is opposite to the direction of the field and the slip is greater than unity. This may happen if the sequence of the suppl source is reversed, while motoring, so that the direction of the field is also reversed. The developed torque, which is in the same direction as the field, opposes the motion and acts as braking torque. Since $s > 1$, the motor currents will be high, but the developed torque will be low. The energy due to plugging brake must be dissipated within the motor and this may cause excessive heating of the motor. This type of braking is not normally recommended.

At starting, the machine speed is $\omega_m = 0$ and $s = 1$. The staring torque can be found from Eq. (11-18) by setting $s = 1$ as

$$T_s = \frac{3R_rV_s^2}{\omega_s[(R_s + R_r)^2 + (X_s + X_r)^2]} \tag{11-19}$$

The slip for maximum torque, s_m, can be determined by setting $dT_d/ds = 0$ and Eq. (11-18) yields

$$s_m = \pm \frac{R_r}{[R_s^2 + (X_s + X_r)^2]^{1/2}} \tag{11-20}$$

Substituting $s = s_m$ in Eq. (11-18) gives the maximum developed torque during motoring, which is also called *pull-out torque* or *breakdown torque*,

$$T_{mm} = \frac{3V_s^2}{2\omega_s[R_s + \sqrt{R_s^2 + (X_s + X_r)^2}]} \tag{11-21}$$

and the maximum regenerative torque can be found from Eq. (11-18) by letting

$$s = -s_m$$

$$T_{mr} = \frac{3V_s^2}{2\omega_s[-R_s + \sqrt{R_s^2 + (X_s + X_r)^2}]} \tag{11-22}$$

If R_s is considered small compared to other circuit impedances, which is usually a valid approximation for motors of more than 1 kW rating, the corresponding expressions become

$$T_d = \frac{3R_rV_s^2}{s\omega_s[(R_r/s)^2 + (X_s + X_r)^2]} \tag{11-23}$$

$$T_s = \frac{3R_rV_s^2}{\omega_s[R_r^2 + (X_s + X_r)^2]} \tag{11-24}$$

$$s_m = \pm \frac{R_r}{X_s + X_r} \tag{11-25}$$

$$T_{mm} = -T_{mr} = \frac{3V_s^2}{2\omega_s(X_s + X_r)} \tag{11-26}$$

Normalizing Eqs. (11-23) and (11-24) with respect to Eq. (11-26) gives

$$\frac{T_d}{T_{mm}} = \frac{2R_r(X_s + X_r)}{s[(R_r/s)^2 + (X_s + X_r)^2]} = \frac{2ss_m}{s_m^2 + s^2} \tag{11-27}$$

and

$$\frac{T_s}{T_{mm}} = \frac{2R_r(X_s + X_r)}{R_r^2 + (X_s + X_r)^2} = \frac{2s_m}{s_m^2 + 1} \tag{11-28}$$

If $s < 1$, $s^2 << s_m^2$ and Eq. (11-27) can be approximated to

$$\frac{T_d}{T_{mm}} = \frac{2s}{s_m} = \frac{2(\omega_s - \omega_m)}{s_m\omega_s} \tag{11-29}$$

which gives the speed as a function of torque,

$$\omega_m = \omega_s\left(1 - \frac{s_m}{2T_{mm}}T_d\right) \tag{11-30}$$

It can be noticed from Eqs. (11-29) and (11-30) that if the motor operates with small slip, the developed torque is proportional to slip and the speed decreases with torque. The speed and torque of induction motors can be varied by one of the following means:

1. Stator voltage control
2. Rotor voltage control
3. Frequency control
4. Stator voltage and frequency control
5. Stator current control
6. Voltage, current, and frequency control

To meet the torque-speed duty cycle of a drive, the voltage, current and frequency control are normally used.

Example 11-1

A three-phase 460-V 60-Hz four-pole Y-connected induction motor has the following equivalent-circuit parameters: $R_s = 0.42\ \Omega$, $R_r = 0.23\ \Omega$, $X_s = X_r = 0.82\ \Omega$, and $X_m = 22\ \Omega$. The no-load loss, which is $P_{\text{no load}} = 60$ W, may be assumed constant. The rotor speed is 1750 rpm. Use the approximate equivalent circuit in Fig. 11-2 to determine the (a) synchronous speed, ω_s; (b) slip, s; (c) input current, I_i; (d) input power, P_i; (e) input power factor of the supply, PF_s; (f) gap power, P_g; (g) rotor copper loss, P_{ru}; (h) stator copper loss, P_{su}; (i) developed torque, T_d, (j) efficiency; (k) starting current, I_{rs}, and starting torque, T_s; (l) slip for maximum torque, s_m; (m) maximum developed torque in motoring, T_{mm}; (n) maximum regenerative developed torque, T_{mr}; and (o) T_{mm} and T_{mr} if R_s is neglected.

Solution $f = 60$ Hz, $p = 4$, $R_s = 0.42\ \Omega$, $R_r = 0.23\ \Omega$, $X_s = X_r = 0.82\ \Omega$, $X_m =$

22 Ω, and N = 1750 rpm. The phase voltage is $V_s = 460/\sqrt{3} = 265.58$ V, $\omega = 2\pi \times 60 = 377$ rad/s, and $\omega_m = 1750\ \pi/30 = 183.26$ rad/s.

(a) From Eq. (11-1), $\omega_s = 2\omega/p = 2 \times 377/4 = 188.5$ rad/s.

(b) From Eq. (11-4), $s = (188.5 - 183.26)/188.5 = 0.028$.

(c) From Eq. (11-15),

$$\mathbf{Z}_i = \frac{-22(0.82 + 0.82) + j22(0.42 + 0.23/0.028)}{0.42 + 0.23/0.028 + j(22 + 0.82 + 0.82)} = 7.732\ \angle 30.9°$$

$$\mathbf{I}_i = \frac{V_s}{Z_i} = \frac{265.58}{7.732}\ \angle -30.9° = 34.35\ \angle -30.9°\ \text{A}$$

(d) The power factor of the motor is

$$\text{PF}_m = \cos(-30.9°) = 0.858\ \text{(lagging)}$$

From Eq. (11-13),

$$P_i = 3 \times 265.58 \times 34.35 \times 0.858 = 23\,482\ \text{W}$$

(e) The power factor of the input supply is $\text{PF}_s = \text{PF}_m = 0.858$ (lagging) which is the same as the motor power factor, PF_m, because the supply is sinusoidal.

(f) From Eq. (11-17), the rotor current is

$$I_r = \frac{265.58}{[(0.42 + 0.23/0.028)^2 + (0.82 + 0.82)^2]^{1/2}} = 30.1\ \text{A}$$

From Eq. (11-9),

$$P_g = \frac{3 \times 30.1^2 \times 0.23}{0.028} = 22{,}327\ \text{W}$$

(g) From Eq. (11-7), $P_{ru} = 3 \times 30.1^2 \times 0.23 = 625$ W.

(h) The stator copper loss, $P_{su} = 3 \times 30.1^2 \times 0.42 = 1142$ W.

(i) From Eq. (11-12a), $T_d = 22{,}327/188.5 = 118.4$ N·m.

(j) $P_0 = P_g - P_{ru} - P_{\text{no load}} = 22{,}327 - 625 - 60 = 21{,}642$ W.

(k) For $s = 1$, Eq. (11-17) gives the starting rotor current,

$$I_{rs} = \frac{265.58}{[(0.42 + 0.23)^2 + (0.82 + 0.82)^2]^{1/2}} = 150.5\ \text{A}$$

From Eq. (11-19),

$$T_s = \frac{3 \times 0.23 \times 150.5^2}{188.5} = 82.9\ \text{N·m}$$

(l) From Eq. (11-20), the slip for maximum torque (or power),

$$s_m = \pm \frac{0.23}{[0.42^2 + (0.82 + 0.82)^2]^{1/2}} = \pm 0.1359$$

(m) From Eq. (11-21), the maximum developed torque,

$$T_{mm} = \frac{3 \times 265.58^2}{2 \times 188.5[0.42 + \sqrt{0.42^2 + (0.82 + 0.82)^2}]}$$

$$= 265.64\ \text{N·m}$$

(n) From Eq. (11-22), the maximum regenerative torque is

$$T_{mr} = -\frac{3 \times 265.58^2}{2 \times 188.5[-0.42 + \sqrt{0.42^2 + (0.82 + 0.82)^2}]}$$

$$= 440.94\,\text{N·m}$$

(o) From Eq. (11-25),

$$s_m = \pm \frac{0.23}{0.82 + 0.82} = \pm 0.1402$$

From Eq. (11-26),

$$T_{mm} = -T_{mr} = \frac{3 \times 265.58^2}{2 \times 188.5(0.82 + 0.82)} = 342.2\ \text{N·m}$$

11-2.2 Stator Voltage Control

Equation (11-18) indicates that the torque is proportional to the square of the stator supply voltage and a reduction in stator voltage will produce a reduction in speed. If the terminal voltage is reduced to bV_s, Eq. (11-18) gives the developed torque

$$T_d = \frac{3R_r(bV_s)^2}{s\omega_s[(R_s + R_r/s)^2 + (X_s + X_r)^2]}$$

where $b \leq 1$.

Figure 11-4 shows the typical torque–speed characteristics for various values of b. The points of intersection with the load line define the stable operating points. In any magnetic circuit, the induced voltage is proportional to flux and frequency, and the rms air-gap flux can be expressed as

$$V_a = bV_s = K_m\omega\phi$$

or

$$\phi = \frac{V_a}{K_m\omega} = \frac{bV_s}{K_m\omega} \tag{11-31}$$

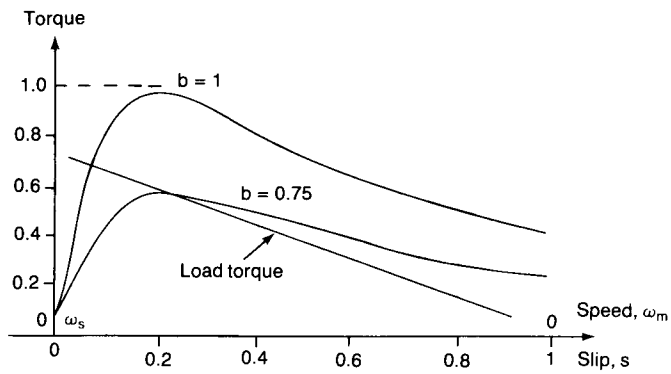


Figure 11-4 Torque–speed characteristics with variable stator voltage.

where K_m is a constant and depends on the number of turns of the stator winding. As the stator voltage is reduced, the air-gap flux and the torque are also reduced. At a lower voltage, the current will be peaking at a slip of $s_a = \frac{1}{3}$. The range of speed control depends on the slip for maximum torque, s_m. For a low-slip motor, the speed range is very narrow. This type of voltage control is not suitable for a constant-torque load and is normally applied to applications requiring low starting torque and a narrow range of speed at a relatively low slip.

The stator voltage can be varied by three-phase (1) ac voltage controllers, (2) voltage-fed variable dc link inverters, or (3) PWM inverters. However, due to limited speed range requirements, the ac voltage controllers are normally used to provide the voltage control. The ac voltage controllers are very simple. However, the harmonic contents are high and the input power factor of the controllers is low. They are used mainly in low power applications, such as fans, blowers, and centrifugal pumps, where the starting torque is low. They are also used for starting high-power induction motors to limit the in-rush current.

Example 11-2

A three-phase 460-V 60-Hz four-pole Y-connected induction motor has the following parameters: $R_s = 1.01\ \Omega$, $R_r = 0.69\ \Omega$, $X_s = 1.3\ \Omega$, $X_r = 1.94\ \Omega$, and $X_m = 43.5\ \Omega$. The no-load loss, $P_{\text{no load}}$, is negligible. The load torque, which is proportional to the speed squared, is 41 N·m at 1740 rpm. If the motor speed is 1550 rpm, determine the (a) load torque, T_L; (b) rotor current, I_r; (c) stator supply voltage, V_a; (d) motor input current, I_i; (e) motor input power, P_i; (f) slip for maximum current, s_a; (g) maximum rotor current, $I_{r(\max)}$; (h) speed at maximum rotor current, ω_a; and (i) torque at the maximum current, T_a.

Solution $p = 4$, $f = 60$ Hz, $V_s = 460/\sqrt{3} = 265.58$ V, $R_s = 1.01\ \Omega$, $R_r = 0.69\ \Omega$, $X_s = 1.3\ \Omega$, $X_r = 1.94\ \Omega$, and $X_m = 43.5\ \Omega$, $\omega = 2\pi \times 60 = 377$ rad/s, and $\omega_s = 377 \times 2/4 = 188.5$ rad/s. Since torque is proportional to speed squared,

$$T_L = K_m \omega_m^2 \tag{11-32}$$

At $\omega_m = 1740\ \pi/30 = 182.2$ rad/s, $T_L = 41$ N·m and Eq. (11-32) yields $K_m = 41/182.2^2 = 1.235 \times 10^{-3}$ and $\omega_m = 1550\ \pi/30 = 162.3$ rad/s. From Eq. (11-4), $s = (188.5 - 162.3)/188.500 = 0.139$.

(a) From Eq. (11-32), $T_L = 1.235 \times 10^{-3} \times 162.3^2 = 32.5$ N·m.

(b) From Eqs. (11-10) and (11-32),

$$P_d = 3I_r^2 \frac{R_r}{s}(1 - s) = T_L \omega_m + P_{\text{no load}} \tag{11-33}$$

For negligible no-load loss,

$$I_r = \left[\frac{sT_L\omega_m}{3R_r(1 - s)}\right]^{1/2} = \left[\frac{0.139 \times 32.5 \times 162.3}{3 \times 0.69\ (1 - 0.139)}\right]^{1/2} = 20.28\ \text{A} \tag{11-34}$$

(c) The stator supply voltage,

$$V_a = I_r\left[\left(R_s + \frac{R_r}{s}\right)^2 + (X_s + X_r)^2\right]^{1/2}$$
$$= 20.28\left[\left(1.01 + \frac{0.69}{0.139}\right)^2 + (1.3 + 1.94)^2\right]^{1/2} = 139.34 \quad (11\text{-}35)$$

(d) From Eq. (11-15),

$$\mathbf{Z}_i = \frac{-43.5(1.3 + 1.94) + j43.5(1.01 + 0.69/0.139)}{1.01 + 0.69/0.139 + j(43.5 + 1.3 + 1.94)} = 6.28 \angle 35.74°$$

$$\mathbf{I}_i = \frac{V_a}{\mathbf{Z}_i} = \frac{139.34}{6.28} \angle -35.74° = 22.2 \angle -35.74° \text{ A}$$

(e) $PF_m = \cos(-35.74°) = 0.812$ (lagging). From Eq. (11-13),

$$P_i = 3 \times 139.34 \times 22.2 \times 0.812 = 7535.4 \text{ W}$$

(f) Substituting $\omega_m = \omega_s(1 - s)$ and $T_L = K_m\omega_m^2$ in Eq. (11-34) yields

$$I_r = \left[\frac{sT_L\omega_m}{3R_r(1 - s)}\right]^{1/2} = (1 - s)\omega_s\left(\frac{sK_m\omega_s}{3R_r}\right)^{1/2} \quad (11\text{-}36)$$

The slip at which I_r becomes maximum can be obtained by setting $dI_r/ds = 0$, and this yields

$$s_a = \tfrac{1}{3} \quad (11\text{-}37)$$

(g) Substituting $s_a = \frac{1}{3}$ in Eq. (11-36) gives the maximum rotor current,

$$I_{r(\max)} = \omega_s\left(\frac{4K_m\omega_s}{81R_r}\right)^{1/2}$$
$$= 188.5\left(\frac{4 \times 1.235 \times 10^{-3} \times 188.5}{81 \times 0.69}\right)^{1/2} = 24.3 \text{ A} \quad (11\text{-}38)$$

(h) The speed at the maximum current,

$$\omega_a = \omega_s(1 - s_a) = (2/3)\omega_s = 0.6667\omega_s$$
$$= 188.5 \times 2/3 = 125.27 \text{ rad/s} \quad \text{or} \quad 1200 \text{ rpm} \quad (11\text{-}39)$$

(i) From Eqs. (11-9), (11-12a), and (11-36),

$$T_a = 9I_{r(\max)}^2\frac{R_r}{\omega_s}$$
$$= 9 \times 24.3^2 \times \frac{0.69}{188.5} = 19.45 \text{ N·m} \quad (11\text{-}40)$$

11-2.3 Rotor Voltage Control

In a wound-rotor motor, an external three-phase resistor may be connected to its slip rings as shown in Fig. 11-5a. The developed torque may be varied by varying the resistance, R_x. If R_x is referred to the stator winding and added to R_r, Eq.

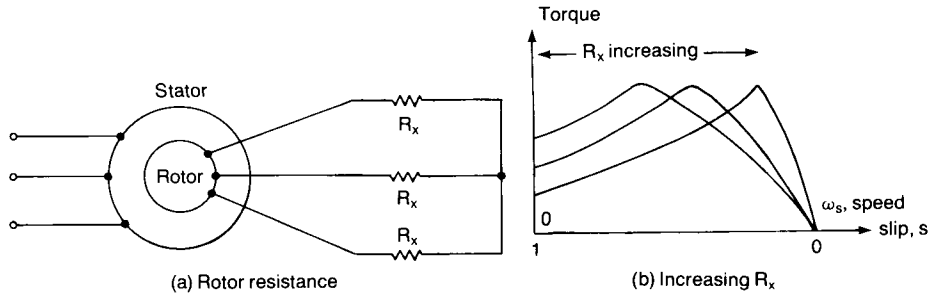


Figure 11-5 Speed control by rotor resistance.

(11-18) may be applied to determine the developed torque. The typical torque–speed characteristics for variations in rotor resistance are shown in Fig. 11-5b. This method increases the starting torque while limiting the starting current. However, this is an inefficient method and there would be unbalances in voltages and currents if the resistances in the rotor circuit are not equal.

The three-phase resistor may be replaced by a three-phase diode rectifier and a chopper as shown in Fig. 11-6a, where the GTO operates as a chopper switch. The inductor, L_d, acts as a current source, I_d, and the chopper varies the effective resistance, which can be found from Eq. (10-45):

$$R_e = R(1 - k) \tag{11-41}$$

where k is the duty cycle of the chopper. The speed can be controlled by varying the duty cycle.

The slip power in the rotor circuit may be returned to the supply by replacing the chopper and resistance, R, with a three-phase full converter as shown in Fig. 11-6b. The converter is operated in the inversion mode with delay range of $\pi/2 \leq \alpha \leq \pi$, thereby returning energy to the source. The variation of the delay angle permits power flow and speed control. This type of drive is known as a *static Kramer* drive. Again, by replacing the bridge rectifiers by three three-phase dual converters (or cycloconverters) as shown in Fig. 11-6c, the slip power flow in either direction is possible and this arrangement is called a *static Scherbius* drive. The static Kramer and Scherbius drives are used in large power pump and blower applications where limited range of speed control is required. Since the motor is connected directly to the source, the power factor of these drives is generally high.

Example 11-3

A three-phase 460-V 60-Hz six-pole Y-connected wound-rotor induction motor whose speed is controlled by slip power as shown in Fig. 11-6a has the following parameters: $R_s = 0.041\ \Omega$, $R_r = 0.044\ \Omega$, $X_s = 0.29\ \Omega$, $X_r = 0.44\ \Omega$, and $X_m = 6.1\ \Omega$. The turns ratio of the rotor to stator windings is $n_m = N_r/N_s = 0.9$. The inductance L_d is very large and its current I_d has negligible ripple. The values of R_s, R_r, X_s, and X_r for the equivalent circuit in Fig. 11-2 can be considered negligible compared to the effective impedance of L_d. The no-load loss of the motor is negligible. The losses in the rectifier, inductor L_d and the GTO chopper are also negligible.

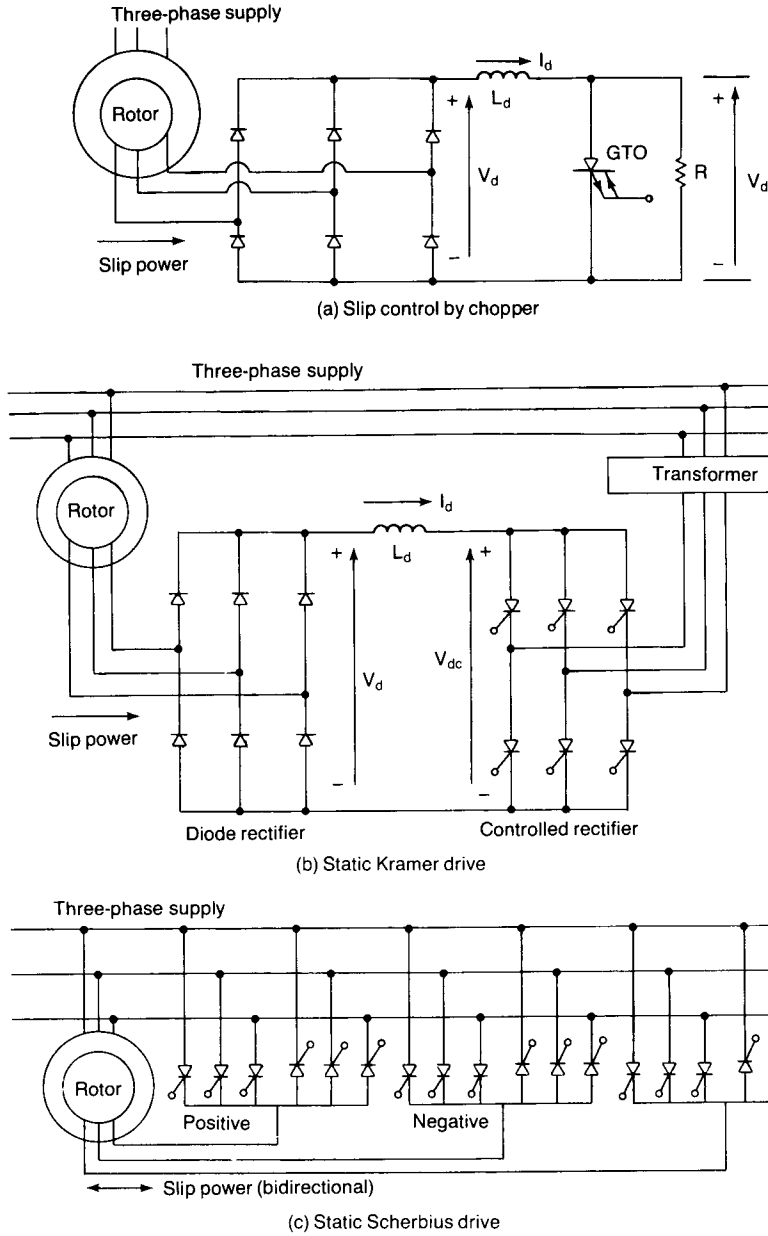


Figure 11-6 Slip power control.

The load torque, which is proportional to speed squared, is 750 N·m at 1175 rpm. (a) If the motor has to operate with a minimum speed of 800 rpm, determine the resistance, R. With this value of R, if the desired speed is 1050 rpm, calculate the (b) inductor current, I_d; (c) duty cycle of the chopper, k; (d) dc voltage, V_d; (e) efficiency; and (f) input power factor of the drive, PF_s.

Solution $V_a = 460/\sqrt{3} = 265.58$ V, $p = 6$, $\omega = 2\pi \times 60 = 377$ rad/s, and $\omega_s = 2 \times 377/6 = 125.66$ rad/s. The equivalent circuit of the drive is shown in Fig. 11-7a, which is reduced to Fig. 11-7b provided the motor parameters are neglected. From Eq. (11-41), the dc voltage at the rectifier output is

$$V_d = I_d R_e = I_d R(1 - k) \tag{11-42}$$

and

$$E_r = sV_s \frac{N_r}{N_s} = sV_s n_m \tag{11-43}$$

For a three-phase rectifier, Eq. (2-77) relates E_r and V_d as

$$V_d = 1.6542 \times \sqrt{2}\, E_r = 2.3394 E_r$$

From Eq. (11-43),

$$V_d = 2.3394 sV_s n_m \tag{11-44}$$

If P_r is the slip power, the gap power,

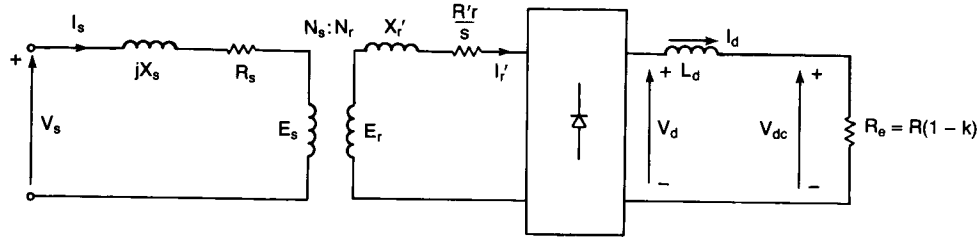
$$P_g = \frac{P_r}{s}$$

and Eq. (11-9) gives the developed power as

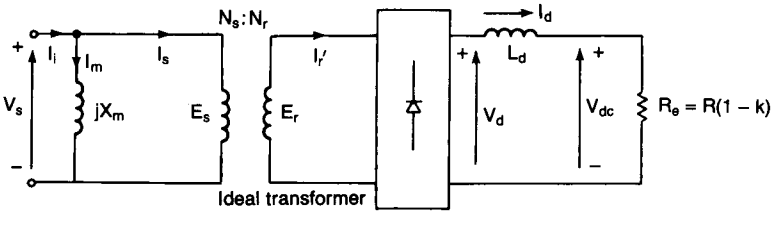
$$P_d = 3(P_g - P_r) = 3\left(\frac{P_r}{s} - P_r\right) = \frac{3P_r(1 - s)}{s} \tag{11-45}$$

Since the total slip power is $3P_r = V_d I_d$ and $P_d = T_L \omega_m$, Eq. (11-45) becomes

$$P_d = \frac{(1 - s)V_d I_d}{s} = T_L \omega_m = T_L \omega_s (1 - s) \tag{11-46}$$



(a) Equivalent circuit



(b) Approximate equivalent circuit

Figure 11-7 Equivalent circuits for Example 11-3.

Substituting Eq. (11-44) in Eq. (11-46) and solving for I_d gives

$$I_d = \frac{T_L \omega_s}{2.3394 V_s n_m} \tag{11-47}$$

which indicates that the inductor current is independent of the speed. Equating Eq. (11-42) to Eq. (11-44) gives

$$2.3394 s V_s n = I_d R(1 - k)$$

which gives

$$s = \frac{I_d R(1 - k)}{2.3394 V_s n_m} \tag{11-48}$$

The speed can be found from Eq. (11-48) as

$$\omega_m = \omega_s(1 - s) = \omega_s\left[1 - \frac{I_d R(1 - k)}{2.3394 V_s n_m}\right] \tag{11-49}$$

$$= \omega_s\left[1 - \frac{T_L \omega_s R(1 - k)}{(2.3394 V_s n_m)^2}\right] \tag{11-50}$$

For a fixed value of duty cycle, the speed decreases with load torque. By varying k from 0 to 1, the speed can be varied from a minimum value to ω_s.

(a) $\omega_m = 800\ \pi/30 = 83.77$ rad/s. From Eq. (11-32) the torque at 900 rpm is

$$T_L = 750 \times \left(\frac{800}{1175}\right)^2 = 347.67\ \text{N·m}$$

From Eq. (11-47), the corresponding inductor current is

$$I_d = \frac{347.67 \times 125.66}{2.3394 \times 265.58 \times 0.9} = 78.13\ \text{A}$$

The speed will be minimum when the duty cycle k is zero and Eq. (11-49) gives the minimum speed,

$$83.77 = 125.66\left(1 - \frac{78.13R}{2.3394 \times 265.58 \times 0.9}\right)$$

and this yields $R = 2.3856\ \Omega$.

(b) At 1050 rpm

$$T_L = 750 \times \left(\frac{1050}{1175}\right)^2 = 598.91\ \text{N·m}$$

$$I_d = \frac{598.91 \times 125.66}{2.3394 \times 265.58 \times 0.9} = 134.6\ \text{A}$$

(c) $\omega_m = 1050\ \pi/30 = 109.96$ rad/s and Eq. (11-49) gives

$$109.96 = 125.66\left[1 - \frac{134.6 \times 2.3856(1 - k)}{2.3394 \times 265.58 \times 0.9}\right]$$

which gives $k = 0.782$.

(d) Slip,

$$s = \frac{125.66 - 109.96}{125.66} = 0.125$$

From Eq. (11-44),

$$V_d = 2.3394 \times 0.125 \times 265.58 \times 0.9 = 69.9 \text{ V}$$

(e) The power loss,

$$P_1 = V_d I_d = 69.9 \times 134.6 = 9409 \text{ W}$$

The output power,

$$P_o = T_L \omega_m = 598.91 \times 109.96 = 65\,856 \text{ W}$$

The rotor current referred to the stator is

$$I_r = \sqrt{\frac{2}{3}} I_d n_m = \sqrt{\frac{2}{3}} \times 134.6 \times 0.9 = 98.9 \text{ A}$$

The rotor copper loss, $P_{ru} = 3 \times 0.044 \times 98.9^2 = 1291$ W, and the stator copper loss, $P_{su} = 3 \times 0.041 \times 98.9^2 = 1203$ W. The input power,

$$P_i = 65{,}856 + 9409 + 1291 + 1203 = 77{,}759 \text{ W}$$

The efficiency is 65,856/77,759 = 85%.

(f) From Eq. (4-62), the fundamental component of the rotor current referred to the stator is

$$I_{r1} = 0.7797 I_d \frac{N_r}{N_s} = 0.7797 I_d n_m$$

$$= 94.45 \text{ A}$$

and the current through the magnetizing branch is

$$I_m = \frac{V_a}{X_m} = \frac{265.58}{6.1} = 43.54 \text{ A}$$

The fundamental component of the input current is

$$I_1 = \left[(0.7797 I_d n_m)^2 + \left(\frac{V_a}{X_m}\right)^2\right]^{1/2}$$
$$= (94.45^2 + 43.54^2)^{1/2} = 104 \text{ A} \tag{11-51}$$

The power factor angle is given by

$$\theta_m = -\tan^{-1} \frac{V_a / X_m}{0.7797 I_d n_m}$$
$$= -\tan^{-1} \frac{43.54}{94.45} = \underline{\angle -24.74°} \tag{11-52}$$

The input power factor, $PF_s = \cos(-24.74°) = 0.908$ (lagging).

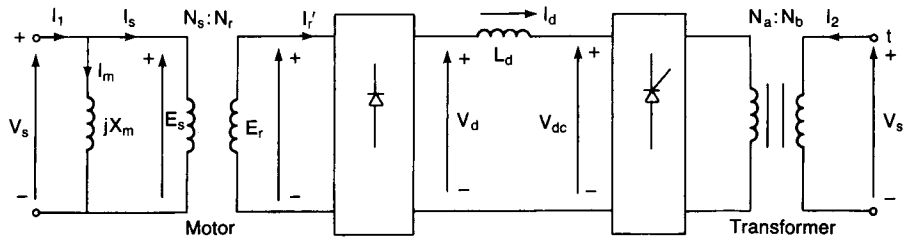


Figure 11-8 Equivalent circuit for static Kramer drive.

Example 11-4

The induction motor in Example 11-3 is controlled by a static Kramer drive as shown in Fig. 11-6b. The turns ratio of the converter ac voltage to supply voltage is $n_c = N_d/N_b = 0.40$. The load torque is 750 N·m at 1175 rpm. If the motor is required to operate at a speed of 1050 rpm, calculate the (a) inductor current, I_d; (b) dc voltage, V_d; (c) delay angle of the converter, α; (d) efficiency; and (e) input power factor of the drive, PF_s. The losses in the diode rectifier, converter, transformer and inductor L_d are negligible.

Solution $V_a = 460/\sqrt{3} = 265.58$ V, $p = 6$, $\omega = 2\pi \times 60 = 377$ rad/s, $\omega_s = 2 \times 377/6 = 125.66$ rad/s, and $\omega_m = 1050\ \pi/30 = 109.96$ rad/s. Then

$$s = \frac{125.66 - 109.96}{125.66} = 0.125$$

$$T_L = 750 \times \left(\frac{1050}{1175}\right)^2 = 598.91 \text{ N·m}$$

(a) The equivalent circuit of the drive is shown in Fig. 11-8, where the motor parameters are neglected. From Eq. (11-47), the inductor current is

$$I_d = \frac{598.91 \times 125.66}{2.3394 \times 265.58 \times 0.9} = 134.6 \text{ A}$$

(b) From Eq. (11-44),

$$V_d = 2.3394 \times 0.125 \times 265.58 \times 0.9 = 69.9 \text{ V}$$

(c) Since $V_a = n_c V_s$, Eq. (4-57) gives the average voltage at the dc side of the converter as

$$V_{dc} = -\frac{3\sqrt{3}\sqrt{2}\, n_c V_s}{\pi} \cos\alpha = -2.3394 n_c V_s \cos\alpha \qquad (11\text{-}53)$$

Since $V_d = V_{dc}$, Eqs. (11-44) and (11-53) give

$$2.3394 s V_s n_m = -2.3394 n_c V_s \cos\alpha$$

and

$$s = \frac{-n_c \cos\alpha}{n_m} \qquad (11\text{-}54)$$

The speed, which is independent of torque, becomes

$$\omega_m = \omega_s(1 - s) = \omega_s\left(1 + \frac{n_c \cos\alpha}{n_m}\right) \tag{11-55}$$

$$109.96 = 125.66\left(1 + \frac{0.4 \cos\alpha}{0.9}\right)$$

and the delay angle, $\alpha = 106.3°$.

(d) The power fed back,

$$P_1 = V_d I_d = 69.9 \times 134.6 = 9409 \text{ W}$$

The output power,

$$P_o = T_L\omega_m = 598.91 \times 109.96 = 65{,}856 \text{ W}$$

The rotor current referred to the stator is

$$I_r = \sqrt{\frac{2}{3}} I_d n_m = \sqrt{\frac{2}{3}} \times 134.6 \times 0.9 = 98.9 \text{ A}$$

$$P_{ru} = 3 \times 0.044 \times 98.9^2 = 1291 \text{ W}$$

$$P_{su} = 3 \times 0.041 \times 98.9^2 = 1203 \text{ W}$$

$$P_i = 65{,}856 + 1291 + 1203 = 68{,}350 \text{ W}$$

The efficiency is 65,856/68,350 = 96%.

(e) From part (f) in Example 11-3, $I_{r1} = 0.7797 I_d n_m = 94.45$ A, $I_m = 265.58/6.1 = 43.54$ A, and $\mathbf{I}_1 = 104 \angle -24.74°$. From Example 4-9, the rms current fed back to the supply is

$$\mathbf{I}_2 = \sqrt{\frac{2}{3}} I_d n_c \angle -\alpha = \sqrt{\frac{2}{3}} \times 134.6 \times 0.4 \angle -\alpha = 41.98 \angle -106.3°$$

The effective input current of the drive is

$$\mathbf{I}_i = \mathbf{I}_1 + \mathbf{I}_2 = 104 \angle -24.74° + 41.98 \angle -106.3° = 117.7 \angle -45.4° \text{ A}$$

The input power factor is $PF_s = \cos(-45.4°) = 0.702$ (lagging).

Note. The efficiency of this drive is higher than that of the rotor resistor control by a chopper. The power factor is dependent on the turns ratio of the transformer (e.g., if $n_c = 0.9$, $\alpha = 97.1°$ and $PF_s = 0.51$).

11-2.4 Frequency Control

The torque and speed of induction motors can be controlled by changing the supply frequency. We can notice from Eq. (11-31) that at the rated voltage and rated frequency, the flux will be the rated value. If the voltage is maintained fixed at its rated value while the frequency is reduced below its rated value, the flux will increase. This would cause saturation of the air-gap flux, and the motor parameters would not be valid in determining the torque–speed characteristics. At low fre-

quency, the reactances will decrease and the motor current may be too high. This type of frequency control is not normally used.

If the frequency is increased above its rated value, the flux and torque would decrease. If the synchronous speed corresponding to the rated frequency is called the *base speed*, ω_b, the synchronous speed at any other frequency becomes

$$\omega_s = \beta\omega_b$$

and

$$s = \frac{\beta\omega_b - \omega_m}{\beta\omega_b} \tag{11-56}$$

The torque expression in Eq. (11-18) becomes

$$T_d = \frac{3R_r V_a^2}{s\beta\omega_b[(R_s + R_r/s)^2 + (\beta X_s + \beta X_r)^2]} \tag{11-57}$$

The typical torque–speed characteristics are shown in Fig. 11-9 for various values of β. The three-phase inverter in Fig. 8-5a can vary the frequency at a fixed voltage. If R_s is negligible, Eq. (11-26) gives the maximum torque at the base speed as

$$T_{mb} = \frac{3V_a^2}{2\omega_b(X_s + X_r)} \tag{11-58}$$

The maximum torque at any other frequency is

$$T_m = \frac{3}{2\omega_b(X_s + X_r)}\left(\frac{V_a}{\beta}\right)^2 \tag{11-59}$$

and from Eq. (11-25), the corresponding slip is

$$s_m = \frac{R_r}{\beta(X_s + X_r)} \tag{11-60}$$

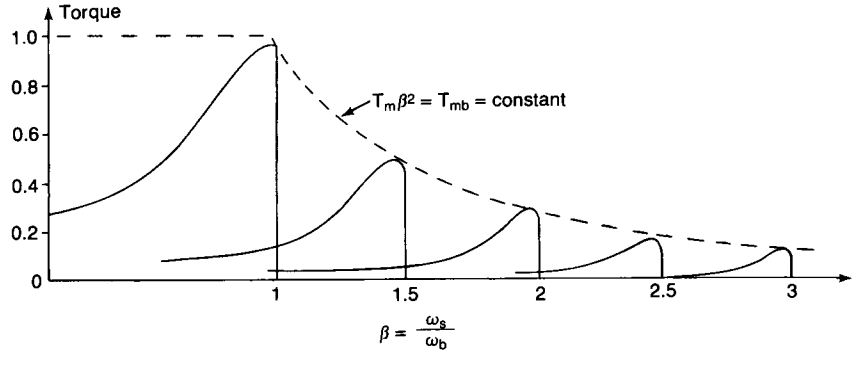


Figure 11-9 Torque–speed characteristics with frequency control.

Normalizing Eq. (11-59) with respect to Eq. (11-58) yields

$$\frac{T_m}{T_{mb}} = \frac{1}{\beta^2} \tag{11-61}$$

and

$$T_m\beta^2 = T_{mb} \tag{11-62}$$

Thus from Eqs. (11-61) and (11-62), it can be concluded that the maximum torque is inversely proportional to frequency squared, and $T_m\beta^2$ remains constant, similar to the behavior of dc series motors. In this type of control, the motor is said to be operated in a *field-weakening mode.*

Example 11-5

A three-phase 11.2-kW 1750-rpm 460-V 60-Hz four-pole Y-connected induction motor has the following parameters: $R_s = 0$, $R_r = 0.38\ \Omega$, $X_s = 1.14\ \Omega$, $X_r = 1.71\ \Omega$, and $X_m = 33.2\ \Omega$. The motor is controlled by varying the supply frequency. If the breakdown torque requirement is 35 N·m, calculate the (a) supply frequency, and (b) speed, ω_m.

Solution $\omega_b = 2\pi \times 60 = 377$ rad/s, $p = 4$, $P_0 = 11{,}200$ W, $T_{mb} \times 1750\ \pi/30 = 11{,}200$, $T_{mb} = 61.11$ N·m, and $T_m = 35$ N·m.

(a) From Eq. (11-62),

$$\beta = \sqrt{\frac{T_{mb}}{T_m}} = \sqrt{\frac{61.11}{35}} = 1.321$$

$$\omega_s = \beta\omega_b = 1.321 \times 377 = 498.01 \text{ rad/s}$$

From Eq. (11-1), the supply frequency is

$$\omega = \frac{4 \times 498.01}{2} = 996.2 \text{ rad/s} \quad \text{or} \quad 158.55 \text{ Hz}$$

(b) From Eq. (11-60), the slip for maximum torque is

$$s_m = \frac{R_r/\beta}{X_s + X_r} = \frac{0.38/1.321}{1.14 + 1.71} = 0.101$$

$$\omega_m = 498.01(1 - 0.101) = 447.711 \text{ rad/s} \quad \text{or} \quad 4275 \text{ rpm}$$

11-2.5 Voltage and Frequency Control

If the ratio of voltage to frequency is kept constant, the flux in Eq. (11-31) remains constant. Equation (11-59) indicates that the maximum torque, which is independent of frequency, can be maintained approximately constant. At a low frequency, the air-gap flux is reduced due to the drop in the stator impedance and the voltage has to be increased to maintain the torque level. This type of control is usually known as *volts/hertz* control.

If $\omega_s = \beta\omega_b$, and the voltage-to-frequency ratio is constant so that

$$\frac{V_a}{\omega_s} = d \tag{11-63}$$

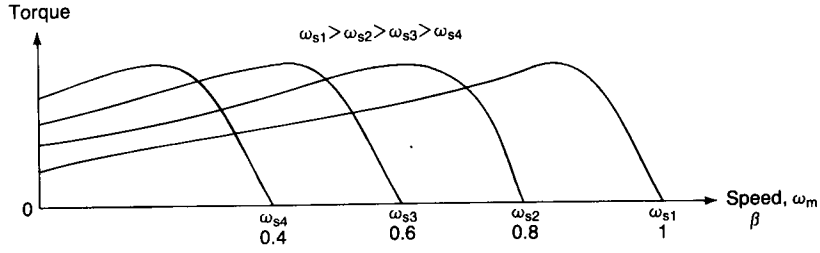


Figure 11-10 Torque–speed characteristics with volts/hertz control.

substitution of Eq. (11-56) in Eq. (11-57) yields

$$T_d = \frac{3R_r d^2 \omega_b^2 (\beta\omega_b - \omega_m)}{\omega_b^2 (R_s + R_r)^2 + [(\beta\omega_b - \omega_m)(X_s + X_r)]^2} \tag{11-64}$$

and the slip for maximum torque is

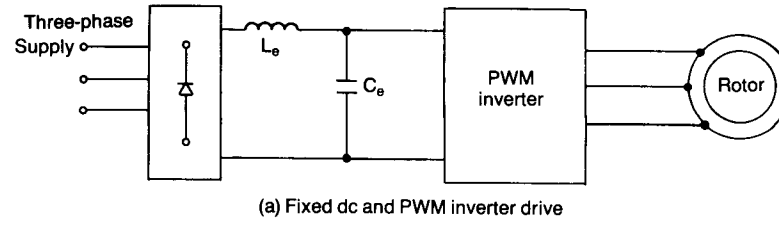
$$s_m = \frac{R_r}{[R_s^2 + \beta^2 (X_s + X_r)^2]^{1/2}} \tag{11-65}$$

The typical torque–speed characteristics are shown in Fig. 11-10. As the frequency is reduced, β decreases and the slip for maximum torque increases. For a given torque demand, the speed can be controlled according to Eq. (11-64) by changing the frequency. Therefore, by varying both the voltage and frequency, the torque and speed can be controlled. The torque is normally maintained constant while the speed is varied. The voltage at variable frequency can be obtained from three-phase inverters or cycloconverters. The cycloconverters are used in very large power applications (e.g., locomotives and cement mills), where the frequency requirement is one-half or one-third of the line frequency.

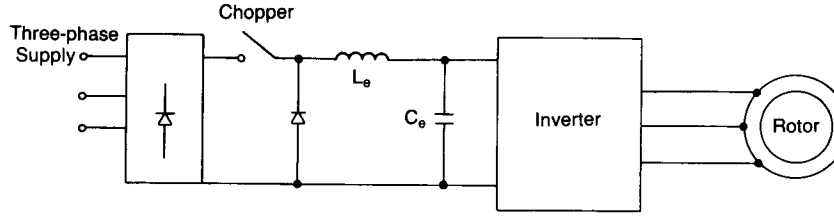
Three possible circuit arrangements for obtaining variable voltage and frequency are shown in Fig. 11-11. In Fig. 11-11a, the dc voltage remains constant and the PWM techniques are applied to vary both the voltage and frequency within the inverter. Due to diode rectifier, regeneration is not possible and the inverter would generate harmonics into the ac supply. In Fig. 11-11b, the chopper varies the dc voltage to the inverter and the inverter controls the frequency. Due to the chopper, the harmonic injection into the ac supply is reduced. In Fig. 11-11c, the dc voltage is varied by the dual converter and frequency is controlled within the inverter. This arrangement permits regeneration; however, the input power factor of the converter is low, especially at a high delay angle.

Example 11-6

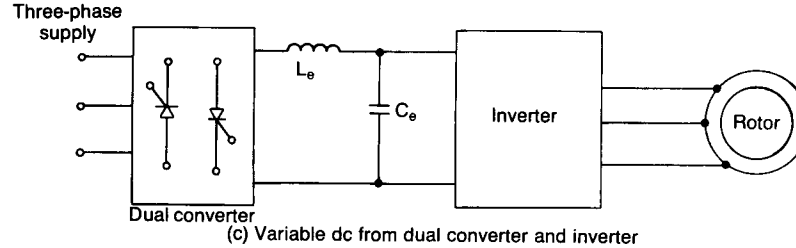
A three-phase 11.2-kW 1750-rpm 460-V 60-Hz four-pole Y-connected induction motor has the following parameters: $R_s = 0.66\ \Omega$, $R_r = 0.38\ \Omega$, $X_s = 1.14\ \Omega$, $X_r = 1.71\ \Omega$, and $X_m = 33.2\ \Omega$. The motor is controlled by varying both the voltage and frequency. The volts/hertz ratio, which corresponds to the rated voltage and rated frequency, is maintained constant. (a) Calculate the maximum torque, T_m, and the corresponding speed, ω_m, for 60 Hz and 30 Hz. (b) Repeat part (a) if R_s is negligible.



(a) Fixed dc and PWM inverter drive



(b) Variable dc and inverter



(c) Variable dc from dual converter and inverter

Figure 11-11 Voltage-source induction motor drives.

Solution $p = 4$, $V_a = 460/\sqrt{3} = 265.58$ V, $\omega = 2\pi \times 60 = 377$ rad/s, and from Eq. (11-1), $\omega_b = 2 \times 377/4 = 188.5$ rad/s. From Eq. (11-63), $d = 265.58/188.5 = 1.409$.

(a) At 60 Hz, $\omega_b = \omega_s = 188.5$ rad/s, $\beta = 1$, and $V_a = d\omega_s = 1.409 \times 188.5 = 265.58$ V. From Eq. (11-65),

$$s_m = \frac{0.38}{[0.66^2 + (1.14 + 1.71)^2]^{1/2}} = 0.1299$$

$$\omega_m = 188.5 \times (1 - 0.1299) = 164.01 \text{ rad/s} \quad \text{or} \quad 1566 \text{ rpm}$$

From Eq. (11-21), the maximum torque is

$$T_m = \frac{3 \times 265.58^2}{2 \times 188.5[0.66 + 0.66^2 + (1.14 + 1.71)^2]} = 156.55 \text{ N·m}$$

At 30 Hz, $\omega_s = 2 \times 2 \times \pi\ 30/4 = 94.25$ rad/s, $\beta = 30/60 = 0.5$, and $V_a = d\omega_s = 1.409 \times 94.25 = 132.79$ V. From Eq. (11-65), the slip for maximum torque is

$$s_m = \frac{0.38}{[0.66^2 + 0.5^2(1.14 + 1.71)^2]^{1/2}} = 0.242$$

$$\omega_m = 94.25 \times (1 - 0.242) = 71.44 \text{ rad/s} \quad \text{or} \quad 682 \text{ rpm}$$

$$T_m = 125.82 \text{ N·m}$$

(b) At 60 Hz, $\omega_b = \omega_s = 188.5$ rad/s and $V_a = 265.58$ V. From Eq. (11-60),

$$s_m = \frac{0.38}{1.14 + 1.71} = 0.1333$$

$$\omega_m = 188.5 \times (1 - 0.1333) = 163.36 \text{ rad/s or } 1560 \text{ rpm}$$

From Eq. (11-59), the maximum torque is $T_m = 196.94$ N·m.

At 30 Hz, $\omega_b = \omega_s = 94.25$ rad/s, $\beta = 0.5$, and $V_a = 132.79$ V. From Eq. (11-60),

$$s_m = \frac{0.38/0.5}{1.14 + 1.71} = 0.2666$$

$$\omega_m = 94.25 \times (1 - 0.2666) = 69.11 \text{ rad/s} \quad \text{or} \quad 660 \text{ rpm}$$

From Eq. (11-59), the maximum torque is $T_m = 196.94$ N·m.

Note. Neglecting R_s may introduce a significant error in the torque estimation, especially at low frequency.

11-2.6 Current Control

The torque of induction motors can be controlled by varying the rotor current. The input current, which is readily accessible, is varied instead of the rotor current. For a fixed input current, the rotor current depends on the the relative values of the magnetizing and rotor circuit impedances. From Fig. 11-2 the rotor current can be found as

$$\bar{\mathbf{I}}_r = \frac{jX_m I_i}{R_s + R_r/s + j(X_m + X_s + X_r)} = I_r \angle \theta_1 \tag{11-66}$$

From Eqs. (11-9) and (11-12a), the developed torque is

$$T_d = \frac{3R_r(X_m I_i)^2}{s\omega_s[(R_s + R_r/s)^2 + (X_m + X_s + X_r)^2]} \tag{11-67}$$

and the starting torque at $s = 1$ is

$$T_s = \frac{3R_r(X_m I_i)^2}{\omega_s[(R_s + R_r)^2 + (X_m + X_s + X_r)^2]} \tag{11-68}$$

The slip for maximum torque is

$$s_m = \pm \frac{R_r}{[R_s^2 + (X_m + X_s + X_r)^2]^{1/2}} \tag{11-69}$$

In a real situation as shown in Fig. 11-1b and c, the stator current through R_s and

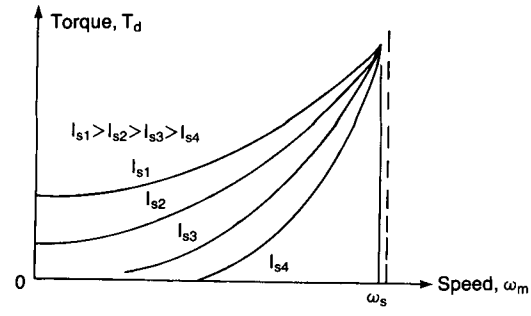


Figure 11-12 Torque–speed characteristics by current control.

X_s will be constant at I_i. Neglecting the values of R_s and X_s, Eq. (11-69) becomes

$$s_m = \pm \frac{R_r}{X_m + X_r} \tag{11-70}$$

and at $s = s_m$, Eq. (11-67) gives the maximum torque,

$$T_m = \frac{3X_m^2}{2\omega_s(X_m + X_r)} I_i^2 = \frac{3L_m^2}{2(L_m + L_r)} I_i^2 \tag{11-71}$$

It can be noticed from Eq. (11-71) that the maximum torque depends on the square of the current and is approximately independent of the frequency. The typical torque–speed characteristics are shown in Fig. 11-12. Since X_m is large as compared to X_s and X_r, the starting torque is low. As the speed increases (or slip decreases), the stator voltage rises and the torque increases. The torque can be

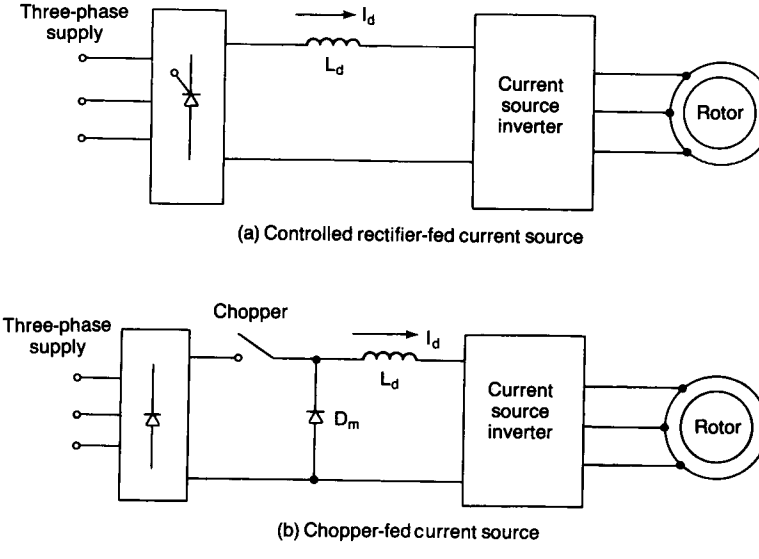


Figure 11-13 Current-source inductor motor drive.

controlled by the stator current and slip. To keep the air-gap flux constant and to avoid saturation due to high voltage, the motor is normally operated on the negative slope of the equivalent torque–speed characteristics with voltage control. The negative slope is in the unstable region and the motor must be operated in closed-loop control. At a low slip, the terminal voltage could be excessive and the flux would saturate. Due to saturation, the torque peaking as shown in Fig. 11-12 will be less than that as shown.

The constant current can be supplied by three-phase current source inverters. The current-fed inverter has the advantages of fault current control and the current is less sensitive to the motor parameter variations. However, they generate harmonics and torque pulsation. Two possible configurations of current-fed inverter drives are shown in Fig. 11-13. In Fig. 11-13a the inductor acts as a current source and the controlled rectifier controls the current source. The input power factor of this arrangement is very low. In Fig. 11-13b the chopper controls the current source and the input power factor is higher.

Example 11-7

A three-phase 11.2-kW 1750-rpm 460-V 60-Hz four-pole Y-connected induction motor has the following parameters: $R_s = 0.66\ \Omega$, $R_r = 0.38\ \Omega$, $X_s = 1.14\ \Omega$, $X_r = 1.71\ \Omega$, and $X_m = 33.2\ \Omega$. The no-load loss is negligible. The motor is controlled by a current-source inverter and the input current is maintained constant at 20 A. If the frequency is 40 Hz and the developed torque is 55 N·m, determine the (a) slip for maximum torque, s_m, and maximum torque, T_m; (b) slip, s; (c) rotor speed, ω_m; (d) terminal voltage per phase, V_a; and (e) power factor, PF_m.

Solution $V_{a(\text{rated})} = 460/\sqrt{3} = 265.58$ V, $I_i = 20$ A, $T_L = T_d = 55$ N·m, and $p = 4$. At 40 Hz, $\omega = 2\pi \times 40 = 251.33$ rad/s, $\omega_s = 2 \times 251.33/4 = 125.66$ rad/s, $R_s = 0.66\ \Omega$, $R_r = 0.38\ \Omega$, $X_s = 1.14 \times 40/60 = 0.76\ \Omega$, $X_r = 1.71 \times 40/60 = 1.14\ \Omega$, and $X_m = 33.2 \times 40/60 = 22.13\ \Omega$.

(a) From Eq. (11-70), $s_m = 0.38/(22.13 + 1.14) = 0.01632$. For $s = s_m$, Eq. (11-71), gives $T_m = 94.64$ N·m.

(b) From Eq. (11-67),

$$T_d = 55 = \frac{3(R_r/s)(22.13 \times 20)^2}{125.66[(0.66 + R_r/s)^2 + (22.13 + 0.76 + 1.14)^2]}$$

which gives $(R_r/s)^2 - 83.74(R_r/s) + 578.04 = 0$, and solving for R_r/s yields

$$\frac{R_s}{s} = 76.144 \text{ or } 7.581$$

and $s = 0.00499$ or 0.0501. Since the motor is normally operated with a large slip in the negative slope of the torque–speed characteristic,

$$s = 0.0501$$

(c) $\omega_m = 125.656(1 - 0.0501) = 119.36$ rad/s or 1140 rpm.

(d) From Fig. 11-2, the input impedance can be derived as

$$\bar{\mathbf{Z}}_i = R_i + jX_i = (R_i^2 + X_i^2)^{1/2} \angle\underline{\theta_m} = Z_i \angle\underline{\theta_m}$$

where

$$R_i = \frac{X_m^2(R_s + R_r/s)}{(R_s + R_r/s)^2 + (X_m + X_s + X_r)^2} \tag{11-72}$$

$$= 6.26\ \Omega$$

$$X_i = \frac{X_m[(R_s + R_r/s)^2 + (X_s + X_r)(X_m + X_s + X_r)]}{(R_s + R_r/s)^2 + (X_m + X_s + X_r)^2} \tag{11-73}$$

$$= 3.899\ \Omega$$

and

$$\theta_m = \tan^{-1}\frac{X_i}{R_i}$$

$$= 31.9° \tag{11-74}$$

$$Z_i = (6.26^2 + 3.899^2)^{1/2} = 7.38\ \Omega$$

$$V_a = Z_i I_i = 7.38 \times 20 = 147.6\ \text{V}$$

(e) $\text{PF}_m = \cos(31.9°) = 0.849$ (lagging).

Note. If the maximum torque is calculated from Eq. (11-71), $T_m = 100.49$ and V_a (at $s = s_m$) is 313 V. For a supply frequency of 90 Hz, recalculations of the values give $\omega_s = 282.74$ rad/s, $X_s = 1.71\ \Omega$, $X_r = 2.565\ \Omega$, $X_m = 49.8\ \Omega$, $s_m = 0.00726$, $T_m = 96.1$ N·m, $s = 0.0225$, $V_a = 316$ V, and V_a (at $s = s_m$) = 699.6 V. It is evident that at high frequency and low slip, the terminal voltage would exceed the rated value and saturated the air-gap flux.

11-2.7 Voltage, Current, and Frequency Control

The torque–speed characteristics of induction motors depend on the type of control. It may be necessary to vary the voltage, frequency, and current to meet the torque–speed requirements as shown in Fig. 11-14, where there are three regions. In the first region, the speed can be varied by voltage (or current) control at constant torque. In second region, the motor is operated at constant current and the slip is varied. In the third region, the speed is controlled by frequency at a reduced stator current.

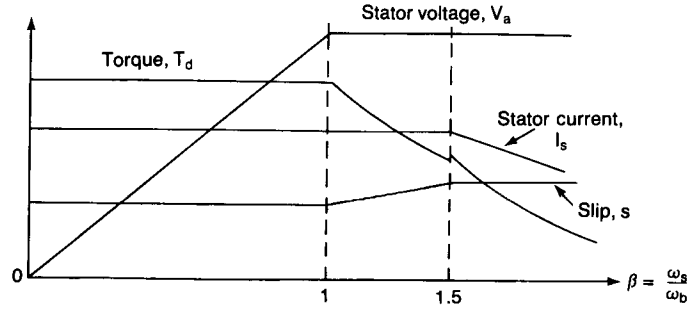


Figure 11-14 Control variables against frequency.

11-2.8 Closed-Loop Control of Induction Motors

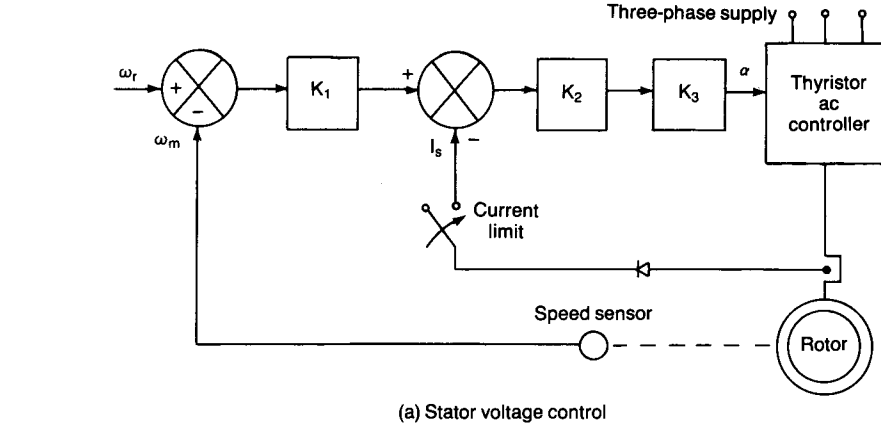
A closed-loop control is normally required to satisfy the steady-state and transient performance specifications of ac drives. The control strategy can be implemented by (1) *scalar control*, where the control variables are dc quantities and only their magnitudes are controlled: (2) *vector control*, where both the magnitude and phase of the control variables are controlled; or (3) *adaptive control*, where the parameters of the controller are continuously varied to adapt to the variations of the output variables.

The dynamic model of induction motors differs significantly from that in Fig. 11-1 and is more complex than dc motors. The design of feedback-loop parameters requires complete analysis and simulation of the entire drive. The control and modeling of ac drives are beyond the scope of this text; and only some of the basic scalar feedback techniques are discussed in this section.

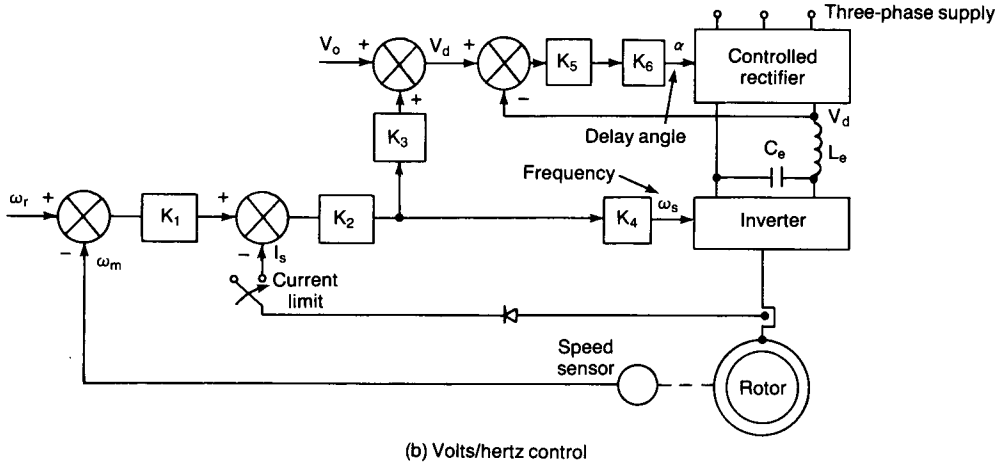
A control system is generally characterized by the hierarchy of the control loops, where the outer loop controls the inner loops. The inner loops are designed to execute progressively faster. The loops are normally designed to have limited command excursion. Figure 11-15a shows an arrangement for stator voltage control of induction motors by ac voltage controllers at fixed frequency. The speed controller, K_1, generates the delay angle of thyristor converter and the inner current-limit loop sets the torque limit indirectly. The current limiter instead of current clamping has the advantage of feeding back the short-circuit current in case of fault. The speed controller, K_1, may be a simple gain (proportional type), proportional-integral type, or a lead-lag compensator. A 187-kW three-phase ac voltage regulator (or controller) for a wire-drawing machine is shown in Fig. 11-16, where the control electronics are mounted on the side panel.

The arrangement in Fig. 11-15a can be extended to volt/hertz control with the addition of a controlled rectifier and dc voltage control loop as shown in Fig. 11-15b. After the current limiter, the same signal generates the inverter frequency and provides input to the dc link gain controller, K_3. A small voltage V_0 is added to the dc voltage reference to compensate for the stator resistance drop at low frequency. The dc voltage V_d acts as the reference for the voltage control of the controlled rectifier. In case of PWM inverter, there is no need of the controlled rectifier and the signal V_d controls the inverter voltage directly. For current monitoring, this arrangement requires a sensor, which introduces a delay in the system response. Fifteen forced-commutated inverter cubicles for controlling the undergrate cooler fans of a cement kiln are shown in Fig. 11-17, where each unit is rated at 100 kW.

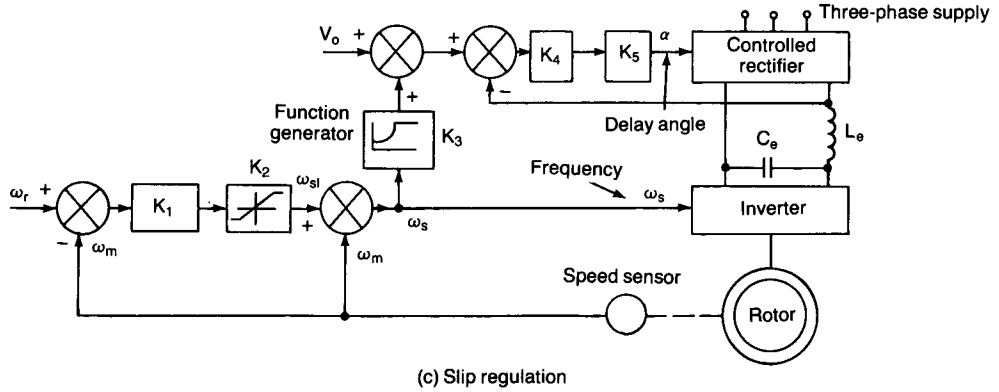
Since the torque of induction motors is proportional to the slip frequency, $\omega_{sl} = s\omega_s$, the slip frequency instead of the stator current can be controlled. The speed error generates the slip frequency command as shown in Fig. 11-15c, where the slip limits set the torque limits. The function generator, which produces command signals for voltage control in response to the frequency, ω_s, can take into account the compensating drop at low frequency. However, the compensating drop V_o is shown in Fig. 11-15c. For a step change in the speed command, the motor accelerates or decelerates within the torque limits to a steady-state slip value



(a) Stator voltage control



(b) Volts/hertz control



(c) Slip regulation

Figure 11-15 Closed-loop control of induction motors.

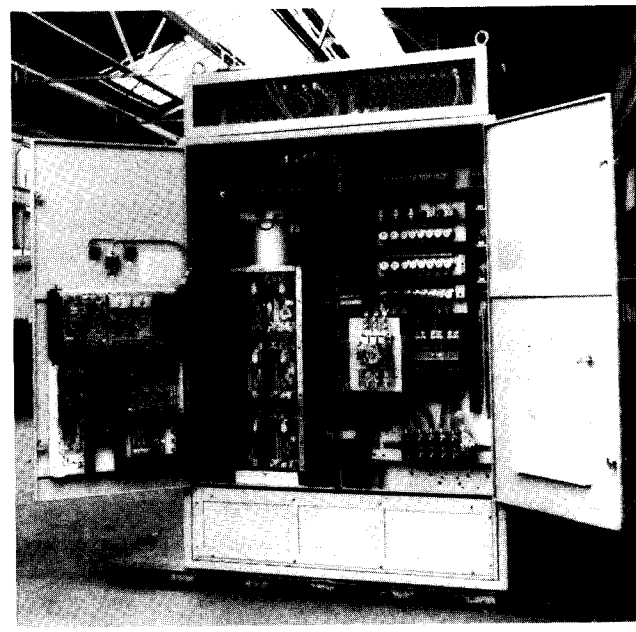


Figure 11-16 A 187-kW three-phase ac voltage regulator. (*Reproduced by permission of Brush Electrical Machines Ltd., England*)

corresponding to the load torque. This arrangement controls the torque indirectly within the speed control loop and does not require the current sensor.

A simple arrangement for current control is shown in Fig. 11-18. The speed error generates the reference signal for the dc link current. The slip frequency, $\omega_{sl} = \omega_s - \omega_m$, is fixed. With a step speed command, the machine accelerates with a high current which is proportional to the torque. In the steady state the

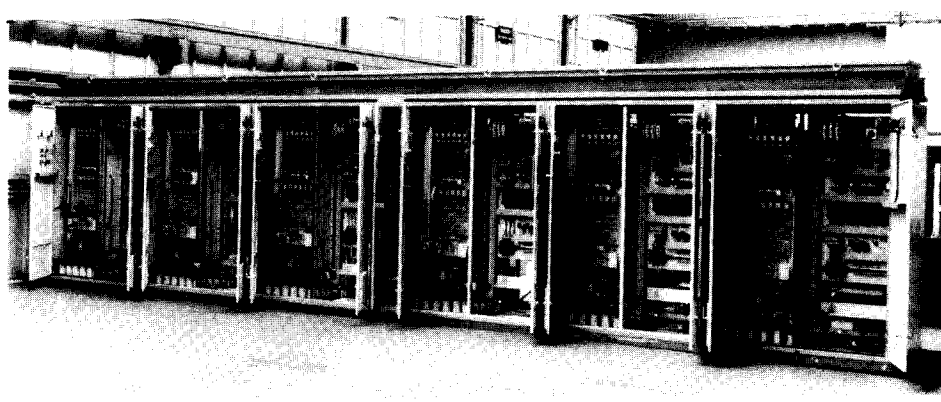


Figure 11-17 Fifteen forced-commutated inverter cubicles for a cement kiln. (*Reproduced by permission of Brush Electrical Machines Ltd., England*)

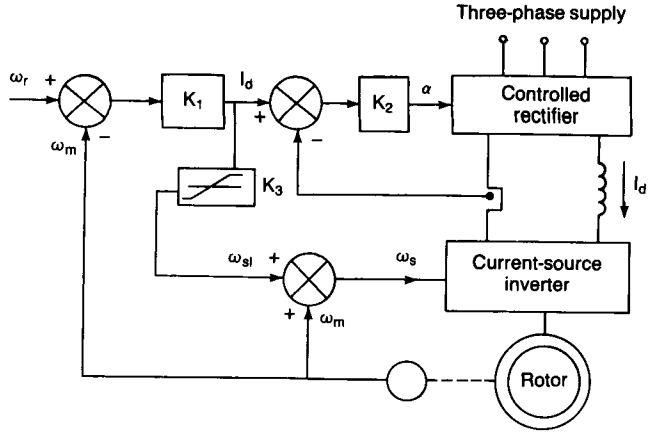


Figure 11-18 Current control with constant slip.

motor current is low. However, the air-gap flux fluctuates, and due to varying flux at different operating points, the performance of this drive is poor.

A practical arrangement for current control, where the flux is maintained constant, is shown in Fig. 11-19. The speed error generates the slip frequency, which controls the inverter frequency and the dc link current source. The function generator produces the current command to maintain the air-gap flux constant, normally at the rated value.

The arrangement in Fig. 11-15a for speed control with inner current control loop can be applied to a static Kramer drive as shown in Fig. 11-20, where the torque is proportional to the dc link current I_d. The speed error generates the dc link current command. A step increase in speed clamps the current to the maximum value and the motor accelerates at a constant torque which corresponds to the maximum current. A step decrease in the speed sets the current command to zero and the motor decelerates due to the load torque. A 110-kW static Kramer drive for fans in cement works is shown in Fig. 11-21.

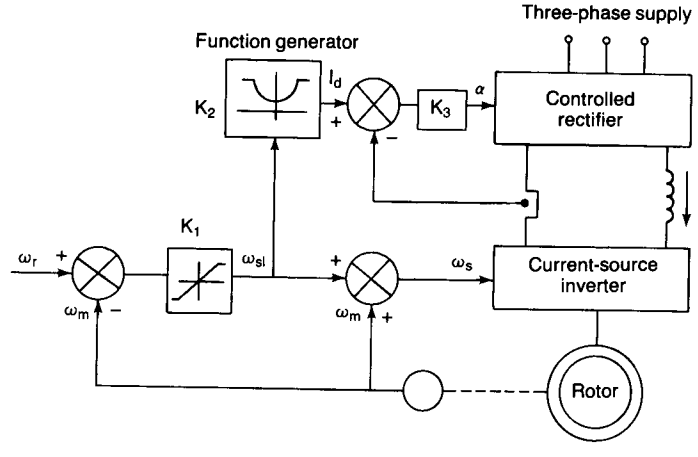


Figure 11-19 Current control with constant flux operation.

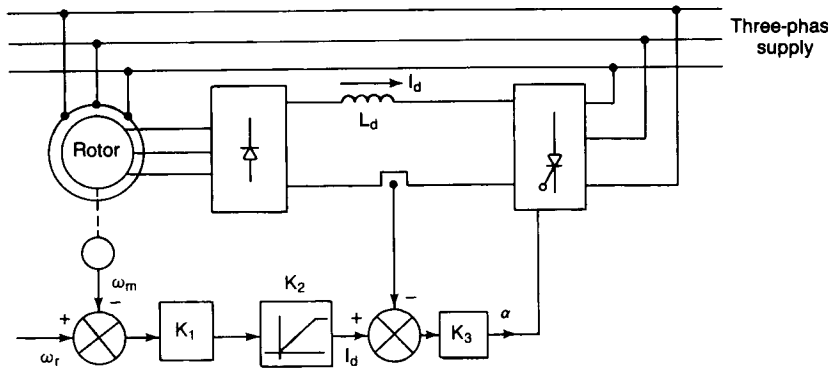


Figure 11-20 Speed control of static Kramer drive.

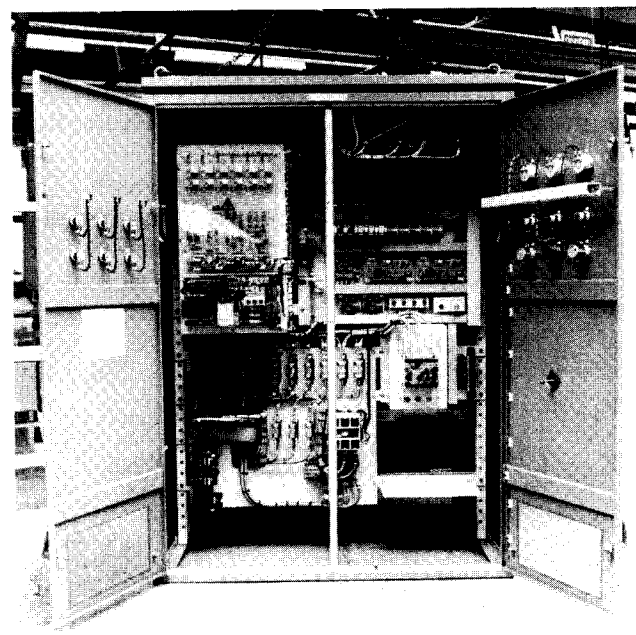


Figure 11-21 A 110-kW static Kramer drive. (*Reproduced by permission of Brush Electrical Machines Ltd., England*)

11-3 SYNCHRONOUS MOTOR DRIVES

Synchronous motors have a polyphase winding on the stator, also known as armature, and a field winding carrying a dc current on the rotor. There are two mmfs involved: one due to the field current and other due to the armature current.

The resultant mmf produces the torque. The armature is identical to the stator of induction motors, but there is no induction in the rotor. A synchronous motor is a constant-speed machine and always rotates with zero slip at the synchronous speed, which depends on the frequency and the number of poles, as given by Eq. (11-1). A synchronous motor can be operated as a motor or generator. The power factor can be controlled by varying the field current. The cycloconverters and inverters are widening the applications of synchronous motors in variable-speed drives. The synchronous motors can be classified into four types:

1. Cylindrical rotor motors
2. Salient-pole motors
3. Reluctance motors
4. Permanent-magnet motors

11-3.1 Cylindrical Rotor Motors

The field winding is wound on the rotor, which is cylindrical, and these motors have a uniform air gap. The reactances are independent on the rotor position. The equivalent circuit per phase, neglecting the no-load loss, is shown in Fig. 11-22a, where R_a is the armature resistance per phase and X_s is the *synchronous reactance* per phase. V_f, which is dependent on the field current, is known as *excitation* or *field* voltage.

The power factor depends on the field current. The V-curves, which show the typical variations of the armature current against the excitation current, are shown in Fig. 11-23. For the same armature current, the power factor could be lagging or leading, depending on the excitation current, I_f.

If θ_m is the lagging factor angle, Fig. 11-22a gives

$$\bar{V}_f = V_a \angle 0 - \bar{I}_a (R_a + jX_s) \tag{11-75}$$

$$= V_a \angle 0 - I_a (\cos \theta_m - j \sin \theta_m)(R_a + jX_s)$$

$$= V_a - I_a X_s \sin \theta_m - I_a R_a \cos \theta_m - jI_a(X_s \cos \theta_m - R_a \sin \theta_m) \tag{11-75a}$$

$$= V_f \angle \delta \tag{11-75b}$$

where

$$\delta = \tan^{-1} \frac{-(I_a X_s \cos \theta_m - I_a R_a \sin \theta_m)}{V_a - I_a X_s \sin \theta_m - I_a R_a \cos \theta_m} \tag{11-76}$$

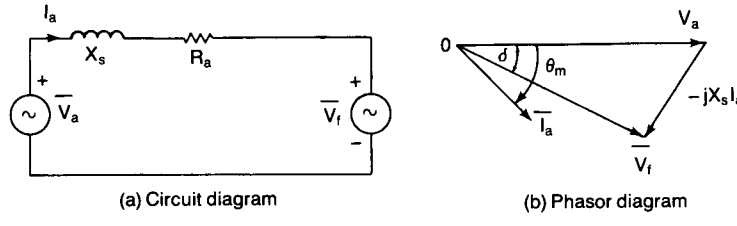


Figure 11-22 Equivalent circuit of synchronous motors.

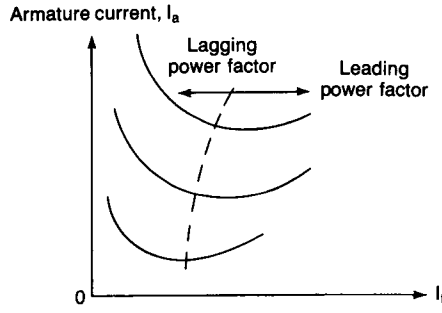


Figure 11-23 Typical *V*-curves of synchronous motors.

and

$$V_f = [(V_a - I_a X_s \sin\theta_m - I_a R_a \cos\theta_m)^2 + (I_a X_s \cos\theta_m - I_a R_a \sin\theta_m)^2]^{1/2} \tag{11-77}$$

and the phasor diagram in Fig. 11-22b yields

$$\bar{\mathbf{V}}_f = V_f(\cos\delta + j \sin\delta) \tag{11-78}$$

$$\bar{\mathbf{I}}_a = \frac{\bar{V}_a - \bar{V}_f}{R_a + jX_s} = \frac{[V_a - V_f(\cos\delta + j\sin\delta)](R_a - jX_s)}{R_a^2 + X_s^2} \tag{11-79}$$

The real part of Eq. (11-79) becomes

$$I_a \cos\theta_m = \frac{R_a(V_a - V_f \cos\delta) - V_f X_s \sin\delta}{R_a^2 + X_s^2} \tag{11-80}$$

The input power can be determined from Eq. (11-80),

$$\begin{aligned} P_i &= 3V_a I_a \cos\theta_m \\ &= \frac{3[R_a(V_a^2 - V_a V_f \cos\delta) - V_a V_f X_s \sin\delta]}{R_a^2 + X_s^2} \end{aligned} \tag{11-81}$$

The stator (or armature) copper loss is

$$P_{su} = 3I_a^2 R_a \tag{11-82}$$

The gap power, which is the same as the developed power, is

$$P_d = P_g = P_i - P_{su} \tag{11-83}$$

If ω_s is the synchronous speed, which is the same as the rotor speed, the developed torque becomes

$$T_d = \frac{P_d}{\omega_s} \tag{11-84}$$

If the armature resistance is negligible, Eq. (11-84) becomes

$$T_d = \frac{3V_a V_f \sin\delta}{X_s \omega_s} \tag{11-85}$$

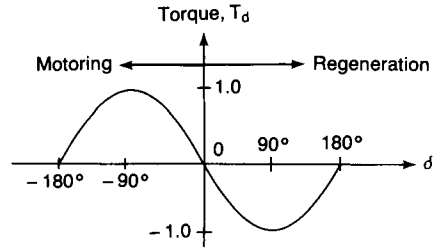


Figure 11-24 Torque against torque angle with cylindrical rotor.

and

$$\delta = -\tan^{-1}\frac{I_a X_s \cos\theta_m}{V_a - I_a X_s \sin\theta_m} \tag{11-86}$$

For motoring δ is negative and torque in Eq. (11-85) becomes positive. In case of generating, δ is positive and the power (and torque) becomes negative. The angle δ is called the *torque angle*. For a fixed voltage and frequency, the torque depends on the angle, δ, and is proportional to the excitation voltage, V_f. For fixed values of V_f and δ, the torque depends on the voltage-to-frequency ratio and a constant volts/hertz control will provide speed control at a constant torque. If V_a, V_f, and δ remain fixed, the torque decreases with the speed and the motor operates in the field weakening mode.

If $\delta = 90°$, the torque becomes maximum and the maximum developed torque, which is called the *pull-out torque*, becomes

$$T_p = T_m = -\frac{3V_a V_f}{X_s \omega_s} \tag{11-87}$$

The plot of developed torque against the angle, δ is shown in Fig. 11-24. For stability considerations, the motor is operated in the positive slope of T_d–δ characteristics and this limits the range of torque angle, $-90° \leq \delta \leq 90°$.

Example 11-8

A three-phase 460-V 60-Hz six-pole Y-connected cylindrical rotor synchronous motor has a synchronous reactance of $X_s = 2.5\ \Omega$ and the armature resistance is negligible. The load torque, which is proportional to the speed squared, is $T_L = 398$ N·m at 1200 rpm. The power factor is maintained at unity by field control and the voltage-to-frequency ratio is kept constant at the rated value. If the inverter frequency is 36 Hz and the motor speed is 720 rpm, calculate the (a) the input voltage, V_a; (b) armature current, I_a; (c) excitation voltage, V_f; (d) torque angle, δ; and (e) pull-out torque, T_p.

Solution PF = $\cos\theta_m = 1.0$, $\theta_m = 0$, $V_{a(\text{rated})} = V_b = 460/\sqrt{3} = 265.58$ V, $p = 6$, $\omega = 2\pi \times 60 = 377$ rad/s, $\omega_b = \omega_s = \omega_m = 2 \times 377/6 = 125.67$ rad/s or 1200 rpm, and $d = V_b/\omega_b = 265.58/125.67 = 2.1133$. At 720 rpm,

$$T_L = 398 \times \left(\frac{720}{1200}\right)^2 = 143.28\ \text{N·m} \qquad \omega_s = \omega_m = 720 \times \frac{\pi}{30} = 75.4\ \text{rad/s}$$

$$P_0 = 143.28 \times 75.4 = 10{,}803\ \text{W}$$

(a) $V_a = d\omega_s = 2.1133 \times 75.4 = 159.34$ V.

(b) $P_0 = 3V_aI_a$ PF = 10,803 or $I_a = 10{,}803/(3 \times 159.34) = 22.6$ A.
(c) From Eq. (11-75),

$$\bar{\mathbf{V}}_f = 159.34 - 22.6(1 + j0)(j2.5) = 169.1 \angle -19.52°$$

(d) The torque angle, $\delta = -19.52°$.
(e) From Eq. (11-87),

$$T_p = \frac{3 \times 159.34 \times 169.1}{2.5 \times 75.4} = 428.82 \text{ N·m}$$

11-3.2 Salient-Pole Motors

The armature of salient-pole motors is similar to that of cylindrical rotor motors. However, due to saliency, the air gap is not uniform and the flux is dependent on the position of the rotor. The field winding is normally wound on the pole pieces. The armature current and the reactances can be resolved into direct and quadrature axis components. I_d and I_q are the components of the armature current in the direct (or d) axis and quadrature (or q) axis, respectively. X_d and X_q are the d-axis reactance and q-axis reactance, respectively. The excitation voltage becomes

$$\bar{\mathbf{V}}_f = \bar{\mathbf{V}}_a - jX_d\bar{\mathbf{I}}_d - jX_q\bar{\mathbf{I}}_q - R_a\bar{\mathbf{I}}_a$$

For negligible armature resistance, the phasor diagram is shown in Fig. 11-25. From the phasor diagram,

$$I_d = I_a \sin(\theta_m - \delta) \tag{11-88}$$

$$I_q = I_a \cos(\theta_m - \delta) \tag{11-89}$$

$$I_dX_d = V_a \cos\delta - V_f \tag{11-90}$$

$$I_qX_q = V_a \sin\delta \tag{11-91}$$

Substituting I_q from Eq. (11-89) in Eq. (11-91), we have

$$\begin{aligned} V_a \sin\delta &= X_qI_a \cos(\theta_m - \delta) \\ &= X_qI_a(\cos\delta \cos\theta_m + \sin\delta \sin\theta_m) \end{aligned} \tag{11-92}$$

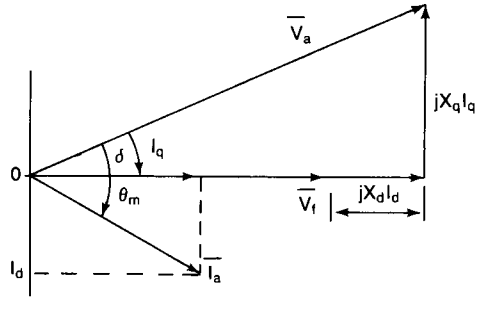


Figure 11-25 Phase diagram for salient-pole synchronous motors.

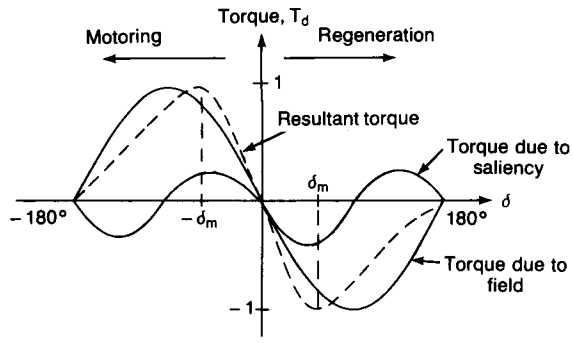


Figure 11-26 Torque against torque angle with salient-pole rotor.

Dividing both sides by cos δ and solving for δ gives

$$\delta = -\tan^{-1} \frac{I_a X_q \cos \theta_m}{V_a - I_a X_q \sin \theta_m} \tag{11-93}$$

where the negative sign signifies that V_f lags V_a. If the terminal voltage is resolved into a d-axis and a q-axis,

$$V_{ad} = -V_a \sin \delta \text{ and } V_{aq} = V_a \cos \delta$$

The input power becomes

$$\begin{aligned} P &= -3(I_d V_{ad} + I_q V_{aq}) \\ &= 3I_d V_a \sin \delta - 3I_q V_a \cos \delta \end{aligned} \tag{11-94}$$

Substituting I_d from Eq. (11-90) and I_q from Eq. (11-91) in Eq. (11-94) yields

$$P_d = -\frac{3V_a V_f}{X_d} \sin \delta - \frac{3V_a^2}{2} \frac{X_d - X_q}{X_d X_q} \sin 2\delta \tag{11-95}$$

Dividing Eq. (11-95) by speed gives the developed torque as

$$T_d = -\frac{3V_a V_f}{X_d \omega_s} \sin \delta - \frac{3V_a^2}{2\omega_s} \frac{X_d - X_q}{X_d X_q} \sin 2\delta \tag{11-96}$$

The torque in Eq. (11-96) has two components. The first component is the same as that of cylindrical rotor if X_d is replaced by X_s and the second component is due to the rotor saliency. The typical plot of T_d against torque angle is shown in Fig. 11-26, where the torque has a maximum value at $\delta = \pm\delta_m$. For stability the torque angle is limited in the range of $-\delta_m \leq \delta \leq \delta_m$ and in this stable range, the slope of T_d–δ characteristic is higher than that of cylindrical rotor motor.

11-3.3 Reluctance Motors

The reluctance motors are similar to the salient-pole motors, except that there is no field winding on the rotor. The armature circuit, which produces rotating magnetic field in the air gap, induces a field in the rotor, which has a tendency to

align with the armature field. The reluctance motors are very simple and are used in applications where a number of motors are required to rotate in synchronism. These motors have low lagging power factor, typically in the range 0.65 to 0.75.

With $V_f = 0$, Eq. (11-96) can be applied to determine the reluctance torque,

$$T_d = -\frac{3V_a^2}{2\omega_s}\frac{X_d - X_q}{X_d X_q}\sin 2\delta \tag{11-97}$$

where

$$\delta = -\tan^{-1}\frac{I_a X_q \cos\theta_m}{V_a - I_a X_q \sin\theta_m} \tag{11-98}$$

The pull-out torque is

$$T_p = -\frac{3V_a^2}{2\omega_s}\frac{X_d - X_q}{X_d X_q} \tag{11-99}$$

11-3.4 Permanent-Magnet Motors

The permanent-magnet motors are similar to that of salient-pole motors, except that there is no field winding on the rotor and the field is provided by permanent magnets. The excitation voltage cannot be varied. For the same frame size, permanent-magnet motors have higher pull-out torque. The equations for the salient-pole motors may be applied to permanent-magnet motors if the excitation voltage, V_f, is assumed constant.

Example 11-9

A three-phase 230-V 60-Hz four-pole Y-connected reluctance motor has $X_d = 22.5\ \Omega$ and $X_q = 3.5\ \Omega$. The armature resistance is negligible. The load torque is $T_L = 12.5$ N·m. The voltage-to-frequency ratio is maintained constant at the rated value. If the supply frequency is 60 Hz, determine the (a) torque angle, δ; (b) line current, I_a; and (c) input power factor, PF.

Solution $T_L = 12.5$ N·m, $V_{a(\text{rated})} = V_b = 230/\sqrt{3} = 132.79$ V, $p = 4$, $\omega = 2\pi \times 60 = 377$ rad/s, $\omega_b = \omega_s = \omega_m = 2 \times 377/4 = 188.5$ rad/s or 1800 rpm, $d = V_b/\omega_b = 132.79/188.50 = 0.7045$, and $V_a = 132.79$ V.

(a) $\omega_s = 188.5$ rad/s. From Eq. (11-97),

$$\sin 2\delta = -\frac{12.5 \times 2 \times 188.5 \times 22.5 \times 3.5}{3 \times 132.79^2 \times (22.5 - 3.5)}$$

and $\delta = -10.84°$.

(b) $P_0 = 12.5 \times 188.5 = 2356$ W. From Eq. (11-98),

$$\tan(10.84°) = \frac{3.5 I_a \cos\theta_m}{132.79 - 3.5 I_a \sin\theta_m}$$

and $P_0 = 2356 = 3 \times 132.79 I_a \cos\theta_m$. From these two equations, I_a and θ_m can be

determined by an iterative method of solution, which yields $I_a = 9.2$ A and $\theta_m = 49.98°$.

(c) PF = cos (49.98°) = 0.643.

11-3.5 Closed-Loop Control of Synchronous Motors

The typical characteristics of torque, current, and excitation voltage against frequency are shown in Fig. 11-27. There are two regions of operation: constant torque and constant power. In the constant-torque region, the volts/hertz is maintained constant, and in the constant-power region, the torque decreases with frequency. Similar to induction motors, the speed of synchronous motors can be controlled by varying the voltage, frequency, and current. There are various configurations for closed loop control of synchronous motors. A basic arrangement for constant volts/hertz control of synchronous motors is shown in Fig. 11-28, where the speed error generates the frequency and voltage command for the PWM inverter. A 3.3-kW soft-start system for synchronous motor compressor drives is

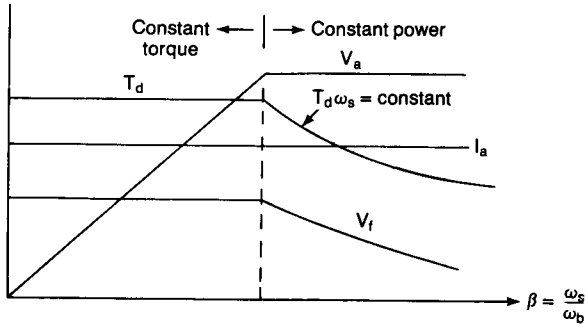


Figure 11-27 Torque–speed characteristics of synchronous motors.

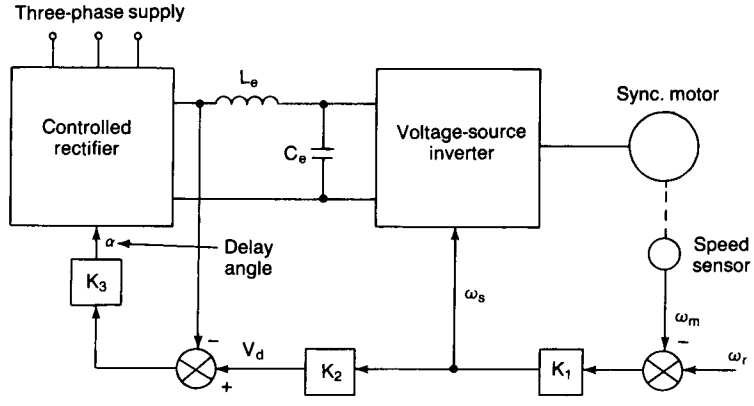


Figure 11-28 Volts/hertz control of synchronous motors.

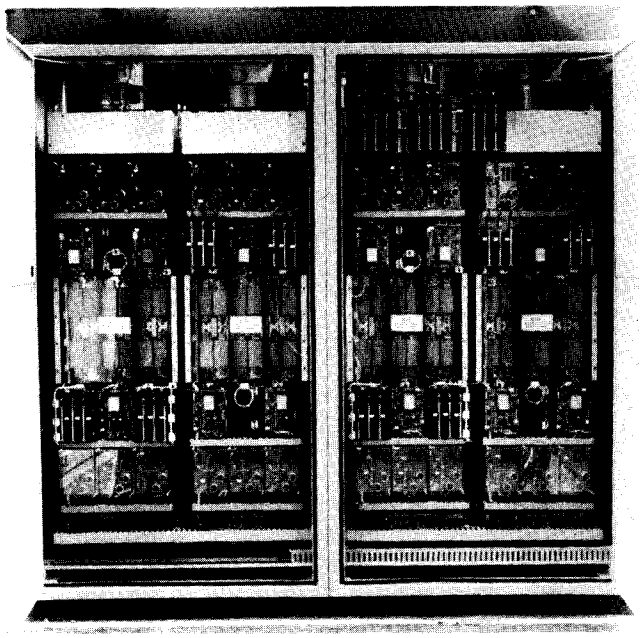


Figure 11-29 A 3.3-MW synchronous motor compressor drive. (*Reproduced by permission of Brush Electrical Machines Ltd., England*)

shown in Fig. 11-29, where two three-phase stacks are connected in parallel to give 12-pulse operation. The control cubicle for the drive in Fig. 11-29 is shown in Fig. 11-30.

SUMMARY

Although ac drives require advanced control techniques for control of voltage, frequency, and current, they have advantages over dc drives. The voltage and frequency can be controlled by voltage-source inverters. The current and frequency can be controlled by current-source inverters. The slip power recovery schemes use controlled rectifiers to recover the slip power of induction motors. The most common method of closed-loop control of induction motors is volts/hertz, flux, or slip control. Both squirrel-cage and wound-rotor motors are used in variable-speed drives. A voltage-source inverter can supply a number of motors connected in parallel, whereas a current-source inverter can supply only one motor.

Synchronous motors are constant-speed machines and their speeds can be controlled by voltage, frequency, and /or current. Synchronous motors are of four types: cylindrical rotors, salient poles, reluctance, and permanent magnets. There is abundant literature on ac drives, so only the fundamentals are covered in this chapter.

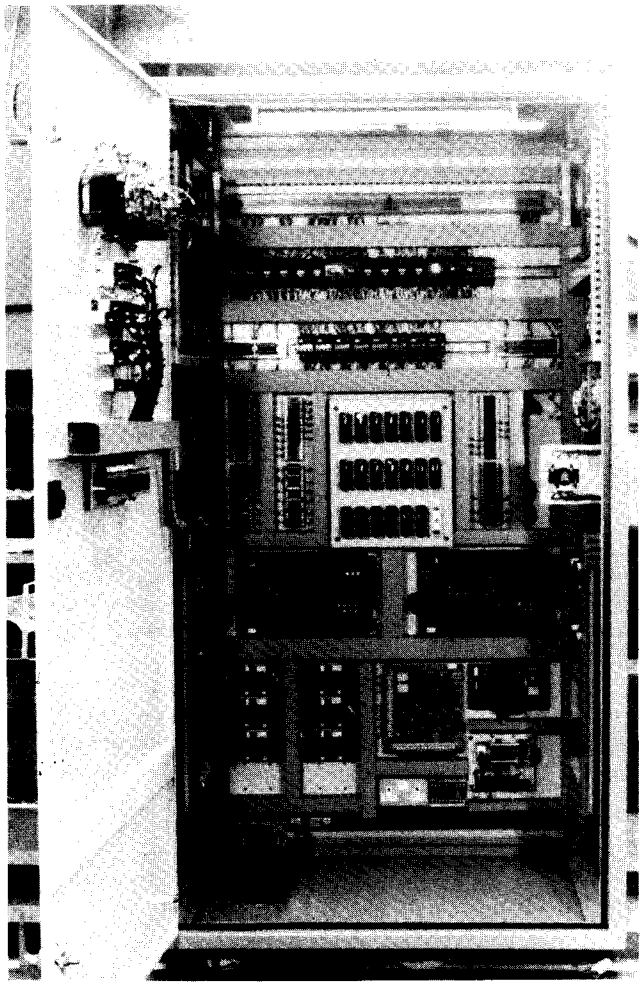


Figure 11-30 Control cubicle for the drive in Fig. 11-29. (*Reproduced by permission of Brush Electrical Machines Ltd., England*)

REFERENCES

1. B. K. Bose, *Power Electronics and AC Drives*. Englewood Cliffs, N.J.: Prentice-Hall, Inc., 1986.
2. B. K. Bose, *Adjustable AC Drives*, New York: IEEE Press, 1980.
3. S. B. Dewan, G. B. Slemon, and A. Straughen, *Power Semiconductor Drives*. New York: John Wiley & Sons, Inc., 1984.
4. W. Leonhard, "Control of ac machines with the help of electronics." *3rd IFAC Symposium on Control in Power Electronics and Electrical Drives*, Lausanne, Switzerland, Tutorial Session, September 1983, pp. 35–58.
5. W. Leonhard, *Control of Electrical Drives*. New York: Springer-Verlag, 1985.

6. Y. D. Landau, *Adaptive Control.* New York: Marcel Dekker, Inc., 1979.
7. H. Le-Huy, R. Perret, and D. Roye, "Microprocessor control of a current-fed synchronous motor drive." *IEEE Industry Applications Society Conference Record*, 1980, pp. 562–569.
8. A. Brickwedde, "Microprocessor-based adaptive speed and position control for electrical drives." *IEEE Industry Applications Society Conference Record*, 1984, pp. 411–417.
9. K. Masato, M. Yano, I. Kamiyana, and S. Yano, "Microprocessor-based vector control system for induction motor drives with rotor time constant identification." *IEEE Transaction on Industry Applications*, Vo. IA22, No. 3, 1986, pp. 453–459.
10. S. K. Biswas, S. Sahtiakumar, and J. Vithayathil, "High efficiency direct torque control scheme for CSI fed induction motor." *IEEE Industry Applications Society Conference Record*, 1986, pp. 216–221.
11. E. Prasad, J. F. Lindsay, and M. H. Rashid, "Parameter estimation and dynamic performance of permanent magnet synchronous motors." *IEEE Industry Applications Society Conference Record*, 1985, pp. 627–633.
12. T. J. E. Miller, "Converter volt-ampere requirements of the switched reluctance motor drive." *IEEE Industry Applications Society Conference Record*, 1984, pp. 813–819.
13. C. Wang, D. V. Novotny, and T. A. Lipo, "An automated rotor time constant measurement system for indirect field oriented drives." *IEEE Industry Applications Society Conference Record*, 1986, pp. 140–146.
14. R. Krishnan and P. Pillay, "Sensitivity analysis and comparison of parameter compensation scheme in vector control induction motor drives." *IEEE Industry Applications Society Conference Record*, 1986, pp. 155–161.
15. B. K. Bose, "Sliding mode control of induction motor." *IEEE Industry Applications Society Conference Record*, 1985, pp. 479–486.
16. A. Smith, "Static Scherbius system of induction motor speed control." *Proceedings IEE*, Vol. 124, 1977, pp. 557–565.

REVIEW QUESTIONS

11-1. What are the types of induction motors?
11-2. What is a synchronous speed?
11-3. What is a slip of induction motors?
11-4. What is a slip frequency of induction motors?
11-5. What is the slip at starting of induction motors?
11-6. What are the torque–speed characteristics of induction motors?
11-7. What are various means for speed control of induction motors?
11-8. What are the advantages of volts/hertz control?
11-9. What is a base frequency of induction motors?
11-10. What are the advantages of current control?

11-11. What is scalar control?

11-12. What is vector control?

11-13. What is adaptive control?

11-14. What is a static Kramer drive?

11-15. What is a static Scherbius drive?

11-16. What is a field-weakening mode of induction motor?

11-17. What are the effects of frequency control of induction motors?

11-18. What are the advantages of flux control?

11-19. What are the various types of synchronous motors?

11-20. What is the torque angle of synchronous motors?

11-21. What are the differences between salient-pole motors and reluctance motors?

11-22. What are the differences between salient-pole motors and permanent-magnet motors?

11-23. What is a pull-out torque of synchronous motors?

11-24. What is the starting torque of synchronous motors?

11-25. What are the torque–speed characteristics of synchronous motors?

11-26. What are the V-curves of synchronous motors?

11-27. What are the advantages of voltage-source inverter-fed drives?

11-28. What are the advantages and disadvantages of reluctance motor drives?

11-29. What are the advantages and disadvantages of permanent-magnet motors?

PROBLEMS

11-1. A three-phase 460-V 60-Hz eight-pole Y-connected induction motor has $R_s = 0.08\ \Omega$, $R_r = 0.1\ \Omega$, $X_s = 0.62\ \Omega$, $X_r = 0.92\ \Omega$, and $R_m = 6.7\ \Omega$. The no-load loss, $P_{\text{no load}} = 300$ W. At a motor speed of 850 rpm, use the approximate equivalent circuit in Fig. 11-2 to determine the (**a**) synchronous speed, ω_s; (**b**) slip, s; (**c**) input current, I_i; (**d**) input power, P_i; (**e**) input power factor of the supply, PF_s; (**f**) gap power, P_g; (**g**) rotor copper loss, P_{ru}; (**h**) stator copper loss, P_{su}; (**i**) developed torque, T_d; (**j**) efficiency; (**k**) starting rotor current, I_{rs}; and starting torque, T_s; (**l**) slip for maximum torque, s_m; (**m**) maximum motoring developed torque, T_{mm}; and (**n**) maximum regerative developed torque, T_{mr}.

11-2. Repeat Prob. 11-1 if R_s is negligible.

11-3. Repeat Prob. 11-1 if the motor has two poles and the parameters are $R_s = 1.02\ \Omega$, $R_r = 0.35\ \Omega$, $X_s = 0.72\ \Omega$, $X_r = 1.08\ \Omega$, and $R_m = 60\ \Omega$. The no-load loss is $P_{\text{no load}} = 70$ W and the rotor speed is 3450 rpm.

11-4. A three phase 460-V 60-Hz six-pole Y-connected induction motor has $R_s = 0.32\ \Omega$, $R_r = 0.18\ \Omega$, $X_s = 1.04\ \Omega$, $X_r = 1.6\ \Omega$, and $X_m = 18.8\ \Omega$. The no-load loss, $P_{\text{no load}}$, is negligible. The load torque, which is proportional to speed squared, is 180 N·m at 1180 rpm. If the motor speed is 950 rpm, determine the (**a**) load torque demand, T_L; (**b**) rotor current, I_r; (**c**) stator supply voltage, V_a; (**d**) motor input current, I_i; (**e**) motor input power, P_i; (**f**) slip for maximum current, s_a; (**g**) maximum rotor current, $I_{r(max)}$; (**h**) speed at maximum rotor current, ω_a; and (**i**) torque at the maximum current, T_a.

11-5. Repeat Prob. 11-4 if R_s is negligible.

11-6. Repeat Prob. 11-4 if the motor has four poles and the parameters are $R_s = 0.25\ \Omega$, $R_r = 0.14\ \Omega$, $X_s = 0.7\ \Omega$, $X_r = 1.05\ \Omega$, and $X_m = 20.6\ \Omega$. The load torque is 121 N·m at 1765 rpm. The motor speed is 1525 rpm.

11-7. A three-phase 460-V 60-Hz six-pole Y-connected wound-rotor induction motor whose speed is controlled by slip power as shown in Fig. 11-6a has the following paramaters: $R_s = 0.11\ \Omega$, $R_r = 0.09\ \Omega$, $X_s = 0.4\ \Omega$, $X_r = 0.6\ \Omega$, and $X_m = 11.6\ \Omega$. The turns ratio of the rotor to stator windings is $n_m = N_r/N_s = 0.9$. The inductance L_d is very large and its current, I_d, has negligible ripple. The values of R_s, R_r, X_s, and X_r for the equivalent circuit in Fig. 11-2 can be considered negligible compared to the effective impedance of L_d. The no-load loss is 275 W. The load torque, which is proportional to speed squared, is 455 N·m at 1175 rpm. (**a**) If the motor has to operate with a minimum speed of 750 rpm, determine the resistance, R. With this value of R, if the desired speed is 950 rpm, calculate the (**b**) inductor current, I_d; (**c**) duty cycle of the chopper, k; (**d**) dc voltage, V_d; (**e**) efficiency; and (**f**) input power factor of the drive, PF_s.

11-8. Repeat Prob. 11-7 if the minimum speed is 650 rpm.

11-9. Repeat Prob. 11-7 if the motor has eight poles and the motor parameters are $R_s = 0.08\ \Omega$, $R_r = 0.1\ \Omega$, $X_s = 0.62\ \Omega$, $X_r = 0.92\ \Omega$, and $R_m = 6.7\ \Omega$. The no-load loss is $P_{\text{no load}} = 300$ W. The load torque, which is proportional to speed, is 604 N·m at 885 rpm. The motor has to operate with a minimum speed of 650 and the desired speed is 750 rpm.

11-10. A three-phase 460-V 60-Hz six-pole Y-connected wound-rotor induction motor whose speed is controlled by a static Kramer drive as shown in Fig. 11-6b has: $R_s = 0.11\ \Omega$, $R_r = 0.09\ \Omega$, $X_s = 0.4\ \Omega$, $X_r = 0.6\ \Omega$, $X_m = 11.6\ \Omega$. The turns ratio of the rotor to stator windings is $n_m = N_r/N_s = 0.9$. The inductance, L_d, is very large and its current, I_d, has negligible ripple. The values of R_s, R_r, X_s, and X_r for the equivalent circuit in Fig. 11-2 can be considered negligible compared to the effective impedance of L_d. The no-load loss is 275 W. The turns ratio of the converter ac voltage to supply voltage is $n_c = N_a/N_b = 0.5$. If the motor is required to operate at a speed of 950 rpm, calculate the (**a**) inductor current, I_d; (**b**) dc voltage, V_d; (**c**) delay angle of the converter, α; (**d**) efficiency; and (**e**) input power factor of the drive, PF_s. The load torque, which is proportional to speed squared, is 455 N·m at 1175 rpm.

11-11. Repeat Prob. 11-10 for $n_c = 0.9$.

11-12. For Prob. 11-10 plot the power factor against the turns ratio n_c.

11-13. A three-phase 56-kW 3560-rpm 460-V 60-Hz two-pole Y-connected induction motor has the following parameters: $R_s = 0$, $R_r = 0.18\ \Omega$, $X_s = 0.13\ \Omega$, $X_r = 0.2\ \Omega$, and $X_m = 11.4\ \Omega$. The motor is controlled by varying the supply frequency. If the breakdown torque requirement is 160 N·m, calculate the (**a**) supply frequency, and (**b**) speed, ω_m.

11-14. If $R_s = 0.07\ \Omega$ and the frequency is changed from 60 Hz to 40 Hz in Prob. 11-13, determine the change in breakdown torque.

11-15. The motor in Prob. 11-13 is controlled by a constant volts/hertz ratio corresponding to the rated voltage and rated frequency. Calculate the maximum torque, T_m, and the corresponding speed, ω_m, for supply frequency of (**a**) 60 Hz, and (**b**) 30 Hz.

11-16. Repeat Prob. 11-15 if R_s is 0.2 Ω.

11-17. A three-phase 40-hp 880-rpm 60-Hz eight-pole Y-connected induction motor has the following parameters: $R_s = 0.19\ \Omega$, $R_r = 0.22\ \Omega$, $X_s = 1.2\ \Omega$, $X_r = 1.8\ \Omega$, and X_m

$= 13\ \Omega$. The no-load loss is negligible. The motor is controlled by a current-source inverter and the input current is maintained constant at 50 A. If the frequency is 40 Hz and the developed torque is 200 N·m, determine the (**a**) slip for maximum torque, s_m, and maximum torque, T_m; (**b**) slip, s; (**c**) rotor speed, ω_m; (**d**) terminal voltage per phase, V_a; and (**e**) power factor, PF_m.

11-18. Repeat Prob. 11-17 if frequency is 80 Hz.

11-19. A three-phase 460-V 60-Hz 10-pole Y-connected cylindrical rotor synchronous motor has a synchronous reactance of $X_s = 0.8\ \Omega$ per phase and the armature resistance is negligible. The load torque, which is proportional to the speed squared, is $T_L = 1250$ N·m at 720 rpm. The power factor is maintained at 0.8 lagging by field control and the voltage-to-frequency ratio is kept constant at the rated value. If the inverter frequency is 45 Hz and the motor speed is 540 rpm, calculate the (**a**) the input voltage, V_a; (**b**) armature current, I_a; (**c**) excitation voltage, V_f; (**d**) torque angle, δ; and (**e**) pull-out torque, T_p.

11-20. A three-phase 230-V 60-Hz 40-kW eight-pole Y-connected salient-pole synchronous motor has $X_d = 2.5\ \Omega$ and $X_q = 0.4$. The armature resistance is negligible. If the motor operates with an input power of 25 kW at a leading power factor of 0.86, determine (**a**) torque angle, δ; (**b**) excitation voltage, V_f; and (**c**) torque, T_d.

11-21. A three-phase 230-V 60-Hz 10-pole Y-connected reluctance motor has $X_d = 18.5\ \Omega$ and $X_q = 3\ \Omega$. The armature resistance is negligible. The load torque, which is proportional to speed, is $T_L = 12.5$ N·m. The voltage-to-frequency ratio is maintained constant at the rated value. If the supply frequency is 60 Hz, determine the (**a**) torque angle, δ; (**b**) line current, I_a; and (**c**) input power factor, PF_m.

12

Power Semiconductor Diodes

12-1 INTRODUCTION

We have seen in the previous chapters that power semiconductor diodes play a significant role in power electronics circuits. A diode acts as a switch to perform various functions, such as freewheeling in switching regulators, charge reversal of capacitor and energy transfer between components in thyristor commutation circuits, isolation in boost regulator, energy feedback from the load to the power source, and trapped energy recovery. The diodes are also used in rectifiers.

Although power diodes are assumed as ideal switches in earlier chapters, practical diodes differ from the ideal characteristics and have certain limitations. The power diodes are similar to *pn*-junction signal diodes. However, the power diodes have larger power-, voltage-, and current-handling capabilities than that of ordinary signal diodes. The frequency response (or switching speed) is low compared to signal diodes.

12-2 DIODE CHARACTERISTICS

A power diode is a two-terminal *pn*-junction device and a *pn*-junction is normally formed by alloying, diffusion, and epitaxial growth. The modern control tech-

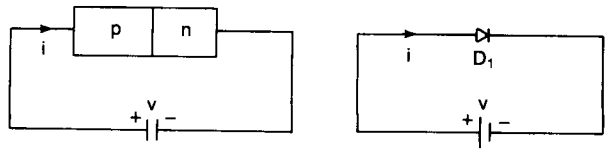


Figure 12-1 *PN*-junction and diode symbol.

niques in diffusion and epitaxial processes permits the desired device characteristics. Figure 12-1 shows the sectional view of a *pn*-junction and diode symbol.

When the anode potential is positive with respect to the cathode, the diode is said to be forward biased and the diode conducts. A conducting diode has a relatively small forward voltage drop across it; and the magnitude of this drop would depend on the manufacturing process and temperature. When the cathode potential is positive with respect to the anode, the diode is said to be reverse biased. Under reverse-biased conditions, a small reverse current (also known as *leakage current*) in the range of micro- or milliampere flows and this leakage current increases slowly in magnitude with the reverse voltage until the avalanche or zener voltage is reached. Figure 12-2 shows the steady-state v–i characteristics of a diode.

The current in a forward-biased junction diode is due to the net effect of majority and minority carriers. Once a diode is in a forward conduction mode and then its forward current is reduced to zero (due to the natural behavior of the diode circuit or by applying a reverse voltage), the diode continues to conduct due to the minority carriers which remain stored in the *pn*-junction and the bulk semiconductor material. The minority carriers require a certain time to recombine with opposite charges and to be neutralized. This time is called the *reverse recovery time* of the diode. Figure 12-3 shows two reverse recovery characteristics of junction diodes. However, the soft recovery type is more common. The reverse recovery time is denoted as t_{rr} and is measured from the initial zero crossing of the diode current to 25% of maximum (or peak) reverse current, I_{RR}. t_{rr} consists of two components, t_a and t_b. t_a is due to the charge storage in the depletion region of the junction and represents the time between the zero crossing and the peak reverse current, I_{RR}. t_b is due to the charge storage in the bulk semiconductor material. The ratio t_b/t_a is known as the *softness factor*, SF. For practical purposes,

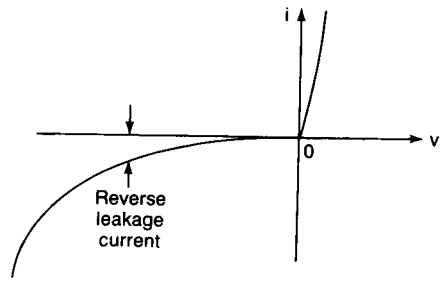


Figure 12-2 v–i characteristics of diode.

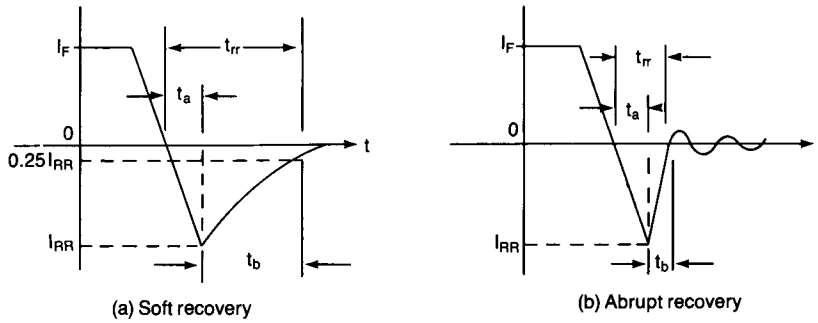


Figure 12-3 Reverse recovery characteristics.

one need be concerned with the total recovery time, t_{rr}, and the value of the peak reverse current, I_{RR}.

$$t_{rr} = t_a + t_b \tag{12-1}$$

The peak reverse current can be expressed in reverse di/dt as

$$I_{RR} = t_a \frac{di}{dt} \tag{12-2}$$

The storage charge which is the area enclosed by the path of the recovery current is approximately

$$Q_{RR} \cong \tfrac{1}{2} I_{RR} t_a + \tfrac{1}{2} I_{RR} t_b = \tfrac{1}{2} I_{RR} t_{rr} \tag{12-3}$$

or

$$I_{RR} \cong \frac{2Q_{RR}}{t_{rr}} \tag{12-4}$$

Equating Eq. (12-2) to Eq. (12-4) gives

$$t_{rr} t_a = \frac{2Q_{RR}}{di/dt} \tag{12-5}$$

If t_b is negligible as compared to t_a, $t_{rr} \approx t_a$,

$$t_{rr} \cong \sqrt{\frac{2Q_{RR}}{di/dt}} \tag{12-6}$$

and

$$I_{RR} = \sqrt{2Q_{RR} \frac{di}{dt}} \tag{12-7}$$

It can be noticed from Eqs. (12-6) and (12-7) that the reverse recovery time and the peak reverse current depend on the storage charge and the reverse (or reap-

plied) di/dt. The storage charge is dependent on the forward diode current, I_F. The peak reverse recovery current, I_{RR}, reverse charge, Q_{RR}, and the softness factor are all of interest to the circuit designer, and these parameters are commonly included in the specification sheets of diodes.

If a diode is in a reverse-biased condition, a leakage current flows due to the minority carriers. Then the application of forward voltage would force the diode to carry current in the forward direction. However, it requires a certain time known as *forward recovery (or turn-on) time* before all the majority carriers over the whole junction can contribute to the current flow. If the rate of rise of the forward current is high and the forward current is concentrated to a small area of the junction, the diode may fail. Thus the forward recovery time limits the rate of rise of the forward current and the switching speed.

Example 12-1

The reverse recovery time of a diode is $t_{rr} = 3$ μs and the rate of fall of the diode current is $di/dt = 30$ A/μs. Determine the (a) storage charge, Q_{RR}, and (b) peak reverse current, I_{RR}.

Solution $t_{rr} = 3$ μs and $di/dt = 30$ A/μs.

(a) From Eq. (12-6),

$$Q_{RR} = \frac{1}{2}\frac{di}{dt}t_{rr}^2 = 0.5 \times 30 \times 3^2 \times 10^{-6} = 135\ \mu C$$

(b) From Eq. (12-7),

$$I_{RR} = \sqrt{2Q_{RR}\frac{di}{dt}} = \sqrt{2 \times 135 \times 30} = 90\ A$$

12-3 POWER DIODE TYPES

Ideally, a diode should have no reverse recovery time. However, manufacturing cost of such a diode would increase. In many applications, the effects of reverse recovery time would not be significant, and inexpensive diodes can be used. Depending on the recovery characteristics and manufacturing techniques, the power diodes can be classified into three categories. The characteristics and practical limitations of each type restrict their applications.

1. Standard or general-purpose diodes
2. Fast-recovery diodes
3. Schottky diodes

12-3.1 General-Purpose Diodes

The general-purpose rectifier diodes have relatively high reverse recovery time, typically 25 μs, and are used in low-speed applications, where recovery time is not critical (e.g., diode rectifiers for low frequency up to 1 kHz applications and line-commutated converters). These diodes cover current ratings from less than 1 A

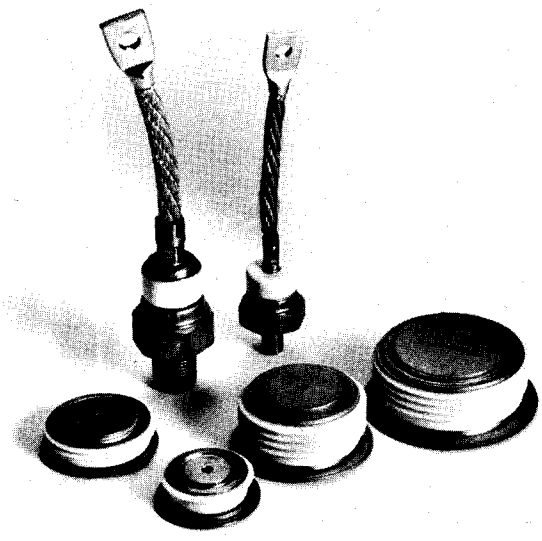


Figure 12-4 Fast-recovery diodes. (*Courtesy of Powerex, Inc.*)

to several thousands of amperes, with voltage ratings from 50 V to around 5 kV. These diodes are generally manufactured by diffusion. However, alloyed types of rectifiers which are used in welding power supplies are most cost-effective and rugged; and their ratings can go up to 300 A and 1000 V.

12-3.2 Fast-Recovery Diodes

The fast-recovery diodes have low recovery time, normally less than 5 μs. They are used in chopper and inverter circuits, where the speed of recovery is often of critical importance. These diodes cover current ratings from less than 1 A to hundreds of amperes, with voltage ratings from 50 V to around 3 kV.

For voltage ratings above 400 V, fast-recovery diodes are generally made by diffusion and the recovery time is controlled by platinum or gold diffusion. For voltage ratings below 400 V, epitaxial diodes provide faster switching speeds than that of the diffused diodes. The epitaxial diodes have a narrow base width, resulting in a fast recovery time of as low as 50 ns. Fast-recovery diodes of various sizes are shown in Fig. 12-4.

12-3.3 Schottky Diodes

The charge storage problem of a *pn*-junction can be eliminated (or minimized) in a Schottky diode. It is accomplished by setting up a "barrier potential" with a contact between a metal and a semiconductor. A layer of metal is deposited on a thin epitaxial layer of *n*-type silicon. The potential barrier simulates the behavior of a *pn*-junction. However, the rectifying action depends on the majority carriers only, and as a result there is no excess minority carriers to recombine. The recovery effect is due solely to the self-capacitance of the semiconductor junction.

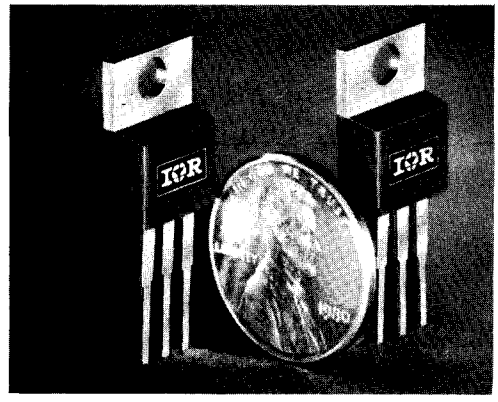


Figure 12-5 20-and 30-Amp dual Schottky center rectifiers. (*Courtesty of International Rectifier*)

The recovered charge of a Schottky diode is much less than that of an equivalent *pn*-junction diode. Since it is due only to the junction capacitance, it is largely independent of the reverse *di/dt*. A Schottky diode has a relatively low forward voltage drop.

The leakage current of a Schottky diode is higher than that of a *pn*-junction diode. A Schottky diode with relatively low conduction voltage has relatively high leakage current, and vice versa. As a result, its maximum allowable voltage is limited to 100 V. The current ratings of Schottky diodes varies from 1 to 300 A. The Schottky diodes are ideal for high-current and low-voltage dc power supplies. However, they are also used in low-current power supplies for increased efficiency. Twenty- and 30-A dual Schottky rectifiers are shown in Fig. 12-5.

12-4 PERFORMANCE PARAMETERS

The semiconductor diodes are characterized by the manufacturers in terms of certain performance parameters. The designer needs to determine the correct semiconductor diode to meet a given requirement. These parameters are nonlinear and dependent on a number of factors. The manufacturers normally provide characteristic curves for important parameters, in the form of a data sheet. Figure 12-6 shows the data sheet of International Rectifier (IR) Diode: 300 A, 800 V, type R23AF. Figure 12-6.1 refers to curve number 1 in Fig. 12-6.

Junction temperature, T_J. T_J is the average temperature over the whole junction. $T_{J(\max)}$ is the maximum junction temperature that a diode can withstand without failing due to thermal runway. This is a very important parameter and influences the ratings of other parameters. The range of T_J is typically -40 to 125°C, where $T_{j(\max)}$ is 125°C. If a diode is operated below its minimum limit (e.g., -40°C), the crystal structure of the silicon wafer may be fractured.

Storage temperature, T_{stg}. T_{stg} defines the range of temperature within which a nonconducting diode can be stored and transported. It is typically -40 to 150°C.

R23AF SERIES
800-600 VOLTS RANGE
REVERSE RECOVERY TIME 0.9μs
300 AMP AVG HOCKEY PUK
SOFT FAST RECOVERY RECTIFIER DIODES

VOLTAGE RATINGS

VOLTAGE CODE (1)	V_{RRM}, V_R - (V) Max. rep. peak reverse and direct voltage	V_{RSM} - (V) Max. non-rep. peak reverse voltage
	T_J = -40° to 125°C	T_J = 25° to 125°C
8	800	900
6	600	700

MAXIMUM ALLOWABLE RATINGS

PARAMETER		VALUE	UNITS	NOTES
T_J	Junction temperature	-40 to 125	°C	
T_{stg}	Storage temperature	-40 to 150	°C	
$I_{F(AV)}$	Max. av. current	300	A	180° half sine wave
	@ Max. T_C	85	°C	
$I_{F(RMS)}$	Nom. RMS current	470	A	
I_{FSM}	Max. peak non-rep. surge current	4980	A	50Hz half cycle sine wave — Initial T_J = 125°C, rated V_{RRM} applied after surge.
		5200		60Hz half cycle sine wave
		5900		50Hz half cycle sine wave — Initial T_J = 125°C, no voltage applied after surge.
		6180		60Hz half cycle sine wave
I^2t	Max. I^2t capability	124	kA^2s	t = 10ms — Initial T_J = 125°C, rated V_{RRM} applied after surge.
		113		t = 8.3ms
		175		t = 10ms — Initial T_J = 125°C, no voltage applied after surge.
		160		t = 8.3ms
$I^2\sqrt{t}$	Max. $I^2\sqrt{t}$ capability	1750	$kA^2\sqrt{s}$	Initial T_J = 125°C, no voltage applied after surge. I^2t for time $t_x = I^2\sqrt{t} \cdot \sqrt{t_x}$, $0.1 \leq t_x \leq 10ms$.
F	Mounting force	4450(1000) ± 10%	N[lbf]	

Figure 12-6 Data sheet for IR diode, type R23AF. (*Courtesy of International Rectifier*)

Ambient temperature, T_A. T_A is the temperature of the cooling medium and is measured with a thermometer close to the diode on the heat sink.

Case temperature, T_C. T_C is the temperature at the case, normally at the base of the diode and it can be measured with a thermocouple.

Sink temperature, T_S. T_S is the temperature of the hottest spot on the heat sink.

CHARACTERISTICS

PARAMETER		MIN.	TYP.	MAX.	UNITS	TEST CONDITIONS
V_{FM}	Peak forward voltage	—	1.50	1.63	V	Initial T_J = 25°C, 50-60Hz half sine, I_{peak} = 940A.
$V_{F(TO)1}$	Low-level threshold	—	—	0.962	V	T_J = 125°C Av. power = $V_{F(TO)} * I_{F(AV)} + r_F * (I_{F(RMS)})^2$ Use low level values for $I_{FM} \leq \pi$ rated $I_{F(AV)}$
$V_{F(TO)2}$	High-level threshold	—	—	1.30		
r_{F1}	Low-level resistance	—	—	0.657	mΩ	
r_{F2}	High-level resistance	—	—	0.353		
t_{rr}	Reverse recovery time					
	"A" suffix	—	0.9	—	μs	T_J = 25°C, I_{FM} = 750A. di_R/dt = 25A/μs for sinusoidal pulse.
	"B" suffix	—	1.1	—		
t_{rr}	Reverse recovery time					
	"A" suffix	—	—	2.20	μs	T_J = 125°C, I_{FM} = 750A. di_R/dt = 25A/μs for sinusoidal pulse.
	"B" suffix	—	—	2.50		
S	"S" Factor (t_b/t_a)					
	"A" suffix	0.59	—	—		
	"B" suffix	0.56	—	—		
$I_{RM(REC)}$	Reverse current					
	"A" suffix	—	—	33	A	
	"B" suffix	—	—	36		
Q_{RR}	Recovered charge					
	"A" suffix	—	—	37	μC	
	"B" suffix	—	—	45		
I_{RM}	Peak reverse current	—	—	35	mA	T_J = 125°C. Max. rated V_{RRM}.
R_{thJC}	Thermal resistance, junction-to-case	—	—	0.08	°C/W	DC operation, double side cooled.
		—	—	0.09	°C/W	180° sine wave, double side cooled.
		—	—	0.09	°C/W	120° rectangular wave, double side cooled.
R_{thCS}	Thermal resistance, case-to-sink	—	—	0.06	°C/W	Mtg. surface smooth, flat and greased. Single side cooled. For double side, divide value by 2.
wt	Weight	—	57[2.0]	—	g[oz.]	
	Case Style	DO-200AA		JEDEC		

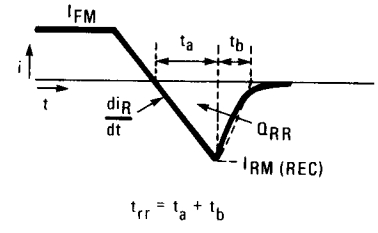


Figure 12-6 (*continued*)

Junction-to-case thermal resistance, R_{thJC}. R_{thJC} is the effective thermal resistance between the junction and the outer case of the device. It is a measure of the heat transfer ability of the materials and mechanical construction of the diode; and it is usually specified in °C/W. Figure 12-6.10 shows the thermal impedance under transient condition. A practical diode has a finite power loss, and this would raise the junction temperature. The junction temperature is maintained within its maximum value by mounting the diode to a heat sink. If P_D is

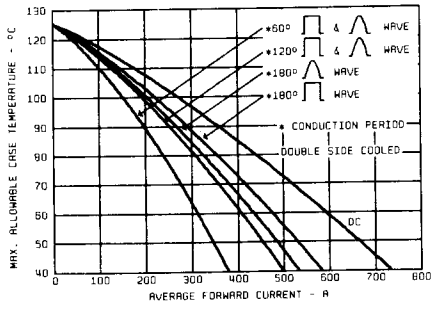


Fig. 1 — Case Temperature Ratings

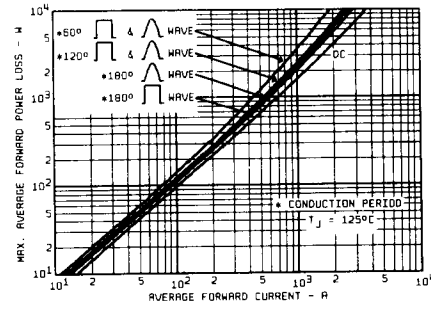


Fig. 2 — Power Loss Characteristics

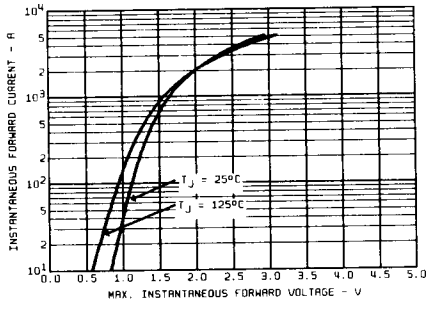


Fig. 3 — Forward Characteristics

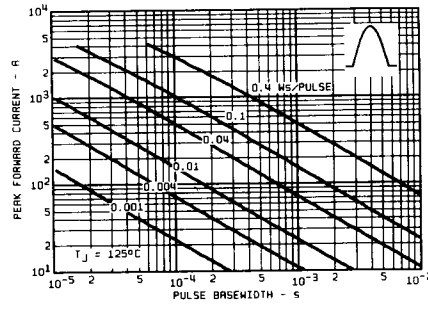


Fig. 4 — Max. Energy Loss Per Pulse — Sinusoidal Waveforms

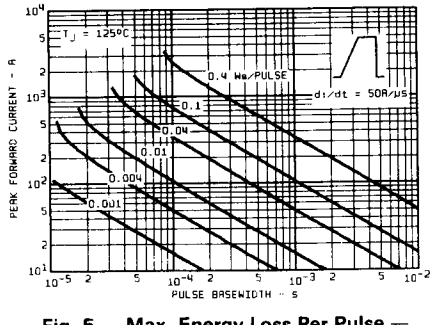


Fig. 5 — Max. Energy Loss Per Pulse — Trapezoidal Waveforms

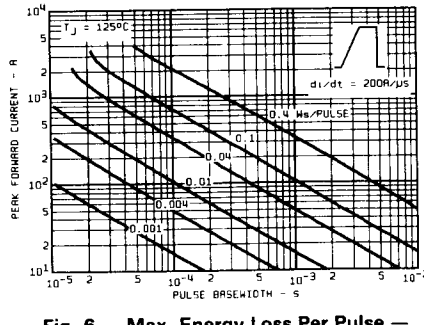


Fig. 6 — Max. Energy Loss Per Pulse — Trapezoidal Waveforms

Figure 12-6 (*continued*)

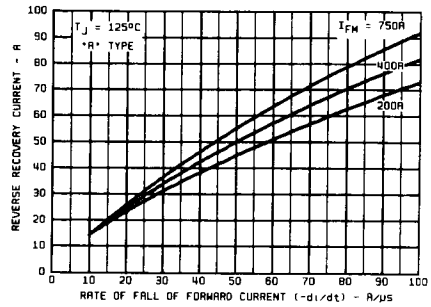


Fig. 7 — Typical Reverse Recovery Current

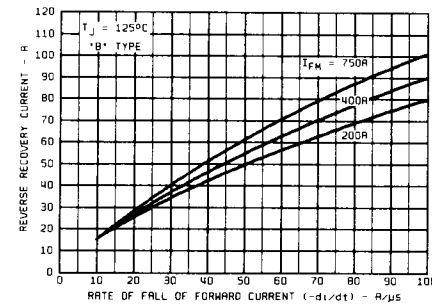


Fig. 7a — Typical Reverse Recovery Current

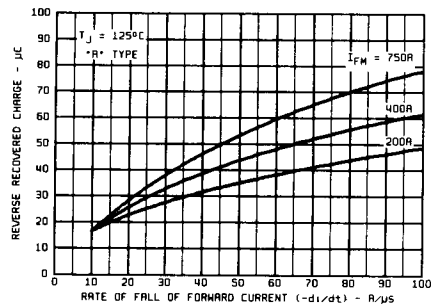


Fig. 8 — Typical Recovered Charge

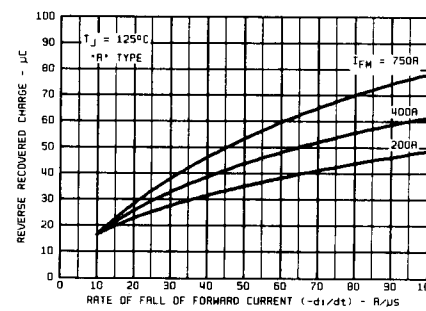


Fig. 8a — Typical Recovered Charge

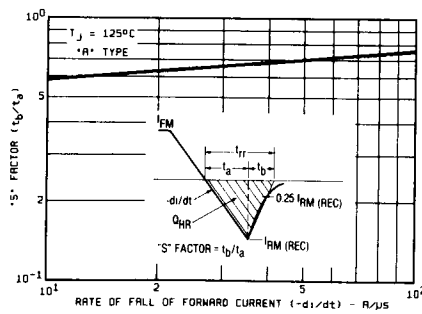


Fig. 9 — Typical "S" Factor (t_b/t_a)

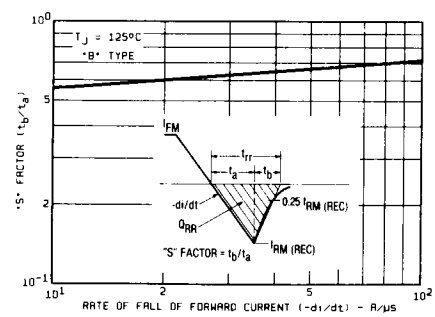


Fig. 9a — Typical "S" Factor (t_b/t_a)

Figure 12-6 *(continued)*

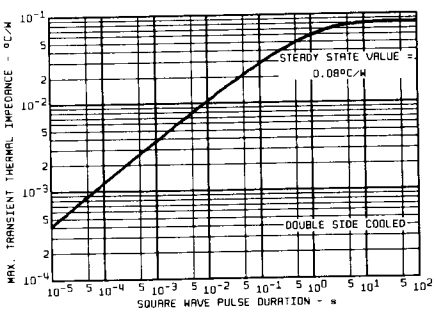


Fig. 10 — Transient Thermal Impedance, Junction-to-Case

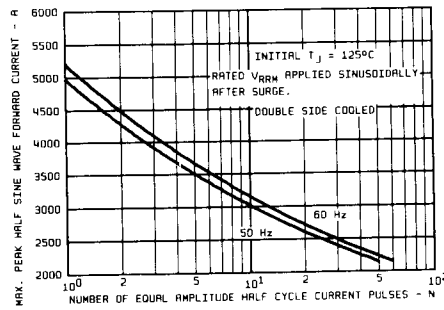


Fig. 11 — Non-Repetitive Surge Current Ratings

ORDERING INFORMATION

TYPE	VOLTAGE		RECOVERY TIME	
	CODE	V_{RRM}	CODE	t_{rr}
R23AF	8	800V	A	0.9μs
	6	600V	B	1.1μs

(1) t_{rr} is typical at 25°C.
Max. t_{rr} is guaranteed at 125°C. See table of Characteristics.

For example, for a device with t_{rr} = 0.9μs, V_{RRM} = 600V, order as R23AF6A.

Figure 12-6 (*continued*)

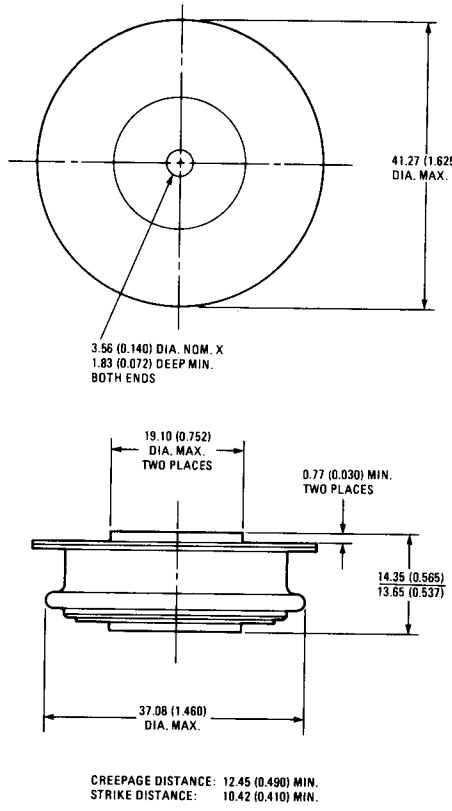
the power dissipated in the diode, R_{thJC} is expressed as

$$R_{thJC} = \frac{T_J - T_C}{P_D} \tag{12-8}$$

The instantaneous case temperature can be calculated from the transient thermal impedance and this is discussed in Section 15-2.

Case-to-sink thermal resistance, R_{thCS}. R_{thCS} is the effective thermal resistance between the case and sink. Its value depends on the nature of the

R23AF SERIES
800-600 VOLTS RANGE



Conforms to JEDEC Outline DO-200AA
All Dimensions in Millimeters and (Inches)

NOTE: OUTLINE DIMENSIONS FOR DEVICES MANUFACTURED IN EUROPE MAY VARY SLIGHTLY FROM THE ABOVE. REFER TO SELECTION GUIDE E1017 FOR DETAILS.

Figure 12-6 (*continued*)

mounting surface (e.g., smoothness, grease). R_{thCS} is expressed as

$$R_{thCS} = \frac{T_C - T_S}{P_D} \tag{12-9}$$

Thermal resistance of sink to ambient, R_{thSA}. R_{thSA}, which is a measure of the heat transfer ability of the heat sink, defines the required thermal resistance of the heat sink to limit the junction temperature within the maximum limit of

R23AF SERIES
1200-1000 VOLTS RANGE
REVERSE RECOVERY TIME 1.0μs
280 AMP AVG HOCKEY PUK
SOFT FAST RECOVERY RECTIFIER DIODES

VOLTAGE RATINGS

VOLTAGE CODE [1]	V_{RRM}, V_R – [V] Max. rep. peak reverse and direct voltage	V_{RSM} – [V] Max. non-rep. peak reverse voltage
	T_J = −40° to 125°C	T_J = 25° to 125°C
12	1200	1300
10	1000	1100

MAXIMUM ALLOWABLE RATINGS

PARAMETER		VALUE	UNITS	NOTES
T_J	Junction temperature	−40 to 125	°C	
T_{stg}	Storage temperature	−40 to 150	°C	
$I_{F(AV)}$	Max. av. current	280	A	180° half sine wave
	@ Max. T_C	85	°C	
$I_{F(RMS)}$	Nom. RMS current	440	A	
I_{FSM}	Max. peak non-rep. surge current	4775	A	50Hz half cycle sine wave — Initial T_J = 125°C, rated V_{RRM} applied after surge.
		5000		60Hz half cycle sine wave
		5680		50Hz half cycle sine wave — Initial T_J = 125°C, no voltage applied after surge.
		5945		60Hz half cycle sine wave
I^2t	Max. I^2t capability	114	kA^2s	t = 10ms — Initial T_J = 125°C, rated V_{RRM} applied after surge.
		104		t = 8.3ms
		161		t = 10ms — Initial T_J = 125°C, no voltage applied after surge.
		147		t = 8.3ms
$I^2\sqrt{t}$	Max. $I^2\sqrt{t}$ capability	1610	$kA^2\sqrt{s}$	Initial T_J = 125°C, no voltage applied after surge. I^2t for time $t_x = I^2\sqrt{t} \cdot \sqrt{t_x}$. $0.1 \leq t_x \leq 10ms$.
F	Mounting force	4450[1000] ± 10%	N[lbf]	

[1] To complete the part number, refer to the Ordering Information table.

Figure 12-6 (*continued*)

$T_{J(\max)}$. The required value of R_{thSA} can be determined from

$$R_{thSA} = \frac{T_S - T_A}{P_D} \tag{12-10}$$

Maximum average forward current, $I_{F(AV)}$. $I_{F(AV)}$ is the maximum allowable value of average forward current at a specified temperature. These data are

CHARACTERISTICS

PARAMETER		MIN.	TYP.	MAX.	UNITS	TEST CONDITIONS
V_{FM}	Peak forward voltage	—	1.60	1.70	V	Initial T_J = 25°C, 50-60Hz half sine, I_{peak} = 880A.
$V_{F(TO)1}$	Low-level threshold	—	—	0.977	V	T_J = 125°C Av. power = $V_{F(TO)} * I_{F(AV)} + r_F * (I_{F(RMS)})^2$ Use low level values for $I_{FM} \leq \pi$ rated $I_{F(AV)}$
$V_{F(TO)2}$	High-level threshold	—	—	1.280		
r_{F1}	Low-level resistance	—	—	0.787	mΩ	
r_{F2}	High-level resistance	—	—	0.501		
t_{rr}	Reverse recovery time					
	"A" suffix	—	1.0	—	µs	T_J = 25°C, I_{FM} = 750A. di_R/dt = 25A/µs for sinusoidal pulse.
	"B" suffix	—	1.2	—		
t_{rr}	Reverse recovery time					
	"A" suffix	—	—	2.50	µs	T_J = 125°C, I_{FM} = 750A. di_R/dt = 25A/µs for sinusoidal pulse.
	"B" suffix	—	—	2.90		
S	"S" Factor (t_b/t_a)					
	"A" suffix	0.60	—	—		
	"B" suffix	0.57	—	—		
$I_{RM(REC)}$	Reverse current					
	"A" suffix	—	—	38	A	
	"B" suffix	—	—	41		
Q_{RR}	Recovered charge					
	"A" suffix	—	—	48	µC	
	"B" suffix	—	—	60		
I_{RM}	Peak reverse current	—	—	35	mA	T_J = 125°C. Max. rated V_{RRM}.
R_{thJC}	Thermal resistance, junction-to-case	—	—	0.08	°C/W	DC operation, double side cooled.
		—	—	0.09	°C/W	180° sine wave, double side cooled.
		—	—	0.09	°C/W	120° rectangular wave, double side cooled.
R_{thCS}	Thermal resistance, case-to-sink	—	—	0.06	°C/W	Mtg. surface smooth, flat and greased. Single side cooled. For double side, divide value by 2.
wt	Weight	—	57(2.0)	—	g(oz.)	
	Case Style		DO-200AA		JEDEC	

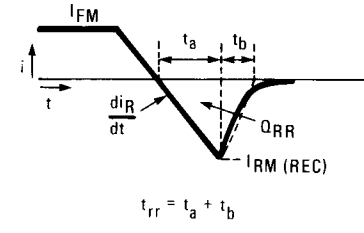


Figure 12-6 (*continued*)

normally quoted for a half-sine wave at a case temperature, T_C = 85°C. Figure 12-6.1 shows the typical variations of average forward current with the maximum case temperature.

Maximum rms forward current, $I_{F(RMS)}$. $I_{F(RMS)}$ is the maximum permissible root-mean-square (rms) value of forward current. This signifies the heating effect due to i^2R dissipation and is limited due to the thermal stress on the device. Figure 12-6.2 shows the maximum average forward power loss against average

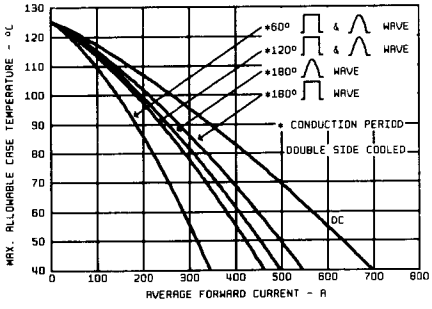


Fig. 1 — Case Temperature Ratings

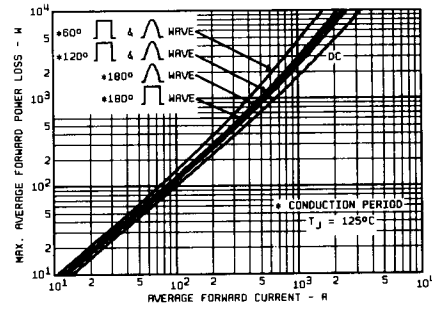


Fig. 2 — Power Loss Characteristics

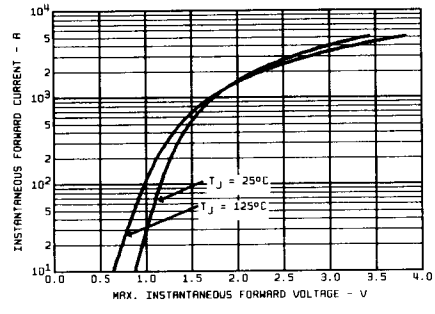


Fig. 3 — Forward Characteristics

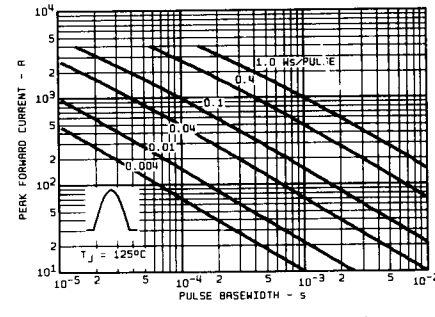


Fig. 4 — Max. Energy Loss Per Pulse — Sinusoidal Waveforms

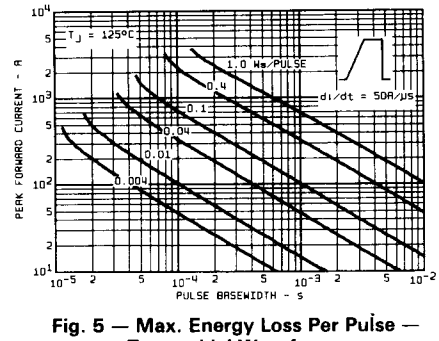


Fig. 5 — Max. Energy Loss Per Pulse — Trapezoidal Waveforms

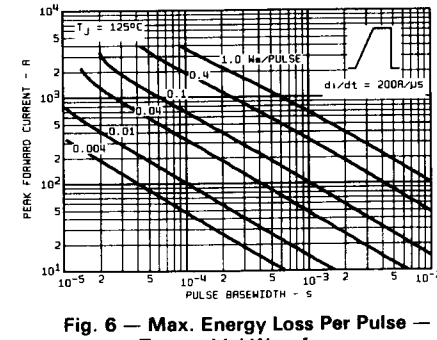


Fig. 6 — Max. Energy Loss Per Pulse — Trapezoidal Waveforms

Figure 12-6 (*continued*)

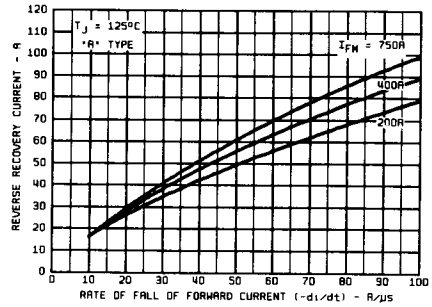


Fig. 7 — Typical Reverse Recovery Current

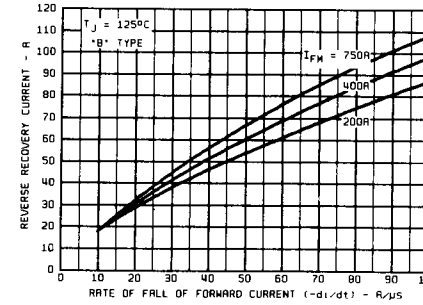


Fig. 7a — Typical Reverse Recovery Current

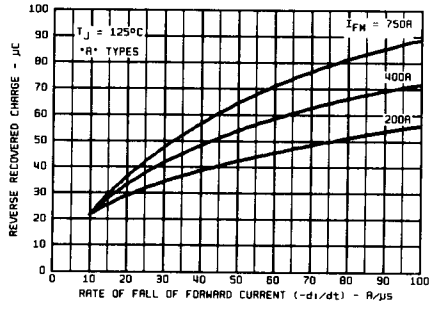


Fig. 8 — Typical Recovered Charge

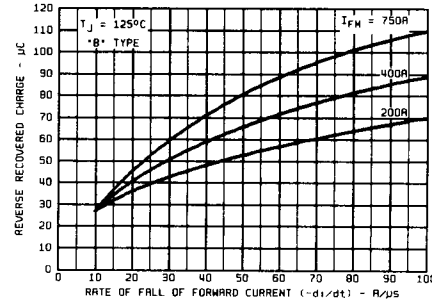


Fig. 8a — Typical Recovered Charge

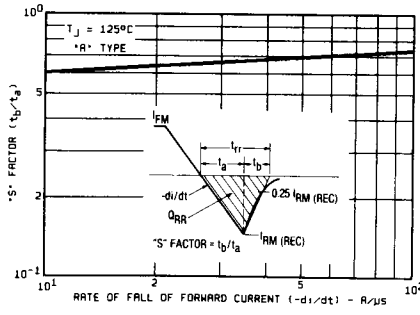


Fig. 9 — Typical "S" Factor (t_b/t_a)

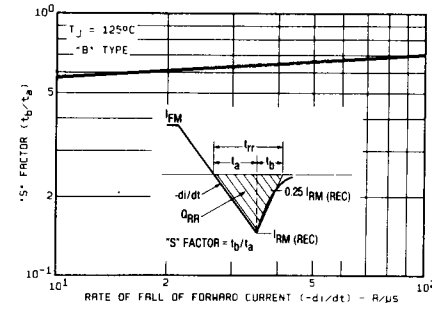


Fig. 9a — Typical "S" Factor (t_b/t_a)

Figure 12-6 *(continued)*

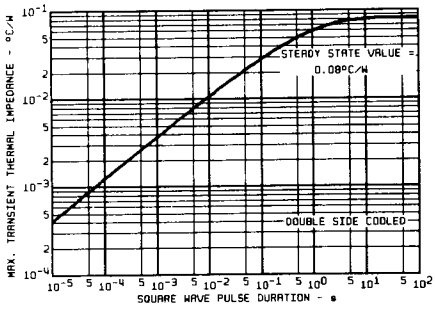


Fig. 10 — Transient Thermal Impedance, Junction-to-Case

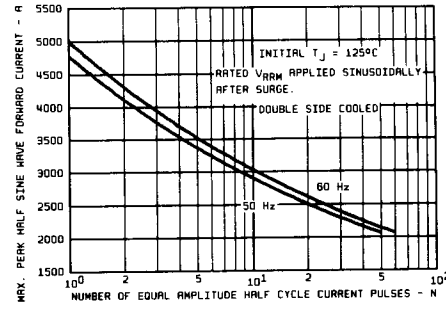


Fig. 11 — Non-Repetitive Surge Current Ratings

ORDERING INFORMATION

TYPE	VOLTAGE		RECOVERY TIME	
	CODE	V_{RRM}	CODE	t_{rr} (1)
R23AF	12	1200V	A	1.0μs
	10	1000V	B	1.2μs

(1) t_{rr} is typical at 25°C.
Max. t_{rr} is guaranteed at 125°C. See table of Characteristics.

For example, for a device with t_{rr} = 1.0μs, V_{RRM} = 1000V, order as R23AF10A.

Figure 12-6 *(continued)*

forward current for sinusoidal and rectangular waveforms at various conduction angles.

Maximum peak repetitive forward current, I_{FRM}. I_{FRM} is the maximum peak permissible current which can be applied on a repetitive basis. This is normally specified for a half-sinusoidal waveform.

Maximum peak one-cycle nonrepetitive forward current, I_{FSM}. I_{FSM} is the maximum peak permissible forward current of half-sine wave with a duration of 10 ms at a specified temperature. A repetition is permissible only after expiration of a minimum interval to reduce the junction temperature to the allowable

range. This peak permissible value varies with the number of repetitions. Figure 12-6.11 shows the maximum nonrepetitive surge current with the number of current pulses.

Maximum repetitive peak reverse voltage, V_{RRM}. V_{RRM} defines the maximum permissible instantaneous value of repetitive applied reverse voltage that the diode can block. This rating is determined by the *pn*-junction and the case type.

Maximum peak nonrepetitive reverse voltage, V_{RSM}. V_{RSM} is the maximum instantaneous peak value of applied reverse voltage under transient conditions. V_{RSM} is typically 25% above V_{RRM}.

Forward voltage drop, V_F. V_F is the instantaneous value of the forward voltage drop and is dependent on the junction temperature, T_J. Figure 12-6.3 shows the instantaneous forward voltage drop against forward current. V_F can be considered as being made up of (1) a value that is independent of the forward current, and (2) a value that is proportional to the instantaneous forward current.

Maximum peak forward voltage, V_{FM}. V_{FM} is the maximum forward voltage drop at a specified forward current and junction temperature.

Threshold voltage, $V_{(TO)}$. $V_{(TO)}$ is the current-independent portion of the forward voltage drop and depends on the temperature.

Forward slope resistance, r_F. r_F is the current dependent portion of the instantaneous forward voltage drop, v_F such that $v_F = V_{(TO)} + ir_F$, where i is the instantaneous diode current.

Maximum peak reverse (or leakage) current, I_{RRM}. I_{RRM} is the maximum reverse current at the maximum junction temperature and maximum repetitive peak reverse voltage. This current would also cause junction heating and a low value is desirable.

Reverse recovery time, t_{rr}. t_{rr} may be defined as the time interval between the instant the current passes through zero during the changeover from forward conduction to reverse blocking condition and the moment the reverse current has decayed to 25% of its peak reverse value, i_{RR}. t_{rr} is dependent on the junction temperature, rate of fall of forward current, and the forward current prior to commutation.

Reverse recovery charge, Q_{RR}. Q_{RR} is the amount of charge carriers which flow across the diode in the reverse direction due to change over from forward conduction to reverse blocking condition. Its value is determined from the area enclosed by the path of the reverse recovery current. Figures 12-6.7 and 12-6.8 show the variations of reverse recovery current and charge with the rate of fall of forward current.

***i²t* for fusing.** The i^2t rating is a measure of the maximum forward nonrecurring overcurrent capability for a given period of 10 ms at a specified junction temperature. It is used to determine the thermal capability of fuses. In cases of a fault (or short-circuit) condition, the diode would offer a resistance; and its junction temperature, which is dependent on the i^2 value and time, would rise. For the protection of the diode, the i^2t rating of the fuse must be less than i^2t of the diode. The coordination of a fuse is discussed in Section 15-7.1.

Example 12-2

Four IR 300-A 800-V diodes of type R23AF are used for the single-phase bridge rectifier in Fig. 2-15a. The rms value of the input voltage is V_s = 208 V at 1.5 kHz and the load resistance is R = 0.47 Ω. The junction temperature and ambient temperature are T_J = 15°C and T_A = 25°C, respectively. Determine the (a) average power loss, P_D; (b) instantaneous forward voltage drop, v_F; (c) recovery charge, Q_{RR}; (d) reverse recovery time, t_{rr}; (e) case temperature, T_C; and (f) thermal resistance of heat sink, R_{thSA}. Assume double-sided cooling and the case-to-sink thermal resistance of R_{thCS} = 0.03°C/W.

Solution V_s = 208 V, $V_m = \sqrt{2} \times 208$ = 294.2 V, f_s = 1500 Hz, R = 0.47 Ω, T_J = 125°, T_A = 25°, and R_{thCS} = 0.03°/W. The solution requires interpolation from the characteristic curves of the device and the results are therefore approximate.

(a) From Eq. (2-59), the average output voltage is

$$V_{dc} = 0.6366V_m = 0.6366 \times 294.2 = 187.29 \text{ V}$$

The average load current, I_{dc} = 187.29/0.47 = 398.5 A, and the average diode forward current, $I_{F(AV)}$ = 398.5/2 = 199.3 A. For 180° conduction, Fig. 12-6.2 gives the average power loss of $P_D \cong$ 240 W.

(b) From Fig. 12-6.3 the threshold voltage is $V_{(TO)}$ = 0.6 V. From Fig. 12-6.3, the slope resistance is

$$r_F \cong \frac{1.1 - 0.6}{200} = 2.5 \text{ m}\Omega$$

The instantaneous diode current is i = (294.2/0.47) sin ωt. Thus the instantaneous forward voltage drop is

$$v_F = 0.6 + 2.5 \times 10^{-3} \times \frac{294.2}{0.47} \sin \omega t$$

$$= 0.6 + 1.565 \sin \omega t \text{ V} \qquad \text{for } 0 \leq \omega t \leq \pi$$

$$= 0 \text{ V} \qquad \text{for } \pi \leq \omega t \leq 2\pi$$

(c) The peak diode current prior to commutation is

$$I_{FM} = \frac{294.2}{0.47} = 625.96 \text{ A}$$

The rate of fall of the diode current is

$$\frac{di}{dt} = \frac{V_m}{R} \omega \cos \omega t$$

The rate of fall of current at the zero crossing of the diode current ($\omega t = \pi$) becomes

$$\left.\frac{di}{dt}\right|_{t=0} = \frac{V_m}{R}\omega = \frac{294.2}{0.47} \times 2\pi \times 1500 = 5.9 \text{ A/}\mu\text{s}$$

For $I_{FM} = 625.96$ A and $di/dt = 5.9$ A/μs, Fig. 12-6.8 gives $Q_{RR} = 12$ μC.

(d) From Fig. 12-6.9, SF $= t_b/t_a = 0.7$. $t_{rr} = t_a + t_b = 1.7t_a$ and from Eq. (12-5)

$$t_{rr} = \sqrt{\frac{2 \times 12 \times 1.7}{5.9}} = 2.63 \text{ μs}$$

(e) From the data sheet of diode, $R_{thJC} = 0.09$°C/W. From Eq. (12-8),

$$T_c = T_J - R_{thJC}P_D = 125 - 0.09 \times 240 = 103.4\text{°C}.$$

(f) From Eqs. (12-8), (12-9), and (12-10),

$$P_D(R_{thJC} + R_{thCS} + R_{thSA}) = T_J - T_A = 125 - 25 = 100$$

or

$$R_{thSA} = \frac{100}{240} - 0.09 - 0.03 = 0.297\text{°C/W}$$

Example 12-3

An IR diode, 300 A, 800 V, of type R23AF is used for charge reversal in a commutation circuit and the equivalent circuit at $t = 0$ is shown in Fig. 12-7. This charge reversal is repeated at a frequency of $f_s = 2.5$ kHz. $C = 72.36$ μF, $L = 14$ μH, and $V_c = 440$ V. If the diode starts conducting at $t = 0$, determine the (a) peak diode current, I_p; (b) width of the current pulse, t_r; and (c) switching loss, P_s.

Solution $f_s = 2500$ Hz, $C = 72.36$ μF, $L = 14$ μH, and $V_c = 440$ V.

(a) From Eq. (2-15), $I_p = 440\sqrt{C/L} = 440\sqrt{72.36/14} = 1000.3$ A.

(b) The pulse width, $t_r = \pi\sqrt{14 \times 72.36} = 99.99$ μs.

(c) The switching loss depends on the peak diode current and the pulse width. Since the pulse width is very small, the power-loss calculation from the average current value (as in Fig. 12-6.2) would be inaccurate. The determination of the switching loss requires the high-frequency data of the device. For $I_p = I_{FM} = 1000.3$ A and $t_r = 99.9$ μs. Fig. 12-6.4 gives the energy per pulse as $W_s = 0.1$ J and the switching loss is $P_s = W_s f_s = 0.1 \times 2500 = 250$ W.

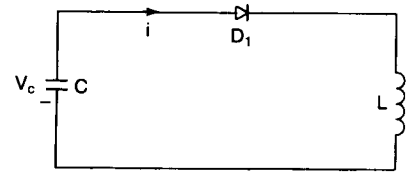


Figure 12-7 Resonant charge reversal circuit.

12-5 EFFECTS OF FORWARD AND REVERSE RECOVERY TIME

The importance of these parameters can be explained with Fig. 12-8a. If the switch, SW, is turned on at $t = 0$ and remains on long enough, a steady-state current of $I_0 = V_s/R$ would flow through the load and the freewheeling diode D_m

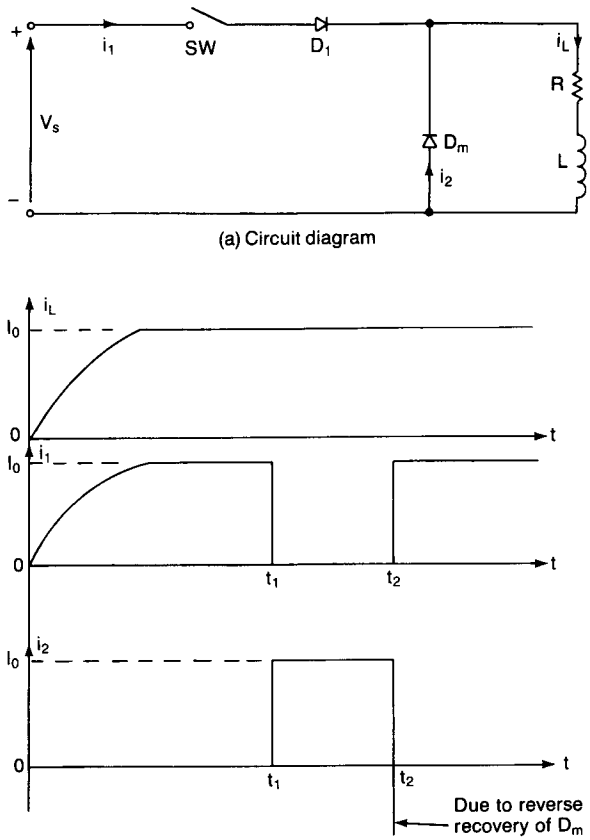
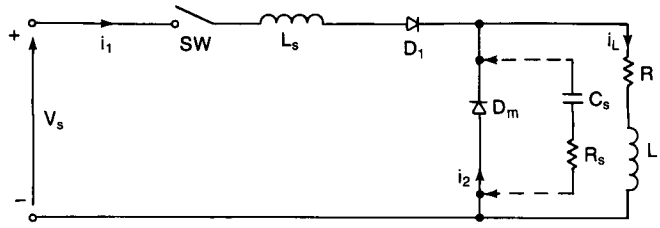


Figure 12-8 Chopper circuit without *di/dt* limiting inductor.

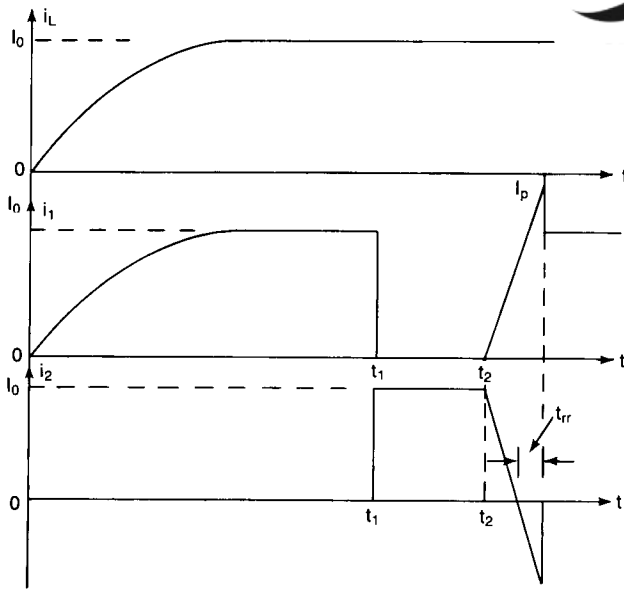
will be reversed biased. If the switch is turned off at $t = t_1$, diode D_m would conduct and the load current would circulate through D_m. Now, if the switch is turned on again at $t = t_2$, diode D_m would behave as a short circuit. The rate of rise of the forward current of the switch (and diode D_1) and the rate of fall of forward current of diode D_m would be very high, tending to be infinity. According to Eq. (12-7), the peak reverse current of diode D_m could be very high, and diodes D_1 and D_m may be damaged. Figure 12-8b shows the various waveforms for the diode currents. This problem is normally overcome by connecting a *di/dt* limiting inductor, L_s as shown in Fig. 12-9a. The practical diodes require a certain turn-on time before the entire area of the junction becomes conductive and the *di/dt* must be kept low to meet the turn-on time limit. This time is sometimes known as *forward recovery time*, t_{rf}.

The rate of rise of current through diode D_1, which should be the same as the rate of fall of the current through diode D_m, is

$$\frac{di}{dt} = \frac{V_s}{L_s} \tag{12-11}$$



(a) Circuit diagram



(b) Waveforms

Figure 12-9 Chopper circuit with *di/dt* limiting inductor.

If t_{rr} is the reverse recovery time of D_m, the peak reverse current of D_m is

$$I_{RR} = t_{rr}\frac{di}{dt} = \frac{t_{rr}V_s}{L_s} \tag{12-12}$$

and the peak current through inductor L_s would be

$$I_p = I_0 + I_{RR} = I_0 + t_{rr}\frac{t_{rr}V_s}{L_s} \tag{12-13}$$

When the inductor current becomes I_p, diode D_m turns off suddenly (assuming abrupt recovery) and breaks the current flow path. Due to highly inductive load, the load current cannot change suddenly from I_0 to I_p. The excess energy stored in L_s would induce a high reverse voltage across D_m and this may damage diode D_m. The excess energy stored as a result of reverse recovery time is found from

$$W_R = \tfrac{1}{2}L_s[(I_0 + I_{RR})^2 - I_0^2] \tag{12-14}$$

POWEREN.IR

$$W_R = \tfrac{1}{2} L_s \left[\left(I_0 + \frac{t_{rr} V_s}{L_s} \right)^2 - I_0^2 \right] \tag{12-15}$$

The waveforms for the various currents are shown in Fig. 12-9b. This excess energy can be transferred from the inductor L_s to a capacitor C_s which is connected across diode D_m. The value of the C_s can be determined from

$$\tfrac{1}{2} C_s V_c^2 = W_R$$

or

$$C_s = \frac{2W_R}{V_c^2} \tag{12-16}$$

where V_c is the allowable reverse voltage of the diode.

A resistor R_s, which is shown in Fig. 12-9a by dashed lines, is connected in series with the capacitor to damp out any transient oscillation. Equation (12-16) is an approximate one and does not take into account the effects of L_s and R_s during the transients for energy transfer. The design of C_s and R_s values is discussed in Section 15-4.

Example 12-4

The diodes in the single-phase full-wave rectifier in Fig. 2-14a have a reverse recovery time of $t_{rr} = 50$ μs and the rms value of input voltage is $V_s = 120$ V. Determine the effect of the reverse recovery time on the average output voltage if the supply frequency is (a) $f_s = 2$ kHz, and (b) $f_s = 60$ Hz.

Solution The reverse recovery time would affect the output voltage of the rectifier. In the full-wave rectifier of Fig. 2-14a, the diode D_1 will not be off at $\omega t = \pi$; rather, it will continue to conduct until $t = \pi/\omega + t_{rr}$. As a result of the reverse recovery time, the average output voltage would be reduced and the output voltage waveform is shown in Fig. 12-10.

If the input voltage is $v = V_m \sin \omega t = \sqrt{2}\, V_s \sin \omega t$, the average output voltage reduction is

$$V_{rr} = \frac{2}{T} \int_0^{t_{rr}} V_m \sin \omega t \, dt = \frac{2V_m}{T} \left[-\frac{\cos \omega t}{\omega} \right]_0^{t_{rr}} \tag{12-17}$$

$$= \frac{V_m}{\pi} (1 - \cos \omega t_{rr})$$

$$V_m = \sqrt{2}\ V_s = \sqrt{2} \times 120 = 169.7 \text{ V}$$

Without any reverse recovery time, Eq. (2-59) gives the average output voltage $V_{dc} = 0.6366 V_m = 108.03$ V.

(a) For $t_{rr} = 50$ μs and $f_s = 2000$ Hz, the reduction of the average output voltage is

$$V_{rr} = \frac{V_m}{\pi} (1 - \cos 2\pi f_s t_{rr})$$

$$= 0.061 V_m = 10.3 \text{ V or } 9.51\% \text{ of } V_{dc}$$

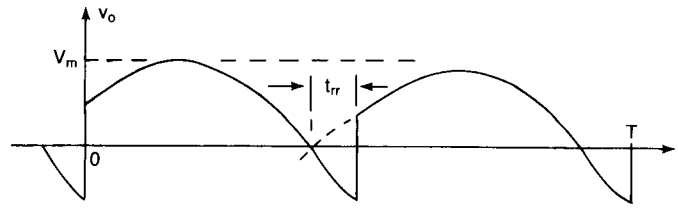


Figure 12-10 Effect of reverse recovery time on output voltage.

(b) For $t_{rr} = 50$ μs and $f_s = 60$ Hz, the reduction of the output dc voltage

$$V_{rr} = \frac{V_m}{\pi}(1 - \cos 2\pi f_s t_{rr}) = 5.65 \times 10^{-5} V_m$$

$$= 9.6 \times 10^{-3} \text{ V} \quad \text{or} \quad 8.88 \times 10^{-3}\% \text{ of } V_{dc}$$

Note. The effect of t_{rr} is significant for high-frequency source and for the case of normal 60-Hz source, its effect can be considered negligible.

Example 12-5

The chopper circuit in Fig. 12-9a is operated at a frequency of $f_s = 2$ kHz and a duty cycle of $k = 50\%$. The load is highly inductive and draws a current of $I_0 = 400$ A. The freewheeling diode D_m is IR type R23AF, 300 A, 800 V. If *di/dt* limiting inductor is $L_s = 4$ μH, dc input voltage is $V_s = 200$ V, and the junction temperature is maintained at $T_J = 125°C$, determine the (a) peak switch current, I_p; (b) value of C_s to limit the peak reverse voltage of diode D_m to 350 V; and (c) average power losses in the diode D_m, P_D.

Solution $V_s = 200$ V, $L_s = 4$ μH, $f_s = 2000$ Hz, $k = 0.5$, $V_c = 350$ V, and $I_0 = 400$ A. From Eq. (12-11), $di/dt = 200/4 = 50$ A/μs.

(a) For $I_{FM} = I_0 = 400$ A and $T_J = 125°$, Fig. 12-6.7 gives $I_{RR} = 50$ A. From Eq. (12-13),

$$I_p = I_0 + I_{RR} = 400 + 50 = 450 \text{ A}$$

(b) From Eq. (12-14), the excess energy due to reverse recovery time is

$$W_R = 0.5 \times 4 \times 10^{-6} \times (450^2 - 400^2) = 85{,}000 \times 10^{-6} \text{ J}$$

From Eq. (12-16),

$$C_s = \frac{2 \times 85{,}000 \times 10^{-6}}{350^2} = 1.39 \text{ μF}$$

(c) For a freewheeling current of $I_0 = 400$ A, Fig. 12-6.3 gives the instantaneous forward voltage drop, $v_F = 1.25$ V. The instantaneous forward power loss becomes $1.25 \times 125 = 500$ W. The average power loss is $P_D = k \times 500 = 0.5 \times 500 = 250$ W.

12-6 SERIES-CONNECTED DIODES

In many high-voltage applications (e.g., HVDC transmission lines), one commercially available diode cannot meet the required voltage rating and diodes are connected in series to increase the reverse blocking capabilities.

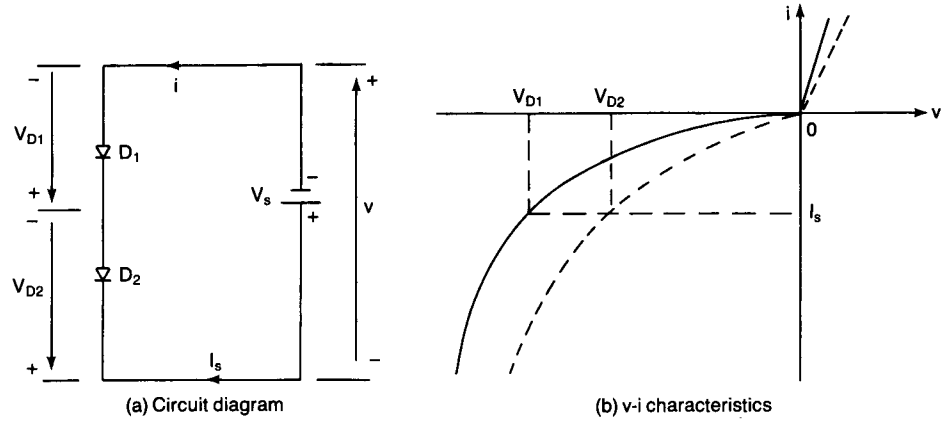


Figure 12-11 Two series-connected diodes.

Let us consider two series-connected diodes as shown in Fig. 12-11a. In practice, the v–i characteristics for the same type of diodes differ due to tolerances in the production process. Figure 12-11b shows two v–i characteristics for such diodes. In the forward-biased condition, both diodes conduct the same amount of current and forward voltage drop of each diode would be almost equal. However, in the reverse blocking condition, each diode has to carry the same leakage current, and as a result the blocking voltages of diodes would differ significantly.

A simple solution to this problem, as shown in Fig. 12-12a, is to force equal voltage sharing by connecting a resistor across each diode. Due to equal voltage sharing, the leakage current of each diode would be different and this is shown in Fig. 12-12b. Since the total leakage current must be shared by a diode and its resistor,

$$I_s = I_{s1} + I_{R1} = I_{s2} + I_{R2} \tag{12-18}$$

But $I_{R1} = V_{D1}/R_1$ and $I_{R2} = V_{D2}/R_2 = V_{D1}/R_2$. Equation (12-18) gives the re-

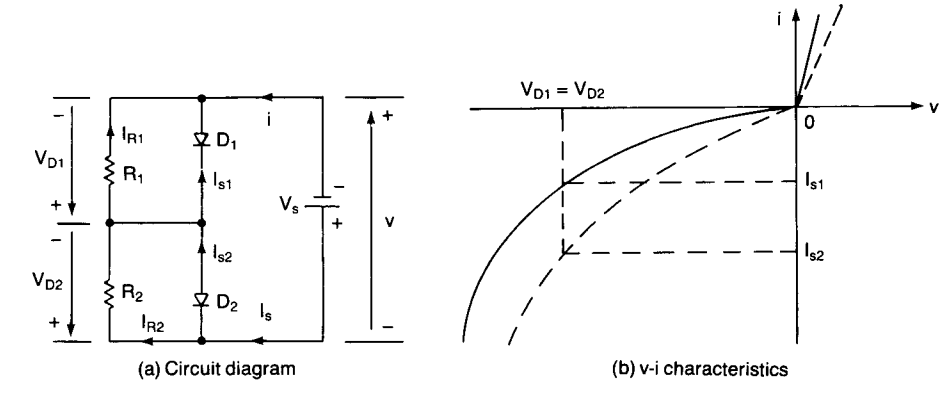


Figure 12-12 Series-connected diodes with steady-state voltage sharing resistors.

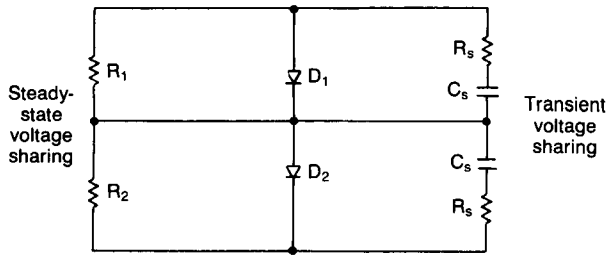


Figure 12-13 Series diodes with voltage-sharing networks under steady-state and transient condition.

lationship between R_1 and R_2 for equal voltage sharing as

$$I_{s1} + \frac{V_{D1}}{R_1} = I_{s2} + \frac{V_{D1}}{R_2} \tag{12-19}$$

If the resistances are equal, $R = R_1 = R_2$ and the two diode voltages would be different slightly depending on the dissimilarities of the two v–i characteristics. The values of V_{D1} and V_{D2} can be determined from Eqs. (12-20) and (12-21):

$$I_{s1} + \frac{V_{D1}}{R} = I_{s2} + \frac{V_{D2}}{R} \tag{12-20}$$

$$V_{D1} + V_{D2} = V_s \tag{12-21}$$

The voltage sharings under transient conditions (e.g., due to switching loads, initial applications of input voltage) are accomplished by connecting capacitors across each diode, which is shown in Fig. 12-13. R_s limits the rate of rise of the blocking voltage.

12-7 PARALLEL-CONNECTED DIODES

In high-power applications, diodes are connected in parallel to increase the current-carrying capability to meet the desired current requirements. The current sharings of diodes would be in according to their respective forward voltage drops. A uniform current sharing can be achieved by providing equal inductances (e.g., in the leads) or by connecting current-sharing resistors (which may not be practical due to power losses); and this is depicted in Fig. 12-14. It is possible to minimize this problem by selecting diodes with equal forward voltage drops or diodes of the

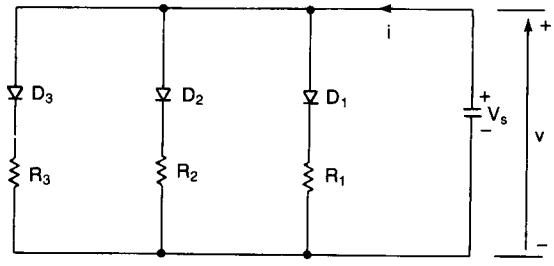


Figure 12-14 Paralled-connected diodes.

same type. Since the diodes are connected in parallel, the reverse blocking voltages of each diode would be the same.

SUMMARY

The characteristics of practical diodes differ from that of ideal diodes. The reverse recovery time plays a significant role, especially at high-speed switching applications. Diodes can be classified into three types: (1) general-purpose diodes, (2) fast-recovery diodes, and (3) Schottky diodes. Although a Schottky diode behaves as a *pn*-junction diode, there is no physical junction; and as a result a Schottky diode is a majority carrier device. On the other hand, a *pn*-junction diode is both a majority and a minority carrier diode.

The manufacturers provide a data sheet describing the characteristics in terms of certain performance parameters. The junction temperature influences these parameters significantly.

If diodes are connected in series to increase the blocking voltage capability, voltage-sharing networks under steady-state and transient conditions are required. When diodes are connected in parallel to increase the current-carrying ability, current-sharing elements are also necessary.

REVIEW QUESTIONS

12-1. What are the types of power diodes?
12-2. What is a leakage current of diodes?
12-3. What is a reverse recovery time of diodes?
12-4. What is a reverse recovery current of diodes?
12-5. What is a softness factor of diodes?
12-6. What are the recovery types of diodes?
12-7. What is the cause of reverse recovery time in a *pn*-junction diode?
12-8. What is the effect of reverse recovery time?
12-9. Why is it necessary to use fast-recovery diodes for high-speed switching?
12-10. What is a forward recovery time?
12-11. What are the main differences between *pn*-junction diodes and Schottky diodes?
12-12. What are the limitations of Schottky diodes?
12-13. What is the typical reverse recovery time of general-purpose diodes?
12-14. What is the typical reverse recovery time of fast-recovery diodes?
12-15. What is the typical maximum junction temperature of diodes?
12-16. What is the purpose of a current-limiting inductor?
12-17. What are the problems of series-connected diodes, and what are the possible solutions?
12-18. What are the problems of parallel-connected diodes, and what are the possible solutions?

12-19. If two diodes are connected in series with equal-voltage sharings, why do the diode leakage currents differ?

PROBLEMS

12-1. The reverse recovery time of a diode is t_{rr} = 5 μs and the rate of fall of the diode current is di/dt = 80 A/μs. If the softness factor is SF = 0.5, determine the **(a)** storage charge, Q_{RR}; and **(b)** peak reverse current, I_{RR}.

12-2. The peak input voltage of a single-phase half-wave diode rectifier is V_m = 169 V at 60 Hz and the load resistance is R_L = 1.2 Ω. The reverse recovery time is t_{rr} = 4 μs. If the softness factor is SF = 0, determine the **(a)** storage charge, Q_{RR}; and **(b)** peak reverse current, I_{RR}.

12-3. Four IR 300-A 800-V diodes of type R23AF are used for the single-phase bridge rectifier in Fig. 2-15a. The rms value of the input voltage is V_s = 120 V at 2 kHz and the load resistance is R = 0.2 Ω. The junction temperature and ambient temperature are T_J = 125°C and T_A = 40°C, respectively. Determine the **(a)** average power loss, P_D; **(b)** instantaneous forward voltage drop, v_F; **(c)** recovery charge, Q_{RR}; **(d)** reverse recovery time, t_{rr}; **(e)** case temperature, T_C; and **(f)** thermal resistance of heat sink, R_{thSA}. Assume double-sided cooling and case-to-sink thermal resistance of R_{thCS} = 0.03°C/W.

12-4. Repeat Prob. 12-3 if T_J = 25°C and T_A = 0°C.

12-5. Six IR 300-A 800-A diodes of type R23AF are used in the three-phase rectifier of Fig. 2-18. The rms value of input line voltage is V_s = 208 V at 60 Hz and the load resistance is R = 0.3 Ω. The junction temperature and ambient temperature are T_J = 125°C and T_A = 25°C respectively. Determine the **(a)** average power loss, P_D; **(b)** instantaneous forward voltage drop; v_F; **(c)** recovery charge, Q_{RR}; ;**(d)** reverse recovery time, t_{rr}; **(e)** case temperature, T_C; and **(f)** thermal resistance of heat sink, R_{thSA}. Assume double-sided cooling and case-to-sink thermal resistance of R_{thCS} = 0.03°C/W.

12-6. A IR diode, 300 A, 800 V, type R23AF, is used for charge reversal in a commutation circuit, and the equivalent circuit is shown in Fig. 12-7. This charge reversal is repeated at a frequency of f_s = 1.5 kHz. C = 80 μF, L = 20 μH, and V_c = 220 V. If the diode starts conducting at t = 0, determine the **(a)** peak diode current, I_p; **(b)** width of the current pulse, t_r; and **(c)** switching loss, P_s.

12-7. The current waveform through a IR diode, 300 A, 800 V, type R23AF, is shown in Fig. P12-7. The frequency switching is f_s = 2 kHz. Determine the switching loss, P_s.

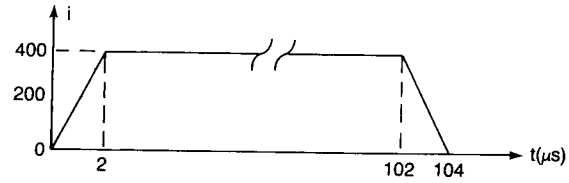


Figure P12-7

12-8. The diodes in the three-phase bridge rectifier of Fig. 2-18a have reverse recovery time, t_{rr} = 50 μs and the rms value of input line voltage, V_s = 208 V. Determine

the effect of the reverse recovery time on the average output voltage if the supply frequency is **(a)** f_s = 2 kHz, and **(b)** f_s = 60 Hz.

12-9. The chopper circuit of Fig. 12-9a is operated at a frequency of f_s = 1.5 kHz and a duty cycle of k = 25%. The load is highly inductive and draws a current of I_0 = 750 A. The freewheeling diode D_m is IR type R23AF, 300 A, 800 V. If di/dt limiting inductor, L_s = 10 μs, dc input voltage, V_s = 400 V, and the junction temperature is maintained at T_J = 125°C, determine the **(a)** peak current of the switch, I_p; **(b)** value of C_s to limit the peak reverse voltage of diode D_m to 600 V; and **(c)** average power losses in the freewheeling diode, P_D.

12-10. Two diodes are connected in series and the voltage across each diode is maintained the same by connecting voltage-sharing resistor, such that $V_{D1} = V_{D2}$ = 2000 V and R_1 = 100 kΩ. The v–i characteristic of the diodes is shown in Fig. P12-10. Determine the leakage currents of each diode and the resistance R_2 across diode D_2.

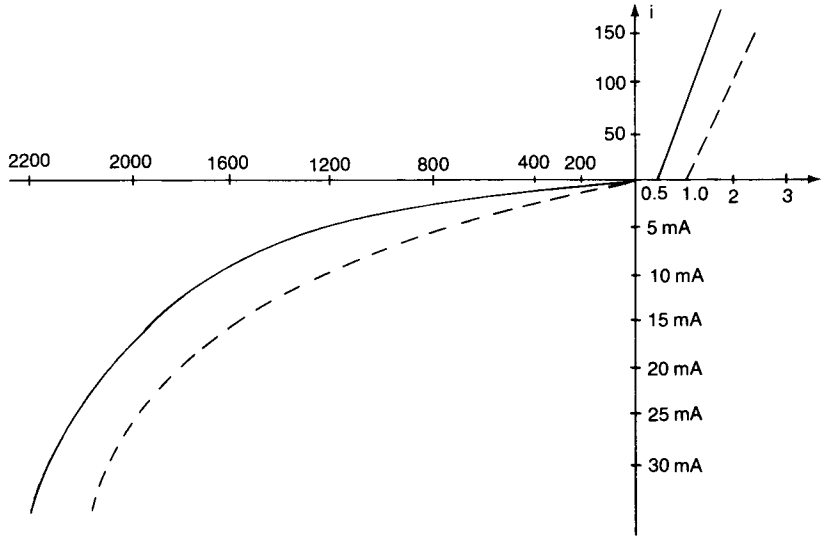


Figure P12-10

12-11. Two diodes are connected in parallel and the forward voltage drop across each diode is 1.5 V. The v–i characteristics of diodes are shown in Fig. P12-10; determine the forward currents through each diode.

12-12. Two diodes are connected in parallel as shown in Fig. 12-14, with current-sharing resistances. The v–i characteristics are shown in Fig. P12-10. The total current is I_T = 200 A. The voltage across a diode and its resistance is v = 2.5 V. Determine the values of resistances R_1 and R_2 if the current is shared equally by the diodes.

12-13. Two diodes are connected in series as shown in Fig. 12-12. The resistance across the diodes are $R_1 = R_2$ = 10 kΩ. The input dc voltage is 5 kV. The leakage currents are I_{s1} = 25 mA and I_{s2} = 40 mA. Determine the voltage across the diodes.

13

Power Transistors

13-1 INTRODUCTION

Power transistors have controlled turn-on and turn-off characteristics. The transistors, which are used as switching elements, are operated in the saturation region, resulting in a low on-state voltage drop. The switching speed of modern transistors is much higher than that of thyristors and they are extensively employed in dc–dc and dc–ac converters, with inverse parallel-connected diodes to provide bidirectional current flow. However, their voltage and current ratings are lower than those of thyristors and transistors are normally used in low to medium power applications. The power transistors can be classified broadly into three categories:

1. Bipolar junction transistors (BJTs)
2. Metal-oxide-semiconductor field-effect transistors (MOSFETs)
3. Metal-oxide-semiconductor insulated-gate transistors (MOSIGTs)

In earlier chapters, BJTs or MOSFETs were assumed as ideal switches to explain the power conversion techniques. It is obvious that a transistor switch is much simpler than a forced-commutated thyristor switch. However, the choice between a BJT and a MOSFET in the converter circuits was not obvious and they were shown simply to demonstrate that either of them can replace a thyristor, provided that their voltage and current ratings meet the output requirements of

the converter. Practical transistors differ from that of ideal devices. The transistors have certain limitations and are restricted to some applications. The characteristics and ratings of each type should be examined to determine its suitability to a particular application.

13-2 BIPOLAR JUNCTION TRANSISTORS

A bipolar transistor is formed by adding a second *p*- or *n*-region to a *pn*-junction diode. With two *n*-regions and one *p*-region, two junctions are formed and it is known as a *npn-transistor*, as shown in Fig. 13-1a. With two *p*-regions and one *n*-region, it is called as a *pnp-transistor*, as shown in Fig. 13-1b. The three terminals are named as *collector*, *emitter*, and *base*. A bipolar transistor has two junctions, collector–base junction (CBJ) and base–emitter junction (BEJ). NPN transistors of various sizes are shown in Fig. 13-2.

13-2.1 Steady-State Characteristics

Although there are three possible configurations—common-collector, common-base, and common-emitter—the common-emitter configuration, which is shown in Fig. 13-3a for a *npn*-transistor, is generally used in switching applications. The typical input characteristics of base current, I_B, against base–emitter voltage, V_{BE}, are shown in Fig. 13-3b. Figure 13-3c shows the typical output characteristics of collector current, I_C, against collector–emitter voltage, V_{CE}. For a *pnp*-transistor, the polarities of all currents and voltages are reversed.

There are three operating regions of a transistor: cutoff, active, and saturation. In the cutoff region, the transistor is off or the base current is not enough to turn it on and both junctions are reverse biased. In the active region, the transistor acts as an amplifier, where the collector current is amplified by a gain and the collector–emitter voltage decreases with the base current. The CBJ is reverse biased and the BEJ is forward-biased. In the saturation region, the base current is sufficiently high so that the collector–emitter voltage is low and the transistor

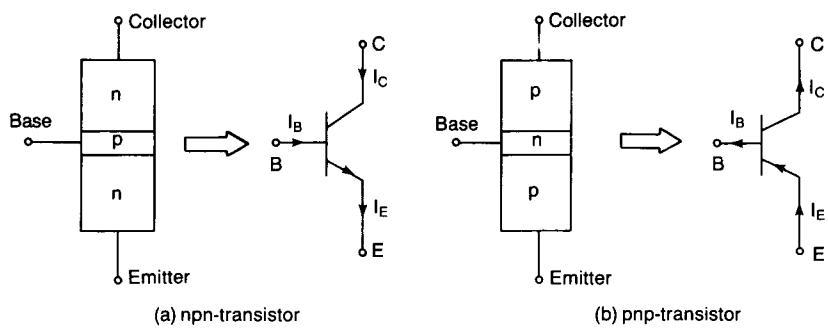


Figure 13-1 Bipolar transistors.

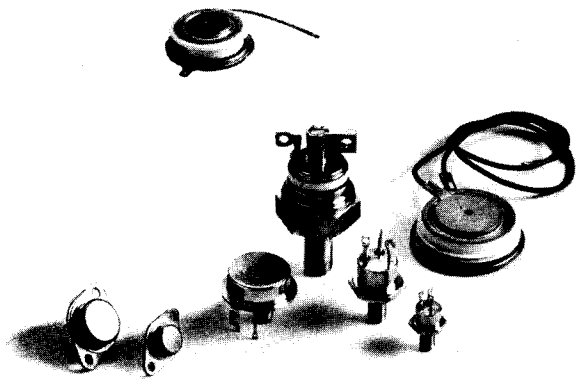


Figure 13-2 *NPN* transistors. (*Courtesy of Powerex, Inc.*)

acts as a switch. Both junctions (CBJ and BEJ) are forward biased. The transfer characteristic, which is a plot of V_{CE} against I_B, is shown in Fig. 13-4.

The model of a *npn*-transistor is shown in Fig. 13-5 under large-signal dc operation. The equation relating the currents is

$$I_E = I_C + I_B \tag{13-1}$$

The base current is effectively the input current and the collector current is the

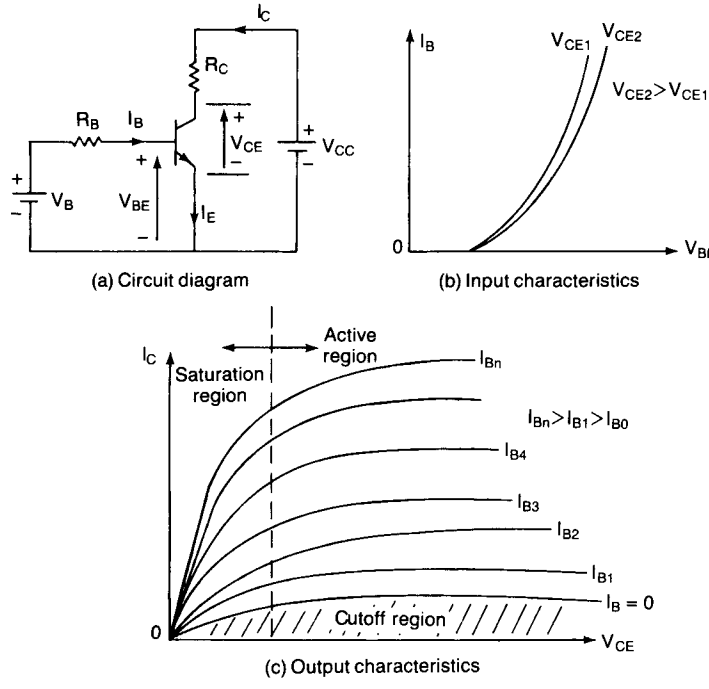


Figure 13-3 Characteristics of *npn*-transistors.

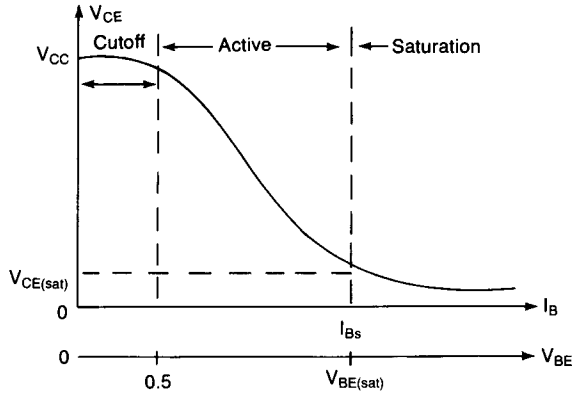


Figure 13-4 Transfer characteristics.

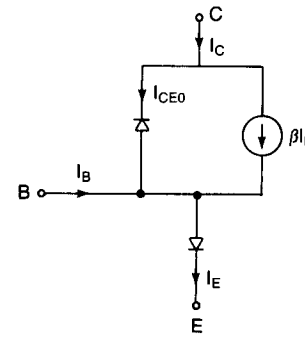


Figure 13-5 Model of *npn*-transistor.

output current. The ratio of the collector current, I_C, to base current, I_B, is known as the *current gain*, β:

$$\beta = h_{FE} = \frac{I_c}{I_B} \tag{13-2}$$

The collector current has two components: one due to the base current and other one is the leakage current of the CBJ.

$$I_C = \beta I_B + I_{CEO} \tag{13-3}$$

where I_{CEO} is the collector-to-emitter leakage current with base open circuit and can be considered negligible compared to βI_B.

From Eqs. (13-1) and (13-3),

$$I_E = I_B(1 + \beta) + I_{CEO} \tag{13-4}$$

$$\approx I_B(1 + \beta) \tag{13-4a}$$

$$I_E \approx I_C\left(1 + \frac{1}{\beta}\right) = I_C\frac{\beta + 1}{\beta} \tag{13-5}$$

The collector current can be expressed as

$$I_C \approx \alpha I_E \tag{13-6}$$

where the constant α is related to β by

$$\alpha = \frac{\beta}{\beta + 1} \tag{13-7}$$

or

$$\beta = \frac{\alpha}{1 - \alpha} \tag{13-8}$$

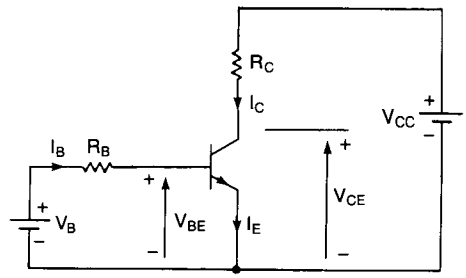


Figure 13-6 Transistor switch.

Let us consider the circuit of Fig. 13-6, where the transistor is operated as a switch.

$$I_B = \frac{V_B - V_{BE}}{R_B} \tag{13-9}$$

$$V_C = V_{CE} = V_{CC} - I_C R_C = V_{CC} - \frac{\beta R_C}{R_B}(V_B - V_{BE}) \tag{13-10}$$

$$V_{CE} = V_{CB} + V_{BE}$$

or

$$V_{CB} = V_{CE} - V_{BE} \tag{13-11}$$

Equation (13-11) indicates that as long as $V_{CE} \geq V_{BE}$, the CBJ will be reverse biased and the transistor will be in the active region. The maximum collector current in the active region, which can be obtained by setting $V_{CB} = 0$ and $V_{BE} = V_{CE}$, is

$$I_{CM} = \frac{V_{CC} - V_{CE}}{R_C} = \frac{V_{CC} - V_{BE}}{R_C} \tag{13-12}$$

and the corresponding value of base current

$$I_{BM} = \frac{I_{CM}}{\beta} \tag{13-13}$$

If the base current is increased above I_{BM}, V_{BE} increases and the collector current will increase and the V_{CE} will fall below V_{BE}. This will continue until the CBJ is forward biased with V_{BC} of about 0.4 to 0.5 V. The transistor then goes into saturation. The *transistor saturation* may be defined as the point above which any increase in the base current does not increase the collector current significantly.

In the saturation, the collector current remains almost constant. If the collector–emitter saturation voltage is $V_{CE(sat)}$, the collector current is

$$I_{CS} = \frac{V_{CC} - V_{CE(sat)}}{R_C} \tag{13-14}$$

and the corresponding value of base current is

$$I_{BS} = \frac{I_{CS}}{\beta} \tag{13-15}$$

Normally, the circuit is designed so that I_B is higher than I_{BS}. The ratio of I_B to I_{BS} is called the *overdrive factor*, ODF:

$$\text{ODF} = \frac{I_B}{I_{BS}} \tag{13-16}$$

and the ratio of I_{CS} to I_B is called as *forced* β, β_f where

$$\beta_f = \frac{I_{CS}}{I_B} \tag{13-17}$$

The total power loss in the two junctions is

$$P_T = V_{BE}I_B + V_{CE}I_C \tag{13-18}$$

A high value of overdrive factor will not reduce the collector–emitter voltage significantly. However, V_{BE} will increase due to increased base current, resulting in increased power loss in the BEJ.

Example 13-1

The bipolar transistor in Fig. 13-6 is specified to have β in the range 8 to 40. The load resistance is $R_C = 11\ \Omega$. The dc supply voltage is $V_{CC} = 200$ V and the input voltage to the base circuit is $V_B = 10$ V. If $V_{CE(\text{sat})} = 1.0$ V and $V_{BE(\text{sat})} = 1.5$ V, find the (a) value of R_B that results in saturation with an overdrive factor of 5; (b) forced β; and (c) power loss in the transistor, P_T.

Solution $V_{CC} = 200$ V, $\beta_{\text{min}} = 8$, $\beta_{\text{max}} = 40$, $R_C = 11\ \Omega$, ODF = 5, $V_B = 10$ V, $V_{CE(\text{sat})} = 1.0$ V, and $V_{BE(\text{sat})} = 1.5$ V. From Eq. (13-14), $I_{CS} = (200 - 1.0)/11 = 18.1$ A. From Eq. (13-15), $I_{BS} = 18.1/\beta_{\text{min}} = 18.1/8 = 2.2625$ A. Equation (13-16) gives the base current for an overdrive factor of 5,

$$I_B = 5 \times 2.2625 = 11.3125 \text{ A}$$

(a) Equation (13-9) gives the required value of R_B,

$$R_B = \frac{V_B - V_{BE(\text{sat})}}{I_B} = \frac{10 - 1.5}{11.3125} = 0.7514\ \Omega$$

(b) From Eq. (13-17), $\beta_f = 18.1/11.3125 = 1.6$.

(c) Equation (13-18) yields the total power loss as

$$P_T = 1.5 \times 11.3125 + 1.0 \times 18.1 = 16.97 + 18.1 = 35.07 \text{ W}$$

Note. For an overdrive factor of 10, $I_B = 22.265$ A and the power loss will be $P_T = 1.5 \times 22.265 + 18.1 = 51.5$ W. Once the transistor is saturated, the collector–emitter voltage is not reduced in relation to the increase in base current. However, the power loss is increased. At a high value of overdrive factor, the

transistor may be damanged due to thermal runway. On the other hand, if the transistor is underdriven ($I_B < I_{CS}$), it may operate in the active region and V_{CE} will increase, resulting in increased power loss.

13-2.2 Switching Characteristics

A forward-biased *pn*-junction exhibits two parallel capacitances: a depletion-layer capacitance and a diffusion capacitance. On the other hand, a reverse-biased *pn*-junction has only depletion capacitance. Under steady-state conditions, these capacitances do not play any role. However, under transient conditions, they contribute to the turn-on and turn-off behavior of the transistor.

The model of a transistor under transient conditions is shown in Fig. 13-7, where C_{cb} and C_{be} are the effective capacitances of the CBJ and BEJ, respectively. The *transconductance*, g_m, of a BJT is defined as the ratio of I_C to V_{BE}. These capacitances are dependent on the junction voltages and physical construction of the transistor. C_{cb} affects the input capacitance significantly due to the Miller multiplication effect [6]. r_{CE} and r_{BE} are the resistances of collector to emitter and base to emitter, respectively.

Due to the internal capacitances, the transistor does not turn on instantly. Figure 13-8 illustrates the waveforms and switching times. As the input voltage v_B rises from zero to V_1 and the base current rises to I_{B1}, the collector current does not respond immediately. There is a delay, known as *delay time*, t_d before any collector current flows. This delay is required to charge up the capacitances of the BEJ to the forward-bias voltage V_{BE} (approximately 0.7 V). After this delay, the collector current rises to the steady-state value of I_{CS}. The rise time, t_r, depends on the time constant determined by input capacitances.

The base current is normally more than that required to saturate the transistor. As a result, the excess minority carrier charge is stored in the base region. The higher the overdrive factor, ODF, the greater is the amount of extra charge stored in the base. This extra charge, which is called the *saturating charge*, is proportional to the excess base drive, I_e:

$$I_e = I_B - \frac{I_{CS}}{\beta} = \text{ODF} \cdot I_{BS} - I_{BS} = I_{BS}(\text{ODF} - 1) \qquad (13\text{-}19)$$

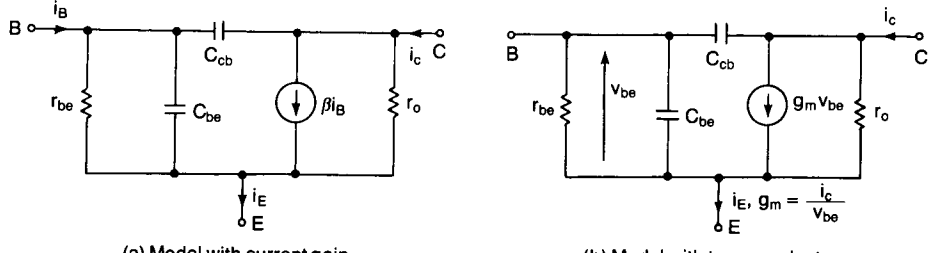


Figure 13-7 Transient model of BJT.

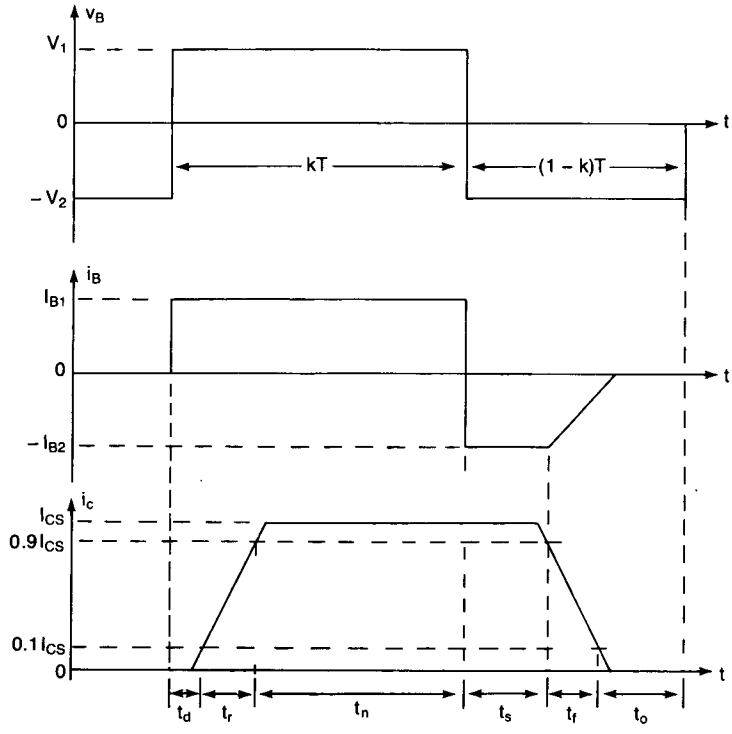


Figure 13-8 Switching times of bipolar transistors.

and the saturating charge is given by

$$Q_s = \tau_s I_e = \tau_s I_{BS}(\text{ODF} - 1) \tag{13-20}$$

where τ_s is known as the *storage time constant* of the transistor.

When the input voltage is reversed from V_1 to $-V_2$ and the base current is also changed to $-I_{B2}$, the collector current does not change for a time, t_s, called the *storage time*. t_s is required to remove the saturating charge from the base. Since v_{BE} is still positive with approximately 0.7 V, the base current reverses its direction due to the change in the polarity of v_B from V_1 to $-V_2$. The reverse current, $-I_{B2}$, helps to discharge the base and remove the extra charge from the base. Without $-I_{B2}$, the saturating charge has to be removed entirely by recombination and the storage time would be longer.

Once the extra charge is removed, the BEJ capacitance charges to the input voltage, $-V_2$, and the base current falls to zero. The fall time, t_f, depends on the time constant, which is determined by the capacitance of the reverse-biased BEJ.

Figure 13-9a shows the extra storage charge in the base of a saturated transistor. During turn-off, this extra charge is removed first in time t_s and the charge profile is changed from *a* to *c* as shown in Fig. 13-9b. During fall time, the charge profile decreases from profile *c* until all charges are removed.

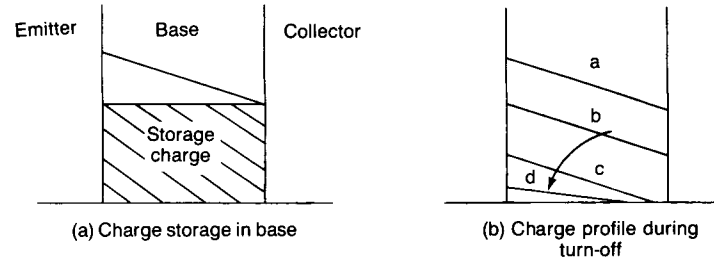


Figure 13-9 Charge storage in saturated bipolar transistors.

The turn-on time, t_{on}, is the sum of delay time, t_d, and rise time, t_r.

$$t_{on} = t_d + t_r$$

and the turn-off time, t_{off}, is the sum of storage tome, t_s, and fall time, t_f,

$$t_{off} = t_s + t_f$$

Example 13-2

The waveforms of the transistor switch in Fig. 13-6 are shown in Fig. 13-10. The parameters are V_{CC} = 250 V, $V_{BE(sat)}$ = 3 V, I_B = 8 A, $V_{CE(sat)}$ = 2 V, I_{CS} = 100 A, t_d = 0.5 μs, t_r = 1 μs, t_s = 5 μs, t_f = 3 μs, and f_s = 10 kHz. The duty cycle is k = 50%. The collector-to-emitter leakage current is I_{CEO} = 3 mA. Determine

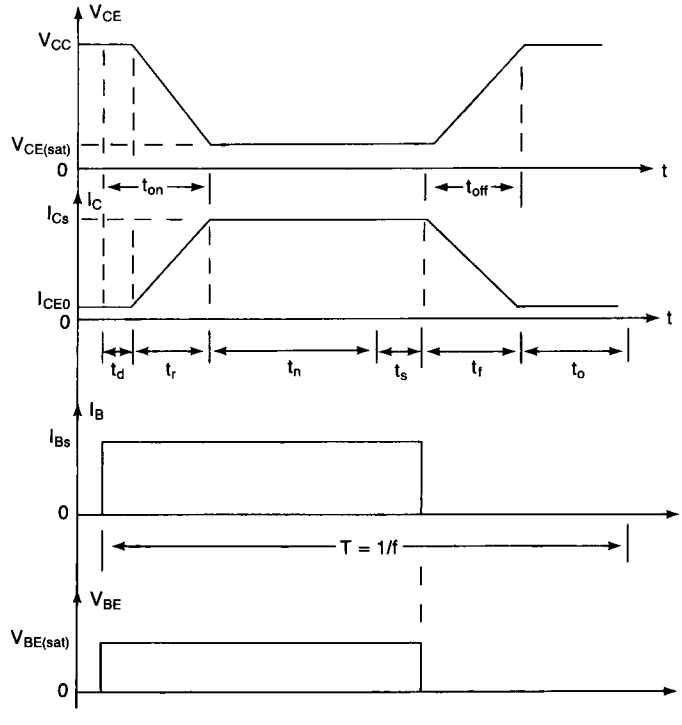


Figure 13-10 Waveforms of transistor switch.

the power loss due to collector current (a) during turn-on, $t_{on} = t_d + t_r$; (b) during conduction period, t_n; (c) during turn-off, $t_{off} = t_s + t_f$; (d) during off-time, t_o; and (e) total average power losses, P_T. (f) Plot the instantaneous power due to collector current, $P_c(t)$.

Solution $T = 1/f_s = 100\ \mu s$, $k = 0.5$, $kT = t_d + t_r + t_n = 50\ \mu s$, $t_n = 50 - 0.5 - 1 = 48.5\ \mu s$, $(1 - k)T = t_s + t_f + t_o = 50\ \mu s$, and $t_o = 50 - 5 - 3 = 42\ \mu s$.

(a) During delay time, $0 \le t \le t_d$:

$$i_c(t) = I_{CEO}$$

$$v_{CE}(t) = V_{CC}$$

The instantaneous power due to the collector current is

$$P_c(t) = i_c v_{CE} = I_{CEO} V_{CC}$$

$$= 3 \times 10^{-3} \times 250 = 0.75\ W$$

The average power loss during the delay time is

$$P_d = \frac{1}{T}\int_0^{td} P_c(t)\,dt = I_{CEO} V_{CC} t_d f_s$$

$$= 3 \times 10^{-3} \times 250 \times 0.5 \times 10^{-6} \times 10 \times 10^3 = 3.75\ mW \tag{13-21}$$

During rise time, $0 \le t \le t_r$:

$$i_c(t) = \frac{I_{CS}}{t_r} t$$

$$v_{CE}(t) = V_{CC} + (V_{CE(sat)} - V_{CC})\frac{t}{t_r}$$

$$P_c(t) = i_c v_{CE} = I_{CS}\frac{t}{t_r}\left[V_{CC} + (V_{CE(sat)} - V_{CC})\frac{t}{t_r}\right] \tag{13-22}$$

The power $P_c(t)$ will be maximum when $t = t_m$, where

$$t_m = \frac{t_r V_{CC}}{2[V_{CC} - V_{CE(sat)}]}$$

$$= 1 \times \frac{250}{2(250 - 2)} = 0.504\ \mu s \tag{13-23}$$

and Eq. (13-22) yields the peak power

$$P_p = \frac{V_{CC}^2 I_{CS}}{4[V_{CC} - V_{CE(sat)}]} \tag{13-24}$$

$$= 250^2 \times \frac{100}{4(250 - 2)} = 6300.4\ W$$

$$P_r = \frac{1}{T}\int_0^{tr} P_c(t)\,dt = f_s I_{CS} t_r \left[\frac{V_{CC}}{2} + \frac{V_{CE(sat)} - V_{CC}}{3}\right] \tag{13-25}$$

$$= 10 \times 10^3 \times 100 \times 1 \times 10^{-6}\left[\frac{250}{2} + \frac{2 - 250}{3}\right] = 42.33\ W$$

The total power loss during the turn-on is

$$P_{on} = P_d + P_r = 0.00375 + 42.33 = 42.33 \text{ W} \tag{13-26}$$

(b) The conduction period, $0 \le t \le t_n$:

$$i_c(t) = I_{CS}$$

$$v_{CE}(t) = V_{CE(sat)}$$

$$P_c(t) = i_c v_{CE} = V_{CE(sat)} I_{CS} = 2 \times 100 = 200 \text{ W}$$

$$P_n = \frac{1}{T}\int_0^{t_n} P_c(t)\,dt = V_{CE(sat)} I_{CS} t_n f_s \tag{13-27}$$

$$= 2 \times 100 \times 48.5 \times 10^{-6} \times 10 \times 10^3 = 97 \text{ W}$$

(c) The storage period, $0 \le t \le t_s$:

$$i_c(t) = I_{CS}$$

$$v_{CE}(t) = V_{CE(sat)}$$

$$P_c(t) = i_c v_{CE} = V_{CE(sat)} I_{CS} = 2 \times 100 = 200 \text{ W}$$

$$P_s = \frac{1}{T}\int_0^{t_s} P_c(t)\,dt = V_{CE(sat)} I_{CS} t_s f_s \tag{13-28}$$

$$= 2 \times 100 \times 5 \times 10^{-6} \times 10 \times 10^3 = 10 \text{ W}$$

The fall time, $0 \le t \le t_f$:

$$i_c(t) = I_{CS}\left(1 - \frac{t}{t_f}\right), \text{ neglecting } I_{CEO}$$

$$v_{CE}(t) = \frac{V_{CC}}{t_f} t, \text{ neglecting } I_{CEO}$$

$$P_c(t) = i_c v_{CE} = V_{CC} I_{CS}\left[\left(1 - \frac{t}{t_f}\right)\frac{t}{t_f}\right] \tag{13-29}$$

This power loss during fall time will be maximum when $t = t_f/2 = 1.5$ μs and Eq. (13-29) gives the peak power,

$$P_p = \frac{V_{CC} I_{CS}}{4} \tag{13-30}$$

$$= 250 \times \frac{100}{4} = 6250 \text{ W}$$

$$P_f = \frac{1}{T}\int_0^{t_f} P_c(t)\,dt = \frac{V_{CC} I_{CS} t_f f_s}{6} \tag{13-31}$$

$$= \frac{250 \times 100 \times 3 \times 10^{-6} \times 10 \times 10^3}{6} = 125 \text{ W}$$

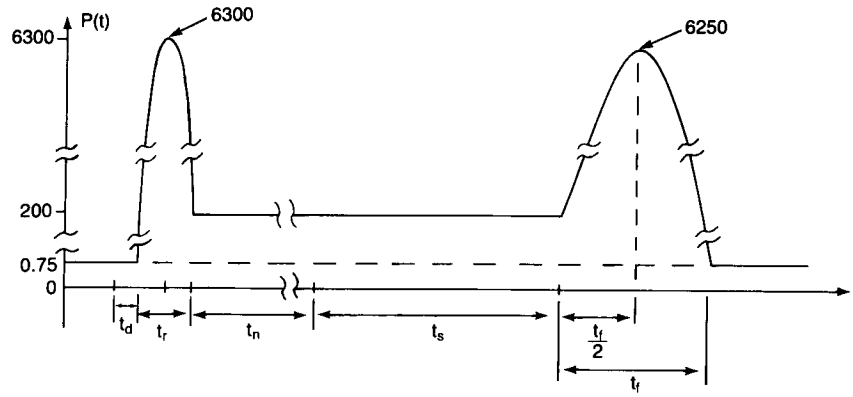


Figure 13-11 Plot of instantaneous power for Example 13-2.

The power loss during turn-off is

$$P_{\text{off}} = P_s + P_f = V_{CC}I_{CS}f_s\left(t_s + \frac{t_f}{6}\right) = 10 + 125 = 135 \text{ W} \tag{13-32}$$

(d) Off-period, $0 \le t \le t_o$:

$$i_c(t) = I_{CEO}$$

$$v_{CE}(t) = V_{CC}$$

$$P_c(t) = i_c v_{CE} = I_{CEO}V_{CC} = 3 \times 10^{-3} \times 250 = 0.75 \text{ W} \tag{13-33}$$

$$P_0 = \frac{1}{T}\int_0^{to} P_c(t)\,dt = I_{CEO}V_{CC}t_o f_s$$

$$= 3 \times 10^{-3} \times 250 \times 42 \times 10^{-6} \times 10 \times 10^3 = 0.315 \text{ W}$$

(e) The total power loss in the transistor due to collector current is

$$P_T = P_{\text{on}} + P_n + P_{\text{off}} + P_0 = 42.33 + 97 + 135 + 0.315 = 274.65 \text{ W} \tag{13-34}$$

(f) The plot of the instantaneous power is shown in Fig. 13-11.

Example 13-3

For the parameters in Example 13-2, calculate the average power loss due to the base current.

Solution $V_{BE(\text{sat})} = 3$ V, $I_B = 8$ A, $T = 1/f_s = 100$ μs, $k = 0.5$, $kT = 50$ μs, $t_d = 0.5$ μs, $t_r = 1$ μs, $t_n = 50 - 1.5 = 48.5$ μs, $t_s = 5$ μs, $t_f = 3$ μs, $t_{\text{on}} = t_d + t_r = 1.5$ μs, and $t_{\text{off}} = t_s + t_f = 5 + 3 = 8$ μs.

During the period, $0 \le t \le (t_{\text{on}} + t_n)$:

$$i_b(t) = I_{BS}$$

$$v_{BE}(t) = V_{BE(\text{sat})}$$

The instantaneous power due to the base current is

$$P_b(t) = i_b v_{BE} = I_{BS} V_{BS(\text{sat})}$$
$$= 8 \times 3 = 24 \text{ W}$$

During the period, $0 \le t \le t_o = (T - t_{\text{on}} - t_n - t_s - t_f)$: $P_b(t) = 0$. The average power loss is

$$P_B = I_{BS} V_{BE(\text{sat})}(t_{\text{on}} + t_n + t_s) f_s \tag{13-35}$$
$$= 8 \times 3 \times (1.5 + 48.5 + 5) \times 10^{-6} \times 10 \times 10^3 = 13.2 \text{ W}$$

13-2.3 Performance Parameters

The characteristics of transistors are normally specified by the manufacturers in terms of certain performance parameters for safe operation. The transistor circuits must be designed so that the operating conditions do not exceed their suggested ratings. Figure 13-12 shows the data sheet of a typical GE-transistor type D67DE, explaining its characteristics.

Dc gain, h_{FE}. h_{FE} (or β) is the ratio of the collector current, I_C to base current, I_B at a specified value of V_{CE}. The gain, which is shown in Fig. 13-12.1 and 13-12.2, is dependent on the temperature. Figure 13-12.1 refers to the characteristic curve number 1 in Fig. 13-12. At the rated collector current, the variation in gain with change in temperature is minimum and the circuit should be designed to operate at the rated value. A high gain would reduce the values of forced β and $V_{CE(\text{sat})}$.

Collector–emitter saturation voltage, $V_{CE(\text{sat})}$. A low value of $V_{CE(\text{sat})}$ will reduce the on-state losses. However, $V_{CE(\text{sat})}$ is a function of the collector current, base current, current gain, and junction temperature. The base drive must be sufficient enough to drive the transistor into saturation, but overdrive will decrease the forced β and increase the losses in the base–emitter junction.

Figure 13-12.3 shows the regions of collector saturation at various collector and base currents. Figure 13-12.4 and 13-12.5 show $V_{CE(\text{sat})}$ against I_C for various forced β. A small value of forced β (or high value of overdrive factor) decreases the value of $V_{CE(\text{sat})}$. However, a higher junction temperature increases the value of $v_{CE(\text{sat})}$.

Collector–base saturation voltage, $V_{BE(\text{sat})}$. A low value of $V_{BE(\text{sat})}$ will decrease the power loss in the base–emitter junction. $V_{BE(\text{sat})}$ increases with collector current and forced β. The transconductance ($g_m = I_C/V_{BE}$) of the transistor can be determined from the curves of $V_{BE(\text{sat})}$ versus I_C as shown in Fig. 13-12.6 and 13-12.7.

Turn-on time, t_{on}. The turn-on time can be decreased by increasing the base drive for a fixed value of collector current. The variations of delay time, t_d, and rise time, t_r, are shown in Fig. 13-12.9. t_d, which is dependent on input capacitances does not change significantly with I_C. However, t_r increases with the increase in I_C.

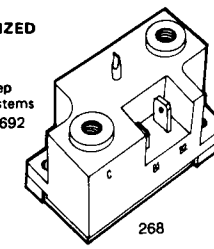
Power Transistors

NPN
D67DE

HI-LINE®
Power Darlington
150 A-PEAK UP TO 500 $V_{CEO(SUS)}$ & 700 V_{CEV}

The General Electric D67DE is a new High Current Power Darlington. It features collector isolation from the heat sink, an internal construction designed for stress-free operation at temperature extremes, hefty screw terminals for emitter and collector connection and quick electrical terminals for B1 and B2. The device is designed to meet UL creep, strike and isolation voltage. Major applications are for motor controls, switching power supplies and UPS systems.

UL RECOGNIZED
- Isolation- 2500 V_{RMS}
- Strike & creep for 460V systems
- File no. E60692



High Voltage: 400 — 500 $V_{CEO(SUS)}$; 500 — 700 V_{CEV}
High Current: 150 Amperes, I_C (Peak)
High Gain: h_{FE} 50 Minimum @ 100 Amperes I_C (h_{FE} 200 typical)

absolute maximum ratings: (T_C = 25°C Unless Otherwise Specified)

		D67DE5	D67DE6	D67DE7	Units
Voltages					
Collector Emitter	V_{CEV}	500	600	700	Volts
Collector Emitter	$V_{CEO\ (SUS)}$	400	450	500	Volts
Emitter Base	V_{EBO}	← 8 →			Volts
Currents					
Collector Current (continuous)	I_C	← 100 →			Amps
Collector Current (peak)	I_C	← 150 →			Amps
Collector Current (Non-Repetitive)	I_{CSM}	← 250 →			Amps
Base Current (continuous)	I_B	← 10 →			Amps
Base Current (peak)	I_B	← 20 →			Amps
Dissipation					
Power Dissipation (T_C = 25°C)	P_D	← 312.5 →			Watts
Temperatures					
Storage	T_{stg}	-40°C to +150°C			
Operating Junction	T_J	-40°C to +150°C			
Isolation Voltage	V_{ISOL}	← 2500 →			Volts (RMS)
Terminal & Mounting Torque Limits Units(1)					
Thermal Resistance	$R_{\Theta JC}$	← .4 →			°C/W

(1) see back page for mounting considerations

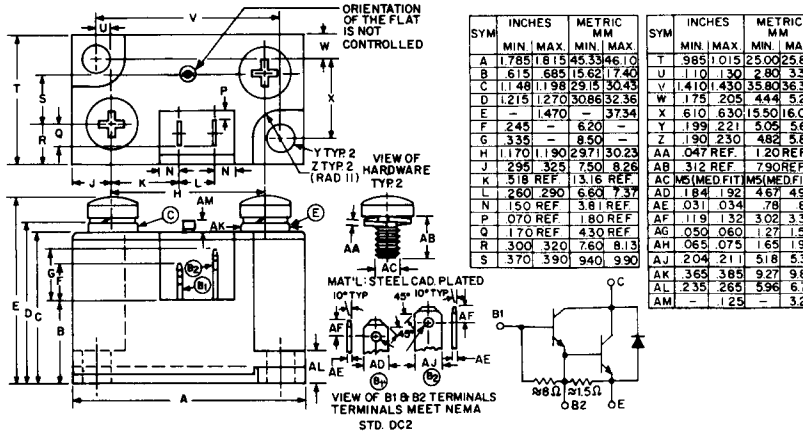
electrical characteristics: (T_C = 25°C Unless Otherwise Specified)

STATIC CHARACTERISTICS		SYMBOL	MIN.	TYP.	MAX.	UNITS
Collector-Emitter Sustaining Voltage						
(I_C = 1A, I_{B1}=I_{B2}=0,)	– D67DE5	$V_{CEO(SUS)}$	400	–	–	Volts
V_{CLAMP} = V_{CEO})	– D67DE6	$V_{CEO(SUS)}$	450	–	–	Volts
	– D67DE7	$V_{CEO(SUS)}$	500	–	–	Volts
Collector Cut-Off Current						
(V_{CEV} = Rated Value,	— T_J = 25°C	I_{CEV}	–	–	2.5	mA
$V_{B1E\ (off)}$ = -1.5V)	— T_J = 150°C	I_{CEV}	–	–	10.0	mA
Emitter-Base Cut-Off Current						
(V_{EB1} = 3.5 V, I_C = O)		I_{EBO}	–	–	500	mA

Figure 13-12 Data sheet of GE transistor, type D67DE. (*Courtesy of General Electric Company*).

STATIC CHARACTERISTICS CONTINUED	SYMBOL	MIN.	TYP.	MAX.	UNITS
DC Current Gain					
(I_C = 150A, V_{CE} = 5V)	h_{FE}	25	90	–	
(I_C = 100A, V_{CE} = 5V)	h_{FE}	50	200	–	
(I_C = 40A, V_{CE} = 5V)	h_{FE}	100	275	–	
Collector-Emitter Saturation Voltage					
(I_C = 150A, I_B = 10A)	$V_{CE(SAT)}$	–	1.9	3.0	Volts
(I_C = 100A, I_B = 8A)	$V_{CE(SAT)}$	–	1.4	2.0	Volts
(I_C = 40A, I_B = 4A)	$V_{CE(SAT)}$	–	1.0	1.5	Volts
Base-Emitter Saturation Voltage					
(I_C = 150A, I_B = 10A)	$V_{BE(SAT)}$	–	2.75	3.5	Volts
(I_C = 100A, I_B = 8A)	$V_{BE(SAT)}$	–	2.3	3.0	Volts
SWITCHING CHARACTERISTICS (Reference Figure 21, Page 474)					
Resistive (V_{CC} = 250V, I_C = 100A, I_{B1} = 5A, $-I_{B1}$ = 10A)					
Delay Time	t_d	–	.105	0.5	μs
Rise Time	t_r	–	.45	1.0	μs
Storage Time	t_s	–	3.2	5.0	μs
Fall Time	t_f	–	1.1	3.0	μs
Inductive (I_C = 100A, V_{CLAMP} = 250V, I_{B1} = 5A, $-I_{B1}$ = 10A, L=100μH)					
Storage Time	t_s	–	3.2	5.0	μs
Fall Time	t_f	–	.6	3.0	μs
Crossover Time	t_c	—	1.8	—	μs
Storage Time (T_J = 150°C)	t_s	—	5.8	—	μs
Fall Time (T_J = 150°C)	t_f	—	1.1	—	μs
Crossover Time (T_J = 150°C)	t_c	—	3.7	—	μs
DIODE CHARACTERISTICS					
Diode Forward Voltage (I_F = 100A)					
— T_J = 25°C	V_F	—	1.9	3.25	Volts
— T_J = 150°C	V_F	—	1.75	3.00	Volts
Diode Reverse Recovery Time (T_J = 25°C)					
(I_F = 100A, di/dt = 25A/μsec, R_{B1E} = .25)	t_{rr}	—	4.5	10.0	μsec
Diode Forward Turn-on Time (T_J = 25°C)					
(I_F = 100A, di/dt = 100A/μsec)	t_{on}	—	1.7	2.5	μsec
Thermal Resistance	$R_{\theta JC}$	–	–	0.4	°C/W

DIMENSIONAL OUTLINE



SYM	INCHES MIN.	INCHES MAX.	METRIC MM MIN.	METRIC MM MAX.
A	1.785	1.815	45.33	46.10
B	.615	.685	15.62	17.40
C	1.148	1.198	29.15	30.43
D	1.215	1.270	30.86	32.36
E	–	1.470	–	37.34
F	.245	–	6.20	–
G	.335	–	8.50	–
H	1.170	1.190	29.71	30.23
J	.295	.325	7.50	8.26
K	.518 REF		13.16 REF	
L	.260	.290	6.60	7.37
N	.150 REF		3.81 REF	
P	.070 REF		1.80 REF	
Q	.170 REF		4.30 REF	
R	.300	.320	7.60	8.13
S	.370	.390	9.40	9.90

SYM	INCHES MIN.	INCHES MAX.	METRIC MM MIN.	METRIC MM MAX.
T	.985	1.015	25.00	25.80
U	1.10	1.30	2.80	3.30
V	1.410	1.430	35.80	36.32
W	.175	.205	4.44	5.20
X	.610	.630	15.50	16.00
Y	.199	.221	5.05	5.61
Z	.190	.230	4.82	5.84
AA	.047 REF.		1.20 REF.	
AB	.312 REF.		7.90 REF.	
AC	MS (MED FIT)		MS (MED FIT)	
AD	1.84	1.92	4.67	4.90
AE	.031	.034	.78	.86
AF	1.19	1.32	3.02	3.35
AG	.050	.060	1.27	1.52
AH	.065	.075	1.65	1.90
AJ	2.04	2.11	5.18	5.36
AK	.365	.385	9.27	9.80
AL	2.35	2.65	5.96	6.73
AM	–	1.25	–	3.20

Figure 13-12 *(continued)*

TYPICAL CHARACTERISTICS

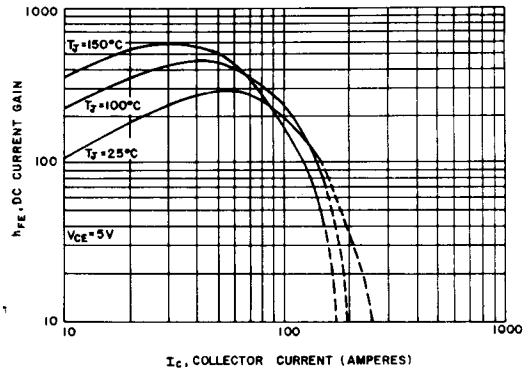


FIGURE 1: DC CURRENT GAIN (V_{CE} = 5V)

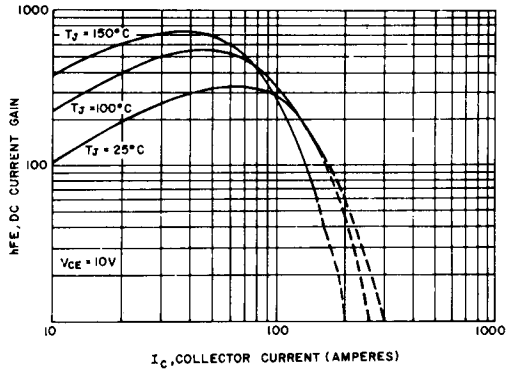


FIGURE 2: DC CURRENT GAIN (V_{CE} = 10V)

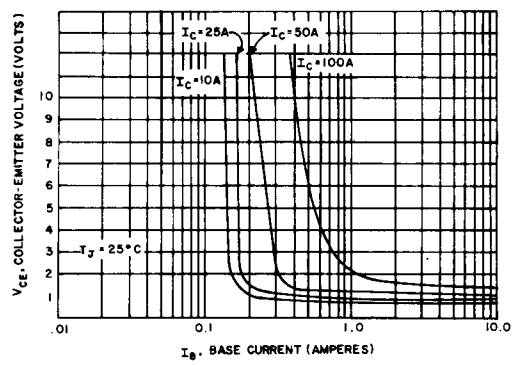


FIGURE 3: COLLECTOR SATURATION REGION

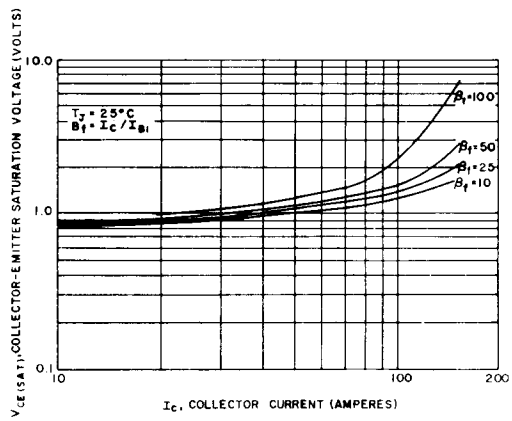


FIGURE 4: $V_{CE(SAT)}$ VS I_C, T_J=25°C

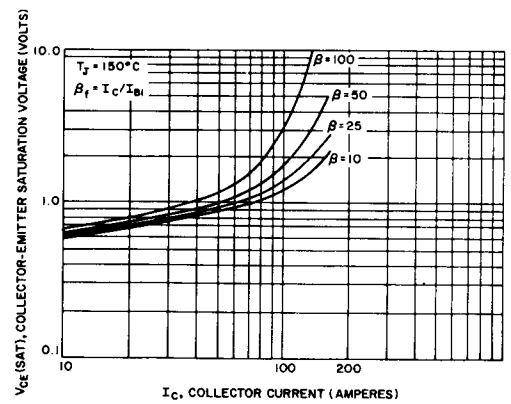


FIGURE 5: $V_{CE(SAT)}$ VS I_C, T_J=150°C

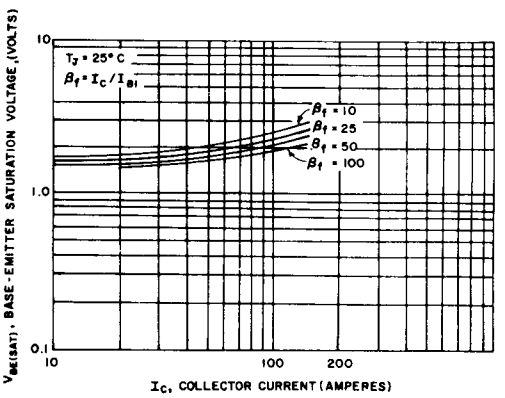


FIGURE 6: $V_{BE(SAT)}$ VS I_C, T_J=25°C

Figure 13-12 (*continued*)

TYPICAL CHARACTERISTICS

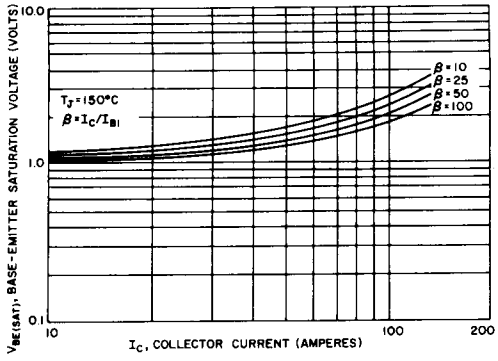


FIGURE 7: $V_{BE(SAT)}$ VS I_C, T_J=150°C

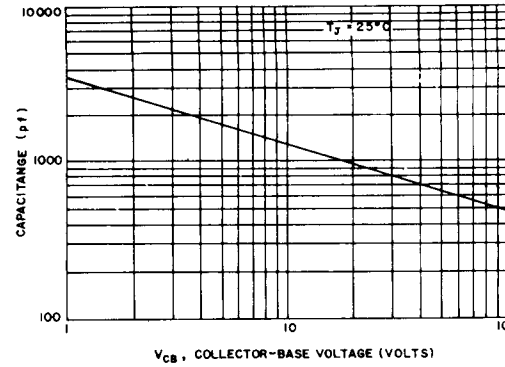


FIGURE 8: CAPACITANCE (C_{CBO})

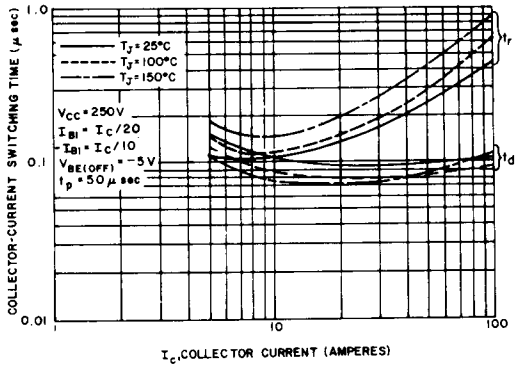


FIGURE 9: TURN-ON TIME (RESISTIVE LOAD)

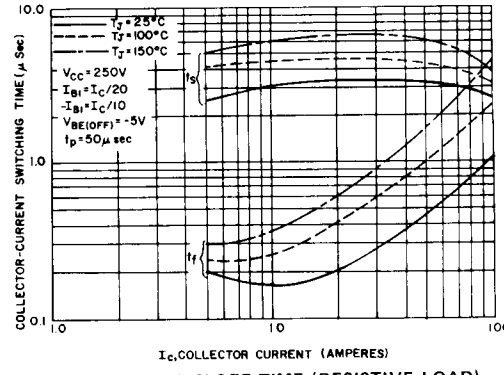


FIGURE 10: TURN-OFF TIME (RESISTIVE LOAD)

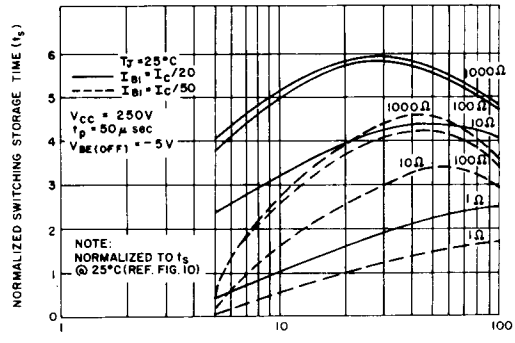


FIGURE 11: NORMALIZED RESISTIVE SWITCHING STORAGE TIME (R_{BE} VARIATIONS) VS COLLECTOR CURRENT

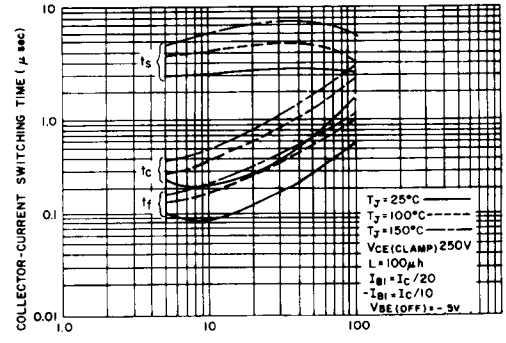


FIGURE 12: CLAMPED INDUCTIVE TURN-OFF TIME

Figure 13-12 *(continued)*

D67DE

TYPICAL CHARACTERISTICS

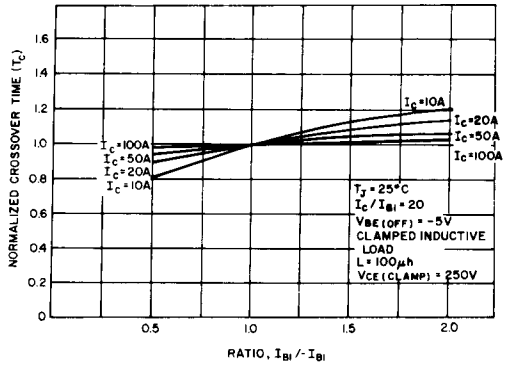


FIGURE 13: CROSSOVER TIME VARIATION WITH $-I_{B1}$

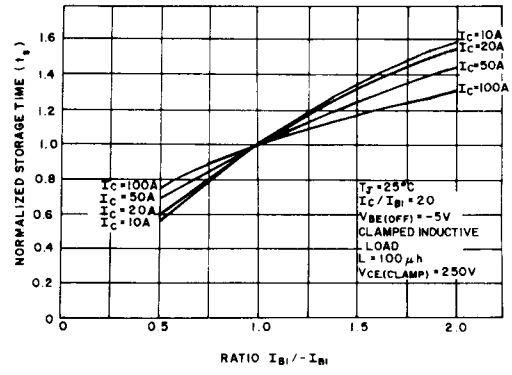


FIGURE 14: STORAGE TIME VARIATION WITH $-I_{B1}$

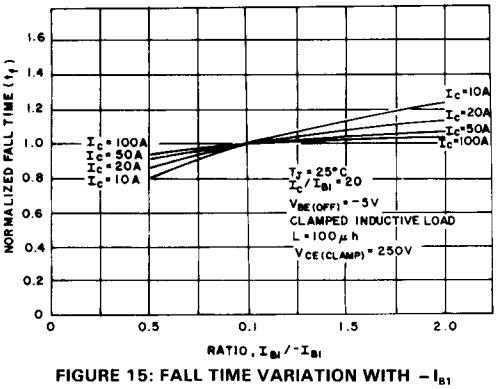


FIGURE 15: FALL TIME VARIATION WITH $-I_{B1}$

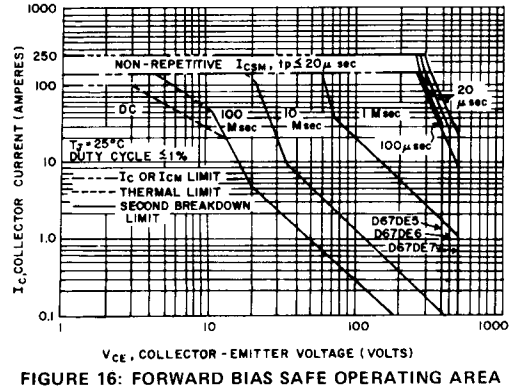


FIGURE 16: FORWARD BIAS SAFE OPERATING AREA

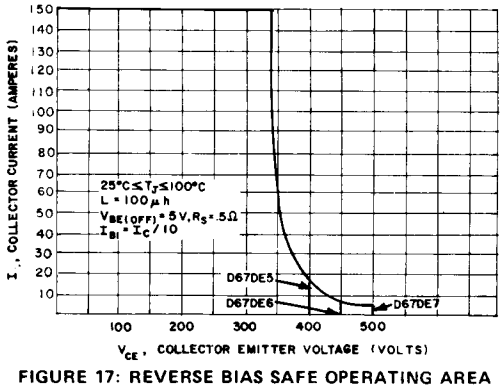


FIGURE 17: REVERSE BIAS SAFE OPERATING AREA (CLAMPED)

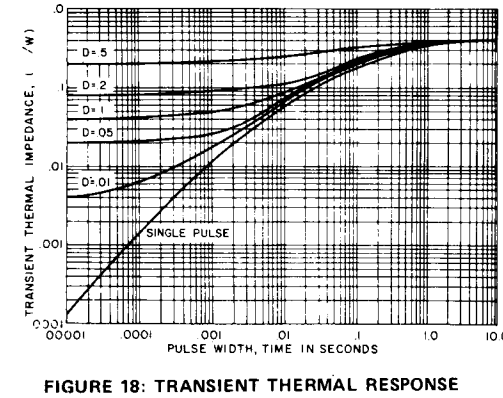


FIGURE 18: TRANSIENT THERMAL RESPONSE

Figure 13-12 *(continued)*

TYPICAL CHARACTERISTICS

D67DE

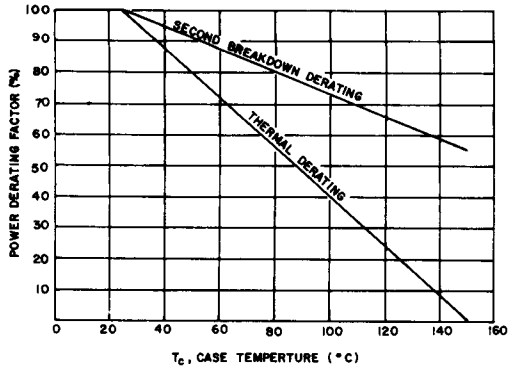


FIGURE 19: POWER DERATING

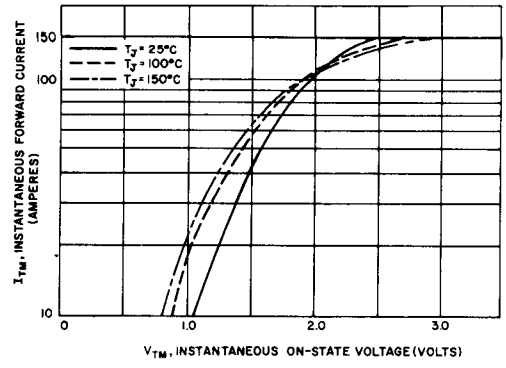


FIGURE 20: DIODE FORWARD CHARACTERISTICS

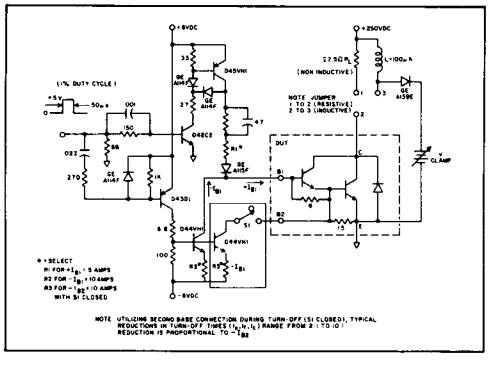
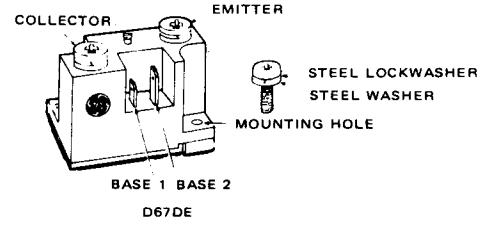


FIGURE 21: SWITCHING TIME TEST CIRCUITS FOR:
- RESISTIVE & INDUCTIVE SWITCHING
- USING BASE 1 ONLY
- USING BASE 1 AND BASE 2



MOUNTING AND ELECTRICAL TERMINATION PROCEDURES

HEAT SINK FLATNESS

Heat sink surfaces must be flat within ±1.5 mils/inch (0.015mm/cm) over the mounting area and must have a surface finish of < 64 micro inches (1.62 microns).

THERMAL COMPOUND

To minimize the effects of flatness differential and/or voids between the base plate and the heat sink, apply a very thin layer of GE #6644 or Dow Corning #4 thermal compound to the back of the base plate and the heat sink. NOTE: excessive thermal compound *will not* squeeze out from underneath the device during mountdown. After applying thermal compound to the device and the heat sink, place the device on the heat sink and rotate slowly to distribute grease. Check both surfaces for uniform coverage before applying torque to mounting screws.

WARNING

THE PRODUCTS DESCRIBED IN THIS SPECIFICATION SHEET SHOULD BE HANDLED WITH CARE. THE CERAMIC PORTION (INTERNAL ISOLATION) OF THIS PRODUCT MAY CONTAIN **BERYLLIUM OXIDE** AS A MAJOR INGREDIENT.

DO NOT CRUSH, GRIND, OR ABRADE THESE PORTIONS OF THE PRODUCT BECAUSE THE DUST RESULTING FROM SUCH ACTION MAY BE HAZARDOUS IF INHALED.

MOUNTING

HARDWARE: Standard #10 or M5
7/16" – ½"OD
(11 " 13mm)OD

TORQUE: 19-25 lb.-in. (2-3 NM)

ELECTRICAL TERMINATION

COLLECTOR & EMITTER:
Screw: M5 × 8mm
Lockwasher: 9.2 – 13mm OD
Torque: 25 – 28 lb. - in.
(2.8 – 3.2 NM)

BASE:
Base 1: FASTON-AMP #640917-1
BASE 2: FASTON-AMP #640903-1
(or equivalents)

Figure 13-12 *(continued)*

NPN
D66GV

HI-LINE®

PWM POWER DARLINGTON

D66GV5,6,7

50 AMPERES
400 TO 500 VOLTS
FAST SWITCHING

The D66GV is a new high voltage NPN High Current Power Darlington especially designed for use in PWM applications where fast and efficient switching is required. This device utilizes GE's latest advances in Bipolar Technology and features the Hi-Line® Industrial Package offering: collector isolation from heat sink, TO-3 mounting compatibility and quick-connect terminals.

The D66GV also features a discrete fast recovery antiparallel high power diode which eliminates the need for an external flyback diode in motor control and other inverter applications such as power supplies and UPS systems.

Features

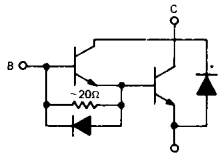
- Fast switching — $t_{f(TYP)}$ 0.5 μs
- High blocking voltage — V_{CEV} 500 to 700 VOLTS
- High current — $I_{C(PEAK)}$ 75 AMPS
- High gain — $h_{FE(MIN)}$ 50 @ 50 AMPS
- Discrete high power fast recovery diode
- UL recognized isolated base package

ISOLATED TO-3 BASE INDUSTRIAL PACKAGE

UL RECOGNIZED
- Isolation- 2500 V_{RMS}
- Strike & creep for 460V systems
- File No. E60692



CIRCUIT DIAGRAM



*NOTE: The collector-emitter diode is a discrete fast-recovery high power diode.

maximum ratings (T_C = 25°C) (unless otherwise specified)

RATING	SYMBOL	D66GV5	D66GV6	D66GV7	UNIT
Collector-Emitter Voltage	V_{CEV}	500	600	700	Volts
Collector-Emitter Voltage	$V_{CER(sus)}$	400	450	500	Volts
Emitter-Base Voltage	V_{EBO}	7			Volts
Collector-Continuous Current	I_C	50			Amps
-Peak (Repetitive)	I_{CM}	75			
-Peak (Non-Repetitive)	I_{CSM}	125			
Base-Continuous Current	I_B	10			Amps
-Peak (Non-Repetitive)	I_{BM}	20			
Power Dissipation (T_C =25°C) Derate Above 25°C	P_D	125 1.0			Watts W/°C
Isolation Voltage	V_{ISOL}	2500			$V_{(RMS)}$

thermal characteristics

Operating and Storage Junction Temperature Range	T_J, T_{STG}	-40°C to +150°C	°C
Thermal Resistance (Transistor) (Diode)	$R_{\theta JC}$	1.0 2.5	°C/W

Figure 13-12 *(continued)*

TYPICAL CHARACTERISTICS

D66DV
D66EV

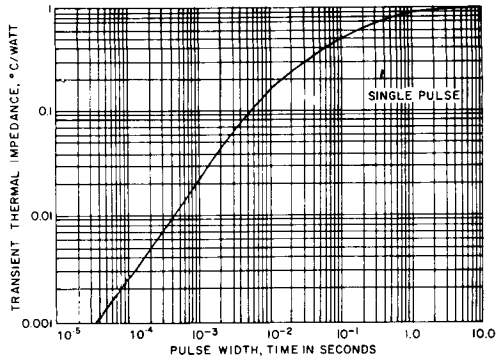


FIGURE 25. TRANSIENT THERMAL RESPONSE

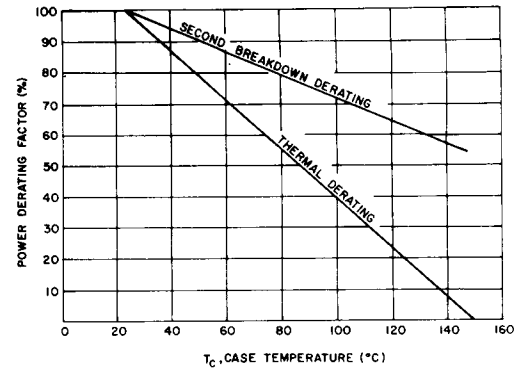


FIGURE 26. POWER DERATING

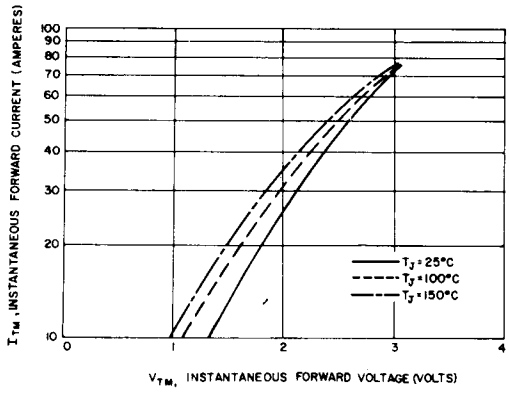


FIGURE 27. DIODE FORWARD CHARACTERISTICS

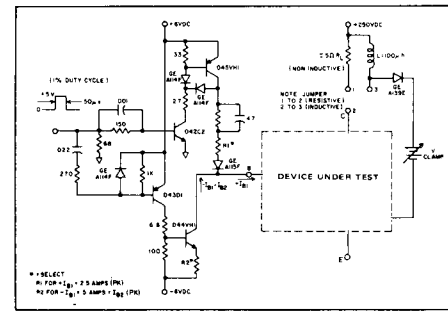


FIGURE 28. SWITCHING TIME TEST CIRCUIT

Figure 13-12 (*continued*)

Turn-off time, t_{off}. The storage time, t_s, which is dependent on the overdrive factor does not change significantly with I_C. The fall time, t_f, which is a function of capacitances increases with I_C as shown in Fig. 13-12.10. t_s and t_f can be reduced by providing negative base drive during turn-off as shown in Fig. 13-12.11 and 13-12.14. However, Fig. 13-12.15 shows that t_f is less sensitive to negative base drive.

Crossover time, t_c. The crossover time, t_c, is defined as the interval during which the collector voltage, V_{CE}, rises from 10% of its peak off-state value and collector current, I_C, falls to 10% of its on-state value. The variations of t_c, which is a function of collector current and negative base drive, are shown in Fig. 13-12.13.

Second breakdown, SB. The secondary breakdown (SB), which is a destructive phenomenon, results from the current flow to a small portion of the base, producing localized hot spots. If the energy in these hot spots is sufficient, the excessive localized heating may damage the transistor. Thus secondary breakdown is caused by a localized thermal runway, resulting from high current concentrations. The current concentration may be caused by defects in the transistor structure. The SB occurs at certain combinations of voltage, current, and time. Since the time is involved, the secondary breakdown is basically an energy dependent phenomenon.

Figure 13-12.16 indicates that the shorter the on-time, the more the applicable FBSOA boundaries extend into higher voltage and current areas. This is also a fact that for very short on-times, the secondary breakdown limit disappears from the FBSOA curves. The SB can occur under forward-bias and reverse-bias conditions. The application of reverse base drive will cause base current in the reverse direction. However, the potential gradients may reverse bias only the periphery of the base, where the center of the base may still be forward biased. The current may be flowing in a small area toward the center of the base, resulting in current concentration forming a hot spot.

Forward-biased safe operating area, FBSOA. During turn-on and on-state conditions, the average junction temperature and second breakdown limit the power-handling capability of a transistor. The manufacturers usually provide the FBSOA curves under specified test conditions. FBSOA indicates the i_c–v_{CE} limits of the transistor; and for reliable operation the transistor must not be subjected to greater power dissipation than that shown by the FBSOA curve.

Figure 13-12.16 shows the typical FBSOA curves at a junction temperature of $T_J = 25°C$. The dc power dissipation in a transistor is $P_T = V_{CE}I_C$. Under dc or continuous current operation, first limit is the peak current (e.g., $I_{CM} = 100$ A for $V_{CE} = 1 - 3$ V). From $V_{CE} = 3 - 14$ V, the collector current has to be reduced to limit the junction temperature within the maximum value. At about $V_{CE} = 14$, the secondary breakdown occurs and for V_{CE} above 14 V, the collector current is reduced due to secondary breakdown limit. Under pulsed operation, the peak power can be more than the average power as long as the junction temperature does not exceed its maximum limit. The FBSOA increases with shorter pulse duration.

Reverse-biased safe operating area, RBSOA. During turn-off, a high current and high voltage must be sustained by the transistor, in most cases with the base-to-emitter junction reverse biased. The collector–emitter voltage must be held to a safe level at or below a specified value of collector current. The manufacturers provide the I_C–V_{CE} limits during reverse-biased turn-off as reverse-biased safe operating area (RBSOA). Figure 13-12.17 shows a typical RBSOA curve.

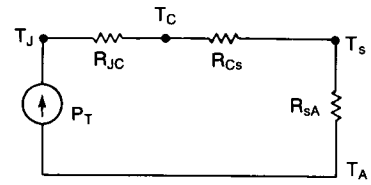


Figure 13-13 Thermal equivalent circuit of a transistor.

Power derating. The thermal equivalent circuit is shown in Fig. 13-13. If the total average power loss is P_T, the case temperature is

$$T_C = T_J - P_T R_{JC}$$

The sink temperature is

$$T_S = T_C - P_T R_{CS}$$

The ambient temperature is

$$T_A = T_S - P_T R_{SA}$$

and

$$T_J - T_A = PT(R_{JC} + R_{CS} + R_{SA}) \tag{13-36}$$

where R_{JC} = thermal resistnace junction to case, °C/W
R_{CS} = thermal resistance case to sink, °C/W
R_{SA} = thermal resistance sink to ambient, °C/W

The maximum power dissipation P_T is normally specified at $T_C = 25°C$. If the ambient temperature is increased to $T_A = T_{J(max)} = 150°C$, the transistor can dissipate zero power. On the other hand, if the junction temperature is $T_C = 0°C$, the device can dissipate maximum power and this is not practical. Therefore, the ambient temperature and thermal resistances must be considered when interpreting the ratings of devices. Figure 13-12.19 shows the derating curves for the thermal derating and second breakdown derating. These derating factors must be considered when using the FBSOA and RBSOA curves.

Breakdown voltages. A *breakdown voltage* is defined as the absolute maximum voltage between two terminals with the third terminal open, shorted, or biased in either forward or reverse direction. At breakdown the voltage remains relatively constant, where the current rises rapidly. The following breakdown voltages are quoted by the manufacturers:

V_{EBO}: the maximum voltage between the emitter terminal and base terminal with collector terminal open circuited. For the transistor in Fig. 13-12, it is 8 V.

V_{CEV} *or* V_{CEX}: the maximum voltage between the collector terminal and emitter terminal at a specified negative voltage applied between base and emitter.

$V_{CEO(SUS)}$: the maximum sustaining voltage between the collector terminal and emitter terminal with the base open circuited. This rating is specified at the maximum collector current and voltage, appearing simultaneously across the device

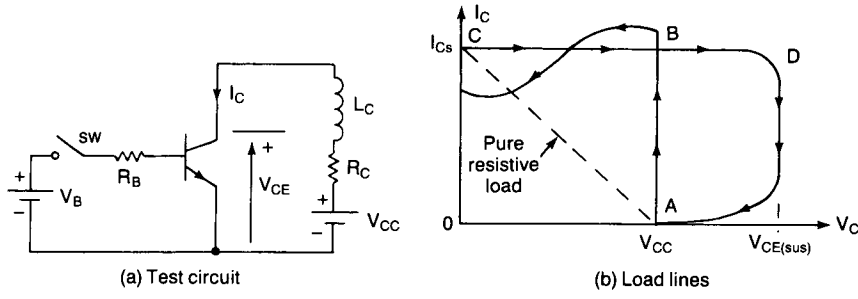


Figure 13-14 Turn-on and turn-off load lines.

with a specified value of load inductance. From Fig. 13-12.17, $V_{CEO(SUS)} = 500$ V for transistor of type D67DE7.

Let us consider the circuit in Fig. 13-14a. When the switch SW is closed, the collector current increases, and after a transient, the steady-state collector current is $I_{CS} = (V_{CC} - V_{CE(sat)})/R_C$. For an inductive load, the load line would be the path ABC shown in Fig. 13-14b. If the switch is opened to remove the base current, the collector current will begin to fall and a voltage of $L(di/dt)$ will be induced across the inductor to oppose the current reduction. The transistor will be subjected to a transient voltage. If this voltage reaches the sustaining voltage level, the collector voltage remains approximately constant and the collector current will fall. After a small time, the transistor will be in the off-state and the turn-off load line is shown in Fig. 13-14b by the path CDA.

Example 13-4

The maximum junction temperature of a transistor is $T_J = 150°C$ and the ambient temperature is $T_A = 25°C$. If the thermal impedances are $R_{JC} = 0.4°C/W$, $R_{CS} = 0.1°C/W$, and $R_{SA} = 0.5°C/W$, calculate the (a) maximum power dissipation, (b) case temperature, and (c) thermal and second breakdown derating factors from Fig. 13-12.19.

Solution (a) $T_J - T_A = P_T(R_{JC} + R_{CS} + R_{SA}) = P_T R_{JA}$, $R_{JA} = 0.4 + 0.1 + 0.5 = 1.0$, and $150 - 25 = 1.0P_T$, which gives the maximum power dissipation as $P_T = 125$ W.

(b) $T_C = T_J - P_T R_{JC} = 150 - 125 \times 0.4 = 100°C$.

(c) For $T_C = 100°C$, Fig. 13-12.19 gives a thermal derating factor of 40% and second breakdown derating factor of 73%.

Example 13-5

A bipolar transistor GE type D67DE is used as a chopper switch for a resistive load. The collector current is $I_C = 50$ A at a forced β of $\beta_F = 25$. If the junction temperature is $T_J = 150°C$, calculate the (a) $V_{CE(sat)}$; (b) $V_{BE(sat)}$; (c) turn-on time, t_{on}; (d) turn-off time, t_{off}; (e) base current to drive the transistor into saturation, I_{BS}; and (f) overdrive factor, ODF.

Solution $\beta_F = 25$ and $I_C = 50$ A.

(a) Figure 13-12.5 gives $V_{CE(sat)} = 0.95$ V.

(b) Figure 13-12.7 gives $V_{BE(sat)} = 1.7$ V.

(c) Figure 13-12.9 gives, $t_r = 0.4$ μs, $t_d = 0.085$ μs; therefore, $t_{on} = t_d + t_r = 0.485$ μs.

(d) Figure 13-12.10 gives $t_f = 1.8$ μs, $t_s = 6$ μs; therefore, $t_{off} = t_s + t_f = 6 + 1.8 = 7.8$ μs.

(e) Figure 13-12.3 indicates that at $I_C = 50$ A the transistor will operate in the saturation region if the base current is approximately, $I_{BS} = 0.4$ A.

(f) If $\beta_F = 25 = 50/I_{B1} = I_C/I_{B1}$, $I_{B1} = I_B = 2$ A. Therefore, the overdrive factor is ODF $= I_B/I_{BS} = 2/0.4 = 5.0$ A.

13-2.4 Base Drive Control

The switching speed can be increased by reducing turn-on time, t_{on}, and turn-off time, t_{off}. t_{on} can be reduced by allowing base current peaking during turn-on, resulting in low forced $\beta(\beta_F)$ at the beginning. After turn-on, β_F can be increased to a suffficiently high value to maintain the transistor in the quasi-saturation region. t_{off} can be reduced by reversing base current and allowing base current peaking during turn-off. Increasing the value of I_{B2} decreases the storage time. A typical waveform for base current is shown in Fig. 13-15.

Apart from a fixed shape of base current as in Fig. 13-15, the forced β may be controlled continuously to match the collector current variations. The commonly used techniques for optimizing the base drive of a transistor are:

1. Turn-on control
2. Turn off-control
3. Proportional base control
4. Antisaturation control

Turn-on control. The base current peaking can be provided by the circuit in Fig. 13-16. When the input voltage is turned on, the base current is limited by resistor R_1 and the initial value of base current is

$$I_{B0} = \frac{V_1 - V_{BE}}{R_1} \tag{13-37}$$

and the final value of the base current is

$$I_{B1} = \frac{V_1 - V_{BE}}{R_1 + R_2} \tag{13-38}$$

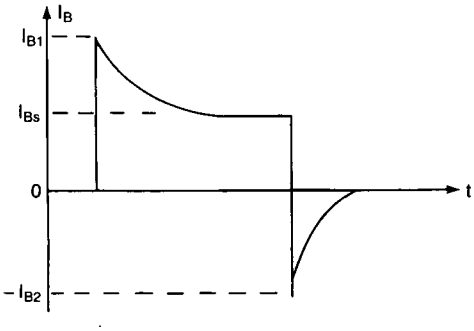


Figure 13-15 Base drive current waveform.

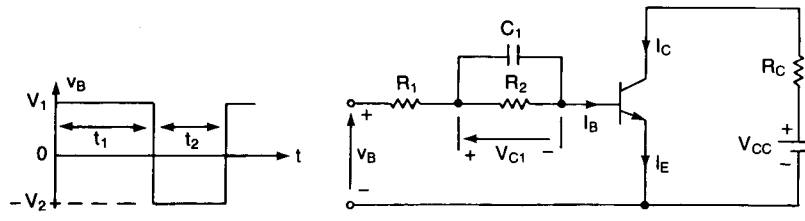


Figure 13-16 Base current peaking during turn-on.

The capacitor C_1 charges up to a final value of

$$V_c \cong V_1 \frac{R_2}{R_1 + R_2} \tag{13-39}$$

The charging time constant of the capacitor is

$$\tau_1 = \frac{R_1 R_2 C_1}{R_1 + R_2} \tag{13-40}$$

Once the input voltage v_B becomes zero, the base–emitter junction is reverse biased and C_1 discharges through R_2. The discharging time constant is $\tau_2 = R_2 C_1$. To allow sufficient charging and discharging times, the width of the base pulse must be $t_1 \geq 5\tau_1$ and the off-period of the pulse must be $t_2 \geq 5\tau_2$. The maximum switching frequency is $f_s = 1/T = 1/(t_1 + t_2) = 0.2/(\tau_1 + \tau_2)$.

Turn-off control. If the input voltage in Fig. 13-16 is changed to $-V_2$ during turn-off, the capacitor voltage V_c in Eq. (13-39) is added to V_2 as a reverse voltage across the transistor. There will be base-current peaking during turn-off. As the capacitor C_1 discharges, the reverse voltage will be reduced to a steady-state value, V_2. If different turn-on and turn-off characteristics are required, a turn-off circuit (using C_2, R_3, and R_4) as shown in Fig. 13-17 may be added. The diode D_1 isolates the forward base drive circuit from the reverse base drive circuit during turn-off.

Proportional base control. This type of control has advantages over the constant drive circuit. If the collector current changes due to change in load demand, the base drive current is changed in proportion to the collector current. A typical arrangement is shown in Fig. 13-18. When switch S_1 is turned on, a pulse current of short duration would flow through the base of transistor Q_1; and

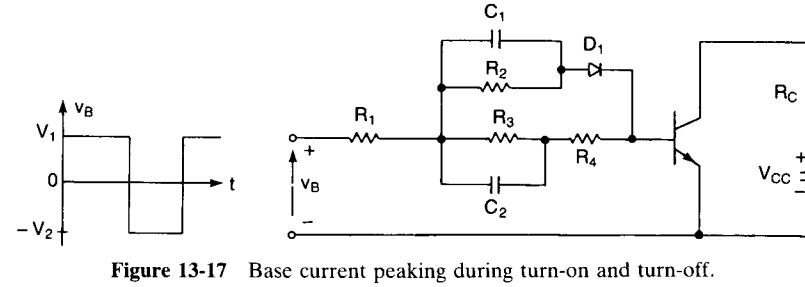


Figure 13-17 Base current peaking during turn-on and turn-off.

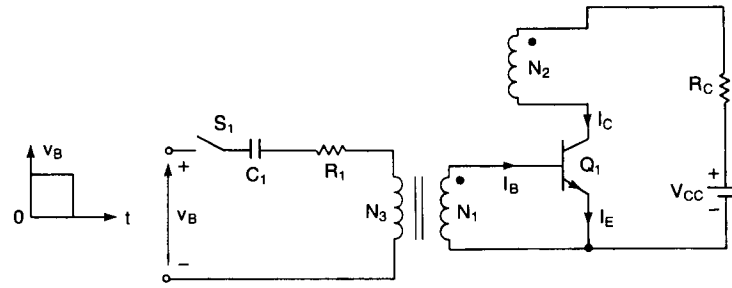


Figure 13-18 Proportional base drive circuit.

Q_1 is turned on into saturation. Once the collector current starts to flow, a corresponding base current is induced due to the transformer action. The transistor would latch on itself, and S_1 can be turned off. The turns ratio is $N_2/N_1 = I_C/I_B = \beta$. For proper operation of the circuit, the magnetizing current, which must be much smaller than the collector current, should be as small as possible. The switch S_1 can be implemented by a small-signal transistor and additional arrangement is necessary to discharge capacitor C_1 and reset the transformer core during turn-off of the power transistor.

Antisaturation control. If the transistor is driven hard, the storage time, which is proportional to the base current, increases and the switching speed is reduced. The storage time can be reduced by operating the transistor in soft saturation rather than hard saturation. This can be accomplished by clamping the collector–emitter voltage to a predetermined level and the collector current is given by

$$I_C = \frac{V_{CC} - V_{cm}}{R_C} \tag{13-41}$$

where V_{cm} is the clamping voltage and $V_{cm} > V_{CE(sat)}$. A typical circuit with clamping action (also known as Baker's clamp) is shown in Fig. 13-19.

The base current, which is adequate to drive the transistor hard, can be found from

$$I_B = I_1 = \frac{V_B - V_{d1} - V_{BE}}{R_B} \tag{13-42}$$

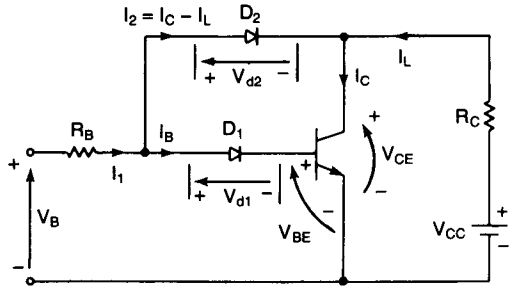


Figure 13-19 Collector clamping circuit.

and the corresponding collector current is

$$I_C = I_L = \beta I_B \tag{13-43}$$

After the collector current rises, the transistor is turned on, and the clamping takes place (due to the fact that D_2 gets forward biased and conducts), then

$$V_{CE} = V_{BE} + V_{d1} - V_{d2} \tag{13-44}$$

The load current is

$$I_L = \frac{V_{CC} - V_{CE}}{R_C} = \frac{V_{CC} - V_{BE} - V_{d1} + V_{d2}}{R_C} \tag{13-45}$$

and the collector current with clamping is

$$\begin{aligned} I_C = \beta I_B &= \beta(I_1 - I_C + I_L) \\ &= \frac{\beta}{1 + \beta}(I_1 + I_L) \end{aligned} \tag{13-46}$$

For clamping, $V_{d1} > V_{d2}$ and this can be accomplished by connecting two or more diodes in place of D_1. The load resistance R_C should satisfy the condition

$$\beta I_B > I_L$$

From Eq. (13-45),

$$\beta I_B R_C > (V_{CC} - V_{BE} - V_{d1} + V_{d2}) \tag{13-47}$$

The clamping action thus results in a reduced collector current and almost elimination of the storage time. At the same time, a fast turn-on is accomplished. However, due to increased V_{CE}, the on-state power dissipation in the transistor is increased, whereas the switching power loss is decreased.

Example 13-6

The base drive circuit in Fig. 13-19 has $V_{CC} = 100$ V, $R_C = 1.5\ \Omega$, $V_{d1} = 2.1$ V, $V_{d2} = 0.9$ V, $V_{BE} = 0.7$ V, $V_B = 15$ V, and $R_B = 2.5\ \Omega$, and $\beta = 16$. Calculate the (a) collector current without clamping; (b) collector-emitter clamping voltage, V_{CE}; and (c) collector current with clamping.

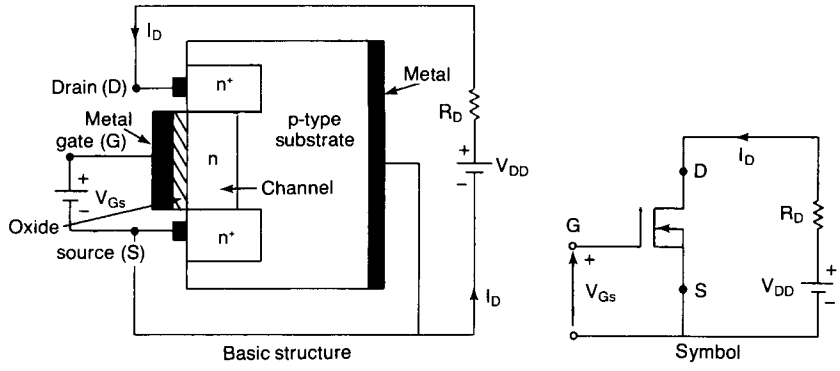
Solution (a) From Eq. (13-42), $I_1 = (15 - 2.1 - 0.7)/2.5 = 4.88$ A. Without clamping, $I_C = 16 \times 4.88 = 78.08$ A.

(b) From Eq. (13-44), the clamping voltage is

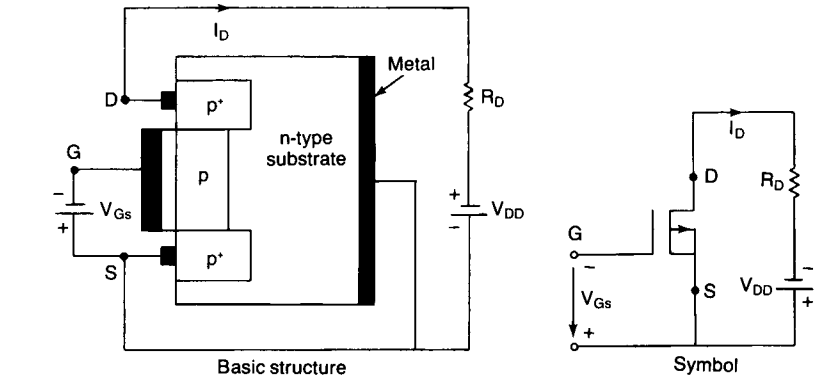
$$V_{CE} = 0.7 + 2.1 - 0.9 = 1.9 \text{ V}$$

(c) From Eq. (13-45), $I_L = (100 - 1.9)/1.5 = 65.4$ A. Equation (13-46) gives the collector current with clamping:

$$I_C = 16 \times \frac{4.88 + 65.4}{16 + 1} = 66.15 \text{ A}$$



(a) n-channel depletion-type MOSFET



(b) p-channel depletion-type MOSFET

Figure 13-20 Depletion-type MOSFETs.

13-3 POWER MOSFETs

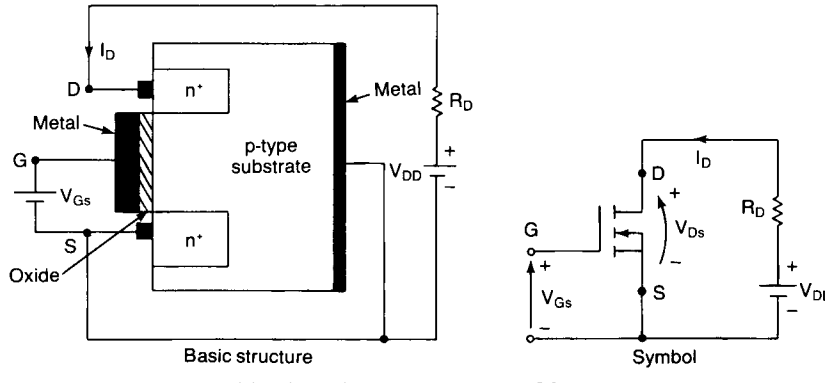
A bipolar junction transistor (BJT) is a current-controlled device and requires base current for current flow in the collector. Since the collector current is dependent on the input (or base) current, the current gain is highly dependent on the junction temperature.

A power MOSFET is a voltage-controlled device and requires only a small input current. The switching speed is very high and the switching times are of the order of nanoseconds. Power MOSFETS are finding increasing applications in low-power high-frequency converters. MOSFETs do not have the problems of second breakdown phenomena as do BJTs. However, MOSFETs have the problems of electrostatic discharge and require special care in handling. In addition, it is relatively difficult to protect them under short-circuited fault conditions.

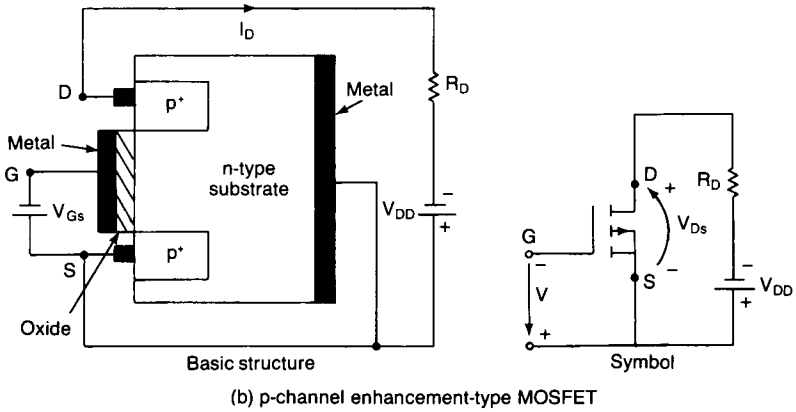
MOSFETs are two types: (1) depletion MOSFETs, and (2) enhancement MOSFETs. An *n*-channel depletion-type MOSFET is formed on a *p*-type silicon substrate as shown in Fig. 13-20a, with two heavily dopped n^+ silicon for low-

resistance connections. The gate is isolated from the channel by a thin oxide layer. The three terminals are called *gate, drain*, and *source*. The substrate is normally connected to the source. The gate-to-source voltage, V_{GS}, could be either positive or negative. If V_{GS} is negative, some of the electrons in the *n*-channel area will be repelled and a depletion region will be created below the oxide layer, resulting in a narrower effective channel and high resistance from the drain to source, R_{DS}. If V_{GS} is made negative enough, the channel will be completely depleted, offering a high value of R_{DS}, and there will be no current flow from the drain to source, $I_{DS} = 0$. The value of V_{GS} when this happens is called *pinch-off voltage*, V_p. On the other hand, V_{GS} is made positive, the channel becomes wider, and I_{DS} increases due to reduction in R_{DS}. With a *p*-channel depletion-type MOSFET, the polarities of V_{DS}, I_{DS}, and V_{GS} are reversed.

An *n*-channel enhancement-type MOSFET has no channel, as shown in Fig. 13-21. If V_{GS} is positive, an induced voltage will attract the electrons from the *p*-substrate and accumulate them at the surface beneath the oxide layer. If V_{GS} is greater than or equal to a value known as *threshold voltage*, V_T, a sufficient number



(a) n-channel enhancement-type MOSFET



(b) p-channel enhancement-type MOSFET

Figure 13-21 Enhancement-type MOSFETs.

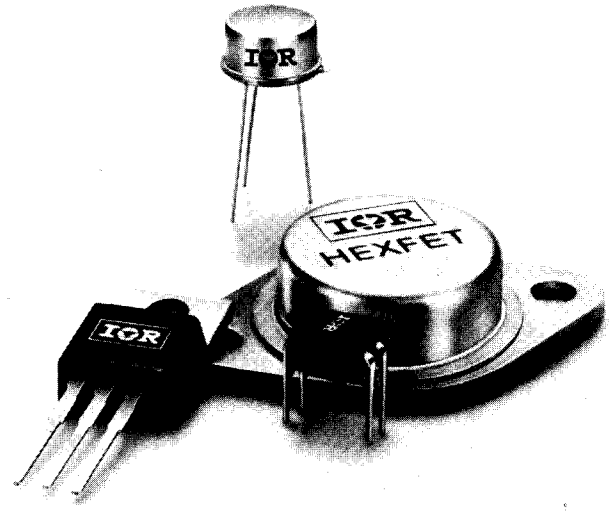


Figure 13-22 Power MOSFETs. (*Courtesy of International Rectifier*).

of electrons are accumulated to form a virtual *n*-channel and the current flows from the drain to source. The polarities of V_{DS}, I_{DS}, and V_{GS} are reversed for a *p*-channel enhancement-type MOSFET. Power MOSFETs of various sizes are shown in Fig. 13-22.

13-3.1 Steady-State Characteristics

The MOSFETs are voltage-controlled devices and have very high input impedance. The gate draws a very small leakage current, in the order of nanoamperes. The current gain, which is the ratio of drain current, I_D, to input gate current, I_G, is typically on the order of 10^9. However, the current gain is not an important parameter. The *transconductance*, which is the ratio of drain current to gate voltage, defines the transfer characteristics and is a very important parameter.

The transfer characteristics of *n*-channel and *p*-channel MOSFETS are shown in Fig. 13-23. Figure 13-24 shows the output characteristics of an *n*-channel enhancement MOSFET. There are three regions of operation: (1) cutoff region, where $V_{GS} \leq V_T$; (2) pinch-off or saturation region, where $V_{DS} \geq V_{GS} - V_T$; and (3) linear region, where $V_{DS} \leq V_{GS} - V_T$. The pinch-off occurs at $V_{DS} = V_{GS} - V_T$. In the linear region, the drain current, I_D varies in proportion to the drain–source voltage, V_{DS}. Due to high drain current and low drain voltage, the power transistors are operated in the linear region for switching actions. In the saturation region, the drain current remains almost constant for any increase in the value of V_{DS} and the transistors are used in this region for voltage amplification. It should be noted that saturation has the opposite meaning to that for bipolar transistors.

The steady-state model, which is the same for both depletion-type and enhancement-type MOSFETs, is shown in Fig. 13-25. The transconductance, g_m, is

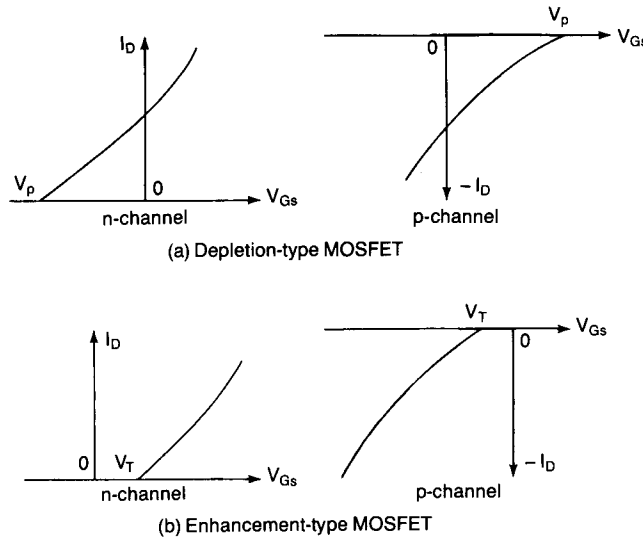


Figure 13-23 Transfer characterisitics of MOSFETs.

defined as

$$g_m = \left.\frac{I_D}{V_{GS}}\right|_{V_{DS}=\text{constant}} \tag{13-48}$$

The output resistance, $r_o = R_{DS}$, which is defined as

$$R_{DS} = \frac{\Delta V_{DS}}{\Delta I_D} \tag{13-49}$$

is normally very high in the pinch-off region, typically on the order of megohms and is very small in the linear region, typically on the order of milliohms.

For the depletion-type MOSFETs, the gate (or input) voltage could be either positive or negative. But the enhancement-type MOSFETs respond to a positive gate voltage only. The power MOSFETs are generally of enhancement type.

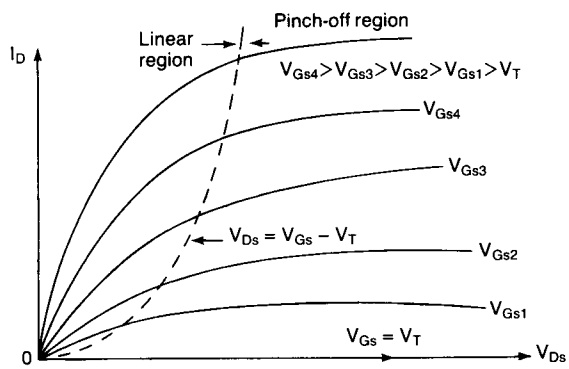


Figure 13-24 Output characteristics of enhancement-type MOSFET.

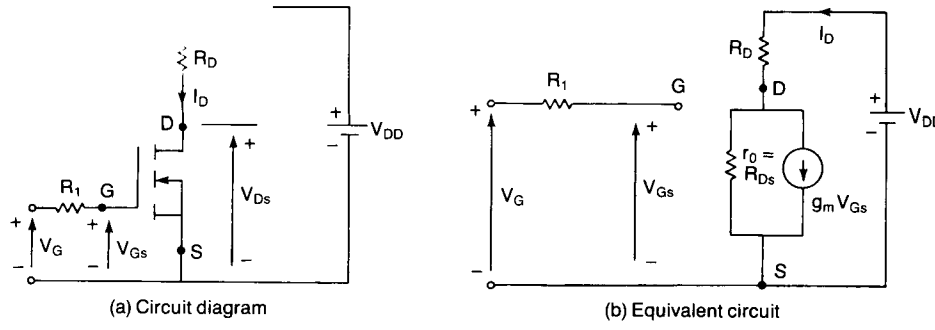


Figure 13-25 Steady-state switching model of MOSFETs.

However, depletion-type MOSFETs would be advantageous and simplify the logic design in some applications which require some form of logic-compatible ac or dc switch that would remain on when the logic supply falls and V_{GS} becomes zero. The characteristics of depletion-type MOSFETs will not be discussed further.

13-3.2 Switching Characteristics

Without any gate signal, an enhancement-type MOSFET may be considered as two diodes connected back to back or as a *npn*-transistor. The gate structure has parasitic capacitances to the source, C_{gs}, and to the drain, C_{gd}. The *npn*-transistor has a reverse-bias junction from the drain to the source and offers a capacitance, C_{ds}. Figure 13-26a shows the equivalent circuit of a parasitic bipolar transistor in parallel with a MOSFET. The base-to-emitter region of *npn*-transistor is shorted at the ship by metalizing the source terminal and the resistance from the base to emitter due to bulk resistance of *n*- and *p*-regions, R_{be}, is small. Hence, a MOSFET may be considered as having an internal diode and the equivalent circuit is shown in Fig. 13-26b. The parasitic capacitances are dependent on their respective voltages.

The switching model of MOSFETs is shown in Fig. 13-27. The typical switching waveforms and times are shown in Fig. 13-28. The *turn-on delay*, $t_{d(on)}$, is the time that is required to charge the input capacitance to threshold voltage level.

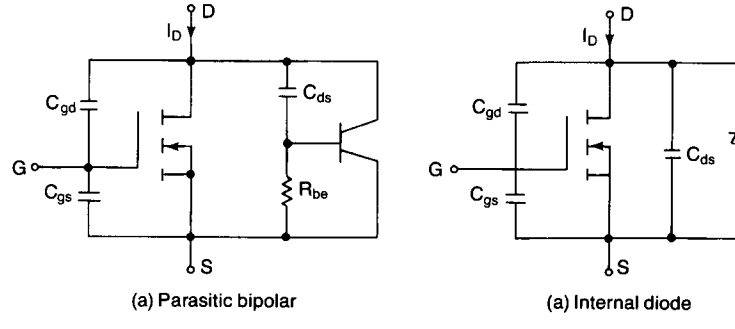


Figure 13-26 Parasitic model of enhancement-type MOSFETs.

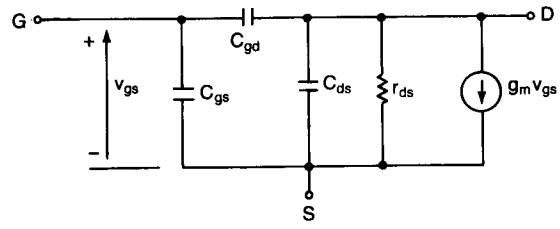


Figure 13-27 Switching model of MOSFETs.

The *rise time*, t_r, is the gate charging time from the threshold level to the full-gate voltage, V_{GSP}, which is required to drive the transistor into the linear region. The *turn-off delay time*, $t_{d(off)}$, is the time required for the input capacitance to discharge from the overdrive gate voltage, V_1, to the pinch-off region. V_{GS} must decrease significantly before V_{DS} begins to rise. The *fall time*, t_f, is the time that is required for the input capacitance to discharge from the pinch-off region to threshold voltage. If $V_{GS} \leq V_T$, the transistor turns off.

13-3.3 Performance Parameters

Figure 13-29 shows the data sheet of typical IR *n*-channel MOSFETs, types IRFZ40 and IRFZ42, which have low voltage and high current ratings.

Output characteristics. The output characteristics, which are the plots of I_D against V_{DS}, are shown in Fig. 13-29.1 for various values of V_{GS}. The threshold voltage is shown as $V_T = 4$ V. For a fixed value of V_{GS}, I_D remains almost constant at the pinch-off region, whereas the output or on-state resistance, ($R_{DS} = \Delta V_{DS}/\Delta I_D$) is approximately constant.

Transfer characteristic. The transfer characteristic, which is a plot of I_D versus V_{GS}, is shown in Fig. 13-29.2 and is temperature dependent.

Transconductance, g_m. This is a measure of the transfer characteristic and decreases with the junction temperature as shown in Fig. 13-29.6.

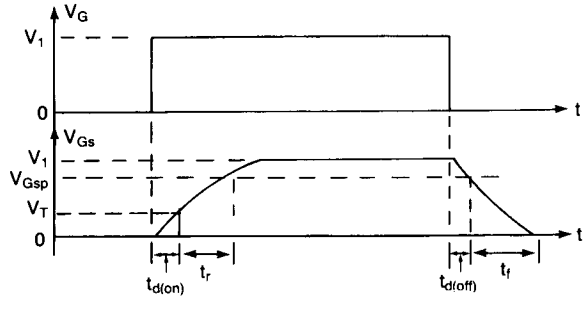
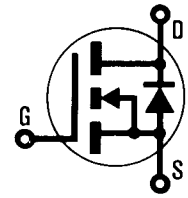


Figure 13-28 Switching waveforms and times.

INTERNATIONAL RECTIFIER IOR

HEXFET® TRANSISTORS IRFZ40 IRFZ42

N-Channel 50 VOLT POWER MOSFETs



50 Volt, 0.028 Ohm HEXFET TO-220AB Plastic Package

The HEXFET technology has expanded its product base to serve the low voltage, very low $R_{DS(on)}$ MOSFET transistor requirements. International Rectifier's highly efficient geometry and unique processing of the HEXFET have been combined to create the lowest on resistance per device performance. In addition to this feature all HEXFETs have documented reliability and parts per million quality!

The HEXFET transistors also offer all of the well established advantages of MOSFETs such as voltage control, freedom from second breakdown, very fast switching, ease of paralleling, and temperature stability of the electrical parameters.

They are well suited for applications such as switching power supplies, motor controls, inverters, choppers, audio amplifiers, high energy pulse circuits, and in systems that are operated from low voltage batteries, such as automotive, portable equipment, etc.

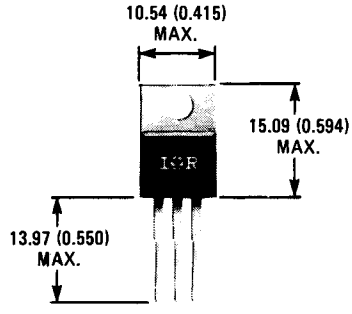
Features:

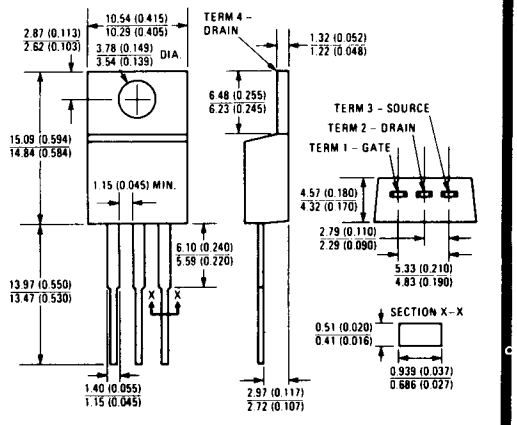
- Extremely Low $R_{DS(on)}$
- Compact Plastic Package
- Fast Switching
- Low Drive Current
- Ease of Paralleling
- No Second Breakdown
- Excellent Temperature Stability
- Parts Per Million Quality

Product Summary

PART NUMBER	V_{DS}	$R_{DS(ON)}$	I_D
IRFZ40	50V	0.028Ω	51A
IRFZ42	50V	0.035Ω	46A

CASE STYLE AND DIMENSIONS





Case Style TO-220AB
Dimensions in Millimeters and (Inches)

Figure 13-29 Data sheet of IR MOSFETS, types IRF240 and IRF242. (*Courtesy of International Rectifier*).

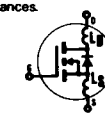
Absolute Maximum Ratings

Parameter		IRFZ40	IRFZ42	Units
V_{DS}	Drain - Source Voltage ①	50	50	V
V_{DGR}	Drain - Gate Voltage (R_{GS} = 20 KΩ) ①	50	50	V
I_D @ T_C = 25°C	Continuous Drain Current	51	46	A
I_D @ T_C = 100°C	Continuous Drain Current	32	29	A
I_{DM}	Pulsed Drain Current ③	160	145	A
V_{GS}	Gate - Source Voltage	±20		V
P_D @ T_C = 25°C	Max. Power Dissipation	125 (See Fig. 14)		W
	Linear Derating Factor	1.0 (See Fig. 14)		W/K
I_{LM}	Inductive Current, Clamped	(See Fig. 15 and 16) L = 100μH		A
		160	145	
T_J T_{stg}	Operating Junction and Storage Temperature Range	−55 to 150		°C
	Lead Temperature	300 (0.063 in. (1.6mm) from case for 10s)		°C

Electrical Characteristics @ T_C = 25°C (Unless Otherwise Specified)

Parameter		Type	Min.	Typ.	Max.	Units	Test Conditions
BV_{DSS}	Drain - Source Breakdown Voltage	IRFZ40	50	–	–	V	V_{GS} = 0V
		IRFZ42	50	–	–	V	I_D = 250 μA
$V_{GS(th)}$	Gate Threshold Voltage	ALL	2.0	–	4.0	V	V_{DS} = V_{GS}, I_D = 250 μA
I_{GSS}	Gate-Source Leakage Forward	ALL	–	–	500	nA	V_{GS} = 20V
I_{GSS}	Gate-Source Leakage Reverse	ALL	–	–	−500	nA	V_{GS} = −20V
I_{DSS}	Zero Gate Voltage Drain Current	ALL	–	–	250	μA	V_{DS} = Max. Rating, V_{GS} = 0V
			–	–	1000	μA	V_{DS} = Max. Rating × 0.8, V_{GS} = 0V, T_C = 125°C
$I_{D(on)}$	On-State Drain Current ②	IRFZ40	51	–	–	A	V_{DS} > $I_{D(on)}$ × $R_{DS(on)max.}$, V_{GS} = 10V
		IRFZ42	45	–	–	A	
$R_{DS(on)}$	Static Drain-Source On-State Resistance ②	IRFZ40	–	0.024	0.028	Ω	V_{GS} = 10V, I_D = 29A
		IRFZ42	–	0.030	0.035	Ω	
g_{fs}	Forward Transconductance ②	ALL	17	22	–	S(℧)	V_{DS} > $I_{D(on)}$ × $R_{DS(on)}$ max., I_D = 29A
C_{iss}	Input Capacitance	ALL	–	2350	3000	pF	V_{GS} = 0V, V_{DS} = 25V, f = 1.0 MHz
C_{oss}	Output Capacitance	ALL	–	920	1200	pF	See Fig. 10
C_{rss}	Reverse Transfer Capacitance	ALL	–	250	400	pF	
$t_{d(on)}$	Turn-On Delay Time	ALL	–	18	25	ns	V_{DD} ≅ 25V, I_D = 29A, Z_o = 4.7Ω
t_r	Rise Time	ALL	–	25	60	ns	See Fig. 17
$t_{d(off)}$	Turn-Off Delay Time	ALL	–	35	70	ns	(MOSFET switching times are essentially independent of
t_f	Fall Time	ALL	–	12	25	ns	operating temperature.)
Q_g	Total Gate Charge (Gate-Source Plus Gate-Drain)	ALL	–	40	60	nC	V_{GS} = 10V, I_D = 64A, V_{DS} = 0.8 Max. Rating.
Q_{gs}	Gate-Source Charge	ALL	–	22	–	nC	See Fig. 18 for test circuit. (Gate charge is essentially
Q_{gd}	Gate-Drain ("Miller") Charge	ALL	–	18	–	nC	independent of operating temperature.)
L_D	Internal Drain Inductance	ALL	–	3.5	–	nH	Measured from the contact screw on tab to center of die.
			–	4.5	–	nH	Measured from the drain lead, 6mm (0.25 in.) from package to center of die.
L_S	Internal Source Inductance	ALL	–	7.5	–	nH	Measured from the source lead, 6mm (0.25 in.) from package to source bonding pad.

Modified MOSFET symbol showing the internal device inductances.



Thermal Resistance

R_{thJC}	Junction-to-Case	ALL	–	–	1.0	K/W	
R_{thCS}	Case-to-Sink	ALL	–	1.0	–	K/W	Mounting surface flat, smooth, and greased.
R_{thJA}	Junction-to-Ambient	ALL	–	–	80	K/W	Free Air Operation

Figure 13-29 (*continued*)

Source-Drain Diode Ratings and Characteristics

I_S	Continuous Source Current (Body Diode)	IRFZ40	–	–	51	A	Modified MOSFET symbol showing the integral reverse P-N junction rectifier.
		IRFZ42	–	–	46	A	
I_{SM}	Pulse Source Current (Body Diode) ③	IRFZ40	–	–	160	A	
		IRFZ42	–	–	145	A	
V_{SD}	Diode Forward Voltage ②	IRFZ40	–	–	2.5	V	T_C = 25°C, I_S = 51A, V_{GS} = 0V
		IRFZ42	–	–	2.2	V	T_C = 25°C, I_S = 46A, V_{GS} = 0V
t_{rr}	Reverse Recovery Time	ALL	–	350	–	ns	T_J = 150°C, I_F = 51A, dI_F/dt = 100A/μs
Q_{RR}	Reverse Recovered Charge	ALL	–	2.1	–	μC	T_J = 150°C, I_F = 51A, dI_F/dt = 100A/μs
t_{on}	Forward Turn-on Time	ALL	Intrinsic turn-on time is negligible. Turn-on speed is substantially controlled by L_S + L_D.				

① T_J = 25°C to 150°C. ② Pulse Test: Pulse width ≤ 300μs, Duty Cycle ≤ 2%. ③ Repetitive Rating: Pulse width limited by max. junction temperature. See Transient Thermal Impedance Curve (Fig. 5).

TO-220A

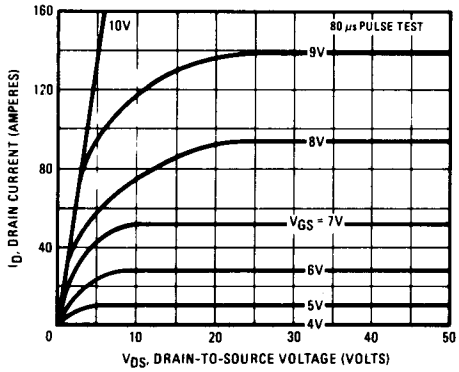


Fig. 1 – Typical Output Characteristics

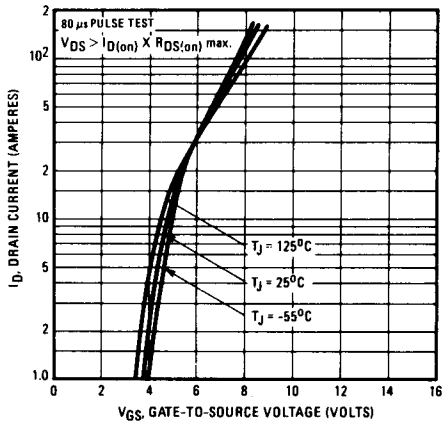


Fig. 2 – Typical Transfer Characteristics

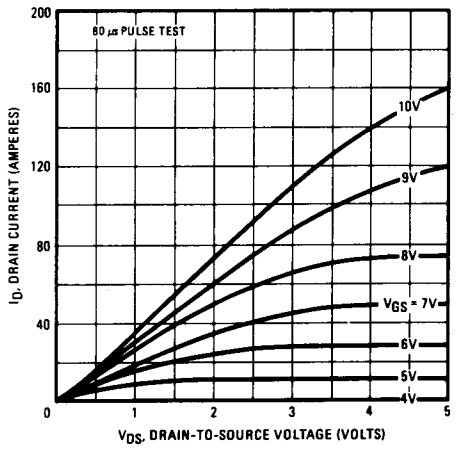


Fig. 3 – Typical Saturation Characteristics

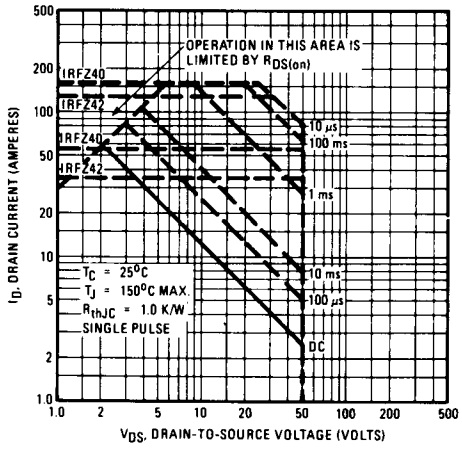


Fig. 4 – Maximum Safe Operating Area

Figure 13-29 (*continued*)

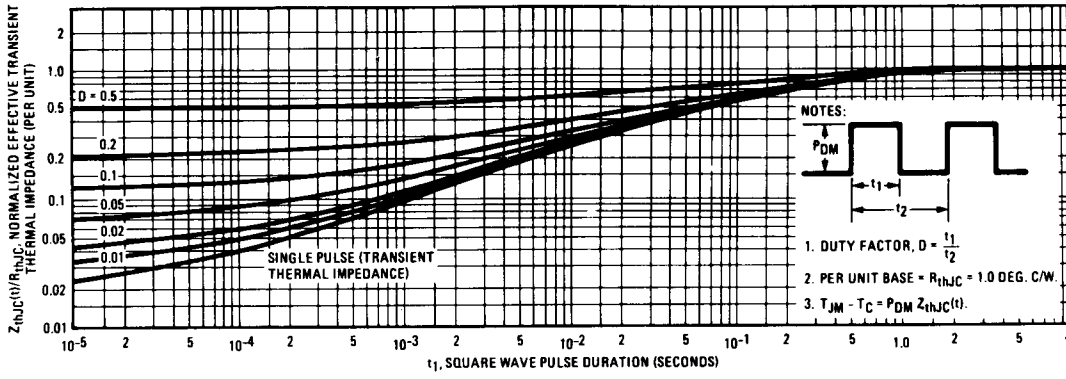


Fig. 5 – Maximum Effective Transient Thermal Impedance, Junction-toCase Vs. Pulse Duration

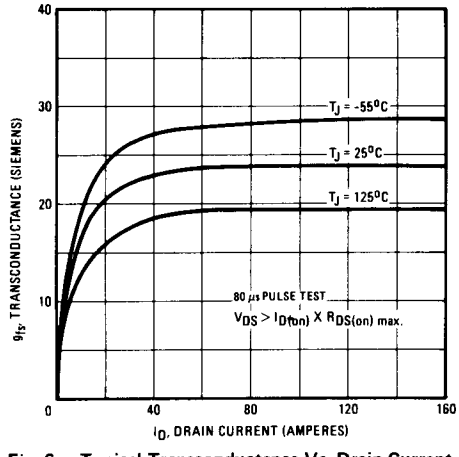


Fig. 6 – Typical Transconductance Vs. Drain Current

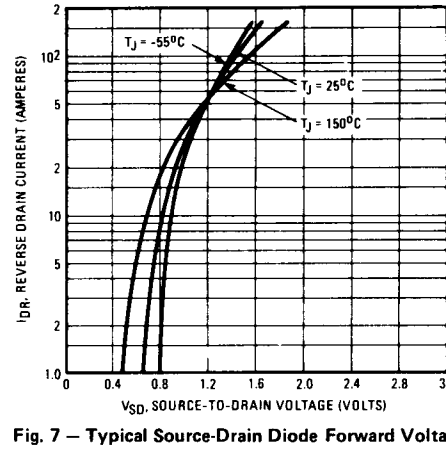


Fig. 7 – Typical Source-Drain Diode Forward Voltage

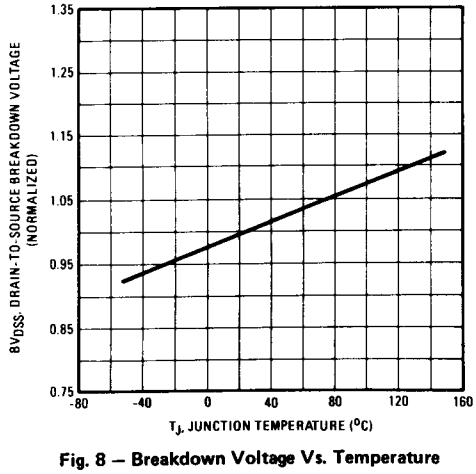


Fig. 8 – Breakdown Voltage Vs. Temperature

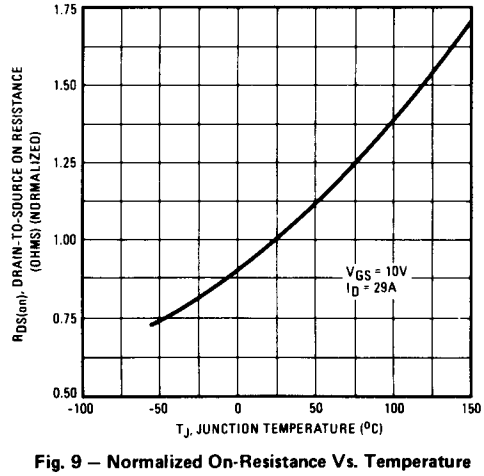


Fig. 9 – Normalized On-Resistance Vs. Temperature

Figure 13-29 (*continued*)

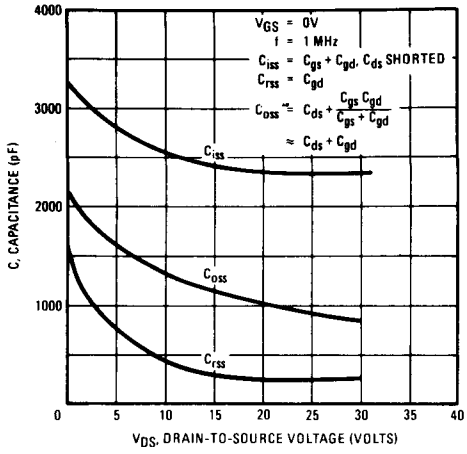


Fig. 10 — Typical Capacitance Vs. Drain-to-Source Voltage

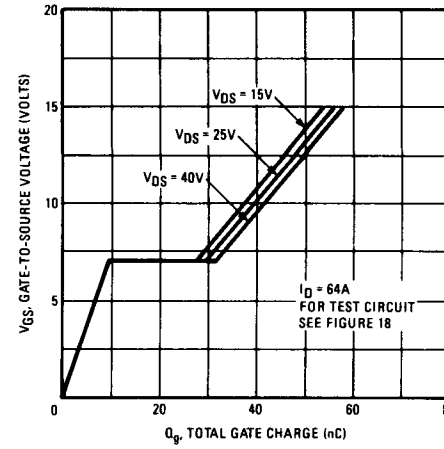


Fig. 11 — Typical Gate Charge Vs. Gate-to-Source Voltage

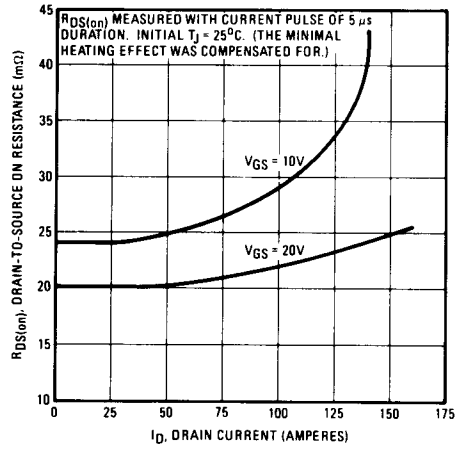


Fig. 12 — Typical On-Resistance Vs. Drain Current

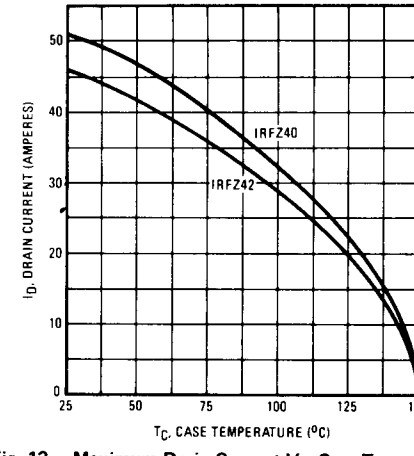


Fig. 13 — Maximum Drain Current Vs. Case Temperature

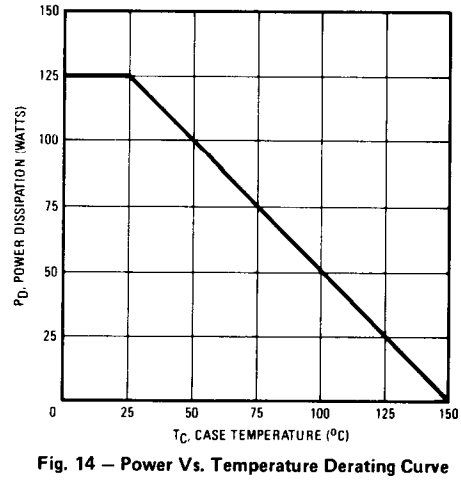


Fig. 14 — Power Vs. Temperature Derating Curve

Figure 13-29 *(continued)*

Linear characteristics. These are the output characteristics at lower values of V_{DS} and are important for switching applications. Since V_{DS} is low in the linear region, they are often identified as saturation characteristics as shown in Fig. 13-29.3, where saturation signifies the low on-state voltage and high on-state current region of operation similar to BJTs.

On-state resistance, R_{DS}. R_{DS} represents the power dissipation when the device is conducting. R_{DS} increases almost linearly with the junction temperature, T_J, as shown in Fig. 13-29.9. The increase of R_{DS} with I_D and V_{GS} as shown in Fig. 13-29.12 is nonlinear. The power dissipation is $P_D = R_{DS}I_D^2 = V_{DS}I_D$. The allowable power dissipation decreases with the case temperature as shown in Fig. 13-29.14.

Safe operating area, SOA. The SOA as shown in Fig. 13-29.4 gives the limit on the maximum value of I_D against the maximum value of V_{DS} during turn-on and turn-off of the device. These are thermal limitations. There is no second breakdown for MOSFETs. But there is a limit on I_D at the lower values of V_{DS} due to increase in the on-state resistance, R_{DS}. For a shorter on-time, the SOA boundaries extend into higher V_{DS} and I_D. The SOA curve is normally specified at $T_J = 150°C$, but the allowable breakdown voltage limit increases with the junction temperature as shown in Fig. 13-29.8.

Input and output capacitances. The manufacturers specify the (1) effective input capacitance as $C_{iss} = C_{gd} \| C_{gs}$, (2) effective output capacitance as $C_{oss} = C_{ds} \| C_{gd}$, and (3) reverse transfer capacitance $C_{rss} = C_{gd}$. These capacitances are dependent on V_{DS}, as shown in Fig. 13-29.10.

Gate charge, Q_g. During turn-on and turn-off, the input capacitance is charged and discharged. The charge stored on the input capacitance depends on the gate-to-source voltage, V_{GS}, as shown in Fig. 13-29.11. The switching loss due to the gate voltage becomes

$$P_G = Q_g V_{GS} f_s \tag{13-50}$$

where f_s is the switching frequency in hertz.

Example 13-7

A IR-MOSFET type IRFZ40 is operated as a switch. The junction temperature is $T_J = 150°C$ at a case temperature of $T_C = 75°C$. The gate-to-source voltage is $V_{GS} = 10$ V. The dc supply voltage is $V_{DD} = 25$ V. Determine the (a) maximum continuous drain current, I_D; (b) maximum power dissipation, P_D; (c) on-state resistance, R_{DS}; (d) gate voltage overdrive factor, ODF; (e) on-state or saturation voltage, V_{DS}; (f) gate power loss if the MOSFET is operated at a frequency of $f_s = 10$ kHz; and (g) peak drain current, I_{DM} (at $V_{DS} = 20$ V, if the pulsed on-time is $t_{on} = 1$ ms).

Solution $T_C = 75°$, $T_J = 150°$, and $V_{GS} = 10$ V.

(a) From Fig. 13-29.13, $I_D = 40$ A.

(b) From Fig. 13-29.14, $P_D = 75$ W.

(c) From Fig. 13-29.12, $R_{DS} = 24.5$ mΩ at $T_J = 25°C$. Figure 13-29.9 gives the temperature factor of 1.7 and at $T_J = 150°C$, $R_{DS} = 24.5 \times 1.7 = 41.65$ mΩ.

(d) From Fig. 13-29.2, V_{GS} = 6.4 V. Therefore, the gate voltage overdrive factor is ODF = 10/6.4 = 1.56.

(e) From Fig. 13-29.3, V_{DS} = 1.1 V.

(f) For V_{GS} = 10 V and V_{DS} = 25 V, Fig. 13-29.11 gives Q_g = 40 nC. From Eq. (13-50), $P_G = 40 \times 10^{-9} \times 10 \times 10 \times 10^3 = 4$ mW.

(g) Figure 13-29.4 gives I_{DM} = 70 A.

13-3.4 Gate Drive

The turn-on time of a MOSFET depends on the charging time of the input or gate capacitance. The turn-on time can be reduced by connecting a *RC* circuit as shown in Fig. 13-30 to charge the gate capacitance faster. When the gate voltage is turned on, the initial charging current of the capacitance is

$$I_G = \frac{V_G}{R_S} \tag{13-51}$$

and the steady-state value of gate voltage is

$$V_{GS} = \frac{R_G V_G}{R_s + R_1 + R_G} \tag{13-52}$$

where R_s is the internal resistance of gate drive source.

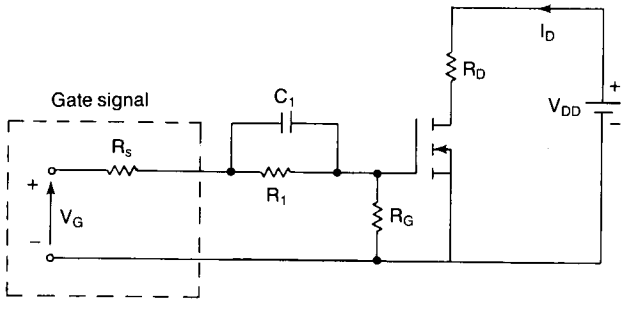


Figure 13-30 Fast-turn-on gate circuit.

13-4 MOSIGTs

A MOSIGT combines the advantages of BJTs and MOSFETS. A MOSIGT has high input impedance, like MOSFETs, and low on-state conduction losses, like BJTs. But there is no second breakdown problem, like BJTs. By chip design and structure, the equivalent drain-to-source resistance, R_{DS}, is controlled to behave like that of a BJT.

The symbol and circuit of a MOSIGT switch are shown in Fig. 13-31. The three terminals are gate, collector, and emitter instead of gate, drain, and source for a MOSFET. The data sheet of a GE-MOSIGT is shown in Fig. 13-32. The parameters and their symbols are similar to that of MOSFETs, except that the subscripts for source and drain are changed to emitter and collector, respectively.

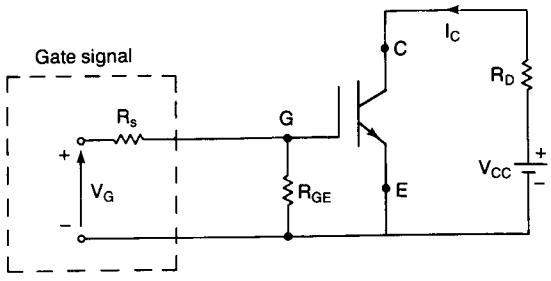


Figure 13-31 Symbol and circuit of a MOSIGT.

Output characteristics. The output characteristics, which are the plots of collector current, I_C, versus collector–emitter voltage, V_{CE}, for various values of gate-emitter voltage, V_{GE}, are shown in Fig. 13-32.1. The gate threshold voltage is $V_{GET} = 4$ V.

Collector–emitter saturation voltage, $V_{CE(sat)}$. $V_{CE(sat)}$ decreases with increasing value of V_{GE}. It is interesting to note from Fig. 13-32.2 that the temperature coefficient for the variations of $V_{CE(sat)}$ could be either positive or negative depending on the collector current. A MOSIGT behaves like a BJT at low value of I_C and similar to a MOSFET at high value of I_C. For a fixed value of I_C, $V_{CE(sat)}$ of a MOSIGT is less than V_{DS} of a comparable MOSFET and equal or greater than $V_{CE(sat)}$ of a comparable BJT.

Transfer characteristics. The transfer characteristics, which are plots of I_C versus V_{GE}, are shown in Fig. 13-32.3. They have temperature coefficients that vary with the collector current. Figure 13-32.4 shows the typical temperature dependence of some parameters.

Forward-biased safe operating area, FBSOA. A typical FBSOA is shown in Fig. 13-32.7. The MOSIGT can conduct continuous current up to the controllable current limit, which is derated due to the temperature limitations. However, there is no second breakdown limit. If the controllable peak current limit is exceeded even for a short time, the device latches on and it cannot be controlled by the gate. In this situation, the device can be turned off by decreasing the load current below the holding current or by reversing the polarity of collector–emitter voltage with an external commutation circuit. Figures 13-32.5 and 13-32.6 show that the peak collector current, I_{CM}, which increases with the gate-emitter resistance, R_{GE}, is less for inductive load. I_{CM} decreases with the maximum junction temperature, T_J.

Switching times. The MOSIGT does not require negative gate voltage for reducing turn-off time. However, the turn-off delay time and fall time are function of R_{GE} and increase with R_{GE}.

Preliminary 26.1, 6/83

POWER-MOS IGT
INSULATED GATE TRANSISTOR

D94FQ4,R4

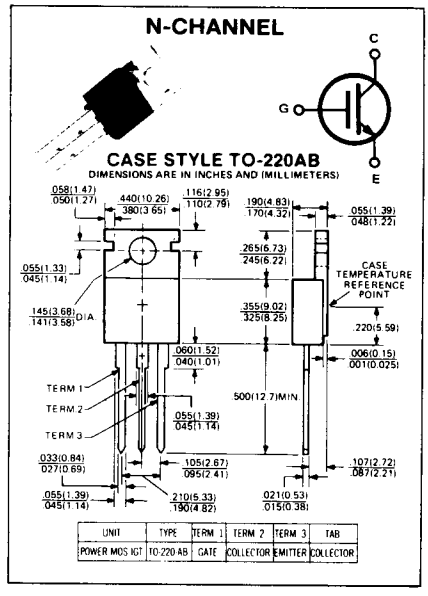
18 AMPERES
400, 500 VOLTS

The D94FQ4, R4 POWER-MOS IGT (Insulated Gate Transistor) is a new type of MOS gate turn on/off power switching device in which the best advantages of power mosfets and bipolar transistors are combined. The result is a device that has high input impedance of mosfets and low on-state conduction losses similar to bipolar transistors. The device design and gate characteristics of the IGT are also similar to power mosfets. An important difference is the equivalent $R_{DS(ON)}$ drain resistance which is modulated to a low value (10 times lower) when the gate is turned on. The much lower IGT on-state voltage drop also varies only moderately between 25°C and 150°C offering extended power handling capability.

The POWER-MOS IGT is ideal for many high voltage switching applications operating at low frequencies and where low conduction losses are essential, such as; AC and DC motor controls, power supplies and drivers for solenoids, relays and contactors.

Features

- Low $V_{CE(SAT)}$ — 2.5V typ @ 10A
- Ultra-fast turn-on — 200 ns typical
- Tailored turn-off times — Down to 1.7 μs t_f
- Polysilicon MOS gate — Voltage controlled turn on/off
- High current handling — 10 amps @ 100°C



maximum ratings (T_C = 25°C) (unless otherwise specified)

RATING	SYMBOL	D94FQ4	D94FR4	UNIT
Collector-Emitter Voltage, R_{GE} = 5KΩ	V_{CER}	400	500	Volts
Collector-Gate Voltage, R_{GE} = 5KΩ	V_{CGR}	400	500	Volts
Continuous Collector Current @ T_C = 25°C @ T_C = 100°C	I_C	18 10	18 10	A A
Pulsed Collector Current(1)	I_{CM}	40	40	A
Gate-Emitter Voltage	V_{GE}	±25	±25	Volts
Total Power Dissipation @ T_C = 25°C Derate Above 25°C	P_D	75 0.6	75 0.6	Watts W/°C
Operating and Storage Junction Temperature Range	T_J, T_{STG}	-55 to 150	-55 to 150	°C

thermal characteristics

Thermal Resistance, Junction to Case	$R_{\theta JC}$	1.67	1.67	°C/W
Thermal Resistance, Junction to Ambient	$R_{\theta JA}$	80	80	°C/W
Maximum Lead Temperature for Soldering Purposes: 1/8" from Case for 5 Seconds	T_L	260	260	°C

(1) Repetitive Rating: Pulse width limited by max. junction temperature.

Figure 13-32 Data sheet of GE MOSIGT, type D94FQ4, R4. (*Courtesy of General Electric Company*)

electrical characteristics (T_C = 25° C) (unless otherwise specified)

CHARACTERISTIC		SYMBOL	MIN	TYP	MAX	UNIT
off characteristics						
Collector-Emitter Breakdown Voltage (R_{GE} = 5KΩ, I_C = 250 μA)	D94FQ4 D94FR4	BV_{CER}	400 500	— —	— —	Volts
Collector Cut-off Current (V_{CE} = Max. Rating, R_{GE} = 5KΩ, T_C = 25° C) (V_{CE} = Max. Rating x 0.8, R_{GE} = 5KΩ, T_C = 150° C)		I_{CER}	— —	— —	250 4.0	μA mA
Gate-Emitter Leakage Current (V_{GE} = ±20V)		I_{GES}	—	—	±500	nA
on characteristics*						
Gate Threshold Voltage (V_{CE} = V_{GE}, I_C = 1 mA)	T_C = 25°C T_C = 150°C	$V_{GE(TH)}$	2 —	3.5 2.4	5 —	Volts
Collector-Emitter Saturation Voltage (V_{GE} = 15V)	I_C = 10 A, T_C = 25°C I_C = 10 A, T_C = 150°C	$V_{CE(SAT)}$	— —	2.5 2.8	2.7 —	Volts
Forward Transconductance (V_{CE} = 10V, I_C = 10A)		g_{FS}	—	1.3	—	mhos
dynamic characteristics						
Input Capacitance	V_{GE} = 0V	C_{ies}	—	630	—	pF
Output Capacitance	V_{CE} = 25V	C_{oes}	—	20	—	pF
Reverse Transfer Capacitance	f = 1 MHz	C_{res}	—	65	—	pF
switching characteristics*						
Turn-on Delay Time	Resistive Load, T_C = 150°C	$t_{d(on)}$	—	100	—	ns
Rise Time	I_C = 10 A, V_{CE} = 400V	t_r	—	120	—	ns
Turn-off Delay Time	V_{GE} = 15V (R_{GE} = 1KΩ) (R_{GE} = 5KΩ)	$t_{d(off)}$	— —	2.5 11.0	— —	μs
Fall Time	$R_{G(on)}$ = 50Ω (R_{GE} = 1KΩ) (R_{GE} = 5KΩ)	t_f	— —	2.0 6.0	— —	μs
Turn-off Delay Time	Inductive Load, T_C = 150°C I_C=10A, $V_{CE(CLAMP)}$=400V (R_{GE} = 5KΩ)	$t_{d(off)}$	—	16.0	—	μs
Fall Time	V_{GE} = 15V $R_{G(on)}$ = 50Ω R_{GE} = 5KΩ (R_{GE} = 5KΩ)	t_f	—	4.4	—	μs
Turn-off Delay Time	Inductive Load, T_C = 150°C I_C=5A, $V_{CE(CLAMP)}$=400V	$t_{d(off)}$	—	3.6	—	μs
Fall Time	V_{GE} = 15V $R_{G(on)}$ = 50Ω R_{GE} = 1KΩ	t_f	—	1.7	—	μs

*Pulse Test: Pulse width ≤ 300 μsec, duty cycle ≤ 2%

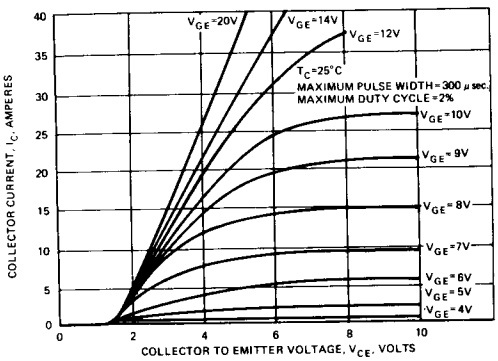


FIGURE 1. TYPICAL OUTPUT CHARACTERISTICS

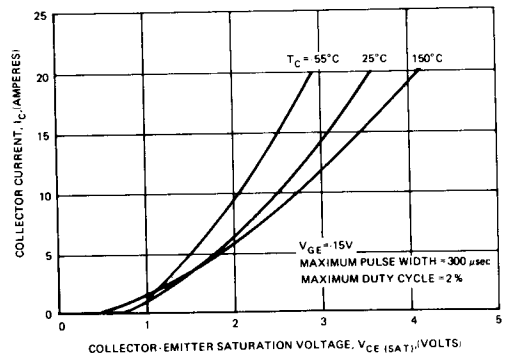


FIGURE 2. TYPICAL COLLECTOR-EMITTER SATURATION VOLTAGE

Figure 13-32 (*continued*)

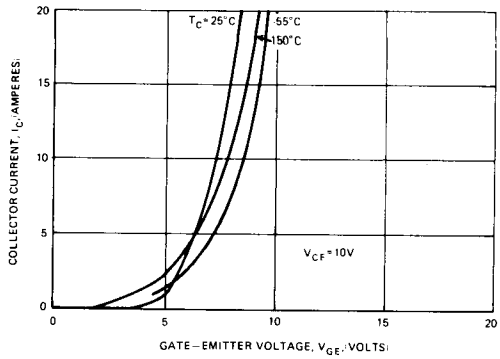


FIGURE 3. TYPICAL TRANSFER CHARACTERISTICS

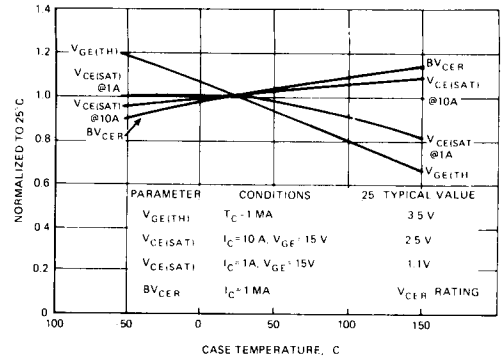


FIGURE 4. TYPICAL TEMPERATURE DEPENDENCE OF PARAMETERS

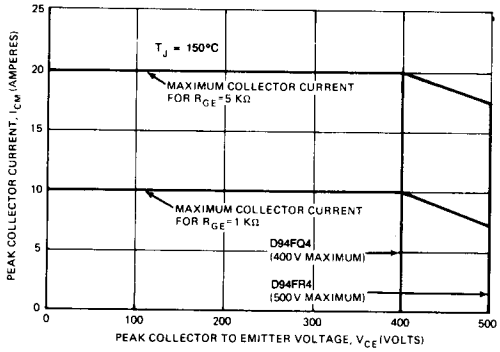


FIGURE 5. MAXIMUM RATED SWITCHING SAFE OPERATING AREA FOR RESISTIVE LOAD

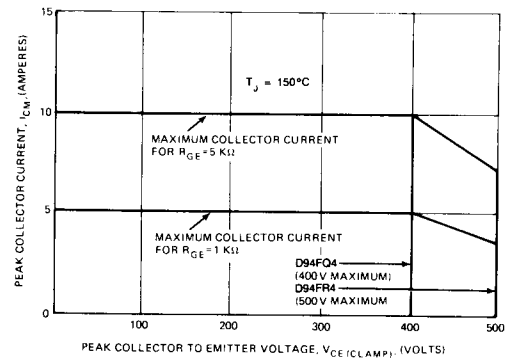


FIGURE 6. MAXIMUM RATED SWITCHING SAFE OPERATING AREA FOR INDUCTIVE LOAD

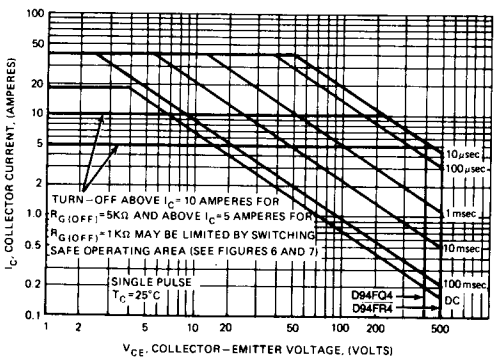


FIGURE 7. MAXIMUM SAFE OPERATING AREA

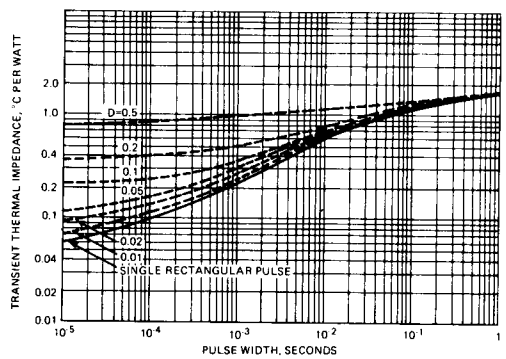


FIGURE 8. MAXIMUM TRANSIENT THERMAL IMPEDANCE

Figure 13-32 (*continued*)

13-5 SERIES AND PARALLEL OPERATION

Transistors may be operated in series to increase the voltage-handling capability. It is very important that the series-connected transistors are turned on and off simultaneously. Otherwise, the slowest device at turn-on and the fastest device at turn-off will be subjected to the full voltage of the collector–emitter (or drain–source) circuit and that particular device may be destroyed due to high voltage. The devices should be matched for gain, transconductance, threshold voltage, on-state voltage, turn-on time, and turn-off time. Even the gate or base drive characteristics should be identical. Voltage-sharing networks similar to diodes could be used.

Transistors are connected in parallel if one device cannot handle the load current demand. For equal current sharings, the transistors should be matched for gain, transconductance, saturation voltage, and turn-on time and turn-off time. But, in practice, it is not always possible to meet these requirements. A reasonable amount of current sharing (45 to 55% with two transistors) can be obtained by connecting resistors in series with the emitter (or source) terminals, as shown in Fig. 13-33.

The resistors in Fig. 13-33 will help current sharing under steady-state conditions. Current sharing under dynamic conditions can be accomplished by connecting coupled inductors as shown in Fig. 13-34. If the current through Q_1 rises, the Ldi/dt across L_1 increases, and a corresponding voltage of opposite polarity is induced across inductor L_2. The result is a low-impedance path through transistor Q_2 and the current is shifted to Q_2. The inductors would generate voltage spikes and they may be expensive and bulky, especially at high currents.

The BJTs have a negative temperature coefficient. During current sharing, if one BJT carries more current, its on-state resistance decreases and its current increases further, whereas MOSFETS have positive temperature coefficient and parallel operation is relatively easy. The MOSFET that initially draws higher current heats up faster and its on-state resistance increases, resulting in current shifting to the other devices. MOSIGTs require special care to match the characteristics due to the variations of the temperature coefficients with the collector current.

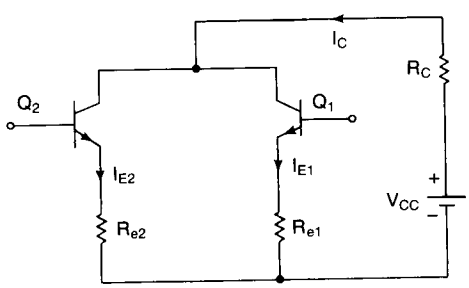


Figure 13-33 Parallel connection of transistors.

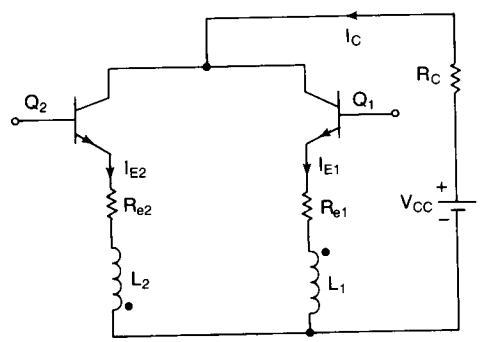


Figure 13-34 Dynamic current sharing.

Example 13-8

Two MOSFETS which are connected in parallel similar to Fig. 13-33 carry a total current of $I_T = 20$ A. The drain-to-source voltage of transistor Q_1 is $V_{DS1} = 2.5$ V and that of transistor Q_2 is $V_{DS2} = 3$ V. Determine the drain current of each transistor and difference in current sharing if the current sharing series resistances are (a) $R_{s1} = 0.3\ \Omega$ and $R_{s2} = 0.2\ \Omega$, and (b) $R_{s1} = R_{s2} = 0.5\ \Omega$.

Solution (a) $I_{D1} + I_{D2} = I_T$ and $V_{DS1} + I_{D1}R_{s1} = V_{DS2} + I_{D2}R_{s2}$. or

$$I_{D1} = \frac{V_{DS2} - V_{DS1} + I_T R_{s2}}{R_{s1} + R_{s2}}$$

$$= \frac{3 - 2.5 + 20 \times 0.2}{0.3 + 0.2} = 9 \text{ A} \quad \text{or} \quad 45\%$$

$$I_{D2} = 20 - 9 = 11 \text{ A} \quad \text{or} \quad 55\%$$

$$\Delta I = 55 - 45 = 10\%$$

$$\text{(b)}\ I_{D1} = \frac{3 - 2.5 + 20 \times 0.5}{0.5 + 0.5} = 10.5\ A \quad or \quad 52.5\%$$

$$I_{D2} = 20 - 10.5 = 9.5 \text{ A} \quad \text{or} \quad 47.5\%$$

$$\Delta I = 52.5 - 47.5 = 5\%$$

13-6 *di/dt* AND *dv/dt* LIMITATIONS

Transistors require certain turn-on and turn-off times. The typical voltage and current waveforms of a BJT switch are shown in Fig. 13-35. During turn-on, the collector current rises and the *di/dt* is

$$\frac{di}{dt} = \frac{I_L}{t_r} = \frac{I_{cs}}{t_r} \tag{13-53}$$

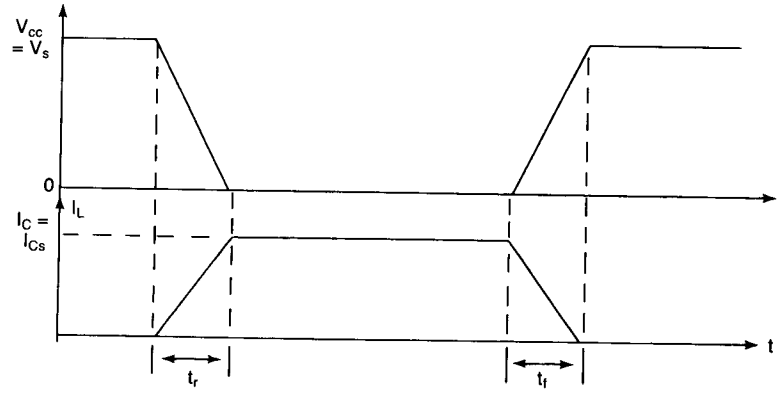


Figure 13-35 Voltage and current waveforms.

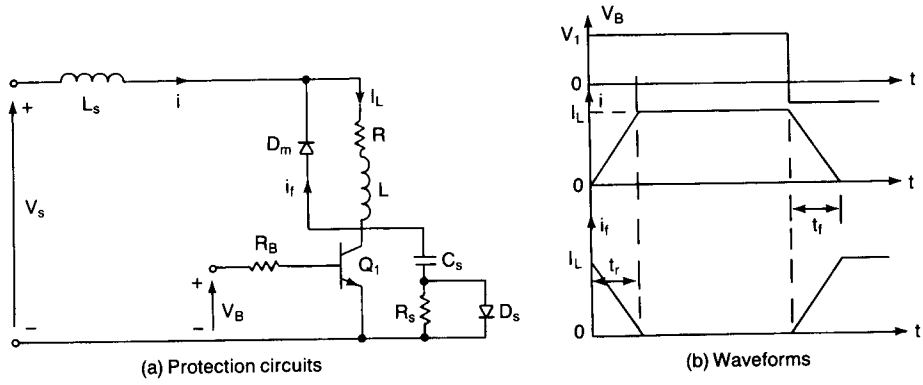


Figure 13-36 Transistor switch with *di/dt* and *dv/dt* protections.

During turn-off, the collector–emitter voltage must rise in relation to the fall of the collector current, and *dv/dt* is

$$\frac{dv}{dt} = \frac{V_s}{t_f} = \frac{V_{cc}}{t_f} \tag{13-54}$$

The conditions in Eqs. (13-53) and (13-54) are set by the transistor switching characteristics and must be satisfied during turn-on and turn-off. Protection circuits are normally required to keep the operating *di/dt* and *dv/dt* within the allowable limits of the transistor. A typical transistor switch with *di/dt* and *dv/dt* protections is shown in Fig. 13-36a, with the operating waveforms in Fig. 13-36b. The *RC* network across the transistor is known as the *snubber circuit* or *snubber* and limits the *dv/dt*. The inductor L_s, which limits the *di/dt*, is sometimes called a *series snubber*.

Let us assume that under steady-state conditions the load current I_L is freewheeling through diode D_m, which has negligible reverse recovery time. When transistor Q_1 is turned on, the collector current rises and current of diode D_m falls. The equivalent circuit during turn-on is shown in Fig. 13-37a and turn-on *di/dt* is

$$\frac{di}{dt} = \frac{V_s}{L_s} \tag{13-55}$$

Equating Eq. (13-53) to Eq. (13-55) gives the value of L_s,

$$L_s = \frac{V_s t_r}{I_L} \tag{13-56}$$

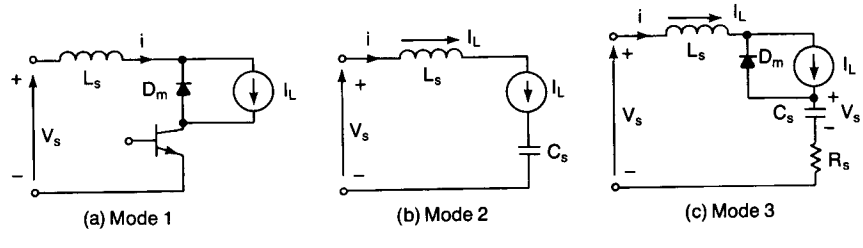


Figure 13-37 Equivalent circuits.

During turn-off, the capacitor C_s will charge by the load current and the equivalent circuit is shown in Fig. 13-37b. The capacitor voltage will appear across the transistor and the dv/dt is

$$\frac{dv}{dt} = \frac{I_L}{C_s} \tag{13-57}$$

Equating Eq. (13-54) to Eq. (13-57) gives the required value of capacitance,

$$C_s = \frac{I_L t_f}{V_s} \tag{13-58}$$

Once the capacitor is charged to V_s, the freewheeling diode will turn on. Due to the energy stored in L_s, there will be a damped resonant circuit as shown in Fig. 13-37c. The transient analysis of RLC circuit is discussed in Section 15-4. The RLC circuit is normally made critically damped to avoid oscillations. For unity critical damping, $\delta = 1$, and Eq. (15-11) yields

$$R_s = 2\sqrt{\frac{L_s}{C_s}} \tag{13-59}$$

The capacitor C_s has to discharge through the transistor and this increases the peak current rating of the transistor. The discharge through the transistor can be avoided by placing resistor R_s across C_s instead of placing R_s across D_s.

The discharge current is shown in Fig. 13-38. In choosing the value of R_s, the discharge time, $R_s C_s = \tau_s$ should also be considered. A discharge time of one-third the switching period, T_s, is usually adequate.

$$3R_s C_s = T_s = \frac{1}{f_s}$$

or

$$R_s = \frac{1}{3f_s C_s} \tag{13-60}$$

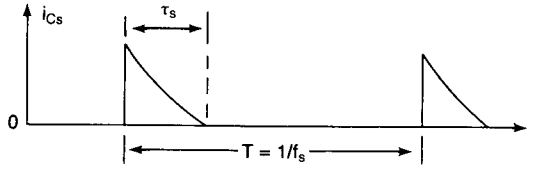


Figure 13-38 Discharge current of snubber capacitor.

Example 13-9

A bipolar transistor is operated as a chopper switch at a frequency of $f_s = 10$ kHz. The circuit arrangement is shown in Fig. 13-36a. The dc voltage of the chopper is $V_s = 220$ V and the load current is $I_L = 100$ A. $V_{CE(sat)} = 0$ V. The switching times are $t_d = 0$, $t_r = 3$ μ, and $t_f = 1.2$ μs. Determine the values of (a) L_s; (b) C_s; (c) R_s for critically damped condition; (d) R_s, if the discharge time is limited to one-third of switching period; (e) R_s, if the peak discharge current is limited to 10% of

load current; and (f) power loss due to RC snubber, P_s, neglecting the effect of inductor L_s on the voltage of snubber capacitor, C_s.

Solution $I_L = 100$ A, $V_s = 220$ V, $f_s = 10$ kHz, $t_r = 3$ μ, and $t_f = 1.2$ μs.

(a) From Eq. (13-56), $L_s = 220 \times 3/100 = 6.6$ μH.

(b) From Eq. (13-58), $C_s = 100 \times 1.2/220 = 0.55$ μF.

(c) From Eq. (13-59), $R_s = 2\sqrt{(6.6/0.55)} = 6.93\ \Omega$.

(d) From Eq. (13-60), $R_s = 10^3/(3 \times 10 \times 0.55) = 60.6\ \Omega$.

(e) $V_s/R_s = 0.1 \times I_L$ or $220/R_s = 0.1 \times 100$ or $R_s = 22\ \Omega$.

(f) The snubber loss, which neglects the loss in diode D_s, is

$$P_s \cong 0.5 C_s V_s^2 f_s \tag{13-61}$$
$$= 0.5 \times 0.55 \times 10^{-6} \times 220^2 \times 10 \times 10^3 = 133.1 \text{ W}$$

13-7 ISOLATION OF GATE AND BASE DRIVES

For operating power transistors as switches, an appropriate gate voltage or base current must be applied to drive the transistors into the saturation mode or low on-state voltage. The control voltage should be applied between the gate and source terminals or between the base and emitter terminals. The power converters generally require multiple transistors and each transistor must be gated individually. Figure 13-39a shows a single-phase bridge inverter. The main dc voltage is V_s with ground terminal G.

The logic circuit in Fig. 13-39b generates four pulses. These pulses as shown in Fig. 13-39c are shifted in time to perform the required logic sequence for power

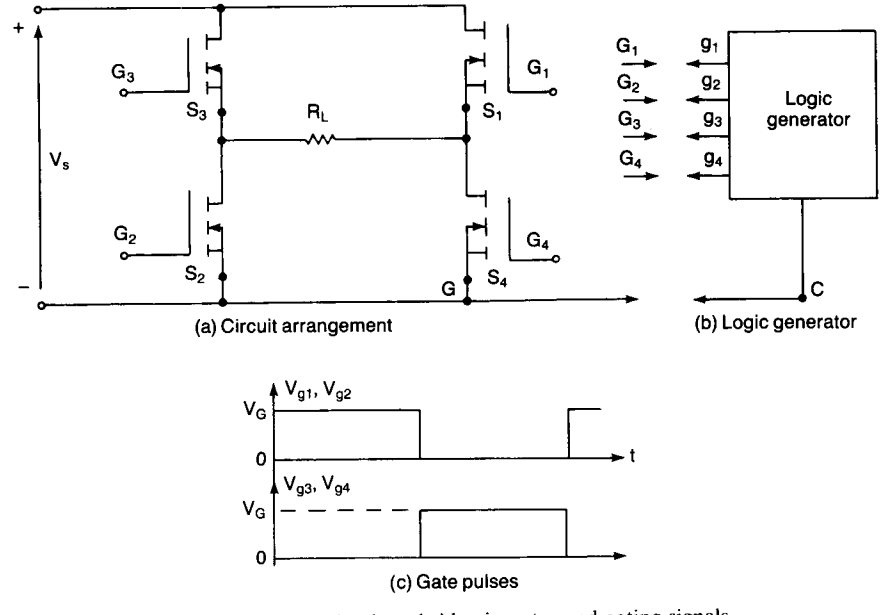


Figure 13-39 Single-phase bridge-inverter and gating signals.

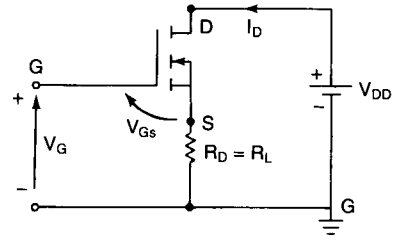


Figure 13-40 Gate voltage between gate and ground.

conversion from dc to ac. However, all of four logic pulses have a common terminal C. The common of the logic circuit may be connected to the ground terminal G of the main dc supply as shown by dashed lines.

The terminal g_1, which has a voltage of V_{g1} with respect to terminal C, cannot be connected directly to gate terminal G_1. The signal V_{g1} should be applied between the gate terminal G_1 and source terminal S_1 of transistor Q_1. There is a need for isolation and interfacing circuits between the logic circuit and power transistors. However, transistors Q_2 and Q_4 can be gated directly without isolation or interfacing circuits if the logic signals are compatible with the gate drive requirements of the transistors.

The importance of gating a transistor between its gate and source rather than applying gating voltage between the gate and common ground can be demonstrated with Fig. 13-40, where the load resistance is connected between the source and ground. The effective gate–source voltage is

$$V_{GS} = V_G - R_L I_D(V_{GS})$$

where $I_D(V_{GS})$ varies with V_{GS}. The effective value of V_{GS} decreases as the transistor turns on and V_{GS} reaches a steady-state value, which is required to balance the load or drain current. The effective value of V_{GS} is unpredictable and such an arrangement is not suitable. There are basically two ways of floating or isolating the control or gate signal with respect to ground.

1. Pulse transformers
2. Optocouplers

13-7.1 Pulse Transformers

Pulse transformers have one primary winding and can have one or more secondary windings. Multiple secondary windings allow simultaneous gating signals to series- and parallel-connected transistors. Figure 13-41 shows a transformer-isolated gate drive arrangement. The transformer should have a very small leakage inductance and the rise time of the output pulse should very small. At a relatively long pulse and low switching frequency, the transformer would saturate and its output would be distorted.

13-7.2 Optocouplers

Optocouplers combine an infrared light-emitting diode (ILED) and a silicon phototransistor. The input signal is applied to the ILED and the output is taken from

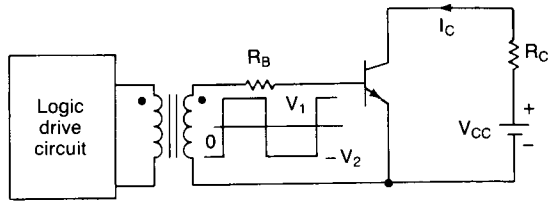


Figure 13-41 Transformer-isolated gate drive.

the phototransistor. The rise and fall times of phototransistors are very small, with typical values of turn-on time, $t_{on} = 2 - 5$ μs, and turn-off time, $t_{off} = 300$ nanoseconds. These turn-on and turn-off times limit the high frequency applications. A gate isolation circuit using phototransistor is shown in Fig. 13-42. The phototransistor could be a Darlington pair. The phototransistors require separate power supply and add to the complexity and cost and weight of the drive circuits.

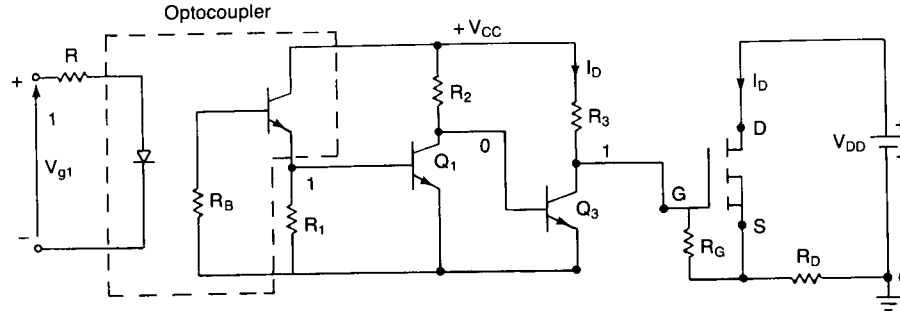


Figure 13-42 Optocoupler gate isolation.

SUMMARY

Power transistors are generally of three types: BJTs, MOSFETs, and MOSIGTs. BJTs are current-controlled devices and their parameters are sensitive to junction temperature. BJTs suffer from second breakdown and require reverse base current during turn-off to reduce the storage time. But they have low on-state or saturation voltage.

MOSFETs are voltage-controlled devices and require very low gating power and their parameters are less sensitive to junction temperature. There is no second breakdown problem and no need for negative gate voltage during turn-off. MOSIGTs, which combined the advantages of BJTs and MOSFETs, are voltage-controlled devices and have low on-state voltage similar to BJTs. MOSIGTs have no second breakdown phenomena.

Transistors can be connected in series or parallel. Parallel operation usually requires current-sharing elements. Series operation requires matching of parameters, especially during turn-on and turn-off. To maintain the voltage and current relationship of transistors during turn-on and turn-off, it is generally necessary to use snubber circuits to limit the *di/dt* and *dv/dt*.

The gate signals can be isolated from the power circuit by pulse transformers or optocouplers. The pusle transformers are simple, but the leakage inductance should be very small. The transformers may be saturated at a low frequency and long pulse. Optocouplers require separate power supply.

REFERENCES

1. E. S. Oxner, *Power FETs and Their Applications*. Englewood Cliffs, N. J.: Prentice-Hall, Inc., 1982.
2. B. J. Baliga and D. Y. Chen, *Power Transistors: Device Design and Applications*. New York: IEEE Press, 1984.
3. Westinghouse Electric, *Silicon Power Transistor Handbook*. Pittsburgh, Pa.: Westinghouse Electric Corporation, 1967.
4. B. R. Pelly, "Power MOSFETs—a status review." *International Power Electronics Conference*, 1983, pp. 10–32.
5. A. Ferraro, "An overview of low cost snubber technology for transistor converters." *IEEE Power Electronics Specialist Conference*, 1982, pp. 466–477.
6. A. S. Sedra and K. C. Smith, *Microelectronics*. New York: CBS College Publishing, 1986.
7. R. Severns and J. Armijos, *MOSPOWER Application Handbook*. Sata Clara, Calif.: Siliconix Corporation, 1984.
8. B. R. Pelly and S. M. Clemente, *Applying International Rectifier's HEXFET Power MOSFETs*, Application Note No. 930A, El Segundo, Calif.: International Rectifier, 1985.
9. T. A. Radomski, "Protection of power transistors in electric vehicle drives." *IEE Power Electronics Specialist Conference*, 1982, pp. 455–465.
10. B. J. Baliga, M. Cheng, P. Shafer, and M. W. Smith, "The insulated gate transistor (IGT)—a new power switching device." *IEEE Industry Applications Society Conference Record*, 1983, pp. 354–363.
11. S. Clemente, and B. R. Pelly, "Understanding power MOSFET switching performance." *Solid-State Electronics*, Vol. 12, No. 12, 1982, pp. 1133–1141.

REVIEW QUESTIONS

13-1. What is a bipolar transistor (BJT)?

13-2. What are the types of BJTs?

13-3. What are the differences between *npn*-transistor and *pnp*-transistors?

13-4. What are the input characteristics of *npn*-transistors?

13-5. What are the output characteristic of *npn*-transistors?

13-6. What are the three regions of operation for BJTs?

13-7. What is a beta (β) of BJTs?

13-8. What is the difference between beta, β, and forced beta, β_F of BJTs?

13-9. What is a transductance of BJTs?
13-10. What is an overdrive factor of BJTs?
13-11. What is the switching model of BJTs?
13-12. What is the cause of delay time in BJTs?
13-13. What is the cause of storage time in BJTs?
13-14. What is the cause of rise time in BJTs?
13-15. What is the cause of fall time in BJTs?
13-16. What is a saturation mode of BJTs?
13-17. What is a turn-on time of BJTs?
13-18. What is a turn-off time of BJTs?
13-19. What is a FBSOA of BJTs?
13-20. What is a RBSOA of BJTs?
13-21. Why is it necessary to reverse bias BJTs during turn-off?
13-22. What is a second breakdown of BJTs?
13-23. What are the base drive techniques for increasing switching speeds of BJTs?
13-24. What is an antisaturation control of BJTs?
13-25. What are the advantages and disadvantages of BJTs?
13-26. What is a MOSFET?
13-27. What are the types of MOSFETs?
13-28. What are the differences between enhancement-type MOSFETs and depletion-type MOSFETs?
13-29. What is a pinch-off voltage of MOSFETs?
13-30. What is a threshold voltage of MOSFETs?
13-31. What is a transconductance of MOSFETs?
13-32. What is the switching model of *n*-channel MOSFETs?
13-33. What are the transfer characteristics of MOSFETs?
13-34. What are the output characteristics of MOSFETs?
13-35. What are the advantages and disadvantages of MOSFETs?
13-36. Why do the MOSFETs not require negative gate voltage during turn-off?
13-37. Why does the concept of saturation differ in BJTs and MOSFETs?
13-38. What is a turn-on time of MOSFETs?
13-39. What is a turn-off time of MOSFETs?
13-40. What is a MOSIGT?
13-41. What are the transfer characteristics of MOSIGTs?
13-42. What are the output characteristics of MOSIGTs?
13-43. What are the advantages and disadvantages of MOSIGTs?
13-44. What are the main differences between MOSFETs and BJTs?
13-45. What are the problems of parallel operation of BJTs?
13-46. What are the problems of parallel operation of MOSFETs?
13-47. What are the problems of parallel operation of MOSIGTs?
13-48. What are the problems of series operation of BJTs?
13-49. What are the problems of series operations of MOSFETs?
13-50. What are the problems of series operations of MOSIGTs?

13-51. What are the purposes of shunt snubber in transistors?

13-52. What is the purpose of series snubber in transistors?

13-53. What are the advantages and disadvantages of transformer gate isolation?

13-54. What are the advantages and disadvantages of optocoupled gate isolation?

PROBLEMS

13-1. The beta (β) of bipolar transistor in Fig. 13-6 varies from 10 to 60. The load resistance is $R_C = 5\ \Omega$. The dc supply voltage is $V_{CC} = 100$ V and the input voltage to the base circuit is $V_B = 8$ V. If $V_{CE(sat)} = 2.5$ V and $V_{BE(sat)} = 1.75$ V, find the **(a)** value of R_B that will result in saturation with an overdrive factor of 20; **(b)** forced β; and **(c)** power loss in the transistor, P_T.

13-2. The beta (β) of bipolar transistor in Fig. 13-6 varies from 12 to 75. The load resistance is $R_C = 1.5\ \Omega$. The dc supply voltage is $V_{CC} = 40$ V and the input voltage to the base circuit is $V_B = 6$ V. If $V_{CE(sat)} = 1.2$ V, $V_{BE(sat)} = 1.6$ V, and $R_B = 0.7\ \Omega$, determine the **(a)** overdrive factor, ODF; **(b)** forced β; and **(c)** power loss in the transistor, P_T.

13-3. A GE transistor, type D67DE with data sheet in Fig. 13-12, is used as a switch and the waveforms are shown in Fig. 13-9. The parameters are $V_{CC} = 200$ V, $V_{BE(sat)} = 3$ V, $I_B = 8$ A, $V_{CE(sat)} = 2$ V, $I_{CS} = 100$ A, $t_d = 0.5\ \mu s$, $t_r = 1\ \mu s$, $t_s = 5\ \mu s$, $t_f = 3\ \mu s$, and $f_s = 10$ kHz. The duty cycle is $k = 50\%$. The collector–emitter leakage current is $I_{CEO} = 3$ mA. Determine the power loss due to the collector current **(a)** during turn-on, $t_{on} = t_d + t_r$; **(b)** during conduction period, t_n; **(c)** during turn-off $t_{off} = t_s + t_f$; **(d)** during off-time, t_o; and **(e)** total average power losses, P_T. **(f)** Plot the instantaneous power due to the collector current, $P_c(t)$.

13-4. The maximum junction temperature of the bipolar transistor in Prob. 13-3 is $T_J = 150°C$ and the ambient temperature is $T_A = 25°C$. If the thermal resistances are $R_{JC} = 0.4°C/W$ and $R_{CS} = 0.05°C/W$, calculate the **(a)** thermal resistance of heat sink, R_{SA}; and **(b)** second breakdown derating factor. (*Hint:* Neglect the power loss due to base drive.)

13-5. For the parameters in Problem 13-3, calculate the average power loss due to the base current, P_B.

13-6. Repeat Prob. 13-3 if $V_{BE(sat)} = 2.3$ V, $I_B = 8$ A, $V_{CE(sat)} = 1.4$ V, $t_d = 0.1\ \mu s$, $t_r = 0.45\ \mu s$, $t_s = 3.2\ \mu s$, and $t_f = 1.1\ \mu s$.

13-7. An IR-MOSFET type IRFZ40 with data sheet in Fig. 13-29 is used as a switch. The parameters are $V_{DD} = 40$ V, $I_D = 35$ A, $R_{DS} = 28\ m\Omega$, $V_{GS} = 10$ V, $t_{d(on)} = 25$ ns, $t_r = 60$ ns, $t_{d(off)} = 70$ ns, $t_f = 25$ ns, $f_s = 20$ kHz. The drain-source leakage current is $I_{DSS} = 250\ \mu A$. The duty cycle is $k = 60\%$. Determine the power loss due to the drain current **(a)** during turn-on $t_{on} = t_{d(n)} + t_r$; **(b)** during conduction period, t_n; **(c)** during turn-off, $t_{off} = t_{d(off)} + t_f$; **(d)** during off-time, t_o; and **(e)** total average power losses, P_T.

13-8. The maximum junction temperature of the MOSFET in Prob. 13-7 is $T_J = 150°C$ and the ambient temperature is $T_A = 30°C$. If the thermal resistances are $R_{JC} = 1°K/W$, and $R_{CS} = 1°K/W$, calculate the thermal resistance of heat sink, R_{SA}. (Note: $°K = °C + 273$).

13-9. A bipolar transistor of GE type D67DE is used a chopper swtich for a resistive load. The collector current is I_C = 80 A at a forced β of β_f = 50. If the junction temperature is T_J = 150°C, calculate the **(a)** $V_{CE(sat)}$; **(b)** $V_{BE(sat)}$; **(c)** turn-on time, t_{on}; **(d)** turn-off time, t_{off}; **(e)** base current to drive the transistor into saturation, I_B; and **(f)** overdrive factor, ODF.

13-10. The base drive circuit in Fig. 13-19 has V_{CC} = 400 V, R_C = 4 Ω, V_{d1} = 3.6 V, V_{d2} = 0.9 V, $V_{BE(sat)}$ = 0.7 V, V_B = 15 V, R_B = 1.1 Ω, and β = 12. Calculate the **(a)** collector current without clamping; **(b)** collector clamping voltage, V_{CE}; and **(c)** collector current with clamping.

13-11. An IR-MOSFET type IRFZ40 is operated as a switch. The junction temperature is T_J = 150°C at a case temperature of T_C = 95°C. The gate-to-source voltage is V_{GS} = 10 V. The dc supply voltage is V_{DD} = 40 V. Determine the **(a)** maximum continuous drain current, I_D; **(b)** maximum power dissipation, P_D; **(c)** on-state resistance, R_{DS}; **(d)** gate voltage overdrive factor, ODF; **(e)** on-state or saturation voltage, V_{DS}; and **(f)** gate power losses if the MOSFET is operated at a frequency of 20 kHz.

13-12. Two BJTs are connected in parallel similar to Fig. 13-33. The total load current of I_T = 200 A. The collector–emitter voltage of transistor Q_1 is V_{CE1} = 1.5 V and that of transistor Q_2 is V_{CE2} = 1.1 V. Determine the collector current of each transistor and difference in current sharing if the current sharing series resistances are **(a)** R_{e1} = 10 mΩ and R_{e2} = 20 mΩ, and **(b)** R_{e1} = R_{e2} = 20 mΩ.

13-13. A bipolar transistor is operated as chopper switch at a frequency of f_s = 20 kHz. The circuit arrangement is shown in Fig. 13-36a. The dc input voltage of the chopper is V_s = 400 V and the load curent is I_L = 100 A. The switching times are t_r = 1 μs and t_f = 3 μs. Determine the values of **(a)** L_s; **(b)** C_s; **(c)** R_s for critically damped condition; **(d)** R_s if the discharge time is limited to one-third of switching period; **(e)** R_s if peak discharge current is limited to 5% of load current; and **(f)** power loss due to *RC* snubber, P_s, neglecting the effect of inductor L_s on the voltage of snubber capacitor, C_s. Assume $V_{CE(sat)}$ = 0.

13-14. A MOSFET is operated as chopper switch at a frequency of f_s = 50 kHz. The circuit arrangement is shown in Fig. 13-36a. The dc input voltage of the chopper is V_s = 30 V and the load current is I_L = 40 A. The switching times are t_r = 60 ns and t_f = 25 ns. Determine the values of **(a)** L_s; **(b)** C_s; **(c)** R_s for critically damped condition; **(d)** R_s if the discharge time is limited to one-third of switching period; **(e)** R_s if peak discharge current is limited to 5% of load current; and **(f)** power loss due to *RC* snubber, P_s, neglecting the effect of inductor L_s on the voltage of snubber capacitor, C_s. Assume $V_{CE(sat)}$ = 0.

14

Thyristors

14-1 INTRODUCTION

A thyristor is the most important type of power semiconductor devices. Thyristors are extensively used in power electronic circuits. They are operated as bistable switches from nonconducting state to conducting state. Although for the development of power conversion techniques in earlier chapters, thyristors are assumed as ideal switches, the practical thyristors exhibit certain characteristics and limitations.

14-2 THYRISTOR CHARACTERISTICS

A thyristor is a four-layer semiconductor device of *pnpn*-structure with three *pn*-junctions. It has three terminals: anode, cathode, and gate. Figure 14-1 shows the sectional view of three *pn*-junctions and the symbol of thyristor. Thyristors are manufactured by diffusion.

When the anode voltage is positive with respect to the cathode, the junctions J_1 and J_3 are forward biased. The junction J_2 is reverse biased, and only the leakage current flows from anode to cathode. The thyristor is then said to be in the *forward blocking* or *off-state* condition and the leakage current is known as *off-*

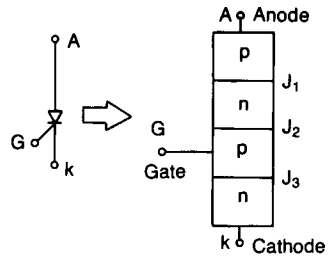


Figure 14-1 Three *pn*-junctions and thyristor symbol.

state current, I_D. If the anode-to-cathode voltage, V_{AK}, is increased to a sufficiently large value, the reverse-biased junction J_2 will break. This is known as *avalanche breakdown* and the corresponding voltage is called *forward breakdown voltage*, V_{BO}. Since the other junctions J_1 and J_3 are already forward biased, there will be free movement of carriers across all three junctions, resulting in large forward anode current. The device will then be in a *conducting state* or *on-state*. The voltage drop would be due to the ohmic drop in the four layers and it is small, typically, 1 V. In the on-state, the anode current is limited by the external impedance or resistance, R_L, as shown in Fig. 14-2a. The anode current must be more than a value known as *latching current*, I_L, to maintain the required amount of carriers flow across the junction; otherwise, the device will revert to the blocking condition as the anode-to-cathode voltage is reduced. The v–i characteristics of a thyristor is shown in Fig. 14-2b.

Once a thyristor conducts, it behaves like a conducting diode and there is no control over the device. The device will continue to conduct because there is no depletion layer on the junction J_2 due to the free movements of carriers. However, if the forward anode current is reduced below a level known as the *holding current*, I_H, a depletion region would develop around junction J_2 due to the reduced number of carriers and the thyristor would be in the blocking state. The holding current is in the order of milliamperes and is less than the latching current, I_L.

When the cathode voltage is positive with respect to the anode, the junction J_2 is forward biased and junctions J_1 and J_3 are reverse biased. This is equivalent

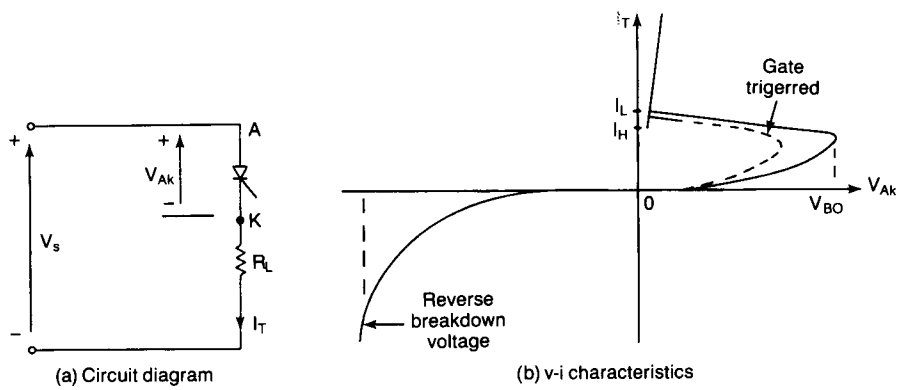


Figure 14-2 Thyristor circuit and v–i characteristics.

to two series-connected diodes with reverse voltage across them. The thyristor will be in the reverse blocking state and a reverse leakage current *known as reverse current*, I_R, would flow through the device.

Although a thyristor can be turned on by increasing the forward voltage beyond V_{BO}, such a turn-on could be destructive. In practice, the forward voltage is maintained below V_{BO} and the thyristor is turned on by applying a positive voltage between the gate and the cathode. This is shown in Fig. 14-2b. Once a thyristor is tuned on by a gating signal and its anode current is greater than the holding current, the device continues to conduct due to positive feedback, even if the gating signal is removed.

14-3 TWO-TRANSISTOR MODEL OF THYRISTOR

The regenerative or latching action due to positive feedback can be demonstrated by using a two-transistor mode of thyristor. A thyristor can be considered as two complementary transistors, one *pnp*-transistor, Q_1, and other *npn*-transistor, Q_2, as shown in Fig. 14-3a.

The collector current, I_C, of a thyristor is related, in general, to the emitter current, I_E, and leakage current of the collector–base junction, I_{CBO}, as

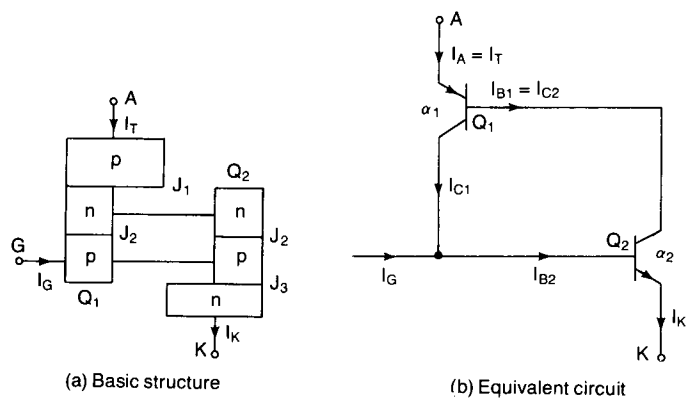
$$I_C = \alpha I_E + I_{CBO} \tag{14-1}$$

and the *common base current* gain is defined as $\alpha \cong I_C/I_E$. For transistor Q_1, collector current is the anode current, I_A, and the collector current can be found from Eq. (14-1):

$$I_{C1} = \alpha_1 I_A + I_{CBO1} \tag{14-2}$$

where α_1 is the current gain and I_{CBO1} is the leakage current for Q_1. For transistor Q_2, the collector current I_{C2} is

$$I_{C2} = \alpha_2 I_K + I_{CBO2} \tag{14-3}$$



(a) Basic structure (b) Equivalent circuit

Figure 14-3 Two-transistor model of thyristor.

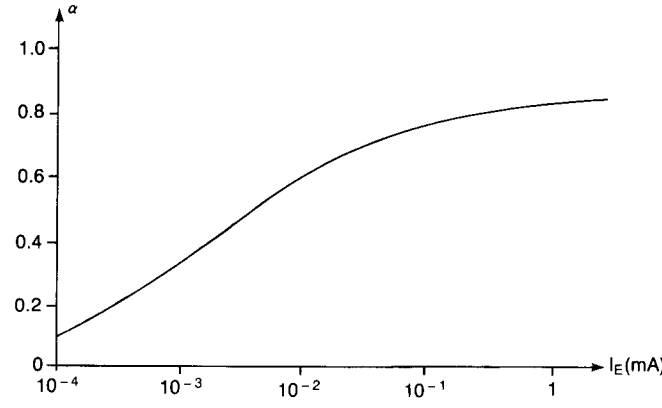


Figure 14-4 Typical variation of current gain with emitter current.

where α_2 is the current gain and I_{CBO2} is the leakage current for Q_2. By combining I_{C1} and I_{C2} gives

$$I_A = I_{C1} + I_{C2} = \alpha_1 I_A + I_{CBO1} + \alpha_2 I_K + I_{CBO2} \tag{14-4}$$

But for a gating current of I_G, $I_K = I_A + I_G$ and solving Eq. (14-4) for I_A gives

$$I_A = \frac{\alpha_2 I_G + I_{CBO1} + I_{CBO2}}{1 - (\alpha_1 + \alpha_2)} \tag{14-5}$$

The curent gain, α_1 varies with the emitter current I_A; and α_2 varies with $I_K = I_A + I_G$. A typical variation of current gain, α, with the emitter current, I_E, is shown in Fig. 14-4. If the gate curent, I_G, is suddenly increased, say from 0 to 1 mA, this would immediately increase anode current, I_A, which would further increase α_1 and α_2. α_2 would depend on I_A and I_G. The increase in the values of α_1 and α_2 would further increase I_A. Therefore, there is a regenerative or positive feedback effect. If $(\alpha_1 + \alpha_2)$ tends to be unity, the denominator of Eq. (14-5) approaches zero, resulting in a large value of anode current, I_A, and the thyristor would turn on with a small gate current.

Under transient conditions, the capacitances of the *pn*-junctions, as shown in Fig. 14-5, will influence the characteristics of the thyristor. If a thyristor is in a blocking state, a rapidly rising voltage applied across the device would cause high current flow through the junction capacitors; and the current through capacitor C_{j2} can be expressed as

$$i_{j2} = \frac{d(q_{j2})}{dt} = \frac{d}{dt}(C_{j2}V_{j2}) = V_{j2}\frac{dC_{j2}}{dt} + C_{j2}\frac{dV_{j2}}{dt} \tag{14-6}$$

where C_{j2} and V_{j2} are the capacitance and voltage of junction J_2, respectively. q_{j2} is the charge in the junction. If the rate of rise of voltage, dv/dt is large, then i_{j2} would be large and this would result in increased leakage currents, I_{CBO1} and I_{CBO2}. According to Eq. (14-5), high enough values of I_{CBO1} and I_{CBO2} may cause $(\alpha_1 +$

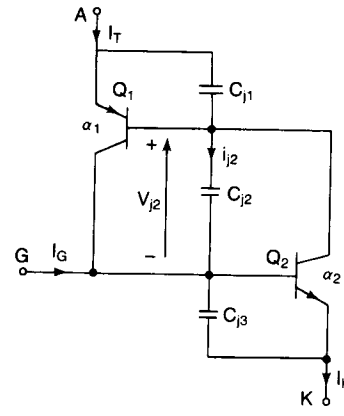


Figure 14-5 Two-transistor transient model of thyristor.

α_2) to tend to unity and results in undesirable turn on the thyristor. However, large values of current through junction capacitors may also damage the device.

14-4 THYRISTOR TURN-ON

A thyristor can be turned on by increasing the anode current. This can be accomplished in one of the following ways.

Thermals. If the temperature of a thyristor is high, there will be an increase in the number of electron–hole pairs, which would increase the leakage currents. This increase in current would cause α_1 and α_2 to increase. Due to the regenerative action, $(\alpha_1 + \alpha_2)$ may tend to be unity and the thyristor may be turned on. This type of turn-on may cause thermal runaway and is normally avoided.

Light. If light is allowed to strike the junctions of a thyristor, the electron–hole pairs will increase; and the thyristor may be turned on. The light-activated thyristors are turned on by allowing light to strike the silicon wafer.

High voltage. If the forward anode-to-cathode voltage is greater than the forward breakdown voltage V_{BO}, a sufficient leakage current will flow to initiate regenerative turn-on. This type of turn-on may be destructive and should be avoided.

dv/dt. It can be noticed from Eq. (14-6) that if the rate of rise of the anode–cathode voltage is high, the charging current of the capacitive junctions may be sufficient enough to turn on the thyristor. A high value of charging current may damage the thyristor and the device must be protected against high *dv/dt*. The manufacturers specify the maximum allowable *dv/dt* of thyristors.

Gate current. If a thyristor is forward based, the injection of gate current by applying positive gate voltage between the gate and cathode terminals would

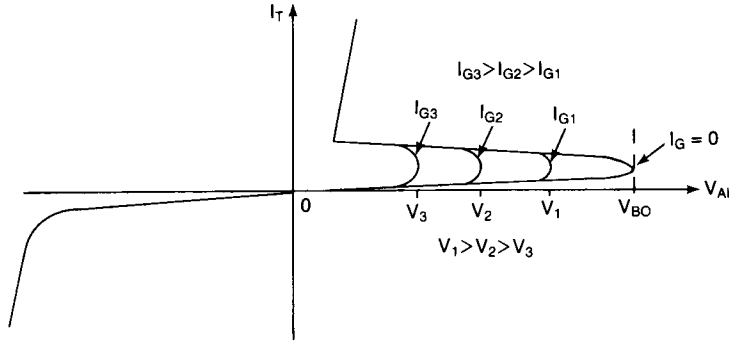


Figure 14-6 Effects of gate current on forward blocking voltage.

turn-on the thyristor. As the gate current is increased, the forward blocking voltage is decreased as shown in Fig. 14-6.

Figure 14-7 shows the waveform of the anode current, following the application of gate signal. There is a time delay known as *turn-on time*, t_{on}, between the application of gate signal and the conduction of a thryistor. t_{on} is defined as the time interval between 10% of steady-state gate current ($0.1I_G$) and 90% of the steady-state thyristor on-state current ($0.9I_T$). t_{on} is the sum of *delay time*, t_d, and *rise time*, t_r. t_d is defined as the time interval between 10% of gate current ($0.1I_G$) and 10% of thyristor on-state current ($0.1I_T$). t_r is the time required for the anode current to rise from 10% of on-state current ($0.1I_T$) to 90% of on-state current ($0.9I_T$). These times are depicted in Fig. 14-7.

The following points should be considered in designing the gate control circuit:

1. The gate signal can be removed after the thyristor is turned on. A continuous gating signal would increase the power loss in the gate junction.

2. While the thyristor is reversed biased, there should be no gate signal; otherwise, the thyristor may fall due to increase leakage current.

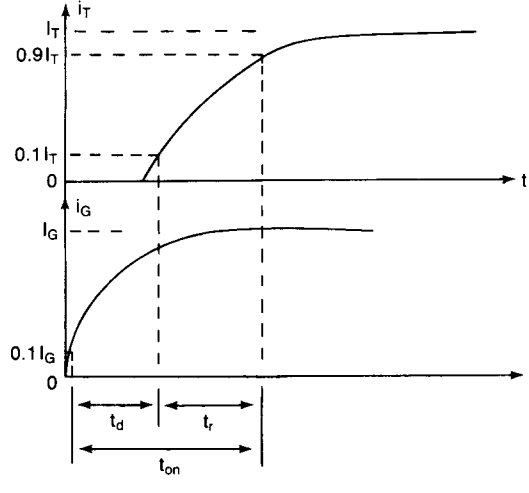


Figure 14-7 Turn-off characteristics.

3. The width of gate pulse, t_G, must be longer than the time required for the anode current to rise to the holding current value. In practice, the pulse width, t_G, is normally made more than the turn-on time of the thyristor, t_{on}.

Example 14-1

The holding current of thyristors in the single-phase full converter of Fig. 14-3a is I_H = 500 mA and the delay time is t_d = 1.5 μs. The converter is supplied from a 120-V 60-Hz supply and has a load of L = 10 mH and R = 10 Ω. The converter is operated with a delay angle of α = 30°. Determine the minimum value of gate pulse width, t_G.

Solution I_H = 500 mA = 0.5 A, t_d = 1.5 μs, α = 30° = π/6, L = 10 mH, and R = 10 Ω. The instantaneous value of the input voltage is $v(t) = V_m \sin \omega t$, where $V_m = \sqrt{2} \times 120 = 169.7$ V.

At $\omega t = \alpha$,

$$V_1 = v(\omega t = \alpha) = 169.7 \times \sin \frac{\pi}{6} = 84.85 \text{ V}$$

The rate of rise of anode current, di/dt, at the instant of triggering is approximately,

$$\frac{di}{dt} = \frac{V_1}{L} = \frac{84.85}{10 \times 10^{-3}} = 8485 \text{ A/s}$$

If di/dt is assumed constant for a short time after the gate triggering, the time required for the anode current to rise to the level of holding current, t_1, is calculated from $t_1 \times (di/dt) = I_H$ or $t_1 \times 8485 = 0.5$ and this gives $t_1 = 0.5/8485 = 58.93$ μs. Therefore, the minimum width of gate pulse is

$$t_G = t_1 + t_d = 58.93 + 1.5 = 60.43 \text{ μs}$$

Example 14-2

The capacitance of reverse-biased junction J_2 in a thyristor is C_{J2} = 20 pF and can be assumed to be independent of the off-state voltage. The limiting value of charging current to turn on the thyristor is 16 mA. Determine the critical value of dv/dt.

Solution C_{j2} = 20 pF and i_{J2} = 16 mA. Since $d(C_{J2})/dt = 0$, we can find the critical value of dv/dt from Eq. (14-6):

$$\frac{dv}{dt} = \frac{i_{J2}}{C_{J2}} = \frac{16 \times 10^{-3}}{20 \times 10^{-12}} = 800 \text{ V/μs}$$

14-5 *di/dt* PROTECTION

A thyristor requires a minimum time to spread the current conduction uniformly throughout the junctions. If the rate of rise of anode current is very fast compared to the spreading velocity of a turn-on process, localized "hot-spot" heating will occur due to high current density and the device may fall, as a result of excessive temperature.

In the earlier chapters it has been assumed that a thyristor can turn on instantaneously and has no di/dt limit. But the practical devices must be protected

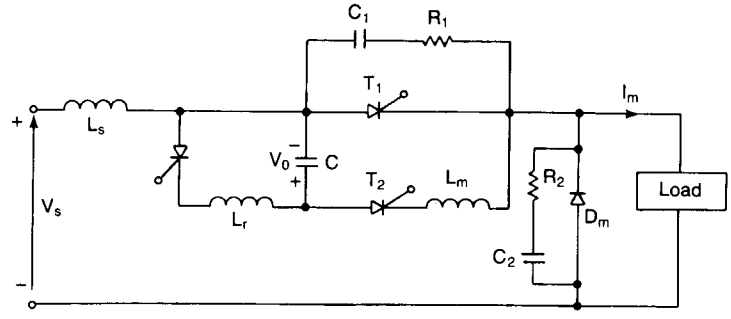


Figure 14-8 Chopper circuit with *di/dt* limiting inductors.

against high *di/dt*. As an example, let us consider the chopper circuit in Fig. 7-17. Under steady-state operation, D_m conducts when thyristor T_1 is off. If T_1 is fired when D_m is still conducting, *di/dt* can be very high and limited only by the stray inductance of the circuit. When T_1 is on and T_2 is fired to turn-off T_1, the discharging current of the commutation capacitor, C, is limited by the stray inductance of the loop formed by T_1, T_2, and C. This reverse *di/dt* of thyristor could also be very high.

In practice, the *di/dt* is limited by adding a series inductor, L_s, as shown in Fig. 14-8. The forward *di/dt* is

$$\frac{di}{dt} = \frac{V_s}{L_s} \tag{14-7}$$

where L_s is the series inductance, including any stray inductance. The reverse *di/dt* is

$$\frac{di}{dt} = \frac{V_0}{L_m} \tag{14-8}$$

where L_m is the reverse *di/dt* limiting inductance and V_0 is the commutation capacitor voltage. For $V_s = 300$ V and forward $di/dt = 100$ A/μs, the required value of limiting inductance is $L_s = V_s/(di/dt) = 300/(100 \times 10^{-6}) = 3$ μH.

Due to reverse recovery time, t_{rr}, of diode D_m, the excess energy, which will be stored in inductor L_s, can be determined from Eq. (12-15) by replacing I_0 with I_m. This energy must be absorbed by capacitor C_2, which is connected across diode D_m as shown in Fig. 14-8. For a load current of I_m, Eq. (12-15) can be applied to calculate the excess energy, which will be stored in inductor L_m due to the reverse recovery time, t_{rr}, of thyristor T_1,

$$W_R = \frac{1}{2} L_m \left[\left(I_m + \frac{t_{rr} V_0}{L_m} \right)^2 - I_m^2 \right] \tag{14-9}$$

and this energy must be absorbed by capacitor C_1 connected across T_1 as shown in Fig. 14-8.

The effects of reverse recovery time of thyristors and diodes on the *di/dt* inductors should be analyzed, especially at high current level. The appropriate

values of energy-absorbing capacitors across the devices should be determined to limit the voltage stress on the devices due to switching transients.

14-6 *dv/dt* PROTECTION

If the switch S_1 in Fig. 14-9a is closed at $t = 0$, a step voltage will be applied across thyristor T_1 and *dv/dt* may be high enough to turn on the device. The *dv/dt* can be limited by connecting capacitor C_s, as shown in Fig. 14-9a. When thyristor T_1 is turned on, the discharge current of capacitor is limited by resistor R_s as shown in Fig. 14-9b.

With a *RC*-snubber circuit, the voltage across the thyristor will rise exponentially as shown in Fig. 14-9c and the circuit *dv/dt* can be found from

$$\frac{dv}{dt} = \frac{0.632V_s}{\tau} = \frac{0.632V_s}{R_sC_s} \tag{14-10}$$

The value of snubber time constant τ ($= R_sC_s$) can be determined from Eq. (14-10) for a known value of *dv/dt*. The value of R_s is found from the discharge current I_{TD}.

$$R_s = \frac{V_s}{I_{TD}} \tag{14-11}$$

It is possible to use different resistors for *dv/dt* and discharging as shown in Fig.

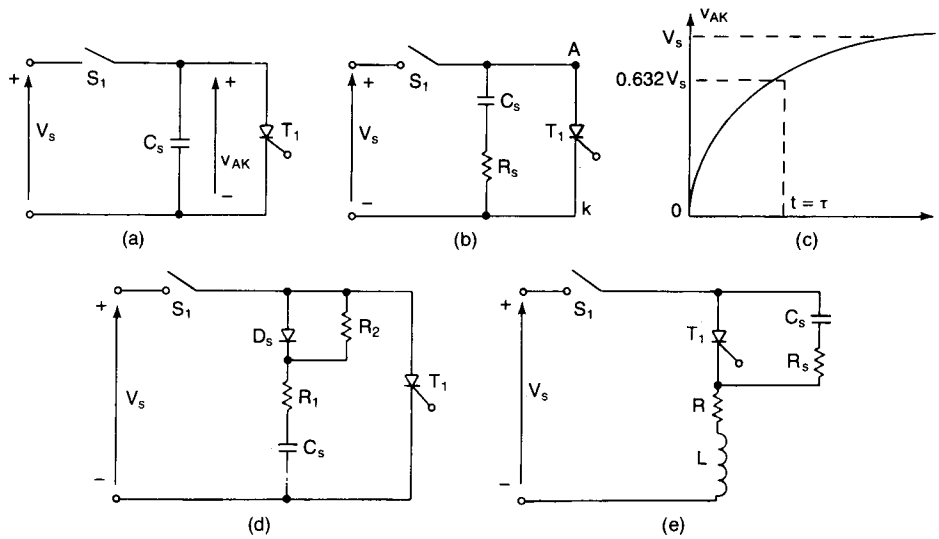


Figure 14-9 *dv/dt* protection circuits.

14-9d. The dv/dt is limited by R_1 and C_s. $(R_1 + R_2)$ limits the discharging current such that

$$I_{TD} = \frac{V_s}{R_1 + R_2} \tag{14-12}$$

The load can form a series circuit with the snubber network as shown in Fig. 14-9e. From Eqs. (2-23) and (2-24), the damping ratio of a second-order equation is

$$\delta = \frac{\alpha}{\omega_0} = \frac{R_s + R}{2}\sqrt{\frac{C_s}{L_s + L}} \tag{14-13}$$

where L_s is the stray inductance and L and R are the load inductance and resistance, respectively.

To limit the peak voltage overshoot applied across the thyristor, the damping ratio in the range 0.5 to 1.0 is used. If the load inductance is high, which is usually the case, R_s can be high and C_s can be small to retain the desired value of damping ratio. A high value of R_s will reduce the discharge current and a low value of C_s reduces the snubber loss. The circuits in Fig. 14-9 should be fully analyzed to determine the required value of damping ratio to limit the dv/dt to the desired value. Once the damping ratio is known, R_s and C_s can be found. The same RC network or snubber is normally used for dv/dt protection and to suppress the transient voltage due to reverse recovery time. The transient voltage suppression is fully analyzed in Section 15-4.

Example 14-3

The input voltage in Fig. 14-9e is $V_s = 200$ V with load resistance of $R = 5\ \Omega$. The load and stray inductances are negligible and the thyristor is operated at a frequency of $f_s = 2$ kHz. If the required dv/dt is 100 V/μs and the discharge current is to be limited to 100 A, determine the (a) values of R_s and C_s, (b) snubber loss, and (c) power rating of snubber resistor.

Solution $dv/dt = 100$ V/μs, $I_{TD} = 100$ A, $R = 5\ \Omega$, $L = L_s = 0$, and $V_s = 200$ V.

(a) From Fig. 14-9e the charging current of the snubber capacitor can be expressed as

$$V_s = (R_s + R)i + \frac{1}{C_s}\int i\,dt + v_c\,(t = 0)$$

With initial condition $v_c\,(t = 0) = 0$, the charging current is found as

$$i(t) = \frac{V_s}{R_s + R}\,e^{-t/\tau} \tag{14-14}$$

where $\tau = (R_s + R)C_s$. The forward voltage across the thyristor is

$$v_T(t) = V_s - \frac{RV_s}{R_s + R}\,e^{-t/\tau} \tag{14-15}$$

At $t = 0$, $v_T(0) = V_s - RV_s/(R_s + R)$ and at $t = \tau$, $v_T(\tau) = V_s - 0.632RV_s/(R_s + R)$:

$$\frac{dv}{dt} = \frac{v_T(\tau) - v_T(0)}{\tau} = \frac{0.368RV_s}{C_s(R_s + R)^2} \tag{14-16}$$

From Eq. (14-11), $R_s = 200/100 = 2\ \Omega$. Equation (14-16) gives

$$C_s = \frac{0.386 \times 5 \times 200 \times 10^{-6}}{(2 + 5)^2 \times 100} = 0.079\ \mu\text{F}$$

(b) The snubber loss,

$$\begin{aligned} P_s &= 0.5C_sV_s^2f_s \\ &= 0.5 \times 0.075 \times 10^{-6} \times 200^2 \times 2000 = 3\ \text{W} \end{aligned} \tag{14-17}$$

(c) Assuming that all the energy stored in C_s is dissipated in R_s only, the power rating of the snubber resistor is 3 W.

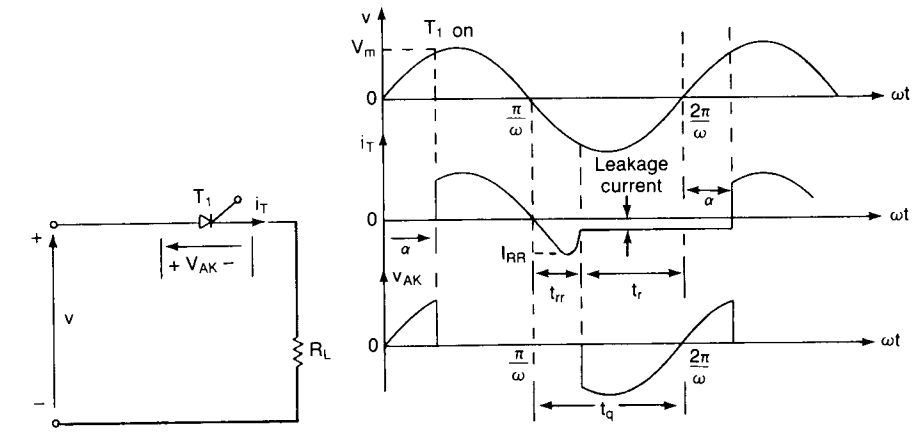
14-7 THYRISTOR TURN-OFF

A thyristor, which is in the on-state, can be turned off by reducing the forward current to a level below the holding current, I_H. There are various techniques for turning off a thyristor, which are discussed in Chapter 3. In all the commutation techniques, the anode current is maintained below the holding current for a sufficiently long time, so that all the excess carriers in the four layers are swept out or recombined.

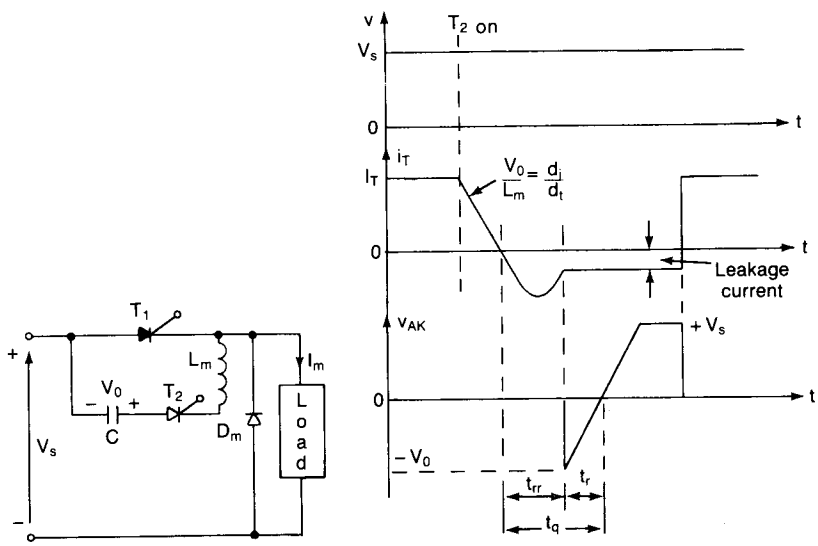
Due to two outer *pn*-junctions, J_1 and J_3, the turn-off characteristics would be similar to that of a diode, exhibiting reverse recovery time, t_{rr}, and peak reverse recovery current, I_{RR}. I_{RR} can be much greater than the normal reverse blocking current, I_R. In a line-commutated circuit where the input voltage is allternating as shown in Fig. 14-10a, a reverse voltage appears across the thyristor immediately after the forward current goes through the zero value. This reverse voltage will accelerate the turn-off process, by sweeping out the excess carriers from *pn*-junctions J_1 and J_3. Equations (12-6) and (12-7) can be applied to calculate t_{rr} and I_{RR}.

The inner *pn*-junction, J_2, will require a time known as *recombination time*, t_r to recombine the excess carriers. A negative reverse voltage would reduce this recombination time. t_r is dependent on the magnitude of the reverse voltage. The turn-off characteristics are shown in Figs. 14-10a and 14-10b for a line commutated circuit and forced-commutated circuit respectively.

The turn-off time, t_q, is the sum of reverse recovery time, t_{rr}, and recombination time, t_r. At the end of turn-off, a depletion layer develops across junction J_2 and the thyristor recovers its ability to withstand forward voltage. In all the commutation techniques in Chapter 3, a reverse voltage is applied across the thyristor during turn-off process.



(a) Line-commutated thyristor circuit



(b) Forced-commutated thyristor circuit

Figure 14-10 Turn-off characteristics.

14-8 THYRISTOR TYPES

Thyristors are manufactured almost exclusively by diffusion. The anode current requires a finite time to propagate to the whole area of the junction, from the point near the gate when the gate signal is initiated for turning on the thyristor. The manufacturers use various gate structures to control the *di/dt*, turn-on time,

and turn-off time. Depending on the physical construction, and turn-on and turn-off behavior, thyristors can, broadly, be classified into eight categories:

1. Phase-control thyristors (SCRs)
2. Fast-switching thyristors (SCRs)
3. Gate-turn-off thyristors (GTOs)
4. Bidirectional triode thyristors (TRIACs)
5. Reverse-conducting thyristors (RCTs)
6. Static induction thyristors (SITHs)
7. Light-activated silicon-controlled rectifiers (LASCRs)
8. FET-controlled thyristors (FET-CTHs)

14-8.1 Phase-Control Thyristors

This type of thyristors generally operates at the line frequency and is turned off by natural commutation. The turn-off time, t_q, is of the order of 50 to 100 μs. This is most suited for low-speed switching applications and is also known as *converter thyristor*. Since the thyristor is basically a silicon-made controlled device, it is also known as *silicon-controlled rectifier* (SCR).

The on-state voltage, V_T, varies typically from about 1.15 V for 600 V to 2.5 V for 4000-V devices; and for a 5500-A, 1200-V thyristor it is typically 1.25 V. The modern thyristors use an amplifying gate, where an auxiliary thyristor, T_A, is gated on by a gate signal and then the amplified output of T_A is applied as a gate signal to the main thyristor, T_M. This is shown in Fig. 14-11. The amplifying gate permits high dynamic characteristics with typical *dv/dt* of 1000 V/μs and *di/dt* of 500 A/μs and simplifies the circuit design by reducing or minimizing *di/dt* limiting inductor and *dv/dt* protection circuits.

14-8.2 Fast-Switching Thyristors

These are used in high-speed switching applications with forced commutation (e.g., choppers and inverters). They have fast turn-off time, generally in the range 5 to 50 μs, depending on the voltage range. The on-state forward drop varies, approximately as an inverse function of the turn-off time, t_q. This type of thyristors is also known as an *inverter thyristor*.

These thyristors have high *dv/dt* of typically 1000 V/μs and *di/dt* of 1000 A/μs. The fast turn-off and high *di/dt* are very important to minimize the size and weight of commutating and /or reactive circuit components. The on-state voltage

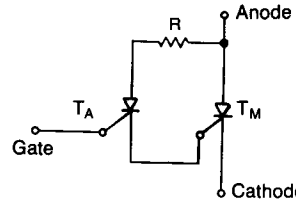


Figure 14-11 Amplifying gate thyristor.

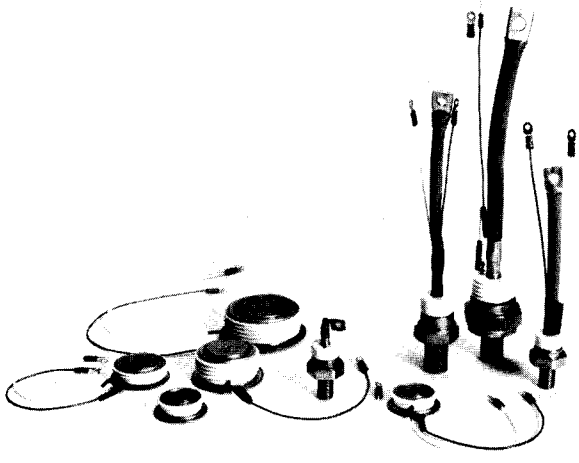


Figure 14-12 Fast-switching thyristors. (*Courtesy of Powerex, Inc.*)

of a 2200-A 1800-V thyristor is typically 1.7 V. Inverter thyristors with a very limited reverse blocking capability, typically 10 V, and a very fast turn-off time between 3 and 5 μs are commonly known as *asymmetrical thyristors* (ASCRs). Fast-switching thyristors of various sizes are shown in Fig. 14-12.

14-8.3 Gate-Turn-Off Thyristors

A gate-turn-off thyristor (GTO) like a SCR can be turned on by applying a positive gate signal. However, it can be turned off by a negative gate signal. A GTO is a latching device and can be built with current and voltage ratings similar to those of a SCR. The GTOs have advantages over SCRs: (1) elimination of commutating components in forced commutation, resulting in reduction in cost, weight, and volume; (2) reduction in acoustic and electromagnetic noise due to the elimination of commutation chokes; (3) faster turn-off, permitting high switching frequencies; and (4) improved efficiency of converters.

In low-power applications, GTOs have the following advantages over bipolar transistors: (1) higher blocking voltage capability; (2) high ratio of peak controllable current to average current; (3) high ratio of peak surge current to average current, typically 10:1; (4) high on-state gain (anode current/gate current), typically 600; and (5) pulsed gate signal of short duration. Under surge conditions, a GTO goes into deeper saturation due to regenerative action. On the other hand, a bipolar transistor tends to come out of saturation.

A GTO has low gain during turn-off, typically 6, and requires a relatively high negative current pulse to turn off. It has higher on-state voltage than that of SCRs. The on-state voltage of a typical 550-A 1200-V GTO is typically 3.4 V. A 160-A 200-V GTO of type 160PFT is shown in Fig. 14-13 and the junctions of this GTO is shown in Fig. 14-14.



Figure 14-13 A 160-A, 200-V GTO. (*Courtesy of International Rectifier*)

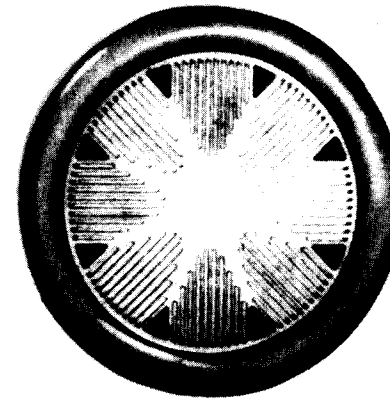


Figure 14-14 Junctions of 160-A GTO in Fig. 14-13. (*Courtesy of International Rectifier*).

14-8.4 Bidirectional Triode Thyristors

A TRIAC can conduct in both directions and is normally used in ac phase control (e.g., ac voltage controllers). It can be considered as two SCRs connected in antiparallel with a common gate connection as shown in Fig. 14-15a. The v–i characteristics are shown in Fig. 14-15c.

Since a TRIAC is a bidirectional device, its terminals cannot be designated as anode and cathode. If terminal MT_2 is positive with respect to terminal MT_1, the TRIAC can be turned on by applying a positive gate signal between gate G and terminal MT_1. If terminal MT_2 is negative with respect to terminal MT_1, it is turned on by applying negative gate signal between gate G and terminal MT_1. It is not necessary to have both polarities of gate signals and a TRIAC can be turned on with either a positive or negative gate signal. In practice, the sensitivities vary from one quadrant to another, and the TRIACs are normally operated in quadrant I^+ (positive gate voltage and gate current) or quadrant III^- (negative gate voltage and gate current).

14-8.5 Reverse-Conducting Thyristors

In many choppers and inverter circuits, an antiparallel diode is connected across an SCR to allow reverse current flow due to inductive load and to improve the turn-off requirement of commutation circuit. The diode clamps the reverse blocking voltage of the SCR to 1 or 2 V under steady-state conditions. However, under

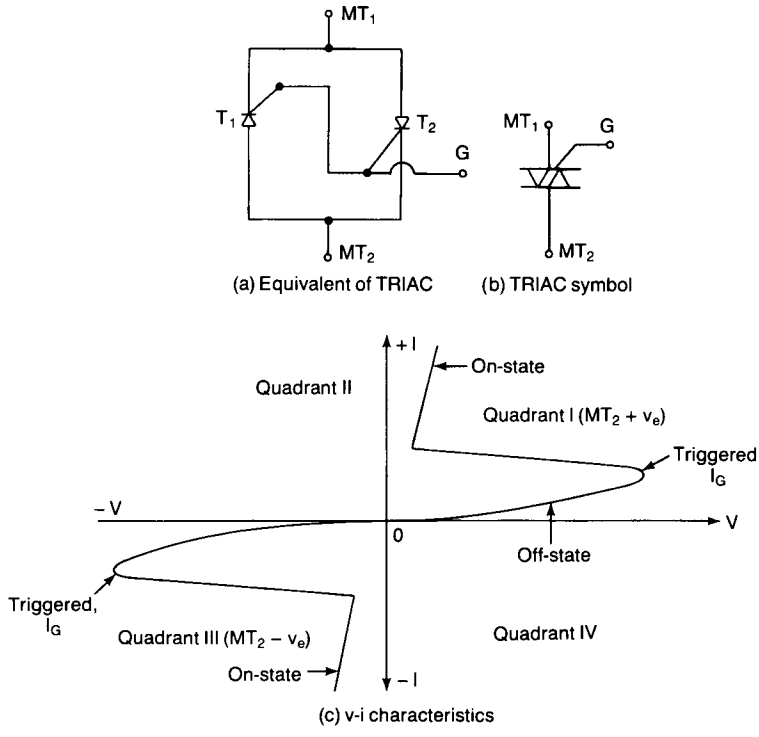


Figure 14-15 Characteristics of TRIAC.

transient conditions, the reverse voltage may rise to 30 V due to induced voltage in the circuit stray inductance within the device.

An RCT is a compromise between the device characteristics and circuit requirement; and it may be considered as a thyristor with a built-in antiparallel diode as shown in Fig. 14-16. An RCT is also called an *asymmetrical thyristor* (ASCR). The forward blocking voltage varies from 400 to 2000 V and the current rating goes up to 500 A. The reverse blocking voltage is typically 30 to 40 V. Since the ratio of forward current through the thyristor to the reverse current of diode is fixed for a given device, their applications will be limited to certain circuit designs.

14-8.6 Static Induction Thryistors

The characteristics of an SITH are similar to those of a MOSFET. An SITH is normally turned on by applying a positive gate voltage like normal thyristors and

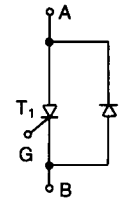


Figure 14-16 Reverse-conducting thyristor.

is turned off by application of negative voltage to its gate. An SITH is a minority-carrier device. As a result, SITH has low on-state resistance or voltage drop and it can be made with higher voltage and current ratings.

SITH has fast switching speeds and high *dv/dt* and *di/dt* capabilities. The switching time is on the order of 1 to 6 μs. The voltage rating can go up to 2500 V and the current rating is limited to 500 A. This device is extremely process sensitive, and small perturbations in the manufacturing process would produce major changes in the device characteristics.

14-8.7 Light-Activated Silicon-Controlled Rectifiers

This device is turned on by direct radiation of silicon with light. Electron–hole pairs which are created due to the radiation produce triggering current under the influence of electric field. The gate structure is designed to provide sufficient gate sensitivity for triggering from practical light sources (e.g., LED and to accomplish high *di/dt* and *dv/dt* capabilities).

The LASRCs are used in high-voltage and high-current applications [e.g., high-voltage (HVDC) transmission and static reactive power or volt-ampere reactive (VAR) compensation. An LASCR offers complete electrical isolation between the light-triggering source and the switching device of the power converter, which floats at a potential of as high as a few hundred kilovolts. The voltage rating of an LASCR could be as high as 4 kV at 1500 A with light-triggering power of less than 100 mW. The typical *di/dt* is 250 A/μs and the *dv/dt* could be as high 2000 V/μs.

14-8.8 FET-Controlled Thyristors

A FET-CTH device combines a MOSFET and a thyristor in parallel as shown in Fig. 14-17. If a sufficient voltage is applied to the gate of the MOSFET, typically 3 V, a triggering current for the thyristor is generated internally. It has high switching speed, high *di/dt*, and high *dv/dt*.

This device can be turned on like conventional thyristors, but it can not be turned off by gate control. This would find applications where optical firing is to be used for providing electrical isolation between the input or control signal and the switching device of the power converter.

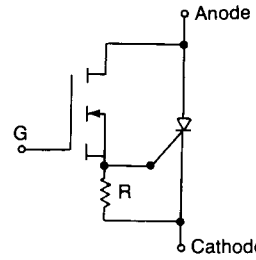


Figure 14-17 FET-controlled thyristor.

14-9 PERFORMANCE PARAMETERS

Thyristors are characterized by certain performance parameters, and the manufacturers specify these parameters in the data sheet of thyristors. Although there are various types of thyristors, the parameters are similar, except the gate characteristics. The characteristic parameters of a diode are applicable to thyristors, except the gate characteristics. The parameters are explained with the data sheets of an SCR and a GTO.

14-9.1 SCR Parameters

Figure 14-18 shows the data sheet of the International Rectifier (IR) Inverter Thyristor: 850 A (RMS), 800 V, types S30EF and S30EFH.

On-state current, $I_{T(AV)}$. $I_{T(AV)}$ is the average on-state current at a specified temperature. These data are normally quoted for a half-sine wave. Figures 14-18.1 and 14-18.2 show the typical variations of average on-state current with the maximum allowable case temperature.

RMS current, $I_{T(RMS)}$. $I_{T(RMS)}$ is the root-mean-square (rms) value of on-state current. This signifies the heating effect due to i^2R dissipation and is limited due to thermal stress on the device. Figures 14-18.3 and 14-18.4 show the maximum average on-state power loss against the average on-state current for sinusoidal and rectangular waveforms at various conduction angles.

Nonrepetitive rate of rise of on-state current, *di/dt*. *di/dt* is the maximum value of the rate of rise of on-state current which the thyristor can withstand without destroying itself.

Maximum repetitive peak reverse voltage, V_{RRM}. V_{RRM} defines the maximum permissible instantaneous value of repetitive applied reverse voltage that a thyristor can block.

Maximum nonrepetitive peak reverse voltage, V_{RSM}. V_{RSM} is the maximum instantaneous peak value of applied reverse voltage under transient conditions and for a specified time duration. V_{RSM} is typically 15% above V_{RRM}.

Maximum repetitive peak off-state voltage, V_{DRM}. V_{DRM} defines the maximum permissible instantaneous value of repetitive applied forward voltage that a thyristor can withstand.

Maximum non-repetitive peak off-state voltage, V_{DSM}. V_{DSM} is the maximum instantaneous peak value of applied forward voltage under transient conditions and for a specified time duration. V_{DSM} is typically 15% above V_{DRM}.

S30EF & S30EFH SERIES
800-600 VOLTS RANGE
STANDARD TURN-OFF TIME 12 μs
850 AMP RMS, RING AMPLIFYING GATE
INVERTER TYPE HOCKEY PUK SCRs

VOLTAGE RATINGS

VOLTAGE CODE [1]	V_{RRM}, V_{DRM} – [V] Max. rep. peak reverse and off-state voltage	V_{RSM} – [V] Max. non-rep. peak reverse voltage $t_p \leq 5ms$	NOTES
	T_J = -40° to max. rated	T_J = 25° to max. rated	
8	800	900	Gate open
6	600	700	

MAXIMUM ALLOWABLE RATINGS

PARAMETER		SERIES	VALUE	UNITS	NOTES
T_J	Junction temperature	S30EF	-40 to 125	°C	
		S30EFH	-40 to 140		
T_{stg}	Storage temperature	ALL	-40 to 150	°C	
$I_{T(AV)}$	Max. av. current	ALL	540	A	180° half sine wave
	● Max. T_C	S30EF	70	°C	
		S30EFH	85		
$I_{T(RMS)}$	Nom. RMS current	ALL	850	A	
I_{TSM}	Max. peak non-repetitive surge current	ALL	8100	A	50Hz half cycle sine wave — Initial T_J = 125°C, rated V_{RRM} applied after surge.
			8500		60Hz half cycle sine wave
			9650		50Hz half cycle sine wave — Initial T_J = 125°C, no voltage applied after surge.
			10000		60Hz half cycle sine wave
I^2t	Max. I^2t capability	ALL	330	kA^2s	t = 10ms — Initial T_J = 125°C, rated V_{RRM} applied after surge.
			300		t = 8.3ms
			465		t = 10ms — Initial T_J = 125°C, no voltage applied after surge.
			425		t = 8.3ms
$I^2\sqrt{t}$	Max. $I^2\sqrt{t}$ capability	ALL	4650	$kA^2\sqrt{s}$	Initial T_J = 125°C, no voltage applied after surge. I^2t for time $t_x = I^2\sqrt{t} \cdot \sqrt{t_x}$. $0.1 \leq t_x \leq 10ms$.
di/dt	Max. non-repetitive rate-of-rise of current	ALL	800	A/μs	T_J = 125°C, $V_D = V_{DRM}$, I_{TM} = 1800A. Gate pulse: 20V, 20Ω, 10μs, 0.5μs rise time. Max. repetitive di/dt is approximately 40% of non-repetitive value.
P_{GM}	Max. peak gate power	ALL	10	W	$t_p \leq 5ms$
$P_{G(AV)}$	Max. av. gate power	ALL	2	W	
$+I_{GM}$	Max. peak gate current	ALL	3	A	$t_p \leq 5ms$
$-V_{GM}$	Max. peak negative gate voltage	ALL	15	V	
F	Mounting force	ALL	8900[2000] ± 10%	N[lbf]	

[1] To complete the part number, refer to the Ordering Information table.

Figure 14-18 Data sheet of SCR, type IR-S30EF, S30EFH. (*Courtesy of International Rectifier*).

CHARACTERISTICS

PARAMETER		SERIES	MIN.	TYP.	MAX.	UNITS	TEST CONDITIONS
V_{TM}	Peak on-state voltage	ALL	—	2.15	2.23	V	Initial T_J = 25°C, 50-60Hz half sine, I_{peak} = 1700A.
$V_{T(TO)1}$	Low-level threshold	ALL	—	—	1.24	V	T_J = max. rated Av. power = $V_{T(TO)} * I_{T(AV)} + r_T * (I_{T(RMS)})^2$ Use low level values for $I_{TM} \leq \pi$ rated $I_{T(AV)}$
$V_{T(TO)2}$	High-level threshold		—	—	1.56		
r_{T1}	Low-level resistance	ALL	—	—	0.57	mΩ	
r_{T2}	High-level resistance		—	—	0.41		
I_L	Latching current	ALL	—	270	—	mA	T_C = 25°C, 12V anode. Gate pulse: 10V, 20Ω, 100µs.
I_H	Holding current	ALL	—	90	500	mA	T_C = 25°C, 12V anode. Initial I_T = 10A.
t_d	Delay time	ALL	—	0.5	1.5	µs	T_C = 25°C, V_D = rated V_{DRM}, 50A resistive load. Gate pulse: 10V, 20Ω, 10µs, 1µs rise time.
t_q	Turn-off time					µs	T_J = max. rated. I_{TM} = 500A, di_R/dt = 25A/µs, V_R = 50V, dv/dt = 200V/µs lin. to 80% rated V_{DRM}. Gate: 0V, 100Ω.
	"A" suffix	S30EF	—	—	12		
	"B" suffix	S30EF/H	—	—	15		
$t_{q(diode)}$	Turn-off time with feedback diode					µs	T_J = max. rated. I_{TM} = 500A, di_R/dt = 25A/µs, V_R = 1V, dv/dt = 800V/µs lin. to 40% V_{DRM}. Gate: 0V, 100Ω.
	"A" suffix	S30EF	—	—	15		
	"B" suffix	S30EF/H	—	—	20		
$I_{RM(REC)}$	Recovery current	ALL	—	47	—	A	T_J = 125°C, I_{TM} = 500A, di_R/dt = 50A/µs.
Q_{RR}	Recovered charge	ALL	—	46	—	µC	
dv/dt	Critical rate-of-rise of off-state voltage	ALL	500	700	—	V/µs	T_J = 125°C. Exp. to 100% or lin. to 80% V_{DRM}, gate open. Higher dv/dt values available.
			1000	—	—		T_J = 125°C. Exp. to 67% V_{DRM}, gate open.
I_{RM}, I_{DM}	Peak reverse and off-state current	S30EF	—	15	40	mA	T_J = max. rated. Rated V_{RRM} and V_{DRM}, gate open.
		S30EFH	—	20	80		
I_{GT}	DC gate current to trigger	ALL	—	—	300	mA	T_C = -40°C +12V anode-to-cathode. For recommended gate drive see "Gate Characteristics" figure.
			50	70	150		T_C = 25°C
V_{GT}	DC gate voltage to trigger	ALL	—	—	3.3	V	T_C = -40°C
			—	1.2	2.5		T_C = 25°C
V_{GD}	DC gate voltage not to trigger	ALL	—	—	0.3	V	T_C = 125°C. Max. value which will not trigger with rated V_{DRM} anode-to-cathode.
R_{thJC}	Thermal resistance, junction-to-case	ALL	—	—	0.040	°C/W	DC operation, double side cooled.
			—	—	0.050	°C/W	180° sine wave, double side cooled.
			—	—	0.053	°C/W	120° rectangular wave, double side cooled.
R_{thCS}	Thermal resistance, case-to-sink	ALL	—	—	0.040	°C/W	Mtg. surface smooth, flat and greased. Single side cooled. For double side, divide value by 2.
wt	Weight	ALL	—	85(3.0)	—	g(oz.)	
	Case Style	ALL	IR A-29				

Figure 14-18 (*continued*)

S30EF & S30EFH SERIES
800-600 VOLTS RANGE

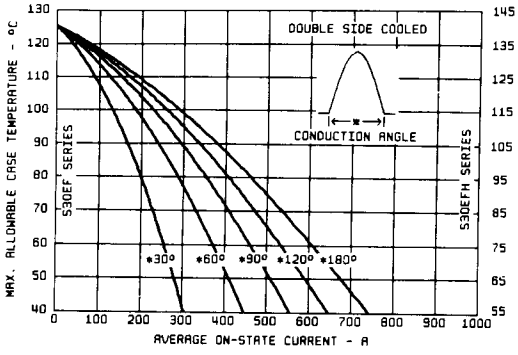


Fig. 1 — Case Temperature Ratings — Sinusoidal Waveforms, 50 to 400 Hz

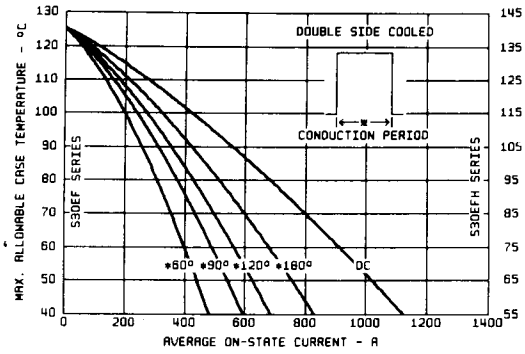


Fig. 2 — Case Temperature Ratings — Rectangular Waveforms, 50 to 400 Hz

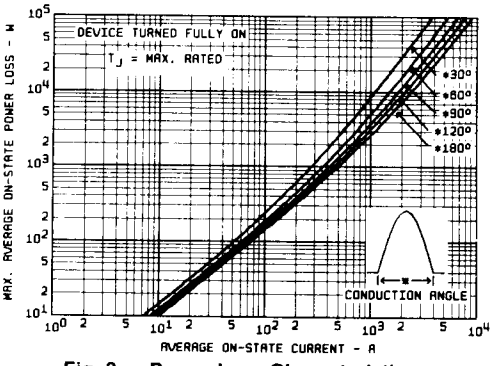


Fig. 3 — Power Loss Characteristics — Sinusoidal Waveforms

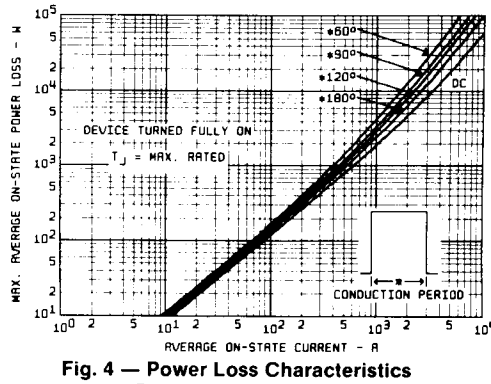


Fig. 4 — Power Loss Characteristics — Rectangular Waveforms

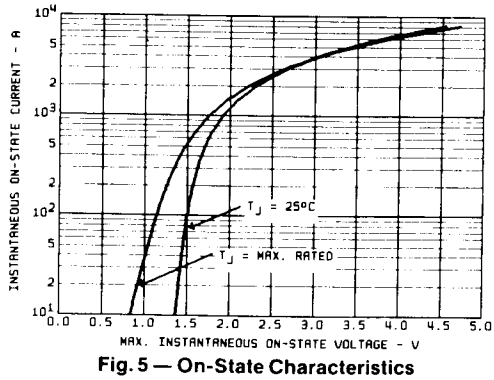


Fig. 5 — On-State Characteristics

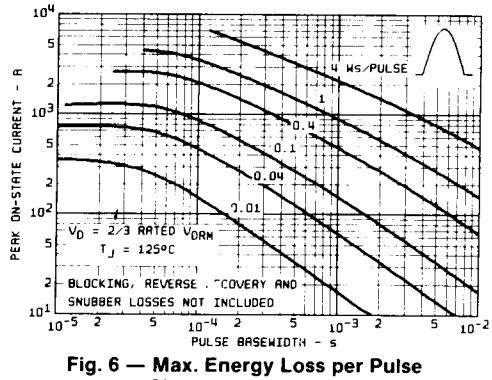


Fig. 6 — Max. Energy Loss per Pulse — Sinusoidal Waveforms

Figure 14-18 (*continued*)

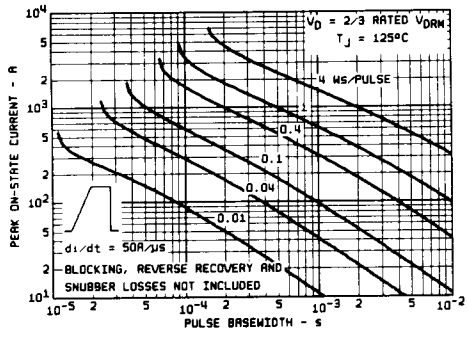


Fig. 7 — Max. Energy Loss per Pulse — Trapezoidal Waveforms, di/dt = 50 A/μs

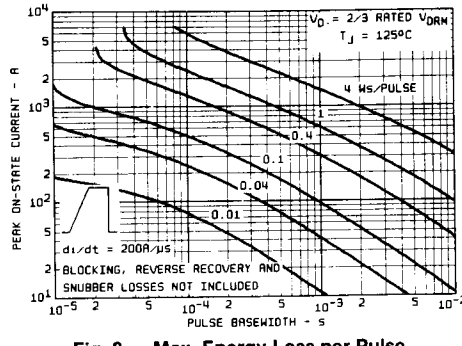


Fig. 8 — Max. Energy Loss per Pulse — Trapezoidal Waveforms, di/dt = 200 A/μs

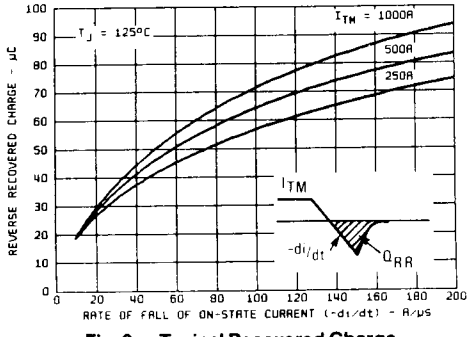


Fig. 9 — Typical Recovered Charge

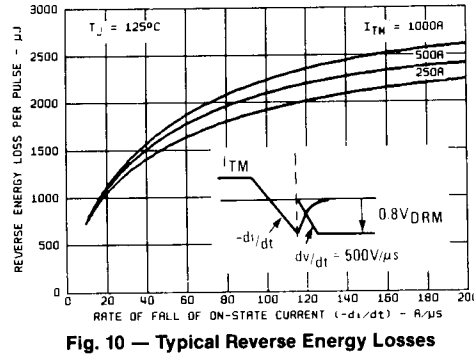


Fig. 10 — Typical Reverse Energy Losses

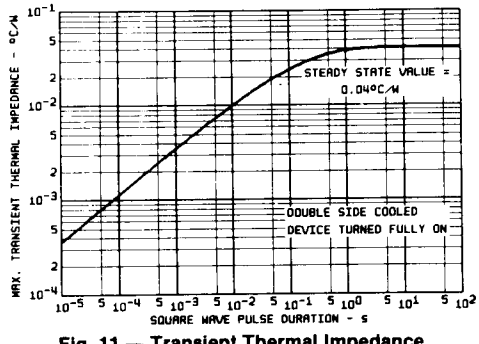


Fig. 11 — Transient Thermal Impedance, Junction-to-Case

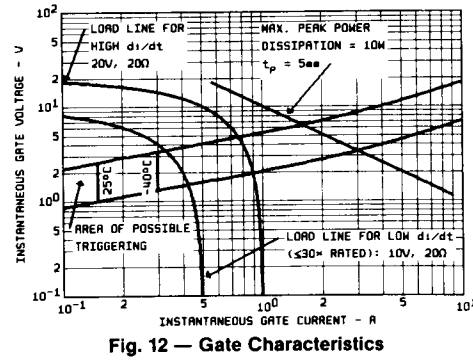


Fig. 12 — Gate Characteristics

Figure 14-18 *(continued)*

S30EF & S30EFH SERIES
800-600 VOLTS RANGE

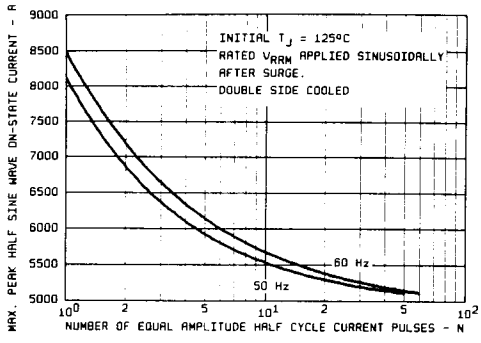


Fig. 13 — Non-Repetitive Surge Current Ratings

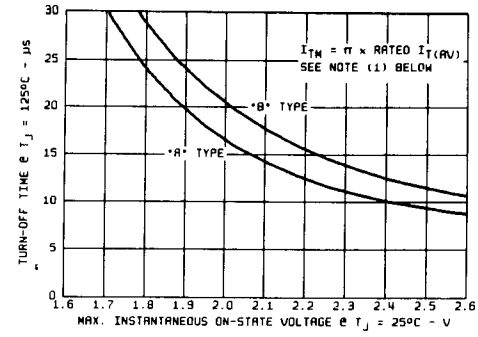


Fig. 14 — Trend for Turn-Off Time vs. On-State Voltage

(1) These curves are intended as a guideline. To specify non-standard t_q/V_{TM} contact factory.

ORDERING INFORMATION

TYPE	TEMPERATURE		VOLTAGE		TURN-OFF	
	CODE	MAX. T_J	CODE	V_{DRM}	CODE	MAX. t_q
S30EF	—	125°C	8	800V	A	12µs
	H	140°C	6	600V	B	15µs

For example, for a device with max. T_J = 125°C, V_{DRM} = 600V, max. t_q = 12µs, order as: S30EF6A.

Figure 14-18 (*continued*)

On-state voltage drop, V_T. V_T is the instantaneous value of on-state voltage drop and is dependent on the junction temperature, T_J. Figure 14-18.5 shows the instantaneous forward voltage drop against forward current. V_T can be considered as being made up of (1) a value which is independent of the forward current, and (2) a value which is proportional to the instantaneous forward current.

Maximum peak on-state voltage, V_{TM}. V_{TM} is the maximum on-state voltage drop at a specified on-state current and junction temperature.

Critical rate of rise of off-state voltage, *dv/dt*. *dv/dt* is the minimum value of the rate of rise of forward voltage which may cause switching from off-state to on-state.

Latching current, I_L. I_L is the minimum anode current which is required to maintain the thyristor in the on-state immediately after a thyristor has been turned on and the gate signal has been removed.

Holding current, I_H. I_H is the minimum anode current to maintain the thyristor in the on-state. The holding current is less than the latching current.

Peak on-state current, I_p. I_p is the peak instantaneous value of on-state current. It depends on the *di/dt* and width of current pulse. The switching losses would depend on the value of I_p, pulse width, and *di/dt* as shown in Fig. 14-18.6.

Peak reverse current, I_{RM}. I_{RM} is the peak value of reverse current at the maximum junction temperature and maximum repetitive peak reverse voltage with gate open. This current would cause junction heating.

Peak off-state current, I_{DM}. I_{DM} is the peak value of off-state current at the maximum junction temperature and maximum repetitive peak reverse voltage with gate open. This current would also cause junction heating.

Reverse recovered charge, Q_{RR}. Q_{RR} is the amount of charge carriers which has to be recovered during the turn-off process. Its value is determined from the area enclosed by the path of the reverse recovery current. The value of Q_{RR} depends on the rate of fall of on-state current and the peak value of on-state current before turn-off. Q_{RR} causes corresponding energy loss within the device. Figure 14-18.9 shows the typical reverse recovered charge and Fig. 14-18.10 shows the reverse energy loss.

Junction-to-case thermal resistance, R_{thJC}. R_{thJC} is the effective thermal resistance between the junction and outer case of the device. It is a measure of the heat transfer ability of materials and mechanical construction of the thyristor. Figure 14-18.11 shows the thermal impedance under transient-condition.

Dc gate current to trigger, I_{GT}. I_{GT} is the recommended value of the gate current at a specified case temperature. The minimum and maximum values of I_{GT} are normally specified, namely 70 to 150 mA. The typical gate characteristics are shown in Fig. 14-18.12.

Dc gate voltage to trigger, V_{GT}. V_{GT} is the recommended value of gate voltage at a specified case temperature. The minimum and maximum values of V_{GT} are normally specified, namely 1.2 to 2.5 V.

Dc gate voltage not to trigger, V_{GD}. V_{GD} is the value of the gate voltage which does not cause the thyristor (with rated V_{DRM} between anode to cathode) to switch from off-state to on-state. It is quoted at specified case temperature,

say 0.3 V at T_C = 125°C. The area of possible triggering is normally marked by the manufacturers in the gate characteristics as shown in Fig. 14-18.9a.

Maximum nonrepetitive surge current, I_{TSM}. I_{TSM} is the maximum permissible peak current of half-sine wave with a duration of normally 10 ms at a specified temperature. A repetition is permissible only after the expiration of a minimum interval to reduce the junction temperature to allowable range. This peak permissible value varies with the number of repetitions. Figure 14-18.13 shows the maximum value of peak surge current with the number of current pulses.

Turn-off time, t_q. t_q is the minimum value of time interval between the instant when the on-state current has decreased to zero and the instant when the thyristor is capable of withstanding forward voltage without turning on. t_q depends on the peak value of on-state current and the instantaneous on-state voltage. Figure 14-18.14 shows the variations of turn-off time against instantaneous on-state voltage.

Example 14-4

The resonant pulse inverter in Fig. 8-27a uses an IR thyristor of type S30EF. The inverter has a dc supply voltage of V_s = 200 V, capacitance of C = 80 μF, inductance of L = 12.8 μH, and resistance of R = 0 Ω. The initial capacitor voltage, V_{c0} = 200 V and the switching frequency, f_s = 4 kHz. Determine the (a) switching loss of thyristor, P_s; (b) reverse recovered charge of thyristor, Q_{RR}; and (c) reverse recovery power loss of thyristor, P_R.

Solution V_s = 200 V, V_{c0} = 200 V, L = 12.8 μH, C = 80 μF, and f_s = 4000 Hz. The current through thyristor T_1 can be found from

$$V_s = L\frac{di}{dt} + \frac{1}{C}\int i\,dt + v_c\,(t = 0)$$

With $v_c\,(t = 0) = -V_{c0} = -V_s$, the thyristor current becomes

$$i(t) = 2V_s\sqrt{\frac{C}{L}}\sin \omega t \qquad (14\text{-}18)$$

where $\omega = 1/\sqrt{LC}$. The current waveform of thyristor T_1 is shown in Fig. 14-19.

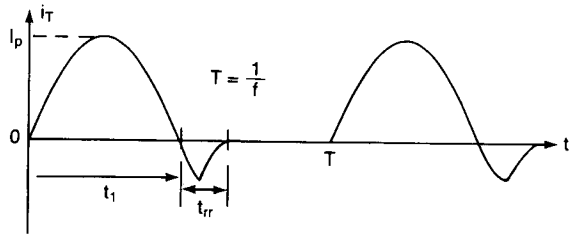


Figure 14-19 Thyristor current in Example 14-4.

The peak current is

$$I_p = 2V_s\sqrt{\frac{C}{L}} = 2 \times 200 \times \sqrt{\frac{80}{12.8}} = 1000 \text{ A}$$

and the conduction time of T_1 is

$$t_1 = \pi\sqrt{LC} = \pi\sqrt{12.8 \times 80} = 100.5 \ \mu\text{s}$$

(a) For $I_p = 1000$ A and $t_1 = 100.5$ μs, Fig. 14-18.6 gives the switching energy loss $W_s \cong 0.15$ J. The switching power loss is $P_s = W_s f_s = 0.15 \times 4000 = 600$ W.

(b) From Eq. (2-17), $di/dt = 2V_s/L = 2 \times 200/12.8 = 31.25$ A/μs. For $I_p = I_{TM} = 1000$ A, Fig. 14-18.9 gives the reverse recovered charge as $Q_{RR} = 37$ μC.

(c) For $di/dt = 31.25$ A/μs and $I_p = 1000$ A, Fig. 14-18.10 gives the reverse energy loss, $W_R = 1400$ μJ $= 0.0014$ J. The reverse recovery power loss, $P_R = W_R f_s = 0.0014 \times 4000 = 5.6$ W.

Note. The reverse recovery loss, P_R (= 5.6 W) is negligible compared to the switching loss, P_s (= 600 W.)

Example 14-5

An IR thyristor of type S30EF carries a current as shown in Fig. 14-20 and the current pulse is repeated at a frequency of $f_s = 50$ Hz. Determine the (a) average on-state power loss, P_T; (b) on-state voltage, V_T; (c) turn-off time, t_q; and (d) reverse recovered charge, Q_{RR}. Assume a junction temperature of $T_J = 125°C$.

Solution $I_p = I_{TM} = 1000$ A, $T = 1/f_s = 1/50 = 20$ ms, and $t_1 = t_2 = 5$ μs. The average on-state current is

$$I_T = \frac{1}{20{,}000}[0.5 \times 5 \times 1000 + (20{,}000 - 2 \times 5) \times 1000 + 0.5 \times 1000]$$

$$= 999.5 \text{ A}$$

(a) Since the switching frequency is low, Fig. 14-18.4 is the appropriate one to find the on-state power loss. For dc operation, $P_T = 2000$ W.

(b) For $I_p = 1000$ A, Fig. 14-18.5 gives the on-state voltage $V_T = 1.8$ V.

(c) For $V_T = 1.8$ V, and type A, Fig. 14-18.14 gives the turn-off time, $t_q = 24$ μs.

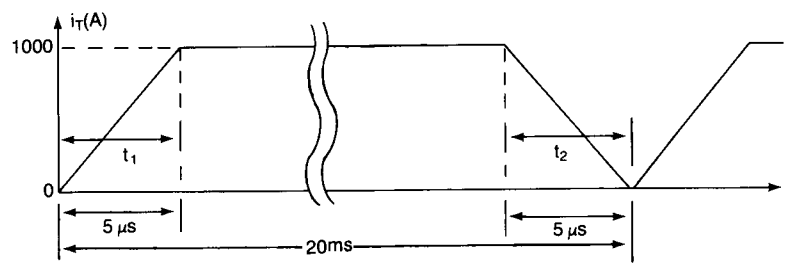


Figure 14-20 Thyristor current waveform.

(d) For $I_p = I_{TM} = 1000$ A and $di/dt = 200$ A/μs. Figure 14-18.9 gives recovery charge, $Q_{RR} = 94$ μC.

14-9.2 GTO Parameters

Figure 14-21 shows the data sheet of the International Rectifier (IR) GTO: 550A RMS, 1600 V, type 350PJT. The on-state and off-state parameters are identical to that of SCR; only the turn-off gate characteristics are different.

Dc gate current to trigger, I_{GT}. I_{GT} is the lowest value of the gate current which will trigger the GTO at a specified case temperature, anode–cathode voltage, and on-state current. Figures 14-21.9 and 14-21.9a show the gate characteristics and the areas of possible triggering points.

Dc gate voltage to trigger, V_{GT}. V_{GT} is the lowest value of gate voltage that will trigger the GTO at a specified case temperature, anode–cathode voltage, and on-state current.

Maximum peak positive gate current, $+I_{GM}$. $+I_{GM}$ is the maximum peak positive gate current at a specified gate pulse width.

Maximum repetitive peak negative gate voltage, $-V_{GRM}$. $-V_{GRM}$ is the maximum peak negative gate voltage that must be applied to the gate immediately after turn-off to prevent retriggering of the GTO.

Maximum peak negative gate current, $-I_{GM}$. $-I_{GM}$ is the maximum allowable peak negative gate current, when the GTO is in the off-state.

Turn-on time, t_{qt}. t_{qt} is the time required to complete the turn-on process. It is measured from the instant of 10% of gate current to the instant at which the anode voltage reaches 10% of the supply voltage with a resistive load. The gate current must be maintained for a long enough time of t_{qt} to ensure that the turn-on is complete. Figure 14.21.10 shows the variation of turn-on time with on-state current, and Fig. 14-21.13 shows the corresponding maximum turn-on energy loss. The turn-on loss depends on the off-state voltage and becomes maximum with resistive load and minimum value of di/dt.

Minimum on-time, t_{on}. t_{on} is the minimum value of on-time to ensure that all cathode islands are fully turned on. This limit is also superimposed on the requirement that the GTO must be on for sufficient time to allow the snubber capacitor to discharge fully.

Maximum fall time, t_f. t_f is the maximum value of time for the on-state current to fall from 90% of on-state current to 10% of on-state current with resistive loads. Figure 14-21.12 shows the variation of fall time with on-state current.

350PJT SERIES

1200A I_{TGQ} Gate Turn-Off Hockey Puk SCRs

Major Ratings

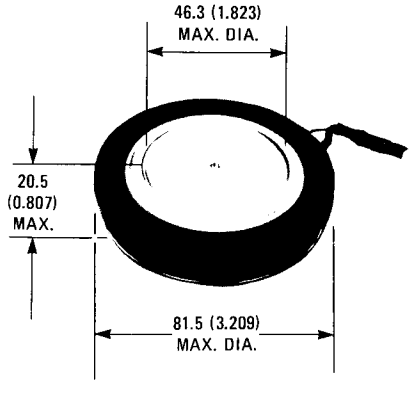
		350PJT	Units
I_{TGQ}		1200	A
$I_{T(RMS)}$		550	A
$I_{T(AV)}$		350	A
@ Max. T_C		80	°C
I_{TSM}	@ 50 Hz	4500	A
	@ 60 Hz	4700	
I^2t	@ 50 Hz	101,000	A^2s
	@ 60 Hz	92,000	
I_{GT}		2	A
dv/dt		1000	V/μs
di/dt		600	A/μs
t_{gq}		15	μs
T_J		-40 to 125	°C
V_{RRM}, V_{DRM}		1000 to 1600V	V

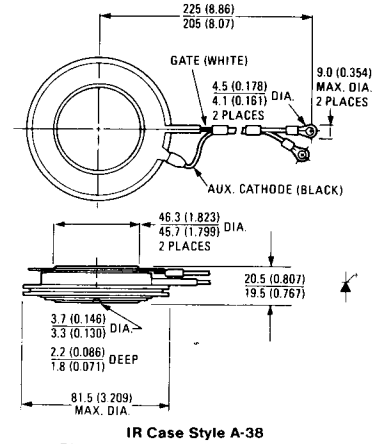
Description/Features

The 350PJT Series of GTO (gate turn-off) thyristors is designed for power control applications such as uninterruptible power supplies (UPS), variable speed ac motor drives, etc. Since they can be turned off by a negative current pulse to the gate, devices in the 350PJT Series allow reductions in overall size, weight, cost and acoustical noise when compared to conventional thyristors that require bulky commutating circuits.

- 350A average current.
- 1200A controllable on-state current.
- Maximum turn-off time of 15 μsec.
- Critical dv/dt of 1000 V/μsec.
- Available with maximum repetitive peak off-state voltage (V_{DRM}) to 1600V.

CASE STYLE AND DIMENSIONS





IR Case Style A-38
Dimensions in Millimeters and (Inches)

Figure 14-21 Data sheet of GTO, type 350PJT. (*Courtesy of International Rectifier*).

VOLTAGE RATINGS ①

Part Number	V_{RRM}, V_{DRM} – Max. Repetitive Peak Reverse and Off-State Voltage (V) ③	V_{RSM}, V_{DSM} – Max. Non-Repetitive Peak Reverse and Off-State Voltage $t_p \leq 5$ ms (V)
	T_J = -40°C to 125°C	T_J = 25°C to 125°C
350PJT100	1000	1200
350PJT120	1200	1400
350PJT140	1400	1600
350PJT160	1600	1750

ELECTRICAL SPECIFICATIONS

		350PJT	Units	Conditions
	ON-STATE			
$I_{T(RMS)}$	Nominal RMS on-state current	550	A	
$I_{T(AV)}$	Max. average on-state current	350	A	180° half sine wave conduction.
	@ Max. T_C	80	°C	
I_{TGQ}	Max. controllable peak on-state current	1200	A	T_J = 125°C, V_{DM} = 1/2 V_{DRM}. G_{GQ} = 5, C_S = 3.0 μF. ② Note: $V_S \leq$ 600V @ T_J = 25°C. $V_S \leq$ 500V @ T_J = 125°C. (V_S is the voltage spike which appears on the dynamic on-state voltage trace during fall time.)
I_{TSM}	Max. peak one cycle, non-repetitive surge current	4500	A	50 Hz half cycle sine wave or 6 ms rectangular pulse. Following any rated load condition, and with rated V_{RRM} applied following surge. SCR turned fully on.
		4700		60 Hz half cycle sine wave or 5 ms rectangular pulse
I^2t	Max. I^2t capability for fusing	101,000	A^2s	t = 10 ms. Rated V_{RRM} applied following surge, initial $T_J \leq$ 125°C.
		92,000		t = 8.3 ms
V_{TM}	Max. peak on-state voltage	3.42	V	T_J = 25°C, $I_{T(AV)}$ = 350A (1100A peak), I_G = 4A
I_L	Typical latching current	30	A	T_J = 25°C
I_H	Typical holding current	30	A	T_J = 25°C
	BLOCKING			
dv/dt	Min. critical rate-of-rise of off-state voltage	1000	V/μs	Gate voltage = -2V; Gate-to-cathode resistance = 2Ω. T_J = 125°C, V_D = 1/2 V_{DRM}
		400		
I_{DM} & I_{RM}	Max. peak off-state and reverse current	80	mA	T_J = 125°C, V_{DM} = rated V_{DRM}. Peak off-state current applies for -2V or more negative gate voltage or for gate-to-cathode resistance = 2Ω.
	SWITCHING			
di/dt	Max. repetitive rate-of-rise of turned-on current	600	A/μs	$di_G/dt \geq$ 5 A/μs, $+I_{GM} \geq$ 10A, $I_{TM} \leq$ 1200A, $V_D \leq$ 1/2 V_{DRM}.
t_{gt}	Max. turn-on time	8	μs	t_{gt} is measured from instant at which i_G = 0.1I_{GM} to instant at which v_D = 0.1V_D with resistive load. T_J = 125°C, I_T = 1200A, $+I_{GM}$ = 10A, di_G/dt = 5 A/μs, V_D = 1/2 V_{DRM}.
t_{on}	Min. permissible on-time	16	μs	t_{on} is the time necessary to ensure that all cathode islands are in conduction. T_J = 125°C, I_T = 1200A, V_D = 1/2 V_{DRM}, I_{GM} = 10A, di_G/dt = 60 A/μs.
t_{gq}	Max. gate-controlled turn-off time	15	μs	t_{gq} is measured from instant at which I_G = 24A to instant at which I_T = 120A with resistive load. T_J = 125°C, I_T = 1200A, di_G/dt = 60 A/μs, G_{GQ} = 5. ②

① Peak off-state voltages apply for -2V or more negative gate voltage or for gate-to-cathode resistance = 2Ω.

② $G_{GQ} = \frac{I_T}{\text{applied } I_{GQ}}$ = forced turn-off gain. I_T = on-state current. Applied I_{GQ} = maximum negative gate current during turn-off interval.

③ Peak reverse voltages apply for zero or negative gate voltage.

Figure 14-21 *(continued)*

ELECTRICAL SPECIFICATIONS (Continued)

		350PJT	Units	Conditions
	SWITCHING (Continued)			
t_f	Max. fall time	1.2	μs	t_f is measured from instant at which I_T = 1080A to instant at which I_T = 120A with resistive load. T_J = 125°C, I_T = 1200A, V_D = 1/2 V_{DRM}, di_G/dt = 60 A/μs, G_{GQ} = 5. ①
t_{off}	Min. permissible off-time	80	μs	t_{off} is measured from the instant at which the turn-off pulse is ① applied to the gate to the earliest instant at which the GTO may be retriggered. T_J = 125°C, I_T = 1200A, di_G/dt = 60 A/μs, G_{GQ} = 5.
	TRIGGERING			
$P_{GF(AV)}$	Max. average forward gate power	30	W	Forward gate power is produced by positive gate current, reverse gate power is produced by negative gate current.
P_{GRM}	Max. peak reverse gate power	18,000	W	$t_p \leq 5$ μs.
$P_{GR(AV)}$	Max. average reverse gate power	80	W	
$+I_{GM}$	Max. peak positive gate current	100	A	$t_p \leq 100$ μs. Positive gate current may not be applied during reverse recovery interval.
$-I_{GM}$	Max. peak negative gate current	50	mA	T_J = 125°C, $-V_{GM}$ = rated $-V_{GRM}$, SCR blocking.
$-V_{GRM}$	Max. repetitive peak negative gate voltage	20	V	SCR blocking.
I_{GT}	Max. required DC gate current totrigger	4.6	A	T_C = -40°C
		2.0		T_C = 25°C
		0.5		T_C = 125°C
				Max. required gate trigger current is the lowest value which will trigger all units with +12 volts anode-to-cathode and I_T = 50A after triggering
V_{GT}	Max. required DC gate voltage to trigger	1.25	V	T_C = -40°C
		1.0		T_C = 25°C
				Max. required gate trigger voltage is the lowest value which will trigger all units with +12 volts anode-to-cathode and I_T = 50A after triggering

THERMAL-MECHANICAL SPECIFICATIONS

T_J	Junction operating temperature range	-40 to 125	°C	
T_{stg}	Storage temperature range	-40 to 125	°C	
R_{thJC}	Max. internal thermal resistance, junction-to-case	0.035	deg. C/W	DC operation; double side cooled, mounting force = 11750N (2650lbf).
R_{thCS}	Thermal resistance, one pole piece to one heat dissipator	0.02	deg. C/W	Mounting surface smooth, flat and greased.
T	Mounting force Min.	10,600 (2400)	N	
	Max.	12,900 (2900)	(lbf)	
wt	Approximate weight	360 (12.7)	g (oz.)	
	Case Style	IR: A-38		

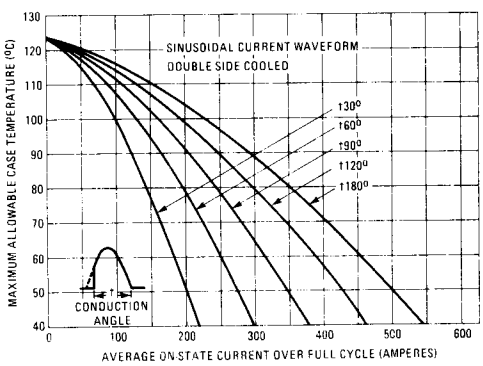


Fig. 1 – Average On-State Current Vs. Maximum Allowable Case Temperature (Sinusoidal Current Waveform)

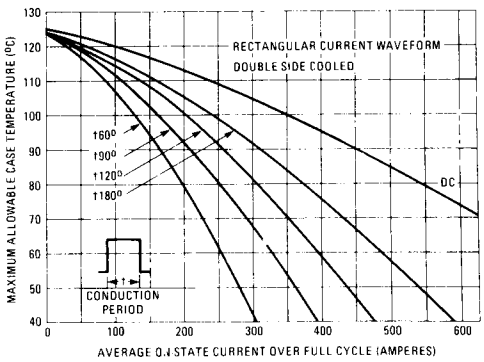


Fig. 2 – Average On-State Current Vs. Maximum Allowable Case Temperature (Rectangular Current Waveform)

Figure 14-21 *(continued)*

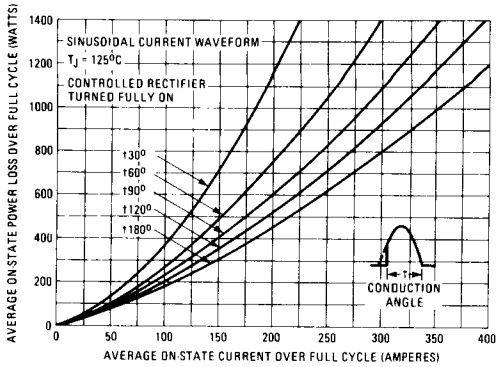


Fig. 3 — Maximum Low Level On-State Power Loss Vs. Average On-State Current (Sinusoidal Current Waveform)

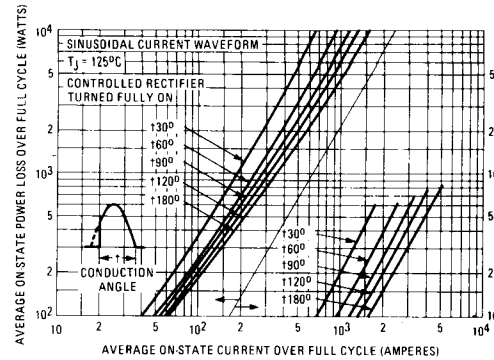


Fig. 4 — Maximum High Level On-State Power Loss Vs. Average On-State Current (Sinusoidal Current Waveform)

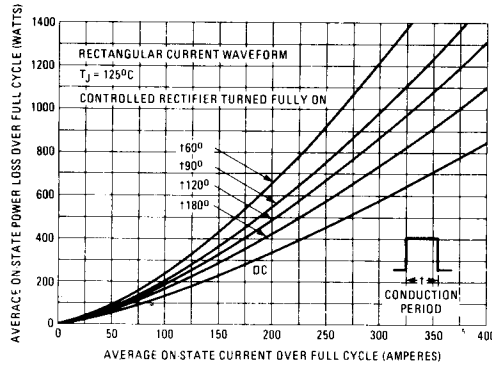


Fig. 5 — Maximum Low Level On-State Power Loss Vs. Average On-State Current (Rectangular Current Waveform)

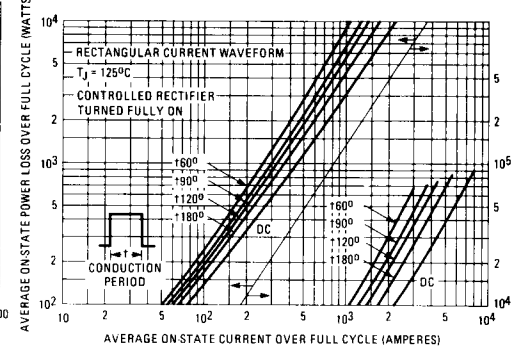


Fig. 6 — Maximum High Level On-State Power Loss Vs. Average On-State Current (Rectangular Current Waveform)

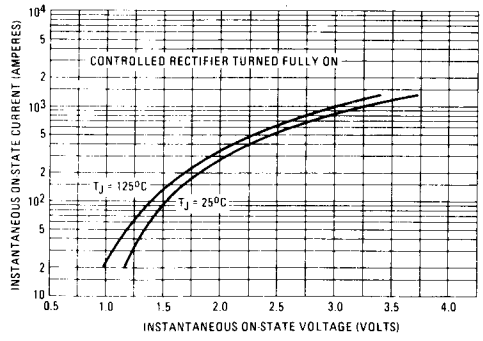


Fig. 7 — Maximum Instantaneous On-State Voltage Vs. Instantaneous On-State Current

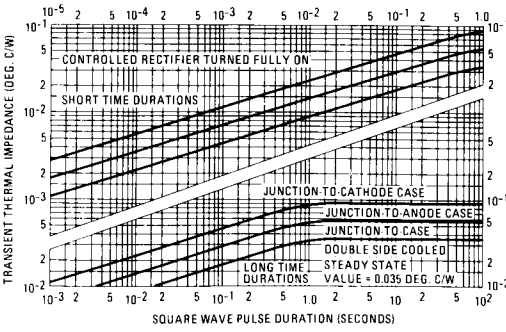


Fig. 8 — Maximum Transient Thermal Impedance Vs. Square Wave Pulse Duration

Figure 14-21 (*continued*)

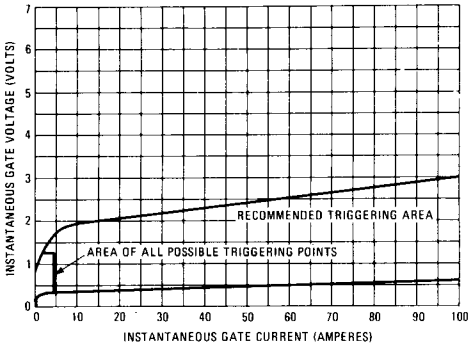


Fig. 9 – Gate Characteristics

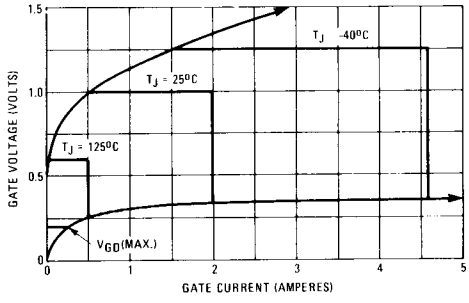


Fig. 9a – Areas of All Possible Triggering Points

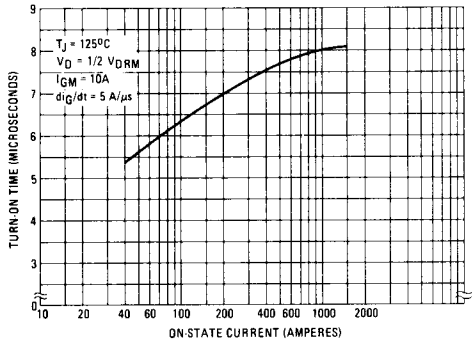


Fig. 10 – Turn-On Time Vs. On-State Current

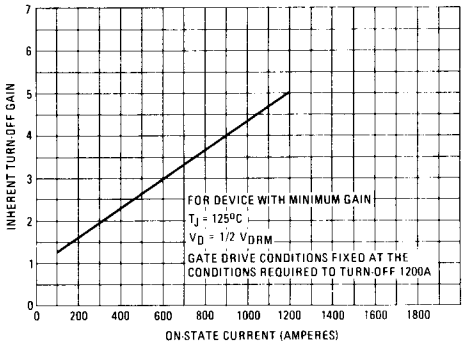


Fig. 11 – Inherent Turn-Off Gain Vs. Instantaneous On-State Current

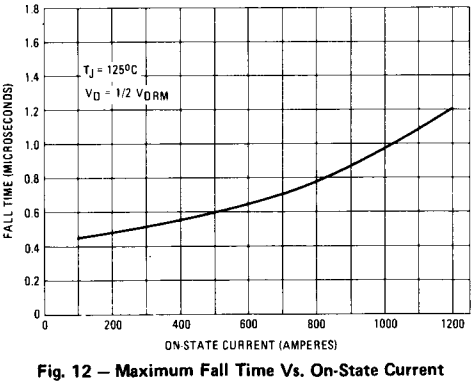


Fig. 12 – Maximum Fall Time Vs. On-State Current

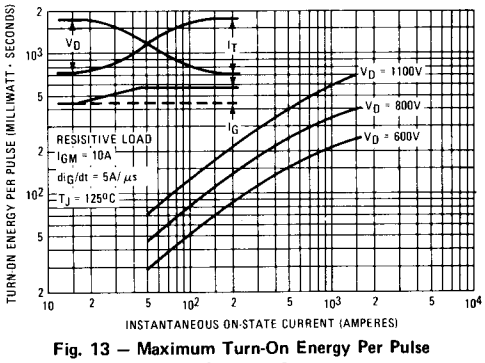


Fig. 13 – Maximum Turn-On Energy Per Pulse Vs. On-State Current

Figure 14-21 (*continued*)

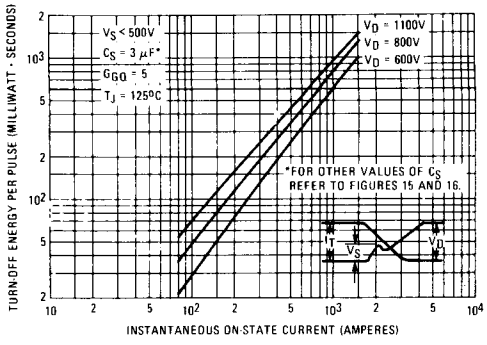


Fig. 14 – Maximum Turn-Off Energy Per Pulse Vs. On-State Current, V_D = 600, 800 & 1100V; C_S = 3 μF

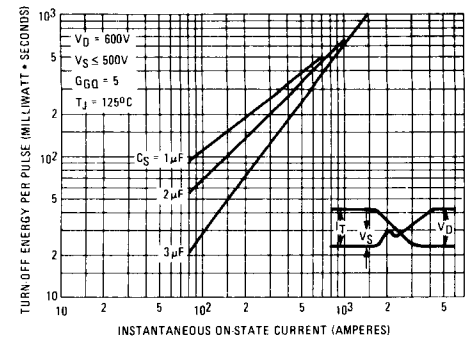


Fig. 15 – Maximum Turn-Off Energy Per Pulse Vs. On-State Current, V_D = 600V; C_S =1, 2, & 3 μF

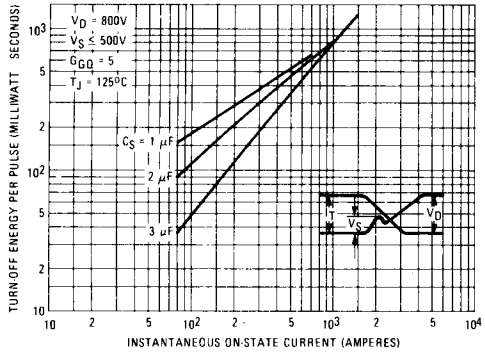


Fig. 16 – Maximum Turn-Off Energy Per Pulse Vs. On-State Current, V_D = 800V; C_S = 1, 2, & 3 μF

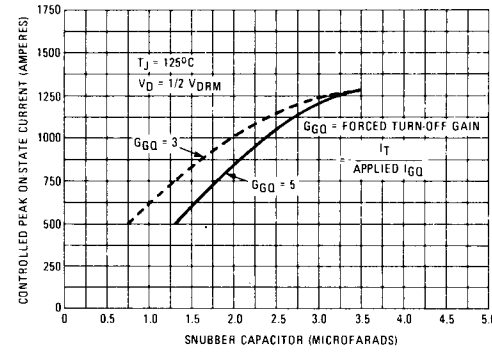


Fig. 17 – Maximum Controllable Peak On-State Current Vs. Snubber Capacitor Value

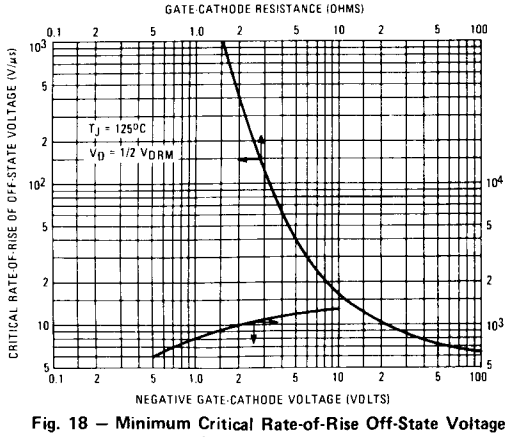


Fig. 18 – Minimum Critical Rate-of-Rise Off-State Voltage Vs. Negative Gate-Cathode Voltage and Vs. Gate-Cathode Resistance

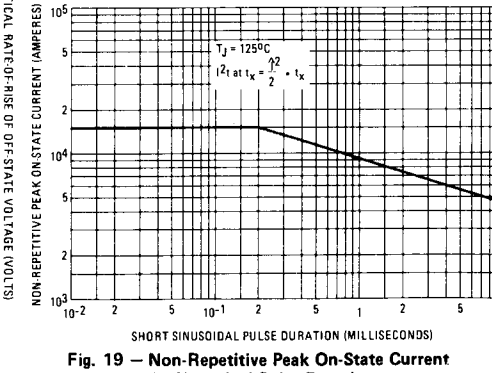
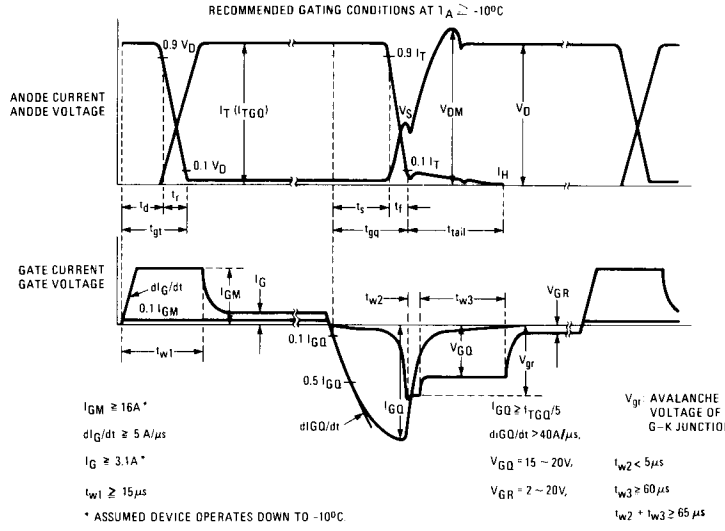


Fig. 19 – Non-Repetitive Peak On-State Current Vs. Sinusoidal Pulse Duration

Figure 14-21 *(continued)*



SNUBBER CAPACITOR Cs (μF)	SNUBBER RESISTOR Rs (Ω)	MINIMUM ON-TIME (μs)
3.0	10	75
	5	45
2.0	10	50
	5	30
1.5	10	38
	5	23

Fig. 20 — Recommended Gating Conditions at $T_A \geq -10^oC$

Figure 14-21 (*continued*)

Maximum gate-controlled turn-off time, t_{gq}. t_{gq} is the maximum value of time between the instant at which the gate current is 10% of its peak negative value and the instant at which the on-state current is reduced to 10% of the on-state current with resistive load. The turn-off loss, which depends on the off-state voltage and the snubber capacitance, is shown in Fig. 14-21.14. An increase in the snubber capacitance increases the *dv/dt* of forward reapplied voltage as the anode current falls; and as a result the turn-off losses are reduced. The turn-off losses in Fig. 14-21.14 do not include the snubber loss, and in fact the switching losses would increase with snubber capacitance. However, the snubber loss is external to the GTO and does not affect the heating of GTO significantly. In practice, the discharging current of the snubber capacitor has to flow through the GTO and contribute to the power loss in the GTO.

Minimum off-time, t_{off}. t_{off} is the minimum value of time for which the GTO must be off before it may be retriggered. It is measured from the instant at which the turn-off pulse is applied to the gate. A GTO requires this time to recombine the excess minority carriers in the cathode islands.

Minimum critical rate of rise of off-state voltage, *dv/dt*. *dv/dt* is the guaranteed rate of rise of forward blocking voltage and depends on the negative gate bias. *dv/dt* is normally quoted for a gate bias of -2 V. Without a negative gate bias, *dv/dt* capability depends on the value of the bypass resistance between the gate and cathode. Figure 14-21.18 shows the variations of *dv/dt* with the negative gate bias and gate–cathode resistance. For example, a gate–cathode resistance of 2 Ω gives $dv/dt = 400$ V/μs and for gate bias voltage of -1 V, $dv/dt = 800$ V/μs.

Controllable peak on-state current, I_{TGQ}. I_{TGQ} is the peak value of on-state current which can be turned off by gate control. Figure 14-21.11 shows the turn-off gain against the instantaneous on-state current. The turn-off gain is low, namely 5 at 1200 A. The off-state voltage is reapplied immediately after turn-off and the reapplied *dv/dt* is only limited by the snubber capacitance. Once a GTO is turned off, the load current, I_L, which is diverted through and charges the snubber capacitor, determines the reapplied *dv/dt*.

$$\frac{dv}{dt} = \frac{I_L}{C_s}$$

where C_s is the snubber capacitance.

To limit the *dv/dt*, the controllable on-state current depends on the snubber capacitance as shown in Fig. 14-21.17. After turn-off time, t_{gq}, a tail of anode current as shown in Fig. 14-21.20 continues to flow for a tail time of $t_{tail} = t_{w2} + t_{w3}$ (namely, 65 μs) and this tail anode current may retrigger the GTO. To prevent this a minimum negative gate bias (namely, -15 V) must be applied for a time of t_{w3} after the turn-off. During the time t_{w2}, an avalanche voltage in the gate-cathode junction exists.

Snubber circuit design considerations. The snubber circuit plays a significant role on the turn-off process of a GTO and Fig. 14-21.20 shows the recommended values of the snubber capacitance and resistance for the GTO of type 350PJT. The voltage step which appears at the beginning of tail anode current (in Fig. 14-21.20) is caused by the stray inductance in the snubber circuit (including the self-inductance of the snubber capacitor). The snubber capacitor must be capable of withstanding high peak current and should have very low inductance. Two or more capacitors may be connected in parallel to give the desired value of capacitance, and the total inductance is reduced due to parallel connection of individual inductances.

The snubber diode should have good forward recovery characteristics and

fast reverse recovery. *di/dt* should be very high for quick transfer of anode current to the snubber circuit.

The snubber resistor must have low value to discharge the snubber capacitor during GTO conduction, whereas the resistance must be high enough to limit the discharge current through GTO to an acceptable value. In addition to dissipating power, the resistor must be able, momentarily, to support high supply voltage.

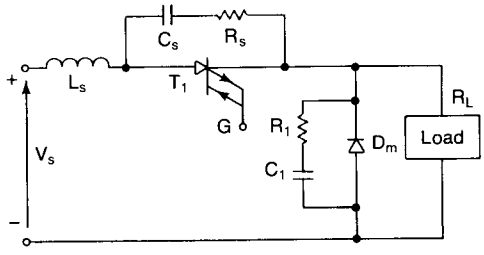


Figure 14-22 GTO chopper.

Example 14-6

A chopper circuit with an IR GTO of type 350PJT is shown in Fig. 14-22. It has a resistive load of $R_L = 1.333\ \Omega$. The dc input voltage is $V_s = 800$ V. The duty cycle is $k = 50\%$ and the switching frequency is $f_s = 2$ kHz. The snubber capacitance is $C_s = 3\ \mu$F and snubber resistance is $R_s = 5\ \Omega$. Determine the (a) turn-on time, t_{on}; (b) turn-off gate current, I_{GQ}; (c) fall time, t_f; (d) turn-on power losses, P_{on}; (e) turn-off power losses, P_{off}; (f) total power loss of GTO, P_T; (g) controllable on-state current, I_{TGQ}; (h) gate current, I_{GT} and gate voltage V_{GT}; and (i) the value of the gate–cathode resistance to limit the critical *dv/dt* to 800 V/μs. Assume a junction temperature of $T_J = 125°C$.

Solution $V_s = 800$ V, $R_L = 1.333\ \Omega$, $k = 0.5$, $f_s = 2$ kHz, $C_s = 3\ \mu$F, $R_s = 5\ \Omega$, and the on-state current, $I_L = 800/1.333 = 600$ A.

(a) For $I_T = I_L = 600$ A, Fig. 14-21.10 gives $t_{on} = 7.8\ \mu$s.

(b) For $I_T = 600$ A, Fig. 14-21.11 gives the turn-on gain, $G_{GQ} = 3$ and $I_{GQ} = I_T/G_{GQ} = 600/3 = 200$ A.

(c) For $I_T = 600$ A, Fig. 14-21.12 gives $t_f = 0.65\ \mu$s.

(d) For $I_T = 600$ A and $V_D = V_s = 800$ V, Fig. 14-21.13 gives the turn-on energy, $W_{on} = 280$ mJ and $P_{on} = W_{on}f_s = 0.28 \times 2000 = 560$ W.

(e) For $I_T = 600$ A, $V_s = 800$ V and $C_s = 3\ \mu$F, Fig. 14-21.16 gives the turn-off energy loss, $W_{off} = 440$ mJ.

$$P_{off} = W_{off}f_s = 0.44 \times 2000 = 880\ \text{W}$$

(f) For $I_{T(AV)} = 600 \times 0.5 = 300$, Fig. 14-21.6 gives $P_0 = 750$ W. The total power loss is

$$P_T = P_{on} + P_{off} + P_0 = 560 + 880 + 750 = 2110\ \text{W}$$

(g) For $C_s = 3\ \mu$F and $G_{GQ} = 3$, Fig. 14-21.17 gives $I_{TGQ} = 1250$ A.

(h) Figure 14-21.9(a) gives $I_{GT} = 0.5$ A and $V_{GT} = 0.6$ V at 125°C. Note: At $T_J = 25°C$, Fig. 14-21.9(a) gives $I_{GT} = 2$ A and $V_{GT} = 1$ V.

(i) For $dv/dt = 800$ V/μs, Fig. 14-21.18 gives a gate–cathode resistance of 1.6 Ω and a negative gate–cathode voltage of 1 V.

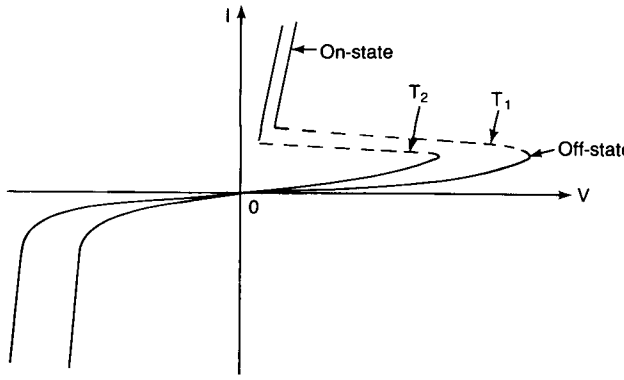


Figure 14-23 Off-state characteristics of two thyristors.

14-10 SERIES OPERATION OF THYRISTORS

For high-voltage applications, two or more thyristors can be connected in series. However, due to the production spread the characteristics of all thyristors of the same type are not identical. Figure 14-23 shows the off-state characteristics of two thyristors. For the same off-state current, their off-state voltages differs.

In case of diodes, only the reverse blocking voltages have to be shared, whereas for thyristors, the voltage-sharing networks are required for both reverse and off-state conditions. The voltage sharing is normally accomplished by connecting resistors across each thyristor as shown in Fig. 14-24. For equal voltage sharing, the off-state currents differ as shown in Fig. 14-25. Let there be n_s thyristors in the string. The off-state current of thyristor T_1 is I_{D1} and that of other thyristors are equal such that $I_{D2} = I_{D3} = I_{Dn}$ and $I_{D1} < I_{D2}$. Since thyristor T_1 has the least off-state current, T_1 will share higher voltage.

If I_1 is the current through the resistor across T_1 and the currents through other resistors are equal so that $I_2 = I_3 = I_n$, the off-state current spread is

$$\Delta I_D = I_{D1} - I_{D2} = I_T - I_2 - I_T + I_1 = I_1 - I_2 \quad \text{or} \quad I_2 = I_1 - \Delta I_D$$

The voltage across T_1 is $V_{D1} = RI_1$. Using Kirchhoff's voltage law,

$$\begin{aligned} V_s &= V_{D1} + (n_s - 1)I_2R = V_{D1} + (n_s - 1)(I_1 - \Delta I_D)R \\ &= V_{D1} + (n_s - 1)I_1R - (n_s - 1)R\,\Delta I_D \\ &= n_sV_{D1} - (n_s - 1)R\,\Delta I_D \end{aligned} \tag{14-19}$$

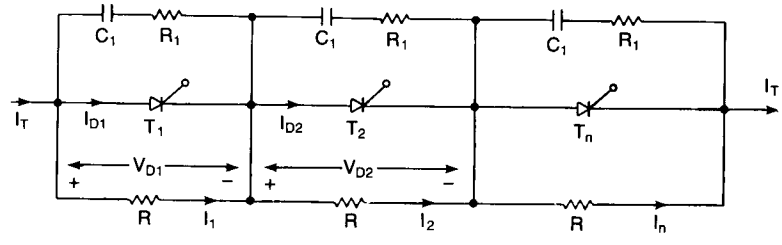


Figure 14-24 Three series-connected thyristors.

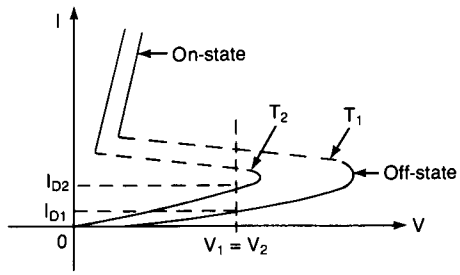


Figure 14-25 Leakage currents with equal voltage sharing.

Solving Eq. (14-19) for the voltage across T_1,

$$V_{D1} = \frac{V_s + (n_s - 1)R\,\Delta I_D}{n_s} \tag{14-20}$$

V_{D1} will be maximum when ΔI_D is maximum. For $I_{D1} = 0$ and $\Delta I_D = I_{D2}$, Eq. (14-20) gives the worst-case steady-state voltage across T_1,

$$V_{DS(\max)} = \frac{V_s + (n_s - 1)RI_{D2}}{n_s} \tag{14-21}$$

During the turn-off, the differences in stored charge causes differences in the reverse voltage sharing as shown in Fig. 14-26. The thyristor with the least recovered charge (or reverse recovery time) will face the highest transient voltage. The junction capacitances which control the transient voltage distributions will not be adequate and it is normally necessary to connect a capacitor, C_1 across each thryistor as shown in Fig. 14-24. R_1 limits the discharge current. The same RC network are generally used for transient voltage sharing and dv/dt protection.

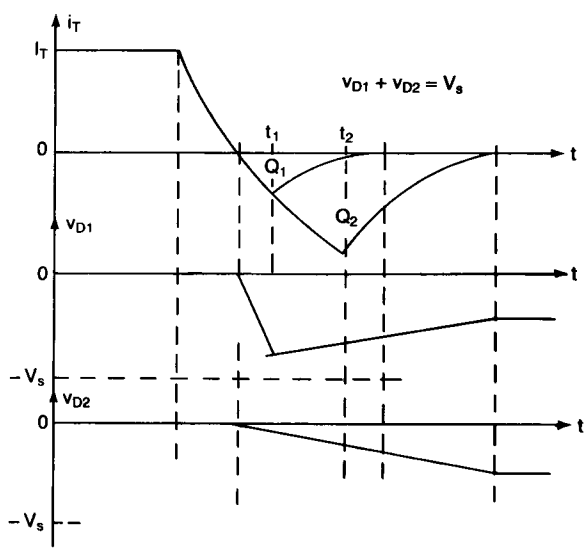


Figure 14-26 Reverse recovery time and voltage sharing.

The transient voltage across T_1 can be determined from Eq. (14-20) by applying the relationship of voltage difference,

$$\Delta V = R\,\Delta I_D = \frac{Q_2 - Q_1}{C_1} = \frac{\Delta Q}{C_1} \tag{14-22}$$

where Q_1 is the stored charge of T_1 and Q_2 is the charge of other thyristors such that $Q_2 = Q_3 = Q_n$ and $Q_1 < Q_2$. Substituting Eq. (14-22) into Eq. (14-20) yields

$$V_{D1} = \frac{1}{n_s}\left[V_s + \frac{(n_s - 1)\,\Delta Q}{C_1}\right] \tag{14-23}$$

The worst-case transient voltage sharing which will occur when $Q_1 = 0$ and $\Delta Q = Q_2$ is

$$V_{DT(\max)} = \frac{1}{n_s}\left[V_s + \frac{(n_s - 1)Q_2}{C_1}\right] \tag{14-24}$$

A derating factor which is normally used to increase the reliability of the string is defined as

$$\text{DRF} = 1 - \frac{V_s}{n_s V_{DS(\max)}} \tag{14-25}$$

Example 14-7

Ten thyristors are used in a string to withstand a dc voltage of $V_s = 15$ kV. The maximum leakage current and recovery charge differences of thyristors are 10 mA and 150 μC, respectively. Each thyristor has a voltage sharing resistance of $R = 56$ kΩ and capacitance of $C_1 = 0.5$ μF. Determine the (a) maximum steady-state voltage sharing, $V_{DS(\max)}$; (b) steady-state voltage derating factor; (c) maximum transient voltage sharing, $V_{DT(\max)}$; and (d) transient voltage derating factor.

Solution $n_s = 10$, $V_s = 15$ kV, $\Delta I_D = I_{D2} = 10$ mA, and $\Delta Q = Q_2 = 150$ μC.

(a) From Eq. (14-21), the maximum steady-state voltage sharing is

$$V_{DS(\max)} = \frac{15{,}000 + (10 - 1) \times 56 \times 10^3 \times 10 \times 10^{-3}}{10} = 2004 \text{ V}$$

(b) From Eq. (14-25), the steady-state derating factor is

$$\text{DRF} = 1 - \frac{15{,}000}{10 \times 2004} = 25.15\%$$

(c) From Eq. (14-24), the maximum transient voltage sharing is

$$V_{DT(\max)} = \frac{15{,}000 + (10 - 1) \times 150 \times 10^{-6}/(0.5 \times 10^{-6})}{10} = 1770 \text{ V}$$

(d) From Eq. (14-25), the transient derating factor is

$$\text{DRF} = 1 - \frac{15{,}000}{10 \times 1770} = 15.25\%$$

14-11 PARALLEL OPERATION OF THYRISTORS

When thyristors are connected in parallel, the total load current is not shared equally due to differences in their characteristics. If a thyristor carries more current than that of the others, its power dissipation increases, thereby increasing the junction temperature and decreasing the internal resistance. This, in turn, will increase its current sharing and may damage the thyristor. This thermal runway may be avoided by having a common heat sink so that all units operate at the same temperature.

Although small resistance, as shown in Fig. 14-27a, may be connected in series with each thyristor to force equal current sharing, there will be considerable power loss in the series resistances. A common approach which is similar to the technique for current sharing of transistors is to use magnetically coupled inductors as shown in Fig. 14-27b. If the current through thyristor T_1 increases, a voltage of opposite polarity will be induced in the windings of thyristor T_2 and the impedance through the path of T_2 will be reduced, thereby increasing the current flow through T_2.

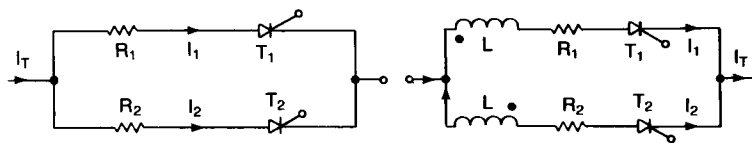


Figure 14-27 Current sharing of thyristors.

14-12 THYRISTOR FIRING CIRCUITS

In thyristor converters, different potentials exist at various terminals. An isolation circuit is required between an individual thyristor and its gate-pulse generating circuit. The isolation can be accomplished by either pulse transformers or optocouplers. A optocoupler could be a phototransistor or photo-SCR as shown in Fig. 14-28. A short pulse to the input of an infrared light-emitting diode (ILED),

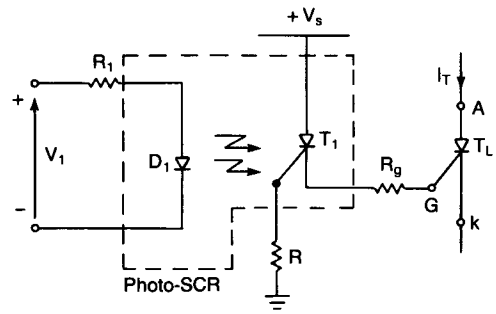


Figure 14-28 Photo-SCR coupled isolator.

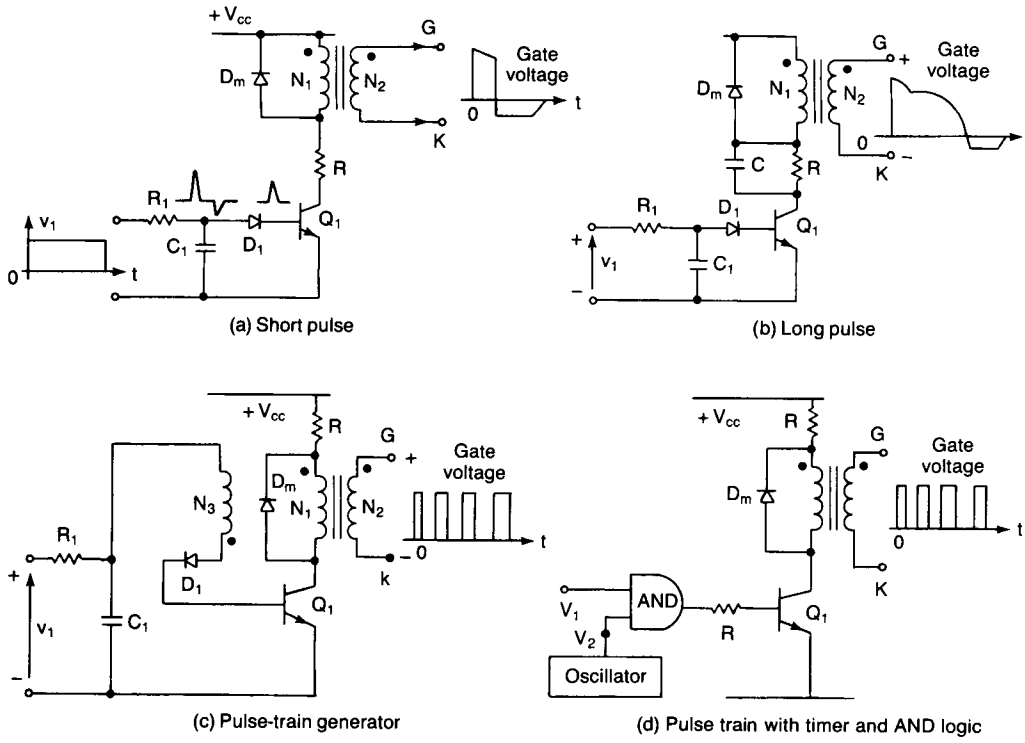


Figure 14-29 Pulse transformer isolation.

D_1, turns on the photo-SCR, T_1; and the power thyristor, T_L, is triggered. This type of isolation requires a separate power supply and increases the cost and weight of the firing circuit.

A simple isolation arrangement with pulse transformers is shown in Fig. 14-29a. When a pulse is applied to the base of switching transistor, Q_1, the transistor saturates and the dc voltage V_{cc} appears across the transformer primary, inducing a pulsed voltage on the transformer secondary, which is applied between the thyristor gate and cathode terminals. When the pulse is removed from the base of transistor Q_1, the transistor turns off and a voltage of opposite polarity is induced across the primary and the freewheeling diode, D_m, conducts. The current due to the transformer magnetic energy decays through D_m to zero. During this transient, a corresponding reverse voltage is induced in the secondary. The pulse width can be made longer by connecting a capacitor cross the resistor, R, as shown in Fig. 14-29b. The transformer carries unidirectional current and the magnetic core will saturate, thereby limiting the pulse width. This type of pulse isolation is suitable for pulses of typically 50 μs.

In many power converters with inductive load, the conduction period of a thyristor depends on the load power factor; therefore, the beginning of thyristor conduction is not well defined. In this situation, it is often necessary to trigger the thyristors continuously. However, continuous gating increases thyristor losses.

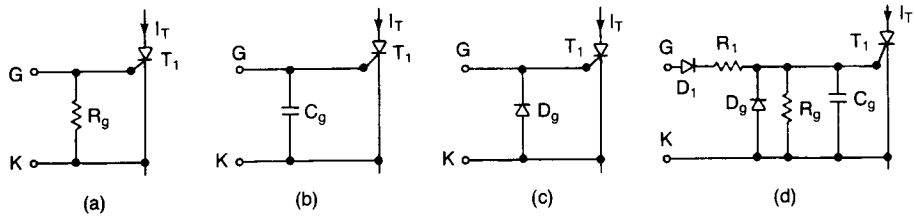


Figure 14-30 Gate protection circuits.

A pulse train which is preferable can be obtained with an auxiliary winding, as shown in Fig. 14-29c. When transistor Q_1 is turned on, a voltage is also induced in the auxiliary winding at the base of transistor Q_1, such that diode D_1 is reverse biased and Q_1 turns off. In the meantime, capacitor C_1 charges up through R_1 and turns on Q_1 again. This process of turn-on and turn-off continues as long as there is an input signal to the isolator. Instead of using the auxiliary winding as blocking oscillator, an AND-logic gate with an oscillator (or a timer) could generate a pulse train as shown in Fig. 14-29d. In practice, the AND gate cannot drive transistor Q_1 directly, and a buffer stage is normally connected before the transistor.

The output of Fig. 14-28 or Fig. 14-29 is normally connected between the gate and cathode along with other gate-protecting components, as shown in Fig. 14-30. The resistor, R_g, in Fig. 14-30a increases the *dv/dt* capability of the thyristor, reduces the turn-off time, and increases the holding and latching currents. The capacitor, C_g, in Fig. 14-30b removes high-frequency noise components and increases *dv/dt* capability and gate delay time. The didoe, D_g, in Fig. 14-30c protects the gate from negative voltage. However, for asymmetrical SCRs, it is desirable to have some amount of negative gate voltage to improve the *dv/dt* capability and also to reduce the turn-off time. All these features can be combined as shown in Fig. 14-30d, where diode D_1 allows only the positive pulses and R_1 damps out any transient oscillation and limits the gate current.

SUMMARY

There are eight types of thyristors. Only the GTOs and SITHs are gate turn-off devices. Each type has advantages and disadvantages. The characteristics of practical thyristors differ significantly from that of ideal devices. Although there are various means of turning on thyristors, the gate control is the most practical. Due to the junction capacitances and turn-on limit, thyristors must be protected from high *di/dt* and *dv/dt* failures. A snubber network is normally used to protect from high *dv/dt*. Due to the recovered charge, some energy is stored in the *di/dt* and stray inductors; and the devices must be protected from this stored energy. The switching losses of GTOs are much higher than those of normal SCRs. The snubber components of GTOs are critical to their performance.

Due to the differences in the characteristics of thyristors of the same type, the series and parallel operations of thyristors require voltage and current-sharing networks to protect them under steady-state and transient conditions. Isolation

between the power circuit and gate signals is necessary. A pulse transformer isolation is simple. For inductive loads, a pulse train that reduces thyristor loss is normally used for gating thyristors instead of a continuous pulse.

REFERENCES

1. General Electric, *SCR Manual*, 6th ed., D. R. Grafham and F. B. Golden, eds. Englewood Cliffs, N.J.: Prentice-Hall, Inc., 1982.
2. D. Grant and A. Honda, *Applying International Rectifier's Gate Turn-Off Thyristors*, Application Note No. AN-315A, El Segundo, Calif.: International Rectifier.
3. C. K. Chu, P. B. Spisak, and D. A. Walczak, "High power asymmetrical thyristors." *IEEE Industry Applications Society Conference Record*, 1985, pp. 267–272.
4. O. Hashimoto, H. Kirihata, M. Watanabe, A. Nishiura, and S. Tagami, "Turn-on and turn-off characteristics of a 4.5-KV 3000-A gate turn-off thyristor." *IEEE Transactions on Industry Applications*, Vol. IA22, No. 3, 1986, pp. 478–482.
5. O. Hashimoto, Y. Takahashi, M. Watanabe, O. Yamada, and T. Fujihira, "2.5-kV, 2000-A monolithic gate turn-off thyristor." *IEEE Industry Applications Society Conference Record*, 1986, pp. 388–392.
6. E. Y. Ho, and P. C. Sen, "Effect of gate drive on GTO thyristor characteristics." *IEEE Transactions on Industrial Electronics*, Vol. IE33, No. 3 (August) 1986, pp. 325–331.
7. H. Fukui, H. Amano, and H. Miya, "Paralleling of gate turn-off thyristors." *IEEE Industry Applications Society Conference Record*, 1982, pp. 741–746.
8. Y. Nakamura, H. Tadano, M. Takigawa, I. Igarashi, and J. Nishizawa, "Very high speed static induction thyristor." *IEEE Transactions on Industry Applications*, Vol. IA22, No. 6, 1986, pp. 1000–1006.

REVIEW QUESTIONS

14-1. What is the v–i characteristic of thyristors?
14-2. What is an off-state condition of thyristors?
14-3. What is an on-state condition of thyristors?
14-4. What is a latching current of thyristors?
14-5. What is a holding current of thyristors?
14-6. What is the two-transistor model of thyristors?
14-7. What are the means of turning-on thyristors?
14-8. What is turn-on time of thyristors?
14-9. What is the purpose of *di/dt* protection?
14-10. What is the common method of *di/dt* protection?
14-11. What is the purpose of *dv/dt* protection?
14-12. What is the common method of *dv/dt* protection?
14-13. What is turn-off time of thyristors?

14-14. What are the types of thyristors?

14-15. What is an SCR?

14-16. What is the difference between an SCR and a TRIAC?

14-17. What is the turn-off characteristic of thyristors?

14-18. What are the advantages and disadvantages of GTOs?

14-19. What are the advantages and disadvantages of SITHs?

14-20. What are the advantages and disadvantages of RCTs?

14-21. What are the advantages and disadvantages of LASCRs?

14-22. What is a snubber network?

14-23. What are the design considerations of snubber networks?

14-24. What is the common technique for voltage sharing of series-connected thyristors?

14-25. What are the common techniques for current sharing of parallel-connected thyristors?

14-26. What is the effect of reverse recovery time on the transient voltage sharing of parallel-connected thyristors?

14-27. What is a derating factor of series-connected thyristors?

PROBLEMS

14-1. The holding current of thyristors in the three-phase full converter in Fig. 4-9a is I_H = 200 mA and the delay time is 2.5 μs. The converter is supplied from a three-phase wye-connected 208-V 60-Hz supply and has a load of L = 8 mH and R = 2 Ω; it is operated with a delay angle of $\alpha = 60°$. Determine the minimum width of gate pulse width, t_G.

14-2. Repeat Prob. 14-1 if $L = 0$.

14-3. The holding current of thyristor T_1 in the chopper circuit in Fig. 7-15 is I_H = 200 mA and the delay time of T_1 is 1.5 μs. The dc input voltage is 220 V and source inductance L_s is negligible. It has a load of L = 10 mH and R = 2 Ω. Determine the minimum width of gate pulse width, t_G.

14-4. The junction capacitance of a thyristor can be assumed to be independent of off-state voltage. The limiting value of charging current to turn on the thyristor is 12 mA. If the critical value of dv/dt is 800 V/μs, determine the junction capacitance.

14-5. The junction capacitance of a thyristor is C_{J2} = 20 pF and can be assumed independent of off-state voltage. The limiting value of charging current to turn on the thyristor is 15 mA. If a capacitor of 0.01 μF is connected across the thyristor, determine the critical value of dv/dt.

14-6. A thyristor circuit is shown in Fig. P14-6. The junction capacitance of thyristor is C_{J2} = 15 pF and can be assumed to be independent of the off-state voltage. The

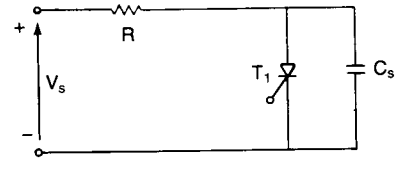


Figure P14-6

limiting value of charging current to turn on the thyristor is 5 mA and the critical value of dv/dt is 200 V/μs. Determine the value of capacitance C_s so that the thyristor will not be turned on due to dv/dt.

14-7. The chopper circuit in Example 7-11 uses the simple RC snubber network, as shown in Fig. 14-9b, for thyristors T_1, T_2, and T_3. If the dv/dt of all thyristors is limited to 200 V/μs and the discharging currents are limited to 10% of their respective peak values, determine the **(a)** values of snubber resistors and capacitors, and **(b)** power ratings of resistors. The effects of load circuit and source inductance L_s can be neglected.

14-8. The input voltage in Fig. 14-9e is $V_s = 200$ V with a load resistance of $R = 10\ \Omega$ and a load inductance of $L = 50$ μH. If the damping ratio is 0.7 and the discharging current of capacitor is 5 A, determine the **(a)** values of R_s and C_s, and **(b)** maximum dv/dt.

14-9. Repeat Prob. 14-8 if the input voltage is ac, $v_s = 179 \sin 377t$.

14-10. The chopper circuit in Example 7-11 uses the IR thyristor of type S30EF for thyristor T_1. Determine the **(a)** switching losses of thyristor, P_s; **(b)** reverse recovery charge of thyristor, Q_{RR}; **(c)** reverse recovery power loss of thyristor, P_R; and **(d)** thermal resistance of the heat sink if the junction and ambient temperatures are $T_J = 125°C$ and $T_A = 25°C$, respectively. Assume $di/dt = 200$ A/μs.

14-11. The IR thyristor of type S30EF carries a current as shown in Fig. P14-11. The switching frequency is $f_s = 50$ Hz. Determine the **(a)** average on-state power loss, P_T; **(b)** on-state voltage, V_T; **(c)** turn-off time, t_q; and **(d)** reverse recovery charge, Q_{RR}. Assume $T_j = 125°C$.

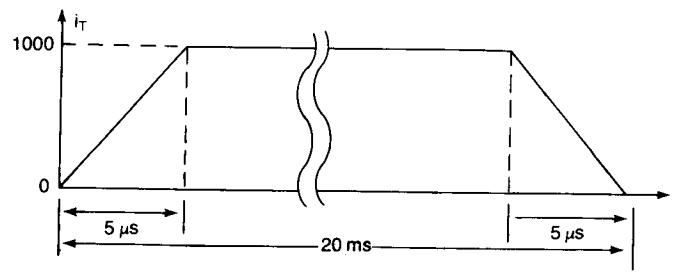


Figure P14-11

14-12. The chopper circuit in Fig. 14-22 uses an IR-GTO of type 350PJT and has a resistive load of $R_L = 1.5\ \Omega$. The dc input voltage is $V_s = 600$ V. The duty cycle is 80% and the switching frequency is $f_s = 1$ kHz. The snubber capacitance is $C_s = 2$ μF and snubber resistance is $R_s = 5\ \Omega$. Determine the **(a)** turn-on time, t_{on}; **(b)** turn-off gate current, I_{GQ}; **(c)** fall time, t_f; **(d)** turn-on power losses, P_{on}; **(e)** turn-off power losses, P_{off}; **(f)** total power loss of GTO, P_T; **(g)** controllable on-state current, I_{TGQ}; **(h)** gate current, I_{GT}, and gate voltage, V_{GT}, at $T_J = 25°C$; and **(i)** the value of the gate–cathode resistance to limit the critical dv/dt to 800 V/μs. Assume a junction temperature of $T_J = 125°C$.

14-13. The resonant pulse inverter in Fig. 8-27a uses an IR GTO of type 350PJT. The inverter has a dc supply voltage, $V_s = 200$ V, capacitance, $C = 80$ μF, inductance, $L = 12.8$ μH, and negligible resistance. The initial capacitor voltage, $V_{c0} = 200$ V and the switching frequency, $f_s = 4$ kHz. Determine the losses of GTO.

14-14. A string of thyristors are connected in series to withstand a dc voltage of $V_s = 15$

kV. The maximum leakage current and recovery charge differences of thyristors are 10 mA and 150 μC, respectively. The derating factor of 20% is applied for the steady-state and transient voltage sharings of thyristors. If the maximum steady-state voltage sharing is 1000 V, determine the **(a)** steady-state voltage sharing resistance, R, for each thyristor; and **(b)** transient voltage capacitance, C_1, for each thyristor.

14-15. Two thyristors are connected in parallel to share a total load current of $I_L = 600$ A. The on-state voltage drop of one thyristor is $V_{T1} = 1.0$ at 300 A and that of other thyristors is $V_{T2} = 1.5$ V at 300 A. Determine the values of series resistances to force current sharing with 10% difference. Total voltage, $v = 2.5$ V.

15

Protection of Devices and Circuits

15-1 INTRODUCTION

Due to the reverse recovery process of power devices and switching actions in the presence of circuit inductances, voltage transients occur in the converter circuits. Even in carefully designed circuits, short-circuit fault conditions may exit, resulting in an excessive current flow through the devices. The heat produced by losses in a semiconductor device must be dissipated sufficiently and effectively to operate the device within its upper temperature limit. The reliable operation of a converter would require ensuring that at all times the circuit conditions do not exceed the ratings of the power devices, by providing protection against overvoltage, overcurrent, and overheating. In practice, the power devices are protected from (1) thermal runway by heat sinks, (2) high dv/dt and di/dt by snubbers, (3) reverse recovery transients, (4) supply and load side transients, and (5) fault conditions by fuses.

15-2 COOLING AND HEAT SINKS

Due to on-state and switching losses, heat is generated within the power device. This heat must be transferred from the device to a cooling medium to maintain the operating junction temperature within the specified range. Although this heat

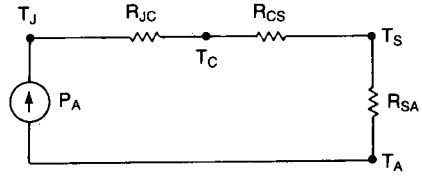


Figure 15-1 Electrical analog of heat transfer.

transfer can be accomplished by conduction, convection, or radiation, natural or forced-air, convection cooling is commonly used in industrial applications.

The heat must flow from the device to the case and then to the heat sink in the cooling medium. If P_A is the average power loss in the device, the electrical analog of a device, which is mounted on a heat sink, is shown in Fig. 15-1. The junction temperature of a device, T_J, is given by

$$T_J = P_A(R_{JC} + R_{CS} + R_{SA}) \tag{15-1}$$

where R_{JC} = thermal resistance from junction to case, °C/W
R_{CS} = thermal resistance from case to sink, °C/W
R_{SA} = thermal resistance from sink to ambient, °C/W
T_A = ambient temperature, °C

R_{JC} and R_{CS} are normally specified by the power device manufacturers. Once the device power loss, P_A, is known, the required thermal resistance of the heat sink can be calculated for a specified ambient temperature, T_A. The next step is to choose a heat sink and its size which would meet the thermal resistance requirement.

A wide variety of extruded aluminum heat sinks are commercially available and they use cooling fins to increase the heat transfer capability. The thermal resistance characteristics of a typical heat sink with natural and forced cooling are shown in Fig. 15-2, where the power dissipation against the sink temperature rise is depicted for natural cooling. In forced cooling, the thermal resistance decreases with the air velocity. However, above a certain velocity, the reduction in thermal resistance is not significant. Heat sinks of various types are shown in Fig. 15-3.

The contact area between the device and heat sink is extremely important to minimize the thermal resistance between the case and sink. The surfaces should be flat, smooth, and free of dirt, corrosion, and surface oxides. Silicone greases are normally applied to improve the heat transfer capability and to minimize the formation of oxides and corrosion.

The device must be mounted properly on the heat sink to obtain the correct mounting pressure between the mating surfaces. The proper installation procedures are usually recommended by the device manufacturers. In case of stud-mounted devices, excessive mounting torques may cause mechanical damage of the silicon wafer; and the stud and nut should not be greased or lubricated because the lubrication increases the tension on the stud.

The device may be cooled by heat pipes partially filled with low-vapor-pressure liquid. The device is mounted on one side of the pipe and a condensing mechanism (or heat sink) on the other side as shown in Fig. 15-4. The heat

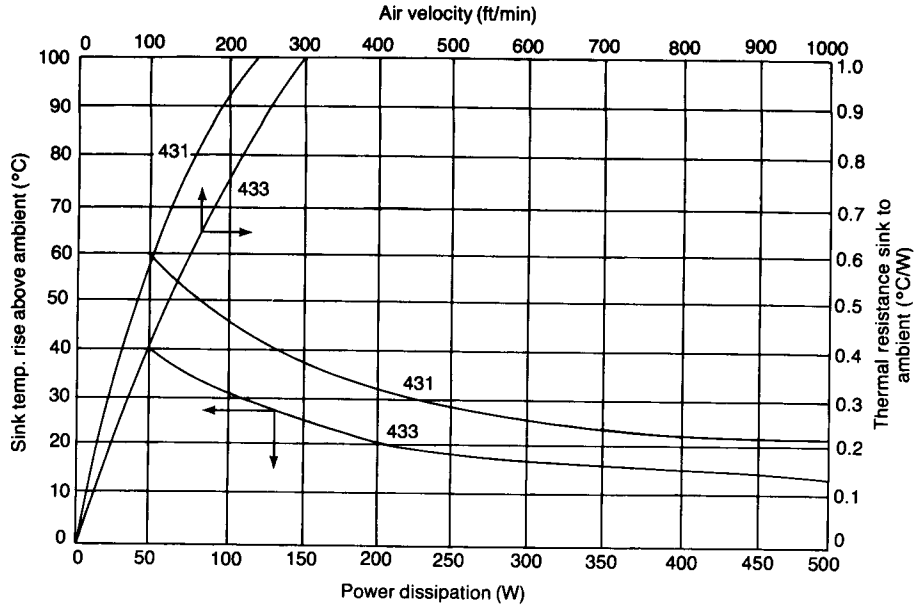


Figure 15-2 Thermal resistance characteristics. (*Courtesy of EG&G Wakefield Engineering*)

produced by the device vaporizes the liquid and the vapor, then flows to the condensing end, where it condenses and the liquid returns to the heat source. The device may be at some distance from the heat sink.

In high-power applications, the devices are more effectively cooled by liquids, normally, oil or water. Water cooling is very efficient and approximately three times more effective than oil cooling. However, it is necessary to use distilled

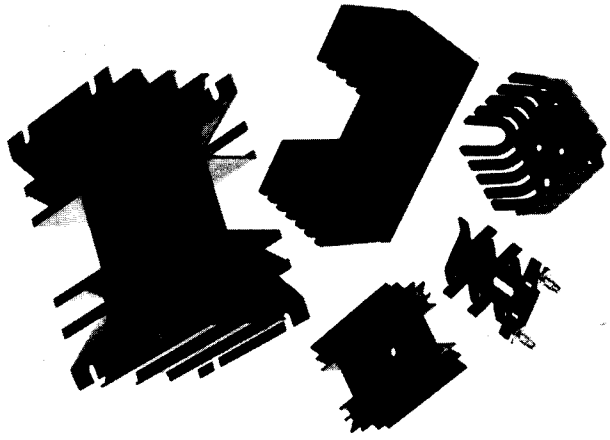


Figure 15-3 Heat sinks. (*Courtesy of EG&G Wakefield Engineering*)

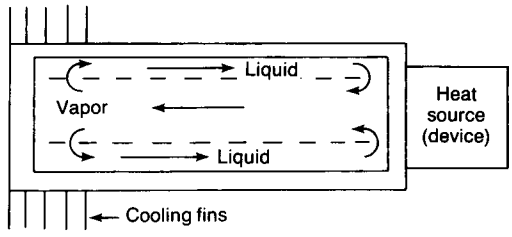


Figure 15-4 Heat pipes.

water to minimize corrosion and antifreeze to avoid freezing. Oil is flammable. Oil cooling, which may be restricted to some applications, provides good insulation and eliminates the problems of corrosion and freezing. Heat pipes and liquid-cooled heat sinks are commercially available. Two water-cooled ac switches are shown in Fig. 15-5. Power converters are available in assembly units as shown in Fig. 15-6.

The thermal impedance of a power device is very small, and as a result the junction temperature of the device varies with the instantaneous power loss. The instantaneous junction temperature must always be maintained lower than the acceptable value. A plot of the transient thermal impedance versus square-wave

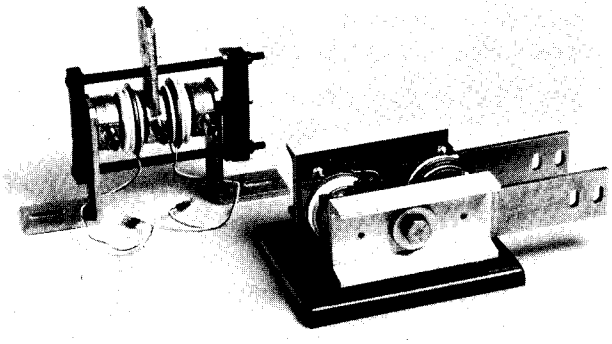


Figure 15-5 Water-cooled ac switches. (*Courtesy of Powerex, Inc.*)

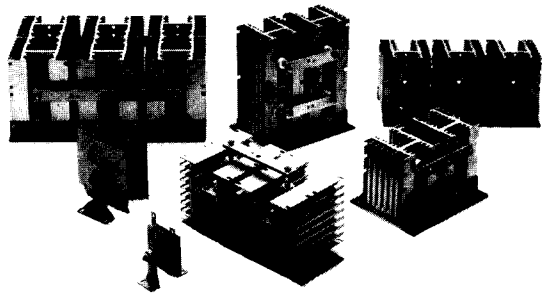


Figure 15-6 Assembly units. (*Courtesy of Powerex, Inc.*)

pulse duration is supplied by the device manufacturers as a part of data sheet as shown in Fig. 14-18.11. From the knowledge of current waveform through a device, a plot of power loss against time can be determined and then the transient impedance characteristics can be used to calculate the temperature variations with time. If the cooling media fails in practical systems, the temperature rise of the heat sinks are normally served to switch off the power converters, especially in high power applications.

The step response of a first order system can be applied to express the transient thermal impedance. If Z_0 is the steady-state junction case thermal impedance, the instantaneous thermal impedance can be expressed as

$$Z(t) = Z_0(1 - e^{-t/\tau_{th}}) \tag{15-2}$$

where τ_{th} is the thermal time constant of the device. If the power loss is P_d, the instantaneous junction temperature rise above the case is

$$T_J = P_d Z(t) \tag{15-3}$$

If the power loss is pulsed type as shown in Fig. 15-7, Eq. (15-3) can be applied to plot the step responses of the junction temperature, $T_J(t)$. If t_n is the duration of nth power pulse, the corresponding thermal impedance at the beginning and end of nth pulse are $Z_0 = Z(t = 0) = 0$ and $Z_n = Z(t = t_n)$, respectively. The thermal impedance $Z_n = Z(t = t_n)$ corresponding to the duration of t_n can be found from the transient thermal impedance characteristics (similar to Fig. 14-18.11). If $P_1, P_2, P_3, \ldots$ are the power pulses with $P_2 = P_4 = \cdots = 0$, the junction temperature at the end of mth pulse can be expressed as

$$\begin{aligned} T_J(t) &= T_{J0} + P_1(Z_1 - Z_2) + P_3(Z_3 - Z_4) + P_5(Z_5 - Z_6) + \cdots \\ &= T_{J0} + \sum_{n=1,3,\ldots}^{m} P_n(Z_n - Z_{n+1}) \end{aligned} \tag{15-4}$$

where T_{J0} is the initial junction temperature. The negative signs of $Z_2, Z_4, \ldots$ signify that the junction temperature falls during the intervals $t_2, t_4, t_6, \ldots$.

The step response concept of junction temperature can be extended to other

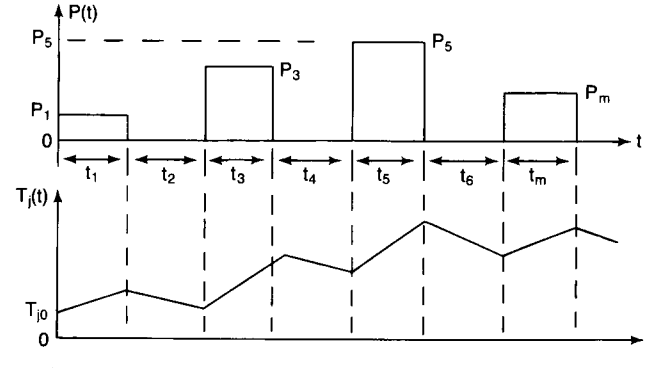


Figure 15-7 Junction temperature with rectangular power pulses.

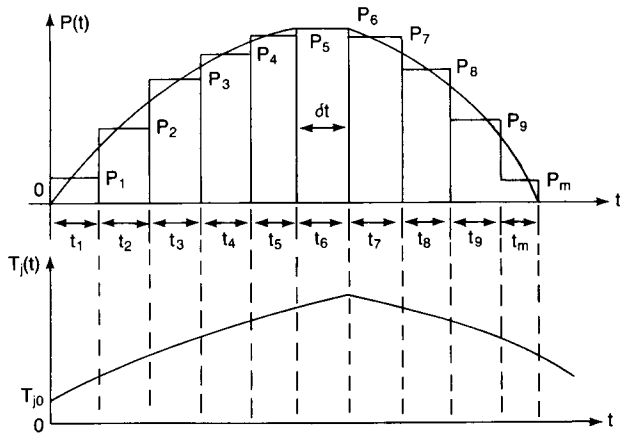


Figure 15-8 Approximation of a power pulse by rectangular pulses.

power waveforms. A waveform of any shape can be represented approximately by rectangular pulses of equal or unequal duration, with the amplitude of each pulse being equal to the average amplitude of the actual pulse over the same period. The accuracy of such approximations can be improved by increasing the number of pulses and reducing the duration of each pulse. This is shown in Fig. 15-8.

The junction temperature at the end of mth pulse can be found from

$$T_J(t) = T_{J0} + Z_1P_1 + Z_2(P_2 - P_1) + Z_3(P_3 - P_2) + \cdots \tag{15-5}$$

$$= T_{J0} + \sum_{n=1,2,\ldots}^{m} Z_n(P_n - P_{n-1})$$

where Z_n is the impedance at the end of nth pulse of duration $t_n = \delta t$. P_n is the power loss for the nth pulse and $P_0 = 0$.

Example 15-1

The power loss in an IR thyristor, type S30EF, is shown in Fig. 15-9. Plot the instantaneous junction temperature rise above the case.

Solution $P_1 = 800$ W, $P_3 = 1200$ W, and $P_5 = 600$ W. For $t_1 = t_3 = t_5 = 1$ ms, Fig. 14-18.11 gives

$$Z\ (t = t_1) = Z_1 = Z_3 = Z_5 = 0.035°\text{C/W}$$

For $t_2 = t_4 = t_6 = 0.5$ ms, Fig. 14-18.11 gives

$$Z\ (t = t_2) = Z_2 = Z_4 = Z_6 = 0.025°\text{C/W}$$

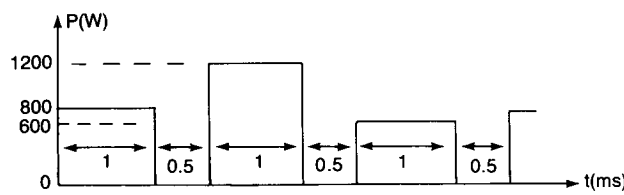


Figure 15-9 Thyristor power loss.

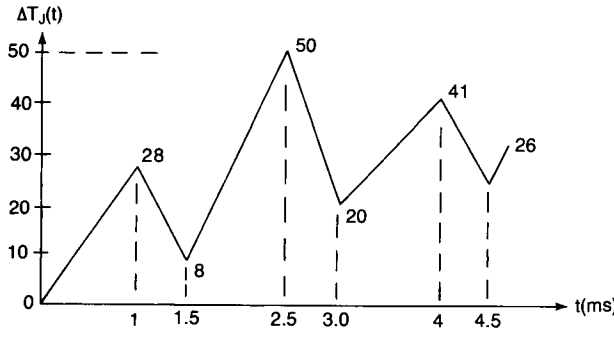


Figure 15-10 Junction temperature rise for Example 15-1.

Equation (15-4) can be applied directly to calculate the junction temperature rise.

$$\Delta T_J(t = 1 \text{ ms}) = T_J(t = 1 \text{ ms}) - T_{J0} = Z_1P_1 = 0.035 \times 800 = 28°C$$

$$\Delta T_J(t = 1.5 \text{ ms}) = 28 - Z_2P_1 = 28 - 0.025 \times 800 = 8°C$$

$$\Delta T_J(t = 2.5 \text{ ms}) = 8 + Z_3P_3 = 8 + 0.035 \times 1200 = 50°C$$

$$\Delta T_J(t = 3 \text{ ms}) = 50 - Z_4P_3 = 50 - 0.025 \times 1200 = 20°C$$

$$\Delta T_J(t = 4 \text{ ms}) = 20 + Z_5P_5 = 20 + 0.035 \times 600 = 41°C$$

$$\Delta T_J(t = 4.5 \text{ ms}) = 41 - Z_6P_5 = 41 - 0.025 \times 600 = 26°C$$

The junction temperature rise above case is shown in Fig. 15-10.

15-3 SNUBBER CIRCUITS

An *RC* snubber is normally connected across a semiconductor device to limit the *dv/dt* within the maximum allowable rating. The snubber could be polarized or unpolarized. A forward-polarized snubber is suitable when a thyristor or transistor is connected with an antiparallel diode as shown in Fig. 15-11a. The resistor, R, limits the forward *dv/dt*; and R_1 limits the discharge current of the capacitor when the device is turned on.

A reverse-polarized snubber which limits the reverse *dv/dt* is shown in Fig.

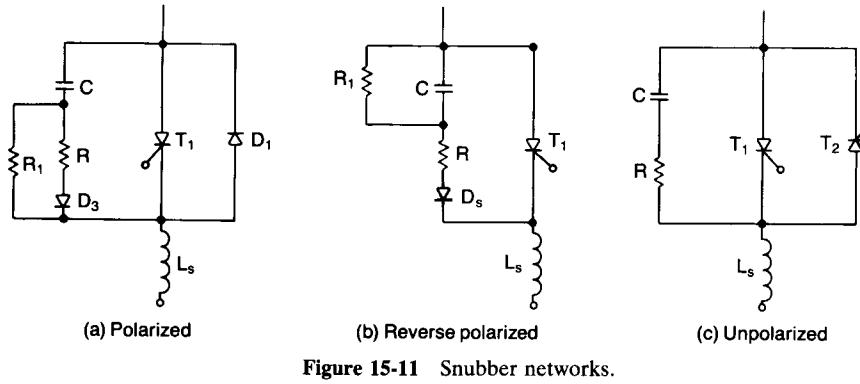


Figure 15-11 Snubber networks.

15-11b, where R_1 limits the discharge current of the capacitor. The capacitor does not discharge through the device, resulting in reduced losses in the device.

When a pair of thyristors are connected in inverse parallel, the snubber must be effective in either direction. An unpolarized snubber is shown in Fig. 15-11c.

15-4 REVERSE RECOVERY TRANSIENTS

Due to the reverse recovery time, t_{rr}, and recovery current, I_R, energy is strapped in the circuit inductances and as a result transient voltage appears across the device. In addition to *dv/dt* protection, the snubber limits the peak transient voltage across the device. The equivalent circuit for a typical circuit arrangement is shown in Fig. 15-12, where initial capacitor voltage is zero and the inductor carries an initial current of I_R. The values of snubber *RC* are selected so that the circuit is slightly underdamped and Fig. 15-13 shows the recovery current and transient voltage. Critical damping usually results in a large value of initial reverse voltage, RI_{RR}; and insufficient damping causes large overshoot of the transient voltage. In the following analysis, it is assumed that the recovery is abrupt and the recovery current is suddenly switched to zero.

The snubber current is expressed as

$$L\frac{di}{dt} + Ri + \frac{1}{C}\int i\,dt + v_c\,(t = 0) = V_s \tag{15-6}$$

(15-7)

$$v = V_s - L\frac{di}{dt}$$

with initial conditions $i(t = 0) = I_R$ and $v_c\,(t = 0) = 0$. We have seen in Section 2-3 that the form of the solution for Eq. (15-6) depends on the values of *RLC*.

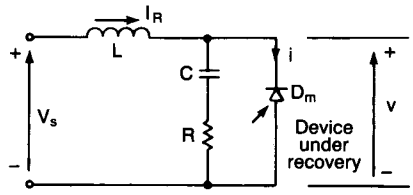


Figure 15-12 Equivalent circuit during recovery.

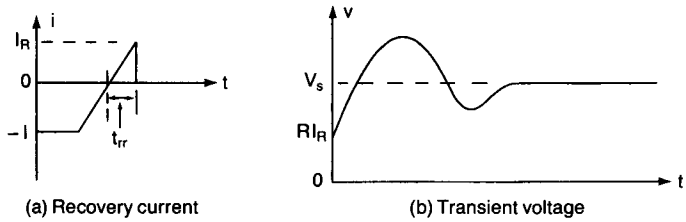


Figure 15-13 Recovery transient.

For an underdamped case, the solutions of Eqs. (15-6) and (15-7) yield the reverse voltage across the device as

$$v(t) = V_s - (V_s - RI_R)\left(\cos \omega t - \frac{\alpha}{\omega} \sin \omega t\right)e^{-\alpha t} + \frac{I_R}{\omega C} e^{-\alpha t} \sin \omega t \tag{15-8}$$

where

$$\alpha = \frac{R}{2L} \tag{15-9}$$

The undamped natural frequency is

$$\omega_0 = \frac{1}{\sqrt{LC}} \tag{15-10}$$

The damping ratio is

$$\delta = \frac{\alpha}{\omega_0} = \frac{R}{2}\sqrt{\frac{C}{L}} \tag{15-11}$$

and the damped natural frequency is

$$\omega = \sqrt{\omega_0^2 - \alpha^2} = \omega_0 \sqrt{1 - \delta^2} \tag{15-12}$$

Differentiating Eq. (15-8) yields

$$\begin{aligned} \frac{dv}{dt} = {} & (V_s - RI_R)\left(2\alpha \cos \omega t + \frac{\omega^2 - \alpha^2}{\omega} \sin \omega t\right)e^{-\alpha t} \\ & + \frac{I_R}{C}\left(\cos \omega t - \frac{\alpha}{\omega} \sin \omega t\right)e^{-\alpha t} \end{aligned} \tag{15-13}$$

The initial reverse voltage and dv/dt can be found from Eqs. (15-8) and (15-13) by setting $t = 0$

$$v\,(t = 0) = RI_R \tag{15-14}$$

$$\left.\frac{dv}{dt}\right|_{t=0} = (V_s - RI_R)2\alpha + \frac{I_R}{C} = \frac{(V_s - RI_R)R}{L} + \frac{I_R}{C}$$

$$= V_s\omega_0(2\delta - 4d\delta^2 + d) \tag{15-15}$$

where

$$d = \frac{I_R}{V_s}\sqrt{\frac{L}{C}} = \frac{I_R}{I_p} \tag{15-16}$$

If the initial dv/dt in Eq. (15-15) is negative, the initial inverse voltage RI_R is the maximum and this may produce a destructive dv/dt. For positive dv/dt, $V_s\omega_0(2\delta - 4d\delta^2 + d) > 0$ or

$$\delta < \frac{1 + \sqrt{1 + 4d^2}}{4d} \tag{15-17}$$

and the reverse voltage will be maximum at $t = t_1$. The time t_1, which can be obtained by setting Eq. (15-13) equal to zero, is found as

$$\tan \omega t_1 = \frac{\omega[V_s - RI_R)2\alpha + I_R/C]}{(V_s - RI_R)(\omega^2 - \alpha^2) - \alpha I_R/C} \tag{15-18}$$

and the peak voltage can be found from Eq. (15-8):

$$V_p = v\ (t = t_1) \tag{15-19}$$

The peak reverse voltage depends on the damping ratio, δ, and the current factor, d. For a given value of d, there is an optimum value of damping ratio, δ_o, which will minimize the peak voltage. However, the dv/dt varies with d and minimizing the peak voltage may not minimize the dv/dt. It is necessary to make a compromise between the peak voltage, V_p, and dv/dt. McMurray [1] proposed to minimize the product $V_p(dv/dt)$ and the optimum design curves are shown in Fig. 15-14,

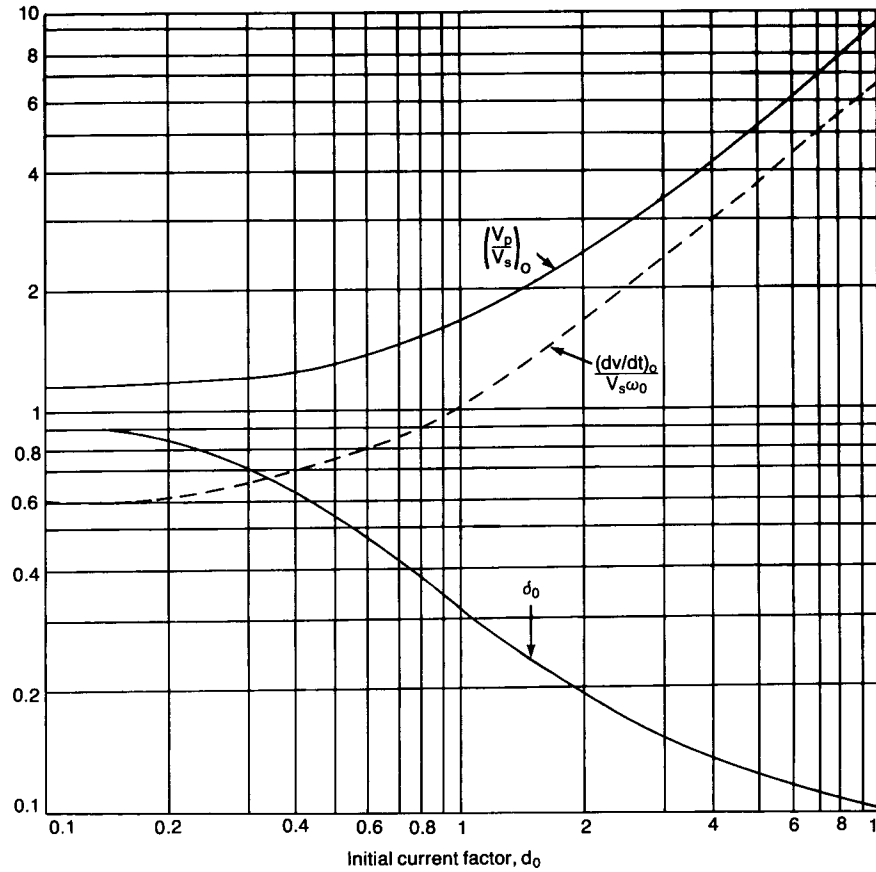


Figure 15-14 Optimum snubber parameters for compromise design. (Reproduced from W. McMurray, "Optimum snubbers for power semiconductors," *IEEE Transactions on Industry Applications*, Vol. 1A8, No. 5, 1972, pp. 503–510, Fig. 7. ©1972 by IEEE)

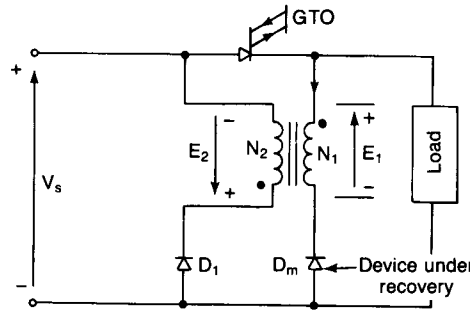


Figure 15-15 Nondissipative snubber.

where dv/dt is the average value over time t_1 and d_o is the optimum value of current factor.

The energy stored in the inductor, L, which is transferred to the snubber capacitor, C, is dissipated mostly in the snubber resistor. This power loss is dependent on the switching frequency and load current. For high-power converters, where the snubber loss is significant, a nondissipative snubber which uses an energy recovery transformer as shown in Fig. 15-15 can improve the circuit efficiency. When the primary current rises, the induced voltage E_2 is positive and diode D_1 is reverse biased. If the recovery current of diode D_m starts to fall, the induced voltage E_2 becomes negative and diode D_1 conducts, returning energy to the dc supply.

Example 15-2

The recovery current of a diode as shown in Fig. 15-12 is $I_R = 20$ A and the circuit inductance is $L = 50$ μH. The input voltage is $V_s = 220$ V. If it is necessary to limit the peak transient voltage to 1.5 times the input voltage, determine the (a) optimum value of current factor α_o; (b) optimum damping factor, δ_o; (c) snubber capacitance, C; (d) snubber resistance, R; (e) average dv/dt; and (f) initial reverse voltage.

Solution $I_R = 20$ A, $L = 50$ μH, $V_s = 220$ V, and $V_p = 1.5 \times 220 = 330$ V. For $V_p/V_s = 1.5$, Fig. 15-14 gives:

(a) The optimum current factor, $d_o = 0.75$.

(b) The optimum damping factor, $\delta_o = 0.4$.

(c) From Eq. (15-16), the snubber capacitance (with $d = d_o$) is

$$C = L\left[\frac{I_R}{dV_s}\right]^2 = 50\left[\frac{20}{0.75 \times 220}\right]^2 = 0.735\ \mu\text{F} \tag{15-20}$$

(d) From Eq. (15-11), the snubber resistance is

$$R = 2\delta\sqrt{\frac{L}{C}} = 2 \times 0.4\sqrt{\frac{50}{0.735}} = 6.6\ \Omega \tag{15-21}$$

(e) From Eq. (15-10),

$$\omega_0 = \frac{10^6}{\sqrt{50 \times 0.735}} = 164{,}957 \text{ rad/s}$$

From Fig. 15-14,

$$\frac{dv/dt}{V_s\omega_0} = 0.88$$

or

$$\frac{dv}{dt} = 0.88V_s\omega_0 = 0.88 \times 220 \times 164{,}957 = 31.9 \text{ V/}\mu\text{s}$$

(f) From Eq. (15-14), the initial reverse voltage is

$$v\ (t = 0) = 6.6 \times 20 = 132 \text{ V}$$

Example 15-3

An *RC*-snubber circuit as shown in Fig. 15-11c has $C = 0.75$ μF, $R = 6.6\ \Omega$, and input voltage, $V_s = 220$ V. The circuit inductance is $L = 50$ μH. Determine the (a) peak forward voltage, V_p; (b) initial dv/dt; and (c) maximum dv/dt.

Solution $R = 6.6\ \Omega$, $C = 0.75$ μF, $L = 50$ μH, and $V_s = 220$ V. By setting $I_R = 0$, the forward voltage across the device can be determined from Eq. (15-8),

$$v(t) = V_s - V_s\left(\cos \omega t - \frac{\alpha}{\omega} \sin \omega t\right]e^{-\alpha t} \tag{15-22}$$

From Eq. (15-13),

$$\frac{dv}{dt} = V_s\left(2\alpha \cos \omega t + \frac{\omega^2 - \alpha^2}{\omega} \sin \omega t\right)e^{-\alpha t} \tag{15-23}$$

The initial dv/dt can be found either from Eq. (15-23) by setting $t = 0$, or from Eq. (15-15) by setting $I_R = 0$

$$\left.\frac{dv}{dt}\right|_{t=0} = V_s 2\alpha = \frac{V_s R}{L} \tag{15-24}$$

The forward voltage will be maximum at $t = t_1$. The time t_1, which can be obtained either by setting Eq. (15-23) equal to zero, or by setting $I_R = 0$ in Eq. (15-18), is found as

$$\tan \omega t_1 = -\frac{2\alpha\omega}{\omega^2 - \alpha^2} \tag{15-25}$$

$$\cos \omega t_1 = -\frac{\omega^2 - \alpha^2}{\omega^2 + \alpha^2} \tag{15-26}$$

$$\sin \omega t_1 = \frac{2\alpha\omega}{\omega^2 + \alpha^2} \tag{15-27}$$

Substituting Eqs. (15-25), (15-26), and (15-27) into Eq. (15-22), the peak voltage is

found as

$$V_p = v\,(t = t_1) = V_s\,(1 + e^{-\alpha t_1}) \tag{15-28}$$

where

$$\alpha t_1 = \frac{\delta}{\sqrt{1 - \delta^2}} \tan^{-1} \frac{-2\delta\sqrt{1 - \delta^2}}{1 - 2\delta^2} \tag{15-29}$$

Differentiating Eq. (15-23) with respect to t, and setting equal to zero, dv/dt will be maximum at $t = t_m$ when

$$-\frac{\alpha(3\omega^2 - \alpha^2)}{\omega} \sin \omega t_m + (\omega^2 - 3\alpha^2) \cos \omega t_m = 0$$

or

$$\tan \omega t_m = \frac{\omega(\omega^2 - 3\alpha^2)}{\alpha(3\omega^2 - \alpha^2)} \tag{15-30}$$

Substituting the value of t_m in Eq. (15-23) and simplifying the sine, and cosine terms yield the maximum value of dv/dt,

$$\left.\frac{dv}{dt}\right|_{\max} = \sqrt{\omega^2 + \alpha^2}\, e^{-\alpha t_m} \tag{15-31}$$

For a maximum to occur, $d(dv/dt)/dt$ must be positive if $t \leq t_m$ and Eq. (15-30) gives the necessary condition as

$$\omega^2 - 3\alpha^2 \geq 0 \quad \text{or} \quad \frac{\alpha}{\omega} \leq \frac{1}{\sqrt{3}} \quad \text{or} \quad \delta \leq 0.5$$

Equation (15-31) is valid for $\delta \leq 0.5$. For $\delta > 0.5$, dv/dt which becomes maximum when $t = 0$ is obtained from Eq. (15-23),

$$\left.\frac{dv}{dt}\right|_{\max} = \left.\frac{dv}{dt}\right|_{t=0} = V_s 2\alpha = \frac{V_s R}{L} \quad \text{for } \delta > 0.5 \tag{15-32}$$

(a) From Eq. (15-9), $\alpha = 6.6/(2 \times 50 \times 10^{-6}) = 66{,}000$ and from Eq. (15-10),

$$\omega_0 = \frac{10^6}{\sqrt{50 \times 0.75}} = 163{,}299 \text{ rad/s}$$

From Eq. (15-11), $\delta = (6.6/2)\sqrt{0.75/50} = 0.404$, and from Eq. (15-12),

$$\omega = 163{,}299\sqrt{1 - 0.404^2} = 149{,}367 \text{ rad/s}$$

From Eq. (15-29), $t_1 = 15.46$ μs; therefore, Eq. (15-28) yields the peak voltage, $V_p = 220(1 + 0.36) = 299.3$ V.

(b) Equation (15-24) gives the initial dv/dt of $(220 \times 6.6/50) = 29$ V/μs.

(c) Since $\delta < 0.5$, Eq. (15-31) should be used to calculate the maximum dv/dt. From Eq. (15-30), $t_m = 2.16$ μs and Eq. (15-31) yields the maximum dv/dt as 31.2 V/μs.

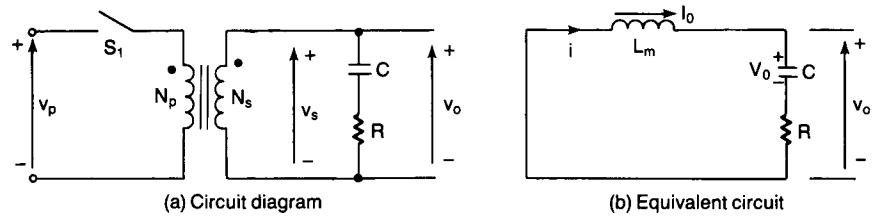


Figure 15-16 Switching off transient.

15-5 SUPPLY- AND LOAD-SIDE TRANSIENTS

A transformer is normally connected to the input side of the converters. Under steady-state condition, energy is stored in the magnetizing inductance, L_m, of transformer, and switching off the supply produces a transient voltage to the input of the converter. A capacitor may be connected across the primary or secondary of the transformer to limit the transient voltage as shown in Fig. 15-16a, and in practice a resistance is also connected in series with the capacitor to limit the transient voltage.

Under steady-state conditions, $v_s = V_m \sin \omega t$ and the magnetizing current is given by

$$L_m \frac{di}{dt} = V_m \sin \omega t$$

which gives

$$i(t) = -\frac{V_m}{\omega L_m} \cos \omega t$$

If the switch is turned off at $\omega t = \theta$, the capacitor voltage at the beginning of switch-off is

$$V_0 = V_m \sin \theta \tag{15-33}$$

and the magnetizing current is

$$I_0 = -\frac{V_m}{\omega L_m} \cos \theta \tag{15-34}$$

The equivalent circuit during the transient condition is shown in Fig. 15-16b and the capacitor current is expressed as

$$L_m \frac{di}{dt} + Ri + \frac{1}{C} \int i \, dt + v_c (t = 0) = 0 \tag{15-35}$$

and

$$v_0 = -L_m \frac{di}{dt} \tag{15-36}$$

with initial conditions $i\ (t = 0) = -I_0$ and $v_c\ (t = 0) = V_0$. The transient voltage $v_0(t)$ can be determined from Eqs. (15-35) and (15-36), for underdamped conditions. A damping ratio of $\delta = 0.5$ is normally satisfactory. The analysis can be simplified by assuming small damping tending to zero, i.e., $\delta = 0$, (or, $R = 0$). Eq. (3-20), which is similar to Eq. (15-35), can be applied to determine the transient voltage, $v_o(t)$. The transient voltage, $v_o(t)$ is the same as the capacitor voltage, $v_c(t)$.

$$v_0(t) = v_c(t) = V_0 \cos \omega_0 t + I_0 \sqrt{\frac{L_m}{C}} \sin \omega_0 t \tag{15-37}$$

$$= \left(V_0^2 + I_0^2 \frac{L_m}{C}\right)^{1/2} \sin (\omega_0 t + \phi)$$

$$= V_m \left(\sin^2 \theta + \frac{1}{\omega^2 L_m C} \cos^2 \theta\right)^{1/2} \sin (\omega_0 t + \phi)$$

$$= V_m \left(1 + \frac{\omega_0^2 - \omega^2}{\omega^2} \cos^2 \theta\right)^{1/2} \sin (\omega_0 t + \phi) \tag{15-38}$$

where

$$\phi = \tan^{-1} \frac{V_0}{I_0} \sqrt{\frac{C}{L_m}} \tag{15-39}$$

and

$$\omega_0 = \frac{1}{CL_m} \tag{15-40}$$

If $\omega_0 < \omega$, the transient voltage in Eq. (15-38) which will be maximum when $\cos \theta = 0$ (or $\theta = 90°$) is

$$V_p = V_m \tag{15-41}$$

In practice, $\omega_0 > \omega$ and the transient voltage, which will be maximum when $\cos \theta = 1$ (or $\theta = 0°$), is

$$V_p = V_m \frac{\omega_0}{\omega} \tag{15-42}$$

Using the voltage and current relationship in a capacitor, the required amount of capacitance to limit the transient voltage can be determined from

$$C = \frac{I_0}{V_p \omega_0} \tag{15-43}$$

Substituting Eq. (15-42) in Eq. (15-43) gives us

$$C = \frac{I_0 V_m}{V_p^2 \omega} \tag{15-44}$$

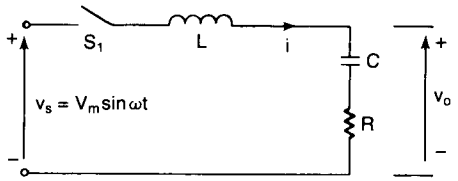


Figure 15-17 Equivalent circuit during switching on the supply.

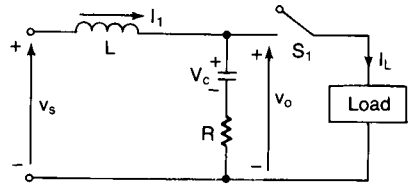


Figure 15-18 Equivalent circuit due to load disconnection.

Now with the capacitor connected across the transformer secondary, the maximum instantaneous capacitor voltage will depend on the instantaneous ac input voltage at the instant of switching on the input voltage. The equivalent circuit during switch-on is shown in Fig. 15-17, where L is the equivalent supply inductance plus the leakage inductance of the transformer.

Under normal operation, energy is stored in the supply inductance and the leakage inductance of the transformer. When the load is disconnected, transient voltages are produced due to the energy stored in the inductances. The equivalent circuit due to load disconnection is shown in Fig. 15-18.

Example 15-4

A capacitor is connected across the secondary of an input transformer as shown in Fig. 15-16a, with zero damping resistance. The secondary voltage is $V_s = 120$ V, 60 Hz. If the magnetizing inductance referred to the secondary is $L_m = 2$ mH and the input supply to the transformer primary is disconnected at an angle of $\theta = 180°$ of the input ac voltage, determine the (a) initial capacitor value, V_0; (b) magnetizing current, I_0; and (c) capacitor value to limit the maximum transient capacitor voltage to $V_p = 300$ V.

Solution $V_s = 120$ V, $V_m = \sqrt{2} \times 120 = 169.7$ V, $\theta = 180°$, $f = 60$ Hz, $L_m = 2$ mH, and $\omega = 2\pi \times 60 = 377$ rad/s.

(a) From Eq. (15-33), $V_c = 169.7 \sin \theta = 0$.

(b) From Eq. (15-34),

$$I_0 = -\frac{V_m}{\omega L_m} \cos \theta = \frac{169.7}{0.002 \times 377} = 225 \text{ A}$$

(c) $V_p = 300$ V. From Eq. (15-44), the required capacitance is

$$C = 225 \times \frac{169.7}{300^2 \times 377} = 1125.3 \ \mu\text{F}$$

15-6 VOLTAGE PROTECTION BY SELENIUM DIODES AND METAL-OXIDE VARISTORS

The selenium diodes may be used for protection against transient overvoltages. These diodes have low forward voltage but well-defined reverse breakdown voltage. The characteristics of selenium diodes are shown in Fig. 15-19. Normally, the

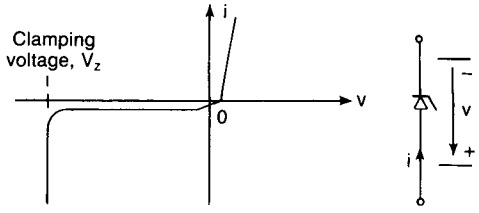


Figure 15-19 Characteristics of selenium diode.

operating point lies before the knee of the characteristic curve and draws very small current from the circuit. However, when an overvoltage appears, the knee point is crossed and the reverse current flow through the selenium increases suddenly, thereby typically limiting the transient voltage to twice the normal voltage.

The selenium diode (or suppresser) must be capable of dissipating the surge energy without undue temperature rise. Each cell of a selenium diode is normally rated at a rms voltage of 25 V, with a clamping voltage of typically 72 V. For protection of dc circuit, the suppresion circuit is polarized as shown in Fig. 15-20a. In ac circuits as in Fig. 15-20b, the suppressers are nonpolarized, so that they can limit overvoltages in both directions. For three-phase circuits, wye-connected-polarized suppressers as shown in Fig. 15-20c can be used.

If a dc circuit of 240 V is to be protected with 25-V selenium cells, then $240/25 \approx 10$ cells would be required and the total clamping voltage would be $10 \times 72 = 720$ V. To protect a single-phase ac circuit of 208 V, 60 Hz, with 25-V selenium cells, $208/25 \approx 9$ cells would be required in each direction and total of $2 \times 9 = 18$ cells would be necessary for nonpolarized suppression. Due to low internal capacitance, the selenium diodes do not limit the dv/dt to the same extent as compared to the RC-snubber circuits. However, they limit the transient voltages to well-defined magnitudes. In protecting a device, the reliability of an RC circuit is better than that of selenium diodes.

Varistors are nonlinear variable-impedance devices, consisting of metal-oxide particles, separated by an oxide film or insulation. As the applied voltage is increased, the film becomes conductive and the current flow is increased. The current is expressed as

$$I = KV^{\alpha} \tag{15-45}$$

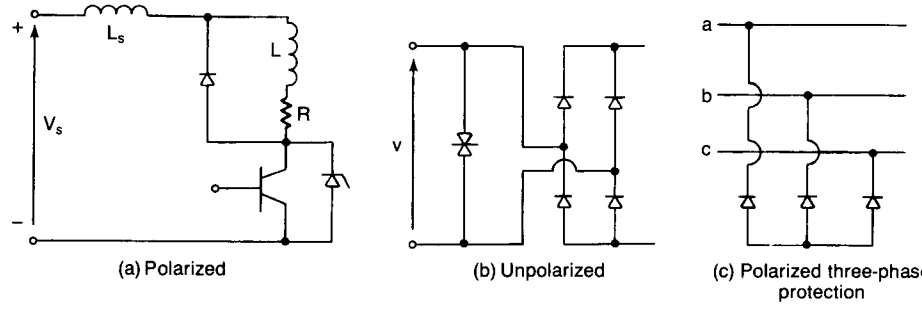


Figure 15-20 Voltage-suppression diodes.

where K is a constant and V is the applied voltage. The value of α varies between 30 and 40.

15-7 CURRENT PROTECTIONS

The power converters may develop short circuits or faults and the resultant fault currents must be cleared quickly. Fast-acting fuses are normally used to protect the semiconductor devices. As the fault current increases, the fuse opens and clears the fault current in few milliseconds.

15-7.1 Fusing

The semiconductor devices may be protected by carefully choosing the locations of the fuses as shown in Fig. 15-21. However, the fuse manufacturers recommend placing a fuse in series with each device as shown in Fig. 15-22. The individual protection which permits better coordination between a device and its fuse, allows superior utilization of the device capabilities and protects from short through faults (e.g., through T_1 and T_4 in Fig. 15-22a). The semiconductor fuses are shown in Fig. 15-23.

When the fault current rises, the fuse temperature also rises until $t = t_m$, at which time the fuse melts and arcs are developed across the fuse. Due to the arc,

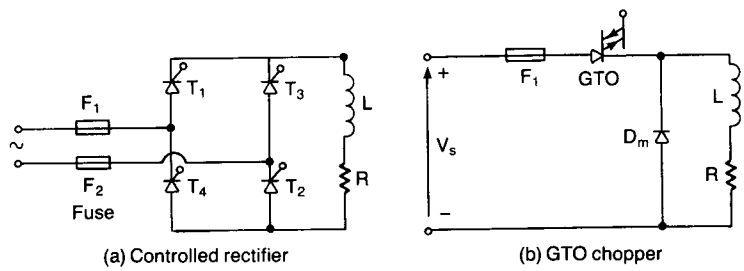


Figure 15-21 Protection of power devices.

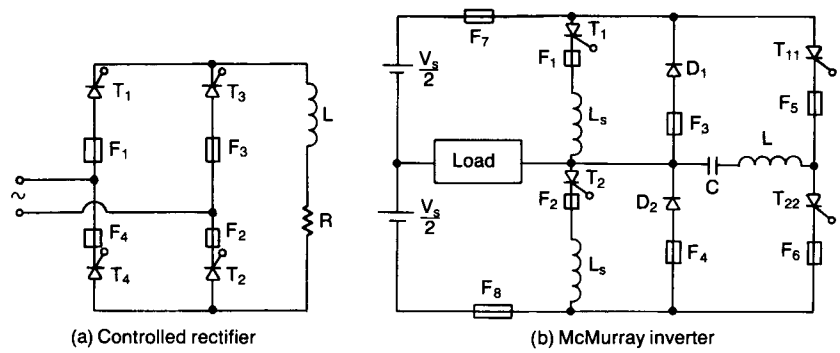


Figure 15-22 Individual protection of devices.

the impedance of the fuse is increased, thereby reducing the current. However, an arc voltage is formed across the fuse. The generated heat vaporizes the fuse element, resulting in increased arc length and further reduction of the current. The cumulative effect is the extinction of the arc in a very short time. When the arcing is complete in time t_a, the fault is clear. The faster the fuse clears, the higher is the arc voltage.

The clearing time t_c is the sum of melting time, t_m, and arc time, t_a. t_m is dependent on the load current, whereas t_a is dependent on the power factor or parameters of the fault circuit. The fault is normally cleared before the fault current reaches its first peak and the fault current, which might have flown if there was no fuse, is called the *prospective fault current*. This is shown in Fig. 15-24.

The current–time curves of devices and fuses may be used for the coordination of a fuse for a device. Figure 15-25a shows the current–time characteristics of a device and its fuse, where the device will be protected over the whole range of overloads. This type of protection is normally used for low-power converters. Figure 15-25b shows the more commonly used system in which the fuse is used for short-circuit protection at the beginning of the fault; and the normal overload protection is provided by circuit breaker or other current-limiting system.

If R is the resistance of the fault circuit and i is the instantaneous fault current between the instant of fault occurring and the instant of arc extinction, the energy fed to the circuit can be expressed as

$$W_e = \int Ri^2\, dt \tag{15-46}$$

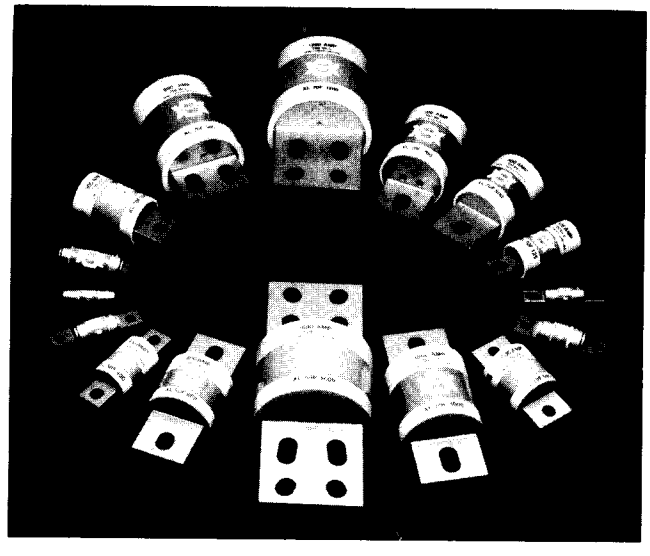


Figure 15-23 Semiconductor fuses. (*Reproduced by permission of Brush Electrical Machines, Ltd., England*)

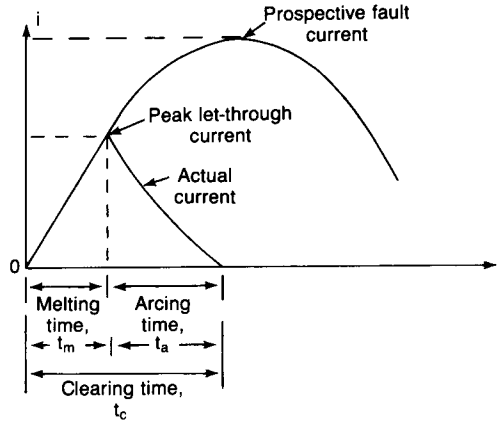


Figure 15-24 Fuse current.

If the resistance, R, remains constant, the value of I^2t is proportional to the energy fed to the circuit. The I^2t value is termed as the *let-through energy* and is responsible for melting the fuse. The fuse manufacturers specify the I^2t characteristic of the fuse and Fig. 15-26 shows the typical characteristics of IR fuses, types TT350.

In selecting a fuse it is necessary to estimate the fault current and then to satisfy the following requirements:

1. The fuse must carry continuously the device rated current.

2. The I^2t let-through value of the fuse before the fault current is cleared must be less than the rated I^2t of the device to be protected.

3. The fuse must be able to withstand the voltage, after the arc extinction.

4. The peak arc voltage must be less than the peak voltage rating of the device.

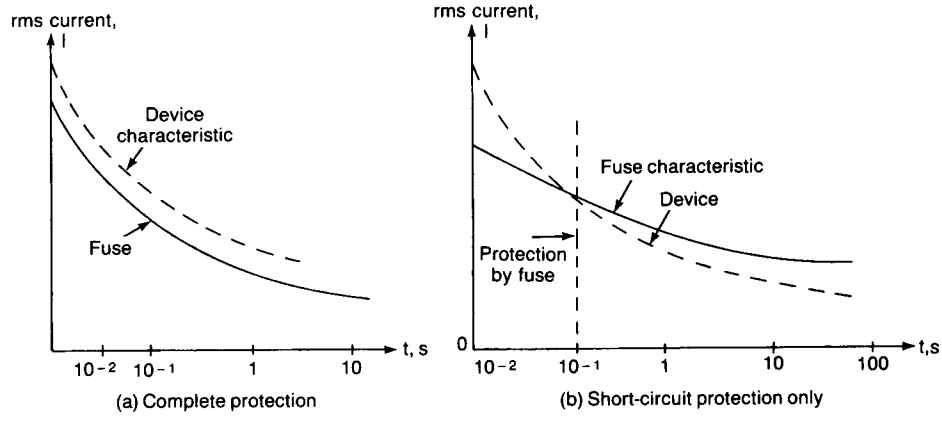


Figure 15-25 Current/time characteristics of device and fuse.

T350 SERIES

290V/175-450A r.m.s. Semiconductor Fuses

Suitable for protecting High Power Semiconductor Devices

Conforms to BS88: Part 4: 1976 and IEC 269-4.
ASTA certificate of short circuit ratings and verification of I^2t cut-off and arc voltage characteristics are available.

IMPORTANT

***Note 1:** Thyristors/diodes are rated in average current while fuses are rated in r.m.s. current. During steady state operation the fuse must not be operated in excess of its maximum r.m.s. rating.*

***Note 2:** The maximum cap temperature and cap temperature rise above ambient of a fuse are critical design parameters. Caution should be taken during installation to ensure that the specified ratings are not exceeded. Some form of heatsink may be necessary.*

The T350 Series of semiconductor fuses are available with I700 indicator fuses already fitted, for dimensional details refer to page E-12. For electrical, thermal and mechanical specifications on I700 refer to page E-5.
To complete part number add prefix "I" e.g. IT350-450.

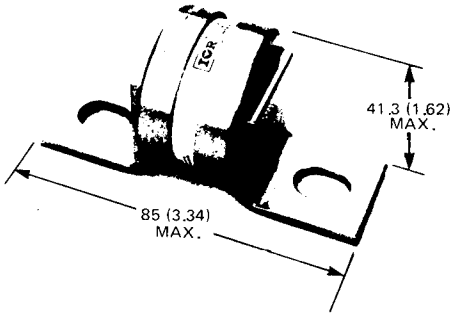
ELECTRICAL SPECIFICATIONS

Maximum r.m.s. voltage rating:	290V
Maximum tested peak voltage	450V
Maximum d.c. voltage rating (L/R≤15ms)	160V
Maximum arcing voltage for AC Supply Voltage = 240V	490V
For variation in arcing voltage with AC Supply Voltage $V_A = 100 + 1.63\ V_S$ where V_A = Peak arc voltage, V_S = AC Supply Voltage	
Fusing Factor	1.25
Force cooling Current uprating factor at 5 m/s	1.2

THERMAL AND MECHANICAL SPECIFICATIONS

Maximum cap temperature:	100°C
Maximum cap temperature rise above ambient	75°C
Weight:	170g (5.95 oz.)

Part number	RMS CURRENT (1) T_{amb} = 25°C	RMS CURRENT (1) T_{amb} = 25°C	MAX. POWER LOSS	PRE-ARCING (2) I^2t	TOTAL I^2t (2) at 120 V_{RMS}	TOTAL I^2t (2) at 240 V_{RMS}	NOTES
	A	A	W	A^2s	A^2s	A^2s	
T350–150	175	155	17	1600	7000	16000	1) Maximum current carrying ability, natural convection cooling using test arrangement as BS88: Part 4: 1976 conductors 1.0 to 1.6 A/mm² attachment. 2) Typical values of I^2t at 20 times rated RMS current
T350–200	210	190	28	2100	10000	20000	
T350–250	250	230	28	4800	20000	40000	
T350–300	315	290	35	9000	34000	70000	
T350–350	355	320	35	13000	50000	100000	
T350–400	400	350	40	20000	75000	160000	
T350–450	450	400	42	30000	110000	220000	



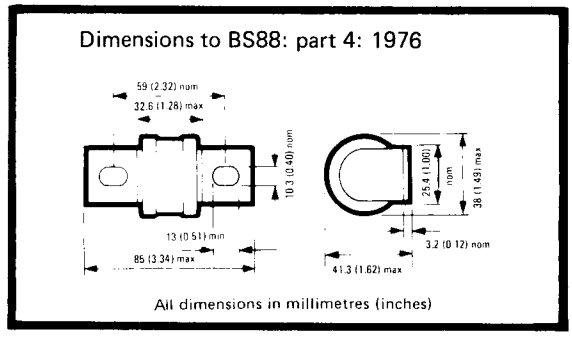


Figure 15-26 Data sheet of IR fuse, type TT350. (*Courtesy of International Rectifier*)

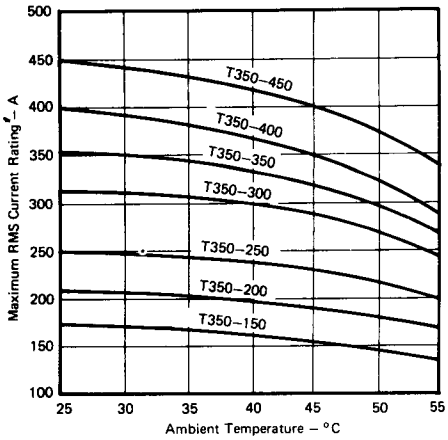


Fig. 1 – Current Rating Characteristic

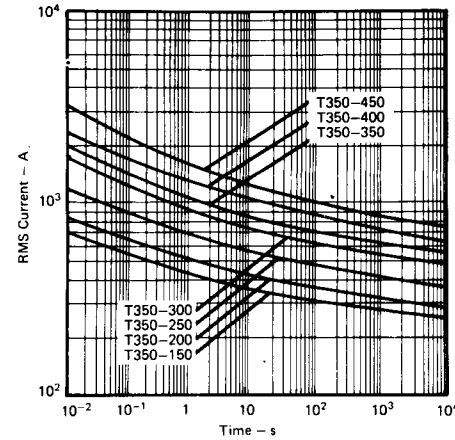


Fig. 2 – Time Current Characteristic

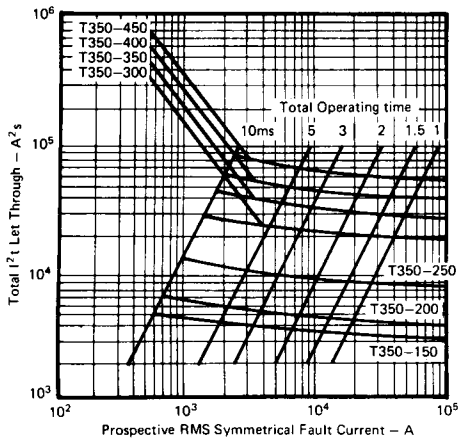


Fig. 3 – I^2t Let Through Characteristic (60V~)

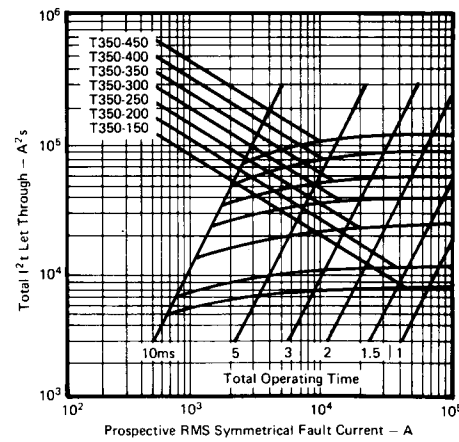


Fig. 4 – I^2t Let Through Characteristic (120V~)

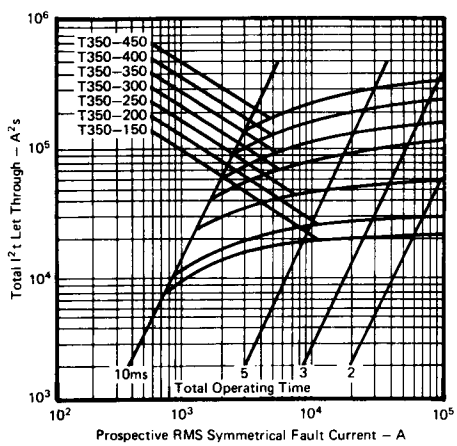


Fig. 5 – I^2t Let Through Characteristic (240V~)

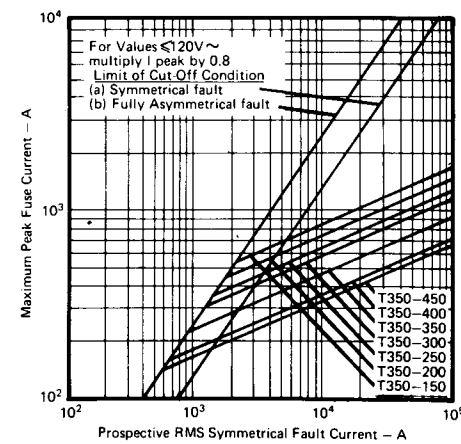


Fig. 6 – Cut-Off Characteristics (240V~)

Figure 15-26 (*continued*)

TT350 SERIES

290V/400-900A r.m.s. Semiconductor Fuses

Suitable for protecting High Power Semiconductor Devices

Conforms to BS88: Part 4: 1976 and IEC 269-4.

IMPORTANT:

Note 1: Thyristors/diodes are calibrated in average current ratings while fuses are calibrated in r.m.s. current ratings. During steady state operation the fuse must not be operated in excess of its maximum r.m.s. rating.

Note 2: The maximum cap temperature and cap temperature rise above ambient of a fuse are critical design parameters. Caution should be taken during installation to ensure that the specified ratings are not exceeded.

The TT350 Series of semiconductor fuses are available with I700 indicator fuses already fitted, for dimensional details refer to page E-67. For electrical, thermal and mechanical specifications refer to page E-66.
To complete part number add prefix "I" e.g. ITT350-900.

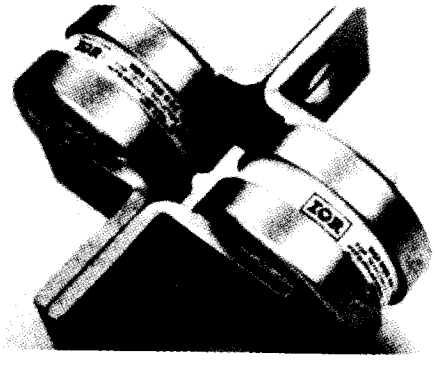
ELECTRICAL SPECIFICATIONS

Maximum r.m.s. voltage rating:	290V
Maximum tested peak voltage:	450V
Maximum d.c. voltage rating (L/R≤15ms)	160V
Maximum arcing voltage for AC Supply Voltage = 240V	490V
For variation in arcing voltage with AC Supply Voltage $V_A = 100 + 1.63\ V_s$	
Where V_A = Peak arc voltage, V_s = AC Supply Voltage	
Fusing Factor:	1.25
Force cooling Current uprating factor at 5 m/s	1.2

THERMAL AND MECHANICAL SPECIFICATIONS

Maximum cap temperature:	100°C
Maximum cap temperature rise above ambient	75°C
Maximum gravitational withstand capability: (for device mounted radially to rotation.)	1500g (52.5 oz.)

Part number	RMS CURRENT (1) T_{amb} = 25°C	RMS CURRENT (1) T_{amb} = 45°C	MAX. POWER LOSS	PRE-ARCING (2) I^2t	TOTAL I^2t (2) at 120 V_{RMS}	TOTAL I^2t (L) at 240 V_{RMS}	NOTES
	A	A	W	kA^2s	kA^2s	kA^2s	
TT350–400	400	350	60	8	35	80	1) Maximum current carrying ability, natural convection cooling using test arrangement as BS88: Part 4: 1976.
TT350–500	500	430	64	19	80	170	
TT350–600	630	540	75	35	150	300	
TT350–700	710	580	77	50	200	420	
TT350–800	800	660	82	70	300	650	2) Typical values of I^2t at 20 times rated RMS Current.
TT350–900	900	740	97	100	400	850	



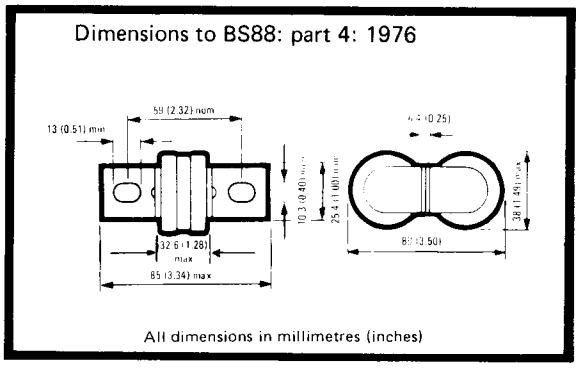


Figure 15-26 (*continued*)

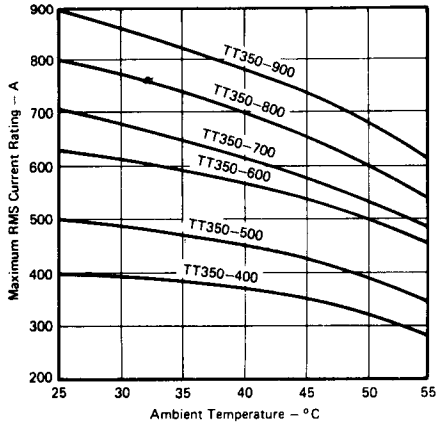


Fig. 1 – Current Rating Characteristic

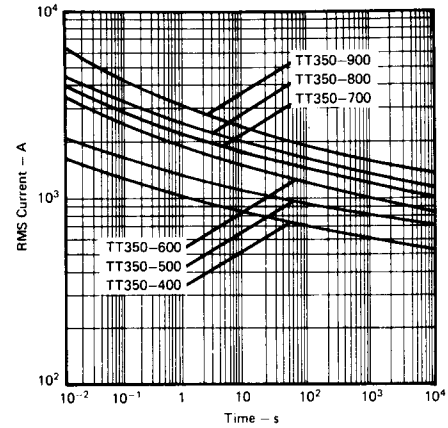


Fig. 2 – Time Current Characteristic

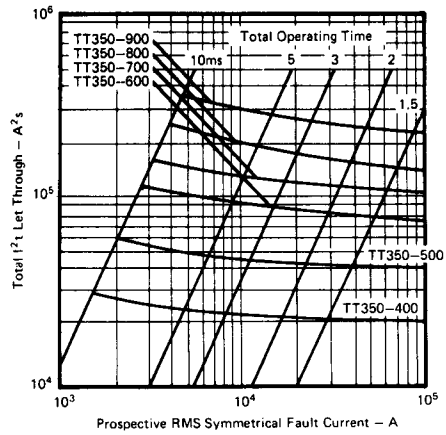


Fig. 3 – I^2t Let Through Characteristic (60V~)

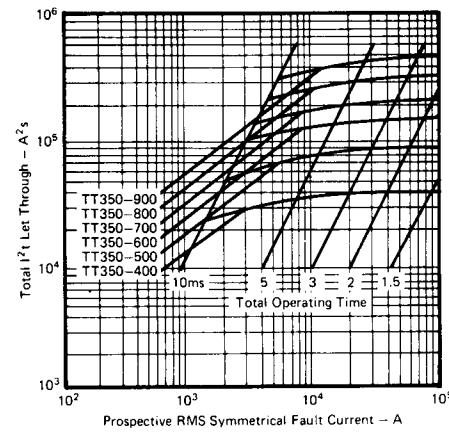


Fig. 4 – I^2t Let Through Characteristic (120V~)

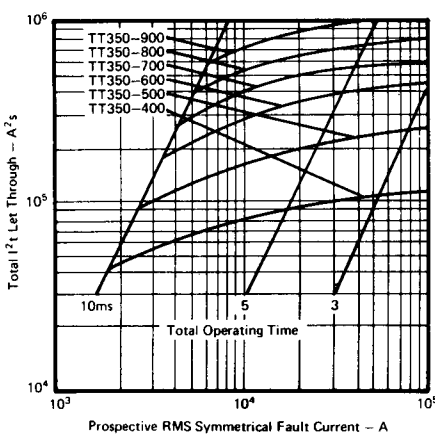


Fig. 5 – I^2t Let Through Characteristics (240V~)

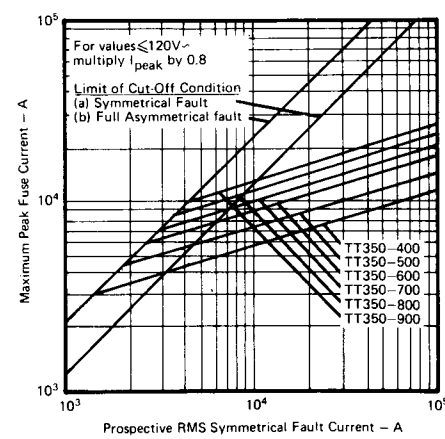


Fig. 6 – Cut-Off Characteristics (240V~)

Figure 15-26 (*continued*)

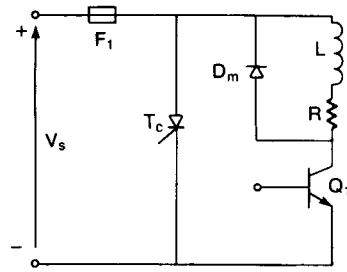


Figure 15-27 Protection by crowbar circuit.

In some applications it may be necessary to add a series inductance to limit the *di/dt* of the fault current and to avoid excessive *di/dt* stress on the device and fuse. However, this inductance may affect the normal performance of the converter.

Thyristors have more overcurrent capability than that of transistors. As a result, it is more difficult to protect transistors than thyristors. Bipolar transistors are gain-dependent and current-control devices. The maximum collector current is dependent on its base current. As the fault current rises, the transistor may go out of saturation and the collector–emitter voltage will rise with the fault current, particularly if the base current is not changed to cope with the increased collector current. This secondary effect may cause higher power loss within the transistor due to the rising collector–emitter voltage and may damage the transistor, even though the fault current is not sufficient enough to melt the fuse and clear the fault current. Thus fast-acting fuses may not be appropriate in protecting bipolar transistors under fault conditions.

Transistors can be protected by a crowbar circuit as shown in Fig. 15-27. A crowbar is used for protecting circuits or equipment under fault conditions, where the amount of energy involved is too high and the normal protection circuits cannot be used. A crowbar consists of a thyristor with a voltage- or current-sensitive firing circuit. The crowbar thyristor is placed across the converter circuit to be protected. If the fault conditions are sensed and crowbar thyristor T_c is fired, a virtual short circuit is created and the fuse link, F_1, is blown, thereby relieving the converter from overcurrent.

MOSFETS are voltage control devices; and as the fault current rises, the gate voltage needs not be changed. The peak current is typically three times the continuous rating. If the peak current is not exceeded and the fuse clears quickly enough, a fast-acting fuse may protect a MOSFET. However, a crowbar protection is also recommended.

15-7.2 Fault Current with AC Source

An ac circuit is shown in Fig. 15-28, where the input voltage is $v = V_m \sin \omega t$. If the switch SW is closed at $\omega t = \theta$, Eq. (6-15) gives the current as

$$i = \frac{V_m}{Z} \sin (\omega t + \theta - \phi) - \frac{V_m}{Z} sin (\theta - \phi) e^{-Rt/L} \qquad (15\text{-}47)$$

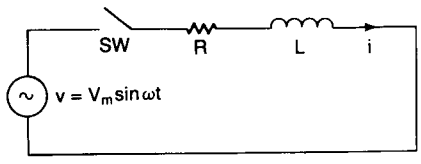


Figure 15-28 *RL* circuit

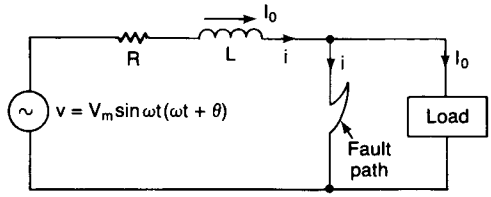


Figure 15-29 Fault in ac circuit.

where $\phi = \tan^{-1}(\omega L/R)$. Figure 15-28 describes the initial current at the beginning of the fault. If there is a fault across the load as shown in Fig. 15-29, Eq. (15-47), which can be applied with an initial current of I_0 at the beginning of the fault, gives the fault current as

$$i = \frac{V_m}{Z}\sin(\omega t + \theta - \phi) + \left(I_0 - \frac{V_m}{Z}\right)\sin(\theta - \phi)e^{-Rt/L} \qquad (15\text{-}48)$$

The fault current will depend on the initial current I_0, power factor of the short-circuit path, ϕ, and angle of fault occurring, θ. Figure 15-30 shows the current and voltage waveforms during the fault conditions in an ac circuit. For a highly inductive fault path, $\phi = 90°$ and $e^{-Rt/L} = 1$, and Eq. (15-48) become

$$i = -I_0\cos\theta + \frac{V_m}{Z}[\cos\theta - \cos(\omega t + \theta)] \qquad (15\text{-}49)$$

If the fault occurs at $\theta = 0$, Eq. (15-49) becomes

$$i = -I_0 + \frac{V_m}{Z}(1 - \cos\omega t) \qquad (15\text{-}50)$$

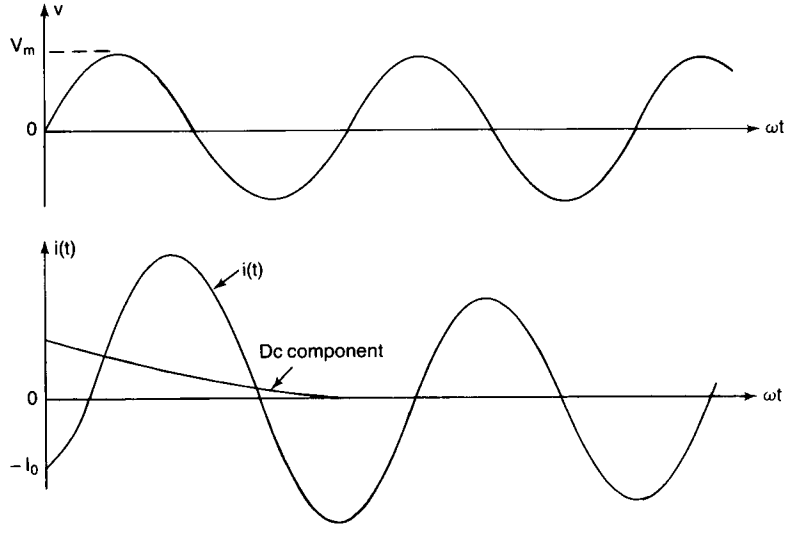


Figure 15-30 Transient voltage and current waveforms.

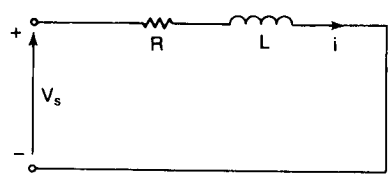


Figure 15-31 Dc circuit.

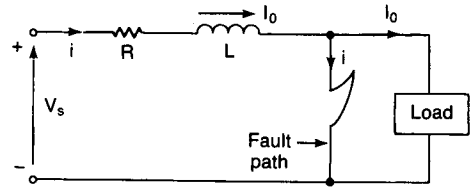


Figure 15-32 Fault in dc circuit.

and Eq. (15-50) gives the maximum peak fault current, $-I_0 + 2V_m/Z$, which occurs $\omega t = \pi$. But in practice, due to damping the peak current will be less than this.

15-7.3 Fault Current with DC Source

The current of a dc circuit in Fig. 15-31 is given by

$$i = \frac{V_s}{R}(1 - e^{-Rt/L}) \tag{15-51}$$

With an initial current of I_0 at the beginning of the fault current as shown in Fig. 15-32, the fault current is expressed as

$$i = I_0 e^{-Rt/L} + \frac{V_s}{R}(1 - e^{-Rt/L}) \tag{15-52}$$

The fault current and the fuse clearing time will be dependent on the time constant of the fault circuit. If the prospective current is low, the fuse may not clear the fault and a slowly rising fault current may produce arcs continuously without breaking the fault current. The fuse manufacturers specify the current–time characteristics for ac circuits and there is no equivalent curves for dc circuits. Since the dc fault currents do not have natural periodic zeros, the extinction of the arc is more difficult. For circuits operating from dc voltage, the voltage rating of the fuse should be typically 1.5 times the equivalent ac rms voltage. The fuse protection of dc circuits requires careful design than that of ac circuits.

Example 15-5

A fuse is connected in series with each IR thyristor of type S30EF in the single-phase full converter as shown in Fig. 4-3a. The input voltage is 208 V, 60 Hz, and the average current of each thyristor is I_a = 400 A. The ratings of thyristors are $I_{T(AV)}$ = 540 A, $I_{T(RMS)}$ = 850 A, I^2t = 300 kA^2s at 8.33 ms, $I^2\sqrt{t}$ = 4650 $kA^2\sqrt{s}$, and I_{TSM} = 10 kA with reapplied V_{RRM} = 0, which will be the case if the fuse opens within a half-cycle. If the resistance of fault circuit is negligible and inductance is L = 0.07 mH, select the rating of a suitable fuse from Fig. 15-26.

Solution V_s = 240 V, f_s = 60 Hz. Let us try an IR fuse, type TT350-600. The short circuit current which is also known as the prospective rms symmetrical fault current is

$$I_{sc} = \frac{V_s}{Z} = 240 \times \frac{1000}{2\pi \times 60 \times 0.07} = 9095 \text{ A}$$

For the 540-A fuse type TT350-600 and I_{sc} = 9095 A, Fig. 15-26.6 gives the maximum peak fuse current of 8500 A, which is less than the peak thyristor current of I_{TSM} = 10 kA. Figure 15-26.5 gives the fuse I^2t of 280 kA^2s and total clearing time of t_c = 8 ms. Since t_c is less than 8.33 ms, the $I^2\sqrt{t}$ rating of the thyristor must be used. If thyristor $I^2\sqrt{t}$ = 4650 × 10^3 $kA^2\sqrt{s}$, then at t_c = 8 ms, thyristor I^2t = 4650 × 10^3 $\sqrt{0.008}$ = 416 kA^2s, which is 48.6% higher than the I^2t rating of the fuse. The I^2t and peak surge current ratings of the thyristor are higher than those of the fuse. Thus the thyristor should be protected by the fuse.

Note. As a general rule of thumb, a fast-acting fuse with a rms current rating equal or less than the average current rating of the thyristor or diode will normally provide adequate protection under fault conditions.

SUMMARY

The power converters must be protected from overcurrents and overvoltages. The junction temperature of power semiconductor devices must be maintained within their maximum permissible values. The heat produced by the device may be transferred to the heat sinks by air and liquid cooling. Heat pipes can also be used. The reverse recovery currents and disconnection of load (and supply line) cause voltage transients due to energy stored in the line inductances.

The voltage transients are normally suppressed by the same *RC*-snubber circuit, which is used for *dv/dt* protection. The snubber design is very important to limit the *dv/dt* and peak voltage transients within the maximum ratings. Selenium diodes and varistors can be used for transient voltage suppression.

A fast-acting fuse is normally connected in series with each device for overcurrent protection under fault conditions. However, fuses may not be adequate for protecting transistors and other protection means, (e.g., a crowbar) may be required.

REFERENCES

1. W. McMurray, "Optimum snubbers for power semiconductors." *IEEE Transactions on Industry Applications*, Vol. IA8, No. 5, 1972, pp. 503–510.
2. W. McMurray, "Selection of snubber and clamps to optimize the design of transistor switching converters." *IEEE Transactions on Industry Applications*, Vol. IA16, No. 4, 1980, pp. 513–523.
3. J. B. Rice, "Design of snubber circuits for thyristor converters." *IEEE Industry General Applications Conference Record*, 1969, pp. 485–489.
4. T. Undeland, "A snubber configuration for both power transistors and GTO PWM inverter." *IEEE Power Electronics Specialist Conference*, 1984, pp. 42–53.
5. C. G. Steyn and J. D. V. Wyk, "Study and application of non-linear turn-off snubber for power electronics switches." *IEEE Transactions on Industry Applications*, Vol. IA22, No. 3, 1986, pp. 471–477.

6. A. Wright and P. G. Newbery, *Electric Fuses*. London: Peter Peregrinus Ltd., 1984.
7. A. F. Howe, P. G. Newbery, and N. P. Nurse, "Dc fusing in semiconductor circuits." *IEEE Transactions on Industry Applications*, Vol. IA22, No. 3, 1986, pp. 483–489.
8. International Rectifiers, *Semiconductor Fuse Applications Handbook* (No. HB50). El Segundo, Calif.: International Rectifiers, 1972.

REVIEW QUESTIONS

15-1. What is a heat sink?
15-2. What is the electrical analog of heat transfer from a power semiconductor device?
15-3. What are the precautions to be taken in mounting a device on a heat sink?
15-4. What is a heat pipe?
15-5. What are the advantages and disadvantages of heat pipes?
15-6. What are the advantages and disadvantages of water cooling?
15-7. What are the advantages and disadvantages of oil cooling?
15-8. Why is it necessary to determine the instantaneous junction temperature of a device?
15-9. What is a polarized snubber?
15-10. What is a nonpolarized snubber?
15-11. What is the cause of reverse recovery transient voltage?
15-12. What is the typical value of damping factor for *RC* snubber?
15-13. What are the considerations for the design of optimum *RC*-snubber components?
15-14. What is the cause of load-side transient voltages?
15-15. What is the cause of supply-side transient voltages?
15-16. What are the characteristics of selenium diodes?
15-17. What are the advantages and disadvantages of selenium voltage suppressers?
15-18. What are the characteristics of varistors?
15-19. What are the advantages and disadvantages of varistors in voltage supressions?
15-20. What is a melting time of a fuse?
15-21. What is an arcing time of a fuse?
15-22. What is a clearing time of a fuse?
15-23. What is a prospective fault current?
15-24. What are the considerations in selecting a fuse for a semiconductor device?
15-25. What is a crowbar?
15-26. What are the problems of protecting bipolar transistors by fuses?
15-27. What are the problems of fusing dc circuits?

PROBLEMS

15-1. The power loss in an IR thyristor, type S30EE, is shown in Fig. P15-1. Plot the instantaneous junction temperature rise above case.

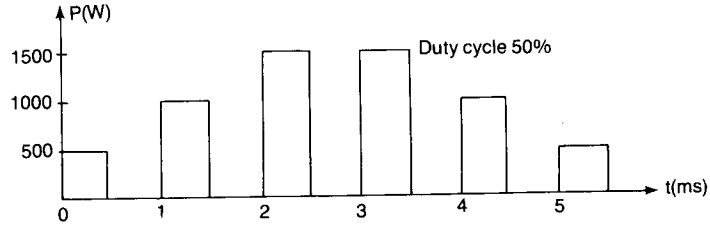


Figure P15-1

15-2. The power loss in an IR thyristor, type S30EF, is shown in Fig. P15-2. Plot the instantaneous junction temperature rise above the case temperature. (*Hint:* Approximate by five rectangular pulses of equal duration.)

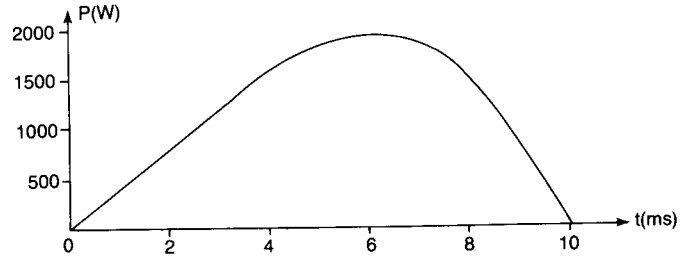


Figure P15-2

15-3. The current waveform through an IR thyristor, type S30EF, is shown in Fig. 14-20. Plot the **(a)** power loss against time, and **(b)** instantaneous junction temperature rise above case. (*Hint:* Assume power loss during turn-on and turn-off as rectangles.)

15-4. The recovery current of a device as shown in Fig. 15-12 is $I_R = 30$ A and the circuit inductance is $L = 20$ μH. The input voltage is $V_s = 200$ V. If it is necessary to limit the peak transient voltage to 1.8 times the input voltage, determine the **(a)** optimum value of current ratio, d_o; **(b)** optimum damping factor, δ_o; **(c)** snubber capacitance, C; **(d)** snubber resistance, R; **(e)** average dv/dt; and **(f)** initial reverse voltage.

15-5. The recovery current of a device as shown in Fig. 15-12 is $I_R = 10$ A and the circuit inductance is $L = 80$ μH. The input voltage is $V_s = 200$ V. The snubber resistance is $R = 2\ \Omega$ and snubber capacitance is $C = 50$ μF. Determine the **(a)** damping ratio, δ; **(b)** peak transient voltage, V_p; **(c)** current ratio, d; **(d)** average dv/dt; and **(e)** initial reverse voltage.

15-6. An *RC*-snubber circuit as shown in Fig. 15-11c has $C = 1.5$ μF, $R = 4.5\ \Omega$, and the input voltage is $V_s = 220$ V. The circuit inductance is $L = 20$ μH. Determine the **(a)** peak forward voltage, V_p; **(b)** initial dv/dt; and **(c)** maximum dv/dt.

15-7. An *RC*-snubber circuit as shown in Fig. 15-11c has a circuit inductance of $L = 20$ μH. The input voltage, $V_s = 200$ V. If it is necessary to limit the maximum dv/dt to 20 V/μs and damping factor is $\delta = 0.4$, determine the **(a)** snubber capacitance, C; and **(b)** snubber resistance, R.

15-8. An *RC*-snubber circuit as shown in Fig. 15-11c has circuit inductance of $L = 50$ μH. The input voltage, $V_s = 220$ V. If it is necessary to limit the peak voltage to 1.5

times the input voltage, and the damping factor, $\alpha = 9500$, determine the **(a)** snubber capacitance, C; and **(b)** snubber resistance, R.

15-9. A capacitor is connected to the secondary of an input transformer as shown in Fig. 15-16a, with zero damping resistance. The secondary voltage, $V_s = 208$ V, 60 Hz, and the magnetizing inductance referred to the secondary is $L_m = 3.5$ mH. If the input supply to the transformer primary is disconnected at an angle of $\theta = 120°$ of the input ac voltage, determine the **(a)** initial capacitor value, V_0; **(b)** magnetizing current, I_0; and **(c)** capacitor value to limit the maximum transient capacitor voltage to $V_p = 350$ V.

15-10. The circuit in Fig. 15-18 has a load current of $I_L = 10$ A and the circuit inductance is $L = 50$ μH. The input voltage is dc with $V_s = 200$ V. The snubber resistance is $R = 1.5$ Ω and snubber capacitance is $C = 50$ μF. If the load is disconnected, determine the **(a)** damping factor, δ; and **(b)** peak transient voltage, V_p.

15-11. Selenium diodes are used to protect a three-phase circuit as shown in Fig. 15-20c. The three-phase voltage is 208 V, 60 Hz. If the voltage of each cell is 25 V, determine the number of diodes.

15-12. The load current at the beginning of a fault in Fig. 15-29 is $I_0 = 10$ A. The ac voltage is 208 V, 60 Hz. The resistance and inductance of the fault circuit are $L = 5$ mH and $R = 1.5$ Ω, respectively. If the fault occurs at an angle of $\theta = 45°$, determine the peak value of prospective current in the first half-cycle.

15-13. Repeat Prob. 15-12 if $R = 0$.

15-14. The current through a fuse is shown in Fig. P15-14. The total i^2t of the fuse is 5400 A^2s. If the arcing time, $t_a = 0.1$ s and the melting time, $t_m = 0.05$ s, determine the peak let-through current, I_p.

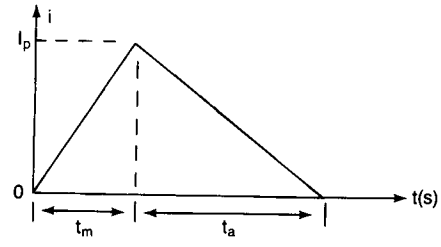


Figure P15-14

15-15. The load current in Fig. 15-32 is $I_0 = 0$ A. The dc input voltage is $V_s = 220$ V. The fault circuit has an inductance of $L = 2$ mH and negligible resistance. The total i^2t of the fuse is 4500 A^2s. The arcing time is 1.5 times the melting time. Determine the **(a)** melting time, t_m; **(b)** clearing time, t_c; and **(c)** peak let-through current, I_p.

A

Three-Phase Circuits

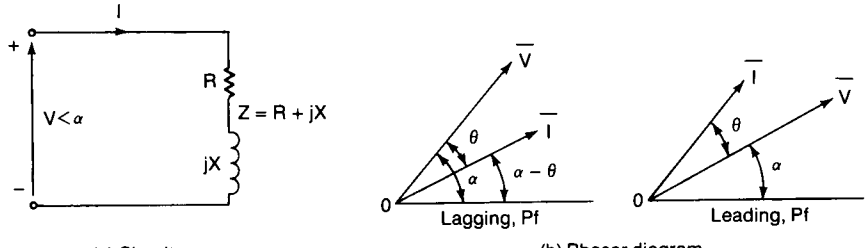
In a single-phase circuit as shown in Fig. A-1a, the current is expressed as

$$\bar{\mathrm{I}} = \frac{V\angle\alpha}{\mathrm{R} + \mathrm{jX}} = \frac{\mathrm{V}\angle\alpha - \theta}{Z} \tag{A-1}$$

where $Z = (R^2 + X^2)^{1/2}$ and $\theta = \tan^{-1}(X/R)$. The power can be found from

$$P = VI \cos\theta \tag{A-2}$$

where cos θ is called the *power factor*, and θ, which is the angle of the load impedance, is known as the *power factor angle*.



(a) Circuit

(b) Phasor diagram

Figure A-1 Single-phase circuit.

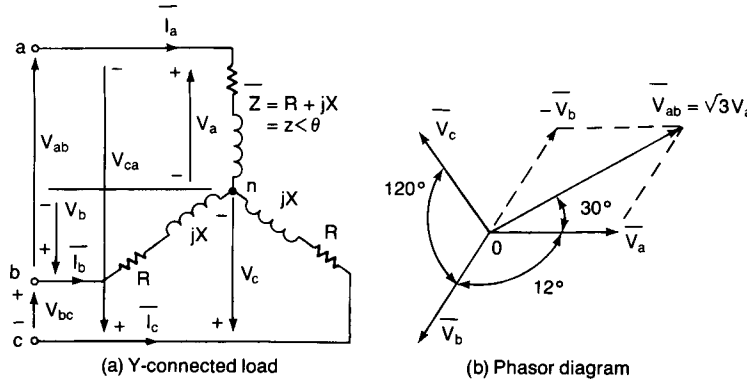


Figure A-2 Y-connected three-phase circuit.

A three-phase circuit consists of three sinusoidal voltages of equal magnitudes and the phase angles between the individual voltages are 120°. A Y-connected load connected to a three-phase source is shown in Fig. A-2a. If the three phase voltages are

$$\bar{\mathbf{V}}_a = V_p \angle 0$$

$$\bar{\mathbf{V}}_b = V_p \angle -120°$$

$$\bar{\mathbf{V}}_c = V_p \angle -240°$$

the line-to-line voltages are

$$\bar{\mathbf{V}}_{ab} = \bar{\mathbf{V}}_a - \bar{\mathbf{V}}_b = \sqrt{3}\, V_p \angle 30° = V_L \angle 30°$$

$$\bar{\mathbf{V}}_{bc} = \bar{\mathbf{V}}_b - \bar{\mathbf{V}}_c = \sqrt{3}\, V_p \angle -90° = V_L \angle -90°$$

$$\bar{\mathbf{V}}_{ca} = \bar{\mathbf{V}}_c - \bar{\mathbf{V}}_a = \sqrt{3}\, V_p \angle -210° = V_L \angle -210°$$

Thus a line-to-line voltage, V_L, is $\sqrt{3}$ times of a phase voltage, V_p. The three line currents, which are the same as phase currents, are

$$\bar{\mathbf{I}}_a = \frac{\bar{\mathbf{V}}_a}{Z_a \angle \theta_a} = \frac{V_p}{Z_a} \angle -\theta_a$$

$$\bar{\mathbf{I}}_b = \frac{\bar{\mathbf{V}}_b}{Z_b \angle \theta_b} = \frac{V_p}{Z_b} \angle -120° - \theta_b$$

$$\bar{\mathbf{I}}_c = \frac{\bar{\mathbf{V}}_c}{Z_c \angle \theta_c} = \frac{V_p}{Z_c} \angle -240° - \theta_c$$

The input power to the load is

$$P = V_a I_a \cos\theta_a + V_b I_b \cos\theta_b + V_c I_c \cos\theta_c \qquad \text{(A-3)}$$

For a balanced supply, $V_a = V_b = V_c = V_p$, Eq. (A-3) becomes

$$P = V_p(I_a \cos\theta_a + I_b \cos\theta_b + I_c \cos\theta_c) \qquad \text{(A-4)}$$

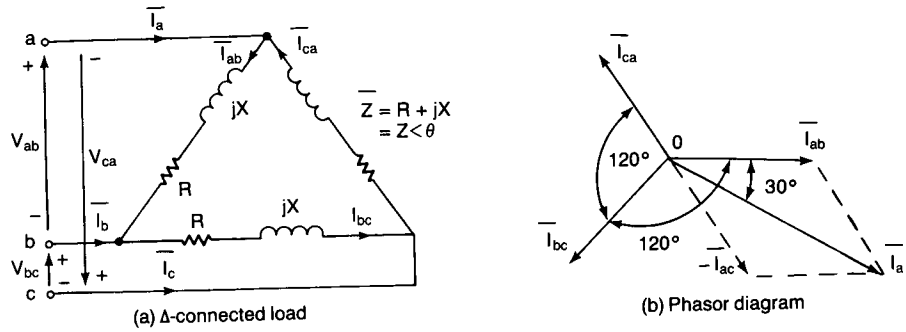


Figure A-3 Delta-connected load.

For a balanced load, $Z_a = Z_b = Z_c = Z$, $\theta_a = \theta_b = \theta_c = \theta$, and $I_a = I_b = I_c = I_p = I_L$, Eq. (A-4) becomes

$$P = 3V_pI_p \cos\theta$$

$$= 3\frac{V_L}{\sqrt{3}} I_L \cos\theta = \sqrt{3}V_LI_L \cos\theta \tag{A-5}$$

A Δ-connected load is shown in Fig. A-3a, where the line voltages are the same as the phase voltages. If the three phase voltages are

$$\bar{\mathbf{V}}_a = \bar{\mathbf{V}}_{ab} = V_L \angle 0 = V_p \angle 0$$

$$\bar{\mathbf{V}}_b = \bar{\mathbf{V}}_{bc} = V_L \angle -120° = V_p \angle -120°$$

$$\bar{\mathbf{V}}_c = \bar{\mathbf{V}}_{ca} = V_L \angle -240° = V_p \angle -240°$$

the three phase-currents are:

$$\bar{\mathbf{I}}_{ab} = \frac{\bar{\mathbf{V}}_a}{Z_a \angle \theta_a} = \frac{V_L}{Z_a} \angle -\theta_a = I_p \angle -\theta_a$$

$$\bar{\mathbf{I}}_{bc} = \frac{\bar{\mathbf{V}}_b}{Z_b \angle \theta_b} = \frac{V_L}{Z_b} \angle -120° - \theta_b = I_p \angle -120° - \theta_b$$

$$\bar{\mathbf{I}}_{ca} = \frac{\bar{\mathbf{V}}_c}{Z_c \angle \theta_c} = \frac{V_L}{Z_c} \angle -240° - \theta_c = I_p \angle -240° - \theta_c$$

and the three line currents are

$$\bar{\mathbf{I}}_a = \bar{\mathbf{I}}_{ab} - \bar{\mathbf{I}}_{ca} = \sqrt{3}\, I_p \angle -30° - \theta_a = I_L \angle -30° - \theta_a$$

$$\bar{\mathbf{I}}_b = \bar{\mathbf{I}}_{bc} - \bar{\mathbf{I}}_{ab} = \sqrt{3}\, I_p \angle -150° - \theta_b = I_L \angle -150° - \theta_b$$

$$\bar{\mathbf{I}}_c = \bar{\mathbf{I}}_{ca} - \bar{\mathbf{I}}_{bc} = \sqrt{3}\, I_p \angle -270° - \theta_c = I_L \angle -270° - \theta_c$$

Therefore, in a Δ-connected load, a line current is $\sqrt{3}$ times of a phase current.

The input power to the load is

$$P = V_{ab}I_{ab} \cos \theta_a + V_{bc}I_{bc} \cos \theta_b + V_{ca}I_{ca} \cos \theta_c \tag{A-6}$$

For a balanced supply, $V_{ab} = V_{bc} = V_{ca} = V_L$, Eq. (A-6) becomes

$$P = V_L(I_{ab} \cos \theta_a + I_{bc} \cos \theta_b + I_{ca} \cos \theta_c) \tag{A-7}$$

For a balanced load, $Z_a = Z_b = Z_c = Z$, $\theta_a = \theta_b = \theta_c = \theta$, and $I_{ab} = I_{bc} = I_{ca} = I_p$, Eq. (A-7) becomes

$$\begin{aligned} P &= 3V_pI_p \cos \theta \\ &= 3V_L \frac{I_L}{\sqrt{3}} \cos \theta = \sqrt{3}\, V_LI_L \cos \theta \end{aligned} \tag{A-8}$$

Note. Equations (A-5) and (A-8), which express power in a three-phase circuit, are the same. For the same phase voltages, the line currents in a Δ-connected load are $\sqrt{3}$ times that of Y-connected load.

B

Magnetic Circuits

A magnetic ring is shown in Fig. B-1. If the magnetic field is uniform and normal to the area under consideration, a magnetic circuit is characterized by the following equations:

$$\phi = BA \tag{B-1}$$

$$B = \mu H \tag{B-2}$$

$$\mu = \mu_r \mu_0 \tag{B-3}$$

$$\mathcal{F} = NI = Hl \tag{B-4}$$

where ϕ = flux, webers
B = flux density, webers/m^2 (or teslas)
H = magnetizing force, ampere-turns/meter
μ = permeability of the magnetic material
μ_0 = permeability of the air ($= 4\pi \times 10^{-7}$)
μ_r = relative permeability of the material
$\mathcal{F}$ = magnetomotive force, ampere-turns (At)
N = number of turns in the winding
I = current through the winding, amperes
l = length of the magnetic circuit, meters

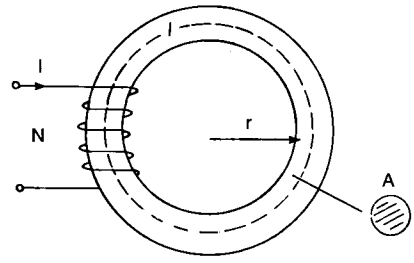


Figure B-1 Magnetic ring.

If the magnetic circuit consists of different sections, Eq. (B-4) becomes

$$\mathcal{F} = NI = \Sigma H_i l_i \tag{B-5}$$

where H_i and l_i are the magnetizing force and length of ith section respectively.

The reluctance of a magnetic circuit is related to the magnetomotive force and flux by

$$\mathcal{R} = \frac{\mathcal{F}}{\phi} = \frac{NI}{\phi} \tag{B-6}$$

and $\mathcal{R}$ depends on the type and dimensions of the core,

$$\mathcal{R} = \frac{l}{\mu_r \mu_0 A} \tag{B-7}$$

The permeability depends on the B–H characteristic and is normally much larger than that of the air. A typical B–H characteristic which is nonlinear is shown in Fig. B-2. For a large value of μ, $\mathcal{R}$ becomes very small, resulting in high value of flux. An air gap is normally introduced to limit the amount of flux.

A magnetic circuit with an air gap is shown in Fig. B-3a and the analogous electric circuit is shown in Fig. B-3b. The reluctance of the air gap is

$$\mathcal{R}_g = \frac{l_g}{\mu_0 A_g} \tag{B-8}$$

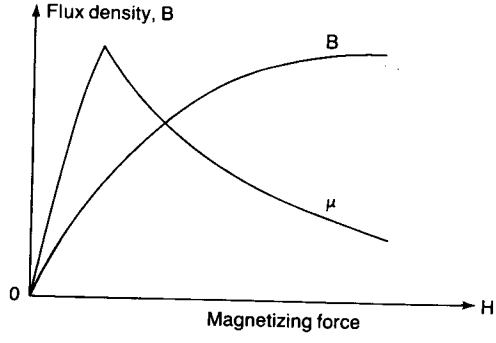


Figure B-2 Typical B–H characteristic.

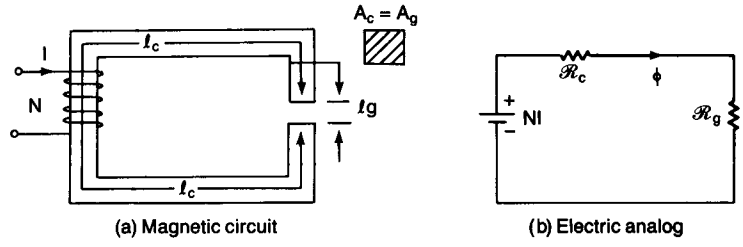


Figure B-3 Magnetic circuit with air gap.

and the reluctance of the core is

$$\mathcal{R}_c = \frac{l_c}{\mu_r \mu_0 A_c} \tag{B-9}$$

where l_g = length of the air gap
l_c = length of the core
A_g = area of the cross section of the air gap
A_c = area of the cross section of the core

The total reluctance of the magnetic circuit is

$$\mathcal{R} = \mathcal{R}_g + \mathcal{R}_c$$

Inductance is defined as the flux linkage (λ) per ampere,

$$L = \frac{\lambda}{I} = \frac{N\phi}{I} \tag{B-10}$$

$$= \frac{N^2\phi}{NI} = \frac{N^2}{\mathcal{R}} \tag{B-11}$$

Example B-1

The parameters of the core in Fig. B-3a are $l_g = 1$ mm, $l_c = 30$ cm, $A_g = A_c = 5 \times 10^{-3}$ m^2, $N = 350$, and $I = 2$ A. Calculate the inductance if (a) $\mu_r = 3500$, and (b) the core is ideal, namely μ_r is very large tending to infinite.

Solution $\mu_0 = 4\pi \times 10^{-7}$ and $N = 350$.
(a) From Eq. (B-8),

$$\mathcal{R}_g = \frac{1 \times 10^{-3}}{4\pi \times 10^{-7} \times 5 \times 10^{-3}} = 159{,}155$$

From Eq. (B-9),

$$\mathcal{R}_c = \frac{30 \times 10^{-2}}{3500 \times 4\pi \times 10^{-7} \times 5 \times 10^{-3}} = 13{,}641$$

$$\mathcal{R} = 159{,}155 + 13{,}641 = 172{,}796$$

From Eq. (B-11), $L = 350^2/172{,}796 = 0.71$ H.
(b) If $\mu \approx \infty$, $\mathcal{R}_c = 0$ and $\mathcal{R} = \mathcal{R}_g = 159{,}155$, $L = 350^2/159{,}155 = 0.77$ H.

B-1 SINUSOIDAL EXCITATION

If a sinusoidal voltage of $v = V_m \sin \omega t = \sqrt{2}\, V_s \sin \omega t$, is applied to the core in Fig. B-3a, the flux can be found from

$$V_m \sin \omega t = -N \frac{d\phi}{dt} \tag{B-12}$$

or

$$\phi = \phi_m \cos \omega t = \frac{V_m}{N\omega} \cos \omega t \tag{B-13}$$

Thus

$$\phi_m = \frac{V_m}{2\pi f N} = \frac{\sqrt{2}\, V_s}{2\pi f N} = \frac{V_s}{4.44 f N} \tag{B-14}$$

The peak flux, ϕ_m, depends on the voltage, frequency, and the number of turns. Equation (B-14) is valid if the core is not saturated. If peak flux is high, the core may saturated and the flux will not be sinusoidal. If the ratio of voltage to frequency is maintained constant, the flux will remain constant, provided that the number of turns is unchanged.

B-2 TRANSFORMER

If a second winding, called the *secondary winding*, is added to the core in Fig. B-3 and the core is excited from sinusoidal voltage, a voltage will be induced in secondary winding. This is shown in Fig. B-4. If N_p and N_s are turns on the primary and secondary windings, respectively, the primary voltage, V_p, and secondary voltage, V_s, are related to each other as

$$\frac{V_p}{V_s} = \frac{I_s}{I_p} = \frac{N_p}{N_s} = a \tag{B-15}$$

where a is the turns ratio.

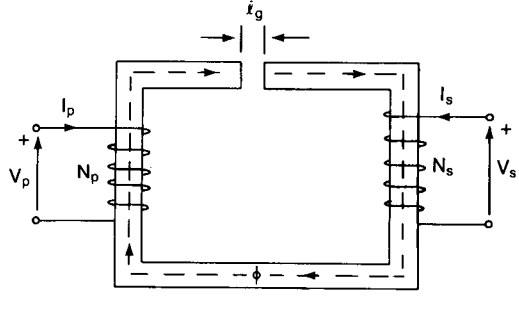


Figure B-4 Transformer core.

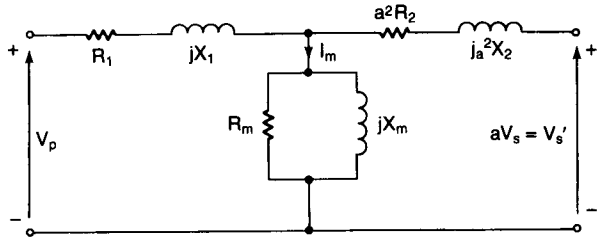


Figure B-5 Equivalent circuit of transformer.

The equivalent circuit of a transformer is shown in Fig. B-5, where all the parameters are referred to the primary. To refer a secondary parameter to the primary side, the parameter is multiplied by a^2. The equivalent circuit can be referred to the secondary side by dividing all parameters of the circuit in Fig. B-5 with a^2. X_1 and X_2 are the leakage reactances of the primary and secondary windings, respectively. R_1 and R_2 are the resistances of the primary and secondary winding, X_m is the magnetizing reactance, and R_m represents the core loss.

The variations of the flux due to ac excitation cause two types of losses in the core: (a) hysteresis loss, and (2) eddy-current loss. The hysteresis loss is expressed empirically as

$$P_h = K_h f B_{\max}^z \tag{B-16}$$

where K_h is a hysteresis constant which depends on the material and $B_{\max}$ is the peak value of flux density. z is the Steinmetz constant, which has a value of 1.6 to 2. The eddy-current loss is expressed empirically as

$$P_e = K_e f^2 B_{\max}^2 \tag{B-17}$$

where K_e is the eddy-current constant and depends on the material. The total core loss is

$$P_c = K_h f B_{\max}^z + K_e f^2 B_{\max}^2 \tag{B-18}$$

Note. If a transformer is designed to operate at 60 Hz and it is operated at a higher frequency, the core loss will increase significantly.

C

Switching Functions of Converters

The output of a converter depends on the switching pattern of the converter switches and the input voltage (or current). Similar to linear system, the output quantities of a converter can be expressed in terms of the input quantities, by spectrum multiplication. The arrangement of a single-phase converter is shown in Fig. C-1a. If $V_i(\theta)$ and $I_i(\theta)$ are the input voltage and current, respectively, the corresponding output voltage and current are $V_o(\theta)$ and $I_o(\theta)$, respectively. The input could be either a voltage source or a current source.

Voltage source. For a voltage source, the output voltage $V_o(\theta)$ can be related to input voltage $V_i(\theta)$ by

$$V_o(\theta) = S(\theta)V_i(\theta) \tag{C-1}$$

where $S(\theta)$ is the switching function of the converter as shown in Fig. C-1b. $S(\theta)$ depends on the type of converter and the gating pattern of the switches. If g_1, g_2, g_3, and g_4 are the gating signals for switches Q_1, Q_2, Q_3, and Q_4, respectively, the switching function is

$$S(\theta) = g_1 - g_4 = g_3 - g_2$$

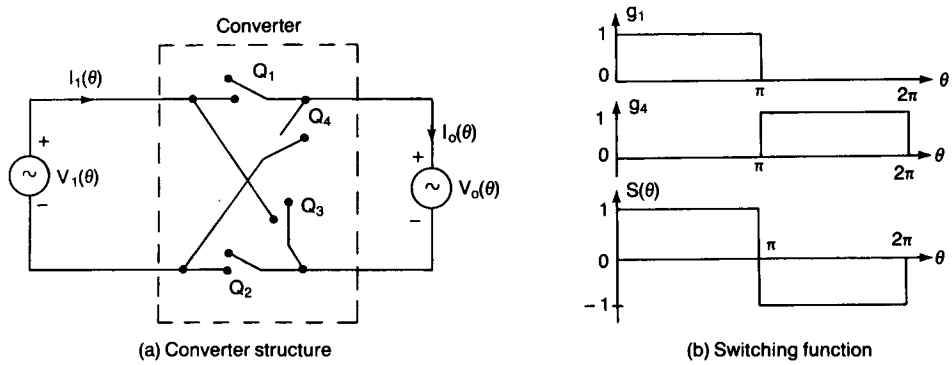


Figure C-1 Single-phase converter structure.

Neglecting the losses in the converter switches gives us

$$V_i(\theta)I_i(\theta) = V_o(\theta)I_o(\theta)$$

$$S(\theta) = \frac{V_o(\theta)}{V_i(\theta)} = \frac{I_i(\theta)}{I_o(\theta)} \tag{C-2}$$

$$I_i(\theta) = S(\theta)I_o(\theta) \tag{C-3}$$

Once $S(\theta)$ is known, $V_o(\theta)$ can be determined. $V_o(\theta)$ divided by the load impedance, gives $I_o(\theta)$; and $I_i(\theta)$ can be found from Eq. (C-3).

Current source. In the case of current source, the input current remains constant, $I_i(\theta) = I_i$ and the output current $I_o(\theta)$ can be related to input current I_i,

$$\begin{aligned} I_o(\theta) &= S(\theta)I_i \\ V_o(\theta)I_o(\theta) &= V_i(\theta)I_i(\theta) \end{aligned} \tag{C-4}$$

which gives

$$V_i(\theta) = S(\theta)V_o(\theta) \tag{C-5}$$

$$S(\theta) = \frac{V_i(\theta)}{V_o(\theta)} = \frac{I_o(\theta)}{I_i(\theta)} \tag{C-6}$$

C-1 SINGLE-PHASE FULL-BRIDGE INVERTERS

The switching function of a single-phase full-bridge inverter in Fig. 8-2a, is shown in Fig. C-2. If g_1 and g_4 are the gating signals for switches Q_1 and Q_4, respectively,

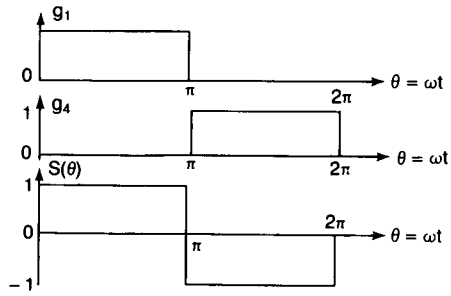


Figure C-2 Switching function of single-phase full-bridge inverter.

the switching function is

$$\begin{aligned} S(\theta) &= g_1 - g_4 \\ &= 1 \qquad \text{for } 0 \le \theta \le \pi \\ &= -1 \qquad \text{for } \pi \le \theta \le 2\pi \end{aligned}$$

If f_0 is the fundamental frequency of the inverter,

$$\theta = \omega t = 2\pi f_0 t \tag{C-7}$$

$S(\theta)$ can be expressed in a Fourier series as

$$\begin{aligned} S(\theta) &= \frac{A_0}{2} + \sum_{n=1,2,\ldots}^{\infty} (A_n \cos n\theta + B_n \sin n\theta) \\ B_n &= \frac{2}{\pi}\int_0^{\pi} S(\theta) \sin n\theta \, d\theta = \frac{4}{n\pi} \qquad \text{for } n = 1, 3, \ldots \end{aligned} \tag{C-8}$$

Due to half-wave symmetry, $A_0 = A_n = 0$.

Substituting A_0, A_n, and B_n in Eq. (C-8) yields

$$S(\theta) = \frac{4}{\pi} \sum_{n=1,3,5,\ldots}^{\infty} \frac{\sin n\theta}{n} \tag{C-9}$$

If the input voltage, which is dc, is $V_i(\theta) = V_s$, Eq. (C-1) gives the output voltage as

$$V_o(\theta) = S(\theta)V_i(\theta) = \frac{4V_s}{\pi} \sum_{n=1,3,5,\ldots}^{\infty} \frac{\sin n\theta}{n} \tag{C-10}$$

which is the same as Eq. (8-9). For a three phase voltage-source inverter in Fig. 8-5, there are three switching functions: $S_1(\theta) = g_1 - g_4$, $S_2(\theta) = g_3 - g_6$, and $S_3(\theta) = g_5 - g_2$. There will be three line-to-line output voltages corresponding to three switching voltages, namely $V_{ab}(\theta) = S_1(\theta)V_i(\theta)$, $V_{bc}(\theta) = S_2(\theta)V_i(\theta)$, and $V_{ca}(\theta) = S_3(\theta)V_i(\theta)$.

C-2 SINGLE-PHASE BRIDGE RECTIFIERS

The switching function of a single-phase bridge rectifier is the same as that of the single-phase full-bridge inverter. If the input voltage is $V_i(\theta) = V_m \sin \theta$, Eqs. (C-1) and (C-9) give the output voltage as

$$V_o(\theta) = S(\theta)V_i(\theta) = \frac{4V_m}{\pi} \sum_{n=1,3,5,\ldots}^{\infty} \frac{\sin \theta \sin n\theta}{n} \tag{C-11}$$

$$= \frac{4V_m}{\pi} \sum_{n=1,3,5,\ldots}^{\infty} \frac{\cos (n-1)\theta - \cos (n+1)\theta}{2n} \tag{C-12}$$

$$= \frac{2V_m}{\pi} \left[1 - \cos 2\theta + \frac{1}{3} \cos 2\theta - \frac{1}{3} \cos 4\theta + \frac{1}{5} \cos 4\theta - \frac{1}{5} \cos 6\theta + \frac{1}{7} \cos 6\theta - \frac{1}{7} \cos 8\theta + \cdots \right]$$

$$= \frac{2V_m}{\pi} \left[1 - \frac{2}{3} \cos 2\theta - \frac{2}{15} \cos 4\theta - \frac{2}{35} \cos 6\theta - \cdots \right]$$

$$= \frac{2V_m}{\pi} - \frac{4V_m}{\pi} \sum_{m=1}^{\infty} \frac{\cos 2m\theta}{4m^2 - 1} \tag{C-13}$$

Equation (C-13) is the same as Eq. (2-63). The first part of Eq. (C-13) is the average output voltage and the second part is the ripple constant on the output voltage.

For a three-phase rectifier in Figs. 2-18a and 4-9a, the switching functions are $S_1(\theta) = g_1 - g_4$, $S_2(\theta) = g_3 - g_6$, and $S_3(\theta) = g_5 - g_2$. If the three input phase voltages are $V_{an}(\theta)$, $V_{bn}(\theta)$, and $V_{cn}(\theta)$, the output voltage becomes

$$V_o(\theta) = S_1(\theta)V_{an}(\theta) + S_2(\theta)V_{bn}(\theta) + S_3(\theta)V_{cn}(\theta) \tag{C-14}$$

C-3 SINGLE-PHASE FULL-BRIDGE INVERTERS WITH SPWM

The switching function of a single-phase full-bridge inverter with sinusoidal pulse-width modulation (SPWM) is shown in Fig. C-3. The gating pulses are generated by comparing a cosine wave with triangular pulses. If g_1 and g_4 are the gating signals for switches Q_1 and Q_4, respectively, the switching function is

$$S(\theta) = g_1 - g_4$$

$S(\theta)$ can be expressed in a Fourier series as

$$S(\theta) = \frac{A_0}{2} + \sum_{n=1,2,\ldots}^{\infty} (A_n \cos n\theta + B_n \sin n\theta) \tag{C-15}$$

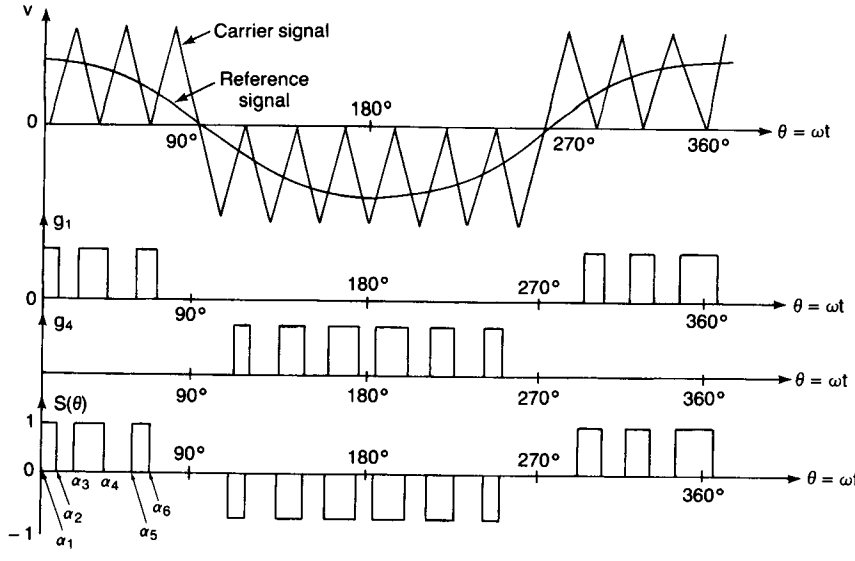


Figure C-3 Switching function with SPWM.

If there are p pulses per quarter cycle and p is an even number,

$$A_n = \frac{2}{\pi}\int_0^{\pi} S(\theta)\cos n\theta\, d\theta$$

$$= \frac{4}{\pi}\int_0^{\pi/2} S(\theta)\cos n\theta\, d\theta$$

$$= \frac{4}{\pi}\left[\int_{\alpha_1}^{\alpha_2}\cos n\theta\, d\theta + \int_{\alpha_3}^{\alpha_4}\cos n\theta\, d\theta + \int_{\alpha_5}^{\alpha_6}\cos n\theta\, d\theta + \cdots\right)$$

$$= \frac{4}{n\pi}\sum_{m=1,2,3,\ldots}^{p}[(-1)^m \sin n\alpha_m] \qquad \text{(C-16)}$$

Due to quarter-wave symmetry, $B_n = A_0 = 0$. Substituting A_0, A_n, and B_n in Eq. (C-15) yields

$$S(\theta) = \sum_{n=1,3,5,\ldots}^{\infty} A_n \cos n\theta$$

$$= \frac{4}{n\pi}\sum_{n=1,3,5,\ldots}^{\infty}\left[\sum_{m=1,2,3,\ldots}^{p}(-1)^m \sin n\alpha_m \cos n\theta\right] \qquad \text{(C-17)}$$

If the input voltage is $V_i(\theta) = V_s$, Eqs. (C-1) and (C-17) give the output voltage as

$$V_o(\theta) = V_s \sum_{n=1,3,5,\ldots}^{\infty} A_n \cos n\theta \qquad \text{(C-18)}$$

If the input voltage is $V_i(\theta) = V_m \cos \theta$, Eqs. (C-1) and (C-17) give the output voltage as

$$V_o(\theta) = V_m \sum_{n=1,3,5,\ldots}^{\infty} A_n \cos n\theta \cos \theta \tag{C-19}$$

$$= \frac{V_m}{2} \sum_{n=1,3,5,\ldots}^{\infty} A_n [\cos (n - 1)\theta + \cos (n + 1)\theta]$$

$$= 0.5V_m[A_1(\cos 0 + \cos 2\theta) + A_3(\cos 2\theta + \cos 4\theta) + A_5(\cos 4\theta + \cos 6\theta) + \cdots]$$

$$= \frac{V_m A_1}{2} + V_m \sum_{n=2,4,6,\ldots}^{\infty} \frac{A_{n-1} + A_{n+1}}{2} \cos n\theta \tag{C-20}$$

The first part of Eq. (C-20) is the average output voltage and the second part is the ripple voltage. Equation (C-20) is valid, provided that the input voltage and the switching function are cosine waveforms.

In the case of sine waves, the input voltage is $V_i(\theta) = V_m \sin \theta$ and the switching function is

$$S(\theta) = \sum_{n=1,3,5,\ldots}^{\infty} A_n \sin n\theta \tag{C-21}$$

Equations (C-1) and (C-2) give the output voltage as

$$V_o(\theta) = V_m \sum_{n=1,3,5,\ldots}^{\infty} A_n \sin \theta \sin n\theta \tag{C-22}$$

$$= \frac{V_m}{2} \sum_{n=1,3,5,\ldots}^{\infty} A_n [\cos (n - 1)\theta - \cos (n + 1)\theta]$$

$$= 0.5V_m [A_1 (\cos 0 - \cos 2\theta) + A_3(\cos 2\theta - \cos 4\theta) + A_5(\cos 4\theta - \cos 6\theta) + \cdots]$$

$$= \frac{V_m A_1}{2} - V_m \sum_{n=2,4,6,\ldots}^{\infty} \frac{A_{n-1} - A_{n+1}}{2} \cos n\theta \tag{C-23}$$

D

DC Transient Analysis

D-1 *RC* CIRCUIT WITH STEP INPUT

When the switch S_1 in Fig. 2-1a is closed at $t = 0$, the charging current of the capacitor can be found from

$$V_s = v_R + v_c = Ri + \frac{1}{C}\int i\,dt + v_c(t = 0) \qquad \text{(D-1)}$$

with initial condition: $v_c(t = 0) = 0$.
Using the Laplace's Table D-1, Eq. (D-1) can be transformed into Laplace's domain of s.

$$\frac{V_s}{s} = R\,I(s) + \frac{1}{C\,s}\,I(s)$$

and solving for the current $I(s)$ gives

$$I(s) = \frac{V_s}{R(s + \alpha)} \qquad \text{(D-2)}$$

where $\alpha = 1/RC$

TABLE D-1 SOME LAPLACE'S TRANSFORMATIONS

$f(t)$	$F(s)$
1	$\frac{1}{s}$
t	$\frac{1}{s^2}$
$e^{-\alpha t}$	$\frac{1}{s + \alpha}$
$\sin \alpha t$	$\frac{\alpha}{s^2 + \alpha^2}$
$\cos \alpha t$	$\frac{s}{s^2 + \alpha^2}$
$f'(t)$	$sF(s) - F(0)$
$f''(t)$	$s^2 F(s) - sF(0) - F'(0)$

Inverse transform of Eq. (D-2) in time domain yields

$$i(t) = \frac{V_s}{R} e^{-\alpha t} \tag{D-3}$$

and the voltage across the capacitor is obtained as

$$v_c(t) = \frac{1}{C} \int_0^t i \, dt = V_s (1 - e^{-\alpha t}) \tag{D-4}$$

In the steady-state (at $t = \infty$),

$$I_s = i(t = \infty) = 0$$

$$V_0 = v_c(t = \infty) = V_s/R$$

D-2 *RL* CIRCUIT WITH STEP INPUT

Two typical *RL* circuits are shown in Figs. 2-2a and 7-3a. The transient current through the inductor in Fig. 7-3a can be expressed as

$$V_s = v_L + v_R + E = L \frac{di}{dt} + R\, i + E \tag{D-5}$$

with initial condition: $i(t = 0) = I_1$. In Laplace's domain of s, Eq. (D-5) becomes

$$\frac{V_s}{s} = L\,s\,I(s) - L\,I_1 + R\,I(s) + \frac{E}{s}$$

and solving for $I(s)$ gives

$$\begin{aligned} I(s) &= \frac{V_s - E}{L\,s\,(s + \beta)} + \frac{I_1}{(s + \beta)} \\ &= \frac{(V_s - E)}{R}\left[\frac{1}{s} - \frac{1}{s + \beta}\right] + \frac{I_1}{s + \beta} \end{aligned} \tag{D-6}$$

where $\beta = R/L$
Taking inverse transform of Eq. (D-6) yields

$$i(t) = \frac{V_s}{R}(1 - e^{-\beta t}) + I_1 e^{-\beta t} \tag{D-7}$$

In the steady state (at $t = \infty$), $I_s = i(t = \infty) = V_s/R$
If there is no initial current on the inductor, (i.e., $I_1 = 0$) and Eq. (D-7) becomes

$$i(t) = \frac{V_s}{R}(1 - e^{-\beta t}) \tag{D-8}$$

In the steady state (at $t = \infty$), $I_s = i(t = \infty) = V_s/R$

D-3 *LC* CIRCUIT WITH STEP INPUT

The transient current through the capacitor in Fig. 3-2a is expressed as

$$V_s = v_L + v_c = L\frac{di}{dt} + \frac{1}{C}\int i\,dt + v_c(t = 0) \tag{D-9}$$

with initial conditions: $v_c(t = 0) = 0$ and $i(t = 0) = 0$. In Laplace's transform, Eq. (D-9) becomes

$$\frac{V_s}{s} = L\,s\,I(s) + \frac{1}{C\,s}I(s)$$

and solving for $I(s)$

$$I(s) = \frac{V_s}{L\,(s^2 + \omega_m^2)} \tag{D-10}$$

where $\omega_m = 1/\sqrt{(LC)}$
The inverse transform of Eq. (D-10) yields the charging current as

$$i(t) = V_s\sqrt{\frac{C}{L}}\sin(\omega_m t) \tag{D-11}$$

and the capacitor voltage is

$$v_c(t) = \frac{1}{C}\int_0^t i(t)\,dt = V_s\,[1 - \cos(\omega_m t)] \tag{D-12}$$

An LC circuit with an initial inductor current of I_m and initial capacitor voltage of V_0 is shown in Fig. 3-18a. The capacitor current is expressed as

$$V_s = L\frac{di}{dt} + \frac{1}{C}\int i\,dt + v_c(t = 0) \tag{D-13}$$

with initial condition: $i(t = 0) = I_m$ and $v_c(t = 0) = V_o$. Note: In Fig. 3-18a, V_0 is shown as equal to $-2V_s$. In Laplace's domain of s, Eq. (D-13) becomes

$$\frac{V_s}{s} = L\,s\,I(s) - L\,I_m + \frac{1}{C\,s} + \frac{V_o}{s}$$

and solving for the current $I(s)$ gives

$$I(s) = \frac{V_s - V_o}{L\,(s^2 + \omega_m^2)} + \frac{s\,I_m}{s^2 + \omega_m^2} \tag{D-14}$$

where $\omega_m = 1/\sqrt{(LC)}$
The inverse transform of Eq. (D-14) yields

$$i(t) = (V_s - V_o)\sqrt{\frac{C}{L}}\sin(\omega_m t) + I_m\cos(\omega_m t) \tag{D-15}$$

and the capacitor voltage as

$$\begin{aligned} v_c(t) &= \frac{1}{C}\int_0^t i(t)\,dt + V_o \\ &= I_m\sqrt{\frac{L}{C}}\sin(\omega_m t) - (V_s - V_o)\cos(\omega_m t) + V_s \end{aligned} \tag{D-16}$$

E

Fourier Analysis

Under steady-state conditions, the output voltage of power converters is, generally, a periodic function of time defined by

$$v_o(t) = v_o(t + T) \tag{E-1}$$

where T is the periodic time
If f is the frequency of the output voltage in Hz, the angular frequency is

$$\omega = \frac{2\pi}{T} = 2\pi f \tag{E-2}$$

and Eq. (E-1) can be rewritten as

$$v_o(\omega t) = v_o(\omega t + 2\pi) \tag{E-3}$$

The Fourier theorem states that a periodic function $v_o(t)$ can be described by a constant term plus an infinite series of sine and cosine terms of frequency $n\omega$, where n is an integer. Therefore, $v_o(t)$ can be expressed as

$$v_o(t) = a_o + \sum_{n=1,2,}^{\infty} [a_n \cos n\omega t + b_n \sin n\omega t] \tag{E-4}$$

where a_o is the average value of the output voltage, $v_o(t)$. The constant a_o, a_n and b_n can be determined from the following expressions:

$$a_o = \frac{1}{T}\int_0^T v_o(t)\,dt = \frac{1}{2\pi}\int_0^{2\pi} v_o(\omega t)\,d(\omega t) \tag{E-5}$$

$$a_n = \frac{1}{T}\int_0^T v_o(t)\cos n\omega t\,dt = \frac{1}{\pi}\int_0^{2\pi} v_o(\omega t)\cos n\omega t\,d(\omega t) \tag{E-6}$$

$$b_n = \frac{2}{T}\int_0^T v_o(t)\sin n\omega t\,dt = \frac{1}{\pi}\int_0^{2\pi} v_o(\omega t)\sin n\omega t\,d(\omega t) \tag{E-7}$$

If $v_o(t)$ can be expressed as an analytical function, these constants can be determined by a single integration. If $v_o(t)$ is discontinuous, which is the usually the case for the output of converters, several integrations (over the whole period of the output voltage) must be performed to determine the constants, a_o, a_n and b_n.

$$a_n \cos n\omega t + b_n \sin n\omega t = [a_n^2 + b_n^2]^{1/2}\left[\frac{a_n}{\sqrt{a_n^2 + b_n^2}}\cos n\omega t + \frac{b_n}{\sqrt{a_n^2 + b_n^2}}\sin n\omega t\right] \tag{E-8}$$

Let us define an angle ϕ_n, whose adjacent side is b_n, opposite side is a_n, and the hypotenuse is $[a_n^2 + b_n^2]^{1/2}$. As a result, Eq. (E-8) becomes

$$a_n \cos n\omega t + b_n \sin n\omega t = [a_n^2 + b_n^2]^{1/2}[\sin\phi_n \cos n\omega t + \cos\phi_n \sin n\omega t]$$

$$= [a_n^2 + b_n^2]^{1/2}\sin(n\omega t + \phi_n) \tag{E-9}$$

$$\text{where} \quad \phi_n = \tan^{-1}\left(\frac{a_n}{b_n}\right) \tag{E-10}$$

Substituting Eq. (E-9) into Eq. (E-4), the series may also be written as

$$v_o(t) = a_o + \sum_{n=1,2,\ldots}^{\infty} C_n \sin(n\omega t + \phi_n) \tag{E-11}$$

$$\text{where} \quad C_n = [a_n^2 + b_n^2]^{1/2} \tag{E-12}$$

C_n and ϕ_n are the peak magnitude and the delay angle of the nth harmonic component of the output voltage, $v_o(t)$, respectively.

If the output voltage has the half-wave symmetry, the number of integrations within the whole period can be reduced significantly. A waveform has the property of half-wave symmetry if the waveform satisfies the following conditions:

$$v_o(t) = -v_o(t + T/2) \tag{E-13}$$

$$\text{or} \quad v_o(\omega t) = -v_o(\omega t + \pi) \tag{E-14}$$

In a waveform with a half-wave symmetry, the negative half-wave is the mirror

image of the positive half-wave, but phase shifted by $T/2$ s (or π rad) from the positive half-wave. A waveform with a half-wave symmetry does not have the even harmonics (that is, $n = 2, 4, 6, \ldots$) and possess only the odd harmonics (that is, $n = 1, 3, 5, \ldots$). Due the half-wave symmetry, the average value is zero, (i.e., $a_o = 0$.) Equations (E-6), (E-7) and (E-11) become

$$a_n = \frac{2}{T}\int_0^T v_o(t) \cos n\omega t \, dt = \frac{1}{\pi}\int_0^{2\pi} v_o(\omega t) \cos n\omega t \, d(\omega t), \quad n = 1, 3, 5, \ldots$$

$$b_n = \frac{2}{T}\int_0^T v_o(t) \sin n\omega t \, dt = \frac{1}{\pi}\int_0^{2\pi} v_o(\omega t) \sin n\omega t \, d(\omega t), \quad n = 1,3,5, \ldots$$

$$v_o(t) = \sum_{n=1,3,5,\ldots}^{\infty} C_n \sin (n\omega t + \phi_n)$$

F

Listing of Computer Programs in IBM-PC BASICA

********* PROG-1 **********

```
20 CLS
30 DIM ALFA(20), ALFAD(20), B(100)
40 REM UNIFORM PWM ANGLE CALCULATION
50 PRINT "No. of pulses per half cycle ?"
60 INPUT NP
70 PRINT "Modulation index less than 1 ?"
80 INPUT AMF
82 PRINT "List of Fourier coefficients? For YES '1' and for NO '2' "
83 INPUT NC
84 PRINT "Highest desired harmonic component less than 100"
85 INPUT NM
87 CLS
90 PI=4!*ATN(1!)
97 PRINT "1987 Copyright by M.H. Rashid"
98 PRINT "Fig. 4-14 AC-DC converter with uniform PWM"
100 DELTAM=(PI/NP)*AMF
110 CENTR=(PI/NP)/2
120 ALFA(1)=CENTR-DELTAM/2
130 ALFAD(1)=ALFA(1)*180/PI
```

```
140 DELTAD=DELTAM*180/PI
170 FOR M=2 TO NP
180 ALFA(M)=ALFA(1)+(PI/NP)*(M-1)
190 ALFAD(M)=ALFA(M)*180/PI
210 NEXT M
220 VMAX=1
230 V=0
240 FOR M=1 TO NP
250 V=(COS(ALFA(M))-COS(ALFA(M)+DELTAM))+V
260 NEXT M
270 VDC=(VMAX/PI)*V/(SQR(2))
290 AN=0
300 IA=1
310 FOR N=1 TO NM
320 C=0
330 FOR M=1 TO NP
340 C=COS(N*ALFA(M))-COS(N*(ALFA(M)+DELTAM))+C
350 NEXT M
360 B(N)=(2*IA/(N*PI))*C
365 IF NC=1 THEN PRINT "B("N") = "B(N)
380 NEXT N
381 PRINT "No. of pulses per half-cycle = "NP
382 PRINT "Modulation index = "AMF
383 PRINT "Pulse width in degrees = "DELTAD
384 FOR M=1 TO NP
386 PRINT "α"M"in degrees = "ALFAD(M)
387 NEXT M
388 PRINT "Average output voltage in % of RMS input voltage = "VDC*100
390 I1=B(1)/SQR(2)
400 PRINT "RMS fundamental input current as % of dc load current = "I1*100
405 SUM=0
410 FOR N=1 TO NM
420 SUM=SUM+B(N)*B(N)/2
430 NEXT N
440 IS=SQR(SUM)
450 PRINT "RMS input current as % of dc load current = "IS*100
460 PF=I1/IS
463 DF=1
465 PRINT "Displacent factor = "DF
470 PRINT "Power factor =" PF
500 END
```

********** PROG-2 **********

```
30 CLS
30 DIM SL(25), C(25), X(90), Y(90), ALFA(25), ALFAD(25), B(50)
40 REM AC-DC CONVERTER WITH SINUSOIDAL PWM
50 PRINT "No. of pulses per half cycle ?"
60 INPUT NP
70 PRINT "Modulation index less than 1 ?"
80 INPUT AMF
```

```
82 PRINT "List of Fourier coefficients? For YES '1' and for NO '2' "
83 INPUT NC
84 PRINT "Highest desired harmonic component less than 100"
85 INPUT NM
87 CLS
90 PI=4!*ATN(1!)
97 PRINT "1987 Copyright by M.H. Rashid"
98 PRINT "Fig. 4-15 AC-DC converter with sinusoidal PWM"
100 NS=2*NP
102 TOL=.001
104 FOR M=1 TO NS
106 SL(M)=((-1)^M)*NS/PI
108 NEXT M
109 FOR M=1 TO NS STEP 2
110 C(M)=M
111 NEXT M
112 FOR M=2 TO NS STEP 2
113 C(M)=-(M-1)
114 NEXT M
116 Y(1)=AMF
118 X(1)=PI/2
119 FOR M=1 TO NS
120 FOR I=1 TO 50
122 K=I+1
124 X(K)=(Y(I)-C(M))/SL(M)
126 Y(K)=AMF*SIN(X(K))
128 XX=ABS(X(K)-X(K-1))
130 IF XX<TOL THEN 134
132 NEXT I
134 ALFA(M)=X(I)
136 NEXT M
138 FOR M=1 TO NS
140 ALFAD(M)=ALFA(M)*180/PI
142 NEXT M
220 VMAX=1
230 V=0
240 FOR M=1 TO NS STEP 2
250 V=(COS(ALFA(M))-COS(ALFA(M+1)))+V
260 NEXT M
270 VDC=(VMAX/PI)*V/(SQR(2))
290 AN=0
300 IA=1
310 FOR N=1 TO NM
320 D=0
330 FOR M=1 TO NS STEP 2
340 D=(COS(N*ALFA(M))-COS(N*ALFA(M+1)))+D
350 NEXT M
360 B(N)=(2*IA/(N*PI))*D
365 IF NC=1 THEN PRINT "B("N") = "B(N)
380 NEXT N
```

```
381 PRINT "No. of pulses per half-cycle = 'NP
382 PRINT "Modulation index = "AMF
384 FOR M=1 TO NS
386 PRINT "α"M"in degrees = "ALFAD(M)
387 NEXT M
388 PRINT "Average output voltage in % of RMS input voltage = "VDC*100
390 I1=B(1)/SQR(2)
400 PRINT "RMS fundamental input current as % of dc load current= "I1*100
405 SUM=0
410 FOR N=1 TO NM
420 SUM=SUM+B(N)*B(N)/2
430 NEXT N
440 IS=SQR(SUM)
450 PRINT "RMS input current as % of dc load current = "IS*100
460 PF=I1/IS
463 DF=1
465 PRINT "Displacent factor = "DF
470 PRINT "Power factor =" PF
500 END
```

********** PROG-3 **********

```
2   CLS
4   REM Solution for example 6-4
5   INPUT "DELAY ANGLE IN DEGREES ? ", ALP1
10  ALP=ALP1*3.1415927#/180
15  INPUT "INPUT VOLTAGE ? ", VS
20  INPUT "INPUT FREQUENCY ? ", F
30  INPUT "LOAD RESITANCE ? ", R
40  INPUT "LOAD INDUCTANCE  IN mH ? ", L
42  PI=4*ATN(1!)
45  W=2*PI*F
50  XL=W*L*.001
55  PRINT "IMPEDANCE OF LOAD INDUCTANCE = ", XL
105 PH=ATN(XL/R)
110 PH1=180*PH/PI
120 PRINT "LOAD ANGLE =", PH1
130 DELB=.25
140 DB=DELB*PI/180
152 BET1=PH
170 N=1
180 Y1=(R/XL)*(ALP-BET1)
190 Y2=EXP(Y1)
195 YX=SIN(ALP-PH)
200 Y3=Y2*YX
210 Y4=SIN(BET1-PH)
215 N=N+1
217 IF N=1000 THEN 360
220 YY=ABS(ABS(Y3)-ABS(Y4))
222 IF YY<.001 THEN  360
230 BET1=BET1+DB
```

```
245 IF Y4<0 THEN  Y4=0
250 GOTO 180
360 BET=180*BET1/PI
365 PRINT "EXTINCTION ANGLE =", BET
380 J=0
384 DEL=(BET1-ALP)/180
390 SUM=0
400 SUMM=0
402 L=L*.001
410 WT=ALP+DEL*J
420 T=WT/W
430 X=-T+ALP/W
440 X=X*R/L
450 X1=EXP(X)
460 X2=SIN(ALP-PH)
470 X3=X2*X1
480 X4=SIN(WT-PH)
490 X5=X4-X3
495 IF X5<0 THEN X5=0
500 XX=X5*X5
510 YY=X5
540 SUM=SUM+XX
550 SUMM=SUMM+YY
555 J=J+1
560 IF WT>BET1 THEN  800
570 IF WT=BET1 THEN 800
580 GOTO 410
800 SUM=SUM*DEL/PI
810 SUMM=SUMM*DEL/PI
811 SUMM=SUMM/SQR(2)
820 Y1=R*R+XL*XL
830 Y1=SQR(Y1)
840 IR=(VS/Y1)*SQR(SUM)
850 ID=(VS/Y1)*SUMM
860 PRINT "IR =  ", IR, "ID = ", ID
870 X=BET1-ALP+.5*SIN(2*ALP)-.5*SIN(2*BET1)
880 VO=VS*SQR(X//PI)
890 PRINT "RMS OF OUTPUT VOLTAGE = ", VO
900 PO=2*IR*IR*R
905 PRINT "OUTPUT POWER  = ", PO
910 PF=PO/(VS*IR*SQR(2))
920 PRINT "POWER FACTOR = ", PF
930 END
```

********** PROG-4 **********

```
5   CLS
8   PRINT "Example 6-7"
10  INPUT "INPUT LINE VOLTAGE ? ", VS
30  INPUT "LOAD RESISTANCE PER PHASE ? ", R
45  INPUT "DELAY ANGLE IN DEGREES ? ", ALP1
```

```
 70  X=4*ATN(1.0)
 80  ALP=ALP1*X/180
 90  IM=SQR(2)*VS/R
 91  AX=X-ALP+SIN(2*ALP)/2
 92  VO=VS*SQR(AX/X)
 93  PRINT "OUTPUT VOLTAGE FROM Eq. (6-35) ", VO
100 NS=360
110 DEL=X/NS
120 SUM=0
122 SUA=0
124 SUC=0
130 J=0
138 T1=ALP
139 IF T1>X/3 OR T1=X/3 THEN T1=X/3
140 Y=DEL*J
150 IA=0
155 IC=IM*SIN(Y-4*X/3)
156 IF ALP>2*X/3 AND Y<(X-ALP) THEN IC=0
158 YY=IA-IC
160 SUM=SUM+YY*YY
162 SUA=SUA+IA*IA
164 SUC=SUC+IC*IC
170 J=J+1
180 IF Y>T1 OR Y=T1 THEN 300
200 GOTO 140
300 T2=X/3
320 Y=DEL*J
322 IA=IM*SIN(Y)
324 IC=IM*SIN(Y-4*X/3)
330 YY=IA-IC
340 SUM=SUM+YY*YY
342 SUA=SUA+IA*IA
344 SUC=SUC+IC*IC
350 J=J+1
360 IF Y>T2 OR Y=T2 THEN  400
370 GOTO 320
400 T3=ALP+X/3
405 Y=DEL*J
410 IA=IM*SIN(Y)
411 IF ALP>X/3 AND Y<ALP THEN  IA=0
412 IC=0
416 YY=IA-IC
420 SUM=SUM+YY*YY
422 SUA=SUA+IA*IA
424 SUC=SUC+IC*IC
430 J=J+1
440 IF Y>T3 OR Y=T3 THEN  500
450 IF Y>X OR Y=X THEN  500
460 GOTO 405
500 T4=X
510 Y=DEL*J
```

```
512 IA=IM*SIN(Y)
514 IC=IM*SIN(Y-4*X/3)
520 YY=IA-IC
530 SUM=SUM+YY*YY
532 SUA=SUA+IA*IA
534 SUC=SUC+IC*IC
540 J=J+1
550 IF Y>T4 OR Y=T4 THEN  600
560 IF Y>X OR Y=X THEN  600
570 GOTO  510
600 PRINT "NO OF SAMPLES =  ", J
620 IA=SQR(SUA/J)
625 PRINT "RMS VALUE OF PHASE A = ", IA
630 IC=SQR(SUC/J)
635 PRINT "RMS CURRENT OF PHASE C = ", IC
640 IL=SQR(SUM/J)
645 PRINT "RMS VALUE OF LINE CURRENT A = ", IL
648 VO=IA*R
649 PRINT "RMS VALUEE OF OUTPUT PHASE VOLTAGE = ", VO
650 PO=IA*IA*R*3
660 PRINT "OUTPUT POWER" , PO
670 VA=3*VS*IA
680 PRINT "VOLT-AMP = ", VA
690 PF=PO/VA
700 PRINT "POWER FACTOR = ", PF
900 END
```

********* PROG-5 **********

```
5 CLS
10 REM "PROG-5"
30 DIM ALFAM(20), ALFAD(20), BN(100), AN(100), V(100)
40 REM UNIFORM PWM ANGLE CALCULATION
50 PRINT "No. of pulses per half cycle ?"
60 INPUT NP
70 PRINT "Modulation index less than 1 ?"
80 INPUT AMF
82 PRINT "List of Fourier coefficients? For YES '1' and for NO '2' "
83 INPUT NC
84 PRINT "Highest desired harmonic component less than 100"
85 INPUT NM
87 CLS
90 PI=4!*ATN(1!)
97 PRINT "1987 Copyright by M.H. Rashid"
98 PRINT "Fig. 8-11 inverter with uniform PWM"
100 DELTA=(PI/NP)*AMF
105 DELTAD=DELTA*180/PI
110 CENTR=(PI/NP)/2
120 ALFAM(1)=CENTR-DELTA/2
130 ALFAD(1)=ALFAM(1)*180/PI
170 FOR M=2 TO NP
```

```
180 ALFAM(M)=ALFAM(1)+(PI/NP)*(M-1)
190 ALFAD(M)=ALFAM(M)*180/PI
210 NEXT M
220 VS=1
225 FOR N=1 TO NM
230 A=0
234 B=0
240 FOR M=1 TO NP
250 A=SIN(N*(ALFAM(M)+DELTA/2))+A
253 B=COS(N*(ALFAM(M)+DELTA/2))+B
260 NEXT M
265 AN(N)=((4*VS/(N*PI))*SIN(N*DELTA/2))*A
270 BN(N)=((4*VS/(N*PI))*SIN(N*DELTA/2))*B
272 V(N)=SQR(AN(N)*AN(N)+BN(N)*BN(N))/SQR(2)
273 IF NC=1 THEN PRINT "AN("N") = "AN(N), "BN("N") = "BN(N), "V("N") = "V(N)
275 NEXT N
381 PRINT "No. of pulses per half-cycle = "NP
382 PRINT "Modulation index = "AMF
383 PRINT "Pulse width in degrees = "DELTAD
384 FOR M=1 TO NP
386 PRINT "α"M"in degrees = "ALFAD(M)
387 NEXT M
388 PRINT "Fundamental RMS output voltage in % of dc input voltage = "V(1)*100
390 VX=VS*SQR(NP*DELTAD/180)
400 PRINT "RMS output voltage as % of dc input voltage = " VX*100
410 HF=(SQR(VX*VX-V(1)*V(1)))/V(1)
420 PRINT "Harmonic factor in % = " HF*100
425 SUM=0
430 FOR N=2 TO NM
440 SUM=SUM+(V(N)/(N^2))^2
450 NEXT N
460 DF=SQR(SUM)/V(1)
465 PRINT "Distortion factor in % = " DF*100
500 END
```

********* PROG-6 **********

```
5 CLS
10 REM "PROG-6"
30 DIM C(25),V(100),Y(90),X(90),ALFA(25),ALFAD(25),AN(50),BN(50)
40 REM SPWM ANGLE CALCULATION
50 PRINT "No. of pulses per half cycle ?"
60 INPUT NP
70 PRINT "Modulation index less than 1 ?"
80 INPUT AMF
82 PRINT "List of Fourier coefficients? For YES '1' and for NO '2' "
83 INPUT NC
84 PRINT "Highest desired harmonic component less than 100"
85 INPUT NM
87 CLS
90 PI=4!*ATN(1!)
```

```
97 PRINT "1987 Copyright by M.H. Rashid"
98 PRINT "Fig. 8-13 inverter with SPWM"
100 NS=2*NP
105 TOL=.0001
110 FOR M=1 TO NS
115 SL(M)=((-1)^M)*((NS+2)/PI)
120 NEXT M
121 FOR M=1 TO NS STEP 2
122 C(M)=M+1
124 NEXT M
125 FOR M=2 TO NS STEP 2
130 C(M)=-M
135 NEXT M
140 Y(1)=AMF
145 X(1)=PI/2
150 FOR M=1 TO NS
155 FOR I=1 TO 90
160 K=I+1
165 X(K)=(Y(I)-C(M))/SL(M)
170 Y(K)=AMF*SIN(X(K))
175 XX=ABS(X(K)-X(K-1))
180 IF XX<TOL THEN GOTO 190
185 NEXT I
190 ALFA(M)=X(I)
195 NEXT M
200 FOR M=1 TO NS
202 ALFAD(M)=ALFA(M)*180/PI
206 NEXT M
220 VS=1
225 FOR N=1 TO NM
230 A=0
234 B=0
240 FOR M=1 TO NS STEP 2
250 A=COS(N*ALFA(M))-COS(N*ALFA(M+1))+A
253 B=SIN(N*ALFA(M+1))-SIN(N*ALFA(M))+B
260 NEXT M
265 AN(N)=((2*VS)/(N*PI))*A
270 BN(N)=((2*VS)/(N*PI))*B
272 V(N)=SQR(AN(N)*AN(N)+BN(N)*BN(N))/SQR(2)
273 IF NC=1 THEN PRINT "AN("N") = "AN(N), "BN("N") = "BN(N), "V("N") = "V(N)
275 NEXT N
381 PRINT "No. of pulses per half-cycle = "NP
382 PRINT "Modulation index = "AMF
383 PRINT "Pulse width in degrees "
384 FOR M=1 TO NS
386 PRINT "α"M"in degrees = "ALFAD(M)
387 NEXT M
388 PRINT "Fundamental RMS output voltage in % of dc input voltage = "V(1)*100
389 VX=0
390 VS=1
391 FOR M=1 TO NS  STEP 2
```

POWEREN.IR

```
392 VX=ALFA(M+1)-ALFA(M)+VX
394 NEXT M
396 VX=VS*SQR(VX/PI)
400 PRINT "RMS output voltage as % of dc input voltage = " VX*100
408 HF=(SQR(VX*VX-V(1)*V(1)))/V(1)
420 PRINT "Harmonic factor in % = " HF*100
425 SUM=0
430 FOR N=2 TO NM
440 SUM=SUM+(V(N)/(N^2))^2
450 NEXT N
460 DF=SQR(SUM)/V(1)
465 PRINT "Distortion factor in % = " DF*100
500 END
```

```
                    ********* PROG-7 **********
5 CLS
10 REM "PROG-7"
30 DIM SL(25),C(25),V(100),Y(90),X(90),ALFA(25),ALFAD(25),AN(50),BN(50)
40 REM SPWM ANGLE CALCULATION
50 PRINT "No. of pulses in the first 60 degrees ?"
60 INPUT NP
70 PRINT "Modulation index less than 1 ?"
80 INPUT AMF
82 PRINT "List of Fourier coefficients? For YES '1' and for NO '2' "
83 INPUT NC
84 PRINT "Highest desired harmonic component less than 100"
85 INPUT NM
87 CLS
90 PI=4!*ATN(1!)
97 PRINT "1987 Copyright by M.H. Rashid"
98 PRINT "Fig. 8-15 inverter with modified SPWM"
100 NS=2*NP
105 TOL=.0001
110 FOR M=1 TO NS
115 SL(M)=((-1)^M)*(3*(NS+1)/PI)
120 NEXT M
121 FOR M=1 TO NS STEP 2
122 C(M)=M+1
124 NEXT M
125 FOR M=2 TO NS STEP 2
130 C(M)=-M
135 NEXT M
136 NAT=2*NS+2
138 NPT=NAT/2
140 Y(1)=AMF
145 X(1)=PI/2
150 FOR M=1 TO NS
155 FOR I=1 TO 90
160 K=I+1
165 X(K)=(Y(I)-C(M))/SL(M)
170 Y(K)=AMF*SIN(X(K))
```

```
175 XX=ABS(X(K)-X(K-1))
180 IF XX<TOL THEN GOTO 184
182 NEXT I
184 ALFA(M)=X(I)
186 NEXT M
188 ALFA(NS+1)=PI/3
190 ALFA(NS+2)=2*PI/3
192 NAS=NS+1
194 FOR M=NAS TO NAT
195 J=NAT-M+1
196 ALFA(M)=PI-ALFA(J)
198 NEXT M
200 FOR M=1 TO NAT
202 ALFAD(M)=ALFA(M)*180/PI
206 NEXT M
220 VS=1
225 FOR N=1 TO NM
230 A=0
234 B=0
240 FOR M=1 TO NAT STEP 2
250 A=COS(N*ALFA(M))-COS(N*ALFA(M+1))+A
253 B=SIN(N*ALFA(M+1))-SIN(N*ALFA(M))+B
260 NEXT M
265 AN(N)=((2*VS)/(N*PI))*A
270 BN(N)=((2*VS)/(N*PI))*B
272 V(N)=SQR(AN(N)*AN(N)+BN(N)*BN(N))/SQR(2)
273 IF NC=1 THEN PRINT "AN("N") = "AN(N), "BN("N") = "BN(N), "V("N") = "V(N)
275 NEXT N
381 PRINT "No. of pulses per half-cycle = "NPT
382 PRINT "Modulation index = "AMF
384 PRINT "Angles are in degrees "
385 FOR M=1 TO NAT
386 PRINT "α"M"in degrees = "ALFAD(M)
387 NEXT M
388 PRINT "Fundamental RMS output voltage in % of dc input voltage = "V(1)*100
389 VX=0
390 VS=1
391 FOR M=1 TO NAT STEP 2
392 VX=ALFA(M+1)-ALFA(M)+VX
394 NEXT M
396 VX=VS*SQR(VX/PI)
400 PRINT "RMS output voltage as % of dc input voltage = " VX*100
408 HF=(SQR(VX*VX-V(1)*V(1)))/V(1)
420 PRINT "Harmonic factor in % = " HF*100
425 SUM=0
430 FOR N=2 TO NM
440 SUM=SUM+(V(N)/(N^2))^2
450 NEXT N
460 DF=SQR(SUM)/V(1)
465 PRINT "Distortion factor in % = " DF*100
500 END
```

Bibliography

BEDFORD, F. E., AND R. G. HOFT, *Principles of Inverter Circuits*. New York: John Wiley & Sons, Inc., 1964.

BIRD, B. M., AND K. G. KING, *An Introduction to Power Electronics*. Chichester, West Sussex, England: John Wiley & Sons Ltd., 1983.

CSAKI, F., K. GANSZKY, I. IPSITS, AND S. MARTI, *Power Electronics*. Budapest: Akadémiai Kiadó, 1980.

DATTA, S. M., *Power Electronics & Control*. Reston, Va.: Reston Publishing Co., Inc., 1985.

DAVIS, R. M., *Power Diode and Thyristor Circuits*. Stevenage, Herts, England: Institution of Electrical Engineers, 1979.

DEWAN, S. B., AND A. STRAUGHEN, *Power Semiconductor Circuits*. New York: John Wiley & Sons, Inc., 1984.

DEWAN, S. B., G. R. SLEMON, AND A. STRAUGHEN, *Power Semiconductor Drives*. New York: John Wiley & Sons, Inc., 1975.

General Electric SCR Manual 6th Ed. GRAFHAN, D. R., AND F. B. GOLDEN, Englewood Cliffs, N.J.: Prentice-Hall, Inc., 1982.

GOTTLIEB, I. M., *Power Control with Solid State Devices*. Reston, Va.: Reston Publishing Co., Inc., 1985.

HEUMANN, K., *Basic Principles of Power Electronics*. New York: Springer-Verlag, 1986.

HNATEK, E. R., *Design of Solid State Power Supplies*. New York: Van Nostrand Reinhold Company, Inc., 1981.

HOFT, R. G., *SCR Applications Handbook*. Segundo, Calif: International Rectifier Corporation, 1974.

HOFT, R. G., *Semiconductor Power Electronics*. New York: Van Nostrand Reinhold Company, Inc., 1986.

KLOSS, A., *A Basic Guide To Power Electronics*. New York: John Wiley & Sons, Inc., 1984.

KUSKO, A., *Solid State DC Motor Drives*. Cambridge, Mass.: The MIT Press, 1969.

LANDER, C. W., *Power Electronics*. Maidenhead, Berkshire, England: McGraw-Hill Book Company (U.K.) Ltd., 1981.

LEONARD, W., *Control of Electrical Drives*. New York: Springer-Verlag, 1985.

LINDSAY, J. F., AND M. H. RASHID, *Electromechanics and Electrical Machinery*. Englewood Cliffs, N.J.: Prentice-Hall, Inc., 1986.

LYE, R. W., *Power Converter Handbook*. Peterborough, Ont.: Canadian General Electric Company Ltd., 1976.

MAZDA, F. F., *Thyristor Control*. Chichester, West Sussex, England: John Wiley & Sons Ltd., 1973.

MCMURRY, W., *The Theory and Design of Cycloconverters*. Cambridge, Mass.: The MIT Press, 1972.

MURPHY, J. M. D., *Thyristor Control of AC Motors*. Oxford: Pergamon Press Ltd., 1973.

PEARMAN, R. A., *Power Electronics–Solid State Motor Control*. Reston, Va.: Reston Publishing Co., Inc., 1980.

PELLY, B. R., *Thyristor Phase Controlled Convertors and Cycloconverters*. New York: John Wiley & Sons, Inc., 1971.

RAMAMOORTY, M., *An Introduction to Thyristors and Their Applications*. London: Macmillan Publishers Ltd., 1978.

RAMSHAW, R. S., *Power Electronics—Thyristor Controlled Power for Electric Motors*. London: Chapman & Hall Ltd., 1982.

RICE, L. R. *SCR Designers Handbook*. Pittsburgh, Pa.: Westinghouse Electric Corporation, 1970.

ROSE, M. J. *Power Engineering Using Thyristors, Vol. 1,* London: Mullard Ltd., 1970.

SEN, P. C., *Thyristor DC Drives*. New York: John Wiley & Sons, Inc., 1981.

SCHAEFER, J., *Rectifier Circuits—Theory and Design*. New York: John Wiley & Sons, Inc., 1965.

SEVERNS, R. P., AND G. BLOOM., *Modern DC-to-DC Switchmode Power Converter Circuits*. New York: Van Nostrand Reinhold Company, Inc., 1985.

STEVEN, R. E., *Electrical Machines and Power Electronics*. Wakingham, Berkshire, England: Van Nostrand Reinhold Ltd., 1983.

SUGANDHI, R. K., AND K. K. SUGANDHI. *Thyristors—Theory and Applications*. New York: Halsted Press, 1984.

TARTER, R. E., *Principles of Solid-State Power Conversion*. Indianapolis, Ind.: Howard W. Sams & Company, Publishers Inc., 1985.

WELLS, R., *Static Power Converters*. New York: John Wiley & Sons, Inc., 1962.

WILLIAMS B. W., *Power Electronics, Devices, Drivers and Applications*, New York: Halsted Press, 1987.

WOOD, P., *Switching Power Converters*. New York: Van Nostrand Reinhold Company, Inc., 1981.

Index

A

Ac drives, 339
  current-source, 363
  induction motors, 340
  synchronous motors, 369
Angle
  commutation or overlap, 49
  delay, 57, 79
  displacement, 30
  extinction, 145
  firing, 79
  power factor, 545
  torque, 372
Avalanche breakdown, 469

B

Base speed, 298
Bipolar junction transistors (BJTs)
  base drive control of, 436
  data sheet of, 426
Bipolar junction transistors (BJTs) (*Contd.*)
  dc gain of, 424
  performance parameters of, 424
  steady-state characteristics of, 413
  switching characteristics of, 418
Blocking mode, 4
Breakdown voltage, 434

C

Capacitance, commutation, 74
Chopper drives, 313
  power control of, 313
  regenerative brake control of, 315
  rheostatic brake control of, 317
  two/four-quadrant, 319
Choppers
  classical, 205
  impulse-commutated, 205, 210
  multiphase, 321
  resonant pulse, 212

Choppers (*Contd.*)
step-down, 180
step-up, 186
thyristor, 204
Commutation, 49, 56
auxiliary, 61
capacitors, 74
complementary, 67, 266
current, 65
external pulse, 69
forced, 57
impulse, 60
line-side, 69
load-side, 69
natural or line, 57
resonant pulse, 64
self, 58
soft, 215
time, 58
voltage, 61
Computer programs, 567
Control
adaptive, 365
antisaturation, 439
base drive, 436
chopper, 313
closed-loop, 323, 365, 376
current, 361
extinction angle, 108
frequency, 356
microcomputer, 332
on-off, 138
phase-locked-loop, 330
phase, 140
phase-displacement, 246
power, 313
proportional base, 437
pulse-width-modulation, 112
regenerative brake, 315
rheostatic brake, 317
rotor voltage, 349
sinusoidal pulse-width modulation, 114
slip power, 351
stator voltage, 347
symmetrical angle, 110
tie, 156
turn-off, 437
turn-on, 436
vector, 365
Control (*Contd.*)
voltage and frequency, 358
volts/hertz, 358
Controllers
ac voltage, 137
polygon-connected, 160
single-phase bidirectional, 142
single-phase, 145
three-phase bidirectional, 157
three-phase full-wave, 154
three-phase half-wave, 148
unidirectional, 140
Converters
ac-ac, 10
ac-dc, 10
dc-ac, 10
dc-dc, 10, 180
dual, 78, 87
flyback, 285
full, 77, 84
full-bridge, 287
half-bridge, 287
one-quadrant, 77
push-pull, 287
semi-, 77
single-phase controlled, 78
single-phase dual, 87
single-phase full, 84
single-phase semi, 80
single-phase series, 90
switching functions of, 554
three-phase dual, 105
three-phase full, 101
three-phase half-wave, 95
three-phase semi, 99
two-quadrant, 77
Cooling, 514
by forced air, 516
by heat pipes, 517
liquid, 516
Crowbar circuit, 538
Current gain, 470, 514
Cycloconverters
single-phase, 166
three-phase, 168

D

Damping factor, 21
Damping ratio, 21, 522

Dc drives, 296
chopper control, 313
closed-loop control of, 323
microcomputer control of, 332
phase-locked-loop control, 330
single-phase control, 300
single-phase dual-converter control, 304
single-phase full-converter control, 303
single-phase half-wave-converter control, 301
single-phase semiconverter control, 302
three-phase control, 307
three-phase dual-converter control, 309
three-phase full-converter control, 308
three-phase half-wave-converter control, 308
three-phase semiconverter control, 308
Dc motors
base speed of, 298
characteristics of, 297
field control of, 298
magnetization characteristics of, 298
series, 299
voltage control of, 298
Dead zone, 255
di/dt, 456
protection, 474
Diodes
characteristics of, 383
commutation of, 33
fast recovery, 387
freewheeling, 17, 23, 228
general purpose, 386
leakage current, 384
parallel connected, 408
performance parameters of, 388
Schottky, 387
series connected, 406
Displacement factor, 30
Distortion
factor, 229
total harmonic, 229
Drives
ac, 339
dc, 296, 369
static Kramer, 350
static Scherbius, 350
Duty cycle, 10
dv/dt, 456
protection, 476

F

Factor
displacement, 30
distortion, 229
form, 30
harmonic, 30, 228
input power, 30
overdrive, 417
power, 107, 545
ripple, 30
softness, 384
transformer utilization, 30
Fault current
with ac source, 538
with dc source, 540
prospective, 531
Filters
ac, 45
dc, 44
Firing circuits of thyristors, 507
Forward breakdown voltage, 469
Fourier analysis, 564
Frequency
damped natural, 522
resonant, 21
ringing, 21
undamped natural, 522
Fuses
current/time characteristics of, 533
data sheet of, 534
Fusing, 531

G

Gate charge, 451
GTOs, 494
characteristics of, 494
data sheet of, 495
snubber circuit of, 502

H

Harmonics
lowest-order, 229
reduction, 248
Heat sinks, 514
Holding current, 469

I

Induction motors, 340
  current control of, 361
  field-weakening of, 358
  frequency control of, 356
  performance characteristics of, 341
  rotor voltage control of, 349
  slip power control of, 350
  stator voltage control of, 347
  voltage and frequency control of, 358
  voltage, current, and frequency control of, 364
Inverters, 11, 226
  auxiliary-commutated, 265
  complementary-commutated, 266
  current-source, 273, 274
  full-bridge series resonant, 256, 260
  gain of, 226
  half-bridge series resonant, 255, 261
  McMurray, 266
  series resonant, 251
  single-phase bridge, 230, 235, 555, 557
  three-phase bridge, 233
  variable dc link, 276
  voltage control, 239, 247
  voltage-source, 274
Isolation
  of gate and base drive, 461
I^2t for fusing, 401

L

Latching current, 469
Let-through energy, 533

M

Magnetic circuits, 549
Modulation
  frequency, 182
  index, 114, 240
  modified sinusoidal pulse-width, 245
  multiple-pulse-width, 241
  pulse-width, 112, 181, 240
  sinusoidal pulse-width, 114, 243
  uniform pulse-width, 241
MOSFETs, 440
  data sheet of, 446
  gate drive of, 452
MOSFETs (*Contd.*)
  performance characteristics of, 445
  steady-state characteristics of, 442
  switching characteristics of, 444
MOSIGTs, 452
  characteristics of, 453
  data sheet of, 454

O

Off-state current, 469
Opticouplers, 462

P

Pinch-off voltage, 441
Power devices, 8
Power electronics, 1
Power factor, 107, 545
Power pulses, 519
Power supplies, 284
  ac, 290
  bidirectional, 289
  bidirectional ac, 291
  dc, 285
  resonant ac, 291
  resonant dc, 288
  switched mode ac, 290
  switched mode dc, 285
Programs, computer, 567
Protections, 514
  by crowbar, 538
  current, 531
  voltage, 527
Pulse transformer, 462

R

Ratio
  damping, 522
  rectification, 30
  turns, 25
Reactance
  circulating current, 89
  commutating, 49
  synchronous, 370
Recovered charge, 385
Rectifiers, 15
  bridge, 33

Rectifiers (*Contd.*)
circuit design of, 44
controlled, 10, 77
efficiency, 30
multiphase star, 38
single-phase bridge, 33, 557, 559
single-phase half-wave, 29
three-phase bridge, 41
Regulators
boost, 193
buck, 190
buck-boost, 196
Cúk, 199
flyback, 196
switching mode, 189
Relays, solid-state, 132
Resistance
on-state, 451
thermal, 391, 515
Reverse current, 470
Reverse recovery, 385

S

Saturating charge, 418
Slip, 341
Snubbers, 459, 520
non-dissipative, 524
optimum design of, 523
Speed
base, 298, 357
synchronous, 340
Static Kramer drive, 350
Static Scherbius drive, 350
Switches
ac static, 11
bidirectional, 143
dc static, 11, 130
single-phase ac, 125
three-phase ac, 127
three-phase reversing, 127
Switching function, 36, 554
Synchronous motors, 369
closed-loop control of, 376
cylindrical rotor, 370
permanent-magnet, 375
reluctance, 374
salient-pole, 373

T

Tap changers
single-phase, 161
synchronous, 164
Thermal impedance, 518
Thermal resistance, 391, 515
Thermal time constant, 517
Threshold voltage, 441
Thyristors
asymmetrical, 483
bidirectional triode, 482
characteristics of, 468
data sheet of, 486
fast switching, 480
FET-controlled, 484
firing circuits of, 507
gate assisted turn-off, 3
gate protection circuits, 509
gate-turn-off, 481
light activated, 484
parallel operation of, 507
performance parameters of, 485
phase-control, 480
reverse conducting, 482
series operation of, 504
static induction, 3, 483
turn-off of, 479
turn-on of, 472
two-transistor model of, 470
types of, 479
Time
available turn-off, 61, 206
circuit turn-off, 61
commutation, 206
delay, 419, 473
fall, 445
forward recovery, 386, 403
reverse recovery, 384, 400
rise, 445, 473
storage, 419
turn-off, 5, 425, 492
turn-off delay, 445
turn-on, 424, 473
Time constant, 325
storage, 419
Torque
developed, 342

POWEREN.IR